CHALCOGEN-NITROGEN CHEMISTRY

From Fundamentals to Applications in Biological, Physical and Materials Sciences

Updated Edition

Tristram Chivers • Risto S. Laitinen

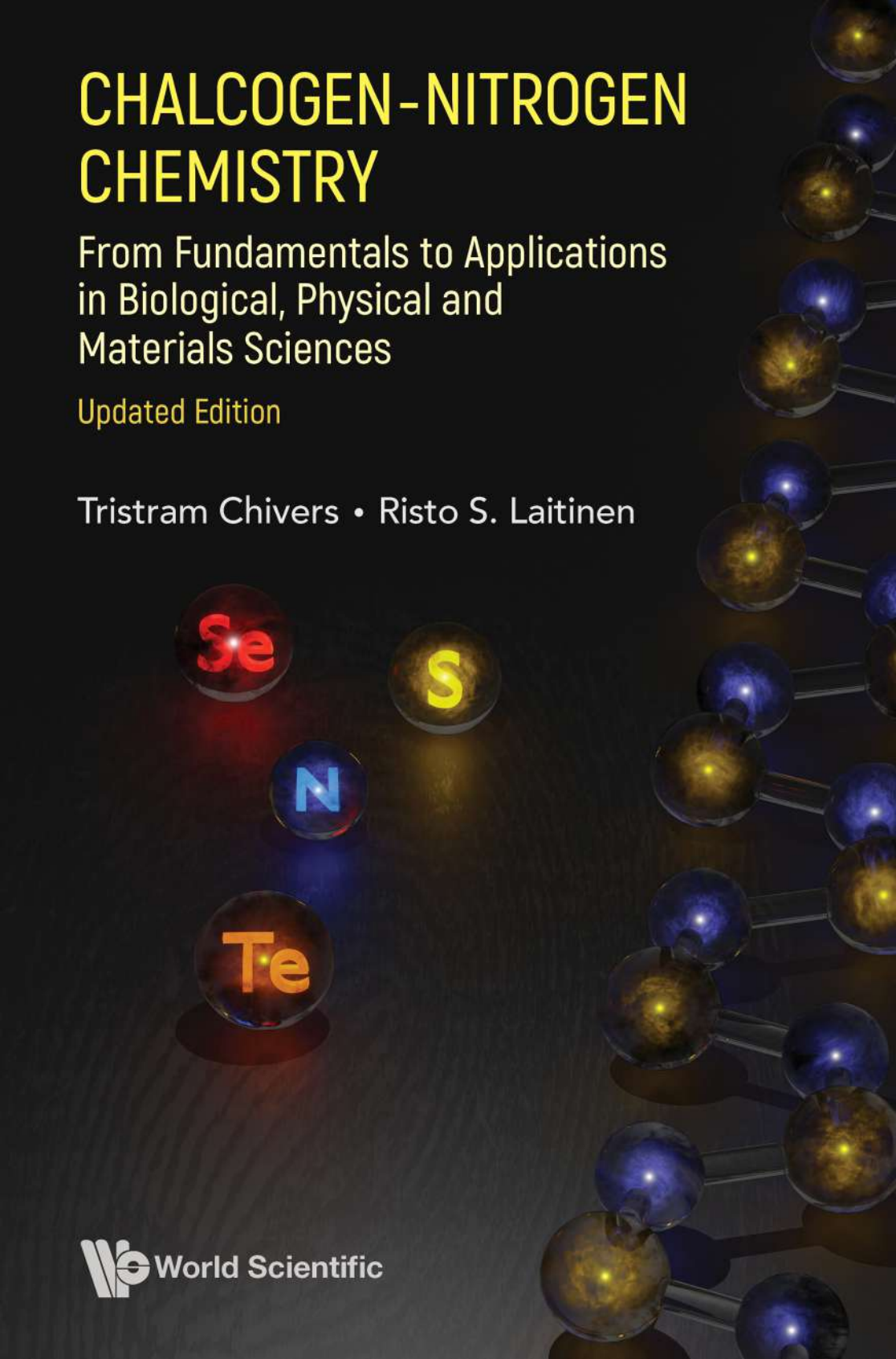

World Scientific

"The diverse and rich chemistry of chalcogen nitrides is brought to life in this compelling book which provides insight and order in an area of chemistry that many find confusing. The combination of fundamentals and applications makes for a very readable and compelling account. This text should be on the shelf of all inorganic and many organic chemists."

J Derek Woollins FRSC FRSE
Professor Emeritus, University of St. Andrews, UK

"An in-depth look at how nitrogen can link to chalcogens, how chalcogen-nitrogen compounds are synthesized, and the properties of these compounds. It is a revised and updated version of the postgraduate text that I have used in teaching for years. This didactically elegant book skillfully spans from classical solid state and molecular chemistry to biochemistry with a steady focus on chalcogen-nitrogen species."

Axel Schulz
Professor of Inorganic Chemistry, University of Rostock, Germany

"Chivers and Laitinen have provided a timely, well-balanced and comprehensive overview of key advances made in chalcogen-nitrogen chemistry during the last 16 years. While developments in fundamental topics like synthetic methods, molecular and electronic structural studies are thoroughly covered, the book also takes on the challenge of addressing broad potential applications in medicine, biology, physics and materials science that is emerging for compounds containing chalcogen-nitrogen units. Thus the book will be an invaluable aid not only to teachers and students of inorganic, organic, physical and materials chemistry, but also to researchers with interests spanning any of these disciplines."

Richard T Oakley FRSC
Professor Emeritus, University of Waterloo, Canada

"Chalcogen-nitrogen chemistry is an important part of contemporary main group chemistry. This book by the world-recognized experts gives a comprehensive discussion of essential achievements of this chemistry and

its applications, together with inspiration towards further research. With about 50 years of experience in the field, I highly recommend this book to the next generations of chemists."

Andrey V Zibarev
Professor of Chemistry, Russian Academy of Sciences, Russia

"This latest edition provides contemporary updates, highlighting the considerable body of work published in the intervening 16 years. The combination of fundamental and advanced topics not only make this an essential text for those working in the field of chalcogen-nitrogen chemistry but will undoubtedly be a strongly recommended text for senior undergraduate courses in main group chemistry."

Jeremy Rawson
Professor of Chemistry, University of Windsor, Canada

CHALCOGEN-NITROGEN CHEMISTRY

From Fundamentals to Applications in Biological, Physical and Materials Sciences

Updated Edition

Other Titles by Tristram Chivers

A Guide to Chalcogen-Nitrogen Chemistry
Inorganic Rings and Polymers of the p-Block Elements: From Fundamentals to Applications (with Ian Manners)

Other Titles by Risto S. Laitinen

Selenium and Tellurium Chemistry: From Small Molecules to Biomolecules and Materials (edited with J. Derek Woollins)
Selenium and Tellurium Reagents — in Chemistry and Materials Science (edited with Raija Oilunkaniemi)

CHALCOGEN-NITROGEN CHEMISTRY

From Fundamentals to Applications in Biological, Physical and Materials Sciences

Updated Edition

Tristram Chivers
University of Calgary, Canada

Risto S. Laitinen
University of Oulu, Finland

World Scientific

NEW JERSEY • LONDON • SINGAPORE • BEIJING • SHANGHAI • HONG KONG • TAIPEI • CHENNAI • TOKYO

Published by

World Scientific Publishing Co. Pte. Ltd.

5 Toh Tuck Link, Singapore 596224

USA office: 27 Warren Street, Suite 401-402, Hackensack, NJ 07601

UK office: 57 Shelton Street, Covent Garden, London WC2H 9HE

Library of Congress Cataloging-in-Publication Data
Names: Chivers, T. (Tristram), 1940– author. | Laitinen, Risto S., author.
Title: Chalcogen-nitrogen chemistry : from fundamentals to applications in biological, physical and materials sciences / Tristram Chivers, University of Calgary, Canada, Risto S. Laitinen, University of Oulu, Finland.
Other titles: Guide to chalcogen-nitrogen chemistry
Description: Updated edition. | New Jersey : World Scientific, [2022] | Includes bibliographical references and index.
Identifiers: LCCN 2021028959 | ISBN 9789811241338 (hardcover) | ISBN 9789811241345 (ebook for institutions) | ISBN 9789811241352 (ebook for individuals)
Subjects: LCSH: Chalcogenides. | Nitrogen compounds. | Chemistry.
Classification: LCC QD169.C5 C48 2022 | DDC 546/.72--dc23
LC record available at https://lccn.loc.gov/2021028959

British Library Cataloguing-in-Publication Data
A catalogue record for this book is available from the British Library.

For any available supplementary material, please visit
https://www.worldscientific.com/worldscibooks/10.1142/12397#t=suppl

Desk Editor: Shaun Tan Yi Jie

Typeset by Stallion Press
Email: enquiries@stallionpress.com

Printed in Singapore

Preface: Updated Edition

In the 16 years since the publication of *A Guide to Chalcogen-Nitrogen Chemistry*, the emphasis of investigations of chalcogen-nitrogen compounds has changed from a focus on fundamental studies to a search for practical applications in areas ranging from biological to materials sciences, and many remarkable advances have been made. Many of these developments have relied on information from early seminal work on the synthesis, molecular and electronic structures, and properties of chalcogen-nitrogen compounds that were discussed in the first edition of this book.

The approach to this updated edition has been to retain the fundamental information from the first edition that continues to be central to the development of our understanding and applications of chalcogen-nitrogen chemistry, while replacing the less important content from the first edition with new material. Thus, chapters 6, 7, 11, 13, 14 and 15 are entirely new and the chapters that have been partially retained from the first edition have been updated with recent findings as outlined below.

From a fundamental perspective, the intricate electronic structures of well-known binary sulfur-nitrogen molecules such as S_2N_2, $[S_3N_3]^-$ and S_4N_4 continue to occupy the attention of computational chemists, particularly with regard to their aromatic and diradical character, as well as the nature of intramolecular π^*–π^* chalcogen-chalcogen interactions in bicyclic compounds. In addition to the importance of the $NS^{\bullet}$ radical as an interstellar species, the cation $[NS]^+$ and the binary anions $[S_xN]^-$ (x = 3, 4) have been detected in astrophysical settings. From a practical

perspective, the well-known polymerisation of S_2N_2 to $(SN)_x$ has been developed as a method for fingerprint detection in forensic science. The equipment is marketed under the name "RECOVER Latent Fingerprint Technology" and has been sold in a dozen countries.

Recent computational studies have predicted unusual optoelectronic properties for nitrogen-rich chalcogen nitrides. Such high-energy materials have been avoided by experimentalists in the past, but the synthesis and structural characterisation of N_2S has been achieved in the last couple of years. Many other small, short-lived sulfur-nitrogen molecules, notably the radicals $[NSO]^{\bullet}$ and $[NSO_2]^{\bullet}$, as well as their conjugate acids, HNSO and $HNSO_2$, have also been identified. These advances have involved the employment of flash photolysis or pyrolysis as a synthetic tool. Characterisation of these ephemeral species utilises vibrational spectroscopy on matrix-isolated products using both natural abundance and ^{15}N-labelled precursors, complemented by density functional methods to elucidate both molecular and electronic structures.

In a biological context, the investigations of the chemistry of thionitrosyls (RSNOs) continue regarding the ability of these labile sulfur-nitrogen compounds to store and transport nitric oxide. In addition, the role of HSNO and ternary S,N,O anions in NO signaling and NO/H_2S "Crosstalk" has become a very active and controversial topic. The synthesis and spectroscopic characterisation of the fundamental anionic species $[SNO]^-$ and $[SSNO]^-$ in the 1980s have provided crucial information for the biological scientists involved in these investigations; curiously, the anion $[SSNO]^-$ also plays a key role in the gunpowder reaction of sulfur with potassium nitrate and carbon.

Organic sulfur-nitrogen compounds continue to attract attention due to their extensive use in the pharmaceutical and agrochemical industries, *e.g.*, sulfonamides, $RS(O)_2NR_2$, are employed for treatment of epilepsy, high blood pressure, arthritis and glaucoma. These widespread applications have stimulated a search for improved syntheses for these important commodities. The sulfinylamine, TrNSO (Tr = trityl), and the *N*-sulfinyl-*O*-hydroxylamine, 4-PhC_6H_4ONSO, are now commercially available reagents for this purpose. From a fundamental perspective, a labile tetraimido analogue of sulfuric acid, $H_2S(N^tBu)_4$, has been isolated and structurally characterised.

The chemistry of carbon-containing chalcogen-nitrogen (E–N; E = S, Se, Te) heterocycles in which the E–N functionality plays a dominant role has expanded enormously, especially in the area of realised and potential applications. The multifarious uses of benzo-2-thia-1,3-diazoles are a major focus of these investigations. Derivatives of these diamagnetic ring systems are employed as muscle relaxants and for the treatment of ocular hypertension and glaucoma, as well as in probes for locating tumour cells. Furthermore, the positive electron affinities and optical properties of these C,N,E heterocycles can be advantageous for applications in light technology, *e.g.*, in organic light-emitting diodes, field-effect transistors or solar cells. From a fundamental perspective, the emphasis has been on increasing our understanding of the influence of replacing sulfur by a heavier chalcogen (Se or Te) on the structures and properties of diamagnetic C,N,E ring systems.

The synthesis, structures and magnetic properties of carbon-poor chalcogen-nitrogen heterocycles, radicals and radical anions, as well as their metal complexes, have been widely investigated as possible functional materials, *e.g.*, in optical switching devices, organic electrodes and lightweight magnetoresistance devices.

Finally, carbon-containing chalcogen-nitrogen heterocycles have played a central role in the emerging area of *chalcogen bonding* involving weak E···N interactions between an electron-rich centre (N) and an electrophilic region on the chalcogen atom (E). These secondary bonding interactions (SBIs) can be either *intra*molecular or *inter*molecular. In the former case, weak E···N interactions are used as an alternative to sterically bulky substituents to stabilise labile functional groups, *e.g.*, in organoselenium(II) azides, organotellurium(IV) compounds with a Te=O unit, or organochalcogen(II) cations. *Inter*molecular E···N SBIs can generate materials with unique conducting, magnetic, optical or mechanical properties. They are especially strong for tellurium leading to supramolecular structures that may participate in host-guest chemistry.

Each chapter in this updated edition is designed to be self-contained, but there are frequent cross-references to a section in another chapter where appropriate. References at the end of each chapter are primarily for the period 2005 to mid-2021, but citations of earlier seminal work are included to provide historical context. In addition to the citations of papers

published in mainstream inorganic, organic, organometallic, physical, theoretical, materials and general chemistry journals, the broadening ambit of chalcogen-nitrogen chemistry is reflected in the following titles among the references: *Icarus, Earth, Moon and Planets, Journal of Atmospheric Chemistry, Solar Energy, Astronomy and Astrophysics, Astrophysical Journal Letters, Space Science Reviews, Dyes and Pigments, Journal of Agricultural and Food Chemistry, Current Opinion in Chemical Biology, Journal of Biological Chemistry, Journal of Medicinal Chemistry, European Journal of Medical Chemistry, Pharmacological Research, Archives of Biochemistry and Biophysics, Free Radical Biology and Medicine, Redox Biology, Photochemical & Photobiological Sciences, Nitric Oxide*, *Interface Focus, Nanoscale, Journal of Physical Chemistry of Solids, Synthetic Metals, Organic Electronics, Applied Magnetic Resonance,* and *Science & Justice*.

A complete list of post-2004 book chapters and review articles is given at the end of Chapter 1.

Preface: First Edition

The quintessential chalcogen-nitrogen compound tetrasulfur tetranitride, S_4N_4, was first detected by Gregory in 1835 just ten years after the discovery of benzene. Its unusual structure, like that of benzene, was not elucidated for over 100 years. The application of diffraction techniques revealed the unusual cage arrangement with two weak cross-ring sulfur–sulfur interactions. The details of the electronic structure of this fascinating molecule are still a matter of debate today.

Pioneering work in Germany, especially by the groups of Becke-Goehring, Weiss and Glemser, in the middle of the previous century uncovered a rich chemistry for inorganic sulfur–nitrogen systems. Their early efforts were notable because of the unavailability of many modern physical techniques for structural characterisation that are commonplace today. The book by Goehring entitled *Ergebnisse und Probleme der Chemie der Schewfelstickstoffverbindungen* deserves special mention for the stimulus that it provided to subsequent workers in the field.

The polymer, $(SN)_x$, was first obtained in 1910 and its metallic character was noted. However, it was the discovery in 1973 by Labes that a polymer comprised only of non-metallic elements behaves as a superconductor at 0.26 K that sparked widespread interest in sulfur-nitrogen (S–N) chemistry. A year earlier Banister proposed that planar S–N heterocycles belong to a class of "*electron-rich aromatics*" that conform to the well-known Hückel $(4n + 2)\pi$-electron rule of organic chemistry. This suggestion, which was based on simple electron-counting concepts, provided an additional impetus for both experimental and theoretical investigations of

S–N systems. The classic book in this field, *The Inorganic Heterocyclic Chemistry of Sulfur, Nitrogen and Phosphorus* by Heal, covered developments up to the end of the 1970s. This opus contributed authoritative insights into the fascinating chemistry of S–N compounds. It used a descriptive approach that drew attention to the many facets of the synthesis, structures and reactions that were poorly understood at that time.

In the first chapter of his book Heal states: "Indeed, the reaction chemistry of these substances (*i.e.*, S–N compounds) deserves to rank with that of boranes for novelty and interest."

In the past 25 years the field of S–N chemistry has reached maturity as a result of contributions from many countries, notably Germany, UK, Canada, Japan and the United States. The combination of structural studies, primarily through X-ray crystallography, spectroscopic information and molecular orbital calculations has provided reasonable rationalisations of the structure-reactivity relationships of these fascinating compounds. The unusual structures and properties of S–N compounds have attracted the attention of numerous theoretical chemists, who continue to address the "aromatic" character of binary S–N systems. Interfaces with other areas of chemistry, *e.g.*, materials chemistry, organic synthesis, biochemistry and coordination chemistry have been established and are under active development. For example, materials with unique magnetic and conducting properties that depend on intermolecular chalcogen-nitrogen interactions between radical species have been designed. Some carbon-nitrogen-sulfur heterocycles exhibit magnetic behaviour that is of potential significance in the construction of organic data-recording devices. In another area of materials chemistry, polymers involving both S–N and P–N linkages in the backbone have been used as components of matrices for oxygen sensors in the aerospace industry. In a biological setting, *S*-nitrosothiols (RSNO) have emerged as important species in the storage and transport of nitric oxide. As NO donors these sulfur–nitrogen compounds have potential medical applications in the treatment of blood circulation problems. In a different, but fascinating, context, thionitrite anions $[S_xNO]^-$ ($x = 1,2$) are implicated in the gunpowder reaction through an explosive decomposition.

The chemistry of selenium– and tellurium–nitrogen compounds has progressed more slowly but, in the last ten years, there have been

numerous developments in these areas also, as a result of the creative contributions of both inorganic and organic synthetic chemists. Significant differences are apparent in the structures, reactivities and properties of these heavier chalcogen derivatives, especially in the case of tellurium. In addition, the lability of Se–N and Te–N bonds has led to applications of reagents containing these reactive functionalities in organic syntheses and, as a source of elemental chalcogen, in the production of metal chalcogenide semi-conductors.

In addition to providing a modern account of developments in chalcogen-nitrogen chemistry, including a comparison of sulfur systems with those of the heavier chalcogens, these interfaces will provide a major focus of this monograph. As implied by the inclusion of "*A Guide to* …." in the title, it is not intended that the coverage of the primary literature will be comprehensive. Rather it provides an overview of the field with an emphasis on general concepts. Each chapter is designed to be self-contained, but there are extensive cross-references between chapters. By the use of selected examples, it is hoped that a reader, who is unfamiliar with or new to the field, will be able to gain an appreciation of the subtleties of chalcogen-nitrogen chemistry. A complete list of review articles is given at the end of Chapter 1. Key references to the primary literature are identified at the end of each chapter for the reader who wishes to pursue an individual topic in detail. The literature is covered up to mid-2004. Apart from two notable exceptions, the coverage of sulfur-nitrogen chemistry in standard inorganic (and organic) chemistry textbooks is sparse and usually limited to brief comments about the neutral binary compounds S_2N_2, S_4N_4 and $(SN)_x$. Those exceptions are the second edition of *Chemistry of the Elements* by N.N. Greenwood and A. Earnshaw (Butterworth-Heinemann, 1997) and the 34th edition of *Inorganic Chemistry* by Hollemann–Wiberg (Academic Press, 2001), which devote 26 and 14 pages, respectively, to this topic. It is hoped that the information in this book will be helpful to those who wish to go beyond the standard textbook treatment of various aspects of this important subject.

Acknowledgements

The invitation to write the updated edition of *A Guide to Chalcogen-Nitrogen Chemistry* was accepted in February 2020 just prior to the imposition of travel and other restrictions necessitated by the global pandemic. The remarkable advances in the influence of chalcogen-nitrogen chemistry across disciplines ranging from Biological Chemistry to Materials Science that have occurred in the last 16 years have made this project a stimulating challenge over the past 15 months.

The final drafts of this book benefitted from the input of expertise and encouragement from scientists in many countries who are active in the field of chalcogen-nitrogen chemistry. The authors acknowledge, with gratitude, helpful comments from the following experts (in alphabetical order): Professor Jens Beckmann (University of Bremen, Germany), Professor René T. Boeré (University of Lethbridge, Canada), Professor Frank T. Edelmann (University of Magdeburg, Germany), Dr. Paul Kelly (Loughborough University, UK), Dr. Alexander Yu. Makarov (Siberian Branch of the Russian Academy of Sciences, Russia), Professor José A. Olabe (University of Buenos Aires, Argentina), Professor Richard T. Oakley (University of Waterloo, Canada), Professor Kathryn E. Preuss (University of Guelph, Canada), Professor Oleg A. Rakitin (Russian Academy of Sciences, Russia), Professor Jeremy M. Rawson (University of Windsor, Canada), Dr. Nikolay A. Semenov (Siberian Branch of the Russian Academy of Sciences, Russia). Professor Harkesh B. Singh (Indian Institute of Technology Bombay, India), Professor Ignacio Vargas-Baca (McMaster University, Canada), Professor J. Derek Woollins

(University of St. Andrews, UK), and Professor Andrey V. Zibarev (Siberian Branch of the Russian Academy of Sciences, Russia). Their perceptive suggestions have enhanced the quality and accuracy of the final version of this edition substantially. Nevertheless, there are undoubtedly shortcomings in the form of errors or omissions for which the authors are entirely responsible.

Special thanks are accorded to the following who, in addition to their invaluable input, provided graphics and other images that have been used in the book: Dr. Roberto S. P. King (Foster & Freeman Ltd., Evesham, UK) (Figure 5.2), Professor José A. Olabe (Figures 7.1 and 7.7, Scheme 7.7), Professor Jeremy M. Rawson (Figure 13.5), Professor Richard T. Oakley (Schemes 11.6 and 11.8, Figure 13.3 and Table 13.1) and Professor Ignacio Vargas-Baca (Figure 3.17 and Chart 11.1). We are also most grateful to Marko Rodewald (University of Jena, Germany) who designed the artwork on the front cover, and to Professor Richard Oakley for helpful suggestions on the presentation of the image.

The retention of the structure of poly(sulfur nitride) from the cover of the first edition is appropriate in view of the impetus that the discovery of this unique polymer had on the field of chalcogen-nitrogen chemistry and its contemporary role in the development of new technology for fingerprint detection. The unfailingly prompt advice of the editor, Shaun Tan Yi Jie at World Scientific Publishing Co., Singapore, is sincerely appreciated.

Finally, we thank Sue and Marita for their continuing support and patience.

Tris Chivers
Calgary, May 2021

Risto Laitinen
Oulu, May 2021

About the Authors

Tristram Chivers is Professor Emeritus of Chemistry at University of Calgary, Canada. He is an elected Fellow of the Royal Society of Canada, the Chemical Institute of Canada and the Royal Society of Chemistry, UK. He is the author of 450 peer-reviewed articles, 32 book chapters and two books: *A Guide to Chalcogen-Nitrogen Chemistry* (World Scientific, 2005) and *Inorganic Rings and Polymers of the p-Block Elements* with Ian Manners (Royal Society of Chemistry, 2009). He served as President of the Canadian Society for Chemistry (CSC) in 2000–2001. He received the Alcan Lecture Award of the CSC in 1987, the Royal Society of Chemistry Award (UK) for Main-Group Element Chemistry in 1993, the E.W.R. Steacie Award from the CSC in 2001, the Montreal Medal of the Chemical Institute of Canada in 2004, an Honourary Doctorate (DSc) from University of Oulu, Finland in 2006, and the ASTech Outstanding Leadership in Alberta Science Award in 2008. His primary research interests are in main-group element chemistry with an emphasis on the chalcogens. He received BSc, PhD and DSc degrees all from the University of Durham, UK.

Risto S Laitinen is Professor Emeritus of Chemistry at University of Oulu, Finland. He has been a member of Finnish Academy of Science and Letters since 2003. He has published 250 peer-reviewed articles, 30 popular articles, 15 book chapters, and has edited two books: *Selenium and Tellurium Reagents — in Chemistry and Materials Science* with Raija Oilunkaniemi (Walther de Gruyter, 2019) and *Selenium and Tellurium Chemistry: From Small Molecules to Biomolecules and Materials* with Derek Woollins (Springer, 2011). He is the Secretary of the Division of Chemical Nomenclature and Structure Representation, International Union of Pure and Applied Chemistry, for the term 2016–2023. He served as Chair of the Board of Union of Finnish University Professors in 2007–2010. In 2017, he received an award from the Finnish Cultural Foundation (North Ostrobothnia Regional Fund) for excellence in his activities for science and music. His research interests are directed to synthetic, structural, and computational chemistry of chalcogen compounds, focusing on selenium and tellurium. He received MSc and PhD degrees from Helsinki University of Technology (currently Aalto University).

Contents

Chapter 1

Introduction

1.1 General Considerations

Oxygen, sulfur, selenium and tellurium are members of Group 16 in the Periodic Table. These elements, which are known as chalcogens, are isovalent. Consequently, some similarities between nitrogen-oxygen and other chalcogen-nitrogen (E–N; E = S, Se, Te) species might be expected. On the other hand, the fundamental properties of the chalcogens differ significantly and this diversity can be expected to lead to disparities between the structures and properties of N–O molecules and ions and those of their heavier chalcogen-nitrogen counterparts. The fundamental properties of chalcogens that contribute to these differences are discussed in this section. The subsequent sections in this chapter illustrate these divergences for various classes of E–N compounds. The titles of general reviews and book chapters on this topic, as well as for specific types of E–N compounds, are listed at the end of the chapter.

(a) The Pauling electronegativities for N, O, S, Se and Te are 3.04, 3.44, 2.58, 2.55 and 2.10, respectively. As a result, an N–O bond will be polarised with a partial negative charge on oxygen, whereas an E–N (E = S, Se, Te) bond will be polarised in the opposite direction.
(b) The preference for σ-bonding over π-bonding is a common feature of the chemistry of the heavier *p*-block elements. For example, in their elemental forms oxygen and nitrogen exist as the diatomic molecules O=O and N≡N, respectively, whereas both sulfur and selenium form a variety of cyclic allotropes with only single E–E (E = S, Se) bonds.

(c) E–N bond dissociation energies decrease down the series: S–N > Se–N > Te–N

(d) Both oxygen and sulfur can adopt a variety of oxidation states in the formation of molecules or ions. These range from –2 to +2 for oxygen and from –2 to +6 for sulfur. The ability to achieve oxidation states >2, especially +4 and +6, gives rise to sulfur–nitrogen species that have no N–O analogues. The higher oxidation states are more stable for Se and Te.

(e) The size of Group 16 elements (chalcogens) increases down the series: O < S < Se < Te. The covalent radii are 0.73, 1.03, 1.17 and 1.35 Å, respectively. The van der Waals radii for S, Se and Te are 1.80, 1.90 and 2.06 Å.

(f) The sum of covalent radii and (in parentheses) van der Waals radii for S–N, Se–N and Te–N are 1.77 (3.35), 1.91 (3.45) and 2.10 (3.61) Å, respectively.

(g) Unlike sulfur, both selenium and tellurium have spin ½ nuclei (^{77}Se 7.58%; ^{125}Te 6.99%; ^{123}Te 0.87%), which can be employed to monitor the synthesis and reactions of Se–N and Te–N compounds by NMR spectroscopy and to provide structural information.

1.2 Binary Species

1.2.1 *Neutral molecules*

The most common oxides of nitrogen are the gases nitric oxide, NO, nitrous oxide, N_2O, and nitrogen dioxide, NO_2. The latter dimerises to N_2O_4 in the liquid or solid states. The sulfur and selenium analogues of these binary systems are all unstable under ambient conditions. Thiazyl and selenazyl monomers have only a transient existence in the gas phase, although these diatomic molecules can be stabilised through bonding to a transition metal (Sec. 5.3). Some examples of sulfur-nitrogen species are shown in Chart 1.1. The dimer S_2N_2 (**1.1**), a colourless solid, exists as a square-planar molecule which undergoes ring-opening to give the blue-black polymer $(SN)_x$ (**1.2**) at room temperature (Sec. 5.4). Although direct applications for this unique, superconducting inorganic material have not been achieved, the formation of **1.2** from the four-membered ring **1.1** has been developed as a practical alternative to current methods for

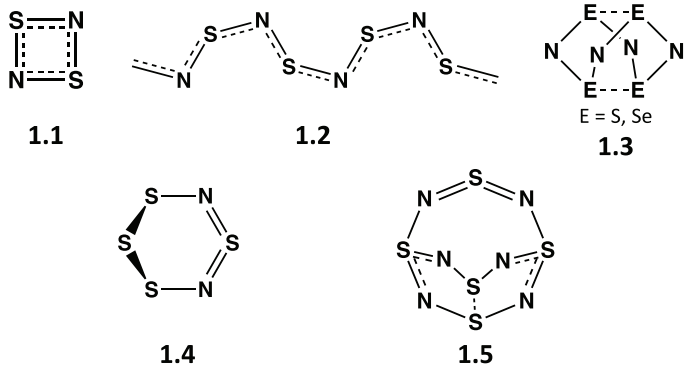

Chart 1.1. Some examples of common sulfur-nitrogen compounds.

fingerprint detection (Sec. 5.4.2). The selenium analogue Se_2N_2 is only known in adducts with Lewis acids. The tetramers E_4N_4 (**1.3**, E = S, Se) adopt unusual cage structures (Sec. 5.5), whereas the corresponding tellurium nitride has the composition Te_3N_4 (Sec. 5.7.6). Both the six-membered ring S_4N_2 (**1.4**) and the nitrogen-rich polycyclic molecule S_5N_6 (**1.5**) are well-characterised (Secs. 5.6.3 and 5.7.4). In general, however, nitrogen-rich sulfur nitrides, *e.g.*, SN_4 and S_3N_4, have low thermodynamic and kinetic stability (Secs. 5.7.2 and 5.7.3). Nevertheless, the ephemeral molecules N_2E (E = S, Se) have been generated from the elements under high pressures and structurally characterised as a matrix-isolated species (Secs. 5.7.1 and 5.7.5).

1.2.2 *Cations*

There are some similarities for binary N–O and S–N cations, especially for acyclic systems. For example, salts of the sulfur analogues of the well-known nitrosyl and nitronium cations, $[NS]^+$ and $[SNS]^+$, are easily prepared. These species are important reagents in S–N chemistry (Secs. 5.8.1 and 5.8.2). The related selenium and tellurium cations are not known. On the other hand, sulfur and nitrogen form an extensive series of cyclic cations that have no N–O analogues. The π-electron count for the examples **1.6–1.10** (Chart 1.2), which are all planar systems, is assigned on the assumption that nitrogen contributes one and sulfur affords two electrons to the overall π-system. The electronic structures of binary S–N rings are

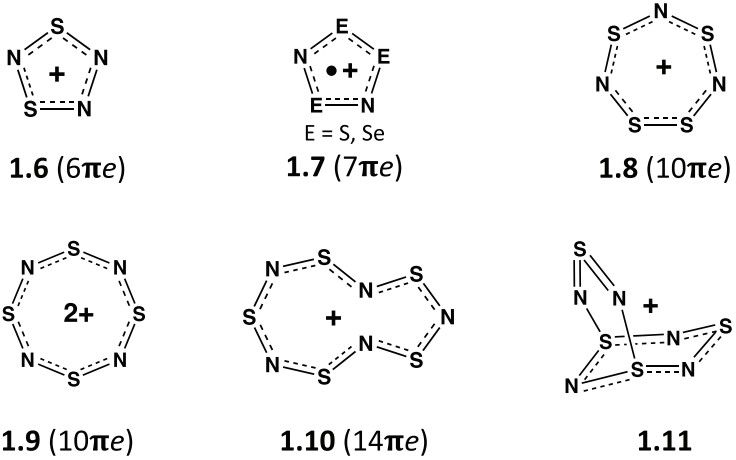

Chart 1.2. Delocalised π-electron count in some cyclic S–N cations.

discussed in detail in Secs. 4.1–4.7. The examples shown above include two five-membered rings, the nitrogen-rich $[S_2N_3]^+$ (**1.6**) and the radical cation $[E_3N_2]^{\bullet+}$ (E = S, Se, **1.7**) (Secs. 5.8.3 and 5.8.4), as well as the seven-, eight- and ten-membered systems, $[S_4N_3]^+$ (**1.8**), $[S_4N_4]^{2+}$ (**1.9**) and $[S_5N_5]^+$ (**1.10**), respectively (Sec. 5.5.5). The tricyclic system $[S_4N_5]^+$ (**1.11**) is also well-characterised (Sec. 5.5.6).

1.2.3 *Anions*

Sulfur and nitrogen form an intriguing variety of both acyclic and cyclic anions. The most common oxo-anions of nitrogen are the nitrite $[NO_2]^-$ and the nitrate anion $[NO_3]^-$. The sulfur analogue of nitrite $[NS_2]^-$ has not been isolated (Sec. 5.9.2), but salts of the $[NS_3]^-$ anion have been characterised. In contrast to nitrate, which has a branched structure (**1.12**), the sulfur analogue $[SNSS]^-$ (**1.13**) forms a chain with a terminal sulfur-sulfur bond, as shown in Chart 1.3 (Sec. 5.9.3). The biologically important $[ONSS]^-$ anion (**1.14**) adopts a similar unbranched arrangement (Sec. 7.9). The structurally analogous peroxynitrite $[ONOO]^-$ can be isolated as a tetramethylammonium salt, but it is more labile than nitrate. The tendency of sulfur to catenate is further manifested by the structure of the deep blue $[SSNSS]^-$ anion (**1.15**), which has two sulfur-sulfur bonds (Sec. 5.9.4). The unbranched structures of $[SSNS_x]^-$ (x = 1, 2) reflect the higher

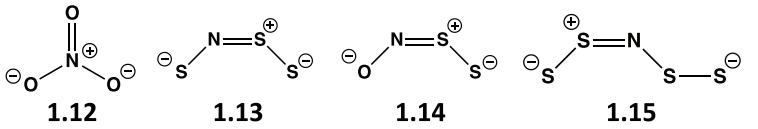

Chart 1.3. Comparison of N, S, O and N, S anions with NO_3^-.

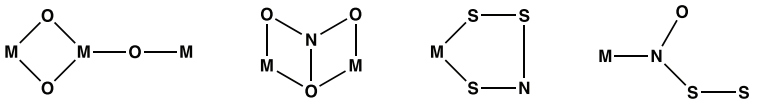

Chart 1.4. Coordination modes for $[NO_3]^-$, $[SNSS]^-$ and $[SNSO]^-$.

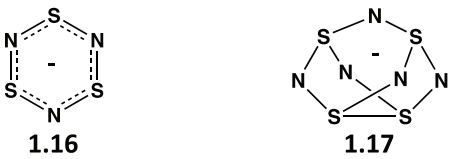

Chart 1.5. Examples of cyclic S–N anions.

electronegativity of N compared to S, since this arrangement allows for the dispersal of negative charge on N as well as S. In the branched structure of $[NO_3]^-$ the negative charge is accommodated entirely on the more electronegative O atoms.

An interesting consequence of the structural differences between N–O and N–S anions is that the latter almost invariably behave as chelating ligands towards a single metal site (Chart 1.4). By contrast, the nitrate ion is able to function as a bridging ligand in a variety of coordination modes, as well as a chelating bidentate ligand, as a result of its branched structure. It has been proposed on the basis of spectroscopic and computational evidence that the ternary anion $[ONSS]^-$ coordinates to iron in an *N*-monodentate fashion in the Gmelin reaction (Sec. 7.9.3).

A unique feature of sulfur-nitrogen anions is the formation of the cyclic systems $[S_3N_3]^-$ (**1.16**) and $[S_4N_5]^-$(**1.17**) (Chart 1.5), which can be isolated as salts with alkali-metals or large organic cations (Secs. 5.9.8 and 5.9.9). The latter are preferred because of the explosive nature of these S–N anions. The electronic structure of **1.16**, a 10π-electron system, is discussed in Sec. 4.3.

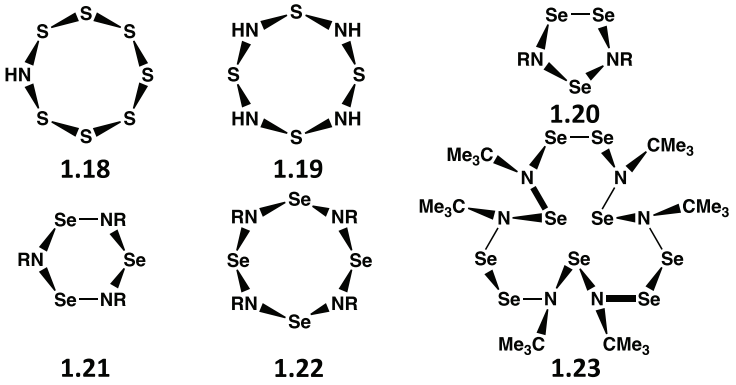

Chart 1.6. Cyclic chalcogen imides.

1.3 Cyclic Chalcogen Imides

Cyclic chalcogen imides provide compelling examples of the tendency of sulfur and selenium to catenate. In the case of S–N systems these heterocycles are structurally related to *cyclo*-S_8 by the replacement of a sulfur atom by one or more NH groups, as illustrated by the examples S_7NH (**1.18**) and $S_4(NH)_4$ (**1.19**) shown in Chart 1.6. The diimide isomers 1,3-, 1,4- and 1,5-$S_6(NH)_2$ and the triimides 1,3,5- and 1,3,6-$S_5(NH)_3$ are also known (Sec. 9.3.1). In the case of selenium, a wider range of ring sizes, including five, six, seven, eight and 15-membered rings with bulky alkyl groups (^{t}Bu or Ad) attached to nitrogen are known (Sec. 9.4). These include both trimeric and tetrameric forms of RNSe monomers (**1.21** and **1.22**, respectively) as well as monomeric and trimeric forms of $[Se_3(NR)_2]_n$ (**1.20**, $n = 1$; **1.23**, $n = 3$) (Chart 1.6); the eight-membered ring, 1,5-$Se_6(NR)_2$, has also been characterised. The six-membered ring, $Te_3(N^tBu)_3$, is the only known cyclic tellurium imide.

1.4 Organic Derivatives

1.4.1 *Acyclic systems*

C-Thionitroso and *C*-selenonitroso compounds RN=E (E = S, Se; R = alkyl, aryl) are short-lived species that can be trapped as Diels-Alder adducts (Sec. 9.2). However, the strong mesomeric effect of the NMe_2

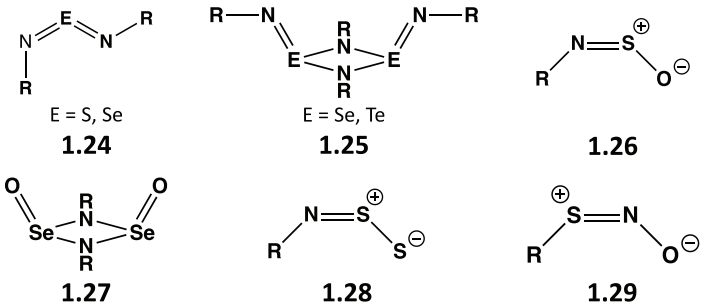

Chart 1.7. Imidochalcogen derivatives and *S*-nitrosothiols.

group in Me_2NNS allows this derivative to be isolated as a low-melting, deep purple solid. Cyclic trimers and tetramers of the type $(RNE)_n$ (E = S, n = 4; E = Se, n = 3,4) are discussed in the previous Section.

A wide variety of monomeric sulfur(IV) diimides RN=S=NR (**1.24**, E = S; R = alkyl, aryl, $SiMe_3$; Chart 1.7) have an extensive chemistry (Sec. 10.4). The trimethylsilyl derivative $Me_3SiN{=}S{=}NSiMe_3$ is an especially important reagent for the synthesis of both inorganic and organic S–N compounds (Scheme 10.11). Selenium(IV) diimides RN=Se=NR (**1.24**, E = Se) are also monomeric, but they have low thermal stability due to redox disproportionation reactions to give cyclic selenium imides (Sec. 9.4). However, metal complexes of dimeric selenium(IV) diimides are formed under the influence of Group 12 metal dihalides (Sec. 10.4.3). In contrast to the lighter chalcogens, tellurium(IV) diimides adopt dimeric structures $RNTe(\mu\text{-}NR)_2TeNR$ (**1.25**) in the solid state (Sec. 10.4.2).

Thionylamines RNSO (**1.26**) are isoelectronic with sulfur(IV) diimides and exist as thermally stable monomeric species for a wide variety of R groups; the selenium analogues adopt a dimeric structure $O{=}Se(\mu\text{-}NR)_2Se{=}O$ (**1.27**) in the solid state (Sec. 10.2). In contrast to organic nitro compounds RNO_2 (R = alkyl, aryl), the dithionitro analogues known as thiosulfinylamines adopt an unbranched arrangement RN=S=S (**1.28**); thermally stable aryl derivatives exist as deep purple solids (Sec. 10.3).

S-Nitrosothiols (or thionitrites) RSNO (**1.29**) incorporate a thermally labile S–N bond with a low dissociation energy. These chalcogen-nitrogen compounds are especially interesting in view of their important role in the biological storage and transportation of nitric oxide; naturally occurring

examples include *S*-nitrosocysteine and *S*-nitrosoglutathione (Sec. 7.7, Chart 7.2). *S*-Nitrosothiols with bulky tertiary alkyl groups (R = CPh_3) or very bulky aryl groups can be isolated and structurally characterised; the latter strategy is also successful for the selenium analogues RSeNO (Sec. 7.9).

1.4.2 *Chains and polymers*

In addition to the unique polymer $(SN)_x$ (**1.2**, Chart 1.1), the formation of chains is another characteristic of chalcogen-nitrogen compounds that distinguishes them from their oxygen analogues. A variety of poly(thiazyl) chains end-capped with organic (usually aryl) groups have been investigated for possible applications as molecular wires. This family of compounds can be viewed as extensions of sulfur(IV) diimides by the successive addition of S or N atoms (Chart 1.8). Thus, chains that incorporate –S–N=S=N–, –S–N=S=N–S–, –N=S=N–S–N=S=N–, –S–N=S=N–S–N=S=N– and –S–N=S=N–S–N=S=N–S– linkages have been characterised. Representative examples are the five-atom chain in PhE–N=S=N–EPh (**1.30**) (Sec. 10.4.2), the seven-atom sequence in $Me_3SiN{=}S{=}N{-}E{-}N{=}S{=}NSiMe_3$ (**1.31**, E = S, Se) and the nine-atom chain in ArS–N=S=N–S–N=S=N–SAr (**1.32**).

1.4.3 *Cyclic systems*

Perhaps the most notable difference between E–N (E = S, Se, Te) and N–O compounds is the existence of a wide range of cyclic compounds for the heavier chalcogens. In this treatise the discussion of C,N,E

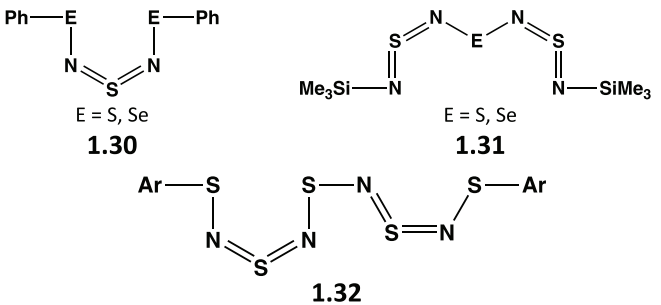

Chart 1.8. Extensions of sulfur(IV) diimides.

heterocycles is limited to those that incorporate an E–N bond and in which the sum of E and N atoms exceeds the number of C atoms in the ring. This area of heterocyclic chemistry has expanded enormously over the past two decades in view of their wide-ranging applications and unique properties, especially for the selenium and tellurium derivatives, as discussed in Chapters 11–15.

The most common C,N,E heterocycles are five, six, seven or eight-membered rings. The representative examples **1.33**–**1.42** (Chart 1.9) are

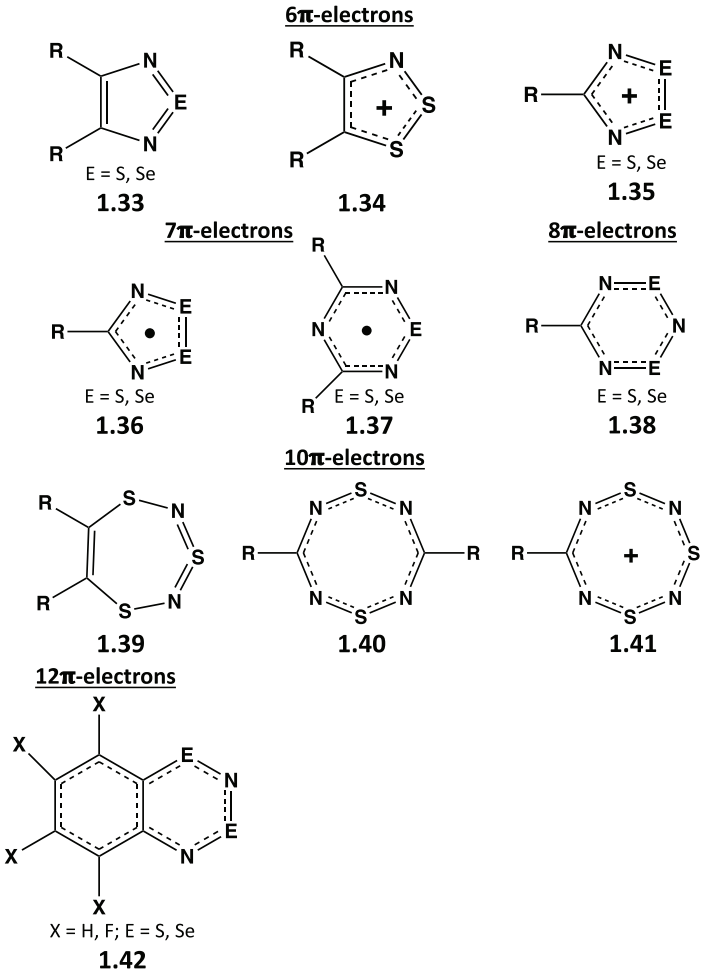

Chart 1.9. Representative examples of C,N,E heterocycles.

all planar in the solid state and are grouped according to their π-electron count assuming that an RC group contributes one electron to the overall π-system. Thus, several C,N,S ring systems are isoelectronic with cyclic S–N cations, *e.g.*, the paramagnetic five-membered rings $[RCN_2S_2]^{\bullet}$ (**1.36**) with $[S_3N_2]^{\bullet+}$ (**1.7**, E = S) and the diamagnetic eight-membered heterocycle 1,5-$(RC)_2N_4S_2$ (**1.40**) with $[S_4N_4]^{2+}$ (**1.9**). The electronic structures of monocyclic C,N,E systems are discussed in more detail in the context of the Hückel $(4n + 2)\pi$-electron rule in Sec. 4.2. The formation of dimeric structures from the radicals **1.36** and **1.37** *via* intermolecular π^*–π^* interactions is described under the rubric "Pancake Bonding" in Sec. 4.10. The synthesis, spectroscopic characterisation, structures and properties of diamagnetic C,N,E heterocycles are the focus of Chapters 11 and 12. Paramagnetic C,N,E ring systems are discussed in Chapter 13.

1.5 Ligand Chemistry and Metal Complexes

The ligand chemistry of both binary chalcogen nitrides and acyclic organic derivatives with either transition-metal or main-group element halides is very extensive. The coordination modes may involve nitrogen and/or sulfur donor sites depending on the nature of the acceptor molecules. A wide variety of metal complexes of binary chalcogen-nitrogen and ternary S,N,O anions are also known, some of which have only been obtained in coordination complexes.

1.5.1 *Neutral chalcogen-nitrogen ligands*

Binary sulfur and selenium nitrides behave as Lewis bases *via* the donor-nitrogen centres in the formation of adducts with Lewis acids and transition-metal complexes. This property has been used to stabilise short-lived or labile molecules. For example, thiazyl monomer NS and, in rare cases, NSe can be stabilised by coordination to a metal (Sec. 5.3.2). S_2N_2 (**1.1**) forms both mono and di-adducts with Lewis acids MCl_3 (M = B, Al, Sb) as well as a variety of transition-metal halides. This property has been employed to stabilise the labile four-membered ring Se_2N_2 as a complex

with $AlBr_3$ or palladium halides (Sec. 5.4.3). S_4N_4 (**1.2**, E = S) also forms a wide variety of *N*-bonded adducts with metal or non-metal halides, which are discussed in Sec. 5.5.2.

Monomeric chalcogen(IV) diimides (**1.24**) have a very extensive coordination chemistry that can involve both nitrogen and sulfur donor sites in a wide variety of coordination modes (Sec. 10.4.4). The ability of the dimers $RNE(\mu\text{-}NR)_2ENR$ (**1.25**, E = Se, Te) to form *N*,*N*′-chelated complexes or to act as bridging ligands in coinage metal complexes adds another dimension to this coordination behaviour (Sec. 10.4.4). Metal complexes of C,N,E (E = S, Se, Te) heterocycles are discussed in Chapter 14.

Organic thionylamines RNSO (**1.26**) form a variety of complexes with transition metals involving the S and/or N donor sites, while coordination of Me_3SiNSO with main-group acceptors may involve either the N or O atoms (Sec. 10.2.3). Complex formation has been applied to the stabilisation of the highly labile, parent thionyl imide HNSO, which has been isolated and structurally characterised as an *N*-bonded adduct with $B(C_6F_5)_3$ (Sec. 6.4).

Coordination complexes of *S*-nitrosothiols RSNO (**1.29**) are of particular interest in view of the influence of transition metals on the bioregulatory function of these vasodilators. In this context, *N*-bonded Cu(I) and Ir(IV) complexes have been isolated and structurally characterised; however, coordination to a strong boron Lewis acid involves donation from the O atom (Secs. 7.7.4 and 7.7.5).

1.5.2 *Metal complexes of chalcogen-nitrogen anions*

Some metal complexes of acyclic S–N anions, *e.g.*, $[NSN]^{2-}$ and $[SNSS]^-$, can be prepared by metathesis of their salts with transition-metal halides. A wider variety of cyclometallathiazenes with the general formula LMS_xN_y are obtained from fragmentation reactions of S_4N_4 with transition-metal reagents. The most common examples involve the dianion $[S_2N_2]^{2-}$ or its monoprotonated derivative $[S_2N_2H]^-$ in *N*,*S*-chelated complexes (Sec. 5.9.7). However, rare examples of complexes with longer anionic chains, *e.g.*, $[S_3N_x]^{2-}$ (x = 2, 4), $[S_4N_3]^-$ and $[S_4N_4]^{2-}$ have been structurally characterised. The unknown Se–N anions $[Se_3N]^-$,

$[Se_2N_2]^{2-}$ and $[Se_2N_2H]^-$ have also been identified in transition-metal complexes. They are generated by fragmentation of Se_4N_4 or, more safely, by *in situ* formation of these anions in solutions of $SeCl_4$ or $SeOCl_2$ in liquid ammonia prior to metathesis with metal halides.

1.6 Chalcogen-Nitrogen Compounds with the Chalcogen in Higher Oxidation States

1.6.1 *Acyclic systems*

The accessibility of the formal +4 and +6 oxidation states for the chalcogens gives rise to both acyclic and cyclic E–N compounds that have no parallels in N–O chemistry, *e.g.*, chalcogen(IV) diimides $E(=NR)_2$ (Secs. 1.4.1 and 10.4) and sulfur(VI) triimides $S(=NR)_3$ (Sec. 10.7). Other examples of acyclic compounds with sulfur in the formal +6 oxidation state include the triply bonded thiazyl trifluoride $N{\equiv}SF_3$ (Sec. 8.3) and sulfonimidoyl fluorides $RN{=}S(O)F_2$ (**1.43**) (Chart 1.10). The latter are important reagents for the synthesis of sulfonamides $RSO_2N(R'R'')$ (**1.44**) (Scheme 8.2), which have numerous pharmaceutical and agricultural applications. The commercially available, hydrophilic lithium salt of the resonance-stabilised bis(trifluoromethylsulfonyl)imide anion $[(CF_3SO_2)_2N]^-$ (**1.45**) (Chart 1.10) is used in lithium-ion batteries and the calcium salt serves as a catalyst in the synthesis of sulfonamides (Scheme 2.3a).

1.6.2 *Cyclic systems*

Stable heterocyclic systems with sulfur in a high oxidation state include the cyclothiazyl halides $(NSX)_n$ (**1.46a**, X = Cl, F, n = 3; **1.46b**, X = F, n = 4) (Sec. 8.7) and the trimeric sulfanuric halides $[NS(O)X]_3$ (**1.47**,

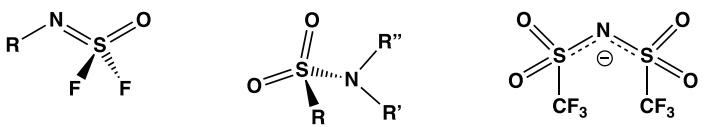

1.43 **1.44** **1.45**

Chart 1.10. Acyclic sulfur(VI)-nitrogen compounds.

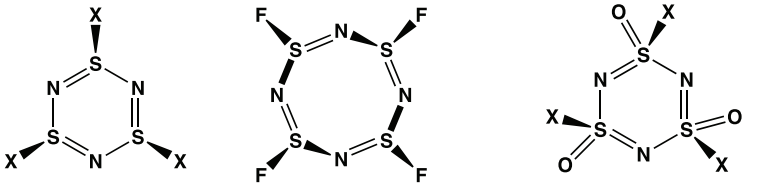

Chart 1.11. Cyclic thiazyl halides and sulfanuric halides.

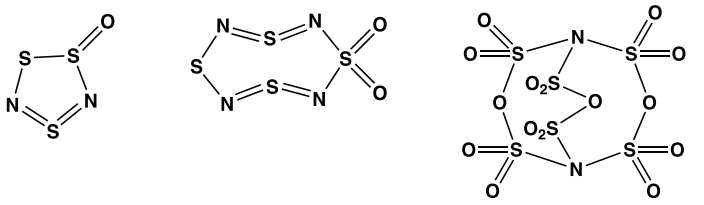

Chart 1.12. Cyclic sulfur-nitrogen oxides.

X = Cl, F) (Sec. 8.9), which are shown in Chart 1.11. Selenium or tellurium analogues of these sulfur-nitrogen halides are unknown.

Cyclic sulfur-nitrogen oxides with sulfur in the +4 or +6 oxidation states are also known, *e.g.*, the well-known monocyclic systems S_3N_2O (**1.48**) and $S_4N_4O_2$ (**1.49**) (Scheme 8.3), and the nitrogen-poor tricyclic molecule $S_6N_2O_{15}$ (**1.50**) (Chart 1.12) [D. van Gerven and M. S. Wickleder, *Angew. Chem. Int. Ed.*, **59**, 17169 (2020)].

1.7 Content and Objectives of Updated Edition

In this updated edition of *A Guide to Chalcogen-Nitrogen Chemistry*, fundamental information from the first edition that describes the most important classes of chalcogen-nitrogen compounds together with appropriate references to early seminal work have been retained. At the same time chapters or sections from the first section on topics that have seen little or no progress since the publication of the first edition in early 2005 have been deleted. In keeping with developments in chalcogen-nitrogen chemistry over the past 16 years, the updated edition puts more emphasis

on selenium- and tellurium-nitrogen compounds and, as the title indicates, on applications of chalcogen-nitrogen compounds in biological, physical and material sciences. The contents of this treatise are summarised in the following paragraph.

The preceding introductory summary of the most important chalcogen-nitrogen compounds is followed by two general chapters (Chapters 2 and 3) outlining (a) the methods for the formation of chalcogen-nitrogen bonds and (b) the techniques used for the characterisation of chalcogen-nitrogen compounds. In both the chapters many of the examples used in the first edition are replaced by more recent illustrations. Chapter 4 discusses developments in our understanding of the electronic structures and bonding in chalcogen-nitrogen compounds and introduces the concepts of bishomoaromaticity and pancake bonding. Chapter 5, which describes the chemistry of binary neutral, cationic and anionic species, has been updated with many recent advances, especially for nitrogen-rich chalcogen nitrides. The new Chapter 6 discusses the methods used for the synthesis and characterisation of short-lived chalcogen-nitrogen molecules, including ternary S,N,O radicals and isomers of S_2N_2 and S_4N_4. Chapter 7 is also a new chapter that focuses on ternary S,N,O anions and *S*-nitrosothiols and their important role in biological signaling and NO/H_2S crosstalk. Chapter 8 on chalcogen-nitrogen halides is retained with updates in view of the importance of these reagents in the synthesis of other chalcogen-nitrogen compounds. The discussion of cyclic chalcogen imides in Chapter 9 has been expanded by the inclusion of significant new findings for cyclic selenium imides. This is followed by a discussion of the chemistry of acyclic C,N,E compounds in which the main focus is chalcogen(IV) diimides, chalcogen(VI) triimides and related polyimido anions (Chapter 10); Chapters 11–13 have been entirely revamped in order to cover both fundamental and practical advances in the extremely active area of C,N,E heterocycles. However, the discussion is limited to those ring systems which contain an E–N bond and in which the number of heteroatoms exceeds the number of carbon atoms in the ring. The topics discussed in these three chapters are diamagnetic five-membered C,N,E (E = S, Se, Te) rings: from fundamentals to functional devices (Chapter 11), diamagnetic six-, seven- and eight-membered C,N,E (E = S, Se, Te) rings: aromaticity (Chapter 12), and paramagnetic C,N,E rings: magnetic materials (Chapter 13). Chapter 14 describes

recent work on the coordination modes of metal complexes of diamagnetic and paramagnetic C,N,E heterocycles. A final chapter (Chapter 15) is devoted to intra- and inter-molecular secondary bonding interactions in chalcogen-nitrogen compounds, including supramolecular systems. In this chapter an exception is made to the restricted definition of C,N,E heterocycles, because some of the most important examples of this phenomenon involve tellurium-nitrogen heterocycles that contain fewer heteroatoms than carbon atoms.

This introductory chapter concludes with a bibliographic listing of books, book chapters and review articles published during the period 2005–2021 that are devoted primarily to chalcogen-nitrogen compounds or contain significant sections on that topic. They are listed in chronological order under sub-headings showing the particular aspect of chalcogen-nitrogen chemistry that is discussed.

Books

T. Chivers, *A Guide to Chalcogen-Nitrogen Chemistry*, World Scientific Publishing Co., Singapore (2005).

Book Chapters and Reviews

(a) General Reviews

T. Chivers, Sulfur-Nitrogen Compounds, in *Encyclopedia of Inorganic Chemistry*, 2nd Edition, Ed. R. B. King, John Wiley & Sons (2005), Vol. 8, pp. 5378–5403.

T. Chivers and R. S. Laitinen, Chalcogen-Nitrogen Chemistry, in *Handbook of Chalcogen Chemistry: New Perspectives in Sulfur, Selenium and Tellurium*, Ed. F. Devillanova, Royal Society of Chemistry (2006), Ch. 4, pp. 223–285.

D. Stalke, Polyimido Sulfur Anions and Ylides, *Chem. Commun*., **48**, 9559–9573 (2012).

T. Chivers and R. S. Laitinen, Chalcogen-Nitrogen Chemistry, in *Handbook of Chalcogen Chemistry: New Perspectives in Sulfur, Selenium and Tellurium*, Ed. F. Devillanova, Royal Society of Chemistry, 2nd Edition (2013), Ch. 4, pp. 191–237.

W. Spillane and J-B. Malaubier, Sulfamic Acid and Its N-and O-Substituted Derivatives, *Chem. Rev*., **114**, 2507–2586 (2014).

V. Bizet, R. Kowalczyk and C. Bolm, Fluorinated Sulfoximines: Synthesis, Properties and Applications, *Chem. Soc. Rev*., **43**, 2426–2438 (2014).

V. Bizet, C. M. M. Hendriks and C. Bolm, Sulfur Imidations: Access to Sulfimides and Sulfoximes, *Chem. Soc. Rev*., **44**, 3378–3390 (2015).

P. K. Chinthakindi, T. Naicker, N. Thota, T. Govender, H. G. Kruger and P. I. Arvidsson, Sulfonimidamides in Medicinal and Agricultural Chemistry, *Angew. Chem. Int. Ed*., **56**, 4100–4109 (2017).

T. Chivers and R. S. Laitinen, Insights into the Formation of Inorganic Heterocycles via Cyclocondensation of Primary Amines with Group 15 and 16 Halides, *Dalton Trans*., **46**, 1357–1367 (2017).

W. Zhao and J. Sun, Triflimide ($HNTf_2$) in Organic Synthesis, *Chem. Rev*., **118**, 10349–10392 (2018).

T. Chivers and R. S. Laitinen, Neutral Binary Chalcogen-Nitrogen and Ternary S,N,P Molecules: New Structures, Bonding Insights and Potential Applications, *Dalton Trans*., **49**, 6532–6547 (2020).

H. Zhang, H. Wang, Y. Jiang, F. Cao, W. Gao, L. Zhu, Y. Yang, X. Wang, Y. Wang, J. Chen, Y. Feng, X. Deng, Y. Lu, X. Hu, J. Zhang, T. Chi and X. Wang, Recent Advances in Iodine-Promoted C–S and N–S Bond Formation, *Chem. Eur. J*., **26**, 17289–17317 (2020).

E-C. Koch and M. Sućeska, Analysis of the Explosive Properties of Tetrasulfur Tetranitride, *Z. Anorg. Allg. Chem*., **647**, 192–199 (2021).

T. Q. Davies and M. C. Willis, Rediscovering Sulfinylamines as Reagents for Organic Synthesis, *Chem. Eur. J.*, **27**, 8918–8927 (2021).

(b) Chalcogen-Nitrogen Radicals

J. M. Rawson, J. Luzon and F. Palacio, Magnetic Exchange Interactions in Perfluorophenyl Dithiadiazolyl Radicals, *Coord. Chem. Rev*., **249**, 2631–2641 (2005).

J. M. Rawson, A. Alberola and A. Whalley, Thiazyl Radicals: Old Materials for New Molecular Devices, *J. Mater. Chem*., **16**, 2560–2575 (2006).

K. Awaga, T. Tanaka, T. Shirai, M. Fujimori, Y. Suzuki, H. Yoshikawa and W. Fujita, Multi-Dimensional Crystal Structures and Unique Solid-State Properties of Heterocyclic Thiazyl Radicals and Related Materials, *Bull. Chem. Soc. Jpn*., **79**, 25–34 (2006).

R. T. Boeré, H. M. Tuononen, T. Chivers and T. L. Roemmele, Structures and EPR Spectra of Binary S-N Radicals from DFT Calculations, *J. Organomet. Chem*., **692**, 2683–2696 (2007).

R. G. Hicks, The Synthesis and Characterisation of Stable Radicals Containing the Thiazyl (SN) Fragment and Their Use as Building Blocks for Advanced Functional Materials, in *Stable Radicals: Fundamental and Applied Aspects of Odd-Electron Compounds*, Ed. R. B. Hicks, John Wiley & Sons (2010), Ch. 9, pp. 317–380.

O. A. Rakitin, Stable Heterocyclic Radicals, *Russ. Chem. Rev.*, **80**, 647–659 (2011).

D. A. Haynes, Crystal Engineering with Dithiazolyl Radicals, *CrystEngComm*, **13**, 4793–4805 (2011).

N. P. Gritsan and A. V. Zibarev, Chalcogen-Nitrogen π-Heterocyclic Radical Anion Salts: The Synthesis and Properties, *Russ. Chem. Bull*., **60**, 2131–2140 (2011).

A. V. Zibarev and R. Mews, A New Class of Paramagnetics: 1,2,5-Chalcogenadiazolidyl Salts as Potential Building Blocks for Molecular Magnets and Conductors, in *Frontiers of Selenium and Tellurium Chemistry: From Small Molecules to Biomolecules and Materials*, Eds. J. D. Woollins and R. S. Laitinen, Springer (2011), Ch. 6, pp. 123–149.

N. P. Gritsan, A. Yu. Makarov and A. V. Zibarev, A New Approach to Chalcogen-Nitrogen π-Heterocyclic Radicals, *Appl. Magn. Reson*., **41**, 449–466 (2011).

K. V. Shuvaev and J. Passmore, $[RCNSSS]^{\bullet+}$: A Novel Class of Stable Sulfur-Rich Radical Cations, *Coord. Chem. Rev*., **257**, 1067–1091 (2013).

J. M. Rawson and J. J. Howard, Stable Chalcogen Radicals, in *Handbook of Chalcogen Chemistry: New Perspectives in Sulfur, Selenium and Tellurium*, Ed. F. Devillanova, Royal Society of Chemistry, 2nd Edition (2013), Ch. 11.1, pp. 69–98.

R. T. Boeré and T. L. Roemmele, Chalcogen-Nitrogen Radicals, in *Comprehensive Inorganic Chemistry II,* Ed. T. Chivers, Elsevier (2013), Vol. 1, Ch. 1.14, pp. 375–411.

K. E. Preuss, Pancake Bonds: π-Stacked Dimers of Organic and Light-Atom Radicals, *Coord. Chem. Rev*., **79**, 1–15 (2014).

J. M. Rawson and C. P. Constantinides, Thiazyl Magnets, in *World Scientific Reference on Spin in Organics,* Ed. J. S. Miller, World Scientific Publishing Co. (2018), Vol. 4, pp. 95–124.

Y. M. Volkova, A. Yu. Makarov, E. A. Pritchina, N. P. Gritsan and A. V. Zibarev, Herz Radicals: Chemistry and Materials Science, *Mendeleev Commun*., **30**, 385–394 (2020).

D. F. Yuan, W. Liu and Z. Zhu, Design and Applications of Single-Component Radical Conductors, *Chem*, **7**, 1–25 (2021).

(c) *S*-Nitrosothiols and Sulfur-Nitrogen-Oxygen Anions

H. Wang and M. Xian, Chemical Methods to Detect *S*-Nitrosation, *Curr. Opin. Chem. Biol*., **15**, 32–37 (2011).

B. C. Smith and M. A. Marletta, Mechanism of *S*-Nitrosothiol Formation and Selectivity in Nitric Oxide Signaling, *Curr. Opin. Chem. Biol*., **16**, 498–506 (2012).

K. A. Broniowska and N. Hogg, The Chemical Biology of *S*-Nitrosothiols, *Antioxidants & Redox Signaling*, **17**, 969–980 (2012).

A. Zeida, C. M. Guardia, P. Lichtig, L. L. Perissonitti, L. A. Defilipe, A. Turjanski, R. Radi, M. Trujillo and D. A. Estrin, Thiol Redox Chemistry: Insights from Computer Simulations, *Biophys. Rev*., **6**, 27–46 (2014).

M. M. Cortese-Krott, B. O. Fernandez, M. Kelm, A. R. Butler and M. Feelisch, On the Chemical Biology of the Nitrite/Sulfide Interaction, *Nitric Oxide — Chemistry and Biology*, **46**, 14–24 (2016).

J. Yi, P. Coppens, D. R. Powell and G. B. Richter-Addo, Linkage Isomerization in Nitrosothiols (RSNOs): The X-Ray Crystal Structure of an *S*-Nitrosocysteine and DFT Analysis of its Metastable MS_1 and MS_2 Isomers, *Comments Inorg. Chem*., **36**, 81–91, (2016).

M. M. Cortese-Krott, A. R. Butler, J. D. Woollins and M. Feelisch, Inorganic Sulfur-Nitrogen Compounds: From Gunpowder Chemistry to the Forefront of Biological Signalling, *Dalton Trans*., **45**, 5908–5919 (2016).

T. Chivers and R. S. Laitinen, Fundamental Chemistry of Binary S,N and Ternary S,N,O Anions: Analogues of Sulfur Oxides and N,O Anions, *Chem. Soc. Rev*. **46**, 5182–5192 (2017).

D. Tsikas and A. Böhmer, *S*-Nitrosation Reactions of Hydrogen Sulfide (H_2S/HS^-/S^{2-}) with *S*-Nitrosated Cysteinyl Thiols in Phosphate Buffer of pH 7.4: Results and Review of the Literature, *Nitric Oxide*, **65**, 22–36 (2017).

J. P. Marcolongo, A. Zeida, L. D. Slep and J. A. Olabe, Thionitrous Acid/Thionitrite and Perthionitrite Intermediates in the "Crosstalk" of NO and H_2S, *Adv. Inorg. Chem.*, **70**, 277–309 (2017).

C. Zhang, T. D. Biggs, N. O. Devarie-Baez, S. Shuang, C. Dong and M. Xian, *S*-Nitrosothiols: Chemistry and Reactions, *Chem. Commun*., **53**, 11266–11277 (2017).

I. Ivanovic-Burmazovic and M. R. Filipovic, Saying NO to H_2S: A Story of HNO, HSNO and $SSNO^-$, *Inorg. Chem*., **58**, 4039–4051 (2019).

J. P. Marcolongo, M. F. Venancio, W. R. Rocha, F. Doctorovich and J. A. Olabe, NO/H_2S "Crosstalk" Reactions. The Role of Thionitrites (SNO^-) and Perthionitrites ($SSNO^-$), *Inorg. Chem*., **58**, 14981–14997 (2019).

M. Xiam, Y. Wang and S. Xu, Specific Reactions of RSNO/HSNO/NO and their Applications in the Design of Fluorescent Probes, *Chem. Eur. J.*, **26**, 11673–11683 (2020).

(d) Carbon-Nitrogen-Chalcogen Heterocycles

M. P. Donzello, C. Ercolani and P. A. Stuzhin, Novel Families of Phthalocyanine-like Macrocycles; Porphyrazines with Annulated Strongly Electron-withdrawing 1,2,5-Thia/Selenodiazole Rings, *Coord. Chem. Rev.*, **250**, 1530–1561 (2006).

F. Blockhuys, N. P. Gritsan, A. Yu. Makarov, K. Tersago and A. V. Zibarev, A Brave New World: The Heteroatom Chemistry of 1,3,2,4- Benzothiadiazenes and Related Compounds, *Eur. J. Inorg. Chem.*, **2008**, 655–672 (2008).

L. S. Konstantinova and O. A. Rakitin, Synthesis and Properties of 1,2,3-Dithiazoles, *Russ. Chem. Rev.*, **77**, 521–546 (2008).

M. P. Cava, M. V. Lakshmikantham, R. Hofmann and R. M. Williams, R. B. Woodward's Unfinished Symphony: Designing Organic Superconductors, *Tetrahedron*, **67**, 6771–6797 (2011).

A. V. Lonchakov, O. A. Rakitin, N. P. Gritsan and A. V. Zibarev, Breathing Some New Life into an Old Topic: Chalcogen-Nitrogen π-Heterocycles as Electron Acceptors, *Molecules*, **18**, 9850–9900 (2013).

B. A. D. Neto, A. A. M. Lapis, E. N. da Silva Jr. and J. Dupont, 2,1,3-Benzothiadiazole Derivatives; Synthesis, Properties, Reactions, and Applications in Light Technology of Small Molecules, *Eur. J. Org. Chem.*, **2013**, 228–255 (2013).

R. Gleiter, G. Haberhauer and S. Woitschetzki, From Eight-Membered 10π Electron Sulfur-Nitrogen Cycles to Bicycles and Cages: A Theoretical Approach, *Chem. Eur. J.*, **20**, 13801–13810 (2014).

B. A. D. Neto, P. H. P. R. Carvalho and J. R. Correa, Benzothiadiazole Derivatives as Fluorescence Imaging Probes: Beyond Classical Scaffolds, *Acc. Chem. Res.*, **48**, 1560–1569 (2015).

J. Du, M. C. Biewer and M. C. Stefan, Benzothiadiazole Building Units in Solution-Processable Small Molecules for Organic Photovoltaics, *J. Mater. Chem. A*, **4**, 15771–15787 (2016).

O. A. Rakitin and A. V. Zibarev, Synthesis and Applications of Five-membered Chalcogen-Nitrogen π-Heterocycles with Three Heteroatoms, *Asian. J. Org. Chem.*, **7**, 2396–2416 (2018).

E. A. Chulanova, N. A. Semenov, N. A. Pushkarevsky, N. P. Gritsan and A. V. Zibarev, Charge-Transfer Chemistry of Chalcogen-Nitrogen π-Heterocycles, *Mendeleev Commun.*, **28**, 453–469 (2018).

E. A. Pritchina, N. P. Gritsan, O. A. Rakitin and A. V. Zibarev, 2,1,3-Benzochalcogendiazoles: Regularities and Peculiarities over a Whole Chalcogen Pentad O, S, Se, Te and Po, in *Targets in Heterocyclic Systems*, Eds. O. A. Attanasi, P. Merino and D. Spinelli, Italian Chemical Society (2019), Vol. 23, Ch. 7, 143–153.

T. S. Sukikh, D. S. Ogienko, D. A. Bashirov and S. N. Konchenkoa, Luminescent Complexes of 2,1,3-Benzothiadiazole Derivatives, *Russ. Chem. Bull.*, **68**, 651–661 (2019).

N. Biot and D. Bonifazi, Chalcogen-Bond Driven Molecular Recognition at Work, *Coord. Chem. Rev*., **413**, 213243 (2020).

P. C. Ho, J. Z. Wang, F. Meloni and I. Vargas-Baca, Chalcogen Bonding in Materials Chemistry, *Coord. Chem. Rev*., **422**, 21364 (2020).

P. G. Joshi, M. S. More, A. A. Jadhav and P. K. Khanna, Materials and Biological Applications of 1,2,3-Selenadiazoles, *Mater. Today Chem.*, **16**, 100255 (2020).

(e) Selenium- and Tellurium-Nitrogen Chemistry

A. F. Cozzolino, P. J. W. Elder and I. Vargas-Baca, A Survey of Tellurium-Centered Secondary-Bonding Supramolecular Synthons, *Coord. Chem. Rev*., **255**, 1426–1438 (2011).

J. L. Dutton and P. J. Ragogna, Recent developments in the Lewis Acid Chemistry of Selenium and Tellurium Halides and Pseudo-Halides, in *Frontiers of Selenium and Tellurium Chemistry: From Small Molecules to Biomolecules and Materials*, Eds. J. D. Woollins and R. S. Laitinen, Springer (2011), Ch. 6, pp. 123–149.

R. Oilunkaniemi, R. S. Laitinen and T. Chivers, Synthesis, Structures, Bonding, and Reactions of Imido-Selenium and -Tellurium Compounds, in *Frontiers of Selenium and Tellurium Chemistry: From Small Molecules to Biomolecules and Materials*, Eds. J. D. Woollins and R. S. Laitinen, Springer (2011), Ch. 8, pp. 179–199.

J. L. Dutton and P. J. Ragogna, Recent Developments in the Synthesis and Isolation of p-Block Centered Polycations, *Coord. Chem. Rev*., **255**, 1414–1425 (2011).

T. M. Klapötke, B. Krumm and R. Moll, Compounds of Selenium and Tellurium with Nitrogen Bonds, in *PATAI's Chemistry of Functional Groups*, John Wiley & Sons (2011), pp. 1–27.

T. Chivers and R. S. Laitinen, Tellurium: A Maverick among the Chalcogens, *Chem. Soc. Rev*., **44**, 1725–1739 (2015).

J. Vasiljeva and P. Arsenyan, Synthesis of Se–N and Te–N Bond-Containing Heterocycles, *Chem. Heterocycl. Compd*., **53**, 1061–1067 (2017).

T. Chivers and R. S. Laitinen, Selenium- and Tellurium-Nitrogen Reagents, in *Selenium and Tellurium Reagents — In Chemistry and Materials Science*, de Gruyter (2019), Ch. 4, pp. 123–150; *Phys. Sci. Rev.*, **4**, 20170125 (2019).

E. R. T. Tiekink, Supramolecular Aggregation Patterns featuring Se···N Secondary-bonding Interactions in Mono-nuclear Selenium Compounds: A Comparison with their Congeners, *Coord. Chem. Rev.*, **443**, 214031 (2021).

(f) Metal Complexes of Chalcogen-Nitrogen Ligands

K. E. Preuss, Metal Complexes of Thiazyl Radicals, *Dalton Trans*., **2007**, 2357–2369 (2007).

K. E. Preuss, Metal-Radical Coordination Complexes of Thiazyl and Selenazyl Ligands, *Coord. Chem. Rev*., **289**, 49–61 (2015).

A. Døssing, The Electronic Structure and Photochemistry of Transition Metal Thionitrosyl Complexes, *Coord. Chem. Rev*., **306**, 544–557 (2015).

L. M. T. Frija, A. J. L. Pombeiro and M. N. Kopylovich, Coordination Chemistry of Thiazoles, Isothiazoles and Thiadiazoles, *Coord. Chem. Rev.*, **308**, 32–55 (2016).

Chapter 2

Formation of Chalcogen-Nitrogen Bonds

This chapter will provide an overview of the methods available for the formation of chalcogen-nitrogen bonds with an emphasis on the synthesis of the most widely used reagents. The applications of these reagents in the synthesis of inorganic and organic chalcogen-nitrogen compounds will be illustrated in reaction schemes in the appropriate chapters. The following recent reviews provide details on the synthesis of specific classes of chalcogen-nitrogen compounds: (a) binary chalcogen-nitrogen molecules,[1] (b) chalcogen-nitrogen radicals,[2,3] (d) chalcogen-nitrogen-oxygen species,[4–6] (d) cyclic chalcogen imides,[7] (e) carbon-nitrogen-chalcogen heterocycles,[8–13] and (f) acyclic and cyclic selenium-nitrogen and tellurium-nitrogen compounds.[14–17]

2.1 From Ammonia and Ammonium Salts

The cyclocondensation reaction of ammonia gas (or ammonium salts) with sulfur halides is the most important route to S–N heterocycles, since it provides an easy preparation of several key starting materials (Scheme 2.1).[18] The polarity of the solvent has a remarkable influence on the outcome of this reaction. When conducted in carbon tetrachloride or methylene chloride, this method is the standard synthesis of S_4N_4 which, in turn, is used for the preparation of numerous S–N ring systems (Sec. 5.5.3, Scheme 5.2). Reaction of $SeBr_4$ with ammonia at high pressure

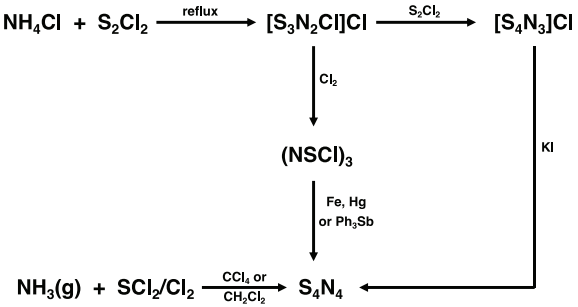

Scheme 2.1. Preparation of S–N heterocycles from ammonia or ammonium salts and sulfur halides.

provides a source of tetraselenium tetranitride Se_4N_4,[19] which has been used for the synthesis of binary Se–N cations and anions, as well as selenium-nitrogen halides (Scheme 5.3), but it must be handled with great care in view of its explosive nature.

The sulfur-nitrogen chlorides $[S_3N_2Cl]Cl$ and $(NSCl)_3$ formed as intermediates in the synthesis of S_4N_4 are important reagents in sulfur-nitrogen chemistry. $[S_3N_2Cl]Cl$ is best prepared by the treatment of S_2Cl_2 with sulfur and ammonium chloride at 150–160°C (Sec. 8.6, Eq. 8.16). This method is useful for the synthesis of ^{15}N-labelled S–N compounds for NMR studies (Sec. 3.2), since $[S_3N_2Cl]Cl$ can be chlorinated with SO_2Cl_2 to give $(NSCl)_3$, which is reduced to S_4N_4 by $SbPh_3$.[20] Examples of the versatility of the reagent $(NSCl)_3$ for the synthesis of inorganic and organic sulfur-nitrogen compounds are depicted in Scheme 8.4.

When the reaction of S_2Cl_2 with ammonia gas is carried out in a polar solvent, *e.g.*, DMF, the hydrolysis of the reaction mixture with aqueous HCl produces a mixture of the cyclic sulfur imides S_7NH, 1,3-, 1,4- and 1,5-$S_6(NH)_2$ and 1,3,5- and 1,3,6-$S_5(NH)_3$, which can be separated by chromatography on silica gel using CS_2 as eluant (Sec. 9.3.1).[21]

Solutions of chalcogen halides or chalcogen-nitrogen halides in liquid ammonia are a convenient source of otherwise inaccessible binary chalcogen-nitrogen anions, which can be used as *in situ* reagents for the preparation of metal complexes. For example, the dianion $[S_2N_2]^{2-}$ is formed in liquid ammonia solutions of $[S_4N_3]Cl$.[22] Solutions of $SeOCl_2$ in liquid ammonia generate the selenium-nitrogen anions $[Se_2N_2]^{2-}$ and $[Se_2N_2H]^-$ as

Scheme 2.2. Preparation of triflimide $(HNTf)_2$.

in situ reagents.[23a,b] By contrast, the addition of a THF solution of $SOCl_2$ to liquid ammonia has been used as an efficient source of the $[NSO]^-$ anion for the synthesis of metal complexes (Sec. 7.2.2, Chart 7.1).[23c]

The strong Brønsted acid bis(trifluoromethylsulfonyl)imide $(CF_3SO_2)_2NH$, known as triflimide $(HNTf_2)$, is used widely in organic synthesis.[24] The first synthesis of this water-soluble, white solid involved ammonia gas as a reagent in a multi-step process from methanesulfonyl chloride *via* $CF_3SO_2NH_2$.[25] More recently, a simpler high-yield preparation of this commercially available reagent from the reaction of trifluoromethyl sulfonyl fluoride with a combination of ammonia and trimethylamine has been reported (Scheme 2.2).[26]

2.2 From Amines

The reactions of amines with chalcogen halides, oxo halides or sulfur dioxide provide a convenient source of a variety of acyclic and cyclic chalcogen-nitrogen compounds. Sulfonamides, $RSO_2NR'R''$, are widely used in the pharmaceutical and agrochemical industries. The traditional route to these important commodities, the reaction of an amine with a sulfonyl chloride, has been replaced by the use of more stable sulfonyl fluorides (Scheme 2.3a).[27a] Sulfonyl fluorides can be activated toward nucleophilic addition with amines by the presence of a stoichiometric amount of the Lewis acid calcium triflimide, $Ca[N(SO_2CF_3)_2]$.[27b] This activation can also be achieved by using a catalytic amount of 1-hydroxybenzotriazole (HOBt) which is especially effective for sterically hindered substrates.[27c] Alternatively, sulfonamides can be prepared from amines and an SO_2 surrogate in combination with arylboronic acids and Cu(II)-catalyst (Scheme 2.3b)[27d] or aryl iodides (Scheme 2.3c).[27e] Sulfonamides have also been obtained directly from SO_2 *via* an electrochemical process using functionalised arenes in a 1:1 hexafluoroisopropanol:MeCN solvent mixture.[27f] Electrochemical oxidation and amination of dimethyl sulfoxide

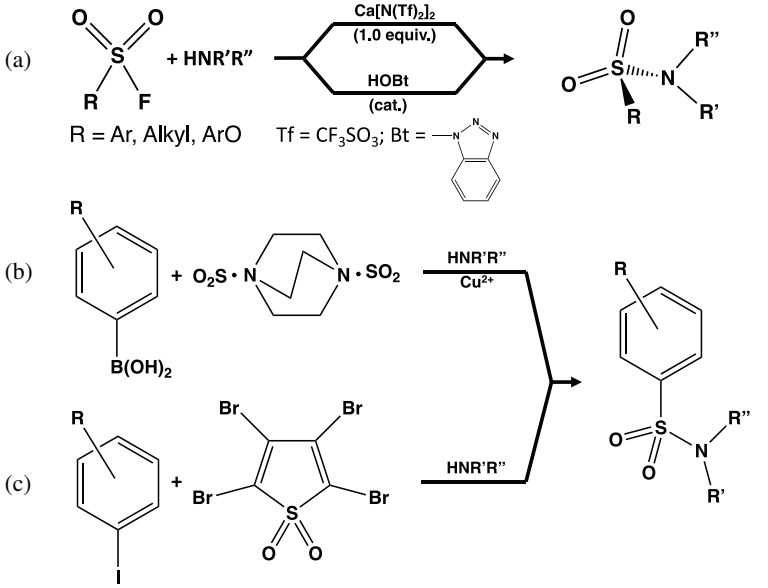

Scheme 2.3. Preparation of sulfonamides from amines and (a) sulfonyl fluorides or (b and c) SO_2 surrogates.

using a platinum anode and nickel cathode is a convenient synthesis of sulfonamides.[27g] Symmetrical sulfonamides $SO_2(NHAr)_2$ (Ar = aryl) can be prepared directly from anilines and SO_2 by using electrochemical methods.[27h]

Compounds containing the structural units –N=SCl_2, –N=S=O or –N=S=S may be prepared from primary amines and sulfur halides. For example, the reaction of $^tBuNH_2$ with SCl_2 in boiling hexane produces $^tBuNSCl_2$.[28] The classical route for the preparation of sulfinyl derivatives RNSO is shown in Eq. 2.1, although silylated amines may be preferred (Sec. 10.2.1).[29a] The related reaction of $SeOCl_2$ with $^tBuNH_2$ produces the selenium analogue as the dimer $OSe(\mu\text{-}N^tBu)_2SeO$.[29b]

$$RNH_2 + SOCl_2 \rightarrow RNSO + 2HCl \qquad (2.1)$$

N-Thiosulfinylanilines ArNSS (Ar = 4-$Me_2NC_6H_4$ or bulky aryl groups) are conveniently prepared by condensing the arylamine with S_2Cl_2 in the presence of a base (Sec. 10.3, Eq. 2.2).[30]

$$ArNH_2 + S_2Cl_2 \rightarrow ArNSS + 2HCl \qquad (2.2)$$

Under appropriate conditions, reactions of chalcogen halides with primary amines proceed *via* cyclocondensation to produce cyclic chalcogen imides.[7] Thus, reactions of aqueous methylamine with dichlorosulfanes S_xCl_2 (x = 1, 2, 3, 5, 7) give rise to a wide range of *N*-methyl cyclic sulfur imides.[31] By contrast, cyclocondensation of RNH_2 (R = Et, Bz) with S_2Cl_2 in diethyl ether under high-dilution conditions yields six-membered rings 1,4-$S_4(NR)_2$.[32]

Cyclocondensation reactions with $^tBuNH_2$ are especially fruitful when selenium(II) dihalide $SeCl_2$ prepared *in situ* by oxidising elemental selenium with SO_2Cl_2 in THF is employed.[33] This reaction provides a rich source of cyclic selenium imides depending on the stoichiometry of the reagents. A series of acyclic, imidoselenium dichlorides $ClSe[N(^tBu)Se]_nCl$ (n = 1, 2, 3) have been isolated as intermediates in the cyclocondensation process and shown to serve as building blocks for the subsequent formation of five-, six-, seven-, eight- and 15-membered cyclic selenium imides (Sec. 9.4, Scheme 9.2).[7,33]

Cyclocondensation of chalcogen halides with bifunctional amines can be used for the preparation of C,N,E (E = S, Se, Te) heterocycles. This is the most common route to 1-thia-2,5-diazoles (Sec.11.2.1).[12] It has also been used to generate benzo-2-selena-1,3-diazoles and benzo-2-tellura-1,3-diazoles from reactions of 1,2-diaminobenzenes with the chalcogen(IV) tetrachloride (Scheme 2.4).[11,34]

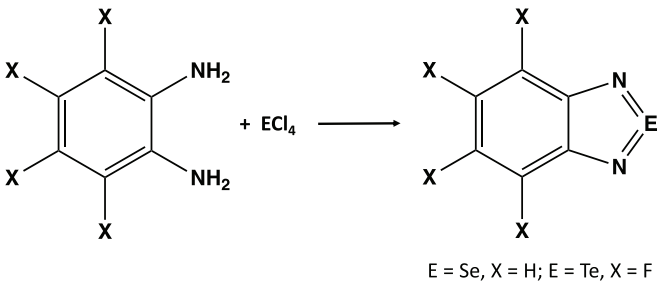

Scheme 2.4. Preparation of benzo-2-chalcogena-1,3-diazoles.

2.3 From Amido-Lithium or Sodium Reagents

The treatment of amido-lithium compounds with chalcogen halides provides a convenient source of a variety of important chalcogen-nitrogen reagents. Reactions of $LiN(SiMe_3)_2$ with SCl_2, Se_2Cl_2 or $TeCl_4$ in hexane or diethyl ether produce the chalcogen(II) diamides $E[N(SiMe_3)_2]_2$ (E = S, Se, Te)[35,36] in good yields (Eq. 2.3–2.5).

$$2LiN(SiMe_3)_2 + SCl_2 \rightarrow S[N(SiMe_3)_2]_2 + 2LiCl \quad (2.3)$$

$$2LiN(SiMe_3)_2 + Se_2Cl_2 \rightarrow Se[N(SiMe_3)_2]_2 + 1/8\ Se_8 + 2LiCl \quad (2.4)$$

$$4LiN(SiMe_3)_2 + TeCl_4 \rightarrow Te[N(SiMe_3)_2]_2 \quad (2.5)$$

The reactivity of the Si–N bonds in these reagents towards chalcogen halides can be utilised in the synthesis of chalcogen-nitrogen compounds *via* elimination of volatile trimethylsilyl halides. For example, the reaction of $S[N(SiMe_3)_2]_2$ with an equimolar mixture of SCl_2 and SO_2Cl_2 provides a convenient source of S_4N_4.[35] In a similar vein, the reaction of $LiN(SiMe_3)_2$ with a mixture of Se_2Cl_2 and $SeCl_4$ (1:4 molar ratio) provides a safer alternative to the explosive selenium nitride Se_4N_4 than the $SeBr_4$-NH_3 reaction.[37]

N,N′-Bis(trimethylsilyl)sulfur(IV) diimide $Me_3SiN{=}S{=}NSiMe_3$ is an especially useful source of the N=S=N functionality in the formation of both acyclic and cyclic S–N compounds. It is conveniently prepared by the reaction of $NaN(SiMe_3)_2$ and thionyl chloride (Eq. 2.6).[38] $Me_3SiN{=}S{=}NSiMe_3$ is a versatile reagent for the preparation of a variety of inorganic and organic sulfur-nitrogen compounds (Scheme 10.11).

$$2NaN(SiMe_3)_2 + SOCl_2 \rightarrow S(NSiMe_3)_2 + (Me_3Si)_2O + 2NaCl \quad (2.6)$$

The selenium analogue $Me_3SiN{=}Se{=}NSiMe_3$ is thermally unstable, but it has been used as an *in situ* reagent to incorporate an N=Se=N unit into heterocycles.[39] The tellurium congener $Me_3SiN{=}Te{=}NSiMe_3$ is unknown, but the *tert*-butyl derivative $^tBuNTe(\mu\text{-}N^tBu)_2TeN^tBu$,

which is a dimer, can be prepared in excellent yield by the reaction of lithium *tert*-butylamide with $TeCl_4$ in THF (Eq. 2.7 and Sec. 10.4.1).[40]

$$8LiNH^tBu + 2TeCl_4 \rightarrow {}^tBuNTe(N^tBu)_2TeN^tBu + 4^tBuNH_2 + 8LiCl \quad (2.7)$$

2.4 From Silicon-Nitrogen and Tin-Nitrogen Reagents

Condensation reactions involving the combination of chalcogen halides and reagents with one or more Si–N functionalities represent a very versatile approach to a wide range of cyclic and acyclic chalcogen-nitrogen compounds, including C,N,E (E = S, Se, Te) and P,N,E (E = S, Se) heterocycles. The driving force for these reactions is the formation of volatile trimethylsilyl halides, which are more easily separated from the other reaction products than the ammonium halides that are formed when ammonia or amines are used as the nitrogen source.

For example, reaction of $(Me_3Sn)_3N$ with S_2Cl_2 produces the cyclostannathiazene $(Me_2SnS_2N_2)_2$ (Eq. 2.8).[38] The butyl derivative of this reagent $Bu_2SnS_2N_2$ has been used for the preparation of a wide variety of metal complexes of the $[S_2N_2]^{2-}$ dianion (Sec. 5.9.7).

$$4S_2Cl_2 + 4(Me_3Sn)_3N \rightarrow (Me_2SnS_2N_2)_2 + 2Me_4Sn + 8Me_3SnCl + 1/2S_8 \quad (2.8)$$

Acyclic Se–N chlorides are formed by reaction of $(Me_3Si)_3N$ with $SeCl_4$ (Eq. 2.9).[15] The bifunctional selenium-nitrogen chloride [ClSeNSeCl]Cl is a useful building block for the generation of cyclic Se–N cations (Sec. 8.4).

$$2SeCl_4 + (Me_3Si)_3N \rightarrow [ClSeNSeCl]Cl + 3Me_3SiCl + Cl_2 \quad (2.9)$$

The sulfinylamine Me_3SiNSO is obtained by treatment of $(Me_3Si)_3N$ with $SOCl_2$ (Eq. 2.10).[41] It is a versatile reagent for the synthesis of ionic or covalent NSO derivatives, *e.g.*, salts of the $[NSO]^-$ anion or the chalcogen derivatives $E(NSO)_2$ (E = S, Se) (Sec. 10.2.1).

$$(Me_3Si)_3N + SOCl_2 \rightarrow Me_3SiNSO + 2Me_3SiCl \quad (2.10)$$

Soluble, high molecular weight poly(oxothiazenes) of the type $[RS(O)=N]_n$ (R = Me, Et, Ph, *p*-MeC_6H_4) are obtained by ambient temperature *in situ* polymerisation of *N*-silylsulfonimidoyl chlorides $ClSR(O)NSiMe_3$ in the presence of a PCl_5 catalyst (Eq. 2.11).[42]

$$ClSR(O)NSiMe_3 \rightarrow [RS(O)=N]_n + Me_3SiCl \qquad (2.11)$$

The treatment of the Si–N reagents $ArN=S=NSiMe_3$ with SCl_2 followed by electrophilic *ortho*-cyclisation of the intermediate [ArN=S=NSCl] is a general route to benzo-1,3-dithia-2,4-diazines, including fluorinated derivatives (Scheme 2.5 and Sec. 12.2.1).[8,43]

The reactions of trifunctional Si–N reagents with chalcogen halides are especially productive for the generation of carbon- or phosphorus-containing S–N or Se–N heterocycles. The combination of trisilylated benzamidines $ArCN_2(SiMe)_3$ with SCl_2 or $SeCl_2$ (generated *in situ*) gives rise to the five-membered cyclic cations $[ArCN_2E_2]^+$ (E = S, Se) (Sec. 11.4).[44a] However, in the reaction with $TeCl_4$ only one Si–N bond in the reagent is cleaved resulting in a four-membered CN_2Te ring (Scheme 2.6).[44b]

Phosphorus(V) can also be introduced into chalcogen-nitrogen rings *via* cyclocondensation reactions using the reagents $R_2PN_2(SiMe)_3$. In this case eight-membered rings of the type 1,5-$R_2P(NEN)_2PR_2$ (E = S, Se) with a cross-ring E···E interaction are formed; these heterocycles are of interest in the context of the concept of bis-homoaromaticity (Sec. 4.9.2). The reagents of choice are $SOCl_2$ (E = S)[45] or a mixture of $SeCl_4$ and Se_2Cl_2 (E = Se); the 1,3-isomer is also formed in the latter case (Scheme 2.7).[46]

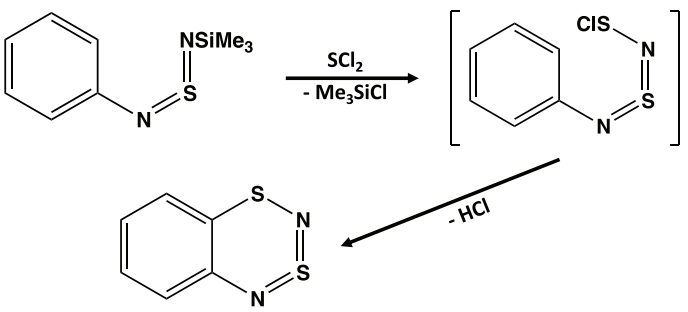

Scheme 2.5. Preparation of benzo-1,3-dithia-2,4-diazines by electrophilic cyclisation.

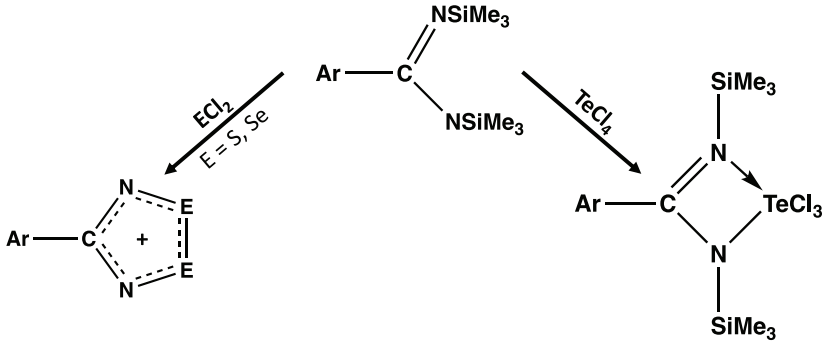

Scheme 2.6. Reactions of trisilylated benzamidines with chalcogen halides.

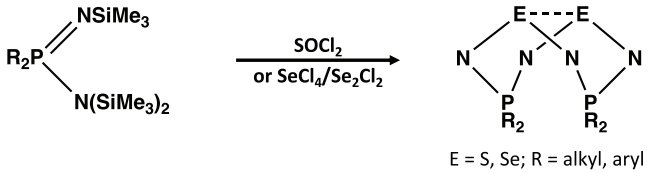

Scheme 2.7. Reactions of $R_2PN_2(SiMe)_3$ with chalcogen halides.

2.5 From Azides

2.5.1 *Inorganic chalcogen-nitrogen compounds*

Reactions of ionic or covalent azides with chalcogen halides or, in the case of sulfur, with the elemental chalcogen provide an alternative route to certain chalcogen-nitrogen compounds. For example, the reaction of sodium azide with *cyclo*-S_8 in hexamethylphosphoric triamide is a more convenient synthesis of S_7NH than the S_2Cl_2/NH_3 reaction (Sec. 9.3.1).[47] Moreover, the azide route can be used for the preparation of 50% ^{15}N-enriched S_7NH.

The polymer $(SN)_x$ may also be made in a two-step process using azide reagents. Thus the reaction of S_2Cl_2 with sodium azide in acetonitrile followed by treatment of the $[S_3N_2]Cl$ produced with Me_3SiN_3 yields $(SN)_x$ as a black solid.[48] By contrast, the explosive and insoluble black compound $Se_3N_2Cl_2$ is prepared by the treatment of Se_2Cl_2 with trimethylsilyl azide in CH_2Cl_2 (Eq. 2.12 and Sec. 8.6).[49]

$$3Se_2Cl_2 + 2Me_3SiN_3 \rightarrow 2Se_3N_2Cl_2 + 2Me_3SiCl + N_2 \qquad (2.12)$$

Chalcogen-nitrogen cations can be generated by reactions of homopolyatomic chalcogen cations with azides. For example, the treatment of $[S_8]^{2+}$ with sodium azide in liquid SO_2 is a source of $[SNS]^+$.[50] By contrast, the reaction of $[Te_4]^{2+}$ with potassium azide in SO_2 gives the tris(azido) tellurium(IV) cation $[Te(N_3)_3][SbF_6]$ as a stable salt.[51]

Explosive selenium(IV) or tellurium(IV) tetraazides $E(N_3)_4$ (E = Se, Te) are obtained by reactions of the corresponding tetrafluoride with trimethylsilyl azide in dichloromethane or SO_2 at low temperatures (Eq. 2.13 and Sec. 5.7.7).[52–54]

$$EF_4 + 4Me_3SiN_3 \rightarrow E(N_3)_4 + 4Me_3SiF \qquad (2.13)$$
$$(E = Se, Te)$$

The use of azide reagents is also important for the synthesis of cyclic sulfur(VI)-nitrogen systems. The reaction of $SOCl_2$ with sodium azide in acetonitrile at –35°C provides a convenient preparation of the trimeric sulfanuric chloride $[NS(O)Cl]_3$ (Eq. 2.14).[55] The phenyl derivative of the six-membered ring $[NS(O)Ph]_3$ can be prepared from lithium azide and PhS(O)Cl.[56]

$$3NaN_3 + 3SOCl_2 \rightarrow [NS(O)Cl]_3 + 3NaCl + 3N_2 \qquad (2.14)$$

Thionyl azide $SO(N_3)_2$ is generated by the heterogeneous reaction of thionyl chloride vapour with silver azide.[57] More recently, sulfuryl diazide $SO_2(N_3)_2$, a colourless liquid, has been prepared on a small scale by reaction of SO_2Cl_2 with sodium azide in acetonitrile (Eq. 2.15 and Sec. 6.2.1).[58]

$$2NaN_3 + SO_2Cl_2 \rightarrow SO_2(N_3)_2 + 2NaCl \qquad (2.15)$$

Fluorosulfonyl azide FSO_2N_3 and trifluoromethylsulfonyl azide $CF_3SO_2N_3$ have been obtained by reactions of sodium azide with the corresponding acid anhydrides (Sec. 6.2.1).[59] The flash photolysis of trifluoromethylsulfonyl azide has been exploited for the generation of $[NSO]^\bullet$ and $[NSO_2]^\bullet$ radicals as discussed in Sec. 6.3.[60,61]

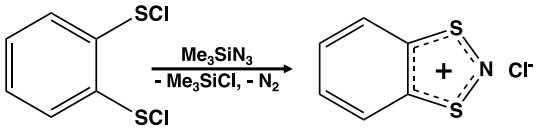

Scheme 2.8. Preparation of benzo-1,3-dithia-2-azolium cations.

2.5.2 *Carbon-nitrogen-chalcogen compounds*

Covalent organochalcogen(II) azides may be generated by treatment of the corresponding halides with Me_3SiN_3 or AgN_3. Simple aryl derivatives are thermally unstable due to loss of N_2, but the introduction of very bulky substituents on the chalcogen or the presence of intramolecular heteroatom coordination generates Se and Te derivatives that can be isolated and structurally characterised (Sec. 10.10).[62,63]

The instability of organosulfur(II) azides has been exploited for the synthesis of C,N,S heterocycles. For example, the cyclocondensation of trimethylsilyl azide with a bis(sulfenyl chloride) is an efficient synthesis of benzo-1,3-dithia-2-azolium cations (Scheme 2.8).[64]

Covalent organoselenium(IV) and organotellurium(IV) azides with two or three azido groups, $R_{4-n}E(N_3)_n$ (E = Se, Te; n = 2, 3), are obtained by metathesis of the corresponding fluorides with Me_3SiN_3 in CH_2Cl_2 (Eq. 2.16).[65,66] However, the organoselenium(IV) azides are thermally unstable, whereas the tellurium analogues can be isolated and structurally characterised (Sec. 10.10).

$$R_2TeF_2 + 2Me_3SiN_3 \rightarrow R_2Te(N_3)_2 + 2Me_3SiF \quad (2.16)$$
(R = Me, Et, ^{n}Pr, ^{i}Pr, Cy)

2.6 From Nitriles

Cycloaddition reactions of nitriles with certain sulfur-nitrogen reagents provide access to heterocycles containing one carbon atom (Scheme 2.9). For example, organic nitriles undergo cycloaddition with the cation $[SNS]^+$ or $(NSCl)_3$ to give excellent yields of the five-membered rings $[RCN_2S_2]^+$ or the six-membered rings $(RCN)(NSCl)_2$, respectively.[67,68]

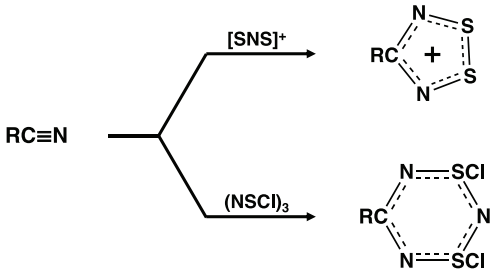

Scheme 2.9. Preparation of C,N,S heterocycles *via* cycloaddition reactions of nitriles.

Cycloaddition reactions of the *in situ* reagent $[S_3]^{\bullet+}$ generated from a stoichiometric mixture of polysulfur cations with nitriles in liquid SO_2 is a general route to salts of the five-membered 1,2,3-trithia-4-azolium radical cations $[RCNSSS]^{\bullet+}$ for nitriles that have high ionisation potentials (Eq. 2.17 and Sec. 13.7).[69]

$$RCN + 1/4S_8[AsF_6]_2 + 1/4S_4[AsF_6]_2 \rightarrow [RCNSSS][AsF_6] \quad (2.17)$$
$$(R = CF_3, C_2F_5, CCl_3, Cl, Br, I)$$

References

1. T. Chivers and R. S. Laitinen, *Dalton Trans*., **49**, 6532 (2020).
2. R. G. Hicks, in *Stable Radicals: Fundamental and Applied Aspects of Odd-Electron Compounds*, Ed. R. B. Hicks, John Wiley & Sons (2010), Ch. 9, pp. 317–380.
3. R. T. Boeré and T. L. Roemmele, in *Comprehensive Inorganic Chemistry II*, Ed. T. Chivers, Elsevier (2013), Vol. 1, Ch. 1.14, pp. 375–411.
4. M. M. Cortese-Krott, A. R. Butler, J. D. Woollins and M. Feelisch, *Dalton Trans*., **45**, 5908 (2016).
5. T. Chivers and R. S. Laitinen, *Chem. Soc. Rev*., **46**, 5182 (2017).
6. C. Zhang, T. D. Biggs, N. O. Devarie-Baez, S. Shuang, C. Dong and M. Xian, *Chem. Commun*., **53**, 11266 (2017).
7. T. Chivers and R. S. Laitinen, *Dalton Trans*., **46**, 1357 (2017).
8. F. Blockhuys, N. P. Gritsan, A. Yu. Makarov, K. Tersago and A. V. Zibarev, *Eur. J. Inorg. Chem*., **2008**, 655 (2008).

9. L. S. Konstantinova and O. A. Rakitin, *Russ. Chem. Rev*., **77**, 521 (2008).
10. N. P. Gritsan and A. V. Zibarev, *Russ. Chem. Bull*., **60**, 2131 (2011).
11. A. V. Zibarev and R. Mews, in *Frontiers of Selenium and Tellurium Chemistry: From Small Molecules to Biomolecules and Materials*, Ed. J. D. Woollins and R. S. Laitinen, Springer (2011), Ch. 6, pp. 123–149.
12. A. V. Lonchakov, O. A. Rakitin, N. P. Gritsan and A. V. Zibarev, *Molecules*, **18**, 9850 (2013).
13. O. A. Rakitin and A. V. Zibarev, *Asian J. Org. Chem*., **7**, 2396 (2018).
14. R. Oilunkaniemi, R. S. Laitinen and T. Chivers, in *Frontiers of Selenium and Tellurium Chemistry: From Small Molecules to Biomolecules and Materials*, Ed. J. D. Woollins and R. S. Laitinen, Springer (2011), Ch. 8, pp. 179–199.
15. T. M. Klapötke, B. Krumm and R. Moll, in *PATAI's Chemistry of Functional Groups*, John Wiley & Sons (2011), pp. 1–27.
16. J. Vasiljeva and P. Arsenyan, *Chem. Heterocycl. Compd*., **53**, 1061 (2017).
17. T. Chivers and R. S. Laitinen, in *Selenium and Tellurium Reagents in Chemistry and Materials Science*, Ed. R. S. Laitinen and R. Oilunkaniemi, de Gruyter (2019), Ch. 4, pp. 123–150.
18. T. Chivers, *Chem. Rev*., **85**, 341 (1985).
19. P. K. Gowik and T. M. Klapötke, *Spectrochim. Acta*, **46A**, 1371 (1990).
20. T. Chivers, R. T. Oakley, O. J. Scherer and G. Wolmershäuser, *Inorg. Chem*., **20**, 914 (1981).
21. H. G. Heal and J. Kane, *Inorg. Synth*., **11**, 192 (1968).
22. V. Matuska, K. Tersago, P. Kilian, C. van Alsenoy, F. Blockhuys, A. M. Z. Slawin and J. D. Woollins, *Eur. J. Inorg. Chem*., **2009**, 4483 (2009).
23. (a) I. P. Parkin and J. D. Woollins, *J. Chem. Soc. Dalton Trans*., 925 (1990); (b) V. C. Ginn, P. F. Kelly and J. D. Woollins, *J. Chem. Soc. Dalton Trans*., 2129 (1992); (c) L. J. R. McGeachie, C. L. Carpenter-Warren, D. B. Cordes, M. Bühl, S. J. Gray, G. Hua, A. M. Z. Slawin and J. D. Woollins, *Z. Anorg. Chem. Allg*., **646**, 1795 (2020).
24. W. Zhao and J. Sun, *Chem. Rev*., **118**, 10349 (2018).
25. (a) J. Foropoulos and D. D. Desmarteau, *Inorg. Chem*., **23**, 3720 (1984); (b) D. D. DesMarteau and M. Witz, *J. Fluorine Chem*., **52**, 7 (1991).
26. L. Conte, G. Gambaretto, G. Caporiccio, F. Alessadrini and S. Passerini, *J. Fluorine Chem*., **125**, 243 (2004).
27. (a) J. Dong, L. Krasnova, M. G. Finn and K. B. Sharpless, *Angew. Chem. Int. Ed*., **53**, 9430 (2014); (b) P. Mukherjee, C. P. Woroch, L. Cleary, M. Rusznak, R. W. Franzese, M. R. Reese, J. W. Tucker, J. M. Humphrey, S. M. Etuk, S. C. Kwan, C. W. am Ende and N. D. Ball, *Org. Lett*., **20**, 3943 (2018);

(c) M. Wei, D. Liang, X. Cao, W. Luo, G. Ma, Z. Liu and L. Li, *Angew. Chem. Int. Ed.*, **60**, 7397 (2021); (d) Y. Chen, P. R. D. Murray, A. T. Davies and M. C. Willis, *J. Am. Chem. Soc.*, **140**, 8781 (2018); (e) X. Jia, S. Kramer, T. Skrydstrup and Z. Lian, *Angew. Chem. Int. Ed.*, **60**, 7353 (2021); (f) S. P. Blum, T. Karakaya, D. Schollmeyer, A. Klapars and S. R. Waldvogel, *Angew. Chem. Int. Ed.*, **60**, 5056 (2021); (g) Z. Lin, L. Huang and G. Yuan, *Chem. Commun.*, **57**, 3579 (2021); (h) S. P. Blum, L. Schäffer, D. Schollmeyer and S. R. Waldvogel, *Chem. Commun.*, **57**, 4775 (2021).

28. O. J. Scherer and G. Wolmershäuser, *Z. Anorg. Allg. Chem.*, **432**, 173 (1977).
29. (a) R. Bussas, G. Kresze, H. Münsterer and A. Schwöbel, *Sulfur Rep.*, **2**, 215 (1983); (b) T. Maaninen, R. S. Laitinen and T. Chivers, *Chem. Commun.*, 1812 (2002).
30. K. Goto and T. Kawashima, *J. Synth. Org. Chem. Japan*, **63**, 1157 (2005).
31. W. I. Gordon and H. G. Heal, *J. Inorg. Nucl. Chem.*, **32**, 1863 (1970).
32. R. Jones, D. J. Williams and J. D. Woollins, *Angew. Chem. Int. Ed. Engl.*, **24**, 760 (1985).
33. (a) A. Maaninen, T. Chivers, M. Parvez, J. Pietikäinen and R. S. Laitinen, *Inorg. Chem.*, **38**, 4093 (1999); (b) T. Maaninen, T. Chivers, R. S. Laitinen and E. Wegelius, *Chem. Commun.*, 759 (2000); (c) A. J. Karhu, O. J. Pakkanen, J. M. Rautiainen, R. Oilunkaniemi, T. Chivers and R. S. Laitinen, *Dalton Trans.*, **45**, 6210 (2016).
34. A. F. Cozzolini, P. S. Whitfield and I. Vargas-Baca, *J. Am. Chem. Soc.*, **132**, 17265 (2010).
35. A. Maaninen, J. Siivari, R. S. Laitinen and T. Chivers, *Inorg. Synth.*, **33**, 196 (2002).
36. M. Björgvinsson, H. W. Roesky, F. Pauer, D. Stalke and G. M. Sheldrick, *Inorg. Chem.*, **29**, 5140 (1990).
37. J. Siivari, T. Chivers and R. S. Laitinen, *Inorg. Chem.*, **32**, 1519 (1993).
38. C. P. Warrens and J. D. Woollins, *Inorg. Synth.*, **25**, 43 (1989).
39. K. Bestari, A. W. Cordes, R. T. Oakley and K. M. Young, *J. Am. Chem. Soc.*, **112**, 2249 (1990).
40. T. Chivers, N. Sandblom and G. Schatte, *Inorg. Synth.*, **34**, 42 (2004).
41. E. Parkes and J. D. Woollins, *Inorg. Synth.*, **25**, 48 (1989).
42. V. Aldeva, S. Gezahegn, B. Panahi, M. Shuoprasad, J. Ward, D. A. Foucher, R. A. Gossage and A. R. McWilliams, *Macromolecules*, **46**, 2562 (2013).
43. A. W. Cordes, M. Hojo, H. Koenig, M. C. Noble, R. T. Oakley and W. T. Pennington, *Inorg. Chem.*, **25**, 1137 (1986).

44. (a) P. Del Bel Belluz, A. W. Cordes, E. M. Kristof, P. V. Kristof, S. W. Liblong and R. T. Oakley, *J. Am. Chem. Soc.*, **111**, 6147 (1989); (b) E. Hey, C. Ergezinger and K. Dehnicke, *Z. Naturforsch.*, **44B**, 205 (1989).
45. T. Chivers, D. D. Doxsee and R. W. Hilts, in *Inorganic Experiments*, 2nd Edition, Ed. J. D. Woollins, Wiley-VCH (2003), pp. 287–290.
46. T. Chivers, D. D. Doxsee and J. F. Fait, *J. Chem. Soc. Chem. Commun.*, 1703 (1989).
47. J. Bojes, T. Chivers and I. Drummond, *Inorg. Synth.*, **18**, 203 (1978).
48. F. A. Kennett, G. K. MacLean, J. Passmore and M. N. S. Rao, *J. Chem. Soc. Dalton Trans.*, 851 (1982).
49. J. Siivari, T. Chivers and R. S. Laitinen, *Angew. Chem. Int. Ed.*, **31**, 1518 (1992).
50. A. J. Banister, R. G. Hey, G. K. MacLean and J. Passmore, *Inorg. Chem.*, **21**, 1679 (1982)
51. J. P. Johnson, G. K. MacLean, J. Passmore and P. S. White, *Can. J. Chem.*, **67**, 1687 (1989).
52. T. M. Klapötke, B. Krumm, M. Scherr, R. Haiges and K. O. Christe, *Angew. Chem. Int. Ed.*, **46**, 8686 (2007).
53. T. M. Klapötke, B. Krumm, P. Mayer and I. Schwab, *Angew. Chem. Int. Ed.*, **42**, 5843 (2003).
54. R. Haiges, J. A. Boatz, A. Vij, M. Gerken, S. Schneider, T. Schroer and K. O. Christe, *Angew. Chem. Int. Ed.*, **42**, 5847 (2003).
55. H. Klüver and O. Glemser, *Z. Naturforsch.*, **32B**, 1209 (1977).
56. T. J. Maricich, *J. Am. Chem. Soc.*, **90**, 7179 (1968).
57. Z. Xiaoqing, L. Fengyi, S. Qiao, G. Maofa, Z. Jianping, A. Xicheng, M. Lingpeng, Z. Shijun and W. Dianxun, *Inorg. Chem.*, **43**, 4799 (2004).
58. X. Zeng, H. Beckers, E. Bernhardt and H. Willner, *Inorg. Chem.*, **50**, 8679 (2011).
59. X. Zeng, M. Gerken, H. Beckers and H. Willner, *J. Phys. Chem. A*, **114**, 7624 (2010).
60. X. Zeng, H. Beckers and H. Willner, *Angew. Chem. Int. Ed.*, **52**, 7981 (2013).
61. Z. Wu, D. Li, H. Li, B. Zhu, H. Sun, J. S. Francisco and X. Zeng, *Angew. Chem. Int. Ed.*, **55**, 1507 (2016).
62. T. M. Klapötke, B. Krumm and K. Polborn, *J. Am. Chem. Soc.*, **126**, 710 (2004).
63. T. M. Klapötke, B. Krumm, H. Nöth, J. C. Gálvez-Ruiz, K. Polborn. I. Schab and M. Suter, *Inorg. Chem.*, **44**, 5354 (2005).

64. G. Wolmershäuser, M. Schnauber and T. Wilhelm, *J. Chem. Soc. Chem. Commun.*, 573 (1984).
65. T. M. Klapötke, B. Krumm and M. Scherr, *Inorg. Chem.*, **47**, 4712 (2008).
66. (a) T. M. Klapötke, B. Krumm, P. Mayer, H. Piotrowski, O. P. Ruscitti and A. Schiller, *Inorg. Chem.*, **41**, 1184 (2002); (b) T. M. Klapötke, B. Krumm, P. Mayer, H. Piotrowski, O. P. Ruscitti, *Inorg. Chem.*, **39**, 5426 (2000).
67. S. Parsons and J. Passmore, *Acc. Chem. Res.*, **27**, 101 (1994).
68. A. Apblett and T. Chivers, *Inorg. Chem.*, **28**, 4544 (1989).
69. K. V. Shuvaev and J. Passmore, *Coord. Chem. Rev.*, **257**, 1067 (2013).

Chapter 3

Applications of Physical Methods

This chapter will provide an overview, illustrated with recent examples, of some applications of the most commonly used physical methods for the characterisation of chalcogen-nitrogen compounds.

3.1 Diffraction Techniques

3.1.1 *X-ray diffraction*

The structures of chalcogen-nitrogen compounds are frequently unpredictable. For example, the reactions of heterocyclic systems often result in substantial reorganisation of their structural frameworks, *e.g.*, ring expansion or contraction. The formation of acyclic products from ring systems (or *vice versa*) is also observed. Spectroscopic techniques alone are rarely sufficient to provide decisive structural information. The advent of CCD diffractometers that facilitated the determination of atomic arrangements in the solid state in less than one day in many cases has been of paramount importance in the development of chalcogen-nitrogen chemistry.

In addition, the availability of better area detectors and high intensity sources for X-ray crystallography has been pivotal for the interrogation of the details of intermolecular interactions that are prevalent in chalcogen-nitrogen compounds because of the polarity of the E–N bonds (Sec. 4.6). This structural information is vitally important for understanding solid-state physical properties such as conductivity and magnetic behaviour. 1,2-Dichalcogena-3,5-diazolyl radicals, $[RCNEEN]^{\bullet}$ (E = S, Se), are an

especially important class of chalcogen-nitrogen compounds in this regard (Sec. 13.4). The extended structures of these multifunctional derivatives adopt a wide variety of packing arrangements in the solid state which, in turn, give rise to unique properties.[1]

In general, these secondary bonding interactions (SBIs) become stronger along the series S···N < Se···N < Te···N.[2] As an example, the structural trends in the series $E(NMe_2)_2$ (E = S, Se, Te) can be considered. Whereas the sulfur and selenium derivatives are liquids that do not exhibit significant intermolecular interactions, bis(dimethylamino)tellurane $Te(NMe_2)_2$ (**3.1**) is a polymeric solid as a result of Te···N contacts (Chart 3.1).[3] The Te–N distances in the monomeric units of **3.1** are 2.05 Å, while the intermolecular Te···N contacts are 2.96 Å; the sum of van der Waals radii for Te and N is 3.61 Å (Table 3.1).

A similar trend is evident from a survey of the SBIs in the crystal structures of 1-tellura-2,5-diazoles (**3.2**).[4] In Table 3.1 the average SBI distances are compared with the sum of the corresponding van der Waals (vdW) radii for the chalcogen and nitrogen atoms. The two sets of data follow opposite trends, clearly indicating that Te···N SBIs are the

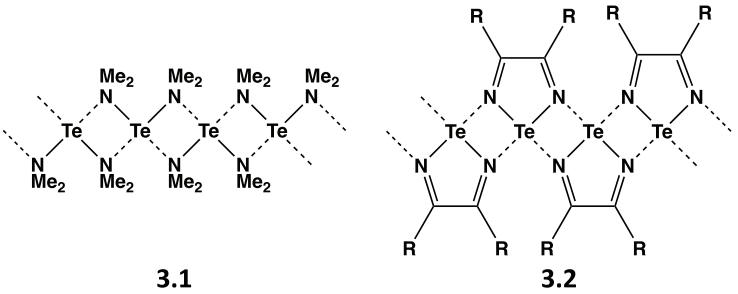

Chart 3.1. Te···N secondary bonding interactions in bis(dimethylamino)tellurane and 1-tellura-2,5-diazoles.

Table 3.1. SBI Distances (Å) in 1-Chalcogena-2,5-diazoles.

E	S	Se	Te
$r_{EvdW} + r_{NvdW}$	3.35	3.45	3.61
E–N (average)	3.20	2.95	2.77

strongest. In practice, selena- and tellura-diazoles form dimers or polymers, while thiadiazoles are generally not associated.

X-ray crystallography has been especially revealing in studies of the solid-state properties of telluradiazoles (Sec. 11.2.2). For example, tetrafluorobenzo-2,1,3-telluradiazole (**3.3**) was shown to exhibit supramolecular chromotropism.[5] Two crystalline phases were identified for the non-solvated structure. The more stable α-**3.3** is comprised of puckered ribbon polymers connected *via* Te···N SBIs and displays a red-orange colour (Fig. 3.1a). The second phase β-**3.3** is yellow and consists of ribbons linked by alternating short and long Te···N SBIs (Fig. 3.1b).[5]

X-ray crystallography is also a powerful technique for investigating polymorphism in 1,2-dithia-3,5-diazolyl radicals. For example, [F(CF_3)C_6H_3-3,5]CN_2S_2 exists as two phases, α and β (Fig. 3.2).[6] In the α phase, the two molecules form a twisted dimer involving S···N and S···S interactions. In the α form, additional S···N interactions link the dimers in quasi-2D structures (Fig. 3.2a). By contrast, the β form is composed of discrete dimers (Fig. 3.2b), in which the two component molecules are rotated by 180°. Structures having more than one equivalent chemical entity in the asymmetric unit occur frequently for 1,2-dithia-3,5-diazolyl radicals (Sec. 13.4.3).[7]

3.1.2 *Electron diffraction*

Electron diffraction studies provide valuable information about structures in the gas phase. Consequently, this method is important for chalcogen-nitrogen compounds that are liquids or gases at room temperature. The application of this technique has provided evidence for the monomeric structures of the 1,2-dithia-3,5-diazolyl radical $[CF_3CNSSN]^{\bullet}$ (**3.4**)[8] and the 1,3-dithia-2-azolyl $[CF_3CSNSCCF_3]^{\bullet}$ (**3.5**), a paramagnetic liquid (Chart 3.2).[9] The structure of the cyclotrithiatriazine $(NSF)_3$ has also been determined in the gas phase by a combination of electron diffraction and microwave spectroscopy, which shows that all three fluorine atoms are axial (**3.6**) (Sec. 8.7).[10]

Since gas-phase structures are not influenced by packing effects, a comparison of the electron diffraction and X-ray diffraction structures for a certain compound allows an evaluation of the influence of packing

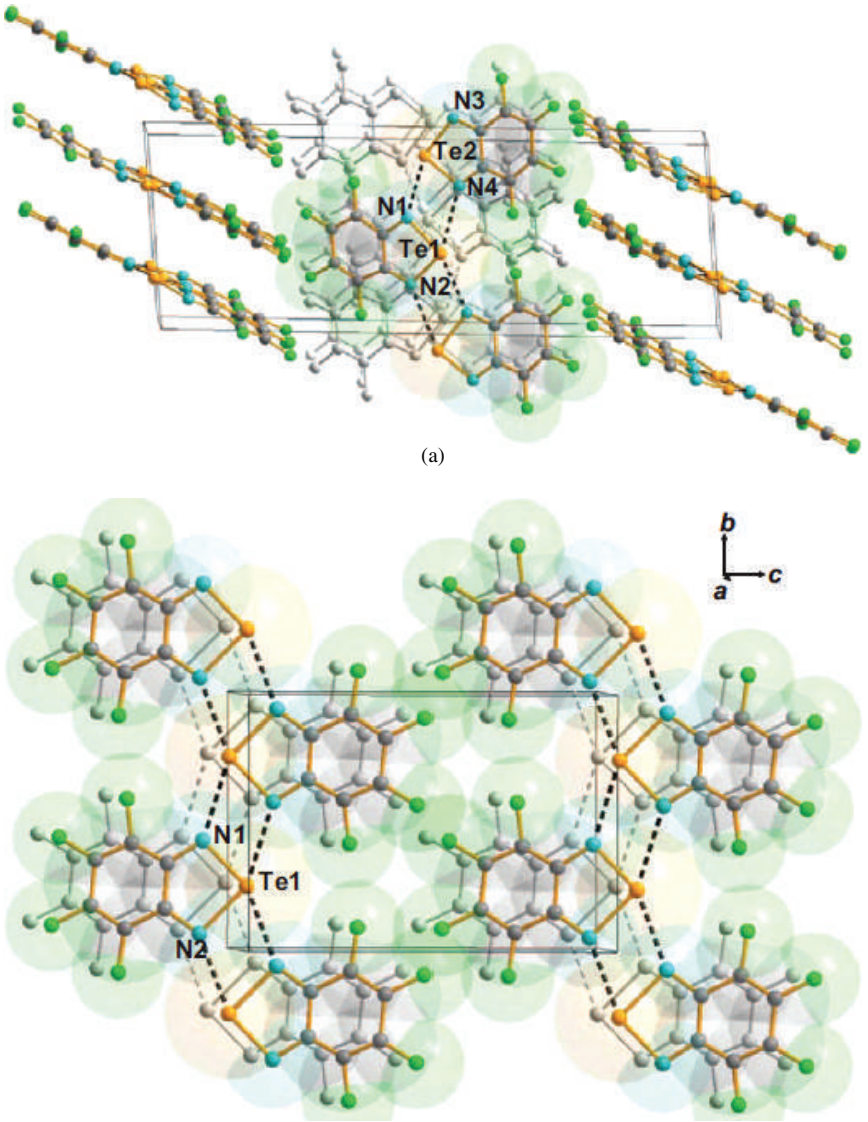

Figure 3.1. Views of the packing along [100] for (a) red and (b) yellow phases of **3.3**.[5] [Reproduced with permission from T. Chivers and R. S. Laitinen, Recent Developments in Chalcogen-Nitrogen Chemistry, in *Handbook of Chalcogen Chemistry: New Perspectives in Sulfur, Selenium and Tellurium*, Eds. F. A. Devillanova and W.-W. du Mont, Royal Society of Chemistry (2013), pp. 191–237. Copyright 2013 Royal Society of Chemistry].

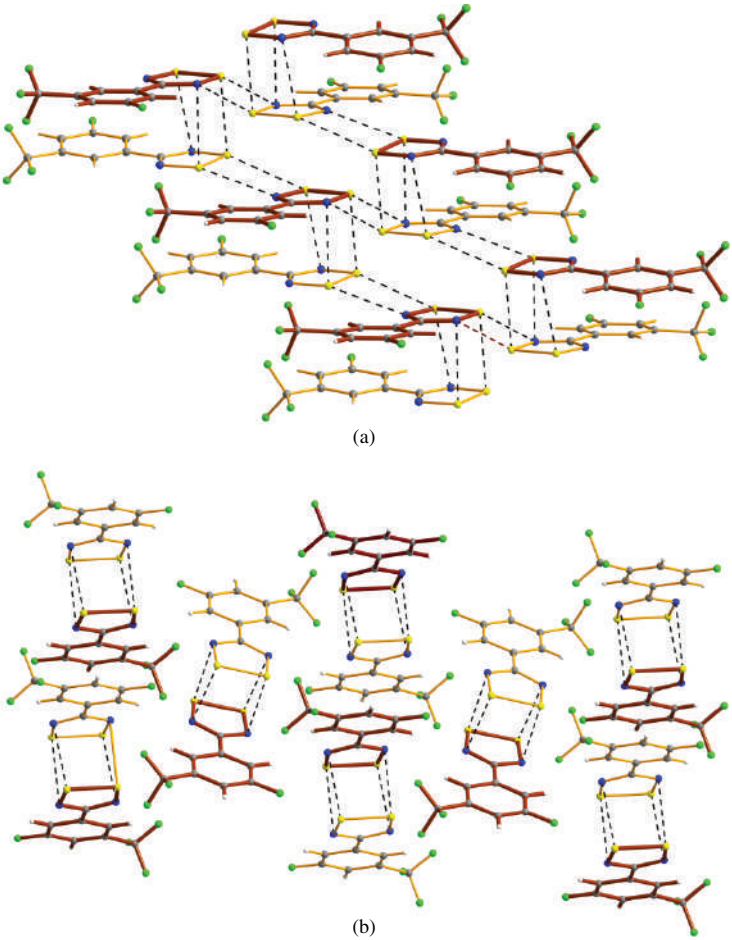

Figure 3.2. Crystal structures of the two polymorphs of $[F(CF_3)C_6H_3\text{-}3,5]CN_2S_2$: (a) the α phase and (b) the β phase.[6]

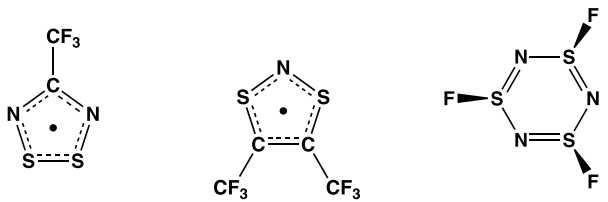

3.4 **3.5** **3.6**

Chart 3.2. The structures of $[CF_3CNSSN]^{\bullet}$, $[CF_3CSNSCCF_3]^{\bullet}$, and $(NSF)_3$.

effects on structural parameters to be made. Recent studies of such structural disparities have focused on the 12π-electron heterocycles benzo-1,3-dithia-2,4-diazines (Sec. 12.2.2).[11] The gas-phase structures of di-, tri-, and tetrafluoro derivatives (Chart 3.3) have been determined by electron diffraction.[12] The difluoro and tetrafluoro derivatives **3.7a** and **3.7c** are planar, whereas the trifluoro derivative **3.7b** and the parent (non-fluorinated) system are non-planar. In the solid state, however, the latter heterocycle is planar,[13] whereas the tetrafluoro derivative **3.7c** is non-planar.[12] This structural dichotomy has been attributed to packing effects; strong intermolecular interactions lead to a planar conformation, whereas non-planar conformations typical of the gas phase are not perturbed by weak interactions.[14] The strength of the intramolecular Te···N interaction in 2-$Me_2N(CH_2)_3TeC_6F_5$ in the solid state and gas phase has been compared based on the X-ray and electron diffraction structural data (Sec. 15.2.1).[15]

In an early application of electron diffraction the sulfur(IV) dimide $S(NSiMe_3)_2$ (**3.8**), a volatile liquid, was shown to adopt a *cis,cis* conformation in the gas phase, as shown in Chart 3.3.[16] By contrast, the *cis,trans* form is the more common arrangement for this class of S–N compounds (Sec. 10.4.2). In this context the structures of the sulfur(IV) diimide $S(N^tBu)_2$ (**3.9**) and the sulfur(VI) triimide $S(N^tBu)_3$ (**3.10**) have been determined both in the gas phase and in the solid state at low temperature.[17,18] Although a small, but significant, lengthening of the S=N bonds (by 0.001–0.002 Å) is observed in the gas phase, the structures of both compounds were found to be similar in both phases (Sec. 4.6).

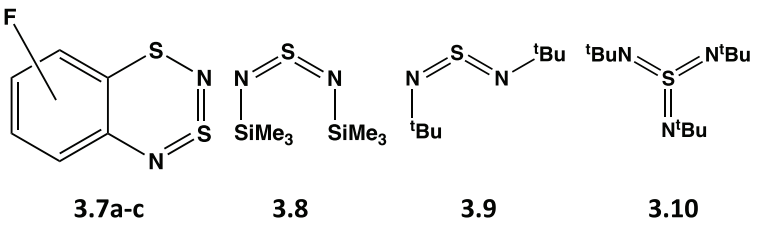

Chart 3.3. Molecular structures of $F_nH_{4-n}C_6S_2N_2$ (n = 2–4), $S(NSiMe_3)_2$, $S(N^tBu)_2$, and $S(N^tBu)_3$.

3.2 ^{14}N and ^{15}N NMR Spectroscopy

The availability of high-field pulsed NMR spectrometers has facilitated nitrogen NMR investigations of chalcogen-nitrogen compounds. Nitrogen has two isotopes, ^{14}N ($I = 1$, 99.6%) and ^{15}N ($I = ½$, 0.4%), that are amenable to NMR studies. The advantages of ^{15}N NMR are narrow, well-resolved lines and the potential ability to observe spin-spin coupling patterns. The disadvantages include the lengthy acquisition times due to long spin-lattice relaxation times and the necessity to prepare isotopically enriched materials in order to observe the effects of spin-spin coupling. Methods for the introduction of ^{15}N into S_4N_4 and Se_4N_4 from ^{15}N-labelled ammonium chloride or ammonia, respectively, have been developed.[19,20] On the other hand, the ^{14}N nucleus gives rise to relatively broad lines, poorer resolution, and loss of coupling information. In order to offset these disadvantages very short delays between pulses are possible in view of the short spin-lattice relaxation times.[21]

Some important early examples of the application of ^{14}N NMR spectroscopy in sulfur-nitrogen chemistry include (a) studies of the $(NSCl)_3 \leftrightharpoons 3NSCl$ equilibrium in solution[22] and (b) identification of the S–N species present in solutions of sulfur in liquid ammonia.[23] The line-width of ^{14}N NMR resonances is dependent on the symmetry of the atomic environment as well as other factors, such as solvent viscosity. The values may vary from *ca.* 10 Hz for solutions of $[SNS][AsF_6]$ in liquid SO_2 to >1000 Hz in metal S–N complexes. However, the chemical shift range for S–N compounds is *ca.* 800 ppm so that useful information may frequently be obtained despite the broad lines.[21] Although common organic solvents, *e.g.*, toluene and CH_2Cl_2, may be used for ^{14}N NMR studies of many chalcogen-nitrogen compounds, solubility considerations or the high reactivity of the species under investigation may require the use of less common solvents for some species. Liquid SO_2 is a particularly good solvent for ^{14}N NMR studies of cationic S–N species,[22] while liquid ammonia is well-suited to investigations of inorganic S–N anions.[21,23]

^{15}N NMR spectroscopy has been used to monitor the formation and identification of sulfur-nitrogen anions in solution. For example, the acyclic $[S_2N_2H]^-$ ion was identified in liquid ammonia by the observation of two characteristic resonances, one of which is a doublet [$^1J(^{15}N–^1H) = 55$ Hz] (Fig. 3.3).[24] The ^{15}N–^{15}N coupling constant between the two

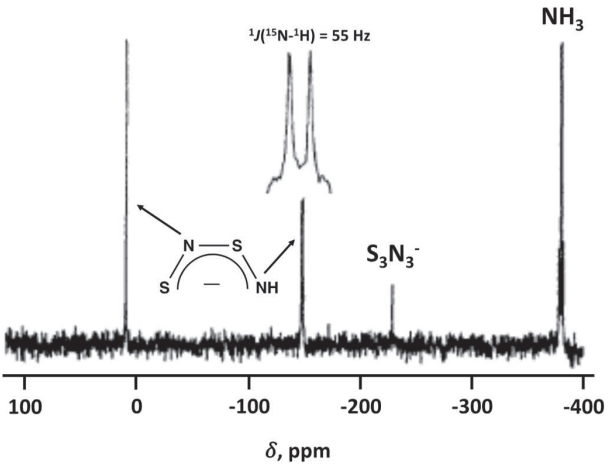

Figure 3.3. ^{15}N NMR spectrum of a solution of $S_4{}^{15}N_4H_4$ + $2KNH_2$ in liquid NH_3 at 25°C.[24] [Reproduced with permission from T. Chivers and R. S. Laitinen, *Chem. Soc. Rev.*, **46**, 5182 (2017). Copyright 2017 Royal Society of Chemistry].

inequivalent nitrogen atoms is *ca.* 2 Hz. The $[S_2N_2H]^-$ ion is well-known in metal complexes, but it has not been structurally characterised in an ion-separated salt (Sec. 5.9.6).

^{15}N NMR spectroscopy has also been used to investigate the formation of S,N,O anions in solution.[25] The reaction of elemental sulfur with nitrite anion results in the generation of the biologically important $[SSNO]^-$ anion (Sec. 7.9). In the gunpowder reaction the combination of these reagents is thought to occur *via* the intermediate $[SNO_2]^-$ anion (Sec. 7.5).[26] The ^{15}N NMR spectrum of the reaction of $[PPN][^{15}NO_2]$ with *cyclo*-S_8 in acetone initially displays a resonance at −67 ppm tentatively attributed to $[SNO_2]^-$; this signal disappears over the course of 24 h and is replaced by a resonance at 348 ppm for the $[SSNO]^-$ anion (Fig. 3.4).[25]

In the absence of ^{15}N-labelling, polarisation transfer techniques can be used to enhance the sensitivity of ^{15}N NMR experiments. For example, the ^{1}H-^{15}N HMQC (heteronuclear multiple quantum coherence) spectrum of a mixture of cyclic sulfur imides containing the diimide isomers 1,3-, 1,4-, and 1,5-$S_6(NH)_2$ and the triimide isomers 1,3,5- and 1,3,6-$S_5(NH)_3$ (Sec. 9.3.1) provides well-resolved ^{1}H and ^{15}N chemical shifts for each component. The $^1J(^{15}N,^1H)$ values are in the range 91–94 Hz and the ^{15}N NMR chemical shifts are determined by the environment of the NH group in these cyclic systems (Fig. 3.5).[27]

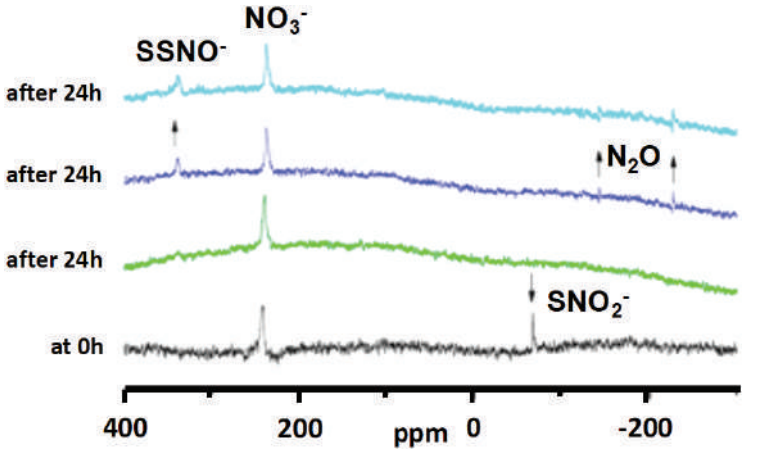

Figure 3.4. ^{15}N NMR spectra of the reaction of [PPN][$^{15}NO_2$] with *cyclo*-S_8 in acetone.[25] [Reproduced with permission from R. Wedmann, A. Zahl, T. E. Shubina, M. Durr, F. W. Heinemann, B. E. C. Bugenhagen, P. Burger, I. Ivanovic-Burmazovic and M. Filipovic, *Inorg. Chem*., **54**, 9367 (2015). Copyright 2015 American Chemical Society].

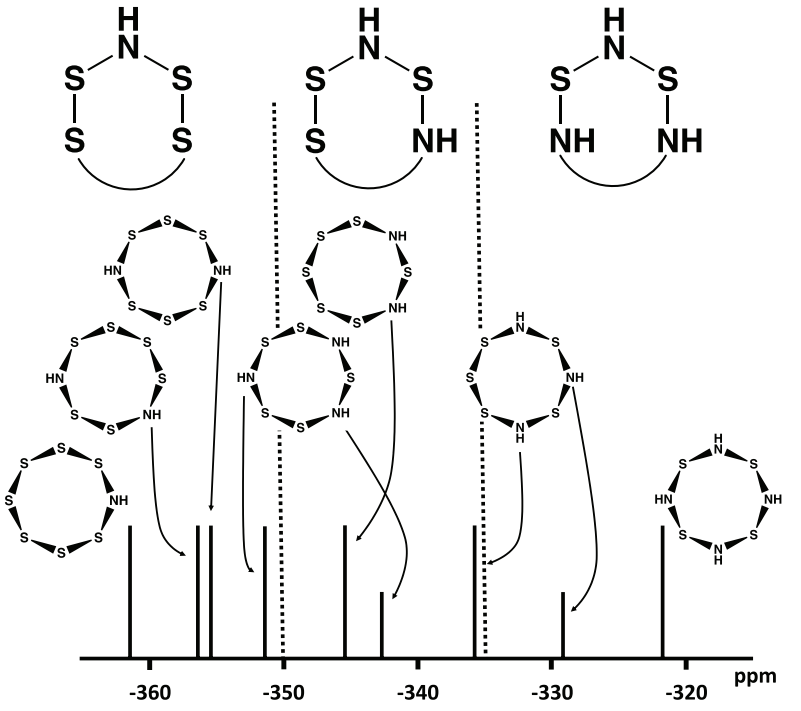

Figure 3.5. ^{15}N NMR chemical shifts for NH groups in cyclic sulfur imides.[27]

The HMQC technique is also informative in discerning the presence of *cis* and *trans* isomers in a D_8-toluene solution of the adduct $HNSO{\cdot}B(C_6F_5)_3$ (Sec. 6.4); the distinctive NMR parameters for the two isomers are $\delta(^1H) = 10.4$ and 10.6 ppm, $\delta(^{15}N) = -95$ and -106 ppm, and $^1J(^{15}N,^1H) = 65$ and 70 Hz.[28]

3.3 ^{77}Se and ^{125}Te NMR Spectroscopy

The only sulfur isotope with a nuclear spin is ^{33}S, which is quadrupolar ($I = 3/2$) and of low natural abundance (0.76%). In view of these inherent difficulties and the low symmetry around the sulfur nuclei in most S–N compounds, ^{33}S NMR spectroscopy has found very limited application in S–N chemistry. On the other hand, both selenium and tellurium have isotopes with $I = ½$ with significant natural abundances (^{77}Se, 7.6% and ^{125}Te, 7.0%). Consequently, NMR studies using these nuclei can provide useful information for Se–N and Te–N systems.

The ^{77}Se NMR chemical shifts of Se–N compounds cover a range of >2500 ppm and the value of the shift is characteristic of the local environment of the selenium atom. As illustrated in Fig. 3.6, a good agreement

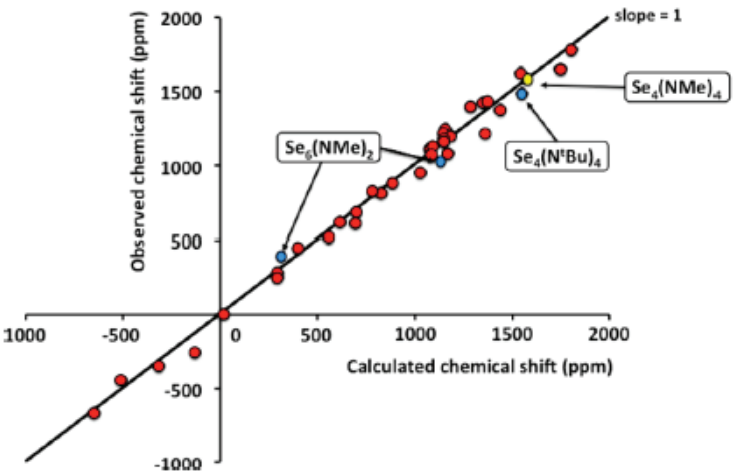

Figure 3.6. Observed and calculated ^{77}Se chemical shifts of Se-containing species.[29] [Reproduced with permission from A. J. Karhu, O. J. Pakkanen, J. M. Rautiainen, R. Oilunkaniemi, T. Chivers and R. S. Laitinen, *Inorg. Chem.*, **54**, 4990 (2015). Copyright 2015 American Chemical Society].

has been established between experimental ^{77}Se NMR chemical shifts for 28 selected selenium compounds and the corresponding calculated values determined at the PBE0/def2-TZVPP level of theory. This correlation together with the structural and spectroscopic characterisation of $Se_4(NMe)_4$ and 1,5-$Se_6(NMe)_2$ enabled the identification of the elusive eight-membered ring $Se_4(N^tBu)_4$.[29]

^{77}Se NMR spectra can also be used to analyse the composition of a complex mixture of Se–N compounds. For example, this technique provides a convenient probe for identifying the medley of cyclic selenium imides formed from the decomposition of selenium(IV) diimides RN=Se=NR (*e.g.*, R = ^{t}Bu);[31] the major decomposition products are the six-membered ring $(SeN^tBu)_3$, the five-membered ring $Se_3(N^tBu)_2$ and 15-membered ring $Se_9(N^tBu)_6$ (Sec. 9.4).[31] In a similar manner the reaction of the imidoselenium(II) dichloride $ClSe[N(^tBu)Se]_2Cl$ with *tert*-butylamine was shown to form $Se_3(N^tBu)_2$ and $(SeN^tBu)_n$ (n = 3, 4) (Fig. 3.7 and Scheme 9.2).[30,31]

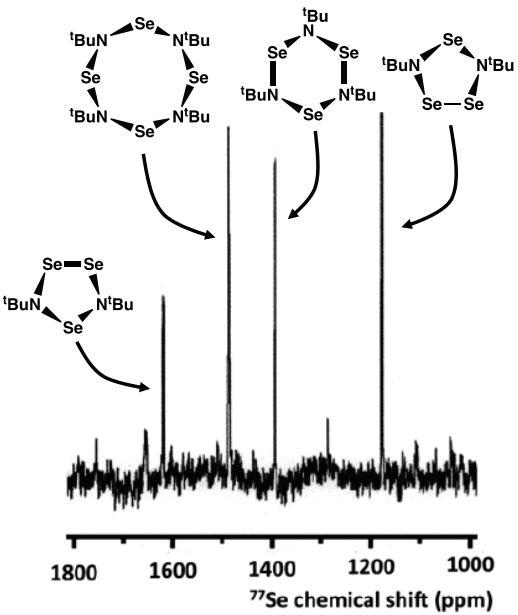

Figure 3.7. ^{77}Se NMR spectrum of the reaction of $ClSe[N(^tBu)Se]_2Cl$ with $^tBuNH_2$ in THF.[31] [Reproduced and modified with permission from A. J. Karhu, O. J. Pakkanen, J. M. Rautiainen, R. Oilunkaniemi, T. Chivers and R. S. Laitinen, *Dalton Trans*., **45**, 6210 (2016). Copyright 2016 American Chemical Society].

Table 3.2. ^{125}Te NMR chemical shifts in [2-(^{t}BuNCH)C_6H_4Te]X (**3.11**).

Species	X	δ (^{125}Te) / ppm
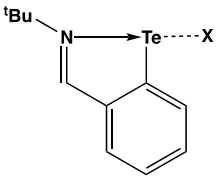 **3.11**	$[O_3SCF_3]^-$	1735
	$[SbF_6]^-$	1896
	$[Al\{OC(CF_3)_3\}_6]^-$	1945

The dependence of the ^{77}Se chemical shift on the chemical environment is clearly demonstrated in Fig. 3.7. The chemical shift appears at higher frequency as the electronegativity of the neighbouring atoms increases.

^{125}Te NMR chemical shifts of tellurium-nitrogen compounds also cover a very wide range of *ca.* 5800 ppm and are sensitive to the environment at the tellurium centre. For example, the ^{125}Te chemical shifts for the aryltellurenyl cation in the salts [2-(^{t}BuNCH)C_6H_4Te]X (**3.11**) in CD_2Cl_2 depend on the strength of the cation-anion interaction in solution (Table 3.2 and Sec. 15.2.4).[32,33]

3.4 Electrochemical Reduction and EPR Spectroscopy

The molecular and electronic structures of chalcogen-nitrogen radicals, including a detailed discussion of the Electron Paramagnetic Resonance (EPR) spectra of binary S–N radicals, have been reviewed recently.[34,35] This section is sub-divided into two parts which describe (a) the EPR spectra of neutral radicals and (b) the application of the technique of Simultaneous Electrochemical Electron Paramagnetic Resonance (SEEPR) spectra to the generation and identification of radical anions. The ^{14}N nucleus ($I = 1$, 99%) has a moderately large magnetic moment and hyperfine splittings from this nucleus are a distinctive feature of the EPR spectra of chalcogen-nitrogen radicals; isotopic labeling with ^{15}N ($I = 1/2$)

is frequently used to confirm identification, especially for fugacious radical anions (Sec. 3.4.2).

3.4.1 *Neutral radicals*

Examples of chalcogen-nitrogen radicals that are monomeric in the solid state are rare. However, arylthio-2,4,6-triphenylanilino radicals (**3.12**, Chart 3.4) can be isolated as dark green or purple crystals.[36] They exhibit a characteristic 1:1:1 triplet in the EPR spectrum as a result of coupling of the unpaired electron with the single nitrogen centre. More commonly, both acyclic and cyclic chalcogen-nitrogen radicals dimerise in the solid state but undergo partial dissociation in solution and, hence, can be characterised by their EPR spectra. For example, the EPR spectra of the well-known *N*,*N*′-(bisarylthio)aminyls (**3.13**) also exhibit 1:1:1 triplets. A particularly pleasing example of the EPR spectra of this type of radical is the 1:1:1 triplet of septets observed for $[(CF_3S)_2N]^{\bullet}$ (**3.14**) in which coupling to the six equivalent fluorine atoms of two CF_3 groups is well-resolved.[38] The isomers of heterocyclic C,N,S radicals, 1,2-dithia-3-azolyl and 1,3-dithia-2-azolyl, are discussed in Secs. 13.2 and 13.3, respectively.

Many of the persistent chalcogen-nitrogen radicals are cyclic C,N,S systems (Chapter 13). For these heterocycles the unpaired electron often occupies a delocalised π-orbital, which may contribute to the stability of the species. In conjunction with molecular orbital calculations, EPR spectra can provide unique information about the electronic structures of these ring systems. For example, the EPR spectra of 1-thia-2,4,6-triazinyls (**3.15**, Chart 3.5) exhibit significantly larger hyperfine couplings to the

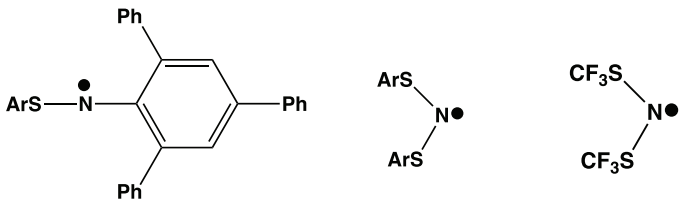

3.12 **3.13** **3.14**

Chart 3.4. Examples of persistent organosulfur-nitrogen radicals.

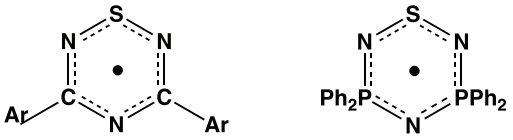

3.15 **3.16**

Chart 3.5. 1-Thia-2,4,6-triazinyl (Ar = 4-$MeOC_6H_4$) and 1-thia-2,4,6-triaza-3,5-diphosphinyl radicals.

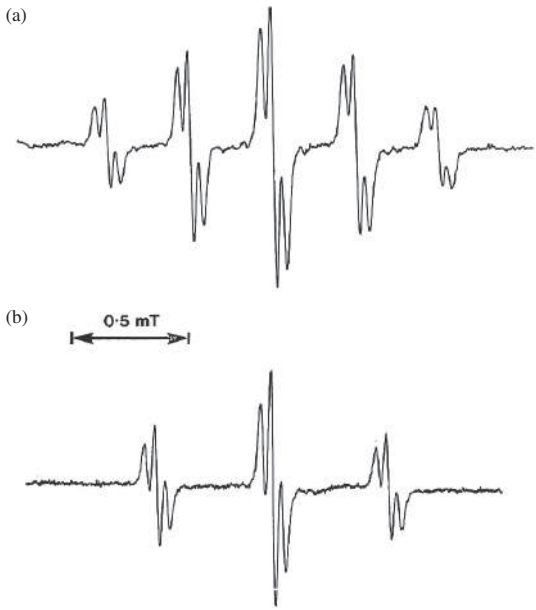

Figure 3.8. EPR spectra of (a) $[Ph_4P_2N_3S]^{\bullet}$ and (b) $[Ph_4P_2{}^{15}N_3S]^{\bullet}$ in CH_2Cl_2.[41] [Reproduced with permission from R. T. Oakley, *J. Chem. Soc., Chem. Commun*., 596 (1986). Copyright 1986 Royal Society of Chemistry].

unique nitrogen, except for Ar = 4-$MeOC_6H_4$, for which accidental equivalence of all three nitrogens is observed (Sec. 13.6).[39,40]

The EPR spectra of the related 1-thia-2,4,6-triaza-3,5-diphosphinyl radicals (**3.16**) reveal a distinctly different electronic structure.[41] The observed spectrum consists of a quintet of triplets consistent with coupling of the unpaired electron with two equivalent nitrogen atoms and two equivalent phosphorus atoms (Fig. 3.8a). This interpretation was

confirmed by the observation that the quintet collapses to a 1:2:1 triplet when the nitrogen atoms in the ring are 99% ^{15}N-enriched (Fig. 3.8b). Thus, the spin delocalisation does not extend to the unique nitrogen atom in the phosphorus-containing system **3.16**.

3.4.2 *Radical anions: SEEPR spectra*

The one-electron electrochemical reduction of sulfur-nitrogen compounds generates short-lived radical anions. The formation of the $[S_4N_4]^{\bullet-}$ from S_4N_4 is a classic early example of this behaviour.[42] This anion radical was characterised by a nine-line EPR spectrum indicating delocalisation of the unpaired electron over four equivalent nitrogen atoms. Subsequently, it was shown that $[S_4N_4]^{\bullet-}$ undergoes a ring-contraction process to generate the six-membered ring $[S_3N_3]^{-}$.[43]

If the electrochemical reduction is carried out in the cavity of an EPR spectrometer it is possible to identify many ephemeral chalcogen-nitrogen radical anions and investigate their decomposition pathways. The power of this technique, which is known as Simultaneous Electrochemical Electron Paramagnetic Resonance (SEEPR), is illustrated below with a few examples. In an SEEPR investigation of tetrasulfur tetranitride in CD_2Cl_2 at −20°C, using both natural abundance and 99% ^{15}N-enriched samples, the nine-line spectrum for $[S_4{}^{14}N_4]^{\bullet-}$ (^{14}N, $I = 1$) became a five-line (1:4:6:4:1) spectrum for $[S_4{}^{15}N_4]^{\bullet-}$, confirming coupling of the unpaired electron with four equivalent ^{15}N nuclei (^{15}N, $I = ½$) (Fig. 3.9).[44]

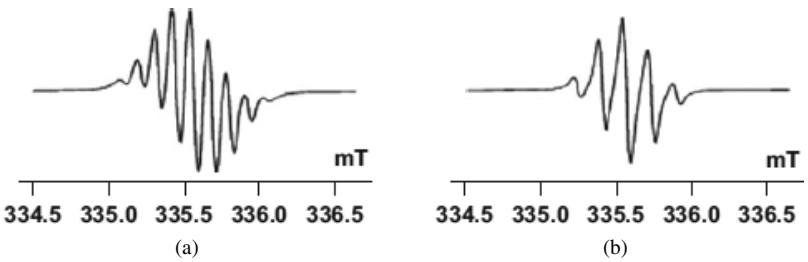

Figure 3.9. EPR spectra of (a) $[S_4{}^{14}N_4]^{\bullet-}$ and (b) $[S_4{}^{15}N_4]^{\bullet-}$ in CD_2Cl_2 at −20°C.[44] [Reproduced with permission from R. T. Boeré, T. Chivers, T. L. Roemmele and H. M. Tuononen, *Inorg. Chem.*, **48**, 7294 (2009). Copyright 2009 American Chemical Society].

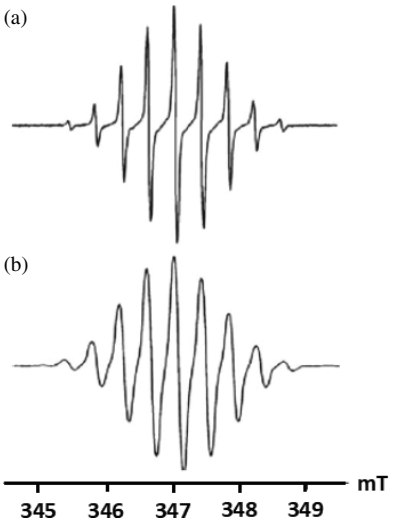

Figure 3.10. EPR spectra of the radical anions (a) $[PhC(NSN)_2CPh]^{\bullet-}$ and (b) $[Me_2NC(NSN)_2CNMe_2]^{\bullet-}$.[46] [Adapted with permission from R. T. Boeré, A. M. Bond, T. Chivers, S. W. Feldberg and T. L. Roemmele, *Inorg. Chem*., **46**, 5596 (2007). Copyright 2007 American Chemical Society].

The radical anion $[S_4N_4]^{\bullet-}$ decays *via* first-order kinetics to give $[S_3N_3]^-$,[44] presumably *via* elimination of the EPR-silent neutral radical $NS^{\bullet}$.[34] A SEEPR investigation of S_2N_2 in both CH_2Cl_2 and CH_3CN resulted in the detection of the characteristic EPR spectrum of $[S_4N_4]^{\bullet-}$.[45]

Short-lived radical anions ($t_{½}$ < 5 s) of the eight-membered rings 1,5-$(RC)_2N_4S_2$ (R = Ph, NMe_2) have been identified using the SEEPR technique. The EPR spectra of both derivatives exhibit nine lines indicating coupling of the unpaired electron with four equivalent nitrogen atoms; the broader lines for the R = NMe_2 derivative result from additional coupling to the N and H nuclei of the NMe_2 groups (Fig. 3.10).[46]

EPR spectroscopy has also played a major role in the characterisation of an extensive series of 1-chalcogena-2,5-diazolidyl radical anions (**3.17**) that are produced upon one-electron chemical or electrochemical reduction of the neutral precursors (**3.18**) (Chart 3.6).[47] For example, the long-lived radical anion [1-thia-2,5-diazolo(3,4-c)][1-thia-2,5-diazolidyl]

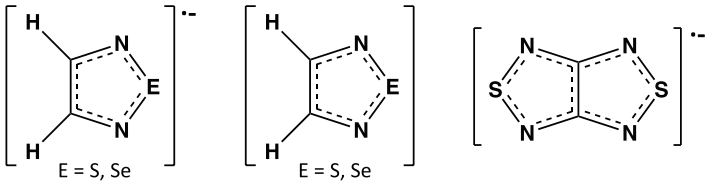

Chart 3.6. 1-Chalcogena-2,5-diazolidyl radical anion (**3.17**), its neutral precursor (**3.18**) and [1-thia-2,5-diazolo(3,4-c)][1-thia-2,5-diazolidyl] radical anion (**3.19**).

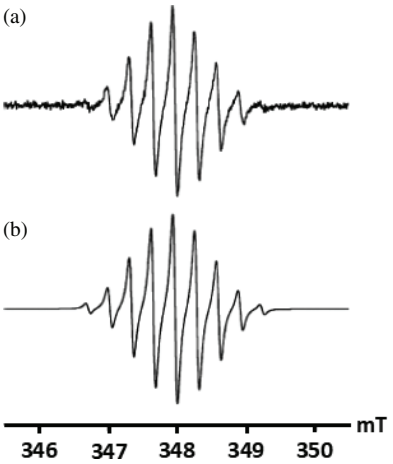

Figure 3.11. (a) Experimental and (b) simulated EPR spectra of **3.19**.[48] [Reproduced with permission from A. Yu. Makarov, I. G. Irtegova, N. V. Vasilieva, I. Yu. Bagryanskaya, T. Bormann, Y. V. Gatilov, E. Lork, R. Mews, W-D. Stohrer and A. V. Zibarev, *Inorg. Chem*., **44**, 7194 (2005). Copyright 2005 American Chemical Society].

(**3.19**) exhibits a nine-line EPR spectrum consistent with delocalisation of the unpaired electron over four equivalent nitrogen atoms in this 10π-electron heterocycle (Fig. 3.11 and Sec. 13.9).[48]

3.5 Photoelectron Spectroscopy

Photoelectron spectra (PES) supply information about the binding energies of either inner core (X-ray PES) or valence-level (UV PES) electrons.

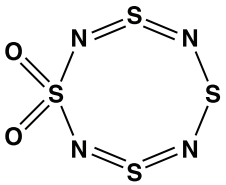

3.20

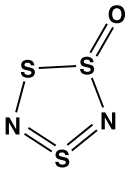

3.21

Chart 3.7. Molecular structures of $S_4N_4O_2$ and S_3N_2O.

PES also provides details of the binding energies of sulfur or nitrogen atoms that are in different environments in a given molecule. For example, in early work the X-ray PES of $S_4N_4O_2$ (**3.20**; Chart 3.7) was found to exhibit distinct binding energy values for the three types of sulfur atoms and two pairs of inequivalent nitrogen atoms consistent with the known structure.[49] Similarly, the X-ray PES of cyclic S_3N_2 derivatives, *e.g.*, S_3N_2O (**3.21**), showed three sulfur (2*p*) and two nitrogen (1*s*) binding energies as expected.[50]

More recently, the PE spectrum of the $[NSO]^-$ anion was investigated in order to measure the electron affinity (EA) and vibrational frequencies of the neutral radical $[NSO]^{\bullet}$.[51,52] The EA of $[NSO]^{\bullet}$ was determined to be 3.11 eV and the vibrational frequencies were assigned as 1202(6) cm^{-1} (ν_1, asymmetric stretch.), 1010(10) cm^{-1} (ν_2, symmetric stretch.) and 300(7) cm^{-1} (ν_3, bend),[52] in excellent agreement with both experimental[53] and calculated values[54] for this triatomic radical (Sec. 6.3). The corresponding fundamental frequencies of the $[NSO]^-$ anion were found to be 1280, 990 and 480 cm^{-1} in good agreement with IR data (Sec. 7.2.1, Table 7.1). The PE spectrum of the isomeric $[SNO]^-$ anion was broad and complicated by photodissociation to give S^- and NO.[52]

UV PES has been used to determine the variation of ionisation energies (IEs) of C,N,E heterocycles as a function of the chalcogen. In an early example, the first IE of the prototypical cyclic radicals $[HCN_2E_2]^{\bullet}$ (E = S, Se) was found to be slightly lower for the selenium derivative.[55] In a more recent UV PES investigation the vertical ionisation energies of benzo-2-chalcogena-1,3-diazoles $C_6H_4N_2E$ (E = S, Se, Te) (Sec. 11.2.2) were compared with the energies of occupied molecular orbitals determined by

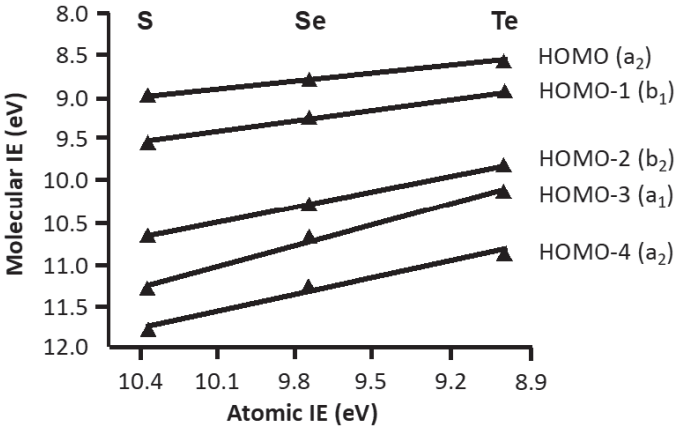

Figure 3.12. Experimental IEs of benzo-2-chalcogena-1,3-diazoles *vs*. first IE of the chalcogen atom.[56] [Reproduced with permission from A. F. Cozzolino, N. E. Gruhn, D. L. Lichtenberger and I. Vargas-Baca, *Inorg. Chem*., **47**, 6220 (2008). Copyright 2008 American Chemical Society].

relativistic DFT methods.[56] As expected, the IEs were found to follow the order Te < Se < S (Fig. 3.12).

3.6 UV-Visible Spectroscopy

In contrast to unsaturated organic systems, many chalcogen-nitrogen compounds exhibit intense colours attributed to low-energy ($\pi^* \rightarrow \pi^*$ or $n \rightarrow \pi^*$) transitions. Consequently, visible spectroscopy can be a powerful technique for monitoring reactions of both cyclic and acyclic chalcogen-nitrogen compounds. For example, solutions of the yellow cyclic anion $[S_3N_3]^-$ (λ_{max} 365 nm) become red upon air oxidation and, subsequently, purple upon exposure to oxygen due to the successive formation of the monoxide $[S_3N_3O]^-$ (λ_{max} 509 nm) and dioxide $[S_3N_3O_2]^-$ (λ_{max} 562 nm) (Fig. 3.13).[57]

Acyclic S,N,O anions also exhibit strong visible absorption bands, *e.g.*, yellow $[SNO]^-$ (λ_{max} 334 nm) and red $[SSNO]^-$ (λ_{max} ~ 445 nm in THF, acetone or MeCN) (Secs. 7.5 and 7.9).[58] Visible spectroscopy has been used to monitor the formation of the biologically significant

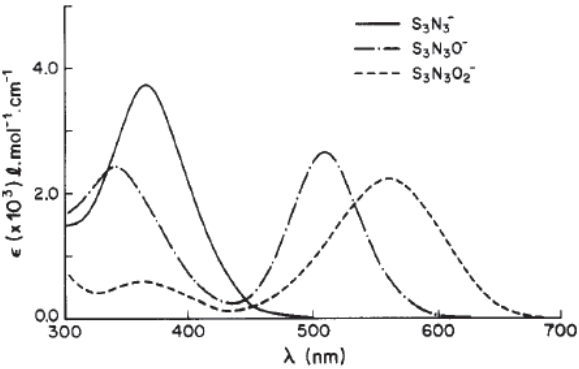

Figure 3.13. Visible spectra of $[S_3N_3]^-$, $[S_3N_3O]^-$ and $[S_3N_3O_2]^-$ in CH_2Cl_2.[57] [Reproduced with permission from T. Chivers, A. W. Cordes, R. T. Oakley and W. T. Pennington, *Inorg. Chem*., **22**, 2429 (1983). Copyright 1983 American Chemical Society].

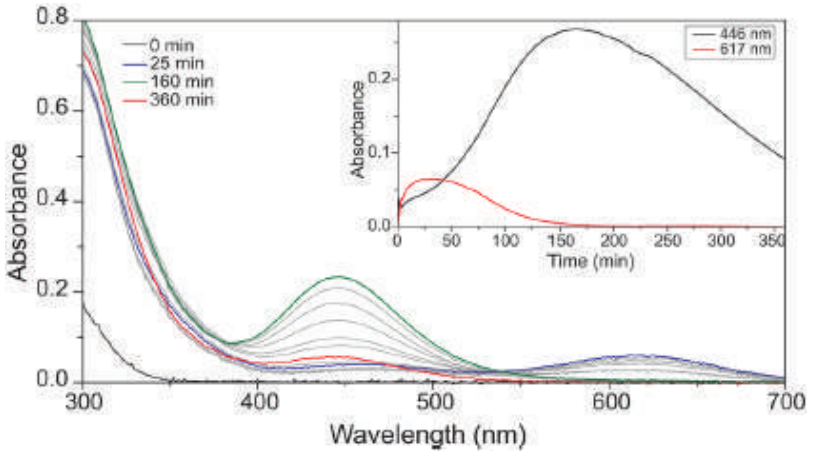

Figure 3.14. UV-visible spectra of reaction of AdSSH with $[NO_2]^-$.[59] [Reproduced with permission from T. S. Bailey, H. A. Henthorn and M. D. Pluth, *Inorg. Chem*., **55**, 12618 (2016). Copyright 2016 American Chemical Society].

$[SSNO]^-$ anion from the reaction of AdSSH (Ad = adamantyl) with nitrite anion in THF.[59] The reaction solution becomes blue-green initially due to the formation of the trisulfide radical anion $S_3^{\bullet-}$ (λ_{max} 617 nm) from the disproportionation of polysulfide dianions S_x^{2-} (x = 3–6). This absorption decays to give a strong band at 446 nm for $[SSNO]^-$ with an isobestic

point at 540 nm (Fig. 3.14). Importantly, the absorbance for $[SSNO]^-$ is highly solvent-dependent and shifts from 446 nm in THF to *ca.* 420 nm in 1:1 THF:water solution, *cf.* calculated values of 458 nm in acetone or acetonitrile and 411 nm in aqueous solutions (Sec. 7.9.2).[59,60] Interestingly, a yellow species (λ_{max} 412 nm) tentatively attributed to the $[SSNO]^-$ anion was observed in early investigations of the reaction of *S*-nitrosoglutathione (GSNO) with the thiolate anion SH^- in aqueous solution (pH 10).[61]

UV-visible spectroscopy has also been used to determine the association constants for the interaction of benzo-2-tellura-1,3-diazoles with halide anions in organic solvents (Sec. 11.2.4).[62] By titration of a solution of $[Bu_4N]Cl$ with the telluradiazole it was established that 1:1 complexes are formed with association constants as high as 29 kJ mol^{-1}.

3.7 Infrared and Raman Spectroscopy

In early work vibrational spectroscopy has been used to identify small chalcogen-nitrogen species that are unstable under ambient conditions.[63,64] The experimental technique involved subjecting nitrogen gas and the chalcogen vapour to a microwave discharge in an argon atmosphere. The products were trapped in the argon matrix at 12 K and, with the aid of isotopic substitution (^{15}N, ^{34}S, ^{76}Se and ^{80}Se), the IR and Raman spectra were assigned to specific molecules. In this way the diatomic species $EN^{\bullet}$ (E = S, Se) (Sec. 5.3.1) and the triatomic molecules SN_2 and $E_2N^{\bullet}$ (E = S, Se) (Sec. 5.6.1) were identified. The strongest absorptions were observed for the antisymmetric stretching vibration of the ENE isomers (E = S, 1225 cm^{-1}; E = Se, 1021 cm^{-1}). The <ENE bond angles were estimated to be 153.5° and 146.5°, respectively. The diatomic species $SN^{\bullet}$ exhibits an absorption at 1209 cm^{-1} and the nitrogen-nitrogen stretching fundamental of SN_2 is observed at 2040 cm^{-1}.[63,64]

More recently, the technique of ^{15}N-enrichment (30%) has been used for the determination of the IR and Raman spectra of S_2N_2 as a solid condensate in N_2 or CH_4 matrices at 15–35 K (Fig. 3.15).[65] It was found that the isolated S_2N_2 molecule has essentially the same square-planar geometry as the crystalline solid; calculations of the stretching force constant indicated a bond order only slightly greater than 1. The use of coupled

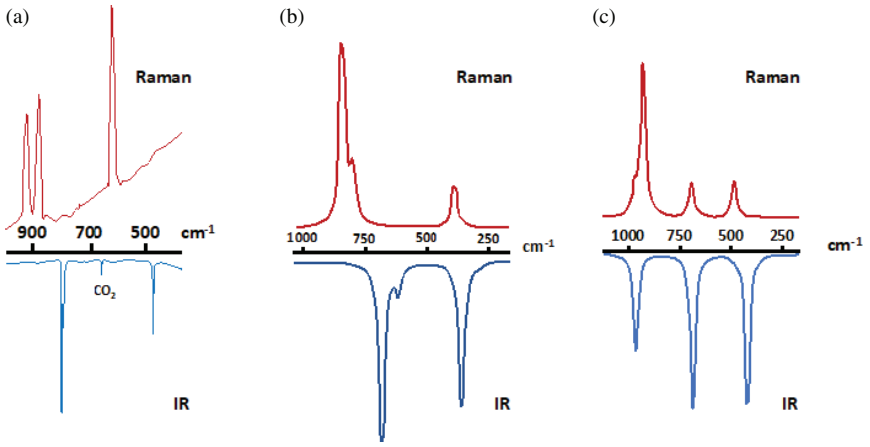

Figure 3.15. IR/Raman spectra of S_2N_2 [65] and the theoretically predicted IR/Raman spectra of (b) Se_2N_2 and (c) $SeSN_2$.[66] [Reproduced with permission from T. Chivers and R. S. Laitinen, *Dalton Trans.*, **49**, 6532 (2020). Copyright 2020 Royal Society of Chemistry].

cluster and multiconfigurational methods gave vibrational frequencies for S_2N_2 that were in reasonable agreement with the experimental values and enabled the prediction of IR and Raman spectra for the putative Se-containing rings Se_2N_2 and $SSeN_2$ (Fig. 3.15).[66]

In the past decade the techniques of matrix isolation combined with a comparison of the IR spectra of natural abundance and ^{15}N-labelled samples have played a major role in the identification of a large variety of short-lived S,N, S,N,O and S,N,P molecules. For example, the acyclic isomers of S_2N_2,[67] as well as isomers of the triatomic combinations, NSO[68] and SPN,[69] have all been characterised in this manner. Full details of the generation, identification and structures of these and related ephemeral chalcogen-nitrogen species are given in Chapter 6.

The power of Raman spectroscopy in chalcogen-nitrogen chemistry is illustrated by its application for the identification of $(SN)_x$ formed *via* polymerisation of S_2N_2 in a zeolitic framework[70] and in the detection of fingerprints on various surfaces (Sec. 5.4.2, Fig. 5.2).[71]

3.8 Mass Spectrometry

A mass spectrum is a plot of the intensity of radical cations that are produced upon ionisation of a molecule (M) as a function of the mass-to-charge (*m*/*z*) ratio of the ions. In a high-resolution mass spectrum the masses of the ions produced are determined to the fourth decimal place and compared to the calculated mass. Consequently, this technique can provide the chemical identity of a molecule from the mass and isotopic composition of the molecular ion $[M]^{\bullet+}$. Both hard and soft ionisation sources are available for the generation of ions. In the former case, the excess energy imparted to the molecule results in fragmentation of the molecular ion and the identification of the fragment ions can provide structural information. Soft ionisation techniques impart lower amounts of residual energy on the molecule and result in relatively little fragmentation. Mass spectrometry is especially useful for the identification of chalcogen-nitrogen compounds for which elemental analyses are difficult to obtain, *e.g.*, oils, volatile liquids, or for those that cannot be crystallised for X-ray diffraction analysis, *e.g.*, powders or high molecular weight macrocycles, as illustrated by the examples below.

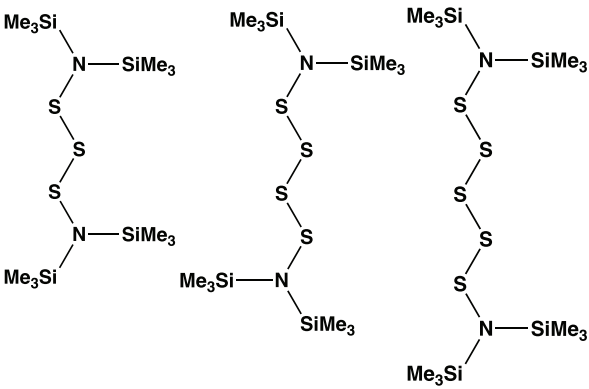

Calcd:	417.1190	449.0911	512.0280
Found:	417.1186	449.0908	512.0241

Figure 3.16. HRMS identification of the series $(Me_3Si)_2NS_xN(SiMe_3)_2$ (x = 3, 4, 5).[72]

3.8.1 *Electron impact (ionisation) mass spectrometry*

Electron impact mass spectrometry (EIMS) involves the collision of high energy electrons (12–70 eV) with a sample molecule. This technique has been crucial for the identification of polysulfides $(Me_3Si)_2NS_xN(SiMe_3)_2$ (x = 3, 4, 5), which were separated as oils by chromatography.[72] The calculated masses for the individual polysulfides were in excellent agreement with the experimental values determined by HRMS (Fig. 3.16).

Although sulfur imide polymers of the type $[SN(R)]_n$ are unknown, the trimethylsilyl derivative $[SN(SiMe_3)]_n$ has been invoked as an intermediate in the formation of metal sulfide nanoparticles, *e.g.*, Ag_2S, CuS, In_2S_3, from metal salts and sulfur in the presence of hexamethyldisilazane (HMDS). This "smelly" polymer is produced more slowly from the direct reaction of sulfur with HMDS in the absence of metal ions. The high-resolution mass spectrum of the product showed a series of ions differing in mass by an SNSi unit attributed to the fragmentation of the polymer $[SN(SiMe_3)]_n$, which was also characterised by gel permeation chromatography.[73]

3.8.2 *Electrospray ionisation mass spectrometry*

Electrospray ionisation mass spectrometry (ESI-MS) is a soft ionisation technique in which the application of a high voltage to a solution of the sample creates an aerosol. ESI-MS has been used to demonstrate the presence of macrocyclic *iso*-tellurazole-*N*-oxides up to the heptamer in solution based on their isotopic patterns; the tetramer and hexamer are shown as examples in Fig. 3.17 (see also, Sec. 15.3.3).[74]

ESI-MS has been also used to detect the formation of the ephemeral species HSNO from the reactions of (a) H_2S with *S*-nitrosoglutathione[75] and (b) nitric oxide with thiosemicarbazides (Fig. 3.18, Sec. 7.6).[76] The latter process has been proposed for the selective detection of NO (Scheme 7.1).

A ruthenium(III) complex of *N*-bonded thionitrous acid $[Ru^{III}(edta)(NOSH)]^-$ (edta = ethylenediamine tetraacetate) has been characterised in aqueous solution by ESI-MS (Fig. 3.19, Sec. 7.6.3).[77]

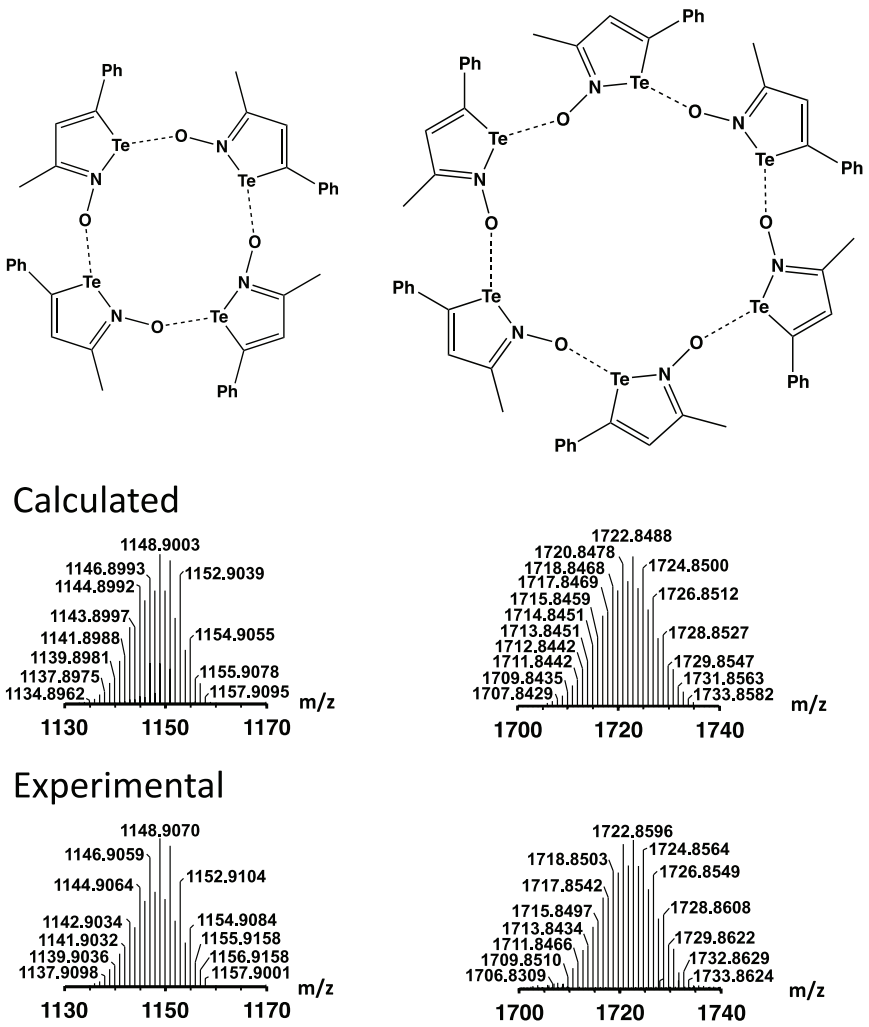

Figure 3.17. The ESI-MS isotopic distributions of the $[M_n\text{-H}]^+$ ions of the macrocyclic tetramer and hexamer of 3-methyl-5-phenyl-*iso*tellurazole *N*-oxide.[74] [Adapted with permission from I. Vargas-Baca].

3.8.3 *Laser desorption ionisation mass spectrometry*

MALDI (Matrix-Assisted Laser Desorption Ionisation) is another soft-ionisation mass spectrometric technique, but most matrices contain acidic

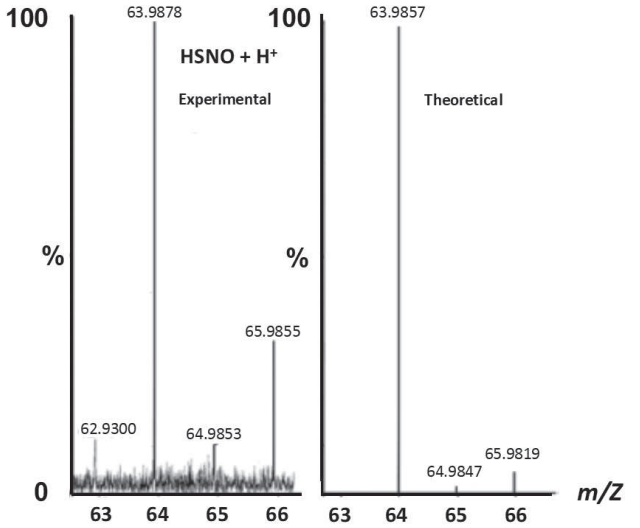

Figure 3.18. ESI-MS spectrum of HSNO formed *in situ* from NO and a thiosemicarbazide in MeCN.[76] [Adapted with permission from A. S. M. Islam, R. Bhowmick, K. Pal, A. Katarkar, K. Chaudhuri, and M. Ali, *Inorg. Chem*., **56**, 4324 (2017). Copyright 2017 American Chemical Society].

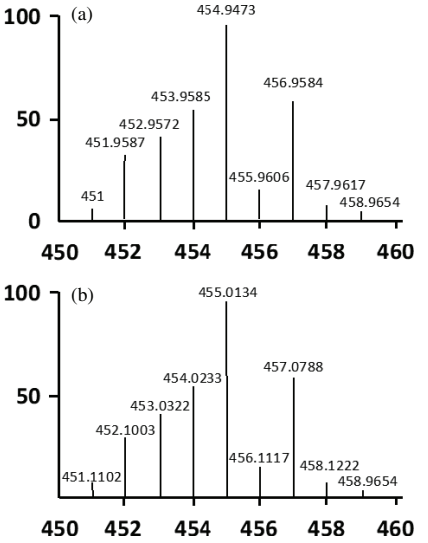

Figure 3.19. (a) Simulated and (b) experimental ESI-MS of $[Ru^{III}(edta)(NOSH)]^-$.[77] [Adapted with permission from D. Chatterjee, C. Chowdhury, A. Datta and R. van Eldik, *New. J. Chem*., **43**, 15311 (2019). Copyright 2019 Royal Society of Chemistry].

protons that would react with chalcogen-nitrogen compounds. However, UVLDI has been used to investigate the association of benzo-2-chalcogena-1,3-diazoles in the gas phase (Sec. 11.2.2.).[78] These chalcogen-nitrogen heterocycles absorb strongly in the UV, thus they can undergo desorption/ionisation without a matrix. In addition to the radical cation $[M]^{\bullet+}$ and the protonated molecular ion $[M + H]^{\bullet+}$, the UVLDI mass spectra of the benzo-2-tellura-1,3-diazoles exhibited ions for dimers of composition $[2M + H]^{\bullet+}$ and $[2M]^{\bullet+}$, which were not observed for the sulfur and selenium analogues. This observation is attributed to stronger Te···N secondary bonding interactions (Sec. 15.3.2).

References

1. For reviews, see (a) D. A. Haynes and J. M. Rawson, *Eur. J. Inorg. Chem*., **2018**, 3554 (2018); (b) D. A. Haynes, *CrystEngComm*, **13**, 4793 (2011); (c) J. M. Rawson, A. Alberola and A. Whalley, *J. Mater. Chem*., **16**, 2560 (2006); (d) J. M. Rawson, J. Luzon and F. Palacio, *Coord. Chem. Rev*., **249**, 2631 (2005).
2. A. F. Cozzolino, P. J. W. Elder and I. Vargas-Baca, *Coord. Chem. Rev*., **255**, 1426 (2011).
3. R. E. Allan, H. Gornitzka, J. Kärcher, M. A. Parver, M-A. Rennie, C. A. Russell, P. R. Raithby, D. Stalke, A. Steiner and D. S. Wright, *J. Chem. Soc., Dalton Trans*., 1727 (1996).
4. A. F. Cozzolino, I. Vargas-Baca, S. Mansour and A. H. Mahmoudkhani, *J. Am. Chem. Soc*., **40**, 4966 (2005).
5. A. F. Cozzolino, P. S. Whitfield and I. Vargas-Baca, *J. Am. Chem. Soc*., **132**, 17265 (2010).
6. D. A. Haynes and J. M. Rawson, *Eur. J. Inorg. Chem.*, **2018**, 3554 (2018).
7. R. T. Boeré and N. D. D. Hill, *CrystEngComm*, **19**, 3698 (2017).
8. H. U. Höfs, J. W. Bats, R. Gleiter, G. Hartman, R. Mews, M. Eckert-Maksić, H. Oberhammer and G. M. Sheldrick, *Chem. Ber*., **118**, 3781 (1985).
9. E. G. Awere, N. Burford, C. Mailer, J. Passmore, M. J. Schriver, P. S. White, A. J. Banister, H. Oberhammer and L. H. Sutcliffe, *J. Chem. Soc., Chem. Commun*., 66 (1987).
10. E. Jaudas-Prezel, R. Maggiulli, R. Mews, H. Oberhammer and W-D. Stohrer, *Chem. Ber*., **123**, 2117 (1990).

11. F. Blockhuys, N. P. Gritsan, A. Yu. Makarov, K. Tersago and A. V. Zibarev, *Eur. J. Inorg. Chem*., **2008**, 655 (2008).
12. (a) F. Blockhuys, S. L. Hinchley, A. Y. Makarov, Y. V. Gatilov, A. V. Zibarev, J. D. Woollins and D. W. H. Rankin, *Chem. Eur. J*., **7**, 3592 (2001); (b) A. R. Turner, F. Blockhuys, C. van Alsenoy, H. E. Robertson, S. L. Hinchley, A. V. Zibarev, A. Yu. Makarov and D. W. H. Rankin, *Eur. J. Inorg. Chem*., **2005**, 572 (2005).
13. A. W. Cordes, M. Hojo, H. Koenig, M. C. Noble, R. T. Oakley and W. T. Pennington, *Inorg. Chem*., **25**, 1137 (1986).
14. I. Yu. Bagryanskaya, E. V. Bartraschevich, D. K. Nikulov, Yu. V. Gatilov and A. V. Zibarev, *J. Struct. Chem*., **50**, 127 (2009).
15. T. Glodde, Y. V. Vishnevsky, L. Zimmermann, H-G. Stammler, B. Neumann and N. W. Mitzel, *Angew. Chem. Int. Ed*., **60**, 1519 (2021).
16. D. G. Anderson, H. E. Robertson, D. W. H. Rankin and J. D. Woollins, *J. Chem. Soc., Dalton Trans*., 859 (1989).
17. S. L. Hinchley, P. Trickey, H. E. Robertson, B. A. Smart, D. W. H. Rankin, D. Leusser, B. Walfort, D. Stalke, M. Buhl and S. J. Obrey, *J. Chem. Soc., Dalton Trans*., 4607 (2002).
18. D. Leusser, J. Henn, N. Kocher, B. Engels and D. Stalke, *J. Am. Chem. Soc*., **126**, 1781 (2004).
19. T. Chivers, R. T. Oakley, O. J. Scherer and G. Wolmerhäuser, *Inorg. Chem*., **20**, 914 (1981).
20. V. C. Ginn, P. F. Kelly and J. D. Woollins, *J. Chem. Soc., Dalton Trans*., 2129 (1992).
21. I. P. Parkin, J. D. Woollins and P. S. Belton, *J. Chem. Soc., Dalton Trans*., 511 (1990).
22. J. Passmore and M. Schriver, *Inorg. Chem*., **27**, 2751 (1988).
23. T. Chivers, D. D. McIntyre, K. J. Schmidt and H. J. Vogel, *J. Chem. Soc., Chem. Commun*., 1341 (1990).
24. T. Chivers and K. J. Schmidt, *J. Chem. Soc., Chem. Commun*., 1342 (1990).
25. R. Wedmann, A. Zahl, T. E. Shubina, M. Durr, F. W. Heinemann, B. E. C. Bugenhagen, P. Burger, I. Ivanovic-Burmazovic and M. Filipovic, *Inorg. Chem*., **54**, 9367 (2015).
26. F. Seel, R. Kuhn, G. Simon and M. Wagner, *Z. Naturforsch. B*, **40b**, 1607 (1985).
27. T. Chivers, M. Edwards, D. D. McIntyre, K. J. Schmidt and H. J. Vogel, *Mag. Reson. Chem*., **30**, 177 (1992).

28. R. Labbow, D. Michalik, F. Reiss, A. Schulz and A. Villinger, *Angew. Chem. Int. Ed*., **55**, 7680 (2016).
29. A. J. Karhu, O. J. Pakkanen, J. M. Rautiainen, R. Oilunkaniemi, T. Chivers and R. S. Laitinen, *Inorg. Chem*., **54**, 4990 (2015).
30. T. Maaninen, T. Chivers, R. S. Laitinen, G. Schatte and M. Nissinen, *Inorg. Chem*., **39**, 5341 (2000).
31. A. J. Karhu, O. J. Pakkanen, J. M. Rautiainen, R. Oilunkaniemi, T. Chivers and R. S. Laitinen, *Dalton Trans*., **45**, 6210 (2016).
32. M. Hejda, E. Lork, S. Mebs, L. Dostál and J. Beckmann, *Eur. J. Inorg. Chem*., **2017**, 3435 (2017).
33. M. Hejda, D. Duvinage, E. Lork, R. Jirásko, A. Lyčka, S. Mebs, L. Dostál and J. Beckmann, *Organometallics,* **39**, 1202 (2020).
34. (a) R. T. Boeré and T. L. Roemmele, in *Comprehensive Inorganic Chemistry II*, Eds. J. Reedijk and K. Poeppelmeier, Elsevier (2013), Vol. 1, Ch.1.14, pp. 375–411; (b) R. G. Hicks, in *Stable Radicals: Fundamental and Applied Aspects of Odd-Electron Compounds*, Ed. R. B. Hicks, John Wiley & Sons (2010), Ch. 9, pp. 317–380.
35. R. T. Boeré, H. M. Tuononen, T. Chivers and T. L. Roemmele, *J. Organomet. Chem*., **692**, 2683 (2007).
36. Y. Miura and A. Tanaka, *J. Chem. Soc., Chem. Commun*., 441 (1990).
37. Y. Miura, N. Makita and M. Kinoshita, *Bull. Chem. Soc. Jpn*., **50**, 482 (1977).
38. K. Schlosser and S. Steenken, *J. Am. Chem. Soc*., **105**, 1504 (1983).
39. R. T. Boeré, R. T. Oakley, R. W. Reed and N. P. C. Westwood, *J. Am. Chem. Soc*., **111**, 1180 (1989).
40. R. T. Boeré and T. L. Roemmele, *Phosphorus, Sulfur and Silicon*, **179**, 875 (2004).
41. R. T. Oakley, *J. Chem. Soc., Chem. Commun*., 596 (1986).
42. R. A. Meinzer, D. W. Pratt and R. J. Myers, *J. Am. Chem. Soc*., **91**, 6623 (1969).
43. T. Chivers and M. Hojo, *Inorg. Chem*., **23**, 1526 (1984).
44. R. T. Boeré, T. Chivers, T. L. Roemmele and H. M. Tuononen, *Inorg. Chem*., **48**, 7294 (2009).
45. T. L. Roemmele, J. Kony, R. T. Boeré and T. Chivers, *Inorg. Chem*., **48**, 9454 (2009).
46. R. T. Boeré, A. M. Bond, T. Chivers, S. W. Feldberg and T. L. Roemmele, *Inorg. Chem*., **46**, 5596 (2007).

47. A. V. Zibarev and R. Mews, in *Selenium and Tellurium Chemistry*: *From Small Molecules to Biomolecules and Materials*, Eds. J. D. Woollins and R. S. Laitinen, Springer (2011), Ch. 6, pp. 123–149.
48. A. Yu. Makarov, I. G. Irtegova, N. V. Vasilieva, I. Yu. Bagryanskaya, T. Bormann, Y. V. Gatilov, E. Lork, R. Mews, W-D. Stohrer and A. V. Zibarev, *Inorg. Chem*., **44**, 7194 (2005).
49. M. V. Andreocci, M. Bossa, V. Di Castro, C. Furlani, G. Maltogno and H. W. Roesky, *Z. Phys. Chem*., **118**, 137 (1979).
50. M. V. Andreocci, M. Bossa, V. Di Castro, C. Furlani, G. Maltogno and H. W. Roesky, *Gazz. Chim. Ital*., **109**, 1 (1979).
51. T. Trabelsi, O. Yazidi, J. S. Francisco, R. Linguern and M. Hichlaf, *J. Chem. Phys*., **143**, 164301 (2015).
52. J. H. Lehman and W. C. Lineberger, *J. Chem. Phys*., **147**, 013943 (2017).
53. Z. Wu, D. Li, H. Li, B. Zhu, H. Sun, J. S. Francisco and X. Zeng, *Angew. Chem. Int. Ed*., **55**, 1507 (2016).
54. R. C. Fortenberry and J. S. Francisco, *J. Chem. Phys*., **143**, 084308 (2015).
55. A. W. Cordes, C. D. Bryan, W. M. Davis, R. H. de Laat, S. H. Glarum, J. D. Goddard, R. C. Haddon, R. G. Hicks, D. K. Kennepohl, R. T. Oakley, S. R. Scott and N. P. C. Westwood, *J. Am. Chem. Soc*., **115**, 7233 (1993)
56. A. F. Cozzolino, N. E. Gruhn, D. L. Lichtenberger and I. Vargas-Baca, *Inorg. Chem*., **47**, 6220 (2008).
57. T. Chivers, A. W. Cordes, R. T. Oakley and W. T. Pennington, *Inorg. Chem*., **22**, 2429 (1983).
58. N. J. Hartmann, G. Wu and T. W. Hayton, *J. Am. Chem. Soc*., **138**, 12352 (2016).
59. T. S. Bailey, H. A. Henthorn and M. D. Pluth, *Inorg. Chem*., **55**, 12618 (2016).
60. J. P. Marcolongo, U. N. Morzan, A. Zeida, D. A. Scherlis and J. A. Olabe, *Phys. Chem. Chem. Phys*., **18**, 30047 (2016).
61. A. P. Munro and D. L. H. Williams, *J. Chem. Soc., Perkin Trans. 2*, 1794 (2000).
62. G. E. Garrett, G. L. Gibson, R. N. Strauss, D. S. Seferos and M. S. Taylor, *J. Am. Chem. Soc*., **137**, 4126 (2015).
63. P. Hassanzadeh and L. Andrews, *J. Am. Chem. Soc*., **114**, 83 (1992).
64. L. Andrews and P. Hassanzadeh, *J. Chem. Soc., Chem. Commun*., 1523 (1994).

65. R. Evans, A. J. Downs, R. Köppe and S. C. Peake, *J. Phys. Chem. A*, **115**, 5127 (2011).
66. H. M. Tuononen, R. Suontamo, J. Valkonen and R. S. Laitinen, *J. Phys. Chem. A*, **109**, 6309 (2005).
67. X. Zeng, A. F. Antognini, H. Beckers and H. Willner, *Angew. Chem. Int. Ed*., **54**, 2758 (2015).
68. Z. Wu, D. Li, H. Li, B. Zhu, H. Sun, J. S. Francisco and X. Zeng, *Angew. Chem. Int. Ed*., **55**, 1507 (2016).
69. X. Zeng, H. Beckers, H. Willner and J. S. Francisco, *Angew. Chem. Int. Ed*., **51**, 3334 (2012).
70. R. S. P. King, P. F. Kelly, S. E. Dann and R. J. Mortimer, *Chem. Commun*., 4812 (2007).
71. P. F. Kelly, R. S. P. King and R. J. Mortimer, *Chem. Commun*., 6111 (2008).
72. K. C. Nicoloau, M. Lu, S. Totokotsopoulos, P. Heretsch, D. Giguère, Y-P. Sun, D. Sarlah, T. H. Nguyen, I. C. Wolf, D. F. Smee, C. W. Day, S. Bopp and E. A. Winzeler, *J. Am. Chem. Soc*., **134,** 17320 (2012).
73. (a) B. G. Kumar and K. Muralidharan, *RSC Adv*., **4**, 28219 (2014); (b) B. G. Kumar and K. Muralidharan, *Eur. J. Inorg. Chem*., **2013**, 2102 (2013); (c) B. G. Kumar and K. Muralidharan, *J. Mater. Chem*., **21**, 11271 (2011).
74. P. C. Ho, P. Szydlowski, J. Sinclair, P. J. W. Elder, J. Kübel, C. Gendy, L. M. Lee, H. Jenkins, J. F. Britten, D. R. Morim and I. Vargas-Baca, *Nature Commun*., **7**, 11299 (2016).
75. M. R. Filipovic, J. Lj. Miljkovic, T. Nauser, M. Royzen, K. Klos, T. Shubina, W. H. Koppenol, S. J. Lippard and I. Ivanović-Burmazović, *J. Am. Chem. Soc*., **134**, 12016 (2012).
76. A. S. M. Islam, R. Bhowmick, K. Pal, A. Katarkar, K. Chaudhuri and M. Ali, *Inorg. Chem*., **56**, 4324 (2017).
77. D. Chatterjee, C. Chowdhury, A. Datta and R. van Eldik, *New. J. Chem*., **43**, 15311 (2019).
78. A. F. Cozzolino, G. Dimopoulos-Italiano, L. M. Lee and I. Vargas-Baca, *Eur. J. Inorg. Chem*., **2013**, 2751 (2013).

Chapter 4

Electronic Structures

4.1 Introduction

Interest in the electronic structures of chalcogen-nitrogen compounds was stimulated initially by the synthesis and structural determination of various binary sulfur nitrides. The unusual cage structure of S_4N_4 (**4.1**)[1] and the planar, cyclic structures of S_2N_2 (**4.2**),[2] $[S_4N_3]^+$ (**4.3**)[3] and $[S_5N_5]^+$ (**4.4**)[4] were prominent among these early findings (Chart 4.1). The discovery of the unique solid-state properties of the polymer $(SN)_x$ (**4.5**)[5] added an important incentive for the need to gain an understanding of the electronic structures of these electron-rich species. In 1972 Banister proposed that planar S–N heterocycles belong to a class of "electron-rich aromatics" which conform to the well-known Hückel $(4n + 2)\pi$-electron rule of organic chemistry.[6] This suggestion has provided a useful guideline to synthetic chemists in their search for novel binary chalcogen-nitrogen ring systems and carbon-nitrogen-chalcogen heterocycles. However, with the advancement in the sophistication of computational methods in the last 15 years it has become apparent that the electronic structures of chalcogen-nitrogen compounds with monocyclic, bicyclic or cage structures involve many subtleties that had not previously been considered.

This chapter will begin with a consideration of general principles that contribute to an understanding of the electronic structures of cyclic and acyclic chalcogen-nitrogen compounds, including carbon-poor sulfur-nitrogen heterocycles, namely (a) Hückel $(4n + 2)\pi$-electron rule,

(b) aromaticity, (c) thermodynamic and kinetic stability, (d) diradical character, and (e) electronegativities. In subsequent sections, these concepts will be applied to a discussion of the polymer $(SN)_x$ and related chain compounds followed by application of the isolobal analogy to carbon-nitrogen-chalcogen heterocycles. The final sections consider weak chalcogen-chalcogen interactions that occur in bicyclic and cage compounds (intramolecular interactions) and radical-radical dimerisation (intermolecular processes).

4.2 Hückel (4n + 2)π-electron Rule

Banister's proposal was based on the reasonable assumption that each sulfur contributes two and each nitrogen one electron to the π-system leading to the description of sulfur nitrides as "electron-rich". In the early 1970s the known species **4.2** (6π), **4.3** (10π) and **4.4** (14π) were cited as examples in support of this contention (Chart 4.1). Subsequently, several additions to this list of planar, monocyclic S–N rings were discovered by synthetic chemists, notably $[S_4N_4]^{2+}$ (**4.6**)[7] and $[S_3N_3]^-$ (**4.7**),[8] both of

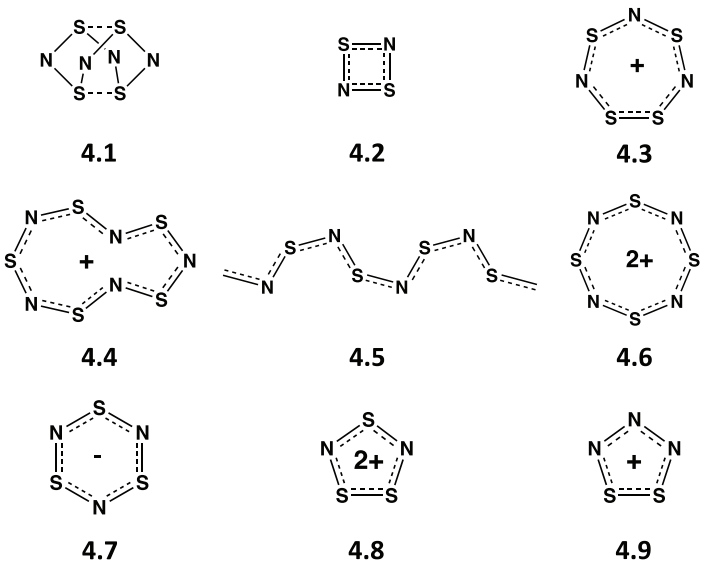

Chart 4.1. Cage, ring, and chain structures of sulfur-nitrogen species.

which are 10π-electron systems, the sulfur-rich dication $[S_3N_2]^{2+}$ (**4.8**)[9] and the nitrogen-rich cation $[S_2N_3]^+$ (**4.9**),[10,11] which are both 6π-electron systems.

4.3 Aromaticity

At first sight the numerous examples of cyclic, binary sulfur-nitrogen species **4.2**–**4.4** and **4.6**–**4.9** that conform to the Hückel (4n + 2)π-electron rule would appear to provide ample justification for the proposal that these ring systems can be regarded as "electron-rich aromatics". However, aromaticity is a more complex phenomenon than is suggested by a simple electron count. Although these planar ring systems have equal S–N bond lengths, which are intermediate between single and double bond distances, the excess electrons are accommodated in nonbonding or antibonding (π^*) orbitals. For example, S_2N_2 (**4.2**) has six π-electrons, four of which occupy a degenerate pair of π orbitals that do not contribute to the bonding; hence, this four-membered ring is essentially a 2π-electron system.[12] More dramatically, four of the electrons in the 10π-electron six-membered ring $[S_3N_3]^-$ occupy a pair of degenerate antibonding (π^*) orbitals, approximately cancelling the contribution from the occupation of the degenerate bonding (π) orbitals.[13–15]

In organic chemistry the criteria for aromaticity include physical data such as heats of formation and diamagnetic ring currents, as well as structural data (planarity and equality of bond lengths) and aromatic stabilisation energies determined either experimentally or theoretically. Modern theoretical methods aimed at understanding aromaticity in inorganic ring systems have employed the determination of ipsocentric ring currents and nuclear-independent chemical shifts (NICS). The criterion of NICS is based on the negative of the computed absolute shielding at ring centres or, preferably, 1 Å above the centre.[12] Negative NICS values of significant magnitude suggest aromaticity, while positive values are indicative of antiaromaticity.

As an example of the application of the criterion of ipsocentric ring currents, the calculated current density maps for the 10π-electron systems $[S_4N_3]^+$ (**4.3**), $[S_4N_4]^{2+}$ (**4.6**) and $[S_3N_3]^-$ (**4.7**), and the 14π-electron system

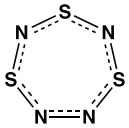

4.10

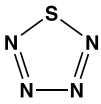

4.11

Chart 4.2. The nitrogen-rich S_3N_4 (10π-electron system) and SN_4 (6π-electron system).

$[S_5N_5]^+$ (**4.4**) were found to support diatropic π currents, reinforced by σ circulations.[14] The binary ring S_3N_4 (**4.10**; Chart 4.2), a 10π-electron system, was also predicted to be aromatic based on this criterion, but this nitrogen-rich binary sulfur nitride is kinetically unstable and has not been isolated (Secs. 4.4 and 5.7.3).

This criterion has also been applied to carbon-poor sulfur-nitrogen heterocycles (heterocyclothiazenes), including the seven-membered rings $S_3N_2(CH)_2$ and $S_3N_3(CH)$ and the eight-membered rings $S_2N_4(CH)_2$ and $S_2N_2(CH)_4$, all of which are 10π-electron systems.[16] The ipsocentric calculations show that these heterocycles support diatropic ring currents and are aromatic on the basis of magnetic criteria. Furthermore, the 24-membered 30π-electron heterocycle $S_6N_{12}(CH)_6$ was found to be aromatic based on this criterion. This macrocycle was predicted by Woodward more than 40 years ago, but it has not been prepared.[17]

Computations of $NICS(0)_{\pi zz}$ values have been used to evaluate the aromaticity of a variety of known and putative sulfur-nitrogen systems. $NICS(0)_{\pi zz}$ values are the most refined NICS index; they are the out-of-plane tensor component of the isotropic NICS(0), but include only the π-orbital component. The $NICS(0)_{\pi zz}$ values of the 6π-electron systems, 1,2- and 1,3-$[S_2N_3]^+$, are −30.6 and −30.5 ppm, respectively, comparable with the value of −35.3 ppm found for the isoelectronic cyclopentadienide anion $[C_5H_5]^-$.[18] However, the 1,2-isomer is kinetically more stable than the 1,3-counterpart (Sec. 4.4). For comparison, the aromaticity of the known dication 1,3-$[S_3N_2]^{2+}$ (**4.8**) is slightly lower based on the $NICS(0)_{\pi zz}$ value of −27.9 ppm.

Calculated $NICS(0)_{\pi zz}$ values have also been used to assess the aromaticity of neutral, nitrogen-rich sulfur nitrides. The value of −33.0 ppm for *cyclo*-SN_4 (**4.11**; Chart 4.2), a 6π-electron system, indicates a high level of aromaticity, but this five-membered ring is kinetically unstable

(Sec. 4.4). Two isomers of the putative six-membered ring S_2N_4 (an 8π-electron antiaromatic system) comprised of a five-membered SN_4 ring with an exocyclic sulfur atom are possible.[18,19] However, their $NICS(0)_{\pi zz}$ values of −10.5 and −13.0 ppm are substantially lower than that of *cyclo*-SN_4.[18]

4.4 Thermodynamic Stability and Kinetic Inertness

In order to understand the "stability" of binary chalcogen-nitrogen systems it is essential to consider both their thermochemical stability and kinetic inertness.[18,19] Although all binary sulfur nitrides are thermodynamically unstable with respect to decomposition to the elements, the ability to isolate a particular species is determined by the value of the activation energy towards dissociation. This caveat is illustrated in the following examples.

The isolation of salts of the $[S_2N_3]^+$ cation as the 1,2-isomer (**4.9**) rather than the thermodynamically more stable 1,3-isomer provides a compelling example of the importance of kinetic inertness.[18] The dissociation of the 1,2-isomer into N_2 and $[NSS]^+$ fragments is only slightly exergonic and has a relatively high barrier (65.3 kJ mol^{-1}), whereas the dissociation of the 1,3-isomer to form N_2 + $[SNS]^+$ is highly exergonic, and the activation energy is only 10.9 kJ mol^{-1} (Fig. 4.1). Hence, the 1,2-isomer is more inert (kinetically more persistent) than its 1,3-counterpart.

Both 1,2- and 1,3-isomers are possible for the dication $[S_3N_2]^{2+}$. The 1,3-isomer (**4.8**) is calculated to be lower in energy than the 1,2-isomer by 67.8 kJ mol^{-1} and salts of **4.8** are obtained from the cycloaddition of $[SN]^+$ and $[SNS]^+$ cations in SO_2.[9,21] The calculated barrier to dissociation of **4.8** into the precursor cations in the gas phase is quite low (< 46 kJ mol^{-1}) and this process is exergonic by 419.7 kJ mol^{-1}.[18,21] However, the dissociation barrier of the 1,2-isomer into $[SS]^{2+}$ and SNN is even lower (6.3 kJ mol^{-1}). Thus, the 1,3-isomer is not only thermodynamically more stable, but it is more persistent kinetically. The isolation of salts of **4.8**, despite the low barrier to dissociation, is attributed to lattice-stabilisation effects.[9] By contrast, the selenium analogue $[Se_3N_2]^{2+}$ does not dissociate into $[SeN]^+$ and $[SeNSe]^+$, but the latter two cations are unknown for selenium.[22]

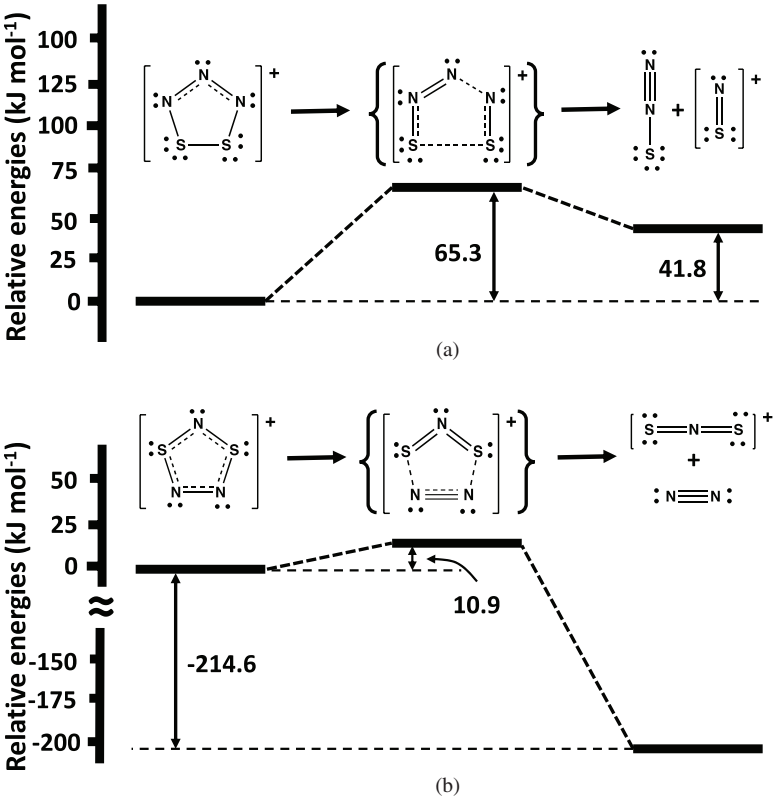

Figure 4.1. Lowest energy dissociation routes for (a) 1,2-$[S_2N_3]^+$ and (b) 1,3-$[S_2N_3]^+$.[18]

Nitrogen-rich binary sulfur nitrides are of interest as high energy-density materials. However, these neutral molecules are thermodynamically unstable and have low barriers to dissociation. Furthermore, unlike chalcogen-nitrogen cations, they cannot be stabilised by lattice effects. For example, *cyclo*-SN_4 (**4.11**) is *ca.* 400 kJ mol^{-1} higher in energy than the decomposition products $1/8S_8 + 2N_2$ and the barrier to dissociation into $N_2 + N_2S$ is very low (29.3 kJ mol^{-1}).[20,23] Similarly, the barrier to dissociation of S_3N_4 (**4.10**) into SNN + S_2N_2 is only 59.0 kJ mol^{-1}.[12] In contrast to these nitrogen-rich systems, *cyclo*-S_2N_2 (**4.2**) has a relatively high dissociation barrier (> 200 kJ mol^{-1}), despite the strain in the four-membered ring.[20]

4.5 Diradical Character

Notwithstanding its long history,[2] the electronic structures of S_2N_2 (**4.2**) and its heavier chalcogen analogues continue to generate controversy regarding their diradical character.[24,25] This four-membered ring is aromatic based on its π CMO-NICS (CMO = canonical molecular orbital) value of –26.2 ppm, but it has a small aromatic stabilisation energy, since only two of the six π electrons contribute to the bonding. On the basis of DFT calculations it was concluded that the diradical character of **4.2** is insignificant on the basis of a large HOMO-LUMO gap (5.1 eV), a large singlet-triplet vertical transition energy (3.6 eV), and the lack of a spin-unrestricted solution.[12] Concurrently, a variety of computational methods were used to investigate the electronic structures of E_2N_2 (E = S, Se, Te) and $SSeN_2$. The authors agreed that these four-membered rings can be described as 2π-electron aromatics, but they found diradical character located solely on the two nitrogen atoms that increased down the series $S_2N_2 < Se_2N_2 < Te_2N_2$.[24,25] The 2$\pi$-electron aromatic Lewis structures and their singlet diradical representations for S_2N_2 are depicted in Fig. 4.2.

CASSCF (Complete Active Space Self-Consistent Field Calculations) estimated that S_2N_2 shows 6% diradical character, while that of Te_2N_2 is 10%.[24b] When the [22,16]-CAS/cc-pVPZ wave function of S_2N_2 was analysed in terms of Lewis-type valence bond structures (Fig. 4.2) using idealised p_z orbitals, it was observed that the diradical representation with

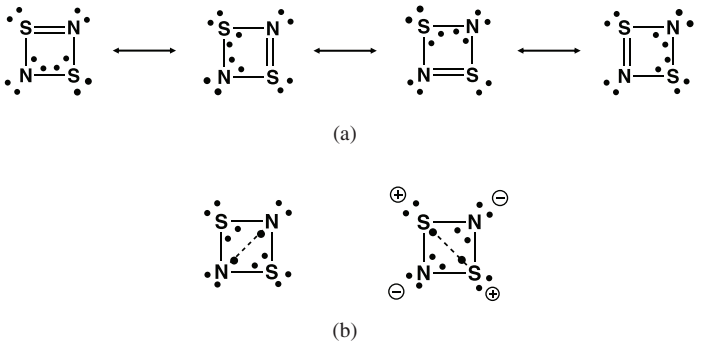

Figure 4.2. (a) 2π-electron aromatic Lewis structure representation and (b) diradicaloid Lewis structures of S_2N_2.

unpaired electrons located at nitrogen atoms has the weight of 34%.[24a] This is in reasonable agreement with the estimates of 40–54% from valence-bond (VB) theory.[25b,c] It should be noted, however, that the relative importance of the different VB structures seems to be dependent on the level of theory (see ref. 25a and references therein).

Calculations of vertical resonance energies for S_2N_2 gave values about 80% of that predicted for benzene and somewhat lower values for E_2N_2 (E = Se, Te), consistent with the notion of aromatic character for S_2N_2. On this basis, it was concluded that diradical character and aromaticity are not mutually exclusive.[25b]

Recently, the bonding and aromaticity in the ground, first triplet excited and lowest triplet electronic states of S_2N_2 were investigated. The results indicated that (a) the S_0 electronic state is aromatic, but rather less so than the electronic ground state of benzene, (b) S_1 is strongly antiaromatic, and T_1 is moderately antiaromatic to a similar extent to that observed in the electronic ground state of square cyclobutadiene.[26] Thus, S_2N_2 is the first example of an inorganic ring for which theory predicts substantial changes in aromaticity upon vertical transition from the ground state to the first singlet or lowest triplet electronic states.

The strength of the intramolecular S···S interactions in S_4N_4 (**4.1**) (d(S–S) = 2.60 Å) has been estimated to be of the order of a hydrogen bond on the basis of the noncovalent bond index.[27] High-level theoretical methods indicated that the elongation of the E···E interaction in E_4N_4 (E = S, Se) compared to a typical single-bond value can be attributed to large correlation effects. Furthermore, there is some singlet diradical character associated with each E···E interaction.[28]

A different aspect of the bonding in **4.1** was revealed by applying QTAIM (quantum theory of atoms in molecules) methodology to all 18 modes of vibration of the cage molecule.[29] A considerable degree of metallicity was found in the S–S and S–N bonds on the basis of delocalisation of the electron density away from the atoms. Notably, considerable metallic behaviour was apparent in the S–S bond critical points for all modes.

4.6 Electronegativity Effects

A fundamental difference between the bonding in unsaturated S–N compounds and organic analogues can be understood from a comparison of

π-systems of the radical $[HSNH]^{\bullet}$ and the ethylene molecule $H_2C{=}CH_2$ (Fig. 4.3). To a first approximation the σ-framework of both molecules can be described in terms of sp^2 hybridisation of the non-hydrogen atoms. In $[HSNH]^{\bullet}$ only two of the sp^2 hybrid orbitals (and two valence electrons) are involved in bonding to neighbouring atoms, while a nonbonding pair of electrons occupies the third sp^2 hybrid orbital. Thus, the sulfur atom has two electrons in a 3*p* orbital and nitrogen has one electron in a 2*p* orbital to contribute to the π system in unsaturated S–N compounds with two-coordinate sulfur. The extra π-electron in $[HSNH]^{\bullet}$ occupies an antibonding level. Consequently, the S=N π-bond is predictably substantially weaker than a C=C π-bond.

In addition, the influence of the electronegativity of the atoms has a two-fold effect on the bonding in sulfur-nitrogen compounds. First, the energies of the π-orbitals in $[HSNH]^{\bullet}$ are lower than those in ethylene as a result of the higher atom electronegativities of sulfur (2.58) and particularly nitrogen (3.04), compared to that of carbon (2.55) (Fig. 4.3). This is especially important for cyclic systems, *e.g.*, $[S_3N_3]^{-}$ (**4.7**), since the lower energies of the molecular orbitals (MOs) compared to those for aromatic analogues are crucial for the stabilisation of π-electron rich rings.[15] Secondly, the disparate electronegativities of S and N result in a π-bonding orbital in $[HSNH]^{\bullet}$ that is polarised towards the nitrogen atom, while the singly occupied π^* orbital has more electron density on sulfur than on nitrogen. In electron-rich sulfur-nitrogen rings, *e.g.*, **4.7**, this results in non-uniform electron distribution in the π MOs due to polarisation

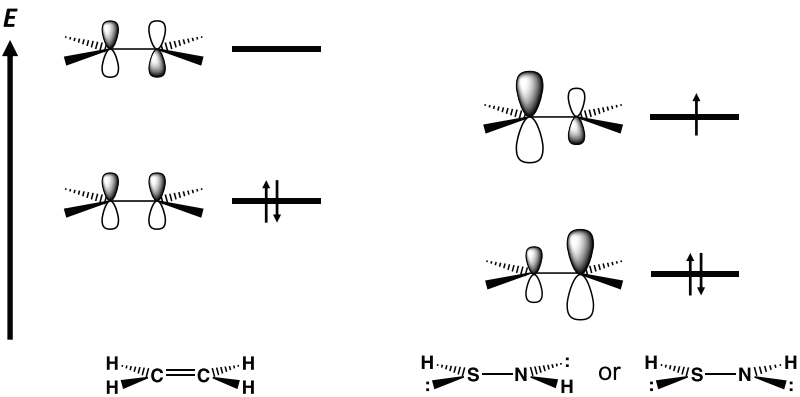

Figure 4.3. Qualitative comparison of the π-orbitals of $H_2C{=}CH_2$ and $[HNSH]^{\bullet}$.

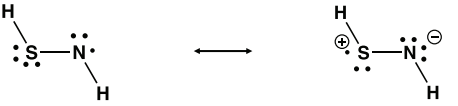

Scheme 4.1. Covalent and ionic resonance structures of the radical [HNSH]$^{\bullet}$.

towards the more electronegative N atoms, which is offset by the presence of electrons in the π^* orbitals.

The [HSNH]$^{\bullet}$ radical can also be represented by two valence bond structures in which both the S and N atoms are divalent (Scheme 4.1). Consequently, in one of these representations the nitrogen atom accommodates the unpaired electron. Since nitrogen has a higher electronegativity than sulfur, a second resonance form depicts a formal oxidation of the S atom by the N atom. High-level quantum chemical calculations [B3LYP and CCSD(T)] for the three possible modes of dimerisation of [HSNH]$^{\bullet}$ reveal that the N–N bonded dimer is more stable than the S–S bond dimer by 173.2 kJ mol^{-1}.[30] However, electronic and steric factors can bring about a reversal of this order of stability, as observed in the cage structure of S_4N_4.

The electronegativity difference between S and N has a major influence on the nature of the S–N bond in acyclic sulfur-nitrogen compounds as revealed by an experimental and theoretical charge density study of the sulfur(IV) diimide $S(N^tBu)_2$ and sulfur(VI) triimide $S(N^tBu)_3$.[31] The S–N framework in both of these molecules is planar and exhibits sulfur-nitrogen bond lengths indicative of S=N double bonds. The natural bond orbital/natural resonance theory analysis (NBO/NRT) reveals sp^2 hybridisation for all S and N atoms with a 3-centre-4-electron π-system for $S(N^tBu)_2$ and a 4-centre-6-electron π-system for $S(N^tBu)_3$. However, the π-orbitals are polarised resulting in a substantial ionic contribution to the S–N bonds, as can be seen from the details depicted in Fig. 4.4.[31]

4.7 Bonding in the Polymer $(SN)_x$ and in Sulfur-Nitrogen Chains

The polymer $(SN)_x$ has remarkable properties for a material that is composed of two non-metallic elements.[5] It has a metallic lustre and

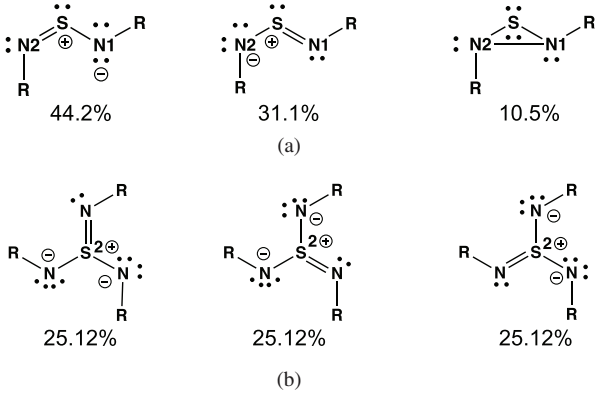

Figure 4.4. (a) NBO/NRT analysis of $S(NR)_2$ (R = ^{t}Bu). Formal atomic charges: S +1.11 e, N1 –0.71 e, N2 –0.77 e. Bond orders: (S–N1) 1.49 (covalent 1.04, ionic 0.45), (S–N2) 1.33 (covalent 0.98, ionic 0.35); (b) NBO/NRT analysis of $S(NR)_3$ (R = ^{t}Bu). Formal atomic charges: S +1.90 e, N –0.63 e. Bond orders: (S–N) 1.33 (covalent 0.97, ionic 0.35).[31a]

behaves as a highly anisotropic conductor at room temperature. The conductivity along the polymer chains is of a similar order of magnitude to that of mercury metal and about 50 times greater than that perpendicular to the chain. The conductivity increases by three orders of magnitude on cooling to 4 K and $(SN)_x$ becomes a superconductor at 0.3 K. The polymer $(SN)_x$ is usually prepared from *cyclo*-S_2N_2 and the topochemical polymerisation process is initiated by cleavage of an S–N bond (Sec. 5.4.2).[32] The metallic behaviour can be understood from the molecular description of the π-bonding in the approximately planar *cis,trans* polymer, which is comprised of an infinite number of acyclic S_2N_2 units, each with two electrons in a π^* orbital (Fig. 4.5). The juxtaposition of these units gives rise to a completely filled valence band and a half-filled conducting band. The electrons in the partially filled band in $(SN)_x$ are free to move under the influence of an applied potential difference and thus conduction occurs along the polymer chain. The S–N distances in the chain are essentially equal, consistent with a delocalised structure. The increase in conductivity with decreasing temperature is characteristic of a metallic conductor. The predicted Peierls distortion is apparently inhibited by weak interactions between the polymer chains (S···S = 3.47–3.70 Å; S···N = 3.26–3.38 Å).[5]

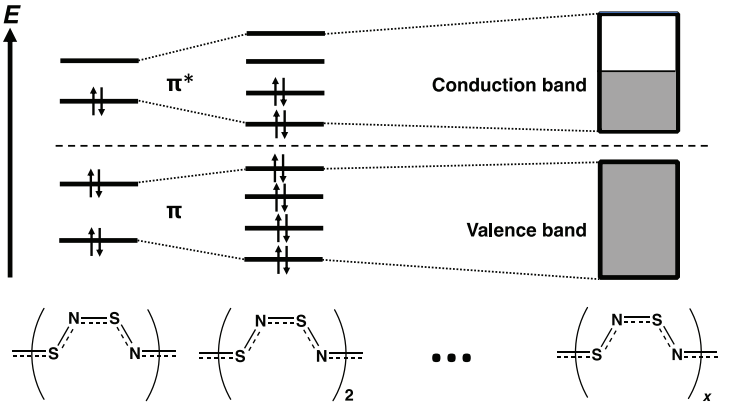

Figure 4.5. Molecular orbital description of the bonding in acyclic S_2N_2 and $(SN)_x$.

Materials that are comprised of small fragments of $(SN)_x$ with organic terminal groups, *e.g.*, ArS_3N_2Ar and ArS_5N_4Ar (Ar = aryl), are of potential interest as molecular wires in the development of nanoscale technology (Sec. 1.4.2).[33] The colours of these compounds are dependent on chain length. The shorter chains are bright yellow or orange (λ_{max} 330–475 nm), whereas the longer chains (more than six heteroatoms) produce deep green, blue or purple solutions (λ_{max} 520–590 nm) and exhibit a metallic lustre in the solid state. This trend can be rationalised by the decrease in the energy gaps between π-orbitals as the chain length (number of SN units) increases. Thus, the five-atom ArS_3N_2Ar chain is yellow or orange whereas the longer ArS_5N_4Ar chain exhibits a deep green, royal blue or purple colour.

4.8 Bonding in Heterocyclothiazenes

4.8.1 *Isolobal analogy*

There is an extensive series of carbon-poor sulfur-nitrogen heterocycles in which an RC group replaces one or more sulfur atoms in an S–N ring (Sec. 1.4.3). Similar to S^+, the three-coordinate carbon in these heterocycles contributes one electron to the π-system. Consequently, there can be an isoelectronic relationship between certain binary S,N cations and C,N,S

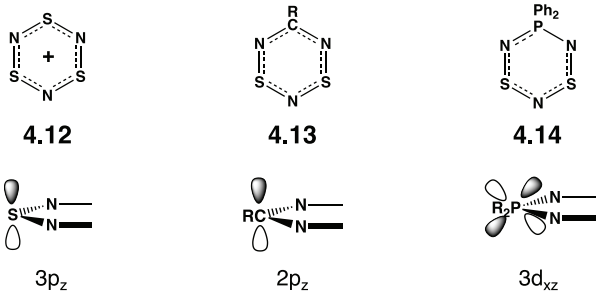

Figure 4.6. The isolobal groups S^+, CR and PR_2.

heterocycles, *e.g.*, $[S_3N_3]^+$ (**4.12**) and $PhCN_3S_2$ (**4.13**). The six-membered ring $PhCN_3S_2$ (**4.13**)[34] and the related phosphorus(V)-containing ring $Ph_2PN_3S_2$ (**4.14**)[35] have been structurally characterised in the solid state, but the cation $[S_3N_3]^+$ (**4.12**) has only been isolated as an adduct with norbornadiene.[36] As illustrated in Fig. 4.6, the groups S^+, CR and PR_2 can be considered as isolobal; each of them contributes one electron to the π-system in an orbital that has similar symmetry properties, but with different energies. In S^+ this electron occupies the $3p_z$ orbital, whereas for the three-coordinate carbon in a CR group it inhabits the $2p_z$ orbital and for the four-coordinate phosphorus in a PR_2 group it inhabits a $3d_{xz}$ orbital. Thus, the heterocycles **4.12**–**4.14** are all 8π-electron "antiaromatic" systems.

In $[S_3N_3]^+$ (**4.12**) with a planar (D_{3h}) structure the π^* orbitals are degenerate and singly occupied.[15] However, the formal replacement of S^+ in **4.12** by a less electronegative E group (E = CR or PR_2) lowers the symmetry of the ring to C_{2v} (if the ring retains planarity) and the degeneracy in the π^* levels (e'') is lifted. The two e″ orbitals transform as b_1 and a_2 representations and the b_1 MO energy is raised relative to a_2, which is nodal at the heteroatom site (Fig. 4.7).[37] With the large perturbation induced by the PR_2 group the b_1-a_2 splitting is sufficient to favour a singlet ground state and monomeric $Ph_2PN_3S_2$ (**4.14**) can be isolated in the solid state (*vide supra*). In the case of an S^+/CR replacement the energy difference between the triplet and singlet states is less pronounced and depends on the nature of the substituent R. Consequently, 1,3-dithia-2,4,6-triazines of the type **4.13** form dimers with weak S···S intermolecular interactions in the solid state (Sec. 4.10).

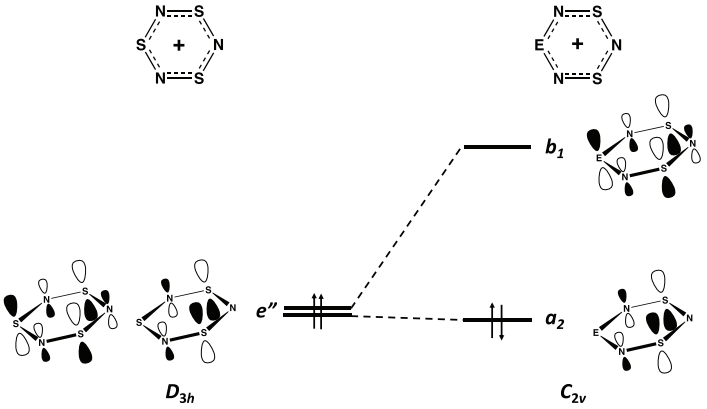

Figure 4.7. Splitting of the degenerate *e″* orbitals of $[S_3N_3]^+$ by incorporation of a less electronegative atom E.

4.8.2 *Cycloaddition reactions*

All three of the 8π-electron heterocycles **4.12–4.14** undergo an *S*,*S´* mode of addition with norbornadiene.[34–36] This regiochemistry is readily explained from frontier orbital considerations. For example, both the HOMO and LUMO of **4.13** are sulfur-based and of the correct symmetry to overlap with the LUMO and HOMO, respectively, of an alkene (Fig. 4.7). Energy considerations indicate that the HOMO (olefin)-LUMO (S–N heterocycle) controls the kinetics of these reactions. The formation of these norbornadiene adducts occurs rapidly and is of practical value in characterising and storing unstable derivatives of **4.14** (R = Me, F, CF_3), since the free heterocycle can be regenerated by mild heating of the adduct.[38] Monomeric 1,3-dithia-2,4,6-triazines **4.13** can also be trapped as norbornadiene adducts.[34,39]

4.9 Weak Chalcogen-Chalcogen Interactions

A characteristic feature of larger chalcogen-nitrogen rings is the formation of folded structures with weak transannular E···E interactions. For sulfur systems the S···S distances are typically in the range 2.50–2.60 Å, about 0.5 Å longer than the S–S bonds in *cyclo*-S_8. The classic example of this

phenomenon is the cage structure of S_4N_4 (**4.1**);[1] the selenium analogue Se_4N_4 has a similar structure.[40] Although the details of the electronic structure of the bonding in **4.1** are still a matter of debate (Sec. 4.5),[28] a simple and useful way of rationalising the molecular structure has been developed recently.[41,42] This protocol is based on counting the valence electrons, as will be illustrated in the following sections for S_4N_4 and related 10π-electron eight-membered rings.

4.9.1 *Tetrasulfur tetranitride*

An early explanation of the structure of S_4N_4[43–45] has been refined in recent years and extended to related bicyclic systems (Sec. 4.9.2).[41,42] The starting point is a planar S_4N_4 molecule with D_{4h} symmetry (Fig. 4.8). The 44 valence electrons in this hypothetical molecule are comprised of σ electrons in eight S–N σ bonds (16 electrons), eight nonbonding ("lone") pairs (16 electrons), and 12 π-electrons. As depicted in Fig. 4.8, this molecule would possess a triplet ground state and hence be susceptible to Jahn-Teller distortion. The distortion of the planar molecule into a D_{2d} structure inverts the ordering of the $2a_{2u}$ LUMO and $2e_g$ HOMOs thereby affording a singlet ground state and, at the same time, allowing the development of a transannular σ bond between two sulfur 3*p* orbitals.[42] The removal of two electrons from planar S_4N_4 by oxidation would give the known dication $[S_4N_4]^{2+}$ (**4.6**), a planar 10π-electron system in which only one antibonding MO ($1b_{1u}$) and four bonding MOs are occupied in the π-manifold.

4.9.2 *Eight-membered phosphorus(III)- and phosphorus(V)-nitrogen-sulfur rings*

The replacement of two antipodal sulfur atoms by phosphorus atoms in the hypothetical planar S_4N_4 molecule generates 1,5-$P_2N_4S_2$ isoelectronic with $[S_4N_4]^{2+}$. This ternary S,N,P molecule would incorporate an unpaired 3*p* electron at each P centre (**4.15**).[41] The diradical species **4.15** would be stabilised by addition of two radicals $R^{\bullet}$ at the phosphorus centres to give

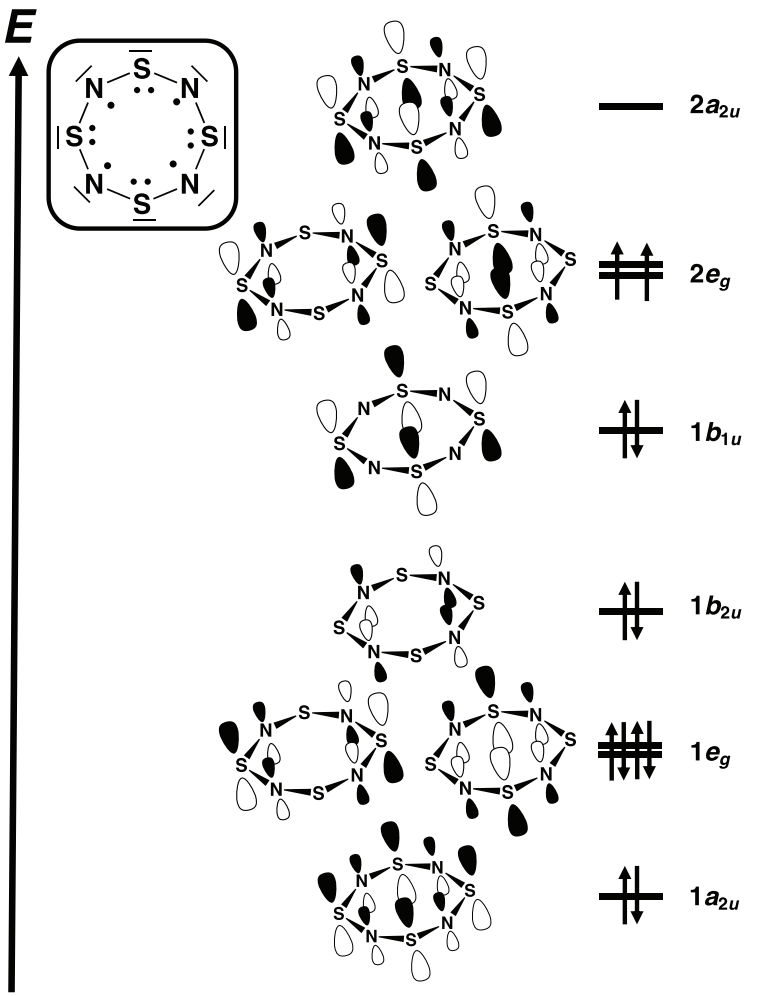

Figure 4.8. Qualitative MO diagram for planar S_4N_4 (D_{4h}).[42]

$RP^{III}(N{=}S{=}N)_2P^{III}R$ (**4.16**) (Scheme 4.2). A comparison of the aromatic character of putative **4.15** with that of the isoelectronic 10π-electron dithiatetrazocine 1,5-$(HC)_2N_4S_2$ using density functional methods revealed that the replacement of two CH groups by the more electronegative P atoms decreases the aromatic character.[46,47] Although **4.16** is not known as a free ligand, metal complexes in which the eight-membered $P_2N_4S_2$ ring is almost planar have been structurally characterised.[48]

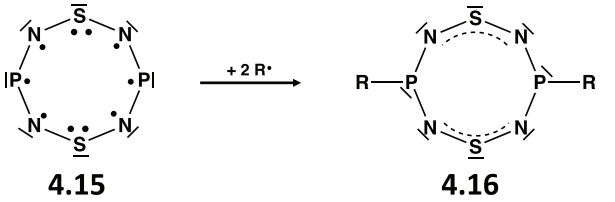

4.15 **4.16**

Scheme 4.2. Stabilisation of $P_2N_4S_2$ by reaction with two $R^{\bullet}$ radicals to give $RP^{III}(N{=}S{=}N)_2P^{III}R$.

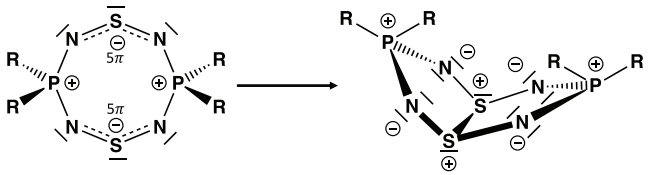

4.17 **4.18**

Scheme 4.3. Distribution of valence π-electrons in planar 1,5-$(R_2P)_2N_4S_2$ (**4.17**) and the folded structure **4.18**.

In contrast to the P^{III}-containing heterocycle **4.16**, the corresponding P^V ring systems $R_2P^V(NSN)_2P^VR_2$ (R = Me, Ph) (**4.18**) are well-known.[49,50] They adopt folded structures with only one transannular S···S interaction of about 2.5 Å. These eight-membered rings are formally derived from S_4N_4 by replacement of two S atoms by R_2P groups in the 1,5-positions. This process results in the redistribution of valence electrons depicted in Scheme 4.3 to give a diradical that incorporates two 5π-electron NSN units (**4.17**), which can be stabilised by ring folding and the formation of a transannular σ bond between two sulfur 3*p* orbitals to give **4.18**.[41]

The transannular S···S interaction in **4.18** has also been described as an inorganic example of *bis*homoaromaticity in which 6-centre-10-electron molecules result from the through-space interaction (homoconjugation) of two 3-centre-5-electron π bonds of the $[NSN]^-$ subunits.[50,51] Figure 4.9 shows the three valence-bond structures that contribute to this interaction. The tetrachlorinated derivative 1,5-$(Cl_2P)_2N_4S_2$ has been prepared, but not structurally characterised; the folded structure is inferred on the basis of the low-field ^{31}P NMR chemical shift characteristic of a structure with a cross-ring S···S interaction.[52,53] Alternatively, it has been suggested that 1,5-$(R_2P)_2N_4S_2$ (**4.18**) should be considered as a

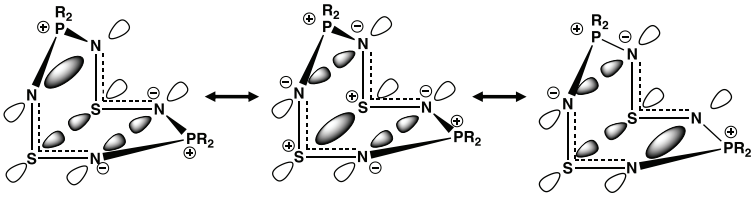

Figure 4.9. Three valence-bond structures for 1,5-$(R_2P)_2S_2N_4$ (R = Me, Ph, Cl).

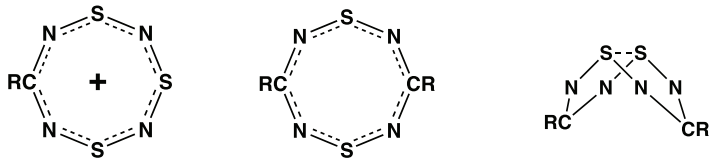

4.19a R = Ph
4.19b R = CF_3
4.19c R = NMe_2

4.20a R = Ph

4.20b R = NMe_2

Chart 4.3. Planar $[RCN_4S_3]^+$ (**4.19**); planar (**4.20a**) and folded (**4.20b**) 1,5-$(RC)_2N_4S_4$.

*tris*homoaroamatic system.[54] On the basis of a fragment-based energy analysis, it has been estimated that the transannular S···S bonding interaction in **4.18** is about half as strong as a typical S–S bond.[55]

4.9.3 *Eight-membered carbon-nitrogen-sulfur rings*

The replacement of an S^+ unit in $[S_4N_4]^{2+}$ by either one or two RC groups generates either the trithiatetrazocine cation $[RCN_4S_3]^+$ (**4.19**) or dithiatetrazocines 1,5-$(RC)_2N_4S_2$ (**4.20**), respectively (Chart 4.3). The cation with either an electron-withdrawing group (**4.19a**, R = Ph; **4.19b**, CF_3) or electron-donating group (**4.19c**, R = NMe_2) can be isolated as hexafluoroarsenate salts.[56] In all cases the eight-membered ring exhibits a planar structure, as expected for a 10π-electron system. However, the NICS values of −17.2 for **4.19b** and −10.4 for **4.19c** indicate reduced aromaticity for the derivative with an electron-donating group. In contrast to the cation **4.19**, the chloro derivative 1,5-$Me_2NC(NSN)_2SCl$ has a folded structure with a transannular S···S distance of 2.43 Å.[57]

The structures of the neutral molecules 1,5-$(RC)_2N_4S_2$ (**4.20**), isoelectronic with **4.19**, are markedly dependent on the nature of the exocyclic substituent R.[58] The $C_2N_4S_2$ ring in the phenyl derivative adopts a planar, delocalised structure (**4.20a**), whereas the dimethylamino substituents give rise to a folded structure (**4.20b**) similar to that observed for the phosphorus-containing systems **4.18**. The parent dithiatetrazocine 1,5-$(HC)_2N_4S_2$ also exhibits a planar structure, consistent with a 10π-electron system, and the aromaticity is corroborated by the low-frequency ^{1}H NMR chemical shift of 9.70 ppm, *cf.* 7.36 ppm for benzene in $CDCl_3$.[47]

The disparity between the structures of **4.20a** and **4.20b** can be explained by the destabilising influence of the π-donor Me_2N substituents on the HOMO of the $C_2N_4S_2$ ring and subsequent second-order Jahn-Teller distortion. This orbital is primarily antibonding with respect to the two NSN units in these eight-membered rings. Ring folding results in an intramolecular π^*-π^* interaction, which is bonding with respect to the sulfur atoms on opposite sides of the ring (Fig. 4.10a). In an alternative

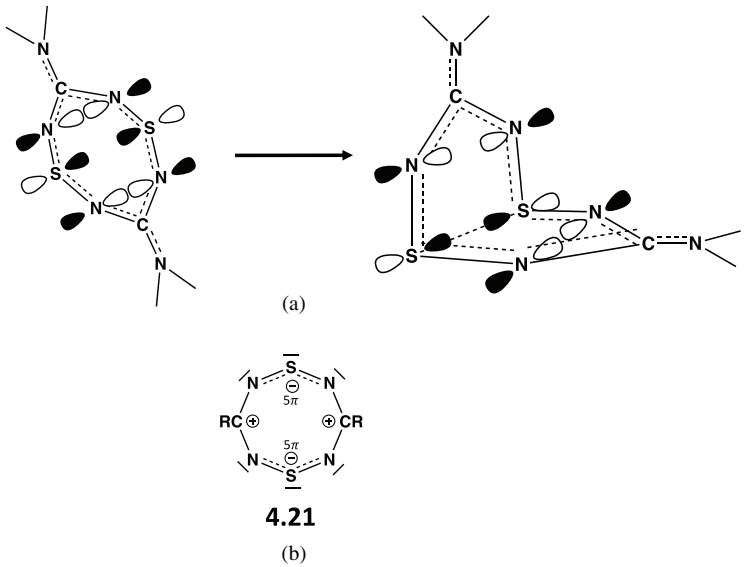

Figure 4.10. (a) The folding of the 1,5-$(Me_2NC)_2N_4S_2$ (**4.20b**) ring due to π^*-π^* interactions and (b) distribution of valence π-electrons in planar 1,5-$(RC)_2N_4S_2$ (R = NMe_2) (**4.21**).

description, the replacement of two S^+ units in $[S_4N_4]^{2+}$ by two RC groups results in the redistribution of valence electrons to give an eight-membered ring that incorporates two 5π-electron NSN units (Fig. 4.10b **4.21**, *cf.* **4.17**).[41] This diradical can be stabilised by ring folding and the formation of a transannular σ bond between two sulfur 3*p* orbitals to give **4.20b**.

4.10 Radical Dimerisation: Pancake Bonding

Weak interactions in which chalcogen-chalcogen distances in chalcogen-nitrogen ring systems are much shorter than the sum of the van der Waals radii may occur between molecules (intermolecular association) as well as within a molecule (intramolecular). The former behaviour is especially significant for odd-electron species, *e.g.*, the radical cations $[E_3N_2]^{\bullet+}$ (**4.22**, E = S, Se) and the neutral radicals 1,2,3,5-$[PhCN_2E_2]^{\bullet}$ (**4.23**, E = S, Se), both of which are 7π-electron molecules (Chart 4.4).

Salts of the binary sulfur nitride radical cation $[S_3N_2]^{\bullet+}$ (**4.22**, E = S) exhibit intermolecular association involving two S···S interactions (d(S···S) ~2.90 Å) as illustrated in Chart 4.5.[59] The resulting dimer adopts a transoid configuration. A similar structure (d(Se···Se) ~ 3.14 Å) is found for the selenium analogue $[Se_6N_4]^{2+}$ (**4.22**, E = Se).[60]

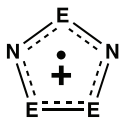

4.22

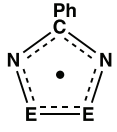

4.23

Chart 4.4. The 7π-electron species $[E_3N_2]^{\bullet+}$ and $[PhCN_2E_2]^{\bullet}$ (E = S, Se).

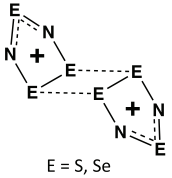

4.22

Chart 4.5. Structure of $[E_6N_4]^{2+}$ (E = S, Se) cation in ion-separated salts.

The formal replacement of an S^+ unit in **4.22** by an RC group generates the isoelectronic 1,2-dithia-3,5-diazolyl $[RCN_2E_2]^\bullet$ (**4.23,** E = S). These neutral radicals represent very important building blocks for the construction of solid-state materials with novel conducting or magnetic properties (Sec. 13.4).[61,62] The SOMO of **4.23** has a similar composition to that of **4.22**, but the substituent attached to carbon influences the dimerisation mode (Fig. 4.11).[63,64] With a flat substituent, *e.g.*, R = aryl, association occurs in a *cis*-cofacial manner with two weak S···S interactions (Fig. 4.11a). In the case of non-planar substituents, *e.g.*, R = CF_3 or Me_2N, the monomer units are held together through one S···S interaction (~3.1 Å) and the rings are in a *twisted* cofacial arrangement, *i.e.*, ~ 90° to one another (Fig. 4.11b).[65] Interestingly, the dimer of the R = 3-$CF_3C_6H_4$ derivative exhibits both of these cofacial motifs within a single crystal structure.[66] A third type of cofacial interaction in which the rings are rotated by ~180° with respect to one another (*trans*-cofacial) is also known for R = 4-IC_6H_4 (Fig. 4.11c).[67] A change in the *para*-substituent to cyano (R = 4-CNC_6H_4) generates a *trans*-antarafacial arrangement in which monomer-monomer interactions only occur through the sulfur atoms

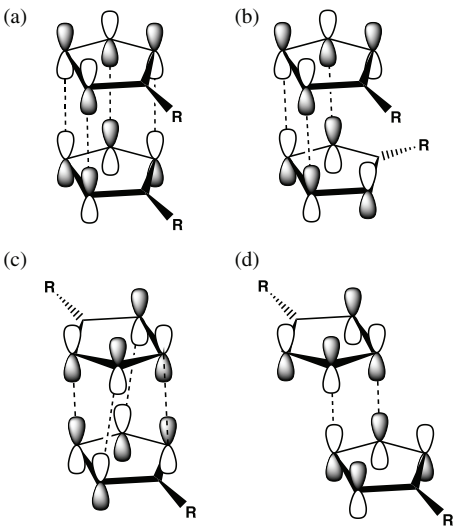

Figure 4.11. Dimerisation motifs of 1,2-dithia-3,5-diazolyl radicals $[RCN_2S_2]^\bullet$ (**4.23**): (a) *cis*-cofacial (b) *twisted* cofacial (c) *trans*-cofacial and (d) *trans*-antarafacial.

(Fig. 4.11d).[68] A fifth, rare orthogonal arrangement is not shown in Fig. 4.11, but is depicted with the other dimeric arrngements in Chart 13.7.[69] The variety of physical properties emanating from the different packing arrangements in these dimers is discussed in Sec. 13.4.4.[62]

The idea of diffuse π^*-π^* overlap was introduced in early work to explain the dimerisation of 1,2-dithia-3,5-diazolyl radicals $[RCN_2S_2]^{\bullet}$, as illustrated for the SOMO-SOMO interaction for a *cis*-cofacial derivative in Fig. 4.12.[70] More recently, the concept of pancake bonding, which was originally invoked to describe 2-electron/multi-centred (2e/mc) bonding in organic systems, has been used to explain the different conformational preferences observed for the prototypical 1,2-dithia-3,5-diazolyl dimer $[HCN_2S_2]_2$ (Fig. 4.11).[71] As illustrated in Fig. 4.12, the π^* SOMO of the radical **4.23** is the source of 2e/mc bonding. The observed geometries of the dimers can be understood in terms of maximising the SOMO-SOMO interaction between the monomers.[64] However, a dispersion interaction also contributes significantly to the binding energy, which is estimated to be *ca.* 75 kJ mol^{-1} in Fig. 4.11(a).[71] The computed interaction energies for the parent radical $[HCN_2S_2]^{\bullet}$ in Fig. 4.11 were found to follow the sequence (a) > (b) > (c) ~ (d). Thus, it can be inferred that the two long S···S contacts in the *trans*-antarafacial arrangement (Fig. 4.11d) provide

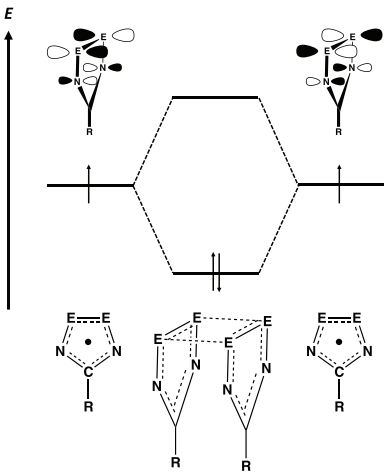

Figure 4.12. Structure and bonding in the *cis*-cofacial dimer $(PhCN_2E_2)_2$ (E = S, Se).

as much binding energy as the *trans*-cofacial interaction in (c), which involves four S···N contacts.

The six-membered rings 1,3-dithia-2,4,6-triazines (**4.13**) also form dimers *via* weak S···S interactions in the solid state (Sec. 4.8.1). In contrast to the five-membered ring $[HCN_2S_2]^{\bullet}$, the prototypical dithiatriazine HCN_3S_2 is not known. In fact, only three aryl derivatives $ArCN_3S_2$ (Ar = Ph, 4-ClC_6H_4 and 3-$CF_3C_6H_4$) have been structurally characterised; all three exist as *cis*-cofacial dimers with *d*(S···S) in the range 2.5–2.6 Å. In early work the dimerisation of **4.13** was described in terms of diffuse π^*-π^* overlap involving four-electron multicentre (4e/mc) interactions as illustrated in Fig. 4.13.[72] More recently the concept of pancake bonding has been extended to "double pancake bonding" to describe these 4e/mc

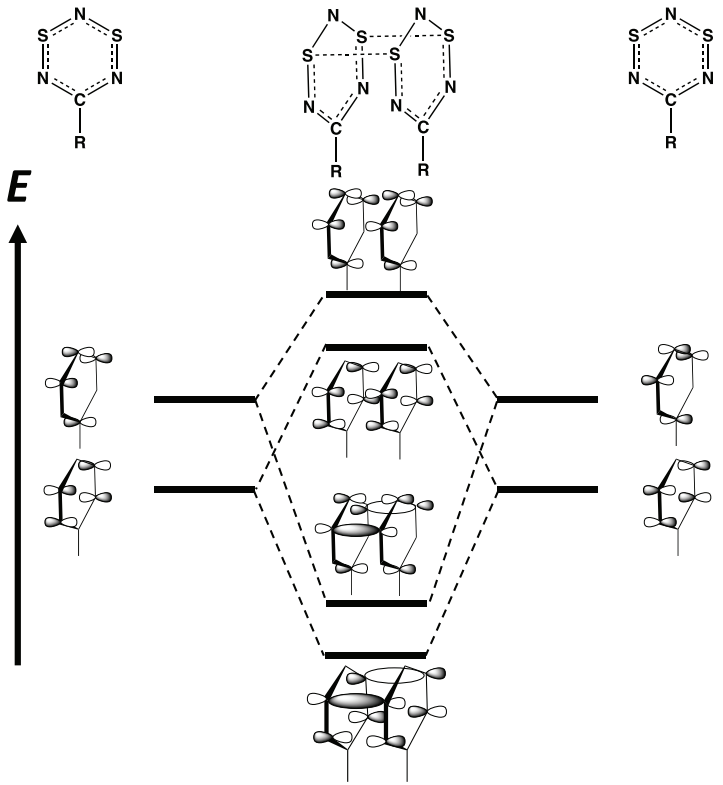

Figure 4.13. Diffuse π^*-π^* bonding between 8π-electron antiaromatic RCN_3S_2 rings.

bonding in the *cis*-cofacial dimer $(HCN_3S_2)_2$ using electron correlation theory combined with multireference effects and dispersion corrections.[73] These calculations also predict strong double pancake bonding for the hypothetical selenium analogue $(HCN_3Se_2)_2$. In addition, the formation of the unknown dimer $(S_3N_3^+)_2$ (**4.12**)$_2$ is estimated to involve S···S contacts of ~2.8 Å and result in an interaction energy of −115.9 kJ mol^{-1}.[73] DFT calculations including dispersion effects for the known phenyl derivative $(PhCN_3S_2)_2$ show that the experimentally determined *cis*-cofacial arrangement is the most stable; the dispersion interaction between the aryl substituents makes a significant contribution to the total interaction energy.

The necessity of the double pancake bonding description for the dimer $(HCN_3S_2)_2$ has been questioned.[30] High-level quantum chemical calculations for the hypothetical monomer HCN_3S_2 predict a preference for a dimer with two S–N σ bonds. However, the order of stability is reversed for the phenyl derivative $PhCN_3S_2$. In this case a dimer with two S–S σ bonds and the phenyl rings placed on top of each other is the most stable with a predicted S–S bond length of 2.57 Å, close to the experimental value of 2.5 Å.[73]

References

1. (a) B. D. Sharma and J. Donohue, *Acta Crystallogr*., **16**, 891 (1963); (b) M. L. Delucia and P. Coppens, *Inorg. Chem*., **17**, 2336 (1978).
2. C. M. Mikulski, P. J. Russo, M. S. Saran, A. G. MacDiarmid, A. F. Garito and A. J. Heeger, *J. Am. Chem. Soc*., **97**, 6358 (1975).
3. (a) J. Weiss, *Z. Anorg. Allg. Chem*., **333**, 314 (1964); (b) A. W. Cordes, R. F. Kruh and E. K. Gordon, *Inorg. Chem*., **4**, 681 (1965).
4. A. J. Banister, P. J. Dainty, A. C. Hazell, R. G. Hazell and J. G. Lomborg, *Chem. Commun*., 1187 (1969).
5. (a) M. M. Labes, P. Love and L. F. Nichols, *Chem. Rev*., **79**, 1 (1979); (b) A. J. Banister and I. B. Gorrell, *Adv. Mater*., **10**, 1415 (1998).
6. A. J. Banister, *Nat. Phys. Sci*., **237**, 92 (1972).
7. R. J. Gillespie, D. R. Slim and J. D. Tyrer, *J. Chem., Soc*., *Chem. Commun*., 253 (1977).
8. J. Bojes and T. Chivers, *J. Chem. Soc., Chem Commun*., 391 (1978).
9. W. V. F. Brooks, T. S. Cameron, S. Parsons, J. Passmore and M. J. Schriver, *Inorg. Chem*. **33**, 6230 (1994).

10. S. Herler, P. Mayer, H. Nöth, A. Schulz, M. Suter and M. Vogt, *Angew. Chem. Int. Ed. Engl.*, **40**, 3173 (2001).
11. A. Haas, *Z. Anorg. Allg. Chem.*, **628**, 673 (2002).
12. Y. Jung, T. Heine, P. v. R. Schleyer and M. Head-Gordon, *J. Am. Chem. Soc.*, **126**, 3132 (2004).
13. (a) J. Bojes, T. Chivers, W. G. Laidlaw and M. Trsic, *J. Am. Chem. Soc.*, **101**, 4517 (1979); (b) T. Chivers, W. G. Laidlaw, R. T. Oakley and M. Trsic, *Inorg. Chim. Acta*, **53**, L189 (1981).
14. F. De Proft, P. W. Fowler, R. W. A. Havenith, P. v. R. Schleyer, G. Van Lier and P. Geerlings, *Chem. Eur. J.*, **10**, 940 (2004).
15. S. De, M. N. K. Sadik and S. Liya, *ChemistrySelect*, **4**, 8807 (2019).
16. P. W. Fowler, C. W. Rees and A. Soncini, *J. Am. Chem. Soc.*, **126**, 11202 (2004).
17. M. P. Cava, M. V. Lakshmikantham, R. Hofmann and R. M. Williams, *Tetrahedron*, **67**, 6771 (2011).
18. G.-H. Zhang, Y.-F. Zhao, J. I. Wu and P. v. R. Schleyer, *Inorg. Chem.*, **48**, 6773 (2009).
19. T. Chivers and R. S. Laitinen, *Dalton Trans.*, **49**, 6532 (2020).
20. G.-H. Zhang, Y.-F. Zhao, J. I. Wu and P. v. R. Schleyer, *Inorg. Chem.*, **51**, 13321 (2012).
21. F. Grein, *Can. J. Chem.*, **71**, 335 (1993).
22. E. G. Awere, J. Passmore and P. S. White, *J. Chem. Soc., Dalton Trans.*, 299 (1993).
23. (a) L. J. Wang, P. G. Mezey and M. Z. Zgierski, *Chem. Phys. Lett.*, **369**, 386 (2003); (b) L. J. Wang and P. G. Mezey, *Chem. Phys. Lett.*, **387**, 233 (2004).
24. (a) H. M. Tuononen, R. Suontamo, J. Valkonen and R. S. Laitinen, *J. Phys. Chem. A*, **108**, 5670 (2004); (b) H. M. Tuononen, R. Suontamo, J. Valkonen and R. S. Laitinen, *J. Phys. Chem. A*, **109**, 6309 (2005).
25. (a) P. Coburger, R. Wolf and H. Grützmacher, *Eur. J. Inorg. Chem.*, **2020**, 3580 (2020); (b) B. Braida, A. Lo and P. C. Hiberty, *ChemPhysChem*, **13**, 811 (2012); (c) R. D. Harcourt, *ChemPhysChem*, **14**, 2859 (2013).
26. P. B. Karadakov, M. A. H. Al-Yassiri and D. L. Cooper, *Chem. Eur. J.*, **24**, 16791 (2018).
27. Contreras-Garcia, E. R. Johnson, S. Keinan, R. Chaudret, J.-P. Piquemal, D. N. Beratan and W. Yang, *J. Chem. Theory Compt.*, **7**, 625 (2011).
28. J. Moilanen, A. J. Karttunen, H. M. Tuononen, and T. Chivers, *J. Chem. Theory Comput.*, **8**, 4249 (2012).
29. Xu, T. Xu, D. Jiajun, S. R. Kirk and S. Jenkins, *Int. J. Quantum Chem.*, **116**, 1025 (2016).

30. G. Haberhauer and R. Gleiter, *Chem. Eur. J*., **22**, 8646 (2016).
31. (a) D. Leusser, J. Henn, N. Kocher, B. Engels and D. Stalke, *J. Am. Chem. Soc*., **126**, 1781 (2004); (b) J. Henn, D. Ilge, D. Leusser, D. Stalke and B. Engels, *J. Phys. Chem. A*, **108**, 9442 (2004); (c) D. Stalke, *Chem. Eur. J*., **17**, 9264 (2011).
32. T. T. Takaluoma, K. Laasonen and R. S. Laitinen, *Inorg. Chem*., **52**, 4648 (2013).
33. F. Blockhuys, N. P. G. Gritsan, A. Yu. Makarov, K. Tersago and A. V. Zibarev, *Eur. J. Inorg. Chem*., **2008**, 655 (2008).
34. R. T. Boeré, C. L. French, R. T. Oakley, A. W. Cordes, J. A. J. Privett, S. L. Craig and J. B. Graham, *J. Am. Chem. Soc*., **107**, 7710 (1985).
35. N. Burford, T. Chivers, A. W. Cordes, W. G. Laidlaw, M. Noble, R. T. Oakley and P. N. Swepston, *J. Am. Chem. Soc*., **104**, 1282 (1982).
36. A. Apblett, T. Chivers, A. W. Cordes and R. Vollmerhaus, *Inorg. Chem*., **30**, 1392 (1991).
37. R. E. Hoffmeyer, W.-T. Chan, J. D. Goddard and R. T. Oakley, *Can. J. Chem*., **66**, 2279 (1988).
38. N. Burford, T. Chivers, R. T. Oakley and T. Oswald, *Can. J. Chem*., **62**, 712 (1984).
39. T. Chivers, F. Edelmann, J. F. Richardson, N. R. M. Smith, O. Treu, Jr., and M. Trsic, *Inorg. Chem*., **25**, 2119 (1986).
40. H. Bärnighausen, T. von Volkmann and J. Jander, *Acta Crystallogr*., **21**, 571 (1966).
41. R. Gleiter, G. Haberhauer and S. Woitschetzki, *Chem. Eur. J*., **20**, 13801 (2014).
42. R. Gleiter and G. Haberhauer, *Coord. Chem. Rev*., **344**, 263 (2017).
43. R. Gleiter, *J. Chem. Soc. A*, 3174 (1970).
44. R. Bartezko and R. Gleiter, *Chem. Ber*., **113**, 1138 (1980).
45. R. Gleiter, *Angew. Chem., Int. Ed. Engl*., **20**, 444 (1981).
46. A. G. Papadopoulos, N. D. Charistos and A. Muñoz-Castro, *New. J. Chem*., **40**, 5090 (2016).
47. K. H. Moock, K. M. Wong and R. T. Boeré, *Dalton Trans*., **40**, 11599 (2011).
48. T. Chivers, K. S. Dhathathreyan, C. Lensink, A. Meetsma, J. C. van de Grampel and J. L. de Boer, *Inorg. Chem*., **28**, 4150 (1989).
49. N. Burford, T. Chivers, P. W. Codding and R. T. Oakley, *Inorg. Chem*., **21**, 982 (1982).
50. T. Chivers, M. Edwards and M. Parvez, *Inorg. Chem*., **31**, 1861 (1992).
51. Q. Zhang, S. Yue, X. Lu, Z. Chen, R. Huang, L. Zheng and P. von R. Schleyer, *J. Am. Chem. Soc*., **131**, 9789 (2009).

52. T. Chivers, R. W. Hilts, P. Jin, Z. Chen and X. Lu, *Inorg. Chem*., **49**, 3810 (2010).
53. T. Chivers, M. Edwards, C. A. Fyfe and L. H. Randall, *Magn. Reson. Chem*., **30**, 1220 (1992).
54. H. S. Rzepa, *Nat. Chem*., **1**, 510 (2009).
55. H. Jacobsen, *Inorg. Chem*., **52**, 11843 (2013).
56. C. Knapp, P. G. Watson, E. Lork, D. H. Friese, R. Mews and A. Decken, *Inorg. Chem*., **47**, 10618 (2008).
57. T. Chivers, J. F. Richardson and N. R. M. Smith, *Inorg. Chem*., **25**, 272 (1986).
58. I. Ernest, W. Holick, G. Rihs, G. Shomburg, G. Shoham, D. Wenkert and R. B. Woodward, *J. Am. Chem. Soc*., **103**, 1540 (1981).
59. R. J. Gillespie, J. P. Kent and J. F. Sawyer, *Inorg. Chem*., **20**, 3784 (1981).
60. (a) E. G. Awere, J. Passmore, P. S. White and T. Klapötke, *J. Chem. Soc., Chem. Commun*., 1415 (1989); (b) E. G. Awere, J. Passmore, and P. S. White, *J. Chem. Soc., Dalton Trans*., 299 (1993).
61. J. M. Rawson, A. J. Banister and I. Lavender, *Adv. Heterocycl. Chem*., **62**, 137 (1995).
62. D. A. Haynes, *CrystEngComm*, **13**, 4793 (2011).
63. R. T. Boeré, *ACS Omega*, **3**, 18170 (2018).
64. K. E. Preuss, *Polyhedron*, **79**, 1 (2014).
65. (a) H.-U. Höfs, J. W. Bats, R. Gleiter, G. Hartmann, R. Mews, M. Eckert-Maksic, H. Oberhammer and G. M. Sheldrick, *Chem. Ber.*, **118**, 3781 (1985); (b) A. W. Cordes, J. D. Goddard, R. T. Oakley and N. P. C. Westwood, *J. Am. Chem. Soc*., **111**, 6147 (1989).
66. R. T. Boeré and N. D. D. Hill, *CrystEngComm*, **19**, 3698 (2017).
67. N. Bricklebank, S. Hargreaves and S. E. Spey, *Polyhedron*, **19**, 1163 (2000).
68. A. W. Cordes, R. C. Haddon, R. G. Hicks, R. T. Oakley and T. T. M. Palstra, *Inorg. Chem*., **31**, 1802 (1992).
69. A. Alberola, E. Carter, C. P. Constantinides, D. J. Eisler, D. M. Murphy and J. M. Rawson, *Chem. Commun*., **47**, 2532 (2011).
70. R. T. Oakley, *Prog. Inorg. Chem*., **36**, 299 (1988).
71. (a) M. Kertesz, *Chem. Eur. J*., **25**, 400 (2019); (b) H. Z. Beneberu, Y.-H. Tian and M. Kertesz, *Phys. Chem. Chem. Phys*., **14**, 10713 (2012).
72. A. W. Cordes, C. D. Bryan, W. M. Davis, R. H. de Laat, S. H. Glarum, J. D. Goddard, R. C. Haddon, R. G. Hicks, D. K. Kennepohl, R. T. Oakley, S. R. Scott, and N. C. Westwood, *J. Am. Chem. Soc*., **115**, 7232 (1993).
73. Z. Cui, H. Lischka, H. Z. Beneberu and M. Kertesz, *J. Am. Chem. Soc*., **136**, 12958 (2014).

Chapter 5

Binary Chalcogen-Nitrogen Neutral Molecules, Cations and Anions

5.1 Introduction

This chapter will deal with species that are comprised of only chalcogen and nitrogen atoms. In contrast to their N–O analogues, for which small molecules such as NO, N_2O and NO_2 are well-known, stable chalcogen-nitrogen molecules of this type often aggregate to form ring or cage structures. The reasons for these differences are considered in Chapter 1. These species can be conveniently classified into neutral species, cations and anions and this classification will be adopted in the ensuing discussion.

5.2 Neutral Molecules of the Type $(NE)_n$ (E = S, Se; n = 1, 2, 4, x)

Thiazyl monomer NS, the sulfur analogue of NO, is a short-lived, gas-phase species.[1] By contrast, the binary sulfur nitrides S_2N_2 (Sec. 5.4) and S_4N_4 (Sec. 5.5) are crystalline solids that exhibit a versatile and well-studied chemistry. In addition, the polymer $(SN)_x$ is well-known for its unique metallic properties (Sec. 4.7). The most common binary selenium nitride is Se_4N_4. Neutral chalcogen-nitrogen molecules are thermodynamically unstable with respect to the formation of the elements or smaller chalcogen-nitrogen fragments. However, some binary chalcogen nitrides

can be isolated and characterised because they are kinetically stable, *i.e.*, have high energy barriers to dissociation (Sec. 4.4).

5.3 Thiazyl, Selenazyl and Tellurazyl Monomers, NE (E = S, Se, Te)

5.3.1 *Structure and spectroscopic characterisation*

Continuing interest in the diatomic thiazyl radical NS stems from its existence in nearly all interstellar environments as well as its role as a ligand in metal complexes.[1] The monomer NS has been detected in interstellar clouds and comets.[2,3] For example, it has been identified in the comet Hale-Bopp by rotational spectroscopy; the abundance of NS relative to water was estimated to be a few hundredths of a percent.[2] The primary source of NS in the gas phase involves the reaction of nitrogen atoms (N) with thiol radicals (SH).[4]

Recent calculations of the bond length in NS gave values of 1.498 Å[5] and 1.497 Å[6], in excellent agreement with the experimental value of 1.496 Å[7] indicating a bond order between two and three. A coupled cluster study estimated the dissociation energy of the strong chalcogen-nitrogen bond in NS to be 468 kJ mol^{-1} and the enthalpy of formation $\Delta_f H$(298 K) = 282 kJ mol^{-1}.[8] The generalised valence bond description indicates that NS possesses a recoupled pair π bond (a two-centre-three-electron interaction) consistent with a short, strong bond.[9] The experimental dipole moment is 1.83 ± 0.03 D, reflecting the difference in the electronegativities of sulfur and nitrogen (Sec. 1.1). The direction of the dipole is opposite to that in NO for which the dipole moment is 0.16 D. The first ionisation potential of NS is 8.87 eV.[10] This ionisation involves loss of an electron from the singly occupied π^* orbital of the NS radical, which is largely localised on the sulfur atom.[9]

Much less is known about the selenazyl monomer, NSe, but it has been characterised by infrared spectroscopy using a combination of matrix isolation techniques and isotopic enrichment (^{15}N, ^{76}Se and ^{80}Se).[11] The tellurium analogue NTe is a reactive fission product from nuclear reactors. It has been produced by laser ablation of elemental tellurium in

the presence of nitrogen gas and identified by FTIR spectroscopy after trapping in an argon matrix.[12a] The bond distance, ionisation energy and stretching frequency of NTe have been determined by quantum chemical calculations.[12b]

5.3.2 *Metal complexes*

The NS monomer is stabilised by coordination to a transition metal and a large number of complexes, primarily with metals from Groups 6, 7, 8 and 9, are known. Details can be found in recent reviews.[7,13] A variety of routes is available for the preparation of metal-thionitrosyl complexes. The most common of these are (a) reaction of nitride complexes with a sulfur source, *e.g.*, elemental sulfur, propylene sulfide or sulfur halides, (b) treatment of $(NSCl)_3$ with transition-metal complexes, and (c) reaction of $[SN]^+$ salts with transition-metal complexes. Some recent findings include several new chromium thionitrosyl complexes $[Cr(NS)(CN)_5]^{3-}$ and $[Cr(NS)(L)_5]^{2+}$ (L = dimethyl sulfoxide, *N*-methylformamide, H_2O)[14,15] and the first vanadium-thionitrosyl complex [V(nacnac)(NS)(OAr)] prepared by method (a) using elemental sulfur.[16]

Until recently, the osmium complex $[OsTp(NSe)Cl_2]$ (Tp = hydrotris(1-pyrazolyl)borate) was the only example of selenonitrosyl-metal complex.[17] However, the iridium complex $[Ir(NSe)\{N(CH{=}CHP^tBu)_2\}][PF_6]$[18] and the ruthenium complex *mer*-$[Ru(NSe)Cl_3(AsPh_3)_2]$[19] have been prepared by method (a) using grey selenium (Scheme 5.1) and structurally characterised (Fig. 5.1). Although no metal complexes of telluronitrosyl NTe are known, several complexes of CTe (isoelectronic with NTe^+) have been prepared and structurally characterised.[20]

Flash photolysis of the chromium complex $[Cr(NS)(CH_3CN)_5]^{2+}$ in acetonitrile generates NS in solution.[15] Photochemically generated NS can be trapped by the iron(II) complex $[Fe(S_2CNEt_2)_2]$. As expected from

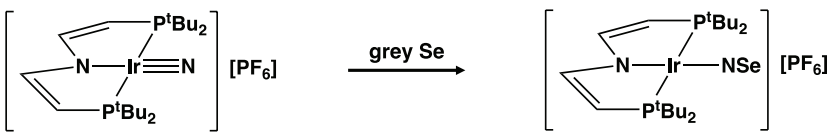

Scheme 5.1. Preparation of a metal-selenonitrosyl from a metal nitride and selenium.

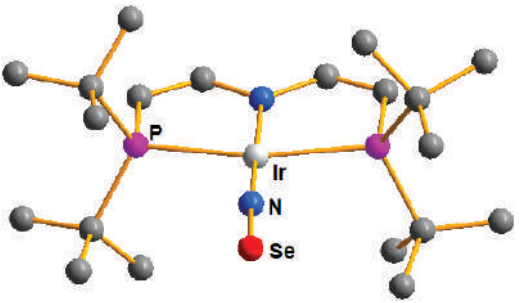

Figure 5.1. Molecular structure of $[Ir(NSe)\{N(CH{=}CHP^tBu)_2\}][PF_6]$.[18]

the discussion in Sec. 5.2, the fundamental difference between the behaviour of NS and NO in solution is the tendency of NS to undergo oligomerisation.[15]

The thionitrosyl and selenonitrosyl ligands in metal complexes are generally coordinated as terminal, nearly linear units in which the bond angle <MNE (E = S, Se) is in the range 169–180°, although [OsTp(NSe)Cl_2] falls outside this range with <OsNSe = 165°.[17] In contrast to transition-metal nitrosyl complexes, for which bridging NO ligands are well known, this bonding mode is uncommon for the NS ligand. However, DFT calculations for the binuclear complex $[Mn_2(NS)_2(CO)_7]$ predict a low energy for a doubly NS-bridged structure.[21]

The nitrogen atom in the (almost) linear metal-thionitrosyl complexes is *sp*-hybridised and the NS ligand behaves as a three-electron donor. The N–S bond distances in metal complexes vary between 1.43 and 1.59 Å[22] (*cf.* 1.44 and 1.495 Å for $[SN]^+$ and NS, respectively). The N–Se bond lengths in metal-selenonitrosyl complexes are in the range 1.63–1.68 Å,[17–19] comparable to that in gas phase NSe (1.65 Å).[9] The metal-nitrogen distances in these chalcogenonitrosyl complexes are generally short, consistent with multiple M–NE bonding. DFT calculations on the hypothetical complexes $[Re(NE)(PH_3)_3Cl_2]$ (E = O, S, Se, Te) indicate that the NO complex should be described as Re=N=E, whereas an Re≡N–E representation is more appropriate for the heavier chalcogens.[22] PM3 molecular orbital calculations for the series of chromium complexes $[CrCp(CO)_2(NE)]$ (E = O, S, Se, Te), which are only known for E = O, S, suggest that metal to ligand π-backbonding increases down the series from NO to NTe.[23]

DFT calculations for the series of iridium cations $[Ir(NE)\{N(CH{=}CHP^tBu)_2\}]^+$ (E = O, S, Se) estimate the π-acceptor ability of the chalcogenonitrosyl ligands to be NS < NSe < NO.[24]

A few reactions of metal complexes that involve the NS ligand rather than the metal centre have been reported. For example, the reaction of the dication $[Re(CO)_5(NS)]^{2+}$ with cesium halides CsX (X = Cl, Br) converts the NS ligand to a thiazyl halide NSX.[25] Oxygen transfer from an NO_2 to an NS ligand on the same metal centre to give a thiazate (NSO) complex occurs in ruthenium porphyrin complexes.[26] The vanadium complex [V(nacnac)(NS)(OAr)] reacts with PPh_3 to produce $SPPh_3$ and regenerate the metal nitride from which it was prepared. Thus, this V-NS complex could be a catalytic source of atomic sulfur.[16]

5.4 Disulfur and Diselenium Dinitride, S_2N_2 and Se_2N_2

5.4.1 *Structure and spectroscopic characterisation*

S_2N_2 forms large, colourless crystals with an iodine-like smell. It detonates with friction or on heating above 30°C, but can be sublimed at 1 Pa at 20°C. It has a square planar structure with S–N bond distance of 1.654 Å and bond angle of 90.0 ± 0.4°.[27] It is prepared by the thermolysis of other cyclic S–N compounds, *e.g.*, S_4N_4 (over silver wool at 220°C),[27] $[S_4N_3]Cl$,[28] or $Ph_3AsNS_3N_3$[29] at *ca.* 130°C. The electronic structure of S_2N_2 is discussed in detail in Sec. 4.5.

Coupled cluster and multiconfigurational approaches, as well as density functional methods, have been used to predict vibrational frequencies of sulfur and selenium nitrides.[30] The calculated IR-active vibrational frequencies are in reasonable agreement with experimental data from the IR and Raman spectra of S_2N_2 obtained as a solid condensate in N_2 or CH_4 matrices at 15–35 K.[31] By the use of 30% ^{15}N-enrichment, it was confirmed that the isolated S_2N_2 molecule has essentially the same square-planar geometry as the crystalline solid (Sec. 3.7).[32] The high-resolution gas-phase FTIR spectrum of S_2N_2 revealed only a small difference between the gas-phase and solid-state structures; in the gas phase the angle at nitrogen <SNS is smaller than <NSN, whereas the opposite is true

in the solid-state structure.[33] A pseudorotation barrier of < 2 kJ mol^{-1} has been computed for S_2N_2 indicative of a floppy molecule, but this does not alter the electronic structure of the four-membered ring.[34]

^{14}N, ^{15}N and ^{77}Se NMR chemical shifts have been calculated for the cyclic chalcogen nitrides S_2N_2, $SeSN_2$ and Se_2N_2.[30] Surprisingly, no experimental NMR data are available for S_2N_2. However, the calculated ^{14}N and ^{15}N NMR chemical shifts for S_4N_4 and the known mixed selenium-sulfur nitride $Se_2S_2N_4$ are in excellent agreement with the experimental data,[30] providing some confidence in the predicted values of 95 ± 20, 125 ± 20 and 185 ± 20 ppm for S_2N_2, $SeSN_2$ and Se_2N_2, respectively.[30]

The experimental UV spectrum of S_2N_2 consists of a broad band in the range 4.5–5.8 eV comprised of two overlapping absorptions centred at approximately 5.0 eV (~250 nm), which is attributed to the $\pi \rightarrow \pi^*$ electronic transition.[35] The calculated band gap energies decrease as the selenium content in the ring increases as evinced by colourless S_2N_2 (3.32 eV, ~375 nm), the predicted orange-yellow colour of $SSeN_2$ (2.50 eV, ~495 nm) and red colour of Se_2N_2 (2.20 eV, ~560 nm).[30]

5.4.2 *Polymerisation*

The spontaneous topochemical polymerisation of S_2N_2 into $(SN)_x$, a polymer with fascinating conducting properties, has been known for more than 40 years.[36] This process can be achieved in the zeolite Na-ZSM-5, which has a pore size that is able to accommodate S_2N_2 as well as infinite channels along the *b*-axis to allow for polymer growth.[36a] Serendipitously, it was observed that the exposure of fingerprints on various surfaces, *e.g.*, glass, metal, paper or ceramic surfaces, to S_2N_2 vapour generates an image of the fingerprint due to the formation of blue-black $(SN)_x$ polymer (Fig 5.2a).[36b,c] This process has now been developed in the form of equipment that is marketed under the name RECOVER Latent Fingerprint Technology (LFT) for applications in forensic science.[37b] Notably, this technique is superior to other methods for fingerprint detection for some applications. For example, RECOVER LFT can yield fingerprints from fired bullet cartridges or metal surfaces that have been submerged in liquids (Fig. 5.2b).[37b]

Molecular dynamics simulations of the topochemical polymerisation of S_2N_2 at high pressures and elevated temperatures in the solid state using

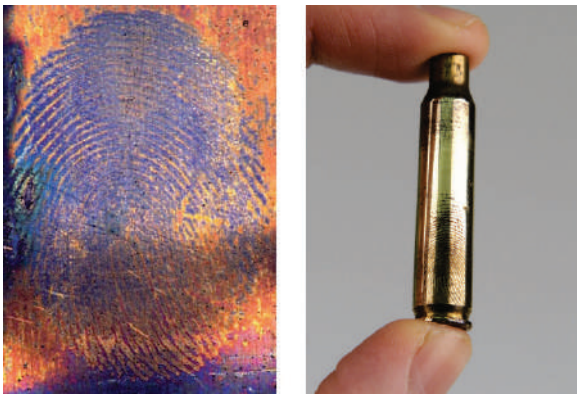

(a) (b)

Figure 5.2. (a) Formation of $(SN)_x$ over latent fingerprints on metallic surfaces.[37] [Reproduced with permission from S. M. Bleay, P. F. Kelly, R. S. P. King, *J. Mater. Chem.*, **20**, 10100 (2010). Copyright 2010 Royal Society of Chemistry]; (b) Fingerprint on fired bullet cartridge. Copyright 2021 Dr. Roberto S. P. King, Chief Technology Officer, foster+freeman®.

DFT methods and periodic functions have been carried out.[38] The formation of $(SN)_x$ is initiated by cleavage of one S–N bond in S_2N_2 followed by a very rapid attack of the resulting open-chain isomer on a neighbouring ring (Fig. 5.3). Propagation occurs along the *a* axis throughout the lattice. The packing changes from the herringbone structure of the S_2N_2 lattice to the layered structure of $(SN)_x$. Although the metrical data for the polymer chain are in good agreement with the experimental crystal structure, there is less long-range order between neighbouring chains.[38] The identification of open-chain isomers formed upon photolysis of S_2N_2 is discussed in Sec. 6.7.

5.4.3 *Adduct formation*

S_2N_2 forms both mono- and di-adducts, $S_2N_2{\cdot}L$ and $S_2N_2{\cdot}2L$, with Lewis acids such as $AlCl_3$, BCl_3 and $SbCl_5$, and with a variety of transition-metal halides (Sec. 1.5).[39a] The S_2N_2 ligand is attached to the Lewis acid through nitrogen in these complexes and bridges two metal centres in the di-adducts; coordination has very little effect on the geometry of the

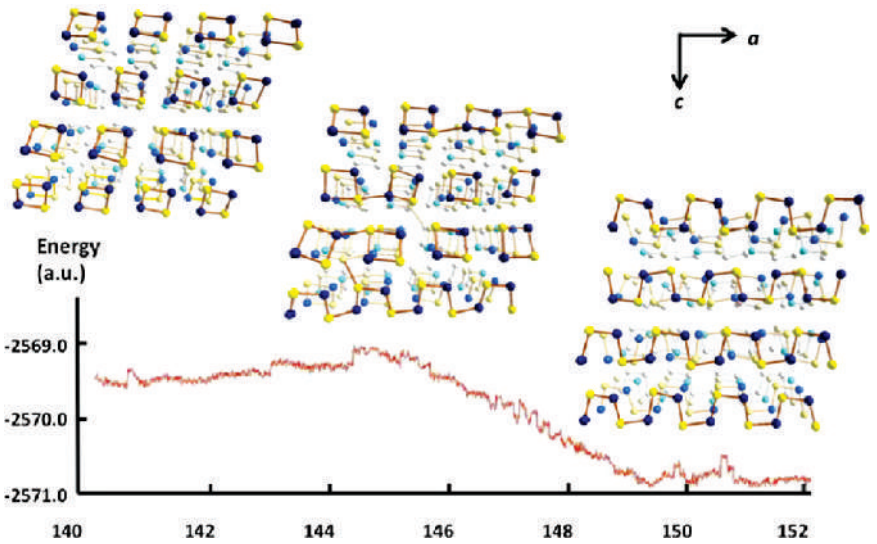

Figure 5.3. Simulated energy profile of the topochemical polymerisation of S_2N_2 rings to $(SN)_x$ at 50 GPa and 600 K. Sulfur atoms are indicated by yellow spheres and nitrogen atoms by blue spheres (*b* axis is directed away from the reader).[38] [Reproduced with permission from T. T. Takaluoma, K. Laasonen and R. S. Laitinen, *Inorg. Chem.*, **52**, 4648 (2013). Copyright 2013 American Chemical Society].

four-membered ring. All these complexes contain one or more halide ligands attached to the metal. A recent EDA-NOCV (Energy Decomposition Analysis — Natural Orbital for Chemical Valence) analysis of the bonding interaction of S_2N_2 with 12- and 14-electron metal halide fragments reveal the versatility of the S_2N_2 ligand, which can behave as a σ and π donor or acceptor.[39b] In the σ system the lone pair on nitrogen is donated to the metal centre and the halide ligand donates to the S–N σ* molecular orbital. In the π system the metal may participate as a donor in Mo–N π-back donation or as an acceptor of electrons from an S_2N_2 π orbital into a vacant *d* orbital as depicted in Fig. 5.4.

Both main group and transition-metal halide adducts of Se_2N_2 have been structurally characterised. The bis-adducts $Se_2N_2{\cdot}2AlBr_3$ and $[X_3Pd(\mu\text{-}Se_2N_2)PdX_3]^{2-}$ (X = Cl, Br) (Fig. 5.5) are prepared by the reaction of Se_4N_4 with $AlBr_3$ or $[ER_4]_2[Pd_2X_6]$ (E = P, N; R = Ph, Bu; X = Cl, Br),

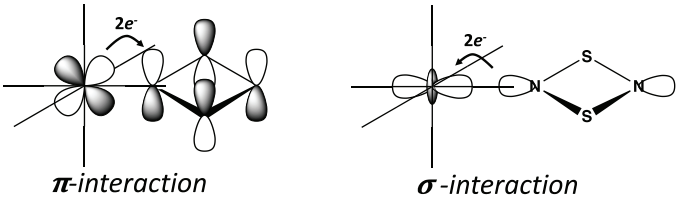

Figure 5.4. Bonding interactions between metal *d* orbitals and S_2N_2 molecular orbitals.

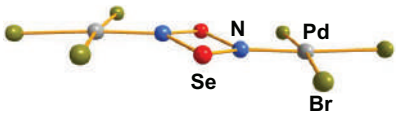

Figure 5.5. X-ray structure of the dianion in $[Bu_4N]_2[Br_3Pd(\mu\text{-}Se_2N_2)PdBr_3]$.[41b]

respectively.[40,41] The mean Se–N bond length in these adducts is *ca.* 1.79 Å.

Although it has not been isolated as the free ligand, evidence for the formation of Se_2N_2 upon treatment of the complex $[Bu_4N]_2[PdBr_3(\mu\text{-}N_2Se_2)PdBr_3]$ with [14]aneS$_4$ has been presented.[41c] Addition of $[Bu_4N]_2[Pd_2Br_6]$ to the yellow product of this reaction regenerated $[Bu_4N]_2[PdBr_3(\mu\text{-}N_2Se_2)PdBr_3]$; Se_4N_4 was formed upon prolonged standing. In addition, treatment of the yellow product with $[PtCl_2(PPhMe_2)_2]$ produced a bis-platinum(II) dihalide adduct of Se_2N_2 identified as $[PtX_2(PPhMe_2)(\mu\text{-}N_2Se_2)PtX_2(PPhMe_2)]$ (X = 50% Cl, 50% Br) by X-ray crystallography.[41c]

Quantum chemical calculations of the interaction of H_2 molecules with S_2N_2 revealed an adduct with two molecules of H_2 which has a low binding energy (< –6.3 kJ mol^{-1}).[42] However, when the ring is doped with a transition metal such as Ni(0), Pd(0) or Pt(0), complexes that incorporate three H_2 molecules for each metal centre were found to have binding energies of –283.3, –78.2 and –341.8 kJ mol^{-1} for M = Ni, Pd and Pt, respectively. Four H atoms appear as hydrides in the Ni and Pd complexes, while one H_2 molecule is η^2-coordinated to the metal. By contrast, in the most stable Pt complex all six hydrogen atoms exist as hydrides.[42] The practicality of using binary S,N compounds as hydrogen storage materials is questionable.

The chemical or electrochemical reduction of S_2N_2 produces the six-membered $[S_3N_3]^-$ anion *via* the short-lived radical anion $[S_4N_4]^{\bullet-}$ (Sec. 3.4.2 and Fig. 3.9).[43]

5.5 Tetrasulfur and Tetraselenium Tetranitride, S_4N_4 and Se_4N_4

5.5.1 *Preparation, properties and structure*

Tetrasulfur tetranitride S_4N_4 is regarded as the quintessential binary sulfur nitride in view of its widespread use as a reagent in the synthesis of inorganic and organic sulfur-nitrogen compounds. The standard synthesis of S_4N_4 involves the treatment of S_2Cl_2 with chlorine, followed by ammonia gas in carbon tetrachloride at 20–50°C (Scheme 2.1). An alternative preparation of S_4N_4 involves the reaction of $[(Me_3Si)_2N]_2S$ with an equimolar mixture of SCl_2 and SO_2Cl_2 (Eq. 5.1).[44] The use of S_4N_4 as a replacement for lead styphnate, a primary explosive in firearms, has been suggested on the basis of an analysis of its explosive and other properties.[45]

Early methods for the synthesis of Se_4N_4 involved the reaction of $(EtO)_2SeO$ or SeX_4 (X = Br, Cl) with ammonia. A synthesis that avoids the use of gaseous reagents is shown in Eq. 5.2.[46] Alternatively, small amounts of pure Se_4N_4 can be obtained in *ca.* 90 % yield from the reaction of elemental selenium with $Ph_2S{=}NBr$.[47] Extreme care and safety precautions are necessary when handling Se_4N_4, which is even more explosive than S_4N_4, *e.g.*, on contact with a metal spatula.

$$[(Me_3Si)_2N]_2S + SCl_2 + SO_2Cl_2 \rightarrow 1/2S_4N_4 + 4Me_3SiCl + SO_2 \quad (5.1)$$

$$12(Me_3Si)_2NLi + 2Se_2Cl_2 + 8SeCl_4 \rightarrow 3Se_4N_4 + 24Me_3SiCl + 12LiCl \quad (5.2)$$

Both tetrasulfur tetranitride and tetraselenium tetranitride adopt cage structures (see **1.3** in Sec. 1.2.1) with equal E–N bond lengths and two weak transannular E···E interactions of *ca.* 2.60 Å and 2.75 Å, respectively, at room temperature. The hybrid tetrachalcogen tetranitride 1,5-$S_2Se_2N_4$ also has a cage structure with transannular chalcogen···

chalcogen contacts of 2.70 Å.[48] Recent advances in our understanding of the electronic structures and, in particular, the nature of the intramolecular π^*-π^* interactions in these cage molecules are discussed in Sec. 4.9.1.

5.5.2 *Adduct formation*

Tetrasulfur tetranitride forms 1:1 *N*-bonded adducts with a variety of Lewis acids. A typical example is $TeCl_4 \cdot S_4N_4$ in which coordination to the nitrogen center results in loss of the transannular S···S bond in the S_4N_4 ring, which adopts a boat conformation (Fig. 5.6); DFT calculations reveal that the π-electron density in the ring is delocalised.[49] The energies of formation of the adducts $L \cdot S_4N_4$ vary from strongly exothermic for L = AsF_5 to thermoneutral for L = $SeBr_4$ and their relative stabilities depend on the ionic character of the M–N bond.[49] However, the reactions of S_4N_4 with metal halides or organometallic reagents more often give rise to cyclometallathiazenes in which the metal becomes part of the S–N ring, *e.g.*, LMS_2N_2 (Sec. 5.9.7).

A computational investigation of the interaction of S_4N_4 with benzene and naphthalene revealed that the σ hole of the sulfur atoms of S_4N_4 engages in non-covalent interactions with the aromatic π systems; the interaction energy of S_4N_4 with three naphthalene rings was estimated to be *ca.* 20 kcal mol^{-1}.[50] The S···π interaction is the main driving force in these complexes of S_4N_4 with only a marginal contribution from the nitrogen centres. The only example of adduct formation between S_4N_4 and an

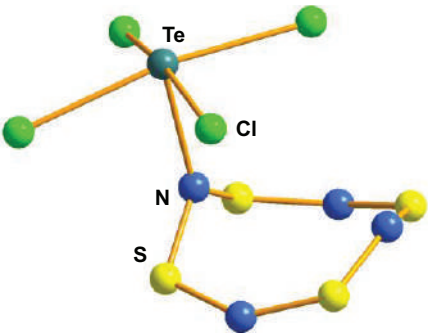

Figure 5.6. X-ray structure of $TeCl_4 \cdot S_4N_4$.[49]

organic compound is the non-stoichiometric complex $C_{60}(S_4N_4)_{1.33}(C_6H_6)_{0.67}$ in which only the sulfur atoms participate in bonding to the fullerene.[51] By contrast, the reactions of S_4N_4 with alkynes generate important C,N,S heterocycles such as the seven-membered 1,3,5-trithia-2,4-diazepines and 1,3,5-trithia-2,4,6-triazepines (Secs. 12.6 and 12.7) in addition to 1-thia-2,5-diazoles, which are the major products.

5.5.3 *Reactions*

The one-electron electrochemical reduction of S_4N_4 to give the radical anion $[S_4N_4]^{\bullet-}$ has been reinvestigated by applying the SEEPR technique (Simultaneous Electrochemical Electron Paramagnetic Resonance) to ^{15}N and ^{33}S-labelled S_4N_4 (Sec. 3.4.2 and Fig. 3.9).[52] The activation energy of the first order decay of $[S_4N_4]^{\bullet-}$ to give $[S_3N_3]^-$ is *ca.* 62 kJ mol^{-1}.[52] This ring contraction occurs *via* an intermediate that is structurally similar to the isomer **6.8** identified in the photochemical study (Sec. 6.9).[53] Ring contraction also occurs in reactions of S_4N_4 with anionic nucleophiles, *e.g.*, azide ion.[54] By contrast, the eight-membered ring is retained on monoprotonation to form $[S_4N_4H]^+$, dichlorination to give 1,5-$Cl_2S_4N_4$, oxidation to the dication $[S_4N_4]^{2+}$ or reduction to the tetraimide $S_4N_4H_4$ (Scheme 5.2).

In spite of the hazardous nature of Se_4N_4, this binary selenium nitride has been used as a source of several important Se–N compounds either *via*

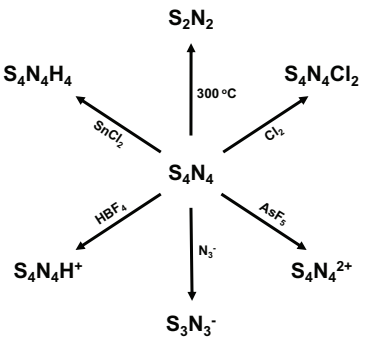

Scheme 5.2. Reactions of S_4N_4 with electrophiles and nucleophiles.

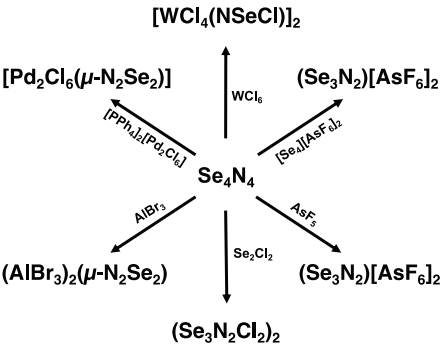

Scheme 5.3. Preparation of Se–N compounds from Se_4N_4.

oxidation or adduct formation (Scheme 5.3). However, safer alternatives to Se_4N_4 are available for the development of Se–N chemistry, *e.g.*, selenium-nitrogen halides and silicon-nitrogen-selenium reagents.

5.6 Chalcogen-rich Nitrides

The only structurally characterised chalcogen-rich binary sulfur nitride is the six-membered ring 1,3-S_4N_2. The isomers of the five-membered rings, 1,2- or 1,3-S_3N_2, would be antiaromatic 8π-electron systems.

5.6.1 *Nitrogen disulfide and diselenide, NS_2 and NSe_2*

The unstable molecules NS_2 and NSe_2 can be produced in an argon/nitrogen/chalcogen microwave discharge, trapped in solid argon at 12 K and characterised by IR spectra of isotopically labelled samples.[56a,b] The more stable isomers have symmetrical bent structures with <ENE bond angles estimated to be 153 ± 5° (E = S) and 146 ± 5° (E = Se).

5.6.2 *Trisulfur dinitride, S_3N_2*

The calculated S–S bond length for the unknown five-membered ring 1,3-S_3N_2 is 2.302 Å (*cf.* 2.05 Å for S–S single bond) and the predicted internal bond angle <NSS = 94.5°, *cf.* 105.2° in the six-membered ring 1,3-S_4N_2.[57] These geometrical parameters indicate an inherent strain in this

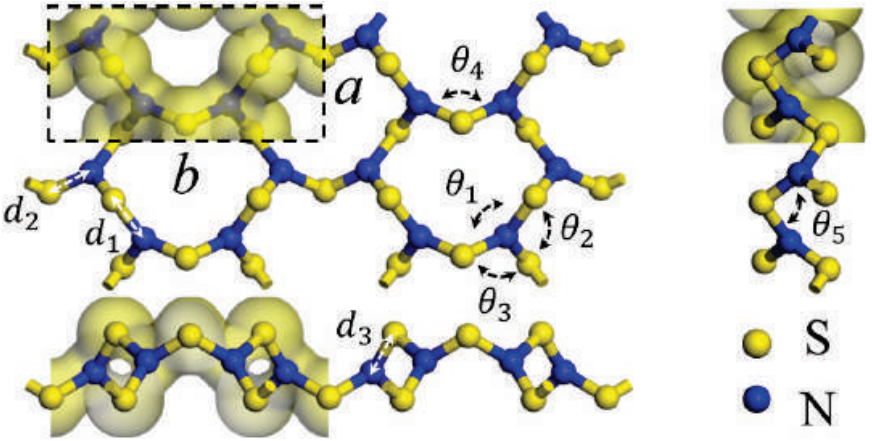

Figure 5.7. The PBE-predicted 2D crystal structure of α-S_3N_2: a = 4.24, b = 8.89 Å; d_1 = 1.81, d_2 = 1.72, d_3 = 1.66 Å; θ_1 = 116.8°, θ_2 = 119.3°, θ_3 = 119.2°, θ_4 = 106.1°, θ_5 = 103.7°.[10a] Bonding is depicted by an isosurface of the electron density.[57] [Reproduced with permission from H. Xiao, X. Shi, X. Liao, Y. Zhang and X. Chen, *Phys. Rev. Mater*., **2**, 024002 (2018). Copyright 2018 American Physical Society].

five-membered ring. As an alternative to a cyclic structure a stable two-dimensional trisulfur dinitride with three polymorphs has been proposed.[58] The crystal structure of the most stable form, α-S_3N_2 (space group $Pmn2_1$), consists of condensed 12-membered (S_6N_6) rings (Fig. 5.7). The S_3N_2 crystal is predicted to be dynamically, thermally and chemically stable on the basis of the computed phonon spectrum and *ab initio* molecular dynamics simulations. Calculations also indicate that α-S_3N_2 will be a wide, direct band gap (3.92 eV) semiconductor with possible optoelectronic applications such as blue or UV light-emitting diodes and photodetectors.[58]

A subsequent study of 2D monolayer crystals of E_3N_2 (E = S, Se) employing DFT calculations predicted α-heart and β-heart structures, which exhibit different mechanical and electrical properties.[59] The former structure resembles that depicted for α-S_3N_2 in Fig. 5.7. The E_3N_2 materials are predicted to have unusual mechanical properties as indicated by the values of negative Poisson's ratios denoting auxetic behaviour. Auxetic materials become thicker when stretched and thinner in response to compression.

5.6.3 *Tetrasulfur dinitride, 1,3-S_4N_2*

Tetrasulfur dinitride forms dark red needles (m.p. 23°C) that sublime readily at room temperature, but it must be stored at –20°C to avoid decomposition. Reaction of S_2Cl_2 with aqueous ammonia is a convenient route to a pure product.[60] The 1,3-S_4N_2 molecule consists of a six-membered ring in a half-chair conformation. There are long S–N bonds (1.68 Å) connecting the –SSS– and –N=S=N– units, which have S–N distances of 1.56 Å.[60] Calculated optimised geometries for 1,3-S_4N_2 are in close agreement with these experimental data.[57]

5.7 Nitrogen-rich Chalcogen Nitrides

Early work on nitrogen-rich sulfur nitrides such as SN_2 and SN_4 was mainly limited to the purported involvement of these species as fleeting intermediates. However, on the basis of recent experimental and theoretical investigations of the formation and structures of this class of sulfur nitrides and their selenium analogues under high pressure, fascinating properties with potential applications in optoelectronics are predicted for these high-energy-density materials.

5.7.1 *The isomers NNS and NSN*

The lowest energy isomer NNS, a heavier analogue of the stable molecule N_2O, decomposes above 160 K. It is generated by flash photolysis of 5-phenyl-1,2,3,4-thiatriazole and has been characterised by high-resolution mass spectrometry and IR spectroscopy.[61]

Recent DFT calculations of the stability, electronic structure and optical properties of a *P*3*m*1 phase of 1*T*-EN_2 (E = S, Se, Te) (1*T* refers to one layer per trigonal unit cell) predict a crystal structure of the two-dimensional material 1*T*-SN_2 comprised of six-coordinated S atoms and three-coordinate N centres (Fig. 5.8a).[62] 1*T*-SN_2 has dynamical stability based on phonon spectra and calculated cohesive energies, but the thermal and mechanical stabilities have yet to be determined. Band-structure calculations revealed indirect band gaps of 2.825, 2.351, and 2.336 eV for 1*T*-SN_2, 1*T*-SeN_2 and 1*T*-TeN_2, respectively, and application of biaxial

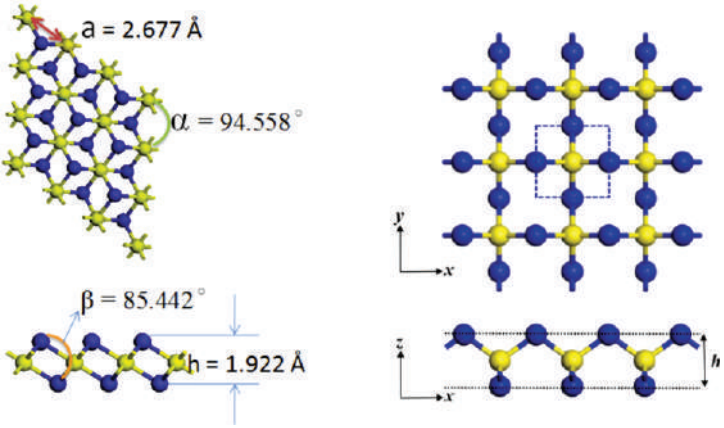

Figure 5.8. Optimised structures of (a) 1*T*-SN_2 [Reproduced with permission from J-H. Lin, H. Zhang, X-L. Cheng and Y. Miyamoto, *Phys. Rev. B*, **94**, 195404 (2016). Copyright 2016 American Physical Society],[62] and (b) *S*-SN_2 [Reproduced with permission from F. Li, X. Lv, J. Gu, K. Tu, J. Gong, P. Jin and Z. Chen, *Nanoscale*, **12**, 85 (2020). Copyright 2020 Royal Society of Chemistry].[63]

strain induced a transition from a wide band gap semiconductor to a metal suggesting possible applications in optoelectronic devices.

A new phase of the SN_2 monolayer, namely *S*-SN_2, was proposed based on first-principles calculations combined with the particle-swarm optimisation method.[63a] The structure of *S*-SN_2 belongs to the space group $P\bar{4}2m$ and incorporates four-coordinate S atoms and two-coordinate nitrogen centres; the prefix *S* indicates a square lattice (Fig. 5.8b). The *S*-SN_2 monolayer is a remarkably stable semiconductor with an indirect band gap of 2.79 eV, *cf.* 2.825 eV for 1*T*-SN_2.[63a] The selenium analogue *S*-SeN_2 has a similar structure and a band gap of 2.21 eV.[63b] These new materials may have applications in mechanical or optoelectronic devices.

Particle-swarm optimisation calculations on the sulfur-nitrogen system up to 200 GPa revealed three binary sulfur-nitrogen solids to be thermodynamically stable: *Pnma* $(SN)_x$, *Pnnm* SN_2, and *C2/c* SN_4 at pressures of 37, 43 and 48 GPa, respectively (Fig. 5.9).[64] A polymeric 3D arrangement was predicted for SN_2 (Fig. 5.9c). Partial density-of-states

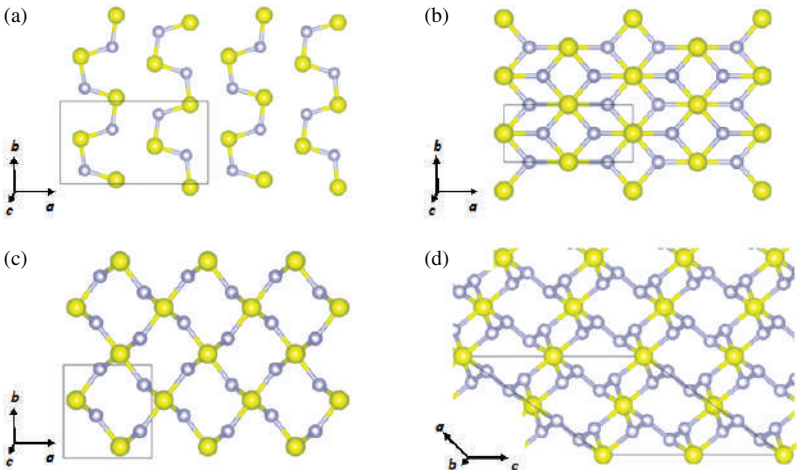

Figure 5.9. Crystal structures of (a) *Pnma* $(SN)_x$, (b) *Immm* $(SN)_x$, (c) *Pnnm* SN_2, and (d) *C2/c* SN_4.[64] [Reproduced with permission from D. Li, F. Tian, Y. Z. Lv, S. Wei. D. Duan, B. Liu and T. Cui, *J. Phys. Chem. C*, **121**, 1515 (2017). Copyright 2017 American Chemical Society].

calculations indicated that SN_2 is a semiconductor with a direct band gap of 0.66 eV at 60 GPa.

A seminal experimental investigation of the formation of sulfur nitrides in the S–N_2 system at high pressures confirmed the predictions for SN_2. Reaction of elemental sulfur and N_2 gas in a diamond anvil cell at pressures above 60 GPa with laser heating produced an orthorhombic (P_{nnm}) SN_2 compound.[65] The lattice parameters of this material obtained from powder diffraction data match closely the theoretically predicted crystalline structure of SN_2.[62] Single crystal X-ray diffraction analysis revealed a $CaCl_2$-type structure composed of edge-sharing SN_6 octahedra with N atoms that are triply coordinated by S atoms (Fig. 5.10).[65] The SN_2 solid was found to be metastable down to *ca.* 20 GPa, at which point it dissociates into the elements.[65]

5.7.2 *Thiatetrazole, SN_4*

The nitrogen-rich thiatetrazole SN_4 has attracted the attention of both experimental and theoretical chemists for more than 20 years. An early attempt to prepare SN_4 from the reaction of $[NS][AsF_6]$ with cesium azide

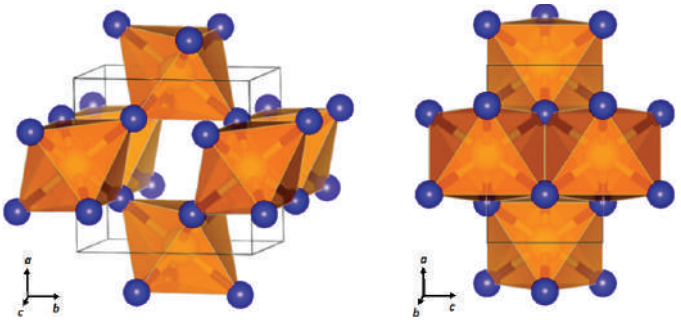

(a) (b)

Figure 5.10. Crystal structure of SN_2 formed at 81.6 GPa showing (a) the cross-linked octahedra and (b) the edge-sharing octahedra and apical S–N bonds.[65] [Reproduced with permission from D. Laniel, M. Bykov, T. Fedotenko, A. V. Ponomareva, I. A. Abrikosov, K. Glazyrin, V. Svitlyk, L. Dubrovinsky and N. Dubrovinskaia, *Inorg. Chem*., **58**, 9195 (2019). Copyright 2019 American Chemical Society].

produced a black precipitate of the polymer $(SN)_x$.[66] Furthermore, no experimental evidence for the formation of SN_4 was garnered from the recent study of the S–N_2 system at high pressures.[65]

The main focus of early theoretical investigations of SN_4 was an estimate of the aromaticity of the cyclic isomer, which is a 6π-electron five-membered ring formally isoelectronic with thiophene. The calculated NICS (nucleus independent chemical shift) and NICS(1) values of −18.40 and −17.48 for *cyclo*-SN_4 are indicative of substantial aromatic character in the ring.[67a] This conclusion is supported by the calculated value of 18.56 for the ASE (aromatic stabilisation energy).[67b]

Nitrogen-rich sulfur nitrides are of considerable interest as high-energy-density materials. The molecular structure, IR and UV spectra (λ_{max} 212 nm) for SN_4 have been calculated by a modification of DFT.[68] However, *cyclo*-SN_4 has low thermodynamic and kinetic stability. The ring system is estimated to be *ca.* 420 kJ mol^{-1} higher in energy than the decomposition products $1/8S_8 + N_2$[69] and the barrier for decomposition into $N_2 + N_2S$ is only 29.3 kJ mol^{-1}.[70]

5.7.3 *Dithiatetrazine, S_2N_4, and trithiatetrazepine, S_3N_4*

A planar six-membered ring *cyclo*-S_2N_4 would be an 8π-electron system. The thermochemical stability and kinetic persistence of various S_2N_4

isomers have been calculated at the B3LYP/6-311+G(3df) DFT level.[57] A boat conformation of 1,4-S_2N_4 (**5.1**) was predicted to be the most stable of the three possible six-membered rings. The other most thermodynamically stable isomers include two five-membered rings SN_4(=S) (**5.2** and **5.3**) and two acyclic species SNSNNN (**5.4** and **5.5**); the acyclic isomers **5.4** and **5.5** differ only in the conformation; the –NNN fragment in **5.4** is oriented above the SNSN plane, whereas **5.5** is planar (Scheme 5.4). On the basis of the kinetic inertness of these five isomers, the acyclic isomer **5.4** is the most viable candidate for synthesis. However, its dissociation barrier to give N_2 and *cyclo*-S_2N_2 is only 90.4 kJ mol^{-1}, *cf.* 213 kJ mol^{-1} for *cyclo*-S_2N_2.

Planar, cyclic trithiatetrazepine 1,2,4,6-S_3N_4 (**5.6**) would be a 10π-electron (aromatic) system (Chart 5.1).[71] However, the energy barrier for dissociation into SNN and S_2N_2 is only 59.0 kJ mol^{-1}.[57] The known compound S_3N_3-N=PPh_3 (**5.7**) can be considered as the triphenylphosphine adduct of S_3N_4[72] and the related derivative S_3N_3–N=S (**6.7**) has

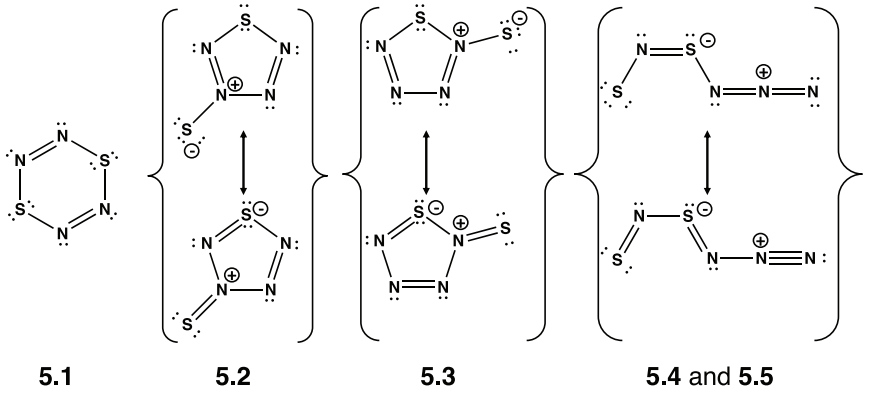

Scheme 5.4. Structures of the five most stable isomers of S_2N_4.

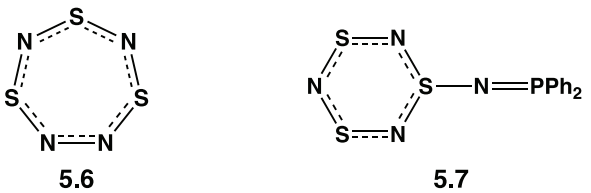

Chart 5.1. 1,2,4,6-S_3N_4 and S_3N_3–N=PPh_3.

been identified as a short-lived intermediate generated upon flash photolysis of S_4N_4.[53]

5.7.4 *Pentasulfur hexanitride, S_5N_6*

Pentasulfur hexanitride is an explosive, air-sensitive orange solid, which is best prepared from reaction of 1,5-$S_4N_4Cl_2$ with $Me_3SiNSNSiMe_3$ (Eq. 5.3).[73] The structure of S_5N_6 resembles a cradle in which an –N=S=N– unit bridges two antipodal sulfur atoms of an S_4N_4 cage *via* S–N single bonds.[74] It decomposes in warm solvents to give S_4N_4.

$$1,5\text{-}S_4N_4Cl_2 + Me_3SiNSNSiMe_3 \rightarrow S_5N_6 + 2Me_3SiCl \qquad (5.3)$$

5.7.5 *Nitrogen-rich selenium nitrides*

Investigations of the high-pressure phase diagrams of the binary selenium-nitrogen system have revealed four stable compounds at high pressures: *Cmc*2_1-SeN_2, *P*2_1/*m*-SeN_3, $P\bar{1}$-SeN_4 and $P\bar{1}$-SeN_5.[75] These novel nitrogen-rich materials are predicted to incorporate a variety of polynitrogen arrangements in the solid state (Fig. 5.11). The binary selenium nitride *Cmc*2_1-SeN_2 has a layer structure (Fig. 5.11a), while *P*2_1/*m*-SeN_3, $P\bar{1}$-SeN_4 and $P\bar{1}$-SeN_5 incorporate N_∞-chains (Fig. 5.11b), oligomeric N_8-chains (Fig. 5.11c) or distorted $[N_6]^{3-}$ anionic rings alternating with layers of N_∞-chains (Fig. 5.11d). The high energy content of the latter three phases is reflected in the values of their energy densities, which are 3.27, 3.26 and 4.08 kJ g^{-1}, respectively.[75]

5.7.6 *Tellurium nitrides*

In contrast to the sulfur and selenium analogues E_4N_4 (E = S, Se), tellurium nitride, a highly explosive material, has the composition Te_3N_4. The reaction of tellurium tetrachloride with tris(trimethysilyl)amine produces the tetra-adduct $[Te_6N_8(TeCl_4)_4]$ (Eq. 5.4).[76] The central core of this complex is a dimer of Te_3N_4, which forms a rhombic dodecahedron comprised of six tellurium atoms at the corners of a distorted octahedron and eight nitrogen atoms on each face of the octahedron as μ_3 ligands (Fig. 5.12).

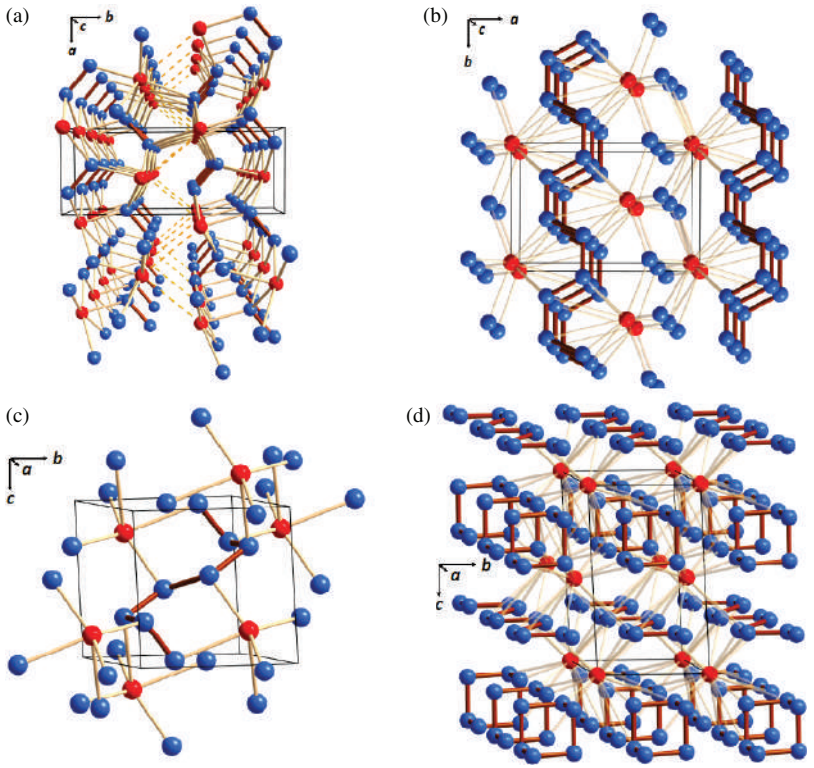

Figure 5.11. Crystal structures of the predicted selenium nitrides: (a) *Cmc*2_1-SeN_2 at 90 GPa (b) $P2_1/m$-SeN_3 at 80 GPa (c) $P\bar{1}$-SeN_4 at 140 GPa and (d) $P\bar{1}$-SeN_5 at 130 GPa. Selenium atoms are depicted in red and nitrogen atoms in blue [redrawn from the structural data in ref. 75; reproduced with permission from T. Chivers and R. S. Laitinen, *Dalton Trans*. **49**, 6532 (2020). Copyright 2020 Royal Society of Chemistry].

$$10TeCl_4 + 8N(SiMe)_3 \rightarrow [Te_6N_8(TeCl_4)_4] + 24Me_3SiCl \qquad (5.4)$$

5.7.7 *Selenium and tellurium azides*

Binary chalcogen azides $E(N_3)_4$ (E = Se, Te) fall under the classification of neutral chalcogen-nitrogen molecules. The selenium(IV) azide $Se(N_3)_4$ and the related anions $[Se(N_3)_5]^-$ and $[Se(N_3)_6]^{2-}$ have been prepared by reactions of the corresponding fluoride and trimethylsilyl azide in dichloromethane or SO_2 at low temperatures (Eq. 5.5).[77] The tellurium analogues $Te(N_3)_4$, $[Te(N_3)_5]^-$ and $[Te(N_3)_6]^{2-}$ were obtained earlier in a similar manner.[78]

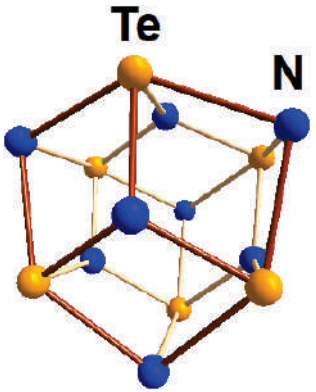

Figure 5.12. Central Te_6N_8 core of the tetra-adduct $[Te_6N_8(TeCl_4)_4]$.[76] [Reproduced with permission from T. Chivers and R. S. Laitinen, *Chem. Soc. Rev.,* **44**, 1725 (2015). Copyright 2015 Royal Society of Chemistry].

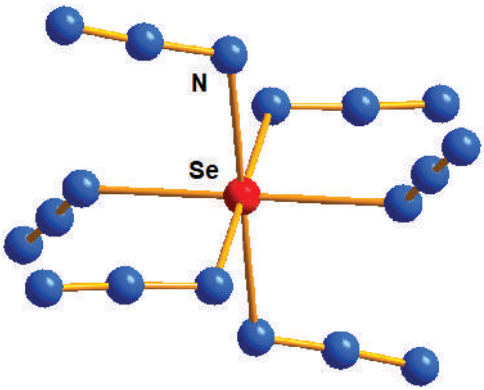

Figure 5.13. Structure of the dianion $[Se(N_3)_6]^{2-}$ in the $[Ph_4P]^+$ salt.[77]

$$SeF_4 + 4Me_3SiN_3 \rightarrow Se(N_3)_4 + 4Me_3SiF \qquad (5.5)$$

The pale yellow tetra-azide $Se(N_3)_4$ is explosive, but salts of the orange $[Se(N_3)_5]^-$ and red $[Se(N_3)_6]^{2-}$ anions with large cations such as $[Ph_4P]^+$ or $[Ph_3PNPPh_3]^+$ can be isolated and structurally characterised.[77] In contrast to the tellurium complex $[Te(N_3)_6]^{2-}$ in which the free electron pair on the Te atom is stereochemically active,[78b] the structure of the selenium analogue $[Se(N_3)_6]^{2-}$ in the $[Ph_4P]^+$ salt exhibits perfect S_6 symmetry (Fig. 5.13).[77]

5.8 Chalcogen-Nitrogen Cations

Investigations of binary sulfur-nitrogen cations have played an important role in the development of S–N chemistry. The simple cations $[SN]^+$ and $[SNS]^+$ are especially useful reagents for the synthesis of other S–N compounds. The planar cyclic cations $[S_2N_3]^+$, $[S_3N_2]^{2+}$, $[S_4N_3]^+$, $[S_4N_4]^{2+}$ and $[S_5N_5]^+$ all conform to the Hückel $(4n + 2)\pi$-electron rule (Secs. 4.1 and 4.2). The only selenium analogue of this series is $[Se_3N_2]^{2+}$ and there are no known tellurium congeners.

5.8.1 *Thiazyl cation, $[SN]^+$*

Thiazyl salts have been known for 50 years. They may be obtained from $(NSCl)_3$ by reaction with (a) $Ag[AsF_6]$ in liquid SO_2 (Eq. 5.6)[79a] or (b) $AlCl_3$ in CH_2Cl_2 under the influence of heat or ultrasound.[79b]

$$(NSCl)_3 + 3Ag[AsF_6] \rightarrow 3[SN][AsF_6] + 3AgCl \qquad (5.6)$$

The $[SN]^+$ cation exhibits a ^{14}N NMR resonance at *ca.* 200 ppm and this technique is useful for monitoring reactions of $[SN]^+$.[79c] The thiazyl cation has been employed for the preparation of other important S–N compounds. For example, the insertion reactions with S_4N_4 or SCl_2 produce $[S_5N_5]^+$ or the acyclic $[ClSNSCl]^+$ cation, respectively.

The $[SN]^+$ cation has been detected spectroscopically as a ubiquitous species in interstellar environments.[80]

5.8.2 *Dithianitronium cation, $[SNS]^+$*

The $[SNS]^+$ cation was first obtained in low yield more than 40 years ago. Several methods are available for the synthesis of this important reagent. The most convenient procedure involves the reaction of a mixture of $(NSCl)_3$ with stoichiometric amounts of sulfur and $Ag[SbF_6]$ in liquid SO_2 (Eq. 5.7).[81] The hexafluoroantimonate salt can be converted to the more soluble red $[SNS][Al\{OC(CF_3)_3\}_4]$ by quantitative anion exchange with $Li[Al\{OC(CF_3)_3\}_4]$.[82]

$$3/8S_8 + (NSCl)_3 + 3Ag[SbF_6] \rightarrow 3[SNS][SbF_6] + 3AgCl \qquad (5.7)$$

Scheme 5.5. Cycloaddition reactions of $[SNS][AsF_6]$ with nitriles and alkynes.

5.8 **5.9**

Chart 5.2. The 1,3- and 1,2-isomers of the $[S_2N_3]^+$ cation.

The $[SNS]^+$ cation is a linear species isoelectronic with CS_2. It exhibits a very narrow ^{14}N NMR resonance at –91 ppm ($\nu_{½} = 8$ Hz) in SO_2. As in the case of $[SN]^+$, this technique is also useful for monitoring reactions of the $[SNS]^+$ cation, which is an important reagent in S–N chemistry. For example, the thermally allowed cycloaddition reactions with organic nitriles and alkynes give quantitative yields of heterocyclic cations (Scheme 5.5).[83]

5.8.3 *Dithiatriazyl cation, $[S_2N_3]^+$*

The cyclic $[S_2N_3]^+$ cation, a 6π-electron system, is the only example of a nitrogen-rich, *monocyclic* S–N cation; it exists as the 1,2-isomer. The thermally stable salt $[S_2N_3]_2[Hg_2Cl_6]$ is obtained from the reaction of $(NSCl)_3$ with $HgCl_2$ in CH_2Cl_2.[84] The bond lengths in the five-membered ring indicate delocalised π-bonding that is attenuated across the S–S bond.

Detailed theoretical calculations showed that the 1,3-isomer (**5.8**) is thermodynamically more stable than the isolated 1,2-isomer (**5.9**) (Chart 5.2). However, the latter is more kinetically inert with a fairly high energy barrier to dissociation into N_2 and NSS^+ fragments. By contrast, the dissociation of the 1,3-isomer into SNS^+ and N_2 has a very low barrier as discussed in Sec. 4.4 and illustrated in Fig. 4.1.[69] NICS analysis reveals considerable 6π-electron aromaticity for both isomers (Sec. 4.3).[69]

5.8.4 *Trichalcogenadiazyl cations $[E_3N_2]^{+\bullet}$, $[E_6N_4]^{2+}$ and $[E_3N_2]^{2+}$ (E = S, Se)*

The binary radical cations $[E_3N_2]^{\bullet+}$ (E = S, Se) (see **1.7** in Chart 1.2) are prepared by oxidation of E_4N_4 with reagents such as AsF_5. In the solid state these five-membered rings form dimers in which the two 7π-electron rings are associated *via* weak intermolecular E···E contacts (π^*-π^* interactions) [d(S···S) = 3.00–3.10 Å, d(Se···Se) = 3.12–3.15 Å] (see Sec. 4.7 and Fig. 4.9). The mixed selenathiadiazolyl radicals $[Se_{(3-n)}S_nN_2]^{+\bullet}$ (n = 1, 2) have also been characterised by their EPR spectra.[85]

The five-membered dication 1,2-$[S_3N_2]^{2+}$ is 67.8 kJ mol^{-1} higher in energy than the 1,3-isomer. The pathway for the exothermic dissociation of 1,3-$[S_3N_2]^{2+}$ into $[SN]^+$ and $[S_2N]^+$ in the gas phase has an energy barrier of only 22.6 kJ mol^{-1}.[69] However, lattice-stabilisation effects allow the isolation of $[MF_6]^-$ salts (M = As, Sb).

5.8.5 *Cyclotrithiazyl cation, $[S_3N_3]^+$*

The $[S_3N_3]^+$ cation is an antiaromatic 8π-electron system with two singly occupied π^* orbitals in the planar (D_{3h}) structure (Sec. 4.8.1).[86a,b] Based on the concept of "pancake bonding" (Sec. 4.10), this binary sulfur-nitrogen cation is predicted to form a dimer $(S_3N_3^+)_2$ with S···S contacts of ~2.8 Å and an interaction energy of −115.9 kJ mol^{-1}.[86b] Experimentally, the monomeric $[S_3N_3]^+$ cation has been obtained as the norbornene adduct, but salts of the free cation have not been isolated.[86c]

5.8.6 *Cyclothiotrithiazyl $[S_4N_3]^+$, cyclotetrathiazyl $[S_4N_4]^{2+}$ and cyclopentathiazyl $[S_5N_5]^+$ cations*

The planar, cyclic cations $[S_4N_3]^+$ and $[S_5N_5]^+$ were discovered in the late 1960s and $[S_4N_4]^{2+}$ was first reported in 1977.[85a] All three cations conform to the Hückel (4n + 2)π-electron rule (Chart 5.3).[85b] The seven-membered ring in $[S_4N_3]^+$ (**5.10**) exhibits approximately equal S–N bond lengths and an S–S single bond (2.08 Å).[87] The $[S_4N_4]^{2+}$ cation (**5.11**) is an eight-membered ring with equal S–N bond lengths (D_{4h}) of *ca.* 1.55 Å. It is a fully delocalised 10π-electron system. The $[S_5N_5]^+$ cation (**5.12**) is a

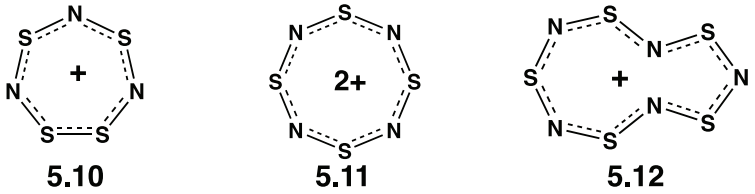

Chart 5.3. Cyclic binary sulfur-nitrogen cations.

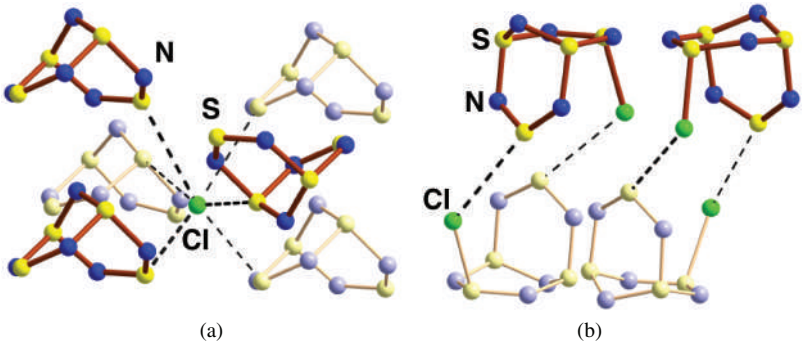

Figure 5.14. Structures of (a) ionic $[S_4N_5]Cl$ and (b) covalent S_4N_5Cl.

14π-electron system. The ten-membered ring has an azulene shape. There are no selenium analogues of these binary S–N cations.

5.8.7 *Tetrasulfur pentanitride cation, $[S_4N_5]^+$*

The nitrogen-rich $[S_4N_5]Cl$ is a yellow-orange, hygroscopic solid which decomposes violently on heating. It is readily prepared from $(NSCl)_3$ and bis(trimethylsilyl)sulfur diimide (Eq. 5.8).[88a] The treatment of $[S_4N_5]Cl$ with AgF_2, $SbCl_5$, or $AgAsF_6$ gives $[S_4N_5]F$, $[S_4N_5][SbCl_6]$ or $[S_4N_5][AsF_6]$, respectively.

$$(NSCl)_3 + Me_3SiNSNSiMe_3 \rightarrow [S_4N_5]Cl + 2Me_3SiCl \qquad (5.8)$$

$[S_4N_5]Cl$ has a polymeric, predominantly ionic, structure in which Cl^- anions show six close contacts to the $[S_4N_5]^+$ cations (**1.11**) in a quasi-octahedral fashion with d(S–Cl) = 2.81–3.37 Å. The unbridged S···S distance is 4.01 Å (Fig. 5.14a).[88a] A covalent modification S_4N_5Cl has also

been structurally characterised (Fig. 5.14b).[88b] The intramolecular S–Cl distance is only 2.23 Å, and the intermolecular S–Cl contacts are in the range 3.43–3.49 Å.

5.9 Chalcogen-Nitrogen Anions

Sulfur and nitrogen are a versatile combination in the formation of binary anions with acyclic (including catenated systems)[89a] and cyclic structures.[89b] In addition, a variety of binary sulfur-nitrogen anions are found only in complexes with transition metals (Sec. 5.9.7). Acyclic anions of the type $[NS_x]^-$ ($x = 2, 3, 4$) are labile in solution and the cyclic anions $[S_3N_3]^-$ and $[S_4N_5]^-$ are explosive in the solid state as alkali-metal salts. Consequently, large organic cations are necessary to isolate stable salts of these anions; bis(triphenylphosphino)iminium $[PPN]^+$ (PPN = $(Ph_3P)_2N$) is especially effective for this purpose.[90] Several binary S,N anions were first obtained serendipitously, but more convenient methods for preparing their salts have subsequently been developed. This section will begin with a discussion of acyclic anions followed by a description of the cyclic species.

Binary selenium-nitrogen anions are unknown in ionic salts, but several selenium analogues of the sulfur-nitrogen anions discussed below can be generated *in situ* and stabilised by chelation to a metal centre, *viz.*, $[Se_3N]^-$, $[Se_2N_2H]^-$ and $[Se_2N_2]^{2-}$.[91]

5.9.1 *Sulfur diimide dianion, $[NSN]^{2-}$*

The simplest binary sulfur-nitrogen anion is the sulfur diimide dianion $[NSN]^{2-}$, isoelectronic with SO_2. The pale yellow salt $K_2[NSN]$ is prepared from bis(trimethylsilyl)sulfur diimide and potassium *tert*-butoxide in boiling dimethoxyethane (Eq. 5.9).[92] The S=N bond distances in the $[K(18\text{-crown-}6)]^+$ salt are *ca.* 0.05 Å longer than the S=O bonds in SO_2 and the <NSN bond angle of 129.9° is *ca.* 12° wider than the corresponding bond angle in SO_2.[93]

$$Me_3SiNSNSiMe_3 + 2KO^tBu \rightarrow K_2[NSN] + 2Me_3SiO^tBu \qquad (5.9)$$

The potassium salt $K_2[NSN]$ has been used for the preparation of numerous other sulfur diimide derivatives *via* metathetical reactions with *p*-block element halides. However, the reagent $Me_3SiNSNSiMe_3$ is usually preferred since volatile trimethylsilyl halides are more easily removed from the sulfur-nitrogen products than KCl.

5.9.2 *$[NS_2]^-$ anion*

Salts of the $[NS_2]^-$ anion have not been isolated. However, the formation of this binary sulfur-nitrogen anion from the electrochemical or chemical (with NH_2^-) reduction of $[SSNS]^-$ (λ_{max} 465 nm) has been proposed to account for the initial appearance of absorption maxima at 375 nm in acetonitrile or 390 nm in liquid ammonia upon reduction.[94,95] Two high-level computational investigations of the geometries, relative stabilities and absorption spectra of the isomers $[NSS]^-$ and $[SNS]^-$ indicate that the unsymmetrical isomer is slightly more stable than the symmetrical form by 10–25 kJ mol^{-1}.[96a,b] The estimated absorption maxima for $[SSN]^-$ and $[SNS]^-$ in acetonitrile are 385 and 423 nm, respectively.[96a] However, there is a relatively low-energy bimolecular process for the isomerisation of $[SNS]^-$ that leads to an equilibrium mixture of both anions.[96b] The electrochemical reduction of $[SSNS]^-$ may give symmetrical $[SNS]^-$ initially *via* cleavage of an S–S bond followed by partial isomerisation to produce an equilibrium mixture of both isomers.[96b]

5.9.3 *$[SSNS]^-$ anion*

The orange-red $[S_3N]^-$ anion (λ_{max} 465 nm) is obtained by the addition of one equivalent of triphenylphosphine to a solution of an $[S_4N]^-$ salt in acetonitrile.[97] It can be isolated in combination with large counterions, *e.g.*, $[Ph_4As]^+$ or $[N(PPh_3)_2]^+$, but it is unstable with respect to the formation of the blue $[S_4N]^-$ anion in solution or in the solid state under the influence of heat or pressure. The vibrational spectra of 30% ^{15}N-enriched $[S_3N]^-$ suggest an unbranched $[SNSS]^-$ arrangement of atoms (**5.13**) (Chart 5.4) in contrast to the branched structure (D_{3h}) of the isoelectronic

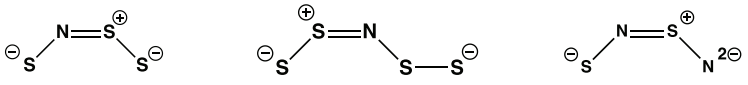

5.13 **5.14** **5.15**

Chart 5.4. Acyclic binary sulfur-nitrogen anions.

$[CS_3]^{2-}$ and the isovalent $[NO_3]^-$ ion (Sec. 1.2). An S–S stretching vibration is observed in the Raman spectrum of $[SNSS]^-$ at *ca.* 570 cm^{-1}.

High-level quantum chemical calculations for $[SNSS]^-$ determined values of 474 nm for the *cis* isomer and 575 nm for the *trans* isomer.[96a] The characteristic absorption of 465 nm is assigned to a $\pi^* \rightarrow \pi^*$ transition for this 6π-electron system.

Many metal complexes are known in which the $[S_3N]^-$ ion is chelated to the metal by two sulfur atoms. Coinage metal (Cu and Ag) complexes are readily obtained by metathetical reactions between the $[S_3N]^-$ ion and the corresponding metal halides.[98]

5.9.4 *[SSNSS]⁻ anion*

The dark blue $[S_4N]^-$ anion (λ_{max} 580 nm) was first obtained from the decomposition of $[^nBu_4N][S_7N]$ produced by treatment of S_7NH with $[^nBu_4N]OH$ in diethyl ether at –78°C.[99] The labile $[S_7N]^-$ ion was subsequently identified in solution by the observation of a ^{14}N NMR resonance at −314 ppm upon deprotononation of S_7NH with $NaNH_2$ in liquid ammonia.[100] The $[S_4N]^-$ ion is more conveniently prepared by the thermolysis of salts of the $[S_3N_3]^-$ ion with large cations in boiling acetonitrile.[101a] The $[SSNSS]^-$ anion (**5.14**) is a planar (*cis,trans*) chain with nitrogen as the central atom and short, terminal S–S bonds (*ca.* 1.90 Å) (Chart 5.4), which give rise to strong bands at *ca.* 565 and 590 cm^{-1} in the Raman spectrum.[101a,b] A high-level quantum chemical calculation determined a value of 580 nm for the visible absorption band in excellent agreement with the experimental data for $[SSNSS]^-$. This characteristic absorption band is assigned to a $\pi^* \rightarrow \pi^*$ transition for this 8π-electron system.[96a]

Investigations of the irradiation of $[NH_4][SH]$ have prompted the suggestion that binary sulfur-nitrogen anions of the type $[S_xN]^-$ ($x = 3, 4$) may

contribute to the colour of Jupiter's great red spot.[102] This assignment is based on the well-established spectroscopic (Raman and visible spectra) data for these anions (*vide supra*).

5.9.5 *Sulfur-nitrogen anions in sulfur-liquid ammonia solutions*

Sulfur dissolves in liquid ammonia to give intensely coloured solutions. The colour is concentration-dependent and the solutions are photosensitive.[103] The primary reduction products are polysulfides $[S_x]^{2-}$ that dissociate to polysulfide radical anions, especially the deep blue $[S_3]^{\bullet-}$ ion (λ_{max} ~ 620 nm).[104] The acyclic anions $[S_xN]^-$ ($x = 3, 4$) have also been detected in these solutions by their characteristic visible and Raman spectra.[101c]

The $[S_4N]^-$ anion has been invoked to explain the complex mixture of products that is formed from bis(anisylphosphonothioyl)disulfanes in methanolic ammonia solutions on the basis of a strong visible absorption band at 563 nm.[105]

5.9.6 *$[S_2N_2H]^-$ anion*

The $[S_2N_2H]^-$ anion is formed by treatment of $S_4N_4H_4$ with potassium amide in liquid ammonia. It has been characterised by ^{14}N and ^{15}N NMR spectroscopy (Sec. 3.2 and Fig. 3.3),[89,98] but not isolated as an ionic salt. However, reaction of $S_4N_4H_4$ with two equivalents of the Wittig reagent $Ph_3P{=}CH_2$ produces a yellow solid, presumably $[Ph_3PMe][S_2N_2H]$, which acts as an *in situ* reagent for the preparation of $Ni(S_2N_2H)_2$ by reaction with $NiCl_2$.[106]

5.9.7 *Metal complexes of acyclic sulfur-nitrogen anions*

A variety of acyclic, binary sulfur-nitrogen anions that are not known in ionic salts have been characterised in metal complexes,[107,108] including the tridentate $[S_4N_4]^{2-}$ dianion (*S,S,N*) in Ir and Pt complexes.[109,110] The most common of these cyclometallathiazenes (Sec. 1.5.2) involve the $[S_2N_2]^{2-}$ dianion (**5.15**, Chart 5.4) or its monoprotonated derivative $[S_2N_2H]^-$, which form numerous complexes with group 8 and 10 metals.[111]

Several synthetic approaches to these transition-metal complexes are available as exemplified by the series $[MCp^*(S_2N_2)]$ (M = Co, Rh, Ir; $Cp^* = C_5Me_5$).[112] The cobalt complex is prepared by reaction of $[CoCp^*(CO)_2]$ with S_4N_4 in toluene at room temperature, while the Rh and Ir complexes are obtained *via* metathesis between $[MCp^*Cl_2]_2$ and $[Sn^nBu_2(S_2N_2)]$ in dichloromethane; a solution of $[S_4N_3]Cl$ in liquid ammonia can also be used as an *in situ* source of $[S_2N_2]^{2-}$ for the synthesis of the Rh complex.[112] DFT calculations for $[CoCp(S_2N_2)]$ indicate complete electron delocalisation in the metallathiazene ring.[113] Protonation of this complex with HBF_4 to give $[CoCp(S_2N_2H)][BF_4]$ occurs at the metal-bonded nitrogen atom and has little effect on the S–N bond lengths.[111] The black heterobimetallic complex $[TiNiCp_2(S_2N_2)_2]$, which also contains the $[S_2N_2]^{2-}$ dianion (**5.15**), has been prepared by metathesis (Scheme 5.6) and adopts a nearly planar $TiNi(S_2N_2)_2$ framework.[114]

A unique binding mode for the $[S_2N_2]^{2-}$ ligand is observed in the lanthanide complexes $[Ln_3I_5(S_2N_2)(S_2)(THF)_{10}]$ (Ln = Nd, Dy) obtained from reactions of iodide-nitride complexes of Nd or Dy with sulfur.[115] The dianionic $[S_2N_2]^{2-}$ ligand in these trinuclear complexes acts as both a chelating and bridging ligand (Fig. 5.15).

In addition to the tin reagent $[Sn^nBu_2(S_2N_2)]$, Group 15 complexes of $[S_2N_2]^{2-}$ have been structurally characterised. The six members of the series $[AsR(S_2N_2)]$ (R = Me, Et, ^{i}Pr, ^{t}Bu, Ph, Mes) are obtained *via* metathesis between the tin reagent and $AsRX_2$ (X = Cl, I).[116] The four alkyl derivatives are volatile orange-red oils, while the aryl derivatives are low-melting solids.[116] The flexible five-membered ring in $[AsR(S_2N_2)]$ is puckered for R = Ph, but planar for the mesityl derivative. The structures of two modifications of $[SbR(S_2N_2)]$ have been reported.[117]

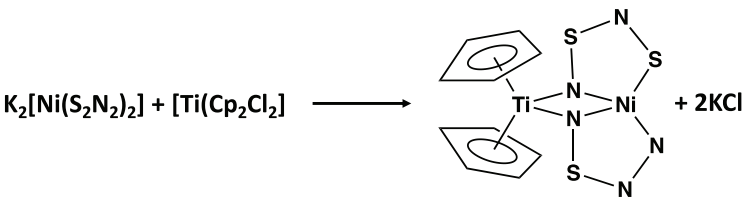

Scheme 5.6. Preparation of a heterobimetallic complex of the $[S_2N_2]^{2-}$ dianion.

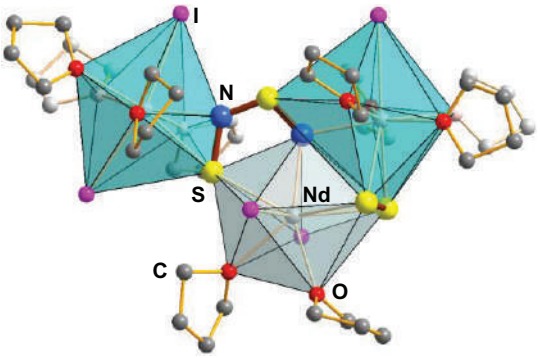

Figure 5.15. Molecular structure of $[Nd_3I_5(S_2N_2)(S_2)(THF)_{10}]$.[115] (Only one trinuclear complex of the asymmetric unit is shown. Hydrogen atoms omitted for clarity).

The aromaticity of planar five-membered NSNSE rings has been evaluated for hypothetical derivatives of the type $(S_2N_2E)X$ (E = B, Al, C, Si; X = H, Cl, CH_3) by using magnetic (^{1}H NMR shifts and NICS values), structural (bond length differences and bond orders), and energetic (HOMO-LUMO gap) criteria.[118] It was found that aromaticity increases on moving to the next group within the same period, but decreases on moving to the next period within the same group or, to a smaller extent, with an increase in the electronegativity of X. Quantum chemical calculations also predict that the sulfur-nitrogen fragment in SiS_2N_2 stabilises both the singlet and the triplet states through extensive delocalisation.[119] This unknown silylene is predicted to resist dimerisation.

The molecular structure of the low-melting sulfoxide $O{=}S(S_2N_2)$, which was first prepared 45 years ago, consists of a puckered S_3N_2 ring with an exocyclic S=O group.[120a,b] The S–S bond distance of 2.216 Å is *ca.* 8% longer than a typical S–S single bond. Theoretical calculations, including NICS values, for this sulfoxide[120a] and the corresponding ketone $O{=}C(S_2N_2)$[121] indicate that they are both aromatic.

5.9.8 *Trisulfur trinitride anion, $[S_3N_3]^-$*

The $[S_3N_3]^-$ anion (**5.16**) was first prepared more than 40 years ago as cesium or tetra-alkylammonium salts and identified by elemental analyses

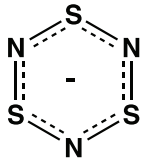

5.16

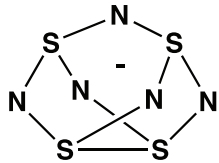

5.17

Chart 5.5. Cyclic binary sulfur-nitrogen anions.

and vibrational (IR and Raman) spectra, which were consistent with D_{3h} symmetry for the anion.[122,123] The best preparation involves the reaction of S_4N_4 with an azide of a large cation, *e.g.*, $[(Ph_3P)_2N]^+$. The $[S_3N_3]^-$ anion is an essentially planar, six-membered ring as confirmed by X-ray crystal structures of the following salts $[^nBu_4N][S_3N_3]$,[124] $[PhCN_2S_2][S_3N_3]$,[125] and $[CoCp_2][S_3N_3]$ (Chart 5.5).[126] The latter was first obtained by reduction of S_4N_4 with cobaltocene[126] and it is also produced upon reduction of S_2N_2 with cobaltocene.[43] In the presence of a crown ether the reducing agents $Na[C_{10}H_8]$ or $Na[Ph_2CO]$ also convert S_2N_2 to the $[S_3N_3]^-$ anion, which is isolated as the $[Na(15\text{-crown-}5)]^+$ salt. In the crystal structure the encrypted Na^+ cations exhibit a strong interaction with one of the nitrogen atoms of the $[S_3N_3]^-$ ring (Fig. 5.16).[43] The structure of $[PPN][S_3N_3{\cdot}HOCH_3]$ has also been determined.[52]

The electronic structure of the 10π-electron six-membered ring system $[S_3N_3]^-$ is discussed in Sec. 4.3. The yellow colour of $[S_3N_3]^-$ (λ_{max} 360 nm) is assigned to a π^*(HOMO) $\rightarrow$ π^*(LUMO) transition.

5.9.9 *Tetrasulfur pentanitride anion, $[S_4N_5]^-$*

The yellow $[S_4N_5]^-$ anion (**5.17**) was first reported in 1975 from the methanolysis of $Me_3SiNSNSiMe_3$.[127a,b] The reaction of $(NSCl)_3$ with dry liquid ammonia at –78°C also generates $[NH_4][S_4N_5]$ in *ca.* 50% yield.[128] The recommended procedure involves the preparation of the piperidinium salt by reaction of S_4N_4 with piperidine, followed by cation exchange, *e.g.*, with [PPN]Cl.[129]

The structure of **5.17** in $[^nBu_4N][S_4N_5]$ is closely related to that of S_4N_4.[127b] In $[S_4N_5]^-$, five of the six edges of the S_4 tetrahedron are bridged

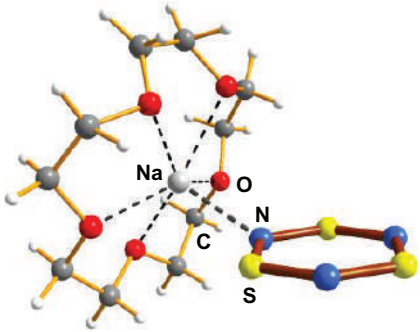

Figure 5.16. Crystal structure of [Na(15-crown-5)][S_3N_3].[43]

by nitrogen atoms (Chart 5.5). The unbridged S···S distance is *ca.* 2.70 Å. A high-resolution VT X-ray diffraction study of [PPN][S_4N_5] as a 1:1 solvate with CH_3CN revealed a similar distance at 100 K.[130]

The carefully controlled thermolysis of solutions of $[S_4N_5]^-$ in boiling acetonitrile generates $[S_3N_3]^-$ and, subsequently, the $[SSNSS]^-$ anion (**5.14**).[101] The reaction of $[S_4N_5]^-$ with bromine or iodine produces pentasulfur hexanitride, S_5N_6, whereas oxidation with chlorine yields $[S_4N_5]Cl$.[131]

References

1. R. T. Boeré and T. L. Roemmele, in *Comprehensive Inorganic Chemistry II,* Ed. T. Chivers, Elsevier (2013), Vol. 1, Ch. 1.14, pp. 375–411.
2. W. M. Irvine, M. Senay, A. J. Lovell, H. E. Mathews, D. McGonagle and R. Meier, *Icarus*, **143**, 412 (2000).
3. M. V. Canaves, A. A. De Almeida, D. C. Boice and G. C. Sanzovo, *Earth, Moon and Planets*, **90**, 335 (2002).
4. (a) J. C. Laas and P. Caselli, *Astron. Astrophys.*, **624**, A108 (2019); (b) D. V. Mifsud, Z. Kañuchová, P. Herczku, S. Ioppolo, Z. Juhász, S. T. Kovács, N. J. Mason, R. W. McCullough and B. Sulik, *Space Sci. Rev*., **217**, 14 (2021).
5. Y. Gao, T. Gao and M. Gong, *J. Quant. Spectrosc. Radiat. Transf*., **129**, 193 (2013).
6. D. H. Shi, W. Xing, J. F. Sun and Z. L. Zhu, *Eur. Phys. J. D*, **66**, 173/1 (2012).

7. A. Døssing, *Coord. Chem. Rev*., **306**, 544 (2015).
8. L. R. Peebles and P. Marshall, *Chem. Phys. Lett*., **366**, 520 (2002).
9. T. Y. Takeshita and T. H. Dunning, Jr., *J. Phys. Chem. A*, **119**, 1446 (2015).
10. S. G. Lias, J. E. Bartmess, J. F. Liebman, J. L. Holmes, R. D. Levin and W. G. Mallard, *J. Phys. Chem. Ref. Data*, **17**, 631 (1988).
11. L. Andrews and P. Hassanzadeh, *J. Chem. Soc., Chem. Commun*., 1523 (1994).
12. (a) K. Sundararajan, K. Sankaran and V. Kavitha, *J. Mol. Struct*., **876**, 240 (2008); (b) M. Rekhis, O. Oumerali, L. Joubert, V. Tognetti and C. Adamo, *J. Mol. Struct*., **863**, 79 (2008).
13. A. Døssing, *Trends Inorg. Chem*., **12**, 1 (2010).
14. J. W. Dethlefsen, A. Døssing and E. D. Hedegärd, *Inorg. Chem*., **49**, 8769 (2010); (b) J. W. Dethlefsen and A. Døssing, *Inorg. Chim. Acta*, **362**, 259 (2009).
15. J. W. Dethlefsen, E. D. Hedegärd, R. D. Rimmers, P. C. Ford and A. Døssing, *Inorg*. *Chem*., **48**, 231 (2009).
16. B. L. Tran, R. Thompson, S. Ghosh, X. Gao, C-H. Chen, M-H. Baik and D. J. Mindiola, *Chem. Commun*., **49**, 2768 (2013).
17. T. J. Crevier, S. Lovell and J. M. Mayer, *J. Am. Chem. Soc*., **120**, 6607 (1998).
18. M. G. Scheibel, I. Klopsch, H. Wolf, P. Stollberg, D. Stalke and S. Schneider, *Eur. J. Inorg. Chem*., **2013**, 3454 (2013).
19. H-Y. Ng, W-M. Cheung, E. K. Huang, K-L. Wong, H. H.-Y. Sung, I. D. Williams and W-H. Leung, *J. Chem. Soc., Dalton Trans*., **44**, 18459 (2015).
20. B. J. Frogley, A. F. Hill, R. A. Manzano and. M. Sharma, *Chem. Commun*., **54**, 1702 (2018).
21. P. Guo, B. Peng, Q. Luo, Q. S. Li, Y. Xie and R. B. King, *Inorg. Chim. Acta*, **406**, 119 (2013).
22. S. F. Vyboishchikov and G. Frenking, *Theor. Chem. Acc*., **102**, 300 (1999).
23. C. M. Teague, T. O'Brien and J. F. O'Brien, *J. Coord. Chem*., **55**, 627 (2002).
24. K. K. Pandey and P. Patidar, *Polyhedron*, **68**, 87 (2014).
25. G. Hartmann and R. Mews, *Z. Naturforsch*., **40B**, 343 (1985).
26. D. S. Bohle, C-H. Hung, A. K. Powell, B. D. Smith and S. Wocadlo, *Inorg. Chem*., **36**, 1992 (1997).
27. C. M. Mikulski, P. J. Russo, M. S. Soran, A. G. MacDiarmid, A. F. Garito and A. J. Heeger, *J. Am. Chem. Soc*., **97**, 6358 (1975).
28. A. J. Banister and Z. V. Hauptman, *J. Chem. Soc., Dalton Trans*., 731 (1980).

29. T. Chivers, A. W. Cordes, R. T. Oakley and P. N. Swepston, *Inorg. Chem*., **20**, 2376 (1981).
30. H. M. Tuononen, R. Suontamo, J. Valkonen and R. S. Laitinen, *J. Phys. Chem. A*, **109**, 6309 (2005).
31. R. Evans, A. J. Downs, R. Köppe and S. C. Peake, *J. Phys. Chem. A*, **115**, 5127 (2011).
32. M. J. Cohen, A. F. Garito, A. J. Heeger, A. G. MacDiarmid, C. M. Mikulski, M. S. Soran and J. Kleppinger, *J. Am. Chem. Soc*., **98**, 3844 (1976).
33. A. Perrin, A. F. Antognini, X. Zeng, H. Beckers, H. Willner and G. Rauhut, *Chem. Eur. J*., **20**, 10323 (2014).
34. W. Zou, D. Izotov and D. Cremer, *J. Phys. Chem. A*, **115**, 8731 (2011).
35. A. J. Bridgeman and B. Cunningham, *Spectrochim. Acta Part A*, **60**, 471 (2004).
36. (a) R. S. P. King, P. F. Kelly, S. E. Dean and R. J. Mortimer, *Chem. Commun*., 4812 (2007); (b) P. F. Kelly, R. S. P. King and R. J. Mortimer, *Chem. Commun.,* 6111 (2008); (c) S. M. Bleay, P. F. Kelly, R. S. B. King, *J. Mater. Chem*., **20**, 10100 (2010).
37. (a) S. M. Bleay, P. F. Kelly, R. S. P. King and S. G. Thorngate, *Science & Justice,* **59**, 606, (2019); (b) http://www.ffsupport.co.uk/Distributor/Brochures/RECOVER_LFT.pdf.
38. T. T. Takaluoma, K. Laasonen and R. S. Laitinen, *Inorg. Chem*., **52**, 4648 (2013).
39. (a) K. Dehnicke and U. Müller, *Transition Metal Chem*., **10**, 361 (1985); (b) M. N. K. Sadik and S. De, *Chemistry Select*, **5**, 12176 (2020)
40. P. F. Kelly and A. M. Z. Slawin, *J. Chem. Soc., Dalton Trans*., 4029 (1996).
41. (a) P. F. Kelly and A. M. A. Slawin, *Angew. Chem. Int. Ed. Engl*., **34**, 1758 (1995); (b) S. M. Aucott, S. H. Dale, M. R. J. Elsegood, K. E. Holmes, S. L. M. James and P. F. Kelly, *Acta Crystallogr. Sect. C*, **60**, m643 (2004); (c) S. M. Aucott, D. Drennan, S. L. M. James, P. F. Kelly and A. M. Z. Slawin, *Chem. Commun.* 3054 (2007).
42. A. Datta, *Phys. Chem. Chem. Phys*., **11**, 11054 (2009).
43. T. L. Roemmele, J. Konu, R. T. Boeré and T. Chivers, *Inorg. Chem*., **48**, 9454 (2009).
44. A. Maaninen, J. Siivari, R. S. Laitinen and T. Chivers, *Inorg. Synth*., **33**, 196 (2002).
45. E-C. Koch and M. Suceska, *Z. Anorg. Allg. Chem*., **647**, 192 (2021).
46. J. Siivari, T. Chivers and R. S. Laitinen, *Inorg. Chem*., **32**, 1519 (1993).
47. W. Clegg, S. H. Dale, D. Drennan and P. F. Kelly, *Dalton Trans*., 3140 (2005).

48. J. Konu, A. Maaninen, K. Paananen, P. Ingman, R. S. Laitinen, T. Chivers and J. Valkonen, *Inorg. Chem*., **41**, 1430 (2002).
49. J. Konu, T. Bajorek, R. S. Laitinen, T. Chivers, R. J. Suontamo and M. Ahlgren, *Eur. J. Inorg. Chem*., **2006**, 2951 (2006).
50. M. K. Si and B. Ganguly, *Chem. Phys. Lett*., **713**, 160 (2018).
51. D. V. Konarev, E. F. Valeev, Y. L. Slovokhotov and R. N. Lyobovskaya, *J. Phys. Chem. Solids*, **58**, 1865 (1997).
52. R. T. Boeré, T. Chivers, T. L. Roemmele and H. M. Tuononen, *Inorg. Chem*., **48**, 7294 (2009).
53. (a) E. A. Pritchina, N. P. Gritsan, A. V. Zibarev and T. Bally, *Inorg. Chem*., **48**, 4075 (2009); (b) E. A. Pritchina, D. S. Terpilovskaya, Y. P. Tsentalovich, M. S. Platz and N. P. Gritsan, *Inorg. Chem*., **51**, 4747 (2012).
54. J. Bojes and T. Chivers, *Inorg. Chem*., **17**, 318 (1977).
55. T. Chivers and R. S. Laitinen, *Phys. Sci. Rev*., **4** (5), 2017–0125 (2019).
56. (a) P. Hassanzadeh and L. Andrews, *J. Am. Chem. Soc*., **114**, 83 (1992); (b) L. Andrews and P. Hassanzadeh. *J. Chem. Soc., Chem. Commun*., 1523 (1994).
57. G-H. Zang, Y-F. Zhao, J. I. Wu and P. v. R. Schleyer, *Inorg. Chem*., **51**, 13321 (2012).
58. H. Xiao, X. Shi, X. Liao, Y. Zhang and X. Chen, *Phys. Rev. Mater.*, **2**, 024002 (2018).
59. Y. Chen, X. Liao, X. Shi, H. Xiao, Y. Liu and X. Chen, *Phys. Chem. Chem. Phys*., **21**, 5916 (2019).
60. T. Chivers, P. W. Codding, W. G. Laidlaw, S. W. Liblong, R. T. Oakley and M. Trsic, *J. Am. Chem. Soc*., **105**, 1186 (1983).
61. C. Wentrup and P. Kambouris, *Chem. Rev*., **91**, 363 (1991).
62. J.-H. Lin, H. Zhang, X-L. Cheng and Y. Miyamato, *Phys. Rev. B*, **94**, 195404 (2016).
63. (a) F. Li, X. Lv, J. Gu, K. Tu, J. Gong, P. Jin and Z. Chen, *Nanoscale*, **12**, 85 (2020); (b) X. Qiao, X. Lv, Y. Yang and F. Li, *Phys. Status Solidi B*, 2100178 (2021).
64. D. Li, F. Tian, Y. Z. Lv, S. Wei, D. Duan, B. Liu and T. Cui, *J. Phys. Chem. C*, **121**, 1515 (2017).
65. D. Laniel, M. Bykov, T. Fedotenko, A. V. Ponomareva, I. A. Abrikosov, K. Glazyrin, V. Svitlyk, L. Dubrovinsky and N. Dubrovinskaia, *Inorg. Chem*., **58**, 9195 (2019).
66. T. Klapötke and A. Schulz, *Polyhedron*, **15**, 4387 (1996).
67. (a) M. K. Cyranski, T. M. Krygowski, A. R. Katritzky and P. v. R. Schleyer, *J. Org. Chem*., **67**, 1333 (2002); (b) M. K. Cyranski, P. v. R. Schleyer, H. Jiao and G. Hohlneicher, *Tetrahedron*, **59**, 1657 (2003).

68. L. J. Wang and P. G. Mezey, *Chem. Phys. Lett.*, **387**, 233 (2004).
69. G-H. Zhang, Y-F. Zhao, J. I. Wu and P. v. R. von Schleyer, *Inorg. Chem.*, **48**, 6773 (2009).
70. D. Glossman-Mitnik, *Theor. Chem. Acc.*, **117**, 57 (2007).
71. P. W. Fowler, C. W. Rees and A. Soncini, *J. Am. Chem. Soc.*, **126**, 11202 (2004).
72. J. Bojes, T. Chivers, I. Drummond and G. MacLean, *Inorg. Chem.*, **17**, 3668 (1978).
73. W. S. Sheldrick, M. N. S. Rao and H. W. Roesky, *Inorg. Chem.*, **19**, 538 (1980).
74. (a) T. Chivers and J. Proctor, *J. Chem. Soc., Chem. Commun.*, 642 (1978); (b) T. Chivers and J. Proctor, *Can. J. Chem.*, **57**, 1286 (1979).
75. W. Wang, H. Wang, Y. Liu, F. Tian, D. Duan, H. Yu and T. Cui, *Inorg. Chem.*, **58**, 2397 (2019).
76. W. Mosa, C. Lau, M. Möhlen, B. Neumüller and K. Dehnicke, *Angew. Chem. Int. Ed. Engl.*, **37**, 2840 (1998).
77. T. M. Klapötke, B. Krumm, M. Scherr, R. Haiges and K. O. Christe, *Angew. Chem. Int. Ed.*, **46**, 8686 (2007).
78. (a) T. M. Klapötke, B. Krumm, P. Mayer and I. Schwab, *Angew. Chem. Int. Ed.*, **42**, 5843 (2003); (b) R. Haiges, J. A. Boatz, A. Vij, M. Gerken, S. Schneider, T. Schroer and K. O. Christe, *Angew. Chem. Int. Ed.*, **42**, 5847 (2003); (c) C. Knapp and J. Passmore, *Angew. Chem. Int. Ed.*, **43**, 4834 (2004).
79. (a) A. Apblett, A. J. Banister, D. Biron, A. G. Kendrick, J. Passmore, M. Schriver and M. Stojanac, *Inorg. Chem.*, **25**, 4451 (1986); (b) A. Apblett, T. Chivers and J. F. Fait, *Inorg. Chem.*, **29**, 1643 (1990); (c) J. Passmore and M. Schriver, *Inorg. Chem.*, **27**, 2751 (1988).
80. J. Cernicharo, B. Lefloch, M. Agúndez, S. Bailleux, L. Margulθs, E. Roueff, R. Bachiller, N. Marcelino, B. Tercero, C. Vastel and E. Caux, *Astrophys. J. Lett.*, **853**, L22 (2018).
81. T. S. Cameron, A. Mailman, J. Passmore and K. V. Shuvaev, *Inorg. Chem.*, **44**, 6524 (2005).
82. C. Knapp, A. Mailman, G. B. Nikiforov and J. Passmore, *J. Fluorine Chem.*, **127**, 916 (2006).
83. S. Parsons and J. Passmore, *Acc. Chem. Res.*, **27**, 101 (1994).
84. (a) S. Herler, P. Mayer, H. Nöth, A. Schulz, M. Suter and M. Vogt, *Angew. Chem. Int. Ed. Engl.*, **40**, 3173 (2001); (b) A. Haas, *Z. Anorg. Allg. Chem.*, **628**, 673 (2002).
85. (a) T. Chivers and R. S. Laitinen, in *Handbook of Chalcogen Chemistry: New Perspectives in Sulfur, Selenium and Tellurium*, Ed. F. Devillanova,

Royal Society of Chemistry (2006), Ch. 4, pp. 223–285; (b) T. Chivers, *Acc. Chem. Res*., **17**, 166 (1984).
86. (a) S. De, M. N. K. Sadik and S. Liya, *ChemistrySelect*, **4**, 8807 (2019); (b) Z. Cui, H. Lischka, H. Z. Beneberu and M. Kertesz, *J. Am. Chem. Soc*., **136**, 12958 (2014); (c) A. Apblett, T. Chivers, A. W. Cordes and R. Vollmerhaus, *Inorg. Chem*., **30**, 1392 (1991).
87. J. R. Galan-Mascaros, A. M. Z. Slawin, J. D. Woollins and D. J. Williams, *Polyhedron*, **15**, 4603 (1996).
88. (a) T. Chivers, L. Fielding, W. G. Laidlaw and M. Trsic, *Inorg. Chem*., **18**, 3379 (1979); (b) C. Knapp, E. Lork, T. Borrmann, W-D. Stohrer and R. Mews, *Z. Anorg. Allg. Chem*., **631**, 1885 (2005).
89. (a) T. Chivers and R. S. Laitinen, *Chem. Soc. Rev*., **46**, 5182 (2017); (b) T. Chivers and R. T. Oakley, *Topics Curr. Chem*., **102**, 117 (1982).
90. R. T. Boeré, T. L. Roemmele and M. K. Krall, *Molecules,* **19**, 1956 (2014).
91. P. F. Kelly, A. M. Z. Slawin, D. J. Williams and J. D. Woollins, *Chem. Soc. Rev*., **21**, 245 (1992).
92. M. Herberhold and W. Ehrenreich, *Angew. Chem. Int. Ed. Engl*., **21**, 633 (1982).
93. T. Borrman, E. Lork, R. Mews, M. M. Shakirov and A. V. Zibarev, *Eur. J. Inorg. Chem*., **2004**, 2452 (2004).
94. T. Chivers and M. Hojo, *Inorg. Chem*., **23**, 2738 (1984).
95. P. Dubois, J. P. Lelieur and G. Lepoutre, *Inorg. Chem*., **28**, 2489 (1989).
96. (a) P. Vilarrubias, *Mol. Phys*., **118**, e1797915 (2020); (b) J. Valjus, H. M. Tuononen, R. S. Laitinen and T. Chivers, *Can. J. Chem*., **96**, 591 (2018).
97. J. Bojes, T. Chivers, W. G. Laidlaw and M. Trsic, *J. Am. Chem. Soc*., **104**, 4837 (1982).
98. J. Bojes, T. Chivers and P. W. Codding, *Chem. Commun*., 1171 (1981).
99. T. Chivers and I. Drummond, *Inorg. Chem*., **13**, 1222 (1974).
100. T. Chivers and K. J. Schmidt, *Can. J. Chem*., **70**, 719 (1992).
101. (a) T. Chivers, W. G. Laidlaw, R. T. Oakley and M. Trsic, *J. Am. Chem. Soc*., **102**, 5773 (1980); (b) N. Burford, T. Chivers, A. W. Cordes, R. T. Oakley, W. T. Pennington and P. N. Swepston, *Inorg. Chem*., **20**, 4430 (1982): (c) T. Chivers and C. Lau, *Inorg. Chem*., **21**, 453 (1982).
102. (a) M. J. Loeffler, R. L. Hudson, N. J. Chanover and A. A. Simon, *Icarus*, **271**, 265 (2016); (b) M. J. Loeffler, R. L. Hudson, N. J. Chanover and A. A. Simon, *Icarus*, **258**, 181 (2015).
103. P. Dubois, J. P. Lelieur and G. Lepoutre, *Inorg. Chem*., **28**, 2489 (1989).
104. (a) T. Chivers and P. J. W. Elder, *Chem. Soc. Rev*., **42**, 5996, (2013); (b) R. Steudel and T. Chivers, *Chem. Soc. Rev*., **48**, 3279 (2019).

105. W. Przychodzen, J. Chojnacki and l. Nierzwicki, *New. J. Chem*., **43**, 15413 (2019).
106. T. Chivers, F. Edelmann, U. Behrens and R. Drews, *Inorg. Chim. Acta*, **116**, 145 (1986).
107. T. Chivers and F. Edelmann, *Polyhedron*, **5**, 1661 (1986).
108. P. F. Kelly and J. D. Woollins, *Polyhedron*, **5**, 607 (1986); (b) J. D. Woollins, in *The Chemistry of Inorganic Ring Systems*, Ed. R. Steudel, Elsevier (1992), Vol. 14, Ch. 18, pp. 349-372.
109. F. Edelmann, H. W. Roesky, C. Spang, M. Noltemeyer and G. M. Sheldrick, *Angew. Chem. Int. Ed. Engl*., **25**, 931 (1986).
110. P. S. Belton, V. C. Ginn, P. F. Kelly and J. D. Woollins, *J. Chem. Soc., Dalton Trans.*, 1135 (1992).
111. R. T. Boeré, *Cryst. Growth Des*., **14**, 814 (2014).
112. V. Matuska, K. Tersago, P. Kilian, C. van Alsenoy, F. Blockhuys, A. M. Z. Slawin and J. D. Woollins, *Eur. J. Inorg. Chem*., **2009**, 4483 (2009).
113. J. Van Droogenbroeck, C. Van Alsenoy, S. M. Aucott, J. D. Woollins, A. D. Hunter and F. Blockhuys, *Organometallics*, **24**, 1004 (2005).
114. F. T. Edelmann, S. Blaurock, V. Lorenz and T. Chivers, *Z. Anorg. Allg. Chem*., **634**, 413 (2008).
115. A. A. Fagin, G. K. Fukin, A. V. Cherkasov, A. F. Shestakov, A. P. Pushkarev, T. V. Balashova, A. A. Maleev and M. N. Bochkarev, *Dalton Trans*., **45**, 4558 (2016).
116. V. Matuska, A. M. Slawin and J. D. Woollins, *Inorg. Chem*., **49**, 3064 (2010).
117. A. M. Slawin, P. G. Waddell and J. D. Woollins, *Acta Cryst. Sect. E Struct. Rep*., **E66**, m418 (2010).
118. J. Van Droogenbroeck, C. Van Alsenoy and F. Blockhuys, *J. Phys. Chem. A*, **109**, 4847 (2005).
119. J. Oláh, T. Veszprémi, J. D. Woollins and F. Blockhuys, *Dalton Trans*., **39**, 3256 (2010).
120. (a) K. Tersago, J. D. Woollins, C. Van Alsenoy and F. Blockhuys, *Chem. Phys. Lett*., **423**, 422 (2006); (b) K. Tersago, V. Matsuka, C. Van Alsenoy, A. M. Z. Slawin, J. D. Woollins and F. Blockhuys, *Dalton Trans*., 4529 (2007).
121. (a) J. Van Droogenbroeck, K. Tersago, C. Van Alsenoy, S. M. Aucott, H. L. Milton, J. D. Woollins and F. Blockhuys, *Eur. J. Inorg. Chem*., **2004**, 3798 (2004); (b) F. Blockhuys, K. Tersago, S. A. Shlykov, A. Konrad and D. Christen, *J. Mol. Struct*., **978**, 147 (2010).
122. J. Bojes and T. Chivers, *J. Chem. Soc., Chem. Commun*., 453 (1977).

123. J. Bojes and T. Chivers, *Inorg. Chem*., **17**, 318 (1978).
124. J. Bojes, T. Chivers, W. G. Laidlaw and M. Trsic, *J. Am. Chem. Soc*., **101**, 4517 (1979).
125. A. J. Banister, M. I. Hansford, Z. V. Hauptman, A. W. Luke, S. T. Wait, W. Clegg and K. A. Jorgensen, *J. Chem. Soc., Dalton Trans*., 2793 (1990).
126. P. N. Jagg, P. F. Kelly, H. S. Rzepa, D. J. Williams, J. D. Woollins and W. Wylie, *J. Chem. Soc., Chem. Commun*., 942 (1991).
127. (a) O. J. Scherer and G. Wolmershäuser, *Angew. Chem. Int. Ed. Engl*., **14**, 485 (1975); (b) W. Flues, O. J. Scherer, J. Weiss and G. Wolmershäuser, *Angew. Chem. Int. Ed. Engl*., **15**, 379 (1976).
128. O. J. Scherer and G. Wolmerhäuser, *Chem. Ber.*, **110**, 3241 (1977).
129. J. Bojes, T. Chivers and R. T. Oakley, *Inorg. Synth*., **25**, 30 (1989).
130. R. T. Boeré, T. L. Roemmele and M. R. Krall, *Molecules*, **19**, 1956 (2014).
131. T. Chivers and J. Proctor, *Can. J. Chem*., **57**, 1286 (1979).

Chapter 6

Short-Lived Chalcogen-Nitrogen Molecules: Matrix Isolation

6.1 Introduction

As a sequel to the discussions on the applications of physical methods to the characterisation of chalcogen-nitrogen compounds (Chapter 3) and the chemistry of binary chalcogen-nitrogen species (Chapter 5), this chapter will deal specifically with the methods used for the generation and identification of short-lived chalcogen-nitrogen molecules, including neutral radical species. In early work simple binary chalcogen nitrides such as NS, NSe, NS_2 and NSe_2 were produced in an argon/nitrogen/chalcogen microwave discharge and trapped in solid argon at 12 K (Secs. 5.3.1 and 5.6.1).[1] The identification of these ephemeral species was accomplished by IR spectroscopy on matrix-isolated samples with the assistance of isotopic substitution (^{15}N, ^{34}S, ^{76}Se and ^{80}Se).

In more recent investigations there has been an intense interest in the synthesis and characterisation of short-lived, ternary S,N,O neutral molecules and anions in view of their importance in fields as diverse as atmospheric chemistry and biological signaling, *cf.* NO/H_2S "crosstalk" (Sec. 7.11). Since these species are often generated from a suitable azide either photochemically by using flash photolysis or thermally *via* pyrolysis, this chapter will begin with a discussion of the synthesis, structures and properties of the sulfonyl azides XSO_2N_3 (X = F, Cl, CF_3) and sulfuryl diazide

$O_2S(N_3)_2$. The subsequent sections will describe (a) $[NSO]^{\bullet}$, $[NSO_2]^{\bullet}$, $[SNO]^{\bullet}$ and $[SSNO]^{\bullet}$ radicals, (b) the conjugate acids HNSO and $HNSO_2$, (c) the isomeric radicals $[H_2NSO]^{\bullet}$ and $[HNSOH]^{\bullet}$, (d) the heterocumulene radicals $[OENSO]^{\bullet}$ (E = C, S), (e) ternary S,N,P molecules, and (f) short-lived isomers of S_2N_2 and S_4N_4. As in the early work, identification of the matrix-isolated molecules is achieved by comparing the IR spectra of natural abundance and ^{15}N-labeled samples. The structures, relative energies of isomers and their interconversion barriers are determined by quantum chemical calculations. The fundamental chemistry of ternary S,N,O anions and their relevance to biological systems are discussed in Chapter 7.

6.2 Sulfonyl Azides, XSO_2N_3 (X = F, Cl, CF_3), and Sulfuryl Diazide, $O_2S(N_3)_2$

6.2.1 *Synthesis and structures*

Fluorosulfonyl azide FSO_2N_3 and trifluoromethylsulfonyl azide $CF_3SO_2N_3$ were first prepared by reactions of sodium azide with the acid anhydrides $(FSO_2)O$ and $(CF_3SO_2)_2O$, respectively.[2a] They are both liquids at room temperature, but X-ray crystal structures have been obtained at very low temperatures. In the solid state these two sulfonyl azides both exist as a single conformer in which one of the S=O bonds is in a *syn*-periplanar position to the NNN group with respect to the S–N bond (Fig. 6.1a).[2a] This arrangement is attributed to negative hyperconjugation (an $n_{\sigma}(N) \rightarrow \sigma^*(S–O)$ interaction) on the basis of DFT calculations. The S–N bond lengths in these sulfonyl azides are both 1.648 Å. Chlorosulfonyl azide $ClSO_2N_3$ has been prepared by the reaction of SO_2Cl_2 with sodium azide in the absence of solvent and characterised by IR and Raman spectroscopy.[2b] Trifluoromethylsulfonyl azide $CF_3SO_2N_3$ is a useful precursor for the generation of N,S,O radicals (Sec. 6.3).

Sulfuryl diazide $O_2S(N_3)_2$ is prepared on a small scale by reaction of SO_2Cl_2 with sodium azide in acetonitrile (Eq. 6.1).[2b] It is a colourless liquid with a melting point of –15°C, but does not decompose at room temperature. Crystal structure determination revealed two

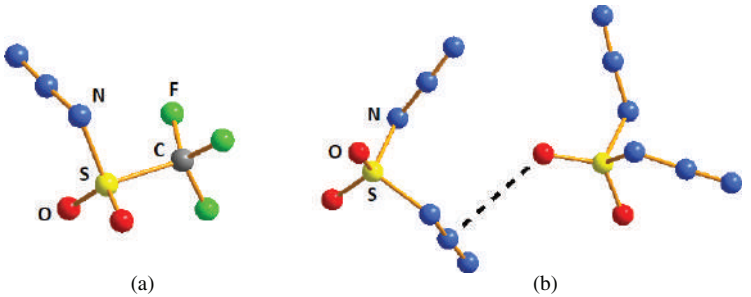

Figure 6.1. Molecular structures of (a) $CF_3SO_2N_3$ [2a] and (b) $O_2S(N_3)_2$.[2b]

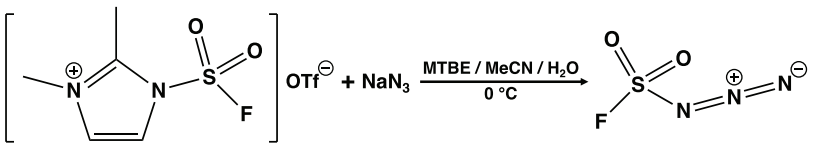

Scheme 6.1. Synthesis of fluorosulfonyl azide.

crystallographically non-equivalent molecules in the unit cell with a very weak N···O interaction between them (Fig. 6.1b). The two azido groups in both molecules are oriented in an *anti* configuration with respect to the NSN plane. The mean S–N bond length is 1.666 Å.

$$O_2SCl_2 + 2NaN_3 \rightarrow O_2S(N_3)_2 + 2NaCl \qquad (6.1)$$

6.2.2 *Applications*

Fluorosulfonyl azide FSO_2N_3 has been used as a diazotising agent for the preparation of a wide variety of azides and 1,2,3-triazoles from primary amines.[3a] For this application the *in situ* reagent is generated in *ca.* 90% yield from the rapid reaction of a commercially available imidazolium fluorosulfonyl triflate salt with sodium azide in a biphasic system of water and methyl *tert*-butyl ether (MTBE)/acetonitrile (Scheme 6.1). Fluorosulfonyl azide has also been used for the amine-to-azide conversion on native RNA.[3b]

6.3 $[NSO]^{\bullet}$, $[NSO_2]^{\bullet}$, $[SNO]^{\bullet}$ and $[SSNO]^{\bullet}$ Radicals

The sulfonyliminyl $[NSO_2]^{\bullet}$ and sulfinyliminyl $[NSO]^{\bullet}$ radicals have been generated by a similar approach.[4] In both cases the precursor is an azide, RSO_2N_3 (R = CH_3, CF_3) and $CF_3S(O)N_3$, respectively. Flash vacuum pyrolysis of $CF_3SO_2N_3$ highly diluted in argon is conducted in a quartz furnace at *ca.* 800°C.[4] Similar experiments using a 1:1 mixture of the ^{15}N-labeled precursors $CF_3SO_2{}^{15}NNN$ and $CF_3SO_2NN^{15}N$ enabled the assignment of the IR spectrum of $[NSO_2]^{\bullet}$, which exhibits strong antisymmetric and symmetric SO_2 stretching vibrations at 1359 and 1217 cm^{-1} and an S–N stretch at 967 cm^{-1}. DFT calculations predict a planar molecule with C_{2v} symmetry for $[NSO_2]^{\bullet}$, d(S=N) = 1.517 Å and d(S=O) = 1.429 Å (Chart 6.1a). The corresponding anion $[O_2SN]^{-}$ has not been structurally characterised in the solid state (Sec. 7.4). However, calculations for the anion reveal a shortened S=N bond length (1.458 Å) and elongated S=O bonds (1.477 Å) (Chart 6.1b), indicating that the unpaired electron in the $[NSO_2]^{\bullet}$ radical is located in a π(NS)-bonding molecular orbital.[4] In a solid argon matrix the $[NSO_2]^{\bullet}$ radical undergoes a photorearrangement into the planar bent isomers, *syn* and *anti* $[OSNO]^{\bullet}$.

Flash vacuum pyrolysis of FSO_2N_3 under similar conditions to those used for $CF_3SO_2N_3$ (*vide supra*) produced triplet fluorosulfonylnitrene FSO_2N, which was trapped in an argon matrix at 16 K and identified by IR and UV-visible spectroscopy in combination with DFT calculations.[5a] The nitrene FSO_2N undergoes a photoinduced rearrangement to $FNSO_2$ in a solid noble gas matrix.[5a] Fluorosulfonylnitrene FSO_2N has also been generated from FSO_2N_3 by laser irradiation (λ = 193 nm).[5b] Photolysis ($\lambda > 320$ nm) of the matrix-isolated nitrene produced the sulfinyl nitrite FS(O)NO.[5b] Sulfinyl nitrites RS(O)NO are thought to play an important

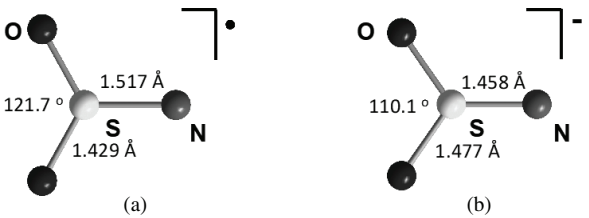

Chart 6.1. Calculated molecular structures of (a) $[NSO_2]^{\bullet}$ and (b) $[NSO_2]^{-}$.[4]

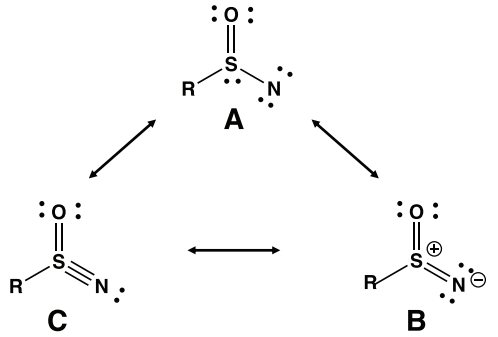

Scheme 6.2. Resonance structures of sulfinylnitrenes RS(O)N.

role in the atmospheric oxidation of volatile organosulfur compounds by oxides of nitrogen.

Flash vacuum pyrolysis of the sulfinyl azide $CF_3S(O)N_3$ at 350°C generated the sulfinylnitrene $CF_3S(O)N$, which was characterised by matrix-isolation IR spectroscopy.[6a] Three resonance structures for sulfinyl nitrenes are shown in Scheme 6.2.[6b] The IR spectrum of $CF_3S(O)N$ indicates that this nitrene prefers the zwitterionic structure (**B**) rather than the alternative forms **A** and **C**.[6a] At 600°C cleavage of the CF_3–S bond in the nitrene produced the sulfinyliminyl radical $[NSO]^{\bullet}$, which was identified by IR spectroscopy. The experimental values of the two stretching vibrations (1198 and 995 cm^{-1}) are in excellent agreement with the calculated data for $[NSO]^{\bullet}$.[6a,7]

The isomeric $[SNO]^{\bullet}$ radical was identified in earlier investigations by IR spectroscopy during the photolysis of HNSO[8a] and the reaction of sulfur atoms with NO in solid noble-gas matrices.[8b,c] High-level coupled cluster calculations predict that $[NSO]^{\bullet}$ is lower in energy than the $[SNO]^{\bullet}$ isomer by *ca.* 7.1 kJ mol^{-1}.[9] The $[SNO]^{\bullet}$ radical is of considerable interest in environmental chemistry, *e.g.*, as an intermediate in the combustion of sulfur-containing fuels.[10a] It has also been suggested that the $[SNO]^{\bullet}$ radical could be formed in the lower atmosphere of Venus.[10b,c]

The $[SSNO]^{\bullet}$ radical has been prepared by the reaction of thermally generated disulfur (S_2) with $^{\bullet}NO$ in the gas phase. It was isolated in argon or N_2 matrices and characterised by vibrational spectroscopy, including ^{15}N-labelled samples, in conjunction with quantum chemical calculations.[11] A bonding analysis shows that the unpaired electron in $[SSNO]^{\bullet}$ is

mainly localised on the SS moiety. Isomerisation of $[SSNO]^{\bullet}$ occurs upon irradiation with a 266 nm laser to give the sulfinyl radicals *cis*- and *trans*-$[NSSO]^{\bullet}$ and the thiyl radicals *cis*- and *trans*-$[OSNS]^{\bullet}$.[11a] Significantly, the $[SSNO]^{\bullet}$ radical is the one-electron oxidation product of the well-characterised perthionitrite anion $[SSNO]^{-}$ (oxidation potential +0.46 V), which may play a role in the Gmelin reaction (Sec. 7.9.3) as well as in NO/H_2S crosstalk in biological signaling (Sec. 7.11).

6.4 Conjugate Acids, HNSO and $HNSO_2$

The neutral molecules HNSO and $HNSO_2$ are formally derived from the $[NSO]^{\bullet}$ and $[NSO_2]^{\bullet}$ radicals by combination with a hydrogen atom. They are the conjugate acids of the ternary anions $[NSO]^{-}$ and $[NSO_2]^{-}$ discussed in Secs. 7.2 and 7.4, respectively. Monomeric HNSO is a gas which, at low temperatures, forms a colourless liquid that quickly polymerises to a brown solid, polythionylimide $(HNSO)_x$, at ambient temperatures.[12] The monomer can be produced *in situ* by protonation of K[NSO] with stearic acid and then stabilised by adduct formation with $B(C_6F_5)_3$ (Scheme 6.3).[13] Transition-metal complexes of the HNSO ligand were prepared from NSF complexes by reaction with Me_3SnOH and characterised by IR and NMR spectra in early work, but no structural information was obtained.[14]

The X-ray structure of the adduct $HNSO{\cdot}B(C_6F_5)_3$ reveals that the HNSO ligand is bonded to the strong Lewis acid $B(C_6F_5)_3$ through the N atom and adopts a *cis* conformation with *d*(S–N) = 1.530 Å, *d*(S=O) = 1.427 Å, and <N–S–O = 114.3° (Fig. 6.2).[13] The corresponding data for the free ligand, *cis*-HNSO, obtained by microwave spectroscopy are *d*(S–N) = 1.5123 Å, *d*(S=O) = 1.4513 Å, and <N–S–O = 120.41°.[15] The co-existence of *cis* and *trans* isomers of the ligand in the adduct was

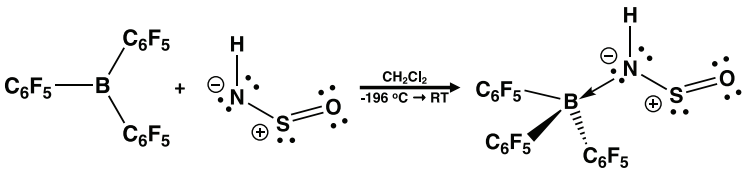

Scheme 6.3. Synthesis of a Lewis acid adduct of *cis*-HNSO.

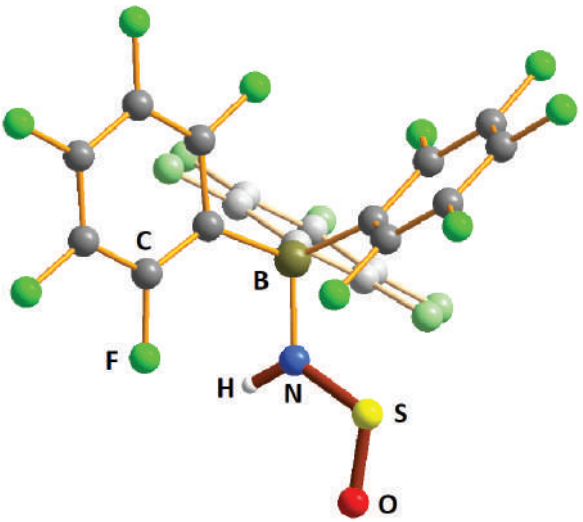

Figure 6.2. Molecular structure of HNSO·B(C_6F_5)$_3$.[13]

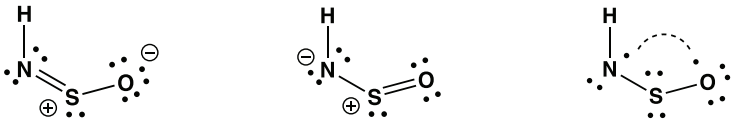

Chart 6.2. Contributions of three resonance structures to the bonding of *cis*-HNSO.[13]

apparent from the temperature-dependent ^{1}H NMR spectra in solution. The estimated energy difference for *cis*- and *trans*-HNSO is ≤8.3 kJ mol^{-1} on the basis of experimental and computational data.[13,16] The structural isomers NSOH and *cis*- or *trans*-HSNO are substantially higher in energy than *cis*-HNSO. The identification and biological significance of the isomer HSNO (thionitrous acid) is discussed in Sec. 7.6. A bonding description for *cis*-HNSO derived from Natural Resonance Theory calculations is shown in Chart 6.2.[13]

The existence of $HNSO_2$ was first proposed in the 1950s.[17] The significance of this short-lived monomer is manifested by its involvement in the medicinal chemistry of sulfamates $ArOSO_2NH_2$ (Ar = aryl),[18] in atmospheric chemistry through the reaction between the radicals $HS^{\bullet}$ and $^{\bullet}NO$,[19] and in biochemistry from the reaction of H_2S with peroxynitrite

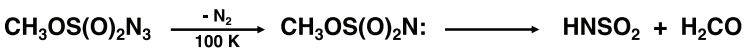

Scheme 6.4. Formation of $HNSO_2$ (g) by photolysis of methoxysulfonyl azide.

$[ONOO]^-$.[20] Although the cyclic trimer $(HNSO_2)_3$ was isolated in early work,[21] the monomer $HNSO_2$ has only been characterised recently.[22]

Similar to the behaviour of HNSO, the parent *N*-sulfonylamine $HNSO_2$ is generated by flash vacuum photolysis of methoxysulfonyl azide at *ca.* 1000 K and characterised by matrix isolation IR spectroscopy.[22] This transformation occurs *via* a nitrene intermediate (Scheme 6.4). Upon 193 nm laser irradiation, $HNSO_2$ forms the structural isomer *N*-hydroxysulfinylamine HONSO.[22] This unbranched isomer is calculated to be significantly higher in energy than the branched arrangement in *N*-sulfonylamine $HNSO_2$, which is isoelectronic with SO_3.[22,23] The structure of the related molecule $HNSOF_2$ has been determined by microwave spectroscopy (Sec. 8.3).[24] The NH and SF_2 groups are in a *cis* arrangement with respect to the S=N bond.

There are nine possible isomers of $HNSO_2$.[23] All of these structural arrangements, with the exception of HSONO, incorporate a sulfur-nitrogen bond. A more detailed study of the photochemistry of $HNSO_2$ and $H^{15}NSO_2$ in cryogenic matrices employing IR and UV-visible spectroscopy supported by quantum chemical calculations led to the identification of several of these isomers, including HSONO and the caged radical pair $HOS^{\bullet}\cdots{}^{\bullet}NO$, in addition to *N*-hydroxysulfinylamine HONSO.[25] The hydrolysis of $HNSO_2$ is a potential source of atmospheric H_2SO_4 and NH_3.[23b]

6.5 $[H_2NSO]^{\bullet}$, *syn*- and *anti*-$[HNSOH]^{\bullet}$ Radicals

Dialkylaminosulfinyl radicals $[R_2NSO]^{\bullet}$ (R = Me, Et) have been detected by EPR spectra of the photolysis of bis(dialkylamino)sulfoxides $(R_2N)_2SO_2$ in the presence of a peroxide at *ca.* 160 K using UV light.[26] The simplest aminosulfinyl radical $[H_2NSO]^{\bullet}$ is generated in the gas phase by high vacuum flash pyrolysis of $CF_3S(O)NH_2$ in N_2 (1:1000) at *ca.* 1000 K.[27] Upon UV-light irradiation (365 nm) in an N_2 or argon matrix at 15 K, 1,3-hydrogen migration occurs to give *cis*- and *trans*-$[HNSOH]^{\bullet}$ radicals

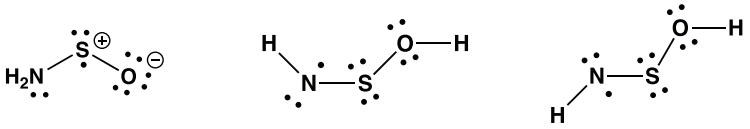

(a) (b) (c)

Chart 6.3. The radicals (a) $[H_2NSO]^{\bullet}$ (b) *cis*-$[HNSOH]^{\bullet}$ and (c) *trans*-$[HNSOH]^{\bullet}$.

(Chart 6.3), which were identified by IR spectroscopy supported by high-level quantum chemical calculations.[27] The calculated S–N bond dissociation energy of $[H_2NSO]^{\bullet}$ is 172.8 kJ mol^{-1} and the barrier to fragmentation of $[HNSOH]^{\bullet}$ into H_2O and $[SN]^{\bullet}$ is 182.0 kJ mol^{-1}. The latter dissociation, accompanied by re-formation of small amounts of $[H_2NSOH]^{\bullet}$, occurs upon 266 nm laser irradiation of $[HNSOH]^{\bullet}$.

The $[HNSOH]^{\bullet}$ radical has one electron more than the diamagnetic, parent sulfur diimide HN=S=NH, which has been shown by ^{1}H NMR spectroscopy to exist as two isomers in solution.[28] In the gas phase *cis,trans* and *cis,cis* isomers of HN=S=NH have been identified by microwave spectroscopy.[29]

6.6 Heterocumulene Radicals, $[OCNSO]^{\bullet}$ and $[OSNSO]^{\bullet}$

The heterocumulene radicals $[OCNSO]^{\bullet}$ and $[OSNSO]^{\bullet}$ are generated from similar precursors and identified by a combination of IR spectroscopy of matrix-isolated species and high-level quantum chemical calculations.[30,31] Flash vacuum pyrolysis of $CF_3S(O)NCO$ in an argon or N_2 atmosphere at *ca.* 1200 K produced the sulfinylisocyanate radical $[OCNSO]^{\bullet}$, which was immediately condensed onto a cold Rh-plated copper block for IR spectroscopic analysis.[30] Both *cis* and *trans* conformers were identified and shown to undergo a reversible interconversion to the more stable *cis* form. Calculated spin densities and atomic charges show that the unpaired electron is located mainly on the sulfinyl moiety for both isomers, with the largest component on the oxygen atom, indicating a major contribution from the ionic resonance form as shown in Fig. 6.3.[30]

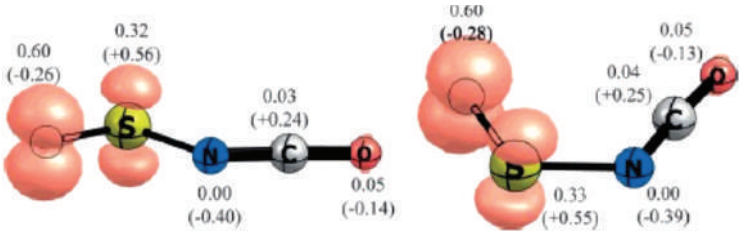

Figure 6.3. UBP86/def2-TVVPP//UCCSD(T)-F12/cc-pVTZ-F12 spin densities and NBO atomic charges (in parentheses) of (a) *trans* and (b) *cis*-[OCNSO]$^{\bullet}$.[30] [Reproduced with permission from Z. Wu, Q. Liu, J. Xu, H. Sun, D. Li, S. Song, D. M. Andrada, G. Frenking, T. Trabelsi, J. S. Francisco and X. Zeng, *Angew. Chem. Int. Ed.*, **56**, 2140 (2017). Copyright 2017 Wiley-VCH Verlag GmbH & Co].

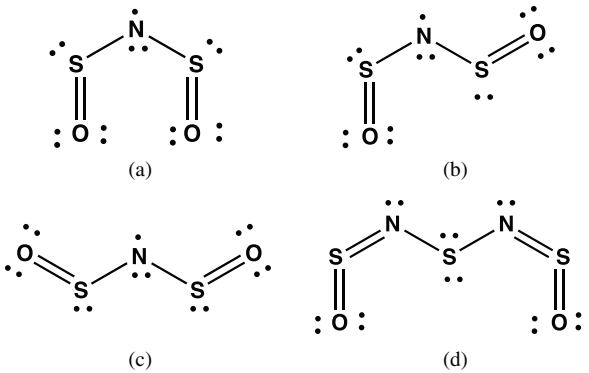

Chart 6.4. Structural arrangements of (a) *cis,cis*-[OSNSO]$^{\bullet}$ (b) *cis,trans*-[OSNSO]$^{\bullet}$ (c) *trans,trans*-[OSNSO]$^{\bullet}$ and (d) OSNSNSO.

In a similar manner flash vacuum pyrolysis of $CF_3S(O)NSO$ at 700 K generated the sulfinylthionylimine radical [OSNSO]$^{\bullet}$ in *cis,cis* and *cis,trans* conformations.[31] The *cis,cis* arrangement is marginally lower in energy than the *cis,trans* conformer and 24.3 kJ mol^{-1} below the *trans,trans* isomer (Chart 6.4a–c).[31] Consistent with electronegativity considerations the central N atom and terminal O atoms carry partial negative charges while the sulfur atoms are positively charged. The spin density values and calculated Wiberg bond indices indicate that the π-bonding in these three conformers is delocalised over the entire molecule.

The diamagnetic bis(sulfinylamino)sulfane OSNSNSO, which is readily prepared by treatment of Me_3SiNSO with SCl_2 (2:1 molar ratio),[32] is formally comprised of $[OSNSO]^{\bullet}$ and $[SN]^{\bullet}$ radicals. In the solid state yellow crystals of OSNSNSO adopt a planar, acyclic structure with a *cis* arrangement about the two S=N bonds (C_{2v} symmetry) (Chart 6.4d).[33,34] The stability of this conformation has been attributed to the electrostatic interaction between the negatively charged terminal O atoms and the positively charged central S atom.[35]

6.7 Ternary S,N,P Molecules

The combination of flash vacuum pyrolysis or photolysis of suitable precursors, including ^{15}N-labelled compounds, followed by IR spectroscopic analysis of matrix-isolated products in conjunction with high-level quantum chemical calculations have enabled the characterisation of short-lived ternary S,N,P molecules.[36] Since a P atom has the same number of electrons as an S^+ cation, these species are isoelectronic with known binary sulfur-nitrogen cations.

The thiophosphoryl triazide $SP(N_3)_3$, a colourless explosive liquid,[37] is a versatile precursor for novel S,N,P species. For example, the pyrolysis of $SP(N_3)_3$ at 1000°C generates the triatomic molecule SPN (Eq. 6.2) together with other nitrogen-containing species, PN, $SN^{\bullet}$ and SN_2.[36a] In an alternative procedure the photolysis of $SP(N_3)_3$ in solid argon generated the most stable isomer SNP as the final product. In both the pyrolysis and photolysis experiments, selective UV irradiations produced linear SPN and *cyclo*-PSN.[36a]

$$SP(N_3)_3 \rightarrow SPN + 4N_2 \qquad (6.2)$$

DFT calculations for linear and cyclic S,P,N isomers indicate that the cyclic isomer is separated from the linear species SNP and SPN by barriers of 138 and 95 kJ mol^{-1}, respectively (Fig. 6.4).[36a] High-level *ab initio* electronic structure calculations for the triatomic molecules E,P,N (E = O, S, Se, Te) confirmed that the nitrogen-centred isomers ENP are the lowest in energy by at least 20.9 kJ mol^{-1}; however, the cyclic isomers become the second lowest-energy isomers for the heavier chalcogens (E = Se, Te).[38]

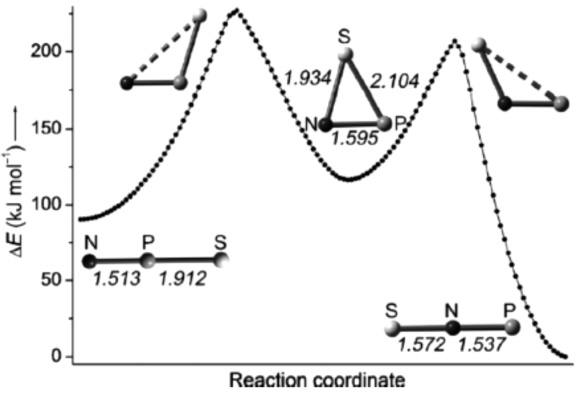

Figure 6.4. Calculated reaction coordinate of S,N,P isomers; bond lengths are given in Å.[36a] [Reproduced with permission from X. Zeng, H. Beckers, H. Willner and J. S. Francisco, *Angew. Chem. Int. Ed.*, **51**, 3334 (2012). Copyright 2012 Wiley-VCH Verlag GmbH & Co].

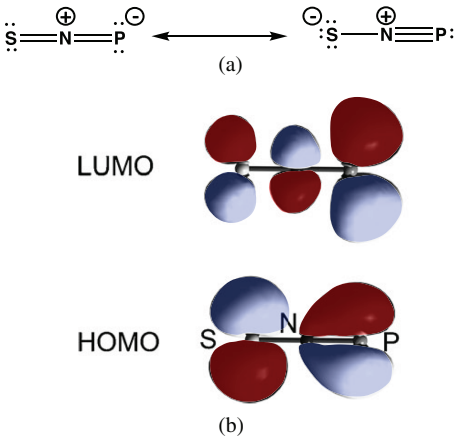

Figure 6.5. (a) Lewis resonance structures and (b) HOMO and LUMO of the isomer SNP.[36a] [Reproduced with permission from X. Zeng, H. Beckers, H. Willner and J. S. Francisco, *Angew. Chem. Int. Ed.*, **51**, 3334 (2012). Copyright 2012 Wiley-VCH Verlag GmbH & Co].

The structure of SNP can be represented by two resonance forms (Fig. 6.5a). This isomer is isoelectronic with the linear sulfur-nitrogen cation $[SNS]^+$ (Sec. 5.8.2), which has an extensive cycloaddition chemistry.[39] The similarity of the frontier orbitals of SNP (Fig. 6.5b) with those

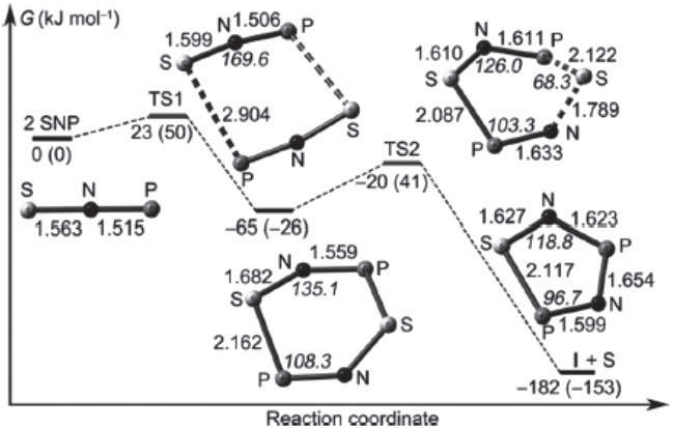

Figure 6.6. Head-to-tail dimerisation of SNP and formation of cyclo-SNPNP; relative energies (kJ mol^{-1}) and computed B3LYP/6-311+G(3df) bond lengths in Å.[36b] [Reproduced with permission from X. Zeng, H. Li, H. Sun, H. Beckers, H. Willner and H. F. Schaefer III, *Angew. Chem. Int. Ed.*, **54**, 1327 (2015). Copyright 2015 Wiley-VCH Verlag GmbH & Co].

of $[SNS]^+$ suggest that the fleeting SNP species could be trapped *via* cycloaddition reactions, *e.g.*, with alkynes or nitriles.[40–42]

A detailed IR analysis of the products of the flash pyrolysis of $SP(N_3)_3$ led to the identification of the five-membered ring, *cyclo*-SNPNP (2,4-diphospha-3,5-diazathiole).[36b] Theoretical calculations support the formation of this cyclic product *via* the head-to-tail dimerisation of SNP to give the six-membered *cyclo*-SNPSNP followed by loss of a sulfur atom (Fig. 6.6). *Cyclo*-SNPNP is a 6π-electron system isoelectronic with the known sulfur-nitrogen dication $[S_3N_2]^{2+}$, which can be isolated as lattice-stabilised salts with $[MF_6]^-$ (M = As, Sb) counter-ions (Sec. 5.8.4).

Molecular electrostatic potentials have been calculated for the three isomers *cyclo*-SNPNP, *cyclo*-SNPPN and *cyclo*-SPNNP and their π-hole interaction energies with EH_3 molecules (E = N, P, As).[43] It was found that these closed-shell non-covalent interactions are stronger than hydrogen bonds.

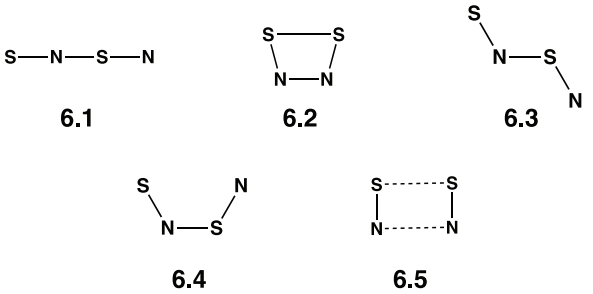

Chart 6.5. Structural arrangements of planar cyclic and acyclic isomers of S_2N_2.

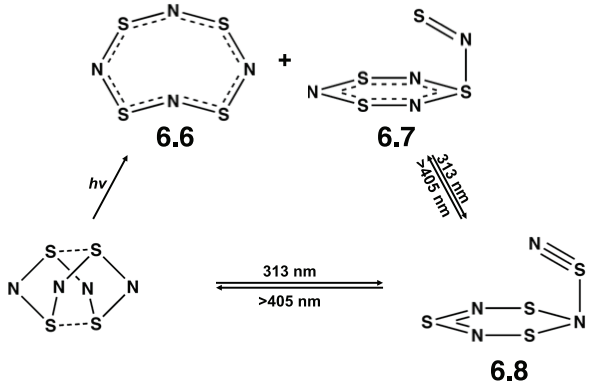

Scheme 6.5. Intermediates formed from photolysis of S_4N_4 in an argon matrix.

6.8 Isomers of S_2N_2

The four-membered ring *cyclo*-S_2N_2 is a precursor of the polymer $(SN)_x$ (Sec. 5.4.2). Although calculations predict both linear SNNS (**6.1**) and cyclic 1,2-dithia-3,4-diazete (**6.2**) (C_{2v}) to be lower in energy than *cyclo*-S_2N_2 (D_{2h}),[44] neither of these isomers has been observed experimentally. Instead, the photolysis of *cyclo*-S_2N_2 using different light sources ($\lambda = 248$ or 255 nm) generated two acyclic, open-shell isomers, *trans*-SNSN (**6.3**) and *cis*-SNSN (**6.4**), together with the closed-shell C_{2v} dimer $(SN)_2$ (**6.5**) as the primary photolysis products.[45] These isomers were identified by

comparing the IR spectra of natural abundance and ^{15}N-enriched samples in solid argon matrices (Chart 6.5). The open-shell isomers **6.3** or **6.4** may be involved in the ring-opening polymerisation of *cyclo*-S_2N_2 to give $(SN)_x$.[46]

6.9 Isomers of S_4N_4

The photochemical behaviour of S_4N_4 in an argon matrix has been investigated in detail and three intermediates (**6.6, 6.7** and **6.8**) were identified by UV-visible and IR spectroscopy in combination with DFT calculations (Scheme 6.5).[47,48] The isomers **6.7** and **6.8** are the result of ring contraction to give a six-membered S_3N_3 ring with an exocyclic thiazyl group. A similar transformation of S_4N_4 to give S_3N_3 derivatives or the anion *cyclo*-$[S_3N_3]^-$ is a common feature of the reaction of S_4N_4 with nucleophiles such as PPh_3 or azide ion, and also occurs in the electrochemical reduction of S_4N_4 (Sec. 3.4.2).[49,50]

References

1. (a) P. Hassanzadeh and L. Andrews, *J. Am. Chem. Soc*., **114**, 83 (1992); (b) L. Andrews and P. Hassanzadeh, *J. Chem. Soc., Chem. Commun*., 1523 (1994).
2. (a) X. Zeng, M. Gerken, H. Beckers and H. Willner, *J. Phys. Chem. A*, **114**, 7624 (2010); (b) X. Zeng, H. Beckers, E. Bernhardt and H. Willner, *Inorg. Chem*., **50**, 8679 (2011).
3. (a) G. Meng, T. Guo, T. Ma, J. Zhang, Y. Shen, K. B. Sharpless and J. Dong, *Nature*, **574**, 86 (2019); (b) O. A. Krasheninina, J. Thaler, M. D. Erlacher and R. Micura, *Angew. Chem. Int. Ed*., **60**, 6970 (2021).
4. X. Zeng, H. Beckers and H. Willner, *Angew. Chem. Int. Ed*., **52**, 7981 (2013).
5. (a) X. Zeng, H. Beckers and H. Willner, *J. Am. Chem. Soc*., **135**, 2096 (2013); (b) X. Zeng, H. Beckers, P. Neuhas, D. Grote and W. Sander, *Z. Anorg. Allg. Chem*., **638**, 526 (2012).

6. (a) Z. Wu, D. Li, H. Li, B. Zhu, H. Sun, J. S. Francisco and X. Zeng, *Angew. Chem. Int. Ed*., **55**, 1507 (2016); (b) T. Q. Davies, M. J. Tilby, J. Ren, N. A. Parker, D. Skole, A. Hall, F. Duarte and M. C. Willis, *J. Am. Chem. Soc*., **142**, 15445 (2020).
7. R. C. Fortenberry and J. S. Francisco, *J. Chem. Phys*., **143**, 084308 (2015).
8. (a) P. O. Tchir and R. D. Spratley, *Can. J. Chem*., **53**, 2331 (1975); (b) L. Andrews, P. Hassanzadeh, G. D. Brabson and A. Citra, *J. Phys. Chem*., **100**, 8273 (1996); (c) M. Bahou and Y.-P. Lee, *J. Chem. Phys*., **115**, 10694 (2011).
9. M. Kumar and J. S. Francisco, *J. Phys. Chem. A*, **121**, 6652 (2017).
10. (a) A. Goumri, D. D. Shao and P. Marshall, *J. Chem. Phys*., **121**, 9999 (2004); (b) V. A. Krasnopolsky, *Icarus*, **191**, 25 (2007); (c) V. A. Krasnopolsky, *Icarus*, **218**, 230 (2012).
11. (a) L. Wang, Z. Wu, B. Lu, A. K. Eckhardt, P. R. Schreiner, T. Tabelsi, J. S. Francisco, Q. Yao, V. Xie, H. Guo and X. Zeng, *J. Chem. Phys*., **153**, 094303 (2020); (b) T. Ayari, N. E. Jaidane, M. M. Al Mogren, J. S. Francisco and M. Hochlaf, *J. Chem. Phys*., **144**, 234316 (2016).
12. P. W. Schenk, *Chem. Ber*., **75**, 94 (1942).
13. R. Labbow, D. Michalik, F. Reiss, A. Schulz and A. Villinger, *Angew. Chem. Int. Ed.,* **55**, 7680 (2016).
14. G. Hartmann, R. Hoppenheit and R. Mews, *Inorg. Chim. Acta*, **76**, L201 (1983).
15. M. Carlotti, G. Di Lonardo, G. Galloni and A. Trombetti, *J. Mol. Spectrosc*., **84**, 155 (1980).
16. T. Trabelsi, O. Yazidi, J. S. Francisco, R. Longuerri and M. Hochlaf, *J. Chem. Phys*., **143**, 164301 (2015).
17. R. Appel and M. Goehring, *Angew. Chem*., **64**, 616 (1952).
18. P. B. Rapp, K. Murai, N. Ichiishi, D. K. Leahy and S. J. Milles, *Org. Lett*., **22**, 168 (2020).
19. (a) R. Kaur and Vikas, *J. Phys. Chem. A*, **122**, 1926 (2018); (b) S. M. Resende, *J. Atmos. Chem*., **56**, 21 (2007).
20. E. Cuevasanta, A. Zeida, S. Carballal, R. Wedmann, U. Morzan, M. Trujillo, R. Radi, D. A. Estrin, M. R. Filipovic and B. Alvarez, *Free Radical Biol. Med*., **80**, 93 (2015).
21. G. Faleschini, E. Nachbaur and F. Belaj, *Phosphorus, Sulfur, Silicon Relat. Elem*., **65**, 147 (1992).
22. G. Deng, Z. Wu, D. Li, R. Linguerri, J. S. Francisco and X. Zeng, *J. Am. Chem. Soc*., **138**, 11509 (2016).

23. (a) M. Mendez, J. S. Francisco and D. A. Dixon, *Chem. Eur. J*., **20**, 10231 (2016); (b) G. Manonmani, L. Sandhiya and K. Senthilkumar, *Int. J. Quantum Chem*., **120**, e26182 (2020).
24. P. Cassoux, R. L. Kuczkowski and R. A. Cresswell, *Inorg. Chem*., **16**, 2959 (1977).
25. C. Chen, L. Wang, X. Zhao, Z. Wu, B. Bernhardt, A. K. Eckhardt, P. R. Schreiner and X. Zeng, *Phys. Chem. Chem. Phys*., **22**, 7975 (2020).
26. J. A. Baban and B. P. Roberts, *J. Chem. Soc. Perkin Trans. 2*, 678 (1978).
27. X. Dong, G. Deng, Z. Wu, J. Xu, B. Lu, T. Trabelsi, J. S. Francisco and X. Zeng, *Angew. Chem. Int. Ed*., **57**, 7513 (2018).
28. M. Herberhold, W. Jellen, W. Bühlmeyer, W. Ehrenreich and J. Z. Reiner, *Z. Naturforsch., B*, **40**, 1229 (1985).
29. R. D. Suenram, F. J. Lovas and W. J. Stevens, *J. Mol. Spectrosc*., **112**, 482 (1985).
30. Z. Wu, Q. Liu, J. Xu, H. Sun, D. Li, S. Song, D. M. Andrada, G. Frenking, T. Trabelsi, J. S. Francisco and X. Zeng, *Angew. Chem. Int. Ed*., **56**, 2140 (2017).
31. Z. Wu, R. Feng, J. Xu, Y. Lu, B. Lu, T. Yang, G. Frenking, T. Trabelsi, J. S. Francisco and X. Zeng, *J. Am. Chem. Soc*., **140**, 1231 (2018).
32. D. A. Armitage and A. W. Sinden, *Inorg. Chem*., **11**, 1151 (1972).
33. G. MacLean, J. Passmore, P. S. White, A. Banister and J. A. Durrant, *Can. J. Chem*., **59**, 187 (1981).
34. R. Steudel, J. Steidel and N. Rautenberg, *Z. Naturforsch*., **35B**, 792 (1980).
35. R. Gleiter and R. Bartetzko, *Z. Naturforsch*., **36B**, 492 (1981).
36. (a) X. Zeng, H. Beckers, H. Willner and J. S. Francisco, *Angew. Chem. Int. Ed*., **51**, 3334 (2012); (b) X. Zeng, H. Li, H. Sun, H. Beckers, H. Willner and H. F. Schaefer III, *Angew. Chem. Int. Ed*., **54**, 1327 (2015).
37. X. Q. Zeng, E. Bernhardt, H. Beckers and H. Willner, *Inorg. Chem*., **50**, 11235 (2011).
38. W. E. Turner II, J. Agarwal and H. F. Schaeffer III, *J. Phys. Chem. A*, **119**, 11693 (2015).
39. S. Parsons and J. Passmore, *Acc. Chem. Res*., **27**, 101 (1994).
40. T. Chivers and R. S. Laitinen, *Dalton Trans*., **49**, 6532 (2020).
41. H-J. Himmel and G. Lintl, *Angew. Chem. Int. Ed*., **51**, 5541 (2012).
42. (a) F. Grein, *Can. J. Chem*., **71**, 335 (1993); (b) W. V. Brooks, T. S. Cameron, S. Parsons, J. Passmore and M. J. Schriver, *Inorg. Chem*., **33**, 6230 (1994).
43. B. Lu, X. Zhang, L. Meng and Y. Zeng, *J. Mol. Model*., **23**, 233 (2017).

44. G.-H. Zhang, Y.-F. Zhao, J. I. Wu and P. v. R Schleyer, *Inorg. Chem*., **51**, 13321 (2012).
45. X. Zeng, A. F. Antognini, H. Beckers and H. Willner, *Angew. Chem. Int. Ed*., **54**, 2758 (2015).
46. T. T. Takaluoma, K. Laasonen and R. S. Laitinen, *Inorg. Chem*., **52**, 4648 (2013).
47. E. A. Pritchina, N. P. Gritsan, A. V. Zibarev and T. Bally, *Inorg. Chem*., **48**, 4075 (2009).
48. E. A. Pritchina, D. S. Terpilovskaya, Y. P. T. Sentalovich, M. S. Platz and N. P. Gritsan, *Inorg. Chem*., **51**, 4747 (2012).
49. J. Bojes and T. Chivers, *Inorg. Chem*., **17**, 318 (1977).
50. R. T. Boeré, T. Chivers, T. L. Roemmele and H. M. Tuononen, *Inorg. Chem*., **48**, 7294 (2009).

Chapter 7

Acyclic S,N,O Anions and *S*-Nitrosothiols: Role in Biological Signaling

7.1 Introduction

Investigations of S,N,O anions and the related *S*-nitrosothiols (RSNO) have ballooned in the past 15 years because of their roles in biological systems. In particular, the realisation that NO and H_2S have similar physiological effects has led to the suggestion of "crosstalk" between these two gasotransmitters (*i.e.*, gaseous molecules that are synthesised in the body) which, in turn, has led to a plethora of studies of the chemical interaction.[1–5] Fundamental knowledge of the structures and spectroscopic properties of the ternary anions $[SNO]^-$ (nitrososulfide, thionitrite) and $[SSNO]^-$ (nitrosodisulfide, perthionitrite), which were first isolated and characterised as salts with large organic cations in the 1980s,[6] has provided a solid foundation for attempts to understand the behaviour of these sulfur-nitrogen-oxygen species in biological environments. At the same time the chemistry and chemical biology of *S*-nitrosothiols continue to be of great interest in view of the ability of these labile molecules to store and transport NO.[7–10] This characteristic is important for the application of these simple organic sulfur-nitrogen compounds as NO donors for the treatment of blood circulation problems (vasodilators). The formation and

properties of the parent HSNO (thionitrous acid) are of especial importance in view of the involvement of this short-lived species in the crosstalk of NO and H_2S.[1]

In light of these exciting developments this chapter will begin with a discussion of the fundamental chemistry of ternary, acyclic S,N,O anions beginning with the sulfur-centred species $[NSO]^-$ and $[NSO_2]^-$, which are formally derived from the short-lived conjugate acids HNSO and $HNSO_2$ that were described in Sec. 6.4. This will be followed by accounts of the synthesis, structures, spectroscopic properties, metal complexes and reactions of the nitrogen-centred anion $[SNO]^-$, the conjugate acid HSNO and *S*-nitrosothiols (RSNOs). The major focus of the final sections is the synthesis, structure and solution behaviour of the $[SSNO]^-$ anion and its controversial roles in the Gmelin reaction and in NO/H_2S crosstalk.

7.2 Thionyl Imide Anion, $[NSO]^-$

7.2.1 *Synthesis and structure*

Alkali-metal thionylimides are prepared by the reaction of Me_3SiNSO with the appropriate alkali-metal *tert*-butoxide in THF (Eq. 7.1).[11,12] The more soluble $[(Me_2N)_3S]^+$ salt has also been reported (Eq. 7.2).[13]

$$MO^tBu + Me_3SiNSO \rightarrow M[NSO] + Me_3SiO^tBu \ (M = Na,K,Rb,Cs) \quad (7.1)$$

$$[(Me_2N)_3S][Me_3SiF_2] + Me_3SiNSO \rightarrow [(Me_2N)_3S][NSO] + 2Me_3SiF \quad (7.2)$$

The tetramethylammonium salt $[Me_4N][NSO]$ is obtained by cation exchange between M[NSO] (M = Rb, Cs) and tetramethylammonium chloride in liquid ammonia.[12b] The bent (C_{2v}) $[NSO]^-$ anion exhibits three characteristic bands in the IR spectrum at *ca.* 1270–1285, 985–1000 and 495–530 cm^{-1}, corresponding to asymmetric and symmetric stretching modes (ν_{as} and ν_s) and a bending mode (δ). The experimental values are compared with those for the isoelectronic species SO_2 and $[NSN]^{2-}$ in Table 7.1. A recent photoelectron spectroscopic study provided values of 1280, 990 and 480 cm^{-1} for $[NSO]^-$, in good agreement with the experimental IR data.[14]

Table 7.1. Fundamental vibrations (cm^{-1}) of isoelectronic species SO_2, $[NSO]^-$, $[NSN]^{2-}$.

	ν_{as} [a]	ν_s [a]	δ
OSO[15]	1360	1151	518
Na[NSO][12a]	1283	999	528
K[NSO][12a]	1276	994	519
Rb[NSO][12a]	1271	986	507
Cs[NSO][12a]	1272	992	511
$[Me_4N][NSO]$[12b]	1268	992	496
$K_2[NSN]$[15]	1198	1001	528

Note: [a]In the salts of $[NSO]^-$,[12a] vibrations ν_{as} and ν_s are primarily (80%) S–N and S–O stretching modes, respectively.

7.2.2 *Metal complexes*

Early or late transition-metal complexes of the $[NSO]^-$ anion are obtained by metathetical reactions between K[NSO] or $[Hg(NSO)_2]$ and transition-metal halides (Eqs. 7.3 and 7.4).[16,17a] The NSO ligand in these complexes is σ-bonded *via* the nitrogen atom in the solid state with N=S and S=O bond lengths in the range 1.46 ± 0.04 Å, indicative of double bond character for both bonds. Characteristic IR bands are observed at 1260–1120, 1090–1010 and 630–515 cm^{-1}.

$$[ZrCp_2Cl_2] + 2K[NSO] \rightarrow [ZrCp_2(NSO)_2] + 2KCl \quad (7.3)$$

$$cis\text{-}[PtCl_2(PR_3)_2] + [Hg(NSO)_2] \rightarrow cis\text{-}[Pt(NSO)_2(PR_3)_2] + HgCl_2 \quad (7.4)$$

Recently, the addition of a THF solution of $SOCl_2$ to liquid ammonia has been shown to be an efficient *in situ* source of the $[NSO]^-$ anion, which has been used to prepare $[MCp^*_2(NSO)_2]$ (M = Ti, Zr, Hf) (Chart 7.1a), the coinage-metal complex $[Cu(bipy)[PPh_3)(NSO)]$ and the novel Group 15 derivatives $[SbAr_3(NSO)_2]$ (Ar = Ph, tolyl, mesityl) (Chart 7.1b).[17b] Reactions of $[TiCp_2(NSO)_2]$ with $[Mo(NBD)(CO)_4]$ (NBD = norbornadiene) or CuX (X = Cl, Br, I) in CH_2Cl_2 produce the bridging thionylimido complexes $TiCp_2(\mu\text{-}NSO)_2Mo(CO)_4$ and

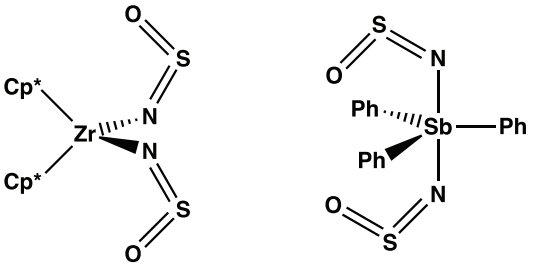

Chart 7.1. Thionylimido complexes of *d*- and *p*-block metals: (a) $[ZrCp^*_2(NSO)_2]$ and (b) $[SbPh_3(NSO)_2]$.

$[TiCp_2(\mu\text{-}NSO)_2Cu(\mu\text{-}X)]_2$, respectively, which exhibit weak metal-metal bonding according to calculated Wiberg bond indices.[17c]

7.3 $[SSNSO]^-$ Anion

The reaction of a yellow solution of $[(Me_2N)_3S][NSO]$ with elemental sulfur in acetonitrile generates a red intermediate (λ_{max} 501 nm), tentatively identified as the $[SSNSO]^-$ anion.[18a] This assignment is supported by recent CR-EOM-CCSD(T) calculations that determined a maximum at 490 nm in the visible spectrum of $[SSNSO]^-$, assuming a structure similar to the known geometry of $[SSNSS]^-$ (Sec. 5.9.4).[18b] Red acetonitrile solutions of $[(Me_2N)_3S][SSNSO]$ become purple in one day at room temperature due to the formation of $[(Me_2N)_3S][SSNSS]$, which was identified by UV-visible and ^{14}N NMR spectra.[18a]

7.4 Sulfuryl Imide, $[NSO_2]^-$, and Azidosulfite, $[SO_2N_3]^-$, Anions

Although the $[NSO_2]^-$ anion, isoelectronic with SO_3, has been generated by the gas-phase reaction of the $[NH_2]^-$ anion with SO_2F_2 (Eq. 7.5) and identified by a combination of experimental and theoretical methods,[19] it has not been characterised as a salt in the solid state. The calculated vibrational frequencies for $[NSO_2]^-$ (g) are: 1188 (symmetric stretching), 1049 (asymmetric stretching), 473 (symmetric bending), and 419 cm^{-1} (asymmetric bending).[19] The formation and spectroscopic characterisation of

matrix-isolated $HNSO_2$, the conjugate acid of $[NSO_2]^-$, are described in Sec. 6.4.

$$[NH_2]^- (g) + SO_2F_2 \rightarrow [NSO_2]^- (g) + 2HF \qquad (7.5)$$

The azidosulfite anion $[SO_2N_3]^-$ has been obtained as thermally unstable cesium or tetramethylammonium salts (Eq. 7.6),[20,21] which are a potential source of $[NSO_2]^-$ *via* loss of N_2. However, mild heating of $Cs[SO_2N_3]$ leads directly to evolution of SO_2 and the formation of cesium azide in preference to the expulsion of N_2 to give $Cs[NSO_2]$.[20] This mode of decomposition is attributed to the remarkably long S–N bond lengths of 1.98–2.00 Å in salts of the $[SO_2N_3]^-$ anion,[20,21] *cf.* ~1.77 Å for an S–N single bond. A white solid, isolated from the hydrolysis of $Me_3SiNSNSiMe_3$ with wet CsF, was first identified as "$Cs[NSO_2]$", but subsequently shown to be Cs[NSO] on the basis of IR and ^{14}N spectroscopic data.[2]

$$[Me_4N]N_3 + SO_2 (l) \rightarrow [Me_4N][SO_2N_3] \qquad (7.6)$$

7.5 Thionitrite, $[SNO]^-$, and Thionitrate, $[SNO_2]^-$, Anions

High-level quantum chemical calculations show that the nitrogen-centered thionitrite anion $[SNO]^-$ is *ca.* 89 kJ mol^{-1} higher in energy than the sulfur-centered isomer $[NSO]^-$.[22,23] This finding is consistent with the general conclusion that species with the NSO motif are thermochemically more stable than those with the SNO arrangement owing to the ability of the central sulfur atom to expand its valency.[24] The $[SNO]^-$ ion was first synthesised and isolated as a green PPN^+ salt (PPN = $(Ph_3P)_2N$) by treatment of [PPN][SSNO] (Sec. 7.9) with one equivalent of triphenylphosphine in acetonitrile (Eq. 7.7).[6]

$$[PPN][SSNO] + PPh_3 \rightarrow [PPN][SNO] + SPPh_3 \qquad (7.7)$$

The $[SNO]^-$ ion has a bent structure, with d(S–N) = 1.695(4) Å, d(N–O) = 1.214(5) Å and <SNO = 120.5(3)°.[6] Similar values were reported later for the acetone adduct of [PPN][SNO], and the solutions

were handled in the dark because of the light sensitivity.[25] The UV-visible spectra showed absorption bands at 332 nm in acetonitrile, and at 350 nm in acetone.[6] A band at ~340 nm was found for the spectra of samples generated by pulse radiolysis of HS^-/nitrite-containing solutions at pH 11.[26] The ^{15}N NMR signal of $[SNO]^-$ appears at 529 ppm (referred to PNP[$^{15}NO_3$]), in an aprotic solvent; theoretical calculations confirm similar values under gas-phase, protic and aprotic conditions.[4] The ^{15}N NMR chemical shift for $[SNO]^-$ is clearly distinct from the values of 334 and 322 ppm estimated for $[SS^{15}NO]^-$ in acetone and water at pH 7.4, respectively.[4]

Although transition-metal complexes of $[SNO]^-$ have not been obtained by metathesis, mass spectrometric evidence indicates the formation of the *S*-bonded ruthenium(III) complex $[Ru(edta)(SNO)]^{2-}$ (edta = ethylenediaminetetraacetate), *via S*-nitrosylation of $[HS]^-$ with NO mediated by $[Ru(edta)(OH)]^{2-}$ in aqueous solution.[27a] The zinc complex [ZnTp(SNO)] (Tp = tris(pyrazolyl)borate) is obtained by treatment of [ZnTp(SSNO)] (Sec. 7.9.1) with PEt_3 in CH_2Cl_2.[27b] In the solid state this *S*-bonded zinc(II) complex exists as a mixture of *syn* (25%) and *anti* (75%) conformers with mean S–N and N–O bond lengths of *ca*. 1.745(11) and 1.208(11) Å, respectively.[27b] [ZnTp(SNO)] is thermally stable in solution up to 75°C, but releases N_2O at room temperature upon treatment with acidic thiols, *e.g.*, C_6F_5SH.[27b]

The gunpowder reaction, which involves the combination of potassium nitrite (produced by reduction of potassium nitrate with charcoal) and sulfur, may involve the formation of potassium thionitrate $K[SNO_2]$ as an intermediate (Eq. 7.8).[28] An investigation of the reaction of [PPN][$^{15}NO_2$] with elemental sulfur in acetone by ^{15}N NMR spectroscopy revealed the initial formation of a resonance at −67 ppm (*cf.* 348 ppm for $[SSNO]^-$), which is associated with a visible absorption band at 428 nm (*cf.* 448 nm for $[SSNO]^-$ in acetone).[29] This resonance was tentatively attributed to the $[SNO_2]^-$ anion (Fig. 3.4).[29] However, this assignment is not supported by high-level quantum chemical calculations, which determined a value of 427 nm for $[SNO_2]^-$ assuming C_s symmetry, but with a very low oscillator strength.[18b] Stable salts of $[SNO_2]^-$ have not been isolated.

$$1/8S_8 + KNO_2 \rightarrow K[SNO_2] \qquad (7.8)$$

7.6 Thionitrous Acid, HSNO, and Isomers

7.6.1 *Synthesis, structure, and spectroscopic properties*

The characterisation of HSNO (thionitrous acid), the conjugate acid of $[SNO]^-$, has assumed great importance in the context of the purported biological relevance of this compound in the crosstalk between the two gasotransmitters NO and H_2S.[3–5] In early work, the photolysis of thionyl imide HNSO in an argon matrix led to a mixture of isomers: HNSO, HOSN, HSNO and HONS (ν_{NO} at 1569 cm^{-1} for HSNO).[30–32] Recently, HSNO has been obtained at room temperature by the spontaneous reaction of NO with H_2S over metallic surfaces; NO undergoes disproportionation to give N_2O_3, which reacts with H_2S to produce HSNO.[33] Fourier transform microwave spectroscopy provided accurate molecular parameters for *cis* and *trans* isomers of HSNO, with S–N bond lengths of 1.834 ± 0.002 and 1.852 ± 0.002 Å, respectively.[33] High-level *ab initio* calculations predicted a value of 1.852 Å for the S–N bond length, and 122.2 kJ mol^{-1} for the homolytic dissociation energy of the S–N bond, consistent with an unusually weak sulfur-nitrogen bond,[34] in comparison with that in CH_3SNO, *cf.* d(S–N) ~1.814 Å and D(S–N) = 135.6 kJ mol^{-1} (Sec. 7.7.2).[35]

Computational studies indicate that fast interconversions of HSNO isomers occur readily in aqueous solution with low energy barriers (< 42 kJ mol^{-1}) *via* proton migration from HSNO to either the N or O atoms to give the Y-isomer SN(H)O or SNOH, respectively.[36] The pK_a of thionitrous acid has been ambiguously described in the literature;[26] given the protonation ability at nonequivalent sites (S,N,O), each with its microscopic acidity constant K_{ai}, the system behaves macroscopically as if only one weak acid exists in the solution, with an apparent equilibrium constant K_{app} dominated by the acid-base couple with the weakest K_{ai}, which would be SNOH, for which an estimation of pK_{ai} ~10–11 seems reasonable. Therefore, aqueous solutions of the isomeric mixtures (referred to as (H)SNO) would deprotonate at pH ≥ 10.[5] The hydrogen bonding interactions in aqueous solutions of $[SNO]^-$ and HSNO determined by QM/MM-MD simulations are illustrated in Fig. 7.1.[4]

The generation of (H)SNO under physiologically relevant conditions (aqueous solution, pH 7.4) has been achieved *via* three routes: (a) reaction

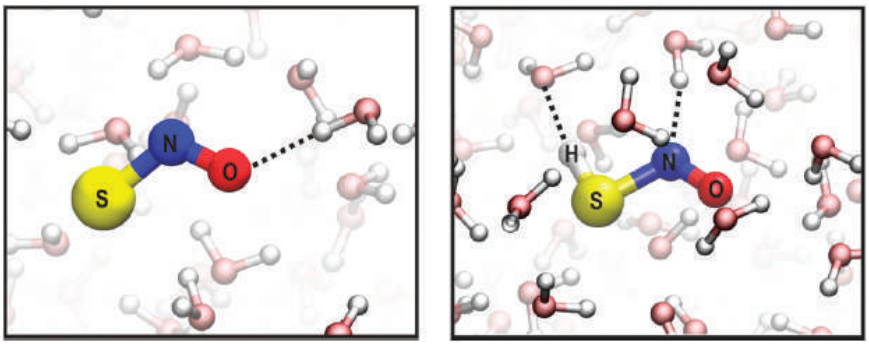

Figure 7.1. Hydrogen bonding interactions (---) in aqueous solutions of $[SNO]^-$ and HSNO.[4] [Reproduced with permission from J. P. Marcolongo, M. F. Venâncio, W. R. Rocha, F. Doctorovich, and J. A. Olabe, *Inorg. Chem*., **58**, 14981 (2019). Copyright 2019 American Chemical Society].

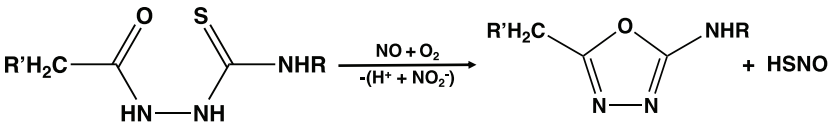

Scheme 7.1. Formation of HSNO from semicarbazide and NO in air.

of the radical $[HS]^{\bullet}$ generated by pulse radiolysis with $^{\bullet}NO$, (b) reaction of H_2S with acidified nitrite, and (c) transnitrosation of *S*-nitrosoglutathione and H_2S.[26] (H)SNO was tentatively identified by ESI-MS, and the UV-visible, FTIR and ^{15}N NMR spectra led to band assignments at 340 nm, 1568 cm^{-1} (ν_{NO}) and 322 ppm, respectively.[26]

A novel approach to the generation of thionitrous acid involves the reaction of thiosemicarbazides with NO, which generates a fluorescent 1,3,4-oxadiazole.[37] This reaction occurs in air and involves N_2O_3 as the reactive species (Scheme 7.1). HSNO was identified by ESI-MS. In addition to the detection of NO, this water-soluble probe could be useful for transforming intracellular NO to HSNO.

7.6.2 *Detection*

HSNO exhibits dual reactivity as (a) an electrophile for thiolate-based nucleophiles, and (b) a transnitrosation agent like RSNOs. This

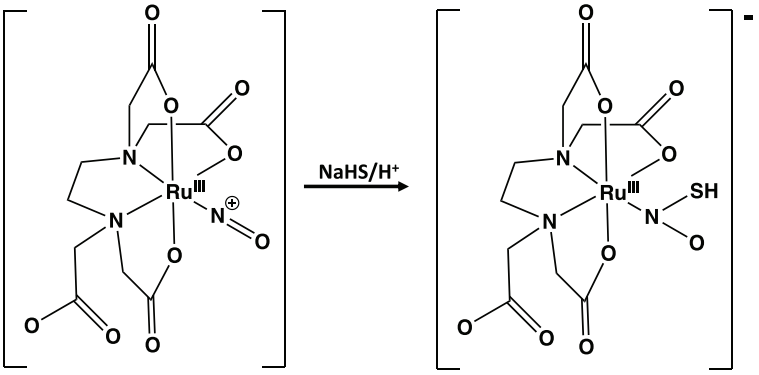

Scheme 7.2. Formation of a Ru^{III}-HSNO complex.

ambivalent behaviour has been used in the design of a sensitive fluorophore for HSNO that incorporates two 2-mercaptobenzoate residues and an *o*-phenylenediamine site on a non-fluorescent scaffold.[38] The interaction of HSNO with these reactive sites in the fluorophore generates a highly fluorescent benzotriazole. This probe shows high selectivity and sensitivity to HSNO in aqueous media and cells, and may serve as a useful tool for understanding the role of HSNO in biological systems.

7.6.3 *Transition-metal complexes*

The nitrosyl complex $[Ru^{III}(edta)(NO^{+})]$ reacts with NaSH in aqueous solution at lower pH (~3.5) to produce an *N*-bonded complex of HSNO, $[Ru^{III}(edta)N(O)SH)]^{-}$ (Scheme 7.2), which was characterised in solution based on spectroscopic data.[39] DFT calculations for $Ru^{III}(edta)$ complexes of HSNO indicate that the *N*-coordinated isomer is of lower energy than the *S*-coordinated analogue and that the energy barrier for conversion of the *S*-bonded to the *N*-bonded isomer is lower than that for the reverse process.[39]

7.7 *S*-Nitrosothiols, RSNO

S-Nitrosothiols (RSNO) are structural isomers of sulfinylimines (RNSO), which are discussed in Sec. 10.2. The formal reversal of the order of the S and N atoms in these organic derivatives of ternary S,N,O anions results

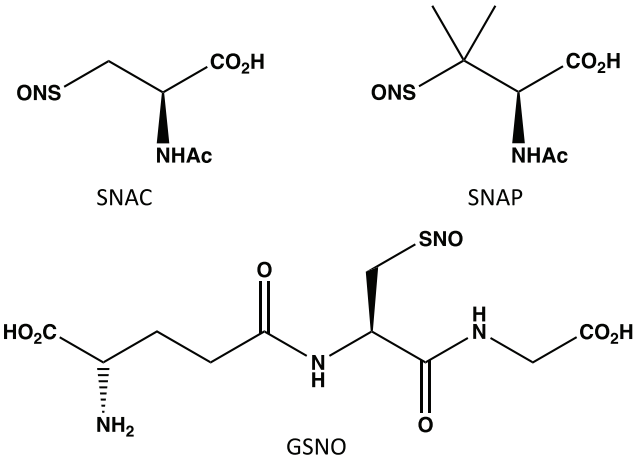

Chart 7.2. Naturally occurring *S*-nitrosothiols: SNAC, SNAP and GSNO.

in completely different properties. *S*-Nitrosothiols are powerful vasodilators that serve as air-stable NO reservoirs which readily release NO due to the relatively weak RS–NO bond strength, 105–146 kJ mol^{-1} depending on the substituent R.[40–42] RSNOs have been the subject of intense investigations because of their important role in NO transport and regulation in biological systems.[7a,b] Several RSNOs occur naturally, *e.g.*, *S*-nitroso-*N*-acetylcysteine (SNAC), *S*-nitroso-*N*-acetylpenicillamine (SNAP) and *S*-nitrosoglutathione (GSNO) (Chart 7.2). The latter participates in protein control *via S*-nitrosation of proteins, an important post-translational modification connected to health and disease.

7.7.1 *Synthesis*

With the exception of GSNO, which is stabilised by the peptide structure, *S*-nitrosothiols containing aliphatic primary or secondary R groups are generally unstable at room temperature owing to thermal or photochemical decomposition to give the corresponding disulfide and NO *via* homolytic cleavage of the weak S–N bond.[10,43,44] However, thermally stable RSNOs with very bulky alkyl or aryl groups can be isolated.

The first preparation of a *S*-nitrosothiol more than a century ago involved the reaction of benzenethiol with nitrosyl chloride to give

PhSNO[45] and that method has been adopted recently for the preparation of CF_3CH_2SNO as a red-brown, photosensitive liquid (Eq. 7.9).[46] More generally, a variety of synthetic methods are available for *S*-nitrosothiol formation including the nitrosation of thiols with an alkyl nitrite or nitrous acid (Eq. 7.10).[47] For example, water-soluble *S*-nitrosothiols are prepared by treatment of a decalin-based thiol with *tert*-butyl nitrite in CH_2Cl_2.[48] Green crystals of the trityl derivative TrSNO (Tr = Ph_3C) are obtained from the corresponding thiol and acidified sodium nitrite[49] and the introduction of a sterically protecting trityl group in TrmSNO (Trm = 3,5-bis(2,6-dimethylphenyl)phenyl) generates a thermally more stable *S*-nitrosothiol.[50] Bowl-shaped aryl groups with two *m*-terphenyl substituents have also been used to stabilise *S*-nitrosothiols and *Se*-nitrososelenols (Sec. 7.8).[51–53]

$$CF_3CH_2SH + NOCl \rightarrow CF_3CH_2SNO + HCl \qquad (7.9)$$

$$RSH + R'NO_2 \rightarrow RSNO + R'OH\ (R' = H, Et, {}^tBu) \qquad (7.10)$$

7.7.2 *Solid-state structures and bonding*

S-Nitrosothiols may adopt either *cis* or *trans* conformations with respect to the S–N bond, as determined by X-ray crystallography.[54] *S*-Nitrosocysteine (as an HCl adduct),[54] *S*-nitrosocaptopril[42] and *S*-nitrosothiols with bulky aryl substituents[51–53] all adopt a *cis* arrangement, while the *trans* isomer pertains in the solid state for SNAP (Chart 7.2)[55] and (decalin)SNO derivatives.[48] The trityl derivative TrSNO also assumes a *trans* conformation,[49] but both *cis* and *trans* isomers are present in crystals of the derivative TrmSNO with a sterically protecting trityl group (Fig. 7.2).[50] The S–N bond lengths in *S*-nitrosothiols are in the range 1.74–1.85 Å typical for a single bond;[10,54] the longer values are associated with the bulky aryl substituents. High-level *ab initio* calculations for CH_3SNO as a model for *S*-nitrosated cysteine (CysSNO) estimate an S–N bond length of 1.814 Å, a low stretching frequency (ν_{S-N} = 387 cm^{-1}), and a dissociation energy (D_o) of 135.6 kJ mol^{-1}.[56]

Despite the inherent weakness of the S–N bond, there is a significant barrier to rotation of 46–53 kJ mol^{-1} around it.[42,51,56] DFT calculations

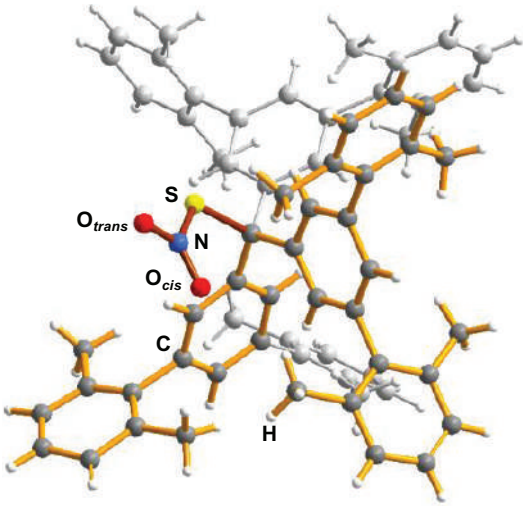

Figure 7.2. Disordered crystal structure of TrmSNO showing both *trans*- and *cis*-CSNO (the site occupancy factors are 0.67 and 0.33 for *trans*- and *cis*-isomers, respectively).[50]

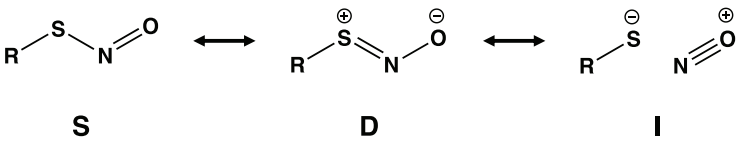

Chart 7.3. Single-bond (**S**), double-bond (**D**) and ionic (**I**) resonance forms of *trans*-RSNO.[57]

(B3P86) indicate that *cis*-RSNO is slightly lower in energy than *trans*-RSNO for R = C_nH_{2n+1}, $n \leq 4$ except for R = ^{t}Bu.[35] *Ab initio* calculations for CH_3SNO estimate the preference for the *cis* isomer to be *ca.* 5.0 kJ mol^{-1},[56] which has been attributed to an intramolecular CH···O interaction in the HOMO of CH_3SNO that does not occur in CF_3SNO.[54]

The weakness of the S–N bond combined with a considerable rotation barrier suggest partial S=N double bond character in RSNOs. This paradox has been attributed to the concomitant contributions of three resonance forms **D**, **S** and **I** to the RSNO electronic structure (Chart 7.3).[57–59] The designation **D** refers to a zwitterionic structure with a double bond that results from delocalisation of a sulfur lone pair *n*(S) into the π^*(NO) orbital (Fig. 7.3a), while **S** represents the conventional single-bond

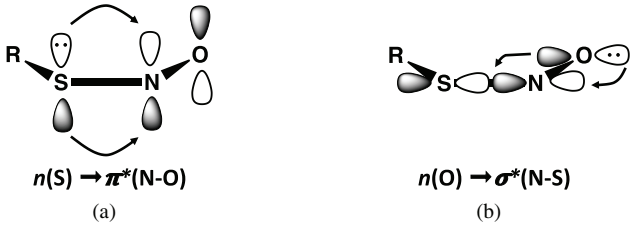

Figure 7.3. Orbital interactions in the (a) **D** and (b) **I** forms of RSNO.[57] [Adapted with permission from Q. K. Timerghazin, A. M. English and G. H. Peslherbe, *Chem. Phys. Lett*., **454**, 24 (2008). Copyright 2008 Elsevier].

structure. The ionic resonance structure **I** arises from the interaction (negative hyperconjugation) between n(O) and σ^*(S–N) orbitals (Fig. 7.3b) and accounts for the weakness of the S–N bond.[59] The resonance forms **D** and **I** are referred to as *antagonistic* structures because they represent opposing bonding patterns and charge distributions. The relative weakness of the S–N bond in aromatic RSNOs is attributed to resonance stabilisation of the ionic form **I**.[59c] The concept of antagonistic structures is important in understanding the reactions of RSNOs with transition metals, nucleophiles and Lewis acids (Secs. 7.7.4 and 7.7.5).[57–59]

7.7.3 *Spectroscopic properties*

IR spectroscopy is a useful technique for the identification of the SNO group. The N–O stretching vibration ν_{NO} for RSNOs occurs in the range 1450–1530 cm^{-1} for alkyl derivatives and 1430–1710 cm^{-1} for corresponding aryls.[5,10] For example, this band is observed at 1514 and 1522 cm^{-1}, respectively, in the IR spectra of the tertiary alkyl derivatives TrSNO[49] and TrmSNO.[50] A detailed experimental and computational investigation of the IR spectra of the primary alkyl derivatives CF_3CH_2SNO (X = H, F) revealed a difference of 22–25 cm^{-1} for the *cis* and *trans* isomers: 1537 and 1559 cm^{-1} for X = H *vs.* 1580 and 1605 cm^{-1} for X = F; the bending vibration δ(SNO) occurs at 629 cm^{-1}, *cf.* computed value of 648 cm^{-1}.[46] The calculated S–N stretching vibration ν_{NS} for RSNO (R = CH_3, CH_3CH_2) in the region 390–400 cm^{-1} is inconsistent with the assignment of 610–650 cm^{-1} for this mode for primary RSNOs.[5,10]

Primary or secondary alkyl thionitrites RSNOs are usually red, while those with R = tertiary alkyl are green. Their UV-visible spectra show a strong absorption at 225–260 nm assigned to a $\pi \rightarrow \pi^*$ transition, a second one in the 330–350 nm region attributed to the $n_O \rightarrow \pi^*$ transition and a very weak absorption at 550–600 nm assigned to the forbidden $n_N \rightarrow \pi^*$ transition, which is responsible for the colour of RSNOs.[10,47] The latter absorption occurs at 560 nm (with a shoulder at 530 nm) for the thermally unstable red derivative $PhCH_2SNO$[60] and at 600 nm for green TrSNO in CH_2Cl_2.[49]

In solution the *cis* and *trans* isomers of RSNOs may co-exist, as demonstrated by independent investigations of the variable temperature ^{15}N NMR spectra of the ethyl and *tert*-butyl derivatives in toluene-d_8.[42,49] In both cases the broad peak observed at room temperature separates into two resonances below −50°C.[49] Solid-state NMR studies have provided the ^{15}N and ^{17}O tensors for SNAP and GSNO (Chart 7.2). The SNO group in these representative examples of RSNOs exhibits very large quadrupolar coupling constants as well as substantial ^{15}N and ^{17}O chemical shift anisotropies.[61] Quantum chemical calculations for the model RSNOs (R = Me, ^tBu) indicate that these anisotropies are due to the magnetic coupling between the HOMO and LUMO in RSNOs.[61]

7.7.4 *Transition-metal complexes*

The structures and reactivities of coordination compounds of RSNOs are of great interest in view of the well-established influence of transition metals on bioregulatory functions. The catalytic decomposition of RSNOs by Cu^+ is well-known,[7,62,63] and it has been demonstrated that PVC or polyurethane films doped with a lipophilic copper(II) complex are capable of catalytically decomposing endogenous RSNO species to NO.[64]

Redox-active copper enzymes, *e.g.*, CuZn-superoxide dismutase, also facilitate the release of NO from RSNOs and nitric oxide synthase activity relies on zinc binding to the tetracysteine thiolate site. In attempts to understand the reactions of RSNOs at these metal centres in biological systems, their reactivity with biomimetic model complexes has been investigated. For example, two-coordinate copper(I) thiolates [Cu(IPr)SR] (IPr is an *N*-heterocyclic carbene with 2,6-$^iPrC_6H_3$ substituents on the

nitrogen atoms) undergo fast reversible transnitrosations with RSNOs.[65] The reaction of tris(pyrazolyl)borate copper(II) thiolates [Cu(^{iPr2}Tp)(SR)] (R = C_6F_5 or CPh_3) with ^{t}BuSNO produces the copper(I) nitrosyl [Cu(^{iPr2}Tp)(NO)] and the disulfide RS–S^{t}Bu; DFT calculations indicate that this is a reversible process involving an *N*-bonded RSNO adduct.[62]

β-Diketiminato Cu(II) complexes react with TrSNO to give NO and the corresponding copper(II) thiolate complex[66] and also activate nitrite ion $[NO_2]^-$ in nitrosation reactions with thiols to give RSNOs (R = Tr).[67] The reactions of model zinc thiolate complexes with NO were found to require the presence of O_2 in order to generate RSNOs.[68,69]

The first structurally characterised metal complex of an *S*-nitrosothiol was a dark red iridium(III) complex prepared in acetonitrile according to Eq. 7.11.[70a] In stark contrast to the facile decomposition of $PhCH_2SNO$ in solution, the metal complex is stable in aqueous solution and an extensive series of water-soluble iridium complexes of RSNOs have been prepared and characterised.[70b] The X-ray structure of *trans*-K[$IrCl_4$(MeCN)N(O)SCH_2Ph] shows the *S*-nitrosothiol is *N*-coordinated to the metal centre in this complex (Fig. 7.4a).[70a] The S–N bond length is shortened by 0.13 Å compared to the calculated value for $PhCH_2SNO$ suggesting increased **D** character and a reduced **I** contribution in the *N*-bonded RSNO ligand (Chart 7.3). The UV-visible spectrum of the metal complex shows a

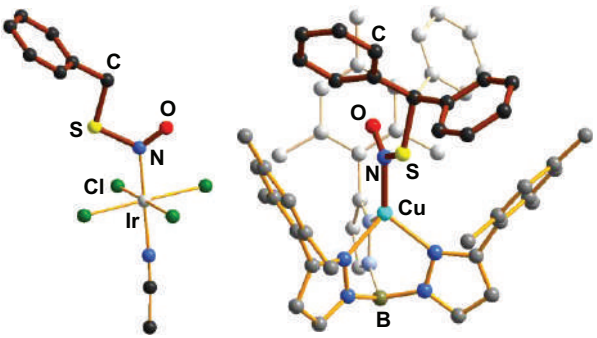

(a) (b)

Figure 7.4. X-ray structures of (a) the anion [$IrCl_4$(MeCN)N(O)SCH_2Ph]$^{-}$[70a] and (b) [Cu^I(^{Mes}Tp)(κ^1-N(O)$SCPh_3$)].[71]

strong absorption at 331 nm and a weak one at 591 nm, *cf.* 560 nm for $PhCH_2SNO$.

$$K[IrCl_5NO] + PhCH_2SH \rightarrow K[IrCl_4(MeCN)N(O)SCH_2Ph] + HCl \quad (7.11)$$

Type 1 Cu sites in multicopper proteins may be involved in the formation of RSNOs from NO and circulating thiols such as glutathione. In model studies it was shown that the addition of NO to the tris(pyrazolyl) borate copper(II) complex $[Cu^{II}(^{Mes}Tp)(SCPh_3)]$ produces $[Cu^{I}(^{Mes}Tp)(N(O)SCPh_3)]$ (Fig. 7.4b), which is also formed by addition of TrSNO to $[Cu^{I}(^{Mes}Tp)(THF)]$.[71] Similar to the Ir(IV) complex, the *S*-nitrosothiol ligand is *N*-bonded to the Cu(II) centre in this complex with a *cis* conformation. The S–N distance is slightly shorter than that in the free Ph_3CSNO ligand (1.755(4) *vs.* 1.792(5) Å) and the N–O bond length is marginally longer (1.206(5) *vs.* 1.177(6) Å). The Cu(I) complex reversibly loses NO with concomitant oxidation of the copper centre to give $[Cu^{II}(^{Mes}Tp)SCPh_3]$.[71] Computational studies show that the uptake and release of NO are low-energy processes.

Treatment of a dinuclear Cu(I)Cu(I) complex with an excess of NO and a thiol RSH was shown to generate a Cu(I)Cu(I) di-*S*-nitrosothiol complex, which readily releases RSNO in high yields (Scheme 7.3). This redox-neutral process occurs *via* a Cu(II)Cu(III) intermediate that has implications for the NO/RSNO interconversion by the copper protein ceruloplasmin.[72]

Reactions of RSNOs with Group 8 metals, *e.g.*, Fe, Ru, are of interest in view of the important role played by *S*-nitrosohemoglobin in vasodilation.[5,73] In that context the formation of HSNO/HNO in the heme

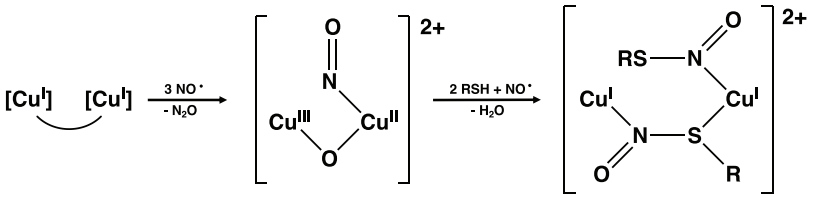

Scheme 7.3. Redox-neutral *S*-nitrosation on a dicopper centre.[72]

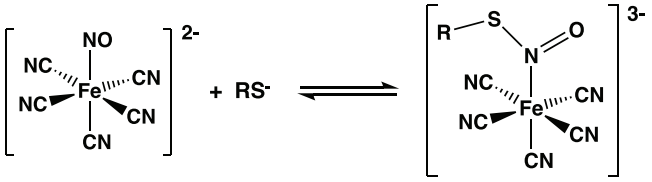

Scheme 7.4. Formation of red product from reaction of thiolate with $[Fe(CN)_5NO]^{2-}$ in aqueous solution (R = alkyl, aryl, 2-mercaptosuccinate).[76,77]

iron-catalysed *S*-nitrosylation of H_2S with nitrite anion has been described.[74] It has also been demonstrated that H_2S can interfere with NO signaling by reacting with NO or $[NO_2]^-$ (Sec. 7.11).[75]

Early kinetic studies for the reactions of nitroprusside $[Fe(CN)_5NO]^{2-}$ and thiolates (RS^-; R = alkyl, aryl) in aqueous solution led to the detection of moderately stable red intermediates formulated as $[Fe(CN)_5N(O)SR]^{3-}$ (*cf.* Gmelin reaction, Sec. 7.9.3), which decomposed to give $[Fe(CN)_5N(O)]^{3-}$ and thiyl radicals, as precursors of alkyl disulfides.[76] More recently, this reaction has been monitored by multinuclear NMR (^{15}N and ^{17}O) by using 2-mercaptosuccinic acid. The unstable red intermediate was tentatively identified as the *N*-bonded complex $[Fe^{II}(CN)_5N(O)SR]^{3-}$ (Scheme 7.4) by comparison of spectroscopic data (UV-Visible, IR and multinuclear NMR) with those of the free ligand RSNO [R = –CH(COO^-)(CH_2)–COO^-)], which was prepared by the reaction of RSH with sodium nitrite.[77]

The reaction of two equivalents of Ph_3CSNO with $TBA_2[Fe^{II}_2Cl_6]$ (TBA = tetrabutylammonium) produces the iron(III) thiolate $[Fe^{III}Cl_3(SCPh_3)]^-$ *via* the rapid release of NO from the putative intermediate $[Fe^{II}Cl_3\{S(NO)CPh_3\}]^-$, which is assigned an *S*-bonded structure based on spectroscopic evidence (Scheme 7.5).[78] The reverse reaction of the product $[Fe^{III}Cl_3(SCPh_3)]^-$ with an excess of NO regenerates Ph_3CSNO.

The results of a stopped flow kinetics investigation of the reaction of RSNO (R = *N*-acetyl-1-amino-2-methypropyl) with the model metalloporphyrin complex $[Ru^{II}(OEP)(CO)]$ (OEP = octaethylporphyrinato dianion) indicated that an *S*-bound RSNO intermediate is formed prior to the production of the addition complex $[Ru^{II}(OEP)(NO)(SR)]$, presumably *via* S–N bond cleavage.[79] The ruthenium complex $[Ru^{III}(edta)(H_2O)]^-$

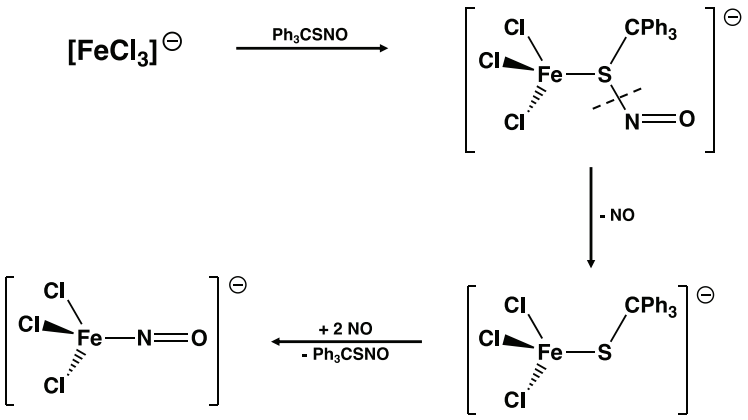

Scheme 7.5. Formation and NO release from $[Fe^{II}Cl_3\{S(NO)CPh_3\}]^-$.

(edta = ethylenediaminetetraacetate tetraanion) has been shown to mediate the *S*-nitrosylation of cysteine in the presence of sodium nitrite at pH 4.5.[80] Formation of the RSNO complex $[Ru^{III}(edta)S(NO)Cy]^-$ was confirmed by ESI-MS analysis (Sec. 3.8.2).[80] This finding suggests that the Ru^{III} complex is able to store NO as an *S*-nitroso (SNO) conjugate of $[Ru^{III}(edta)CyS]^{2-}$, thus mimicking heme-assisted *S*-nitrosylation of a proximal thiolate in a nitric oxide transport protein.[81]

7.7.5 *Reactions with nucleophiles and Lewis acids*

The unusual antagonistic nature of the electronic structure of RSNOs (Chart 7.3) is key to understanding their reactions with nucleophiles (Lewis bases) and Lewis acids.[82a] For example, external electric field effects in biological systems can influence the relative importance of resonance structures **D** and **I** and, hence, the reactivity of RSNOs.[59b] High level *ab initio* and DFT calculations show that RSNOs interact with Lewis bases (electron-pair donors) *via* a σ hole, *i.e.*, a region of positive electrostatic potential on the molecular surface at the extension of the N–S bond.[82a] This interaction at the sulfur atom promotes the contribution from resonance form **D** at the expense of **I**, thereby stabilising the weak N–S bond and making the S atom more electrophilic. Coordination with a Lewis acid through the nitrogen or oxygen atom of RSNOs increases the **D** character and thus strengthens the σ hole bonding.[82]

The reactions between thiols and RSNOs represent a possible biological pathway for the formation of nitroxyl (HNO), the reduced form of the gasotransmitter NO.[83a] DFT calculations for this transformation suggest an initial proton transfer from R–SH to the nitrogen atom of RSNO that promotes the zwitterionic structure **D** (Chart 7.3) and, hence, increases the electrophilicity of the sulfur atom of RSNO. Subsequent nucleophilic attack by RSH generates the charge-separated intermediate $[R'SS]^+[RN(H)O]^-$, which decomposes to give HNO and the disulfide R′SSR.[83b] A kinetic study showed that the rate-limiting step in the transnitrosation of RSNOs, as exemplified by the reaction of thiolate with *S*-nitroso-*N*-acetylcysteine, is nucleophilic attack on the nitrogen atom of the SNO group to give an intermediate with an –SN(O)S– bridge.[84]

The reaction of the strong Lewis acid $B(C_6F_5)_3$ with RSNOs (R = Ad, $MesCH_2$) occurs rapidly in pentane to give 1:1 adducts (Eq. 7.12).[85]

$$RSNO + B(C_6F_5)_3 \rightarrow RSNO{-}B(C_6F_5)_3 \qquad (7.12)$$

In contrast to the *N*-bonded thionylimide complex $HNSO{-}B(C_6F_5)_3$ (Sec. 6.4, Fig. 6.2), the RSNO ligand in the thionitrosyl complexes is *O*-bonded to boron in either a *trans* (R = Ad) or *cis* ($R = MesCH_2$) conformation (Chart 7.4).[85] The S–N bond length is substantially shortened and the N–O distance is lengthened compared to the values in free RSNOs, consistent with an increased contribution from the zwitterionic resonance form **D** (Chart 7.3) in these novel *O*-bonded complexes, as predicted by computational results (*vide supra*).[82]

In contrast to the behaviour of free *S*-nitrosothiols, the one-electron electrochemical reduction of $AdSNO{-}B(C_6F_5)_3$ is quasi-reversible.

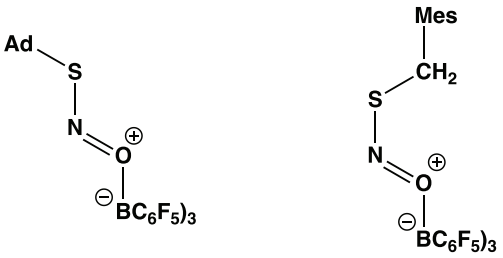

(a) (b)

Chart 7.4. (a) *trans*-$AdSNO{-}B(C_6F_5)_3$ and (b) *cis*-$MesCH_2SNO{-}B(C_6F_5)_3$.

The radical anion $[AdSNO–B(C_6F_5)_3]^{\bullet-}$ exhibits a three-line EPR spectrum that becomes two lines upon isotopic substitution with ^{15}N, consistent with an *N*-centred radical as predicted by DFT calculations.[85] Upon treatment of the adducts $RSNO–B(C_6F_5)_3$ with $[CoCp^*_2]$ the RSNO ligand is reduced to the hyponitrite dianion $[ONNO]^{2-}$, which is stabilised by coordination to the Lewis acid (Eq. 7.13).[85]

$$2RSNO–B(C_6F_5)_3 + [CoCp^*_2] \rightarrow [CoCp^*_2][(C_6F_5)_3BO–N{=}N–OB(C_6F_5)_3] + RSSR \quad (R = Ad, CH_2Mes) \qquad (7.13)$$

The detection of short-lived RSNOs, especially HSNO (Sec. 7.6.2), in biological settings is an important challenge. The widely used biotin switch assay suffers from a number of disadvantages.[10] Consequently, methods based on novel fluorescent probes are being developed, some of which involve phosphine mediation.[86a] The design of these probes is based on the long-known reaction between TrSNO and two equivalents of PPh_3 (Eq. 7.14).[86b] The attachment of an *ortho*-ester group to a phenyl substituent of the phosphine, *i.e.*, $2\text{-}R'O(O)CC_6H_4PPh_2$, entraps the intermediate in this transformation and subsequent hydrolysis generates a sulfonamide.[87] A fluorescent probe based on this reaction showed strong fluorescent responses to small RSNOs like GSNO (Chart 7.2).[88]

$$Ph_3C–S–N{=}O + 2PPh_3 \rightarrow Ph_3C–S–N{=}PPh_3 + O{=}PPh_3 \qquad (7.14)$$

7.8 *Se*-Nitrososelenols, RSeNO

Alkyl derivatives of *Se*-nitrososelenols have a much lower thermal stability than aryl derivatives. Furthermore, the Se–N bond in *Se*-nitrososelenols is even weaker than the S–N bond in *S*-nitrosothiols. Recently, however, the simplest alkyl derivative MeSeNO was generated and identified by using the methodology described in Chapter 6 for the generation and characterisation of short-lived sulfur-nitrogen species. Thus, the $[MeSe]^{\bullet}$ radical was generated by flash-vacuum pyrolysis of $MeSeCH_2CH_2SeMe$ at 840°C and trapped in a solid argon matrix at 10 K. Subsequent reaction of

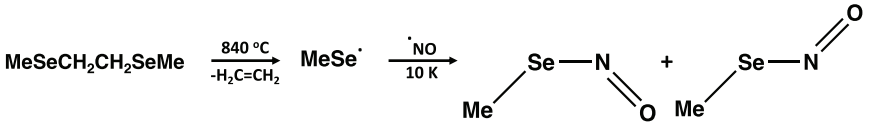

Scheme 7.6. Formation of *cis* and *trans*-MeSeNO *via* reaction of MeSe$^{\bullet}$ with $^{\bullet}$NO.

[MeSe]$^{\bullet}$ radical with NO produced MeSeNO as a mixture of *cis* and *trans* isomers (Scheme 7.6), which were characterised by comparing the IR spectra of natural abundance and ^{15}N-labelled products.[89]

In earlier work the synthesis and characterisation of *Se*-nitrososelenols with very bulky alkyl and aryl groups attached to selenium were reported. The alkyl derivative $(Me_3Si)_3CSeNO$ was generated by the fast nitrosation of $(Me_3Si)_3CSeH$ with *tert*-butyl nitrite at −78°C.[90] This red species exhibited a characteristic IR band at 1459 cm^{-1} (ν_{NO}). It decomposes above –78°C to produce the corresponding di- and tri-selenides $(Me_3Si)_3CSe_xC(SiMe_3)_3$ ($x = 2, 3$); EPR spectra indicated the possible formation of the radical $[(Me_3Si)_3CSe(NO)_2]^{\bullet}$ as an intermediate during this decomposition.

In contrast to the thermal lability of $(Me_3Si)_3CSeNO$, the aryl derivative BpqSeNO (Bpq = 2,6-bis[3,5-bis(2,6-diisopropylphenyl)phenyl]-phenyl) was isolated as reddish purple crystals in high yield from the reaction of BpqSeH with an excess ethyl nitrite (or GSNO) in $CDCl_3$ (Eq. 7.15).[91,92]

$$BpqSeH + C_2H_5ONO \rightarrow BpqSeNO + C_2H_5OH \qquad (7.15)$$

The X-ray structure of bowl-shaped BpqSeNO revealed a *cis* conformation with an Se–N bond length of 2.107(6) Å and an N–O bond length of 1.162(6) Å, consistent with single and double bonds, respectively (Fig. 7.5).[91] The IR spectrum of BpqSeNO shows an N–O stretching band at 1563 cm^{-1}, *cf.* 1548 cm^{-1} for the thionitrosyl analogue BpqSNO. The UV-visible spectrum of BpqSeNO exhibits an absorption band at 485 nm in $CHCl_3$ attributed to the $n \rightarrow \pi^*$ transition, which represents a bathochromic shift of *ca.* 140 nm compared to BpqNSO. The ^{77}Se NMR chemical resonance of BpqSeNO is shifted to lower field by a remarkable

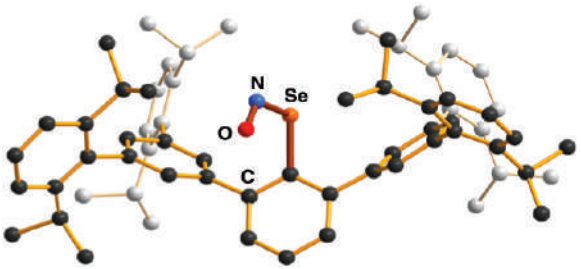

Figure 7.5. Crystal structure of bowl-shaped *cis*-BpqSeNO.[93]

2100 ppm compared to the chemical shift for the corresponding selenol BpqSeH, suggesting a strong magnetic shielding effect of the NO group. The thermolysis of BpqSeNO produced the diselenide BpqSeSeBpq, whereas photolysis generated the tetraselenide BpqSeSeSeSeBpq as the major product.[93]

7.9 Perthionitrite Anion, $[SSNO]^-$

7.9.1 *Synthesis and solid-state structures*

In 1985 the $[SSNO]^-$ anion (λ_{max} 448 nm) was produced in aprotic solvents (*e.g.*, acetone) from the reaction of an ionic nitrite with elemental sulfur or a polysulfide, supposedly $[PPN]_2S_{12}$, and isolated as the red $[PPN]^+$ salt.[6] Almost 35 years later the X-ray structure of $[PPN]_2S_{12}$ confirmed the presence of the dodecasulfide dianion, the longest known ionic polysulfide chain.[94] The reaction of NO with sulfides or disulfides *in aqueous solution* was observed to generate a transient band (λ_{max} 409 nm) attributed tentatively to $[SSNO]^-$.[95]

The planar *cis* conformation of $[SSNO]^-$ in the red $[PPN]^+$ salt was established in an early work.[6] More recently, small amounts of yellow crystals of [PPN][SSNO] were isolated in addition to the usual red ones; however, the structural parameters for both crystal forms were identical within experimental error, with a short S–S distance (1.974(2) Å) and S–N and N–O distances of 1.700(6) Å and 1.242(6) Å, respectively.[29] Orange crystals of [K(18-crown-6)][SSNO] have been isolated in high yield, along with [Ni(L)(NO)] (L = β-diketiminate), from the reaction of

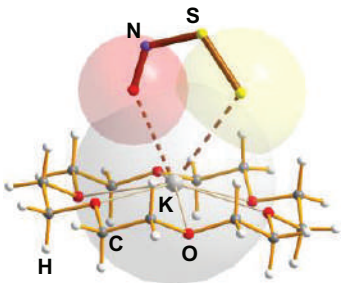

Figure 7.6. Molecular structure of [K(18-crown-6)][SSNO]. The van der Waals radii of O and K atoms are shown as transparent spheres.[96] [Adapted with permission from T. Chivers and R. S. Laitinen, *Chem. Soc. Rev.*, **46**, 5182 (2017). Copyright 2017 Royal Society of Chemistry].

the terminal nickel(II) sulfide complex [K(18-crown-6)][(L)NiS] with an excess of nitric oxide.[96] The $[SSNO]^-$ anion is coordinated to the potassium centre in this salt in a κ^2 (*S,O*) fashion (Fig. 7.6). A similar coordination mode is found for the related sodium salt [Na(15-crown-5)][SSNO], which is obtained as red crystals by addition of ^{t}BuONO to [Na(15-crown-5)][SH] in fluorobenzene.[27b] The reaction of this reagent with [ZnTp(ClO_4)] (Tp = tris(pyrazolyl)borate) in CH_2Cl_2 produces the zinc(II) complex [ZnTp(SSNO)], which exhibits κ^2 (*S,O*) bonding of the $[SSNO]^-$ anion in which the interaction with the sulfur centre is much stronger than that in the alkali-metal salts. [ZnTp(SSNO)] is thermally stable in solution up to 75°C, but releases NO at room temperature upon treatment with an acidic thiol, e.g., C_6F_5SH.[27b]

7.9.2 *Solution behaviour*

A recent investigation using ^{17}O NMR spectroscopy indicated that $[SSNO]^-$ should be the predominant species at physiological pH, based on a proposed pK_a value < 4.7 for the protonated derivative.[97] The rapid conversion of $[SNO]^-$ to $[SSNO]^-$ was also observed in the ^{17}O NMR studies. The identity and stability of *aqueous* $[SSNO]^-$ (at pH 7.4) has been a source of considerable controversy related to its possible biorelevant role,[3,4] arising from different interpretations of the results of the transnitrosation reactions of *S*-nitrosothiols with H_2S (Eq. 7.16).[5,26,98–100]

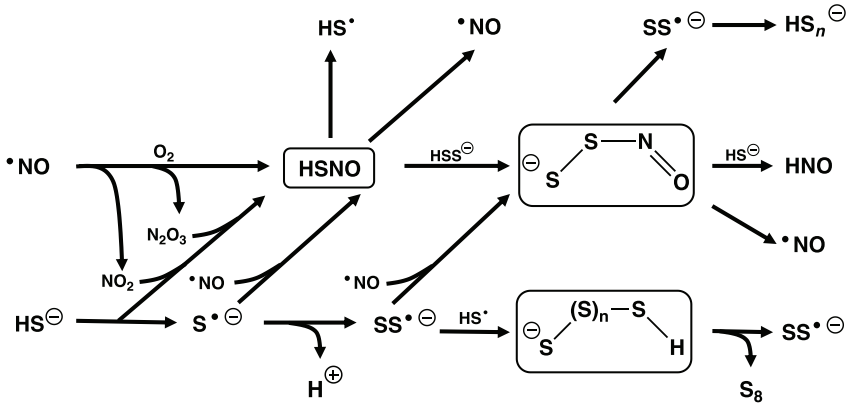

Scheme 7.7. Pathways for the formation and decomposition of (H)SNO and $[SSNO]^-$.[4]

$$RSNO + HS^- \rightarrow (H)SNO + RS^- \qquad (7.16)$$

As illustrated in Scheme 7.7 and discussed in Sec. 7.11, several pathways can lead to (H)SNO. Subsequently, the decomposition of (H)SNO may generate NO through homolysis of the S–N bond together with polysulfides, HS_n^- (n = 2, 3, *etc.*), and colloidal sulfur. Alternatively, in the presence of excess sulfide, HNO and HS_2^- may be formed (Scheme 7.7).[5,23,99]

The transient appearance of a moderately stable yellow intermediate (λ_{max} 412 nm) was attributed to the polysulfide/sulfur mixtures, based on UV-visible, FTIR and ^{15}N NMR data.[26] By contrast, ESI-MS evidence strongly supports the assignment of this band to $[SSNO]^-$,[99] consistent with the previous attribution of a visible absorption band at 409 nm to $[SSNO]^-$ in aqueous solution (Sec. 7.6.1).[95] The reaction of HSNO with HS_2^- (Eq. 7.17 and Scheme 7.7) has been proposed as the main source of $[SSNO]^-$.[5,98]

$$HSNO + HS_2^- \rightarrow [SSNO]^- + HS^- + H^+ \qquad (7.17)$$

In addition, an investigation of the reactions of $[SSNO]^-$ with heme proteins showed that the anion is "relatively stable" in aqueous solution under anaerobic conditions.[101] Furthermore, it was observed that THF solutions of $[SSNO]^-$ generated by treatment of the trisulfide radical ion $[S_3]^{\bullet-}$ with NO persist upon addition of water, but the absorbance of $[SSNO]^-$ at

446 nm in THF shifts substantially with increasing water concentration to *ca.* 420 nm in a 1:1 THF:water solution.[102] Consistently, theoretical evidence (QM-MM simulations, combined with TD-DFT calculations) showed that the visible absorption band of $[SSNO]^-$ moves to lower wavelength upon changing from aprotic to aqueous media, with intermediate values for alcohols.[5,100] The strong solvatochromism was traced to the hydrogen bonding and donor/acceptor interactions of $[SSNO]^-$ with the solvents. Furthermore, calculations indicated that the observed ^{15}N NMR signal at 322 ppm should be attributed to $[SSNO]^-$,[5] rather than $[SNO]^-$ (Sec. 7.5).[28] A detailed comparison of the different structural and spectroscopic data for $[SSNO]^-$ and HSNO/$[SNO]^-$ has been provided.[5]

The influence of solvent on the reactivity of the $[SSNO]^-$ also explains the divergent observations on the reaction of this anion with cyanide. The *aqueous* "$[SSNO]^-$ mix" was unreactive towards cyanide,[98] whereas the reaction of [PPN][SSNO] in *acetone* produces [PPN][SNO] and thiocyanate,[103] *cf.* reaction of $[SSNO]^-$ with PPh_3 (Eq. 7.7).[6] These apparently contrasting results have been attributed to hydrogen bonding to the lone pair at the terminal sulfur atom of $[SSNO]^-$, as indicated by the calculated Mulliken negative charges at terminal sulfur (–0.795 in water, –0.609 in acetone) (Fig. 7.7).[4] In this context, significant changes in reactivity might

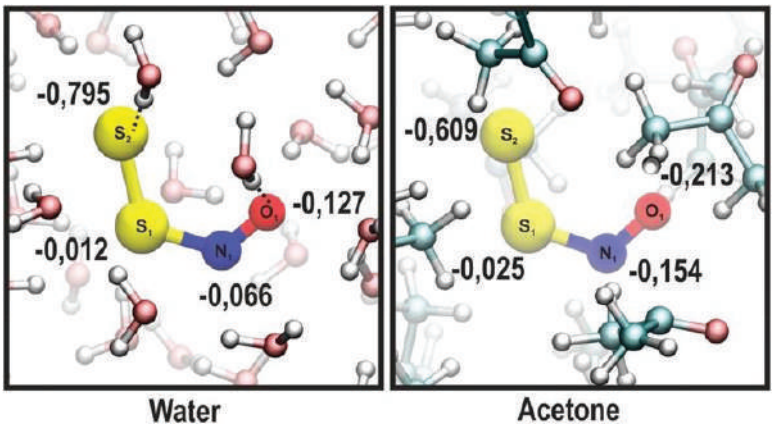

Figure 7.7. Interactions of $[SSNO]^-$ with solvents; dashed lines (---) indicate H-bonding.[100] [Adapted with permission from J. P. Marcolongo, U. N. Morzan, A. Zeida, D. A. Scherlis and J. A. Olabe, *Phys. Chem. Chem. Phys.,* **18**, 30047 (2016). Copyright 2016 Royal Society of Chemistry].

be expected on going from an aqueous medium to a more hydrophobic cellular environment.[104]

In summary, current evidence indicates that $[SSNO]^-$ can survive *transiently* in aqueous solutions for minutes/hours depending on the oxygen concentration and the influence of light.[1,4,5] In addition to the reactivity toward nucleophiles described above, $[SSNO]^-$ (a sulfur analogue of peroxynitrite, $OONO^-$) has been recognised as an NO donor with signaling abilities, through the homolytic cleavage of the S–N bond.

7.9.3 *The "Gmelin" reaction: Iron complexes of $[S_xNO]^-$ (x = 1, 2)*

The longstanding interest in the detailed mechanism of the 178-year-old Gmelin reaction, used for the quantitative determination of sodium nitroprusside (SNP = $Na_2[Fe(CN)_5NO]$), has been renewed because of the biorelevance of the latter nitrosyl complex, as well as of H_2S as a gasotransmitter (Sec. 7.1).[105] At pH 10–13, initial nucleophilic attack of HS^- occurs at the bound NO^+ fragment, with intermediate formation of a moderately stable red-violet coloured species (λ_{max} 535 nm), probably $[Fe(CN)_5NOS]^{4-}$ (Eq 7.18). In the pH range 7–9, a blue transient intermediate (λ_{max} 570 nm) of controversial assignment is additionally formed.[105,106] These coloured species decay further through redox reactions. The formation of an unstable red complex $[Fe(CN)_5N(O)SR]^{3-}$ (λ_{max} ~520 nm) from the reaction of nitroprusside and thiolates is discussed in Sec. 7.7.4 (Scheme 7.4).[77]

$$[Fe(CN)_5NO]^{2-} + HS^- \rightarrow [Fe(CN)_5NOS]^{4-} + H^+ \qquad (7.18)$$

In a recent study the reactions of SNP with either Na_2S or Na_2S_2 in aqueous solution (at pH 12) were monitored by multinuclear NMR (^{17}O, ^{15}N, ^{13}C), UV-visible and IR spectroscopic techniques. The spectroscopic data, in combination with quantum chemical calculations, led to the assignment of the red-violet species as $[Fe(CN)_5NOS]^{4-}$ (λ_{max} 542 nm), whilst the blue species formed through the mixing of aqueous SNP with

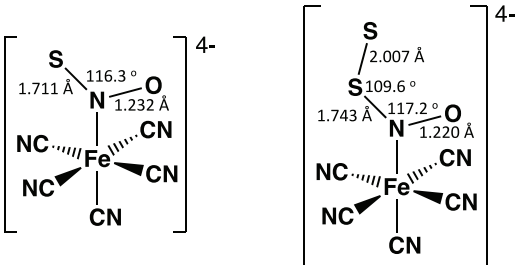

Figure 7.8. Structures of (a) $[Fe(CN)_5N(O)S]^{4-}$ and (b) $[Fe(CN)_5N(O)SS]^{4-}$ fully optimised at the B3LYP/6-311G level.[107] [Adapted with permission from T. Chivers and R. S. Laitinen, *Chem. Soc. Rev.*, **46**, 5182 (2017). Copyright 2017 Royal Society of Chemistry].

Na_2S_2 at pH 7.4 was attributed to $[Fe(CN)_5N(O)SS]^{4-}$ (λ_{max} 570 nm)].[107] The calculated geometries of the two complexes showed that the $[SNO]^-$ and $[SSNO]^-$ anions are both κ^1 (*N*-bonded) to iron, with structural parameters that resemble those found in their $[PPN]^+$ salts (Fig. 7.8).[6,96,107] However, the structural characterisation of these two complexes has not been confirmed and further work on the mechanistic aspects of the Gmelin reaction is also warranted.[5]

7.10 Thiohyponitrite Dianion, $[SN{=}NO]^{2-}$

In contrast to the well-characterised transition-metal complexes of the $[SSNS]^-$ anion, *e.g.*, with coinage metals (Sec. 5.9.3), no metal complexes of $[SSNO]^-$ have been isolated and structurally characterised. However, the reaction of the terminal nickel(II) sulfide complex [K(18-crown-6)][Ni(L)S] with nitrous oxide generates [K(18-crown-6)][Ni(L)(SN=NO)] *via* a [3 + 2] cyclo-addition of N_2O across the Ni–S bond (Chart 7.5).[108] This nickel complex contains the first example of the thiohyponitrite $[SN{=}NO]^{2-}$ ligand. The S–N and O–N distances are 1.787(6) and 1.308(1) Å, respectively, consistent with single bonds, while the N–N bond length of 1.154(9) Å is indicative of a double bond.

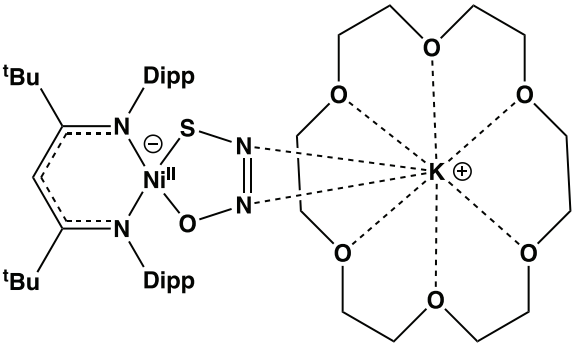

Chart 7.5. Structure of [K(18-crown-6)][Ni(L)(SN=NO)].

7.11 NO/H_2S Crosstalk

The title of this section refers to the biologically relevant interactions of two gasotransmitters that are recognised as endogenously formed species with specific signaling abilities (Sec. 7.1). In fact, the crosstalk significance of the direct NO + H_2S reaction has been extended to the chemistry of H_2S with other NO-containing species, *e.g.*, NO^+, NO^-, NO_2^-, $[ONOO]^-$, RSNOs and metal complexes $[ML_5(NO)]^{n+}$. Early studies of the direct reaction revealed a variety of products including NH_3, N_2O and S_8. A possible first step (Eq. 7.19) is endergonic with $\Delta G° = +\ 142$ kJ mol^{-1}.[3,4]

$$HS^- + NO \rightarrow HNO + S^{\bullet -} \qquad (7.19)$$

A recent combined experimental and computational study showed that aliphatic and aromatic thiols are able to convert NO to HNO under aerobic conditions; the free radical adduct $[RSNOH]^\bullet$ was identified as an intermediate in this process.[110] In 2014 a very fast formation of HNO was observed when the NO and H_2S precursors were co-produced at pH 7.4.[75a]

Comprehensive evidence for the generation of (H)SNO and $[SSNO]^-$ *via* the direct reactions under aerobic and anaerobic conditions has been presented.[98,99] In the former case the proposed formation of N_2O_3 produces (H)SNO and, subsequently, $[SSNO]^-$, upon reaction with $[HS_2]^-$ (Scheme 7.7). Subsequently, HNO, NO and polysulfides are generated. Surprisingly, under anaerobic conditions the formation of similar products

is invoked (Scheme 7.7). However, this route involves the initial endergonic formation of thiyl radical anions $S^{\bullet-}$, which may arise from disulfide impurities in the monosulfide reagent.[99]

7.12 Conclusions

Early sections in this chapter have described the synthesis, spectroscopic properties, molecular and electronic structures, reactions and metal complexes of the $[SNO]^-$ anion and its conjugate acid HSNO (Secs. 7.5 and 7.6, respectively), as well as the $[SSNO]^-$ anion (Sec. 7.9). This information is crucial to an understanding of the role of these labile species in biological systems. The following conclusions can be made:

- The spectroscopic signatures (UV-visible, FTIR, and ^{15}N chemical shifts) of $[SNO]^-$, $[SSNO]^-$ and (H)SNO are reasonably well-established.[4] One or more of these techniques can be used to identify these species or monitor their reactions.
- The production of HSNO as a unique isomer from the reaction of NO and H_2S has enabled the structural characterisation of both the *cis*- and *trans*-isomers at room temperature in the gas phase by FT microwave spectroscopy.[33]
- HSNO coordinates in an *N*-bonded fashion to a Ru(III) centre.[39]
- A mixture of rapidly interconverting isomers (H)SNO can be produced from H_2S in water under physiologically relevant conditions by using the transnitrosation reaction with *S*-nitrosothiols, *e.g.*, GSNO.[3,28] (H)SNO behaves as a reactive species leading to NO ($t_{½}$ = 6 sec) upon dissociation, HNO *via* reaction with sulfide, or $[SSNO]^-$ upon reaction with disulfide $[HS_2]^-$.
- In aqueous solution the ^{15}N NMR chemical shift of $[SSNO]^-$ is 322 ppm and its presence can also be detected by ESI-MS.
- The properties of $[SSNO]^-$ in aprotic solvents are markedly different from those in aqueous solution under physiological conditions (pH = 7.4). For example, the UV-visible absorption maximum shifts from *ca.* 448 nm to 410 nm upon changing the solvent from acetone to water.[100,102] This solvatochromic effect influences the structural

parameters and Mulliken charges and, hence, the reactivity of $[SSNO]^-$ in different solvents.

- The $[SSNO]^-$ anion decomposes faster in water than in non-aqueous solvents *via* S–N bond cleavage.[4] On the other hand, $[SSNO]^-$ is unreactive towards nucleophiles such as cyanide or thiols in water.[98] However, faster reactions occur with nucleophiles in aprotic media and the reaction with PPh_3 in acetone is used for the preparation of salts of the $[SNO]^-$ anion.[6,103]
- HNO (nitroxyl), the conjugate acid of the nitroxide anion $[NO]^-$, can be formed as an intermediate in transnitrosation or direct reactions with H_2S.[3,110,111] It can lead to N_2O or be further reduced to NH_2OH/NH_3, depending on the conditions.

Despite much progress, the roles of $[SNO]^-$, $[SSNO]^-$ and (H)SNO in NO/H_2S crosstalk remain controversial, particularly with regard to mechanistic details of the biological relevance (for detailed discussions, see refs. 3 and 4). Some of the unresolved questions include: (a) the fate of (H)SNO, (b) the role of $[SSNO]^-$ in the crosstalk, (c) the possible involvement of polysulfides $[HS_n]^-$, and (d) the mode of HNO production. From a more fundamental point of view the identity of the blue species (λ_{max} 575 nm) formed in the Gmelin reaction awaits a resolution.

References

1. M. M. Cortese-Krott, A. R. Butler, J. D. Woollins and M. Feelisch, *Dalton Trans*., **45**, 5908 (2016).
2. T. Chivers and R. S. Laitinen, *Chem. Soc. Rev*., **46**, 5182 (2017).
3. I. Ivanovic-Burmazovic and M. R. Filipovic, *Inorg. Chem*., **58**, 4039 (2019).
4. J. P. Marcolongo, M. F. Venâncio, W. R. Rocha, F. Doctorovich, and J. A. Olabe, *Inorg. Chem*., **58**, 14981 (2019).
5. J. P. Marcolongo, A. Zeida, L. D. Slep and J. A. Olabe, *Adv. Inorg. Chem*., **70**, 277 (2017).
6. F. Seel, R. Kuhn, G. Simon, M. Wagner, B. Krebs and M. Dartmann, *Z. Naturforsch*., **40B**, 1607 (1985).

7. (a) D. L. H. Williams, *Acc. Chem. Res*., **32**, 869 (1999): (b) D. L. H. Williams, *Org. Biomol. Chem.*, **1**, 441 (2003).
8. K. A. Broniowska and N. Hogg, *Antioxid. Redox Signal.*, **17**, 969 (2012).
9. B. C. Smith and M. A. Marletta, *Curr. Opin. Chem. Biol*., **16**, 498 (2012).
10. C. Zhang, T. D. Biggs, N. O. Devarie-Baez, S. Shuang, C. Dong and M. Xian, *Chem. Commun*., **53**, 11266 (2017).
11. D. A. Armitage and J. C. Brand, *J. Chem. Soc., Chem. Commun*., 1078 (1979).
12. (a) S. Mann and M. Jansen, *Z. Anorg. Allg. Chem*., **621**, 153 (1995); (b) S. Mann and M. Jansen, *Z. Naturforsch*., **49B**, 1503 (1994).
13. W. Heilemann and R. Mews, *Chem. Ber*., **121**, 461 (1988).
14. J. H. Lehman and W. C. Lineberger, *J. Chem. Phys*., **147**, 013943 (2017).
15. M. Herberhold and W. Ehrenreich, *Angew. Chem. Int. Ed. Engl*., **21**, 633 (1982).
16. H. Plenio, H. W. Roesky, F. T. Edelmann and M. Noltemeyer, *J. Chem. Soc., Dalton Trans*., 1815 (1989).
17. (a) R. Short, M. B. Hursthouse, T. G. Purcell and J. D. Woollins, *J. Chem. Soc., Chem. Commun.,* 407 (1987); (b) L. J. R. McGeachie, C. L. Carpenter-Warren, D. B. Cordes, M. Bühl, S. J. Gray, G. Hua, A. M. Z. Slawin and J. D. Woollins, *Z. Anorg. Chem. Allg*., **646**, 1795 (2020); (c) L. J. R. McGeachie, M. Bühl, D. B. Cordes, A. M. Z. Slawin and J. D. Woollins, *Inorg. Chem*., **60**, 8423 (2021).
18. (a) T. Chivers, K.J. Schmidt, D. D. McIntyre and H. J. Vogel, *Can. J. Chem*., **67**, 1788 (1989); (b) P. Vilarrubias, *Mol. Phys*., **118**, e1797915 (2020).
19. N. H. Morgon, H. V. Linnert and J. M. Riveros, *J. Phys. Chem*., **99**, 11667 (1995).
20. K. O. Christe, J. A. Boatz, M. Gerken, R. Haiges, S. Schneider. T. Schroer, F. S. Tham, A. Vij, V. Vij, R. I. Wagner and W. W. Wilson, *Inorg. Chem*., **41**, 4275 (2002).
21. A. Kornath, O. Blecher and R. Ludwig, *Z. Anorg. Allg. Chem*., **628**, 183 (2002).
22. J. Valjus, H. M. Tuononen, R. S. Laitinen and T. Chivers, *Can. J. Chem*., **96**, 591 (2018).
23. T. Trabelsi, O. Yazidi, J. S. Francisco, R. Linguerri and M. Hochlaf, *J. Chem. Phys*., **143**, 164301 (2015).
24. M. Méndez, J. S. Francisco and D. A. Dixon, *Chem. Eur. J*., **20**, 10231 (2014).

25. E. Victor, *Reactions of S-nitrosothiols with biomimetic iron complexes and other transition metals*, Ph. D. thesis, Massachusetts Institute of Technology, 2014.
26. M. R. Filipovic, J. L. Miljkovic, T. Nauser, M. Royzen, K. Klos, T. Shubina, W. H. Koppenol, S. J. Lippard and I. Ivanović-Burmazović, *J. Am. Chem. Soc*., **134**, 12016 (2012).
27. (a) D. Chatterjee, P. Sarkar, M. Oszajca and R. van Eldik, *Inorg. Chem*., **55**, 5037 (2016); (b) V. Hosseininasab, J. A. Bertke and T. H. Warren, *Angew. Chem. Int. Ed*., [in press], doi: 10.1002/anie.202104906 (2021).
28. F. Seel, in *Sulfur: Its Significance for Chemistry, for the Geo-, Bio- and Cosmophere and Technology*, Eds. A. Müller and B. Krebs, Elsevier (1984), pp. 55–66.
29. R. Wedmann, A. Zahl, T. E. Shubina, M. Dürr, F. W. Heinemann, B. E. C. Bugenhagen, P. Burger, I. Ivananovic-Burmazovic and M. R. Filipovic, *Inorg. Chem*., **54**, 9367 (2015).
30. P. O. Tchir and R. D. Spratley, *Can. J. Chem*., **53**, 2318 (1975).
31. R. P. Müller, M. Nonella, P. Russegger and J. R. Huber, *Chem. Phys*., **87**, 351 (1984).
32. M. Nonella, J. R. Huber and T. K. Ha, *J. Phys. Chem*., **91**, 5203 (1987).
33. M. Nava, M-A. Martin-Drumel, C. A. Lopez, K. N. Crabtree, C. C. Womack, T. L. Nguyen, S. Thorworth, C. C. Cummins, J. F. Stanton and M. C. McCarthy, *J. Am. Chem. Soc*., **138**, 11441 (2016).
34. Q. K. Timerghazin, G. H. Peslherbe and A. M. English, *Phys. Chem. Chem. Phys*., **10**, 1532 (2008).
35. C-H. Lai, E. Y. Li and P-Tai. Chou, *Theor. Chem. Acc*., **117**, 145 (2007).
36. L. V. Ivanova, B. J. Anton and Q. K. Timerghazin, *Phys. Chem. Chem. Phys*., **16**, 1532 (2014).
37. A. S. M. Islam, R. Bhowmick, K. Pal, A. Katarkar, K. Chaudhri and M. Ali, *Inorg. Chem*. **56**, 4324 (2017).
38. W. Chen, T. Matsunaga, D. L. Neill, C-T. Tang, T. Akaike and M. Xian, *Angew. Chem. Int. Ed*., **58**, 16067 (2019).
39. D. Chatterjee, C. Chowdury, A. Datta and R. van Eldik, *New. J. Chem*., **43**, 15311 (2019).
40. M. Flister and Q. K. Timerghazin, *J. Phys. Chem. A*, **118**, 9914 (2014).
41. M. Bartberger, J. D. Mannion, S. C. Powell, J. D. Mannion, J. S. Stamler, K. N. Houk, and E. J. Toone, *J. Am. Chem. Soc*., **122**, 8868 (2001).
42. M. Bartberger, K. N. Houk, S. C. Powell, J. D. Mannion, K. Y. Lo, J. S. Stamler and E. J. Toone, *J. Am. Chem. Soc*., **123**, 5889 (2000).

43. M. Marazzi, A. López-Delgado, M. A. Fernández-González, O. Castaño, L. M. Frutos and M. Temprado, *J. Phys. Chem. A*, **116**, 7039 (2012).
44. J. B. Dorado, B. Z. Dlugogorski, E. M. Kennedy, J. C. Mackie, J. Gore and M. Altrawneh, *RSC Adv*., **5**, 29914 (2015).
45. H. S. Tasker and H. O. Jones, *J. Chem. Soc*., **95**, 1910 (1909).
46. A. Cánneva, C. O. Della Védova, N. W. Mitzel and M. F. Erben, *J. Phys. Chem. A*, **119**, 1524 (2015).
47. J. Lee, L. Chen and G. B. Richter-Addo, *Chem. Rev*., **102**, 1019 (2002).
48. A. C. Spivey, J. Colley, L. Sprigens, S. M. Hancock, D. S. Cameron, K. I. Chigboh, G. Veitch, C. S. Frampton and H. Adams, *Org. Biomol. Chem*., **3**, 1942 (2005).
49. N. Arulsamy, D. S. Bohle, J. A. Butt, G. I. Irvine, P. A. Jordan and E. Sagan, *J. Am. Chem. Soc*., **121**, 7115 (1999).
50. K. Goto, Y. Hino, T. Kawashima, M. Kaminaga, E. Yano, G. Yamamoto, N. Takagi and S. Nagase, *Tetrahedron Lett*., **41**, 8479 (2000).
51. K. Goto and T. Kawashima, *J. Synth. Org. Chem. Japan*, **63**, 1157 (2005).
52. K. Goto, Y. Hino, Y. Takahashi, T. Kawashima, G. Yamamoto, N. Takagi and S. Nagase, *Chem. Lett*., **30**, 1204 (2001).
53. M. Ito, K. Takenaka, R. Okazaki, N. Takeda and N. Tokitoh, *Chem. Lett*., **30**, 1206 (2001).
54. J. Yi, P. Coppens, D. R. Powell and G. B. Richter-Addo, *Comments Inorg. Chem*., **36**, 81 (2016).
55. G. E. Carnahan. P. G. Lenhert and R. Ravichandran, *Acta Crystallogr*., **B34**, 2645 (1978).
56. D. G. Khomyakov and Q. K. Timerghazin, *J. Chem. Phys*., **147**, 044305 (2017).
57. (a) Q. K. Timerghazin, G. H. Peslherbe and A. M. English, *Org. Lett*., **9**, 3049 (2007); (b) Q. K. Timerghazin, A. M. English and G. H. Peslherbe, *Chem. Phys. Lett*., **454**, 24 (2008).
58. E. E. Moran, Q. K. Timerghazin, E. Kwong and A. M. English, *J. Phys. Chem. B*, **115**, 3112 (2011).
59. (a) M. R. Talipov and Q. K. Timerghazin, *J. Phys. Chem. B*, **117**, 1827 (2013); (b) Q. K. Timerghazin and M. R. Talipov, *J. Phys. Chem. Lett*., **4**, 1034 (2013); (c) M. Flister and Q. K. Timerghazin, *J. Phys. Chem. A*, **118**, 9914 (2014)
60. J. Barrett, D. F. Debenham and J. Glauser, *Chem. Commun*., 248 (1965).
61. Y. Gao, Y. Dai and G. Wu, *J. Phys Chem. B,* **121,** 7311 (2017).
62. S. Zhang, N. Çelebi-Ölçüm, M. M. Melzer, K. N. Houk and T. H. Warren, *J. Am. Chem. Soc*., **135**, 16746 (2013).

63. S. Kundu, W. Y. Kim, J. A. Bertke and T. H. Warren, *J. Am. Chem. Soc*., **139**, 1045 (2017).
64. (a) B. K. Oh and M. E. Meyerhoff, *J. Am. Chem. Soc*., **125**, 9552 (2003); (b) S. Hwang, W. Cha and M. E. Meyerhoff, *Angew. Chem. Int. Ed.*, **45**, 2745 (2006).
65. M. M. Melzer, E. Li and T. H. Warren, *Chem. Commun*., 5847 (2009).
66. M. M. Melzer, S. Mossin, A. J. P. Cardenas, K. D. Williams, S. Zhang, K. Meyer and T. H. Warren, *Inorg. Chem*., **51**, 8658 (2012).
67. S. Kundu, W. Y. Kim, J. A. Bertke and T. H. Warren, *J. Am. Chem. Soc*., **139**, 1045 (2017).
68. J. Kozhukh and S. J. Lippard, *Inorg. Chem*., **51**, 7346 (2012).
69. (a) M. S. Varonka and T. H. Warren, *Inorg. Chem*., **48**, 5605 (2009); A. J. P. Cardenas, R. Abelmann and T. H. Warren, *Chem. Commun*., **50**, 168 (2014).
70. (a) L. Perissinotti, D. A. Estrin, G. Leitus and F. Doctorovich, *J. Am. Chem. Soc*., **128**, 2512 (2006); (b) L. Perissinotti, G. Leitus, L. Shimon, D. Estrin and F. Doctorovich, *Inorg. Chem*., **47**, 4723 (2008).
71. S. Zhang, M. M. Melzer, S. S. Nermin, N. Çelebi-Ölçüm and T. H. Warren, *Nat. Chem*., **8**, 663 (2016).
72. W. Tao, C. E. Moore and S. Zhang, *Angew. Chem. Int. Ed*., **60**, 15980 (2021).
73. C. D. Hubbard, D. Chatterjee, M. Oszajca, J. Polazek, O. Impert, M. Chrzanowska, A. Katafias, R. Puchta and R. van Eldik, *Dalton Trans*., **49**, 4599 (2020).
74. J. L. Miljkovic, I. Kenkel, I. Ivanović-Burmazović and M. R. Filipovic, *Angew. Chem. Int. Ed*., **52**, 12061 (2013).
75. (a) M. Eberhardt, M. Dux, B. Namer, J. Miljkovic, N. Cordasic, C. Will, T. I. Kichko, J. de la Roche, M. Fischer, S. A. Suárez, D. Bikiel, K. Dorsch, A. Leffler, A. Babes, A. Lampert, J. K. Lennerz, J. Jacobi, M. A. Marti, F. Doctorovich, E. D. Högestätt, P. M. Zygmunt, I. Ravanovic-Burmazovic, K. Messlinger, P. Reeh and M. R. Filipovic, *Nat. Commun*., **5**, 4381 (2014); (b) R. Wedmann, S. Bertlein, I. Macinkovic, S. Böltz, J. Lj. Miljkovic, L. E. Muñoz, M. Herrmann and M. R. Filipovic, *Nitric Oxide*, **41**, 85 (2014).
76. M. D. Johnson and R. G. Wilkins, *Inorg. Chem*., **23**, 231 (1984).
77. Y. Gao, B. Mossing and G. Wu, *Dalton Trans*., **44**, 20338 (2015).
78. A. L. Poptic and S. Zhang, *Inorg. Chem*., **60**, 5190 (2021).
79. L. V. Andreasen, I. M. Lorkovic, G. B. Richter-Addo and P. C. Ford, *Nitric Oxide*, **6**, 228 (2002).

80. D. Chatterjee, N. Jaiswal, M. Schmeisser and R. van Eldik, *Dalton Trans*., **43**, 18042 (2014).
81. A. Weichsel, E. M. Maes, J. F. Andersen, J. G. Valenzuela, T. K. Shokhireva, F. A. Walker and W. R. Montfort, *Proc. Nat. Acad. Sci. U. S. A*., **102**, 594 (2005).
82. (a) N. Hendinejad and Q. K. Timerghazin, *Phys. Chem. Chem. Phys*., **22**, 6595 (2020); (b) M. R. Talipov, D. G. Khomyakov, M. Xian and Q. K. Timerghazin, *J. Comput. Chem.,* **34**, 1527 (2013).
83. (a) A. Zeida, C. M. Guardia, P. Lichtig, L. L. Perissonitti, L. A. Defilipe, A. Turjanski, R. Radi, M. Trujillo and D. A. Estrin, *Biophys. Rev*., **6**, 27 (2014); (b) L. V. Ivanova, D. Cibich, G. Deye, M. R. Talipov and Q. K. Timerghazin, *ChemBioChem*, **18**, 726 (2017).
84. L. L. Perissinotti, A. G. Turjanski, D. A. Estrin and F. Doctorovich, *J. Am. Chem. Soc*., **127**, 486 (2005).
85. V. Hosseininasab, A. C. McQuilken, A. Bakhoda, J. A. Bertke, Q. K. Timerghazin and T. H. Warren, *Angew. Chem. Int. Ed.*, **59**, 10854 (2020).
86. (a) Y. Wang, S. Xu and M. Xian, *Chem. Eur J.*, **26**, 11673 (2020); (b) M. Haake, *Tetrahedron Lett*., **33**, 3405 (1972).
87. H. Wang and M. Xian, *Angew. Chem. Int. Ed*., **47**, 6598 (2008).
88. D. Zhang, W. Chen, Z. Miao, Y. Ye, Y. Zhao, S. B. King and M. Xian, *Chem. Commun*., **50**, 4806 (2014).
89. L. Song, F. Keul and A. Mardyukov, *Chem. Commun*., **55**, 9943 (2019).
90. C. Wismach, W-W. du Mont, P. G. Jones, L. Ernst, U. Papke, G. Mugesh, W. Kaim, M. Wanner and K. D. Becker, *Angew. Chem. Int. Ed.,* **43**, 3970 (2004).
91. K. Shimada, K. Goto, T. Kawashima, N. Takagi, Y-K. Choe and S. Nagase, *J. Am. Chem. Soc*., **126**, 13238 (2004).
92. K. Goto, K. Shimada and T. Kawashima, *Phosphorus, Sulfur, Silicon Relat. Elem*., **180**, 945 (2005).
93. K. Shimada, K. Goto and T. Kawashima, *Chem. Lett*., **34**, 654 (2005).
94. P. Liebing, M. Kühling, C. Swanson, M. Feneberg, L. Filbert, R. Goldhahn, T. Chivers and F. T. Edelmann, *Chem. Commun*., **55**, 14965 (2019).
95. F. Seel and M. Wagner, *Z. Anorg. Allg. Chem*., **558**, 189 (1988).
96. N. J. Hartmann, G. Wu and T. W. Hayton, *J. Am. Chem. Soc*., **138**, 12352 (2016).
97. X. Zhu and Y. Gao, *RSC Adv*., **10**, 39617 (2020).
98. M. M. Cortese-Krott, B. O. Fernandez, J. L. T. Santos, E. Mergia, M. Grman, P. Nagy, M. Kelm, A. Butler and M. Feelisch, *Redox Biol*., **2**, 234 (2014).

99. M. M. Cortese-Krott, G. G. C. Kuhnle, A. Dyson, B. O. Fernandez, M. Grman, J. F. DuMond, M. P. Barrow, G. McLeod, H. Nakagawa, K. Ondrias, P. Nagy, S. B. King, J. E. Saavedra, L. K. Keefer, M. Singer, M. Kelm, A. R. Butler and M. Feelisch, *Proc. Natl. Acad. Sci. U. S. A.*, **112**, E4651 (2015).
100. J. P. Marcolongo, U. N. Morzan, A. Zeida, D. A. Scherlis and J. A. Olabe, *Phys. Chem. Chem. Phys.,* **18**, 30047 (2016).
101. C. Bolden, S. B. King and D. B. Kim-Shapiro, *Free Radic. Biol. Med.*, **99**, 418 (2016).
102. T. S. Bailey, H. A. Henthorn and M. D. Pluth, *Inorg. Chem.*, **55**, 12618 (2016).
103. R. Wedmann, I. Ivananovic-Burmazovic and M. R. Filipovic, *Interface Focus*, **7**, 20160139 (2017).
104. T. V. Mishanina, M. Libiad and R. Banerjee, *Nat. Chem. Biol.*, **11**, 457 (2015).
105. S. L. Quiroga, A. E. Almaraz, V. T. Amorebieta, L. L. Perissinotti and J. A. Olabe, *Chem. Eur. J.*, **17**, 4145 (2011).
106. M. R. Filipovic and I. Ivanovic-Burmazovic, *Chem. Eur. J.*, **18**, 13538 (2012).
107. Y. Gao, A. Toubaei, X. Kong and G. Wu, *Chem. Eur. J.*, **21**, 17172 (2015).
108. N. J. Hartmann, G. Wu and T. W. Hayton, *Angew. Chem. Int. Ed.*, **54**, 14956 (2015).
109. M. Filipovic, M. Eberhardt, V. Prokopovic, A. Mijuskovic, Z. Orescanin-Dusic, P. Reeh and I. Ivanovic-Burmazovic, *J. Med. Chem.*, **56**, 1499 (2013).
110. S. A. Suarez, M. Muñoz, L. Alvarez, M. F. Venâncio, W. R. Rocha, D. E. Bikiel, M. A. Marti and F. Doctorovich, *J. Am. Chem. Soc.*, **139**, 14483 (2017).
111. L. V. Ivanova, D. Cibich, G. Deye, M. R. Talipov and Q. K. Timerghazin, *ChemBioChem*, **18**, 726 (2017).

Chapter 8

Chalcogen-Nitrogen Halides: Synthetic Reagents

8.1 Introduction

This chapter will deal with both acyclic and cyclic chalcogen-nitrogen compounds that contain chalcogen-halogen bonds. The simplest examples of these ternary systems are the monomeric thiazyl halides N≡S–X (X = F, Cl), which are obtained in the gas phase. These sulfur(IV) compounds exhibit a versatile chemistry, including the preparation of the first $[NS]^+$ salts and the formation of metal complexes, which are also known for NSeCl. The monomers NSX readily oligomerise to form cyclic trimers $(NSX)_3$ (X = F, Cl); selenium analogues $(NSeX)_3$ are unknown. However, the cationic, acyclic chalcogen-nitrogen halides $[N(ECl)_2]^+$ (E = S, Se) and $[N(EX_2)_2]^+$ (E = S, Se; X = F, Cl) are well-characterised for both sulfur and selenium. There are no tellurium analogues of these acyclic chalcogen-nitrogen halides, but cyclic cations that contain $[Cl_3Te–N=TeCl]^+$ units have been structurally characterised.

The sulfur(VI) derivative thiazyl trifluoride $N≡SF_3$ is a colourless gas that reacts readily with nucleophiles or electrophiles and also forms *N*-bonded complexes with a variety of transition metals and Lewis acids. Iminosulfur(VI)-oxydifluorides $RN=S(O)F_2$ are versatile reagents for the synthesis of sulfur(VI)-nitrogen compounds with a variety of medicinal applications.

The cyclic sulfur-nitrogen halides $[S_3N_2Cl]Cl$ and $(NSCl)_3$ are important reagents for the synthesis of both inorganic and organic

sulfur-nitrogen derivatives, *e.g.*, binary sulfur-nitrogen cations, cyclic sulfur-nitrogen oxides, and carbon-containing sulfur-nitrogen heterocycles. Sulfanuric halides $[NS(O)X]_3$ (X = F, Cl) are cyclic sulfur-nitrogen compounds with sulfur atoms in the formal +6 oxidation state.

The series of imidoselenium(II) dihalides $ClSe[N(^tBu)Se]_nCl$ (n = 1–3) with chain structures have no sulfur or tellurium analogues. They are important intermediates in the synthesis of cyclic selenium imides *via* cyclocondensation of *tert*-butylamine with $SeCl_2$ (Sec. 9.4). Imidochalcogen(IV) dihalides $RN{=}EX_2$ (E = S, Se, Te; X = F, Cl, Br) are known for all three chalcogens. However, their thermal stability is strongly dependent on the nature of both the chalcogen and the R group.

Throughout this chapter the emphasis will be on structural aspects and synthetic applications of chalcogen-nitrogen halides.

8.2 Thiazyl Halides, NSX (X = F, Cl, Br)

8.2.1 *Synthesis and structures*

Thiazyl fluoride is a moisture-sensitive, thermally unstable gas.[1] It is conveniently generated by decomposition of compounds which already contain the NSF group, *e.g.*, $FC(O)NSF_2$ (Eq. 8.1) or $[Hg(NSF_2)_2]$ (Eq. 8.2).[2] It forms the cyclic trimer $(NSF)_3$ at room temperature. A high yield synthesis of NSF from $(NSCl)_3$ and KF in tetramethylsulfone at 80°C has been reported.[3]

$$FC(O)NSF_2 \rightarrow NSF + COF_2 \qquad (8.1)$$

$$[Hg(NSF_2)_2] \rightarrow 2NSF + HgF_2 \qquad (8.2)$$

Monomeric NSCl is formed as a greenish-yellow gas by heating the cyclic trimer $(NSCl)_3$ under vacuum or in an inert gas stream.[4] NSCl monomer may also be generated in solutions of $(NSCl)_3$ in liquid SO_2 at room temperature or in CCl_4 at 70°C.[5] It trimerises in the condensed state. Monomeric thiazyl halides NSX (X = Cl, Br) have also been obtained by the pyrolysis of $[S_4N_3]X$ at 120°C (X = Cl) or 90°C (X = Br).[6] This method has been used to produce NSX in an argon matrix at 15 K for the determination of infra-red spectra. The gas-phase structures of NSF[7a] and NSCl[7b] have been determined by microwave spectroscopy. They are bent molecules

(<NSF = 117°, <NSCl = 118°) with sulfur-nitrogen bond lengths of 1.448 and 1.450 Å, respectively, consistent with substantial triple bond character. The sulfur-halogen distances are 1.643 Å (X = F) and 2.161 Å (X = Cl).

Recent generalised valence bond calculations, accompanied by accurate coupled cluster calculations, showed that the NSF arrangement is more stable than the FSN isomer by 164.8 kJ mol^{-1}.[8a] Earlier *ab initio* molecular orbital calculations showed that NSCl is favoured over the hypothetical SNCl by 77.0 kJ mol^{-1}.[8b] Self-consistent field calculations predict that (a) the dimers $(NSX)_2$ (X = F, Cl) are thermodynamically unstable with respect to 2NSX and (b) the trimer $(NSF)_3$ is stable compared to 3NSF, consistent with experimental observations (Sec. 8.7).[9]

8.2.2 *Reactions*

The reaction of NSF with strong fluoride ion acceptors, *e.g.*, MF_5 (M = As, Sb) in liquid SO_2 was the first synthesis of $[SN]^+$ salts (Eq. 8.3).[10] However, other preparative routes to these important reagents have subsequently been developed (Sec. 5.8.1).

$$NSF + MF_5 \rightarrow [SN][MF_6] \qquad (8.3)$$

Thiazyl halide monomers NSX also undergo nucleophilic addition with halide ions to give ternary anions of the type $[NSX_2]^-$. The $[NSF_2]^-$ ion in the salts $Cs[NSF_2]$ and $[(Me_2N)_3S][NSF_2]$ has been characterised by vibrational spectra.[11] The $[NSCl_2]^-$ anion, obtained by chloride addition to NSCl (generated from the cyclic trimer), has been isolated in salts with large counter-anions, *e.g.*, $[Ph_4P]^+$ and $[Me_4N]^+$.[12] The $[NSCl_2]^-$ anion in the $[(Ph_3PN)_2SCl]^+$ salt has a slightly distorted C_s structure with a very short sulfur-nitrogen bond (1.44 Å) and two loosely bound chlorine atoms [d(S–Cl) = 2.42 Å]. The structure can be described by the resonance forms depicted in Chart 8.1.

8.2.3 *Metal complexes*

Monomeric thiazyl halides can be stabilised by coordination to transition metals and a large number of such complexes are known. The NSF complexes are conveniently prepared in SO_2 (Eq. 8.4).[13]

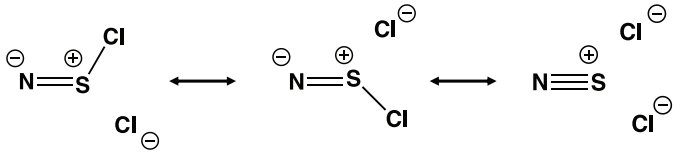

Chart 8.1. Resonance structures of $[NSCl_2]^-$.

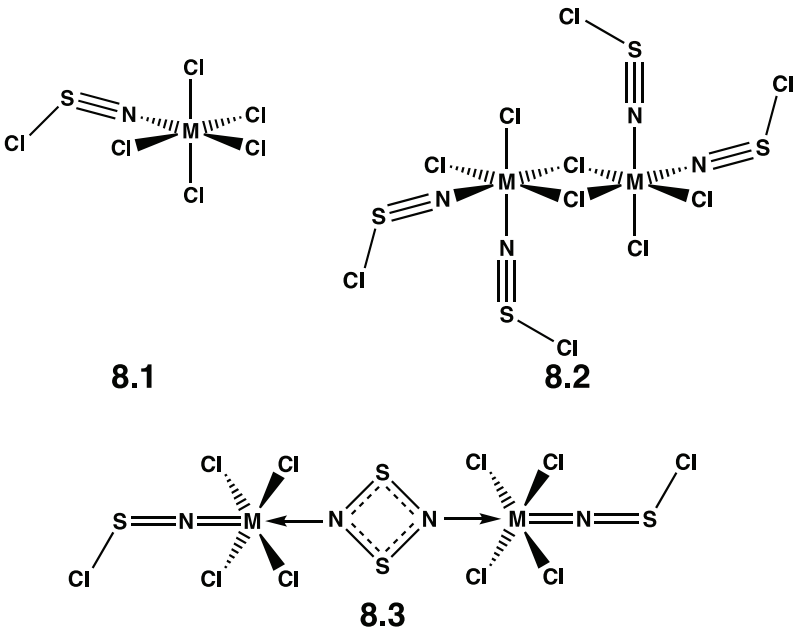

Chart 8.2. Metal complexes of NSCl.

$$[M(SO_2)][AsF_6]_2 + 6NSF \rightarrow [M(NSF)_6][AsF_6]_2 + SO_2 \quad (M = Co, Ni) \qquad (8.4)$$

The most general route to M-NSCl complexes involves the reactions of the cyclic trimer $(NSCl)_3$ with anhydrous metal chlorides in solvents such as CH_2Cl_2 or CCl_4.[14] For example, the 1:1 complexes $[MCl_5(NSCl)]$ (**8.1**, M = Nb, Ta) are formed from MCl_5 and $(NSCl)_3$, whereas VCl_4 yields a dimeric structure $[VCl_3(NSCl)_2]_2$ (**8.2**, M = V) (Chart 8.2).[15] However, the nature of the products obtained from these reactions is markedly dependent on

the reaction conditions. For example, the dimeric complex $[MoCl_4(NSCl)]_2$ is obtained from reaction of Mo_2Cl_{10} with $(NSCl)_3$ in CH_2Cl_2 when the $MoCl_5$:NSCl ratio is 1:1,[16] whereas a dinuclear complex containing a bridging S_2N_2 ligand (**8.3**, M = Mo) (Chart 8.2) is obtained when that ratio is changed to 1:2.[17] In CCl_4 solution the reaction of WCl_6 with $(NSCl)_3$ produces the tungsten analogue **8.3** (M = W), in addition to $[WCl_4(NSCl)]_2$ and the cyclometallathiazene $[WCl_3(S_2N_3)]_2$.[16b]

Both NSCl and NSBr complexes have been prepared by halogen exchange at coordinated NSF using silicon tetrahalides as the reagent and liquid SO_2 as solvent (Eq. 8.5).[18a] Metal complexes of the thiazyl amide ligand $NSNMe_2$ have also been generated by treatment of coordinated NSF with Me_3SiNMe_2.[18b]

$$[Re(CO)_5NSF][AsF_6] + \tfrac{1}{4}SiX_4 \rightarrow [Re(CO)_5NSX][AsF_6] + \tfrac{1}{4}SiF_4 \quad (8.5)$$
$$(X = Cl, Br)$$

Selenazyl halides NSeX have not been characterised either as monomers or cyclic oligomers. However, the monomeric ligand is stabilised in metal complexes of the type $[MCl_4(NSeCl)]_2$ (M = Mo, W), which are obtained from the reactions of $MoCl_5$ or WCl_6 with Se_4N_4 in dichloromethane.[19] The bonding features in the anion $[WCl_5(NSeCl)]^-$ are similar to those in NSCl complexes with a short tungsten-nitrogen bond, a selenium-nitrogen bond length of 1.77 Å, and a bond angle <NSeCl of *ca.* 92°.

8.3 Thiazyl Trifluoride, NSF_3

8.3.1 *Synthesis and structure*

Thiazyl trifluoride, a colourless gas with a pungent odour, is prepared by the oxidative decomposition of $FC(O)NSF_2$ with AgF_2 (Eq. 8.6).[20a] NSF_3 is kinetically very stable even in the liquid form. The chemical inertness of NSF_3 resembles that of SF_6. For example, it does not react with sodium metal below 200°C.[1]

$$FC(O)NSF_2 + 2AgF_2 \rightarrow NSF_3 + 2AgF + COF_2 \quad (8.6)$$

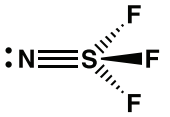

8.4

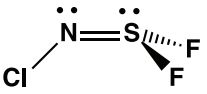

8.5

Chart 8.3. Thiazyl trifluoride and chloroimidosulfur(IV) fluoride.

The structure of NSF_3 (**8.4**) (Chart 8.3) in the gas phase has been determined by microwave spectroscopy to be a distorted tetrahedron with C_{3v} geometry and a S≡N bond length of 1.416 Å, consistent with triple bond character.[20b] The bond angle <FSF is *ca.* 94° and the S–F distance is 1.55 Å indicating a much stronger bond than that in NSF [d(S–F) = 1.64 Å]. The mixed halide derivatives $XNSF_2$ (X = Cl, Br, I) are obtained by the reaction of $Hg(NSF_2)_2$ with halogens (Eq. 8.7).[2] This reaction also gives rise to $FNSF_2$, a structural isomer of NSF_3.[21] The chloro derivative $ClNSF_2$ (**8.5**) (Chart 8.3) has been shown by electron diffraction to have a *cis* arrangement of the lone pairs on the sulfur and nitrogen atoms.[22] The S–N and S–F bond lengths are 1.48 and 1.60 Å, respectively. The isomer $FNSF_2$ is estimated to be less stable than NSF_3 by 15.9 kJ mol^{-1}.[23]

$$[Hg(NSF_2)_2] + 2X_2 \rightarrow 2XNSF_2 + HgX_2 \quad (X = F, Cl, Br, I) \tag{8.7}$$

S,S,S-triphenylthiazyne N≡SPh_3 is obtained as a thermally stable, high-melting solid (d(S≡N) = 1.462 Å) from the reaction of *S,S*-diphenyl *S*-fluorothiazyne, $Ph_2FS{\equiv}N$, with PhLi in THF at low temperature (Eq. 8.8).[24]

$$Ph_2FS{\equiv}N + PhLi \rightarrow NSPh_3 + LiF \tag{8.8}$$

8.3.2 *Metal and Lewis acid complexes*

Complexes with up to four NSF_3 ligands coordinated to a metal centre have been synthesised by the displacement of SO_2 from metal carbonyl complexes (Eq. 8.9) or by direct reaction of NSF_3 with $Ag[AsF_6]$ (Eq. 8.10).[25]

$$[M(CO)_5SO_2][AsF_6] + NSF_3 \rightarrow [M(CO)_5(NSF_3)][AsF_6] \quad (M = Mn, Re) \qquad (8.9)$$

$$Ag[AsF_6] + 2NSF_3 \rightarrow [Ag(NSF_3)_2][AsF_6] \qquad (8.10)$$

In these complexes the S≡N bond length is shortened by *ca.* 0.05 Å compared to the value in free NSF_3. Consistently, the IR stretching frequency ν(NS) occurs at higher wavenumbers, 1575–1650 cm^{-1} compared to the corresponding value of 1515 cm^{-1} for NSF_3.

In a similar fashion NSF_3 forms *N*-bonded adducts with fluoro Lewis acids (L in Eq. 8.11).[1] The S≡N and, especially, the S–F bond lengths are significantly shortened upon adduct formation as revealed by the X-ray structure of $F_5As{\cdot}NSF_3$.[1] By contrast, NSF_3 undergoes halogen exchange with the chloro Lewis acid BCl_3 to produce the acyclic cation $[N(SCl)_2]^+$ as the $[BCl_4]^-$ salt, rather than $NSCl_3$.[26]

$$L + N{\equiv}SF_3 \rightarrow L{\cdot}N{\equiv}SF_3 \quad (L = BF_3, AsF_5, SbF_5) \qquad (8.11)$$

Oxidative addition of an S–F bond in NSF_3 to a metal centre occurs in the reaction with an iridium(I) reagent to give an iridium(III) complex of the thiazyl difluoride anion $[NSF_2]^-$, which is readily hydrolysed to an NSO complex (Scheme 8.1).[27] Metal-NSO complexes are prepared more easily *via* metathetical reactions (Sec. 7.2.2).

8.3.3 *Reactions*

Reactions of NSF_3 with amido-lithium reagents $LiN(SiMe_3)R$ (R = ^{t}Bu, $SiMe_3$) result in a rearrangement to produce sulfur(VI) triimides $S(NR)_3$,[28] which are isoelectronic with SO_3. However, oxidation of the dianion

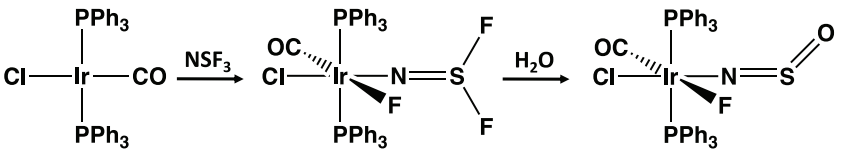

Scheme 8.1. Formation and hydrolysis of an $[NSF_2]^-$ complex.

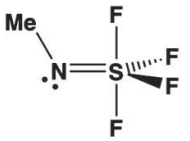

8.6

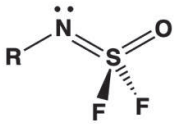

8.7

Chart 8.4. Imidosulfur(VI) tetrafluoride (**8.6**) and oxydifluorides (**8.7**).

$[S(N^tBu_3)]^{2-}$ with halogens is a better route to these sulfur(VI)-nitrogen compounds as described in Sec. 10.7.

Alkylation of NSF_3 with $[MeSO_2][AsF_6]$ produces $[MeNSF_3][AsF_6]$.[29a] This salt reacts with sodium fluoride at elevated temperature to give $MeN{=}SF_4$ (**8.6**, Chart 8.4), which was shown by electron diffraction to have a distorted trigonal bipyramidal structure analogous to that of the isoelectronic molecule $O{=}SF_4$.[1,29b]

8.3.4 *Synthetic applications of imidosulfur(VI) oxydifluorides*

Imidosulfur(VI) oxydifluorides $RN{=}S(O)F_2$ (**8.7**, Chart 8.4) are closely related derivatives of **8.6** that have been known for 60 years. However, the widespread uses of **8.7** for the synthesis of sulfur(VI)-nitrogen compounds of medicinal importance *via* sulfur-fluoride exchange click chemistry have only been discovered in the last five years.[30,31] A large variety of derivatives of **8.7** are readily prepared by the reaction of thionyl tetrafluoride gas with primary amines in acetonitrile in the presence of triethylamine (Eq. 8.12).[30]

$$OSF_4 + RNH_2 \rightarrow RN{=}S(O)F_2 \qquad (8.12)$$

The controlled reactions of **8.7** with an organolithium reagent generate the corresponding sulfonimidoyl fluorides with one S–C linkage (**8.8**). Subsequent treatment of **8.8** with various nucleophiles enables efficient access to a range of sulfoximes (**8.9a**), sulfonimidates (**8.9b**) and sulfonimidamides (**8.9c**), as illustrated in Scheme 8.2.[30]

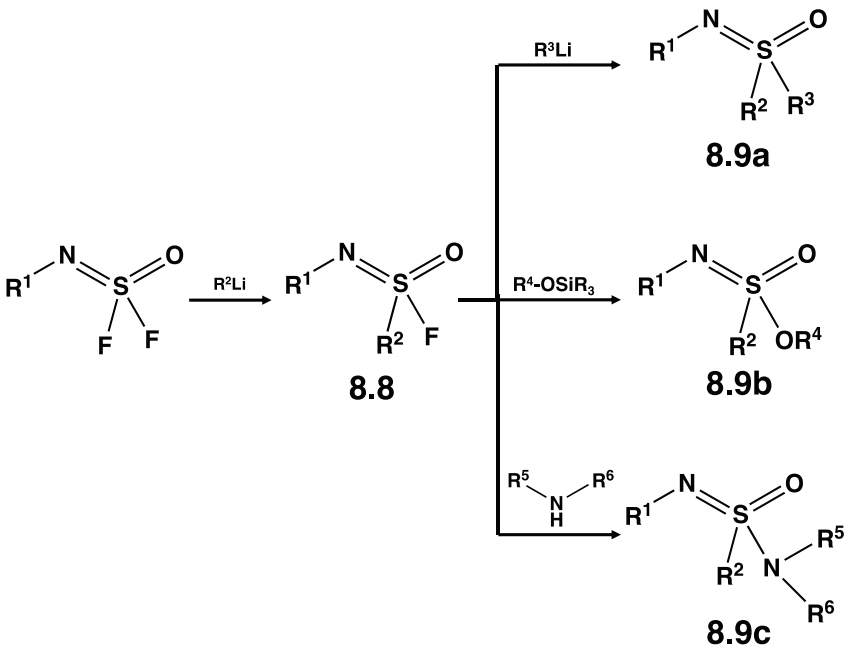

Scheme 8.2. Synthesis of sulfur(VI)-nitrogen compounds from imidosulfur(VI) oxydifluorides.

Imidosulfur oxydifluorides (**8.7**) may also be used to install trifluoromethyl groups on a sulfur(VI) centre *via* reactions with $Si(CF_3)Me_3$ in the presence of potassium bifluoride (KHF_2) in DMSO (Eq. 8.13).[31a] A benzothiazole derivative of the resulting bis(trifluoromethyl)sulfur oxyimines exhibits anticancer properties.[31b]

$$RN{=}S(O)F_2 + 2Me_3SiCF_3 \rightarrow RN{=}S(O)(CF_3)_2 + 2Me_3SiF \qquad (8.13)$$

8.4 Acyclic Chalcogen-Nitrogen-Halogen Cations, $[N(ECl)_2]^+$ (E = S, Se) and $[N(SeCl_2)_2]^+$

The most straightforward route to the acyclic cation $[N(SCl)_2]^+$ (**8.10a**) (Chart 8.5) is the reaction of $[NS]^+$ with SCl_2 (Eq. 8.14).[32] Other

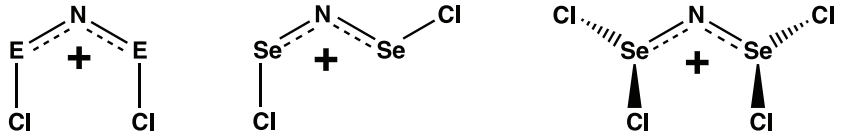

8.10a E = S
8.10b E = Se

8.10b′

8.11

Chart 8.5. Acyclic cationic chalcogen-nitrogen halides.

preparative methods include the reactions of (a) $(NSCl)_3$ with SCl_2 in the presence of a metal chloride (*e.g.*, $AlCl_3$ or $SbCl_5$) or $Ag[AsF_6]$[33a] or (b) an $[SCl_3]^+$ salt with $N(SiMe_3)_3$ in CCl_4.[33b]

$$[NS][SbCl_6] + SCl_2 \rightarrow [N(SCl)_2][SbCl_6] \qquad (8.14)$$

The treatment of $N(SiMe_3)_3$ with $SeCl_4$ in boiling CH_2Cl_2 yields Se_2NCl_3;[34] the bromo derivative Se_2NBr_3 is prepared in a similar manner from $SeBr_4$ and $N(SiMe_3)_3$.[35] Chloride abstraction from Se_2NCl_3 with $GaCl_3$ produces $[N(SeCl)_2]^+$ (**8.10b**) as the $[GaCl_4]^-$ (Chart 8.5).[34] The nature of the counter-ion has a marked effect on the outcome of the reactions of $[SeCl_3]^+$ salts with $N(SiMe_3)_3$. Thus, the reaction of this reagent with an equimolar quantity of $[SeCl_3][AsF_6]$ in $CFCl_3$ produces $[N(SeCl_2)_2]^+$ (**8.11**) (Chart 8.5),[36] whereas $[SeCl_3][SbCl_6]$ generates the cation **8.10b**, which is isolated as the *cis,cis* isomer.[37] On the other hand, the *cis,trans* isomer **8.10b′** is obtained from reaction of $[SeCl_3][FeCl_4]$ with $N(SiMe_3)_3$.[38]

The structures of various salts of **8.10a** have been determined by X-ray diffraction. The cation adopts a U-shaped (C_{2v}) geometry with an <NSN bond angle of 150 ± 1° in the absence of strong cation-anion interactions. The S–N bond lengths are *ca.* 1.53 Å and the S–Cl distances are relatively short at 1.91–1.99 Å. The structures of **8.10b** and **8.11** exhibit Se–N bond lengths that are substantially shorter than the single bond value of 1.86 Å. Negative hyperconjugation [lone pair (N) → σ^* (E–Cl)] (E = S, Se) accounts for the short S–N and Se–N bond lengths in these cations[37,39] and, in the case of the *cis,trans* isomer **8.10b′**, explains the inequality of the Se–N distances.[37]

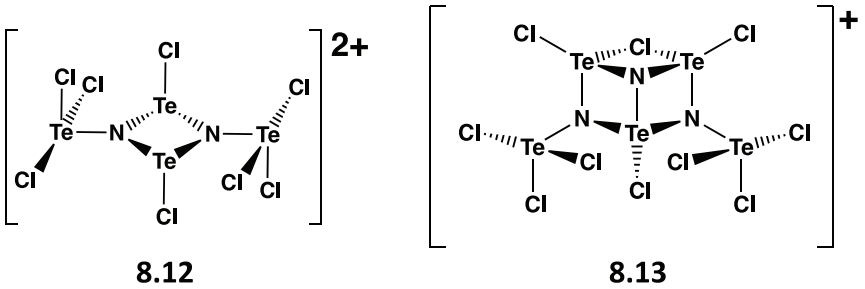

8.12 **8.13**

Chart 8.6. Cyclic cationic tellurium-nitrogen chlorides.

8.5 Tellurium-Nitrogen Chlorides, $[Te_4N_2Cl_8]^{2+}$ and $Te_{11}N_6Cl_{26}$

There are no tellurium analogues of the chalcogen-nitrogen halides described in Sec. 8.4. However, the dication $[Te_4N_2Cl_8]^{2+}$ (**8.12**) (Chart 8.6) is obtained as the $[AsF_6]^-$ salt from the reaction of $TeCl_4$ with $N(SiMe_3)_3$ in a 2:1 molar ratio in acetonitrile.[40] The formation of the four-membered Te_2N_2 ring in **8.12** illustrates the facile self-association of multiply bonded tellurium-nitrogen species. This dication is a dimer of the hypothetical tellurium(IV) imide $[Cl_3Te–N=TeCl]^+$, which is a structural isomer of $[N(TeCl_2)_2]^+$ (the tellurium analogue of **8.11**). This building block also features in the tellurium-nitrogen chloride cation $[Te_5N_3Cl_{10}]^+$ (**8.13**) (Chart 8.6) obtained from the combination of $TeCl_4$ with $N(SiMe_3)_3$ in boiling toluene. The cation **8.13** is comprised of two $[Cl_3Te–N=TeCl]^+$ units bridged by a monomeric NTeCl moiety and a chloride ion.

8.6 Thiodithiazyl and Selenadiselenazyl Dichloride, $[E_3N_2Cl]Cl$ (E = S, Se)

The $[S_3N_2Cl]^+$ cation (**8.14a**) (Chart 8.7) is conveniently obtained by refluxing S_2Cl_2 with dry, finely ground ammonium chloride (Eq. 8.15).[42a] $[S_3N_2Cl]Cl$ may also be prepared from urea and S_2Cl_2.[42b] The selenium analogue $[Se_3N_2Cl]^+$ (**8.14b**) is prepared by the reduction of the acyclic cation **8.10b** with Ph_3Sb.[43] The explosive and insoluble compound

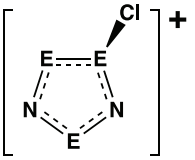

8.14a E = S
8.14b E = Se

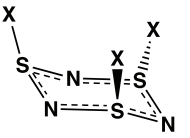

8.15a X = Cl
8.15b X = F

Chart 8.7. Cyclic $[ClE_3N_2]^+$ (E = S, Se) cations and cyclotrithiazyl halides.

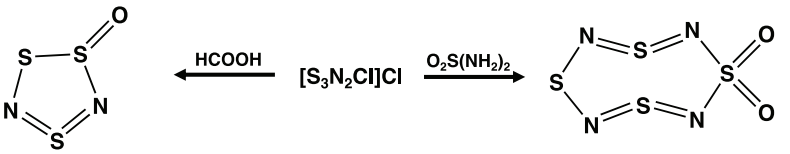

Scheme 8.3. Synthesis of sulfur-nitrogen oxides from $[S_3N_2Cl]Cl$.

$Se_3N_2Cl_2$, which also contains the cyclic cation **8.14b**, is formed in the reaction of Se_2Cl_2 with trimethylsilyl azide in CH_2Cl_2 (Eq. 8.16).[44] X-ray diffraction studies show that **8.14a**, in the $[FeCl_4]^-$ salt,[45] and **8.14b**, in the $[SbCl_6]^-$ salt,[46] consist of slightly puckered five-membered rings.

$$4S_2Cl_2 + 2NH_4Cl \rightarrow [S_3N_2Cl]Cl + 8HCl + \tfrac{5}{8}S_8 \qquad (8.15)$$

$$3Se_2Cl_2 + 2Me_3SiN_3 \rightarrow 2Se_3N_2Cl_2 + 2Me_3SiCl + N_2 \qquad (8.16)$$

Reactions of $[S_3N_2Cl]Cl$ with (a) formic acid or (b) sulfamide produce the cyclic sulfur-nitrogen oxides S_3N_2O[47] and $S_4N_4O_2$,[48] respectively (Scheme 8.3); the photoelectron spectra of these S–N oxides are discussed in Sec. 3.5. Similar to the six-membered ring 1,3-S_4N_2 (Sec. 5.6.3), S_3N_2O is a low-melting (m.p. 18°C) red solid that can be readily sublimed. The X-ray structure reveals a puckered five-membered ring with an exocyclic S=O group and a long S–S bond (2.216(1) Å).[49] The calculated NICS(0) value of –16.8 (Sec. 4.3) is consistent with aromatic character for S_3N_2O.[49]

8.7 Cyclotrithiazyl Halides, $(NSX)_3$ (X = Cl, F)

A safe and convenient procedure for the preparation of $(NSCl)_3$ (**8.15a**) (Chart 8.7) is the chlorination of $[S_3N_2Cl]Cl$ with either Cl_2 or SO_2Cl_2 (Eq. 8.17).[42a,50] The moisture-sensitive, pale-yellow product may be recrystallised from CCl_4 without decomposition provided that the temperature is kept below 50°C. The fluoride $(NSF)_3$ (**8.15b**) can be made in high yield by stirring **8.15a** with AgF_2 in CCl_4 at room temperature.[51] Halogen exchange between **8.15a** and Me_3SiBr produces the polymer $(NSBr_{0.4})_x$ rather than $(NSBr)_3$ (Scheme 8.4).[52]

$$3[S_3N_2Cl]Cl + 3SO_2Cl_2 \rightarrow 2(NSCl)_3 + 3SCl_2 + 3SO_2 \qquad (8.17)$$

The six-membered rings **8.15a** and **8.15b** both adopt a chair conformation with all three halogen atoms in axial positions. This arrangement is stabilised by the delocalisation of the nitrogen lone pair into an S–X σ^* orbital.[53] All the S–N distances are equal within experimental error [$|d$(S–N)| = 1.60 Å (**8.15a**),[54] 1.59 Å (**8.15b**)[55]].

The cyclic trimer **8.15a** is an important reagent in S–N chemistry as a source of both cyclic and acyclic sulfur-nitrogen compounds

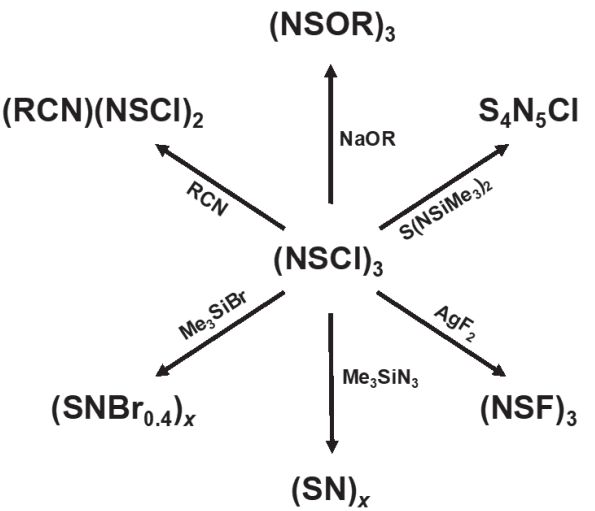

Scheme 8.4. Some reactions of $(NSCl)_3$.

(Scheme 8.4). In some cases, *e.g.*, reactions of $(NSCl)_3$ with sodium alkoxides or AgF_2 to give $(NSOR)_3$[56] or $(NSF)_3$,[51] respectively, the six-membered ring is retained. On the other hand, treatment of $(NSCl)_3$ with trimethylsilyl azide generates the polymer $(SN)_x$.[57] Dissociation of $(NSCl)_3$ into monomeric NSCl occurs readily in solution. This behaviour accounts for the use of **8.15a** in the synthesis of $[NS]^+$ salts (Sec. 5.8.1)[58] as well as the formation of the six-membered rings $(RCN)(NSCl)_2$ in reactions with nitriles (Scheme 8.4).[59] Additional examples of the use of $(NSCl)_3$ as a reagent for the synthesis of carbon-poor sulfur-nitrogen heterocycles are discussed in Chapters 11 and 12. The S_3N_3 ring in $(NSF)_3$ is more robust than that in $(NSCl)_3$ as evinced by isolation of the salts $[N_3S_3F_2][MF_6]$ from reaction of $(NSF)_3$ with MF_5 (M = As, Sb).[60]

8.8 Dihalocyclotetrathiazenes, $S_4N_4X_2$ (X = Cl, F), and Cyclotetrathiazyl Fluoride, $(NSF)_4$

The oxidative addition of one equivalent of X_2 (X = Cl, F) to S_4N_4 under mild conditions produces 1,5-$S_4N_4X_2$ as moisture-sensitive, thermally unstable compounds.[61,62] The structure of 1,5-$S_4N_4Cl_2$ (**8.16**) (Chart 8.8) consists of a folded eight-membered ring [d(S···S) = 2.45 Å] with the exocyclic substituents in *exo,endo* positions.[63] The halogen atoms in **8.16** can be readily replaced by NR_2 groups (R = alkyl) with retention of the eight-membered ring by using trimethylsilylated reagents.[64] The reaction of **8.16** with $Me_3SiN{=}S{=}NSiMe_3$ is the best route to the nitrogen-rich sulfur nitride S_5N_6 (Sec. 5.7.4).

The fluorination of S_4N_4 with an excess of AgF_2 in CCl_4 under reflux gives the tetramer $(NSF)_4$ (**8.17**) as a boat-shaped eight-membered ring with juxtaposed long (1.66 Å) and short (1.54 Å) S–N bonds and fluorine

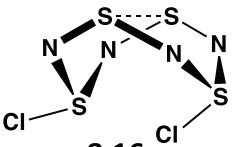

8.16

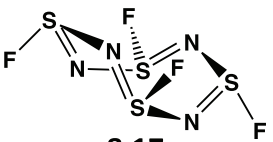

8.17

Chart 8.8. Structures of 1,5-$Cl_2S_4N_4$ and $(NSF)_4$.

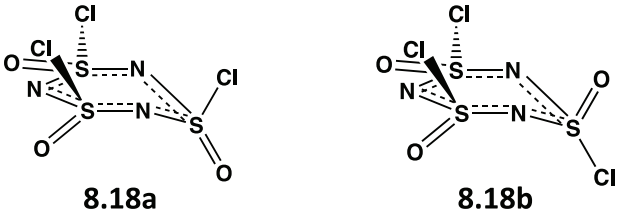

Chart 8.9. Structures of α- and β-isomers of $[NS(O)Cl]_3$.

substituents in alternate axial and equatorial positions (Chart 8.8).[66] Treatment of **8.17** with AsF_5 results in ring contraction to give $[S_3N_3F_2][AsF_6]$ *via* elimination of NSF from the thermally unstable salt $[S_4N_4F_3][AsF_6]$.[1]

8.9 Sulfanuric Halides, $[NS(O)X]_3$ (X = Cl, F)

The sulfanuric halides $[NS(O)X]_3$ are colourless solids (X = Cl) or liquids (X = F), which are stable in dry air. The chloride $[NS(O)Cl]_3$ is best prepared by treatment of $SOCl_2$ with sodium azide in acetonitrile at –35°C (Eq. 8.18).[67] It may also be obtained as a mixture of α- and β-isomers in a two-stage reaction from H_2NSO_3H and PCl_5.[68] The fluoride $[NS(O)F]_3$ is formed as a mixture of isomers by the fluorination of $[NS(O)Cl]_3$ with SbF_3.[69]

$$SOCl_2 + NaN_3 \rightarrow \tfrac{1}{3}[NS(O)Cl]_3 + NaCl + N_2 \qquad (8.18)$$

The isomer α-$[NS(O)Cl]_3$ (**8.18a**) is a six-membered ring in the chair form with equal S–N bond lengths (1.57 Å). The three chlorine atoms are in axial positions on the same side of the ring.[70a] The β-isomer **8.18b** has two axial and one equatorial chlorine atoms (Chart 8.9).[70b]

8.10 Chalcogen-Nitrogen Halides Containing Two Chalcogens

The reaction of $Me_3SiNSNSiMe_3$ with $TeCl_4$ is an especially fruitful source of chalcogen-nitrogen halides that contain both sulfur and

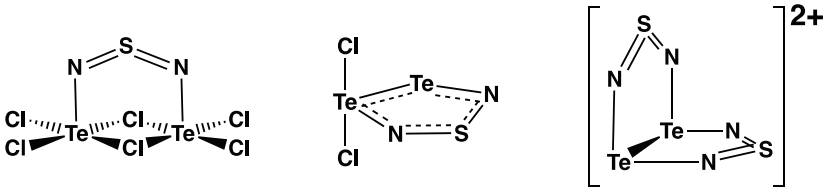

8.19 **8.20** **8.21**

Chart 8.10. Mixed tellurium/sulfur-nitrogen halides and the $[Te_2S_2N_4]^{2+}$ dication.

tellurium.[71] When the reaction is carried out in a 1:2 molar ratio in CH_2Cl_2 at –50°C the bicyclic compound **8.19** is obtained (Chart 8.10). Reduction of **8.19** with $SbPh_3$ produces the five-membered ring (**8.20**, Chart 8.10).[72] In contrast to the related S or Se systems, **8.14a** and **8.14b**, both Cl substituents are attached covalently to Te in **8.20**. Treatment of **8.20** with an excess of AsF_5 in SO_2 produces the eight-membered cyclic dication $[Te_2S_2N_4]^{2+}$ (**8.21**, Chart 8.10) which exhibits a transannular Te–Te bond length of 2.88 Å (*cf.* 2.70 Å for a Te–Te single bond).[72]

8.11 Imidochalcogen(II) Halides

Comprehensive investigations of the cyclocondensation reactions of *tert*-butylamine with $SeCl_2$ using different stoichiometries have resulted in the isolation and characterisation of a homologous series of acyclic imidoselenium(II) dichlorides $ClSe[N(^tBu)Se]_nCl$ (n = 1–3) (Fig. 8.1).[73–76] There are no sulfur or tellurium analogues of this class of chalcogen-nitrogen halides.

As illustrated in Fig. 8.1b, there is a close ClSe···SeCl contact of 2.891 Å (*cf.* sum of van der Waals radii for Se and Cl is 4.0 Å) in $ClSe[N(^tBu)Se]_2Cl$, which is accompanied by a pronounced alternation in the Se–N distances (1.803 and 1.948 Å) and, to a smaller extent, the Se–Cl (2.313 and 2.269 Å) bond lengths.[75] These structural observations can be explained by two lone pair (N) → σ^*(Se–Cl) interactions as depicted in Fig. 8.2. The intramolecular ClSe···SeCl interaction is much weaker in the two polymorphs of the longer chain $ClSe[N(^tBu)Se]_3Cl$ (3.345 and 3.368 Å).[76]

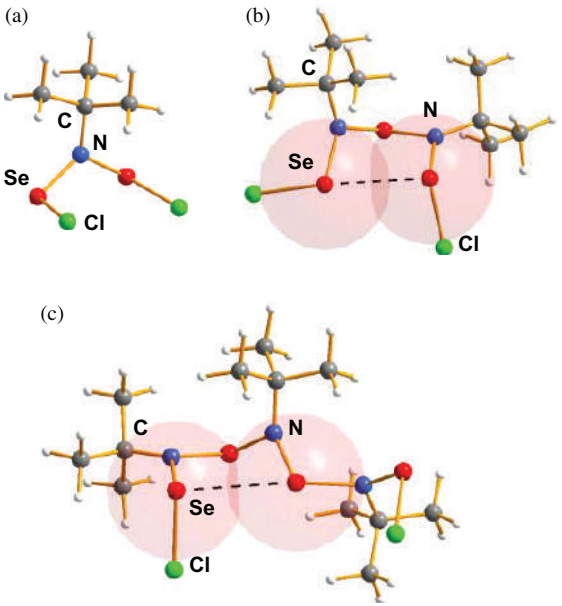

Figure 8.1. Molecular structures of ClSe[N(^{t}Bu)Se]$_n$Cl (a) n = 1; (b) n = 2;[75] (c) n = 3;[76] van der Waals radius of selenium is indicated by large spheres.

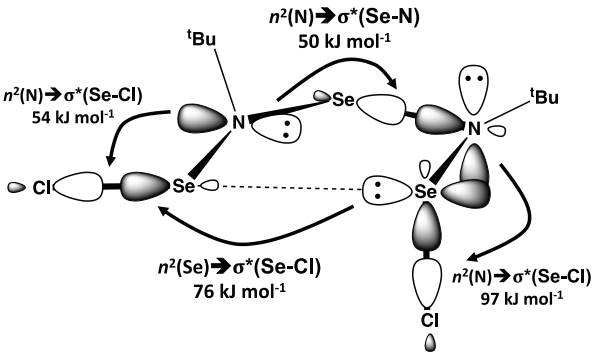

Figure 8.2. Hyperconjugation in ClSe[N(^{t}Bu)Se]$_2$Cl.[76]

A reaction pathway that accounts for the sequential formation of the homologous series ClSe[N(^{t}Bu)Se]$_n$Cl (n = 1–3) is depicted in Scheme 8.5.[73] The initial intermediate ^{t}BuN(H)SeCl has not been isolated, but could serve as a source of "^{t}BuNSe" units in the formation of longer

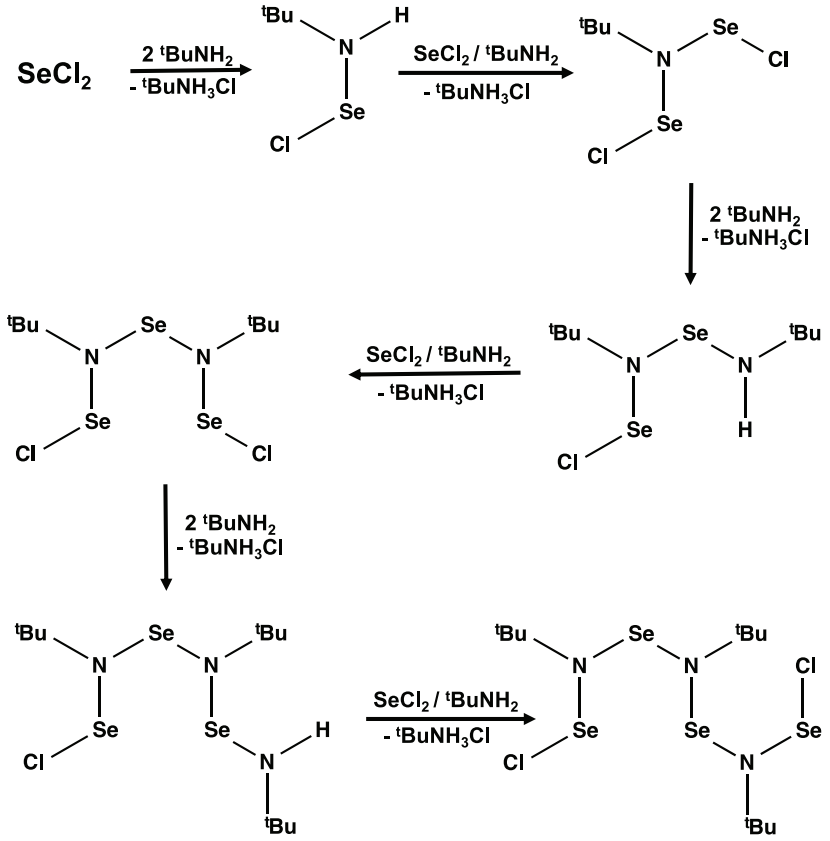

Scheme 8.5. Reaction pathway for the formation of imidoselenium(II) dichlorides $ClSe[N(^tBu)Se]_nCl$ (n = 1–3).

chains. The role of imidoselenium(II) dichlorides in the formation of cyclic selenium imides is discussed in Sec. 9.4 (Scheme 9.3).

The unique imidochalcogen halide $ClSeN(^tBu)Se(O)Cl$ with selenium in different oxidation states is obtained by the reaction of *tert*-butylamine with a mixture of $SeCl_2$ and $SeOCl_2$ in a 6:2:1 molar ratio and the acyclic structure was established by X-ray crystallography as illustrated in Fig. 8.3.[77] The small structural differences between this Se^{II}/Se^{IV} system and the corresponding Se^{II}/Se^{II} derivative $ClSeN(^tBu)SeCl$ (Fig. 8.1a) are attributed to negative hyperconjugation effects involving the p lone pairs of the oxygen atoms. In solution the two different selenium environments

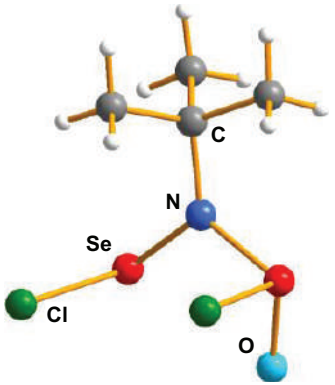

Figure 8.3. Molecular structure of ClSeN(^{t}Bu)Se(O)Cl.[77]

in ClSeN(^{t}Bu)Se(O)Cl are indicated by ^{77}Se NMR chemical shifts of 1435 and 1291 ppm attributed to the N*Se*(O)Cl and N*Se*Cl units, respectively.[77]

8.12 Imidochalcogen(IV) Dihalides

Imidochalcogen(IV) halides of the type $RNECl_2$ (E = S, Se, Te) provide an informative example of the reluctance of the heavier chalcogens to form –N=E< double bonds. The sulfur derivatives $RNSX_2$ (X = F, Cl) are stable, monomeric compounds, *cf.* the chloro derivative $ClNSF_2$ (**8.5**).[78,79] The difluorides are obtained in good yields from the reactions of SF_4 with *N*-silylated primary amines (Eq. 8.19). Halogen exchange, *e.g.*, with $AlCl_3$ in nitromethane, yields the corresponding dichlorides $RN{=}SCl_2$;[78] ^{t}BuNSCl_2 is a yellow oil.[80]

$$RN(SiMe_3)_2 + SF_4 \rightarrow RN{=}SF_2 + 2Me_3SiF \quad (R = Me, Et) \qquad (8.19)$$

Selenium analogues $RN{=}SeCl_2$ are unknown for R = aryl or alkyl and thermally unstable when R = CF_3 or C_2F_5. The perfluoroalkyl derivatives are prepared by the reaction of dichloroamino compounds with Se_2Cl_2 in CCl_3F (Eq. 8.20), but they decompose at room temperature to form the corresponding diazene and a mixture of selenium chlorides.[81]

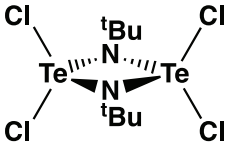

8.22

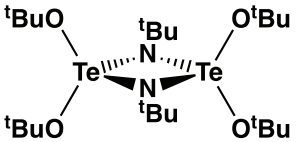

8.23

Chart 8.11. Dimeric imidotellurium(IV) derivatives.

$$3RNCl_2 + 2Se_2Cl_2 \rightarrow 3RN{=}SeCl_2 + SeCl_4 \quad (R = CF_3, C_2F_5) \qquad (8.20)$$

In contrast to the selenium systems, *tert*-butylimidotellurium dihalides $(^tBuNTeX_2)_n$ (X = Cl, Br) are thermally stable in the solid state. They are obtained in good yields in THF solution by a redistribution reaction (Eq. 8.21).[82]

$$^tBuNTe(\mu\text{-}N^tBu)_2TeN^tBu + 2TeX_4 \rightarrow 4/n(^tBuNTeX_2)_n \qquad (8.21)$$

The dichloride forms fragile, lamellar crystals with a golden colour. The X-ray structure reveals a layered arrangement of hexameric units generated by linking three $(^tBuNTeCl_2)_2$ dimers (**8.22**) (Chart 8.11) by chloride bridges. The reaction of $(^tBuNTeCl_2)_n$ with potassium *tert*-butoxide yields $^tBuN{=}Te(O^tBu)_2$, which forms the dimer **8.23** (Chart 8.11) with significantly different Te–N bond lengths (1.943(4) and 2.217(4) Å) in the solid state.[82]

References

1. O. Glemser and R. Mews, *Angew. Chem. Int. Ed. Engl.*, **19**, 883 (1980).
2. O. Glemser, R. Mews and H. W. Roesky, *Chem. Ber.*, **102**, 1523 (1969).
3. A. Haas and M. Rieland, *Chimia*, **42**, 67 (1988).
4. R. C. Patton and W. L. Jolly, *Inorg. Chem.*, **9**, 1079 (1970).
5. J. Passmore and M. J. Schriver, *Inorg. Chem.*, **27**, 2749 (1988).
6. S. C. Peake and A. J. Downs, *J. Chem. Soc. Dalton Trans.*, 859 (1974).
7. (a) W. H. Kirchoff and E. B. Wilson, Jr., *J. Am. Chem. Soc.*, **85**, 1726 (1963); (b) T. Beppu, E. Hirota and Y. Morino, *J. Mol. Spectroscopy*, **36**, 386 (1970).

8. (a) T. Y. Takeshita and T. H. Dunning, Jr., *J. Phys. Chem. A*, **119**,1446 (2015); (b) M. T. Nguyen and R. Flammang, *Chem. Ber*., **129**, 1379 (1996).
9. R. Ahlrichs and C. Ehrhardt, *Chem. Phys*., **107**, 1 (1986).
10. O. Glemser and W. Koch, *Angew. Chem. Int. Ed. Engl*., **10**, 127 (1971).
11. W. Heilemann and R. Mews, *Chem. Ber*., **121**, 461 (1988).
12. E. Kessenich, F. Kopp, P. Mayer and A. Schulz, *Angew. Chem. Int. Ed.*, **40**, 1904 (2001).
13. B. Buss, P. G. Jones, R. Mews, M. Noltemeyer and G. M. Sheldrick, *Angew. Chem. Int. Ed. Engl*., **18**, 231 (1979).
14. K. Dehnicke and U. Müller, *Comments Inorg. Chem*., **4**, 213 (1985).
15. (a) J. Hanich and K. Dehnicke, *Z. Naturforsch*., **39B**, 1467 (1984); (b) G. Beber, J. Hanich and K. Dehnicke, *Z. Naturforsch*, **40B**, 9 (1985).
16. (a) U. Kynast and K. Dehnicke, *Z. Anorg. Allg. Chem*., **502**, 29 (1983); (b) U. Kynast, U. Müller and K. Dehnicke, *Z. Anorg. Allg. Chem*., **508**, 26 (1984).
17. U. Kynast, P. Klingelhofer, U. Müller and K. Dehnicke, *Z. Anorg. Allg. Chem*., **515**, 61 (1984).
18. (a) G. Hartmann and R. Mews, *Z. Naturforsch.*, **40B**, 343 (1985); (b) G. Hartmann, R. Mews and G. M. Sheldrick, *Angew. Chem. Int. Ed. Engl*., **22**, 723 (1983).
19. J. Adel and K. Dehnicke, *Chimia*, **42**, 413 (1988).
20 (a) R. Mews, K. Keller and O. Glemser, *Inorg. Synth*., **24**, 12 (1986); (b) W. H. Kirchoff and E. B. Wilson, Jr., *J. Am. Chem. Soc*., **84**, 334 (1962).
21. O. Glemser, R. Mews and H. W. Roesky, *Chem. Commun*., 914 (1969).
22. J. Haase, H. Oberhammer, W. Zeil, O. Glemser and R. Mews, *Z. Naturforsch*., **25A**, 153 (1970).
23. C. Erhardt and R. Ahlrichs, *Chem. Phys*., **108**, 429 (1986).
24. T. Yoshimura, K. Hamada, M. Imado, K. Hamata, K. Tomoda, T. Fujii, H. Morita, C. Shimasaki, S. Ono, E. Tsukurimichi, N. Furukawa and T. Kimura, *J. Org*. *Chem*., **63**, 3802 (1997).
25. R. Mews, *J. Chem. Soc., Chem. Commun*., 278 (1979).
26. O. Glemser, B. Krebs, J. Wegener and E. Kindler, *Angew. Chem. Int. Ed. Engl*., **8**, 598 (1969).
27. P. G. Watson, E. Lork and R. Mews, *J. Chem. Soc., Chem. Commun*., 1069 (1994).
28. R. Mews, P. G. Watson and E. Lork, *Coord. Chem. Rev*., **158**, 233 (1997).
29. (a) R. Mews, *Angew. Chem. Int. Ed. Engl*., **17**, 530 (1978); (b) R. Bartsch, H. Henle, T. Meier and R. Mews, *Chem. Ber*., **121**, 451 (1988).

30. (a) S. Li, P. Wu, J. E. Moses and K. B. Sharpless, *Angew. Chem. Int. Ed*., **56**, 2903 (2017); (b) B. Gao, S. Li, P. Wu, J. E. Moses and K. B. Sharpless, *Angew. Chem. Int. Ed*., **57**, 1939 (2018).
31. (a) C. J. Smedley, Q. Zheng, B, Gao, S. Li, A. Molino, H. M. Duivenvoorden, B. S. Parker, D. J. D. Wilson, K. B. Sharpless and J. E. Moses, *Angew. Chem. Int. Ed.*, **58**, 4552 (2019); (b) S. Kitamura, Q. Zheng, J. L. Woehl, A. Solania, E. Chen, N. Dillon, M. V. Hull, M. Kotaniguchi, J. R. Cappiello, S. Kitamura, V. Nizet, K. B. Sharpless and D. W. Wolan, *J. Am. Chem. Soc*., **142**, 10899 (2020).
32. R. Mews, *Angew. Chem. Int. Ed. Engl*., **15**, 691 (1976).
33. (a) B. Ayres, A. J. Banister, P. D. Coates, M. I. Hansford, J. M. Rawson, C. E. F. Rickard. M. B. Hursthouse, K. M. Abdul Malik and M. Motevalli, *J. Chem. Soc. Dalton Trans*., 3097 (1992); (b) M. Borschag, A. Schulz and T. M. Klapötke, *Chem. Ber*., **127**, 2187 (1994).
34. R. Wollert, A. H. Ilworth, G. Frenking, D. Fenske, H. Goesman and K. Dehnicke, *Angew. Chem. Int. Ed. Engl*., **31**, 1251 (1992).
35. C. Lau, B. Neumüller, W. Hiller, M. Herker, S. F. Vyboishchikov, G. Frenking and K. Dehnicke, *Chem. Eur. J*., **2**, 1373 (1996).
36. M. Broschag, T. M. Klapötke, I. C. Tornieporth-Oetting and P. S. White, *J. Chem. Soc., Chem. Commun*., 1390 (1992).
37. M. Broschag, T. M. Klapötke, A. Schulz and P. S. White, *Inorg. Chem*., **32**, 5734 (1993).
38. M. Broschag, T. M. Klapötke, A. Schulz and P. S. White, *Chem. Ber*., **127**, 2177 (1994).
39. A. Schulz, P. Buzek, P. von R. Schleyer, M. Broschag, I. C. Tornieporth-Oetting, T. M. Klapötke and P. S. White, *Chem. Ber*., **128**, 35 (1995).
40. J. Passmore, G. Schatte and T. S. Cameron, *J. Chem. Soc., Chem. Commun*., 2311 (1995).
41. C. Lau, B. Neumüller and K. Dehnicke, *Z. Anorg. Allg. Chem*., **622**, 739 (1996).
42. (a) W. L. Jolly and K. D. Maguire, *Inorg. Synth*., **9**, 102 (1967); (b) H. W. Roesky, W. Schaper, O. Petersen and T. Müller, *Chem. Ber*., **110**, 2695 (1977).
43. R. Wollert, B. Neumüller and K. Dehnicke, *Z. Anorg. Allg. Chem*., **616**, 191 (1992).
44. T. Chivers, J. Siivari and R. S. Laitinen, *Inorg. Chem*., **32**, 4391 (1993).
45. (a) H. M. M. Shearer, A. J. Banister, J. Halfpenny and G. Whitehead, *Polyhedron*, **2**, 149 (1983); (b) W. Isenberg, N. K. Homsy, J. Anhaus, H. W. Roesky and G. M. Sheldrick, *Z. Naturforsch*., **38B**, 808 (1983).

46. C. Lau, B. Neumüller and K. Dehnicke, *Z. Naturforsch*., **52B**, 543 (1997).
47. H. W. Roesky, M. Kuhn and M. Witt, *Inorg. Synth*., **25**, 49 (1989).
48. H. W. Roesky, W. Schaper, O. Petersen and T. Müller, *Chem. Ber*., **110**, 2695 (1977).
49. K. Tersago, V. Matuska, C. Van Alsenoy, A. M. Z. Slawin, J. D. Woollins and F. Blockhuys, *Dalton Trans*., 4529 (2007).
50. G. G. Alange, A. J. Banister and B. Bell, *J. Chem. Soc., Dalton Trans*., 2399 (1972).
51. H. Schröder and O. Glemser, *Z. Anorg. Allg. Chem*., **298**, 78 (1959).
52. U. Demant and K. Dehnicke, *Z. Naturforsch*., **41B**, 929 (1986).
53. E. Jaudas-Prezel, R. Maggiulli, R. Mews, H. Oberhammer and W-D. Stohrer, *Chem. Ber*., **123**, 2117 (1990).
54. A. C. Hazell, G. Wiegers and A. Vos, *Acta Crystallogr*., **20**, 186 (1966).
55. B. Krebs and S. Pohl, *Chem. Ber*., **106**, 1069 (1973).
56. R. Jones, I. P. Parkin, D. J. Williams and J. D. Woollins, *Polyhedron*, **6**, 2161 (1987).
57. F. A. Kennett, G. K. MacLean, J. Passmore and M. N. S. Rao, *J. Chem. Soc., Dalton Trans*., 851 (1982).
58. (a) A. Apblett, A. J. Banister, D. Biron, A. G. Kendrick, J. Passmore, M. Schriver and M. Stojanac, *Inorg. Chem*., **25**, 4451 (1986); (b) A. Apblett, T. Chivers and J. F. Fait, *Inorg. Chem*., **29**, 1643 (1990).
59. A. Apblett and T. Chivers, *Inorg. Chem*., **28**, 4544 (1989).
60. W. Isenberg and R. Mews, *Z. Naturforsch*., **37B**, 1388 (1982).
61. L. Zborilova and P. Gebauer, *Z. Anorg. Allg. Chem*., **448**, 5 (1979).
62. I. Ruppert, *J. Fluorine Chem*., **20**, 241 (1982).
63. Z. Zak, *Acta Crystallogr*., **B37**, 23 (1981).
64. (a) H. W. Roesky, M. N. S. Rao, C. Graf, A. Gieren and E. Hädicke, *Angew. Chem. Int. Ed. Engl.* **20**, 592, (1981); (b) H. W. Roesky, C. Pelz, B. Krebs and G. Henkel, *Chem. Ber*., **115**, 1448, (1982).
65. O. Glemser, H. Schröder and H. Haeseler, *Z. Anorg. Allg. Chem*., **279**, 28 (1955).
66. (a) D. Gregson, G. Klebe and H. Fuess, *Acta Crystallogr*., **C47**, 1784 (1991); (b) M. H. Palmer, R. T. Oakley and N. P. C. Westwood, *Chem. Phys*., **131**, 255 (1989).
67. H. Kluver and O. Glemser, *Z. Naturforsch*., **32B**, 1209 (1977).
68. T. J. Maricich and M. H. Khalil, *Inorg. Chem*., **18**, 912 (1979).
69. (a) F. Seel and G. Simon, *Z. Naturforsch*., **19B**, 354 (1964); (b) T-P. Lin, U. Klingebiel and O. Glemser, *Angew. Chem. Int. Ed. Engl*., **11**, 1095 (1972).

70. (a) A. C. Hazell, G. Wiegers and A. Vos, *Acta Crystallogr*., **20**, 186 (1966); (b) E. Lork, U. Behrens, G. Steinke and R. Mews, *Z. Naturforsch*., **49B**, 437 (1994).
71. (a) A. Haas, *J. Organomet. Chem*., **646**, 80 (2002); (b) A. Haas, *Adv. Heterocyclic Chem*., **71**, 115 (1998).
72. (a) A. Haas and M. Pryka, *J. Chem. Soc., Chem. Commun*., 391 (1994); (b) A. Haas and M. Pryka, *Chem. Ber*., **128**, 11 (1995).
73. T. Chivers and R. S. Laitinen, *Dalton Trans*., **46**, 1357 (2017).
74. R. S. Laitinen, R. Oilunkaniemi and T. Chivers, in *Selenium and Tellurium Chemistry*: *From Small Molecules to Biomolecules and Materials*, Eds. J. D. Woollins and R. S. Laitinen, Springer-Verlag (2011), Ch. 5, pp. 103–122.
75. T. Maaninen, T. Chivers, R. Laitinen and E. Wegelius, *Chem. Commun*., 759 (2000).
76. A. J. Karhu, O. J. Pakkanen, J. M. Rautiainen, R. Oilunkaniemi, T. Chivers and R. S. Laitinen, *Dalton Trans*., **45**, 6210 (2016).
77. A. Karhu, J. Jämsä, J. M. Rautiainen, R. Oilunkaniemi, T. Chivers and R. S. Laitinen, *Z. Anorg. Allg. Chem*., **643**, 495 (2017).
78. O. Glemser and R. Mews, *Adv. Inorg. Chem. Radiochem*., **14**, 333 (1970).
79. H. W. Roesky, in *Sulfur in Organic and Inorganic Chemistry*, Ed. A. Senning, Marcel Dekker, Inc. (1982), Vol. 4, pp. 15–45.
80. O. Scherer and G. Wolmershäuser, *Z. Anorg. Allg. Chem*. **432**, 173 (1977).
81. J. S. Thrasher, C. W. Bauknight, Jr. and D. S. Desmarteau, *Inorg. Chem*., **24**, 1598 (1985).
82. T. Chivers, G. D. Enright, N. Sandblom, G. Schatte and M. Parvez, *Inorg. Chem*., **38**, 5431 (1999).

Chapter 9

Cyclic Chalcogen Imides: From Five- to 15-Membered Rings

9.1 Introduction

In contrast to the binary chalcogen-nitrogen heterocycles discussed in Chapter 5, which involve *two-coordinate* nitrogen and exist as cations, anions and neutral molecules, cyclic chalcogen imides incorporate *three-coordinate* nitrogen atoms. In addition to the symmetrical systems $(ENR)_n$ (E = S, $n = 4$; E = Se, $n = 3, 4$; E = Te, $n = 3$; R = alkyl), which are oligomers of the short-lived monomers RNE (Sec. 9.2), a variety of ring systems that incorporate chalcogen-chalcogen bonds are known.

The majority of cyclic sulfur imides are eight-membered rings derived from *cyclo*-S_8 by the replacement of one or more S atoms by NH groups with an almost planar SN(H)S arrangement. Ring systems containing N–N bonds are unknown, but structural isomers exist for derivatives containing two or three NH groups. In early work cyclic sulfur imides were the source of the first salts of certain binary sulfur-nitrogen anions and cations. For example, deprotonation of S_7NH with a strong base generated the $[SSNSS]^-$ anion (Sec. 5.9.4) and oxidation with $SbCl_5$ produced the $[SNS]^+$ cation (Sec. 5.8.2).

Although cyclic selenium imides containing NR (R = H) groups are unknown, a wide variety of ring systems with a bulky alkyl substituent (R = ^{t}Bu or Ad) on nitrogen have been prepared either by cyclocondensation of a primary amine with $SeCl_2$ or decomposition of selenium(IV) diimides.

The well-characterised series of acyclic imidoselenium(II) dichlorides $ClSe[N^tBu)Se]_nCl$ (n = 1–3) (Sec. 8.11) are intermediates in the former synthesis. Several cyclic selenium imides do not have sulfur analogues, *e.g.*, the six-membered ring $Se_3(N^tBu)_3$ and the five- and 15-membered cyclic oligomers $[Se_3(N^tBu)_2]_n$ (n = 1, 3).

9.2 Chalcogenylnitrosyls, RNE (E = S, Se)

In contrast to monomeric thiazyl fluoride NSF (Sec. 8.2.1), generalised valence bond calculations, accompanied by accurate coupled cluster calculations, estimate that the HNS isomer is more stable than the NSH arangement.[1] Although the prototypical chalcogenonitrosyls HNE (E = S, Se) have not been characterised spectroscopically, HNS has been trapped as a bridging ligand in the complex $(HNS)Fe_2(CO)_6$ (**9.1**) (Chart 9.1), which is obtained from the reaction of $Fe_3(CO)_{12}$ with $Me_3SiNSNSiMe_3$.[2a,b] Complex **9.1** is readily deprotonated by ^{n}BuLi to give the corresponding anion **9.2**. This anion undergoes alkylation with trialkyloxonium salts and forms E–N bonds in reactions with a variety of *p*-block element halides (E = B, Si, Ge, Sn, P and As).[2c,d]

The thionitrosyl group is stabilised by a dimethylamino substituent in *N,N′*-dimethylthionitrosoamine Me_2NNS, which is obtained as a low-melting, deep purple solid from the reaction of 1,1-dimethylhydrazine with sulfur (Eq. 9.1) or by the reduction of Me_2NNSO with $LiAlH_4$.[3] This thermally unstable derivative is monomeric in solution.

$$Me_2NNH_2 + 1/4S_8 \rightarrow Me_2NNS + H_2S \qquad (9.1)$$

An alternative approach to thionitrosoarenes involves the reaction of amines with SCl_2.[4] This method has also been adapted to the production of selenonitrosoarenes ArN=Se (Ar = 4-XC_6H_4, X = Br, Me) by using the

9.1

9.2

Chart 9.1. Complexes of HNS and $[NS]^-$ with $Fe_2(CO)_6$.

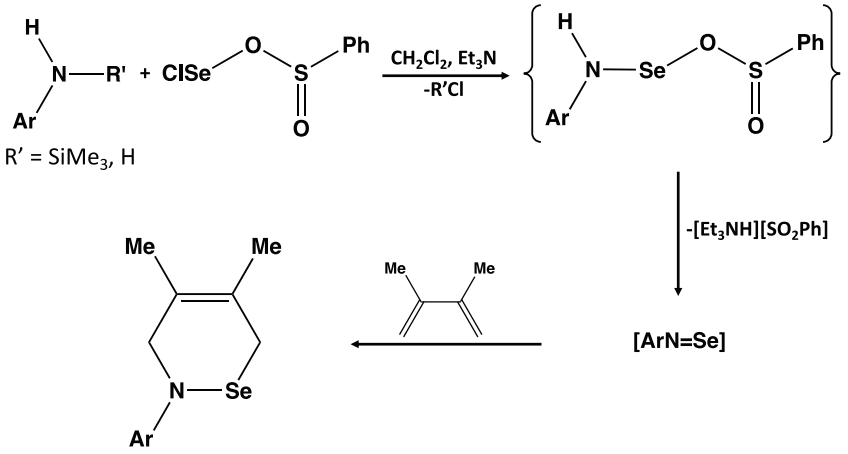

Scheme 9.1. Generation and trapping of selenonitrosoarenes.

selenium(II) synthon $PhSO_2SeCl$ as the Se source (Scheme 9.1).[5] The Diels–Alder cycloaddition of ArN=Se species with dimethylbutadiene gives 1-selena-2-azine derivatives in low yields. The initial product of the reaction of $^tBuNH_2$ with $SeCl_2$ is probably $^tBuN(H)SeCl$, which acts as a source of "^{t}BuNSe" in forming a series of acyclic imidoselenium dichlorides $ClSe[N(^tBu)Se]_nCl$ (n = 1–3) (Sec. 8.11).

9.3 Cyclic Sulfur Imides

9.3.1 *Eight-membered rings*

The best-known examples of cyclic sulfur imides are eight-membered rings in which one or more of the sulfur atoms in *cyclo*-S_8 are replaced by an imido group [NH or NR (R = alkyl)]. This class of compounds has an important place in the history of chalcogen-nitrogen chemistry and the early developments in the field were covered comprehensively in the book by Heal.[6] The formal replacement of a sulfur atom in *cyclo*-S_8 generates S_7NH (**9.3**), the first member of a series of cyclic sulfur imides that includes the three diimides 1,3-, 1,4-, and 1,5-$S_6(NH)_2$ (**9.4**–**9.6**), two triimides 1,3,5- and 1,3,6-$S_5(NH)_3$ (**9.7** and **9.8**), and the tetraimide $S_4(NH)_4$ (**9.9**) (Chart 9.2).

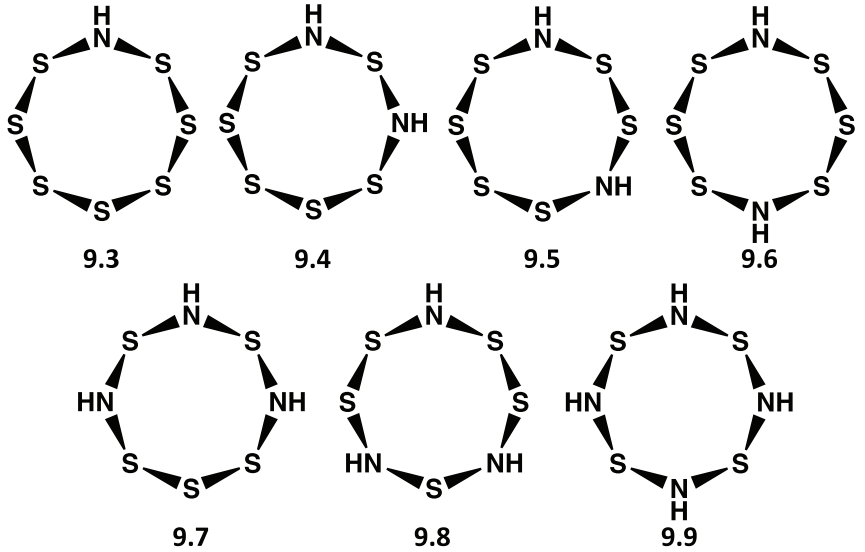

Chart 9.2. Eight-membered cyclic sulfur imides.

The standard preparation of these cyclic sulfur imides, with the exception of $S_4(NH)_4$, involves the reaction of S_2Cl_2 with gaseous ammonia in DMF at *ca.* –10°C, followed by hydrolysis with cold dilute hydrochloric acid.[7] This method gives mainly S_7NH, but the three diimide isomers, **9.4**–**9.6**, and very small amounts of the triimide 1,3,6-$S_5(NH)_3$ (**9.8**) can be separated by chromatography of CS_2 solutions on silica gel or by high-performance liquid chromatography.[8] The reaction of sodium azide with elemental sulfur in $(Me_2N)_3PO$ is an excellent source of S_7NH, which has been employed for making the ^{15}N-enriched ring system.[9] The tetraimide $S_4(NH)_4$ (**9.9**) is prepared in good yields from S_4N_4 by using methanolic $SnCl_2{\cdot}2H_2O$ as the reducing agent.[10]

These ring systems all adopt the crown configuration of *cyclo*-S_8 with S–S bond lengths in the range 2.04–2.06 Å, typical of single bonds. The S–N bond distances (1.66–1.68 Å) are significantly shorter than a S–N single bond and the geometry around nitrogen is almost planar, indicating three-centre π-bonding in the S–N(H)–S units.[11] This conclusion is supported by experimental electron deformation density measurements of S_7NH[12] and $S_4(NH)_4$.[13] The ^1H and ^{15}N NMR chemical shifts of all the

cyclic sulfur imides have been determined by inverse detection methods (as exemplified for ^{15}N NMR chemical shifts depicted in Fig. 3.5).[14] The values of $^{1}J(^{15}N–^{1}H)$ fall within the narrow range 93–96 Hz, consistent with sp^2-hybridised nitrogen atoms.

The cyclic sulfur imides are weak Brønsted acids that are readily deprotonated by strong bases. In the case of S_7NH, deprotonation with $[Bu_4N]OH$ produces the thermally unstable, yellow $[S_7N]^-$ anion, which decomposes to the deep blue acyclic $[SSNSS]^-$ anion, which was first characterised as the $[Bu_4N]^+$ salt (Sec. 5.9.4).[15] The deprotonation of $S_4(NH)_4$ with the Wittig reagent acts as an *in situ* source of the acyclic $[S_2N_2H]^-$ anion (Sec. 5.9.6).[16]

Oxidation of S_7NH with $SbCl_5$ in liquid sulfur dioxide results in rupture of the S_7N ring to generate the $[SNS]^+$ cation.[17] This reaction provided the first synthesis of this important reagent (Sec. 5.8.2).

Alkyl derivatives of cyclic sulfur imides are obtained by cyclocondensation reactions. Thus, the reaction of aqueous methylamine with dichlorosulfanes S_xCl_2 (x = 1, 2, 3, 5, 7) yields S_7NMe, the three diimides 1,3-, 1,4-, and 1,5-$S_6(NMe)_2$, and the two triimides 1,3,5- and 1,3,6-$S_5(NMe)_3$. The relative amounts of these heterocycles are determined by the chain length in S_xCl_2.[18] Cyclocondensation of gaseous $MeNH_2$ with SCl_2 in hexane generates $S_4(NMe)_4$ as the major product together with two isomers of $S_5(NMe)_3$.[19] This mixture of cyclic sulfur imides is difficult to separate from $[MeNH_3]Cl$ by-product. Similar to the parent tetraimide **9.9**, the methyl derivative $S_4(NMe)_4$ is a crown-shaped eight-membered ring with a nearly planar configuration at the nitrogen atoms (Fig. 9.1a).[20] The reaction of arylamines with S_2Cl_2 in the presence of a base gives good yields of S_7NAr derivatives, *e.g.*, Ar = pyrimidin-2-yl, which are of interest for their fungicidal properties.[21]

9.3.2 *Six-, seven-, nine- and ten-membered rings*

The six-membered cyclic sulfur imides 1,4-$S_4(NR)_2$ (R = Et, Bz) are obtained in moderate yields from the cyclocondensation of S_2Cl_2 with the appropriate primary amine in diethyl ether when high-dilution conditions are employed.[22] The crystal structures of 1,4-$S_4(NR)_2$ revealed a cyclohexane-like ring (Fig. 9.1b). However, in contrast to eight-membered

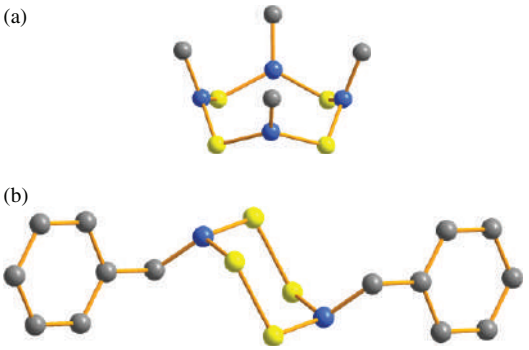

Figure 9.1. Molecular structures of (a) 1,3,5,7-$S_4(NMe)_4$[20] and (b) 1,4-$S_4(NR)_2$ (R = Et, Bz).[22]

tetraimide $S_4(NMe)_4$ (Fig. 9.1a), a substantial degree of pyramidalisation at the nitrogen atoms is observed in the six-membered ring.[22]

Cyclic sulfur imides containing S–S bonds undergo cycloaddition reactions with $[TiCp_2(CO)_2]$ (Sec. 9.5). For example, reaction of this cyclopentadienyl metal dicarbonyl with the eight-membered rings S_7NR (R = H, Me) gives the complexes $[TiCp_2(S_7NR)]$ in which the sulfur imide ligand is *S,S′*-chelated to titanium (Eq. 9.2).[23] Subsequent metathesis of $[TiCp_2(S_7NH)]$ with dichlorosulfanes S_xCl_2 (x = 1 or 2) produces nine- or ten-membered cyclic sulfur imides S_8NH (**9.12**) or S_9NH (**9.13**) (Eq. 9.3) (Chart 9.3).[24] Smaller cyclic sulfur imides with a single NR functionality, S_5NR (**9.10**) and S_6NR (**9.11**) (R = Oct) (Chart 9.3), have also been obtained by this methodology.[25]

$$[TiCp_2(CO)_2] + S_7NR \rightarrow [TiCp_2(S_7NR)] + 2CO \qquad (9.2)$$

$$[TiCp_2(S_7NH)] + S_xCl_2 \rightarrow [TiCp_2Cl_2] + S_{7+x}NH \quad (x = 1, 2) \qquad (9.3)$$

The nine- and ten-membered rings **9.12** and **9.13** are obtained as pale yellow crystals that are soluble in CS_2.[24] They undergo photochemical decomposition in daylight after several days, but can be stored in the dark at 22°C for weeks. The nine-membered ring shows a sequence of torsional angles similar to that found for *cyclo*-S_9. By contrast, the motif of

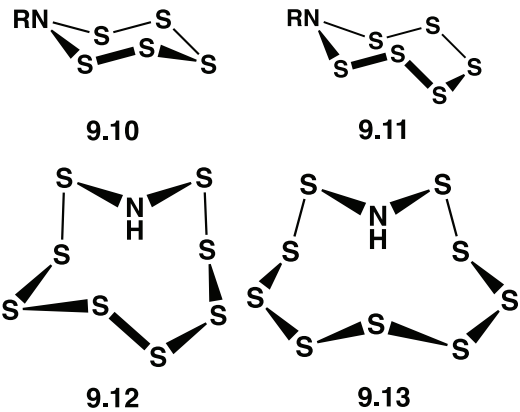

Chart 9.3. Six-, seven-, nine- and ten-membered cyclic sulfur imides.

torsional angles for the ten-membered ring resembles the crown structure of *cyclo*-S_8 with the insertion of an SN(H) unit rather than that of *cyclo*-S_{10}. The S–N bond distances of *ca.* 1.67 Å and the planarity at the nitrogen atoms in **9.12** and **9.13** imply the presence of π-bonding, as found in the eight-membered cyclic sulfur imides (Sec. 9.3.1).

9.4 Cyclic Selenium and Tellurium Imides

There are no selenium analogues of the prototypical cyclic sulfur imides (Chart 9.2), *i.e.*, ring systems that incorporate N(H) functionalities. However, an extensive series of organic derivatives of cyclic selenium imides, most of which do not have sulfur analogues, have been characterised.[26–28] The major sources of these heterocycles are either (a) cyclocondensation reactions of *tert*-butylamine with $SeCl_2$ or (b) decomposition of acyclic selenium(IV) diimides. These two synthetic approaches are compared below. With one exception the ring systems that have been structurally characterised incorporate a bulky *tert*-butyl or adamantyl group attached to selenium. Examples of five-, six-, seven-, eight- and 15-membered rings: $Se_3(NR)_2$ (**9.14**, R = ^{t}Bu, Ad),[29,30] $Se_3(N^tBu)_3$ (**9.15**),[31] $Se_6(N^tBu)_2$ (**9.17**),[32] $Se_4(NMe)_4$ (**9.18**),[33] and $Se_9(N^tBu)_6$ (**9.19**) (Chart 9.4)[32] have been isolated and structurally characterised. The seven-membered ring $Se_4(N^tBu)_3$ (**9.16**) is only known in a metal complex (Sec. 9.5).[34]

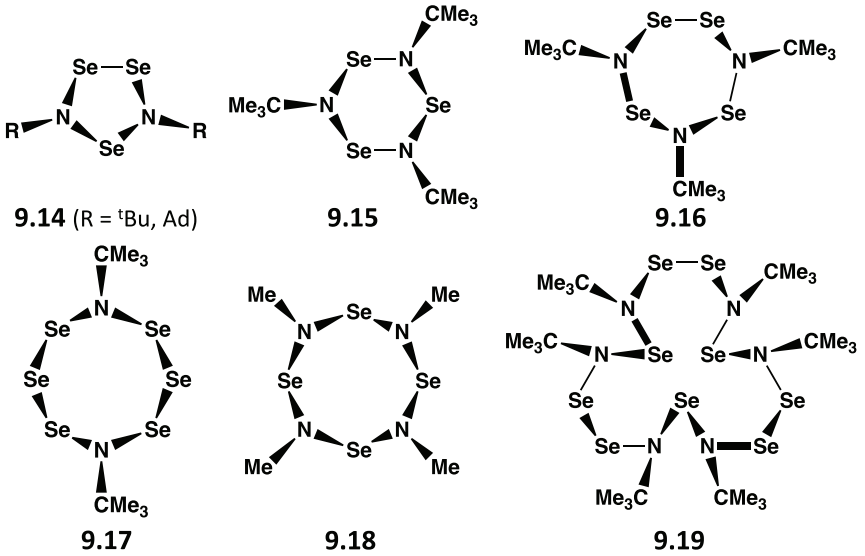

Chart 9.4. Five-, six-, seven-, eight- and 15-membered cyclic selenium imides.

The selenium-rich eight- and 15-membered rings **9.17** and **9.19** were first prepared in 1988 by cyclocondensation reactions between $^{t}Bu(Me_3Si)NLi$ and either Se_2Cl_2 or $SeOCl_2$ in THF.[32] The eight-membered ring $Se_4(NMe)_4$ (**9.18**) is the only member of the series **9.14–9.19** that has a sulfur analogue, *i.e.*, $S_4(NMe)_4$ (Fig. 9.1a). The selenium derivative **9.18** is obtained in excellent yield from the cyclocondensation reaction of $SeCl_2$ with the primary amine equivalent $(Me_3Si)_2NMe$ (Eq. 9.4).[33]

$$(Me_3Si)_2NMe + SeCl_2 \rightarrow 1/4Se_4(NMe)_4 + 2Me_3SiCl \qquad (9.4)$$

A prominent feature of the cyclic selenium imides generated *via* cyclocondensation reactions of primary amines and $SeCl_2$ is the formation of catenated structures with –Se–Se– or –Se–Se–Se– linkages in the ring. A series of acyclic imidoselenium(II) dichlorides $ClSe[N(^{t}Bu)Se]_nCl$ (n = 1–3) have been isolated and identified as intermediates in this process (Sec. 8.11).[35] As illustrated in Scheme 9.2, treatment of these bifunctional building blocks with $^{t}BuNH_2$ occurs by concurrent pathways involving either (a) nucleophilic substitution or (b) reduction. The former route gives rise to the symmetrical ring systems $Se_n(N^{t}Bu)_n$ (n = 3, 4) whereas

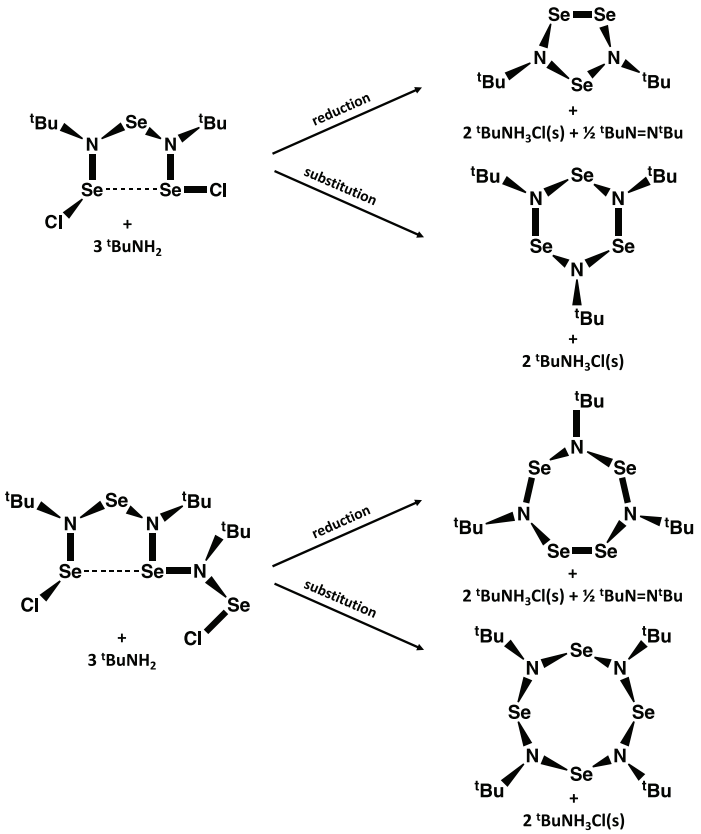

Scheme 9.2. Formation of cyclic selenium imides from reactions of ClSe[N(^{t}Bu)Se]$_n$Cl (n = 2, 3) and ^{t}BuNH2 *via* reduction or nucleophilic substitution.

reduction generates rings with –Se–Se– bonds and is thermodynamically favourable due to the formation of the diazene RN=NR as a by-product.

The ^{77}Se NMR spectra provide an informative analysis of the components of the reaction mixtures in these syntheses of cyclic selenium imides (Sec. 3.3). The oligomeric five- and 15-membered rings **9.14** and **9.19**, show two resonances with relative intensities of 2:1 corresponding to the diselenido and monoselenido bridging units, respectively. The eight-membered ring **9.17** also exhibits two resonances attributable to the two different selenium environments. The characteristic chemical shifts for the different selenium environments in cyclic selenium imides and imidoselenium(II) dichlorides show a marked upfield shift as the

electronegativity of the neighbouring atoms decreases: δ 1620–1725 (N**Se**Cl), 1400–1625 (N**Se**N), 1100–1200(N**Se**Se), and 500–600 (Se**Se**Se).[30] The knowledge of the ^{77}Se NMR chemical shift for $Se_4(NMe)_4$ (**9.18**), prepared according to Eq. 9.4, provided a benchmark for the identification of the elusive *tert*-butyl derivative $Se_4(N^tBu)_4$, which has not been isolated.[33]

The decomposition of thermally unstable selenium(IV) diimides RN=Se=NR (R = ^{t}Bu, Ad) in THF solution at ambient temperatures is also a rich source of cyclic selenium imides.[29,30] The predominant products are the five-membered ring $Se_3(NR)_2$ (**9.14**, R = ^{t}Bu, Ad) and the six-membered ring $Se_3(NR)_3$ (**9.15**, R = ^{t}Bu, Ad); the larger rings $Se_6(N^tBu)_2$ (**9.17**) and $Se_9(N^tBu)_6$ (**9.19**) are also observed by ^{77}Se NMR spectroscopy.[36] The influence of group 12 metal dihalides MCl_2 (M = Cd, Hg) on the cyclodimerisation of selenium(IV) diimides is discussed in Sec. 10.2.3.

The cyclic chalcogen imides **9.14** (R = Ad), **9.15** (R = ^{t}Bu), **9.17, 9.18**, and **9.19** have been structurally characterised by X-ray crystallography. The metrical parameters for the puckered five-membered ring **9.14** are significantly different from those of the larger rings as a result of ring strain. Thus the Se–Se distance in **9.14** is *ca.* 0.07 Å longer than the mean Se–Se bond distance in **9.17**, which has typical Se–Se single bond values of 2.33 Å (*cf.* 2.34 Å in *cyclo*-Se_8).[36] The mean Se–N distance in the N–Se–N unit of **9.14** is *ca.* 0.06 Å longer than the corresponding bonds in the six-membered ring **9.15** (R = ^{t}Bu), which adopts a chair conformation with Se–N bond distances of 1.83 Å indicative of single bonds. Another structural difference between **9.14** and the other cyclic selenium imides involves the geometry at the nitrogen atoms, which is distinctly pyramidal ($\sum$<N = 343–344^o) in the five-membered ring **9.14** compared to the almost planar configurations in **9.15, 9.16** and **9.17**. The eight-membered ring **9.17** crystallises in a crown conformation similar to that of *cyclo*-Se_8.

The only known cyclic tellurium imide is $Te_3(N^tBu)_3$, which is formed as a by-product in the synthesis of the tellurium(IV) diimide ^{t}BuNTe(μ-$N^tBu)_2TeN^tBu$ from the reaction of $TeCl_4$ with $LiNH^tBu$ when the reaction is carried out in toluene (Sec. 10.4).[37] Similar to the selenium analogue **9.15** (R = ^{t}Bu), the six-membered ring $Te_3(N^tBu)_3$ has a chair conformation with Te–N distances of 2.03 Å, consistent with single bonds.

9.5 Metal Complexes of Cyclic Chalcogen Imides

Cyclic chalcogen imides exhibit three types of behaviour in their interactions with metal-containing reagents: (a) deprotonation, (b) oxidative addition and (c) adduct formation:

(a) A simple example of deprotonation involves the reaction of S_7NH with phenylmercury acetate to give $[HgPh(NS_7)]$, which has been investigated as an S_7N transfer agent.[38] By contrast, deprotonation of $S_4(NH)_4$ with the zerovalent platinum complex $[Pt(PPh_3)_4]$ results in ring fragmentation and the formation of the complex $[Pt(PPh_3)_2(S_2N_2)]$ in which the acyclic $[S_2N_2]^{2-}$ ligand is *N,S*-chelated to the platinum (II) centre.[16]

(b) Cyclic sulfur imides containing S–S bonds undergo oxidative addition reactions with $[TiCp_2(CO)_2]$. In the reaction with eight-membered rings S_7NR (R = H, Me) the metal inserts into an S–S bond to give the complexes $[TiCp_2(S_7NR)]$ (Eq. 9.2).[23] Surprisingly, the insertion into S_7NH involves a different S–S bond than the corresponding insertion for S_7NMe. Thus, the structure $[TiCp_2(S_7NMe)]$ incorporates bridging trisulfido and tetrasulfido fragments, whereas $[TiCp_2(S_7NH)]$ contains bridging disulfido and pentasulfido units; the latter complex has been used for the synthesis of *cyclo*-S_8NH and *cyclo*-S_9NH (Eq. 9.3). A different transformation occurs in the reactions of $[TiCp_2(CO)_2]$ with the six-membered cyclic sulfur imides 1,4-$S_4(NR)_2$ (R = Me, Oct).[24] In this case the oxidative addition results in the replacement of one of the NR groups by a Cp_2Ti fragment to give the complexes $[TiCp_2(S_4NR)]$, which have a chair conformation.

(c) Adduct formation rather than deprotonation of $S_4(NH)_4$ occurs with some metal complexes and involves the sulfur centres. For example, a sandwich complex $[S_4(NH)_4]_2{\cdot}AgClO_4$ (**9.20**), in which all four sulfur atoms of both ligands are bonded to silver, has been structurally characterised (Chart 9.5).[39] The tetraimide may also act as an *S*-monodentate ligand as observed in complexes of type $[M(CO)_5\{S_4(NH)_4\}]$ (**9.21**, M = Cr, W), formed by the displacement of the THF ligand in $[M(THF)(CO)_5]$ by $S_4(NH)_4$ (Chart 9.5).[40]

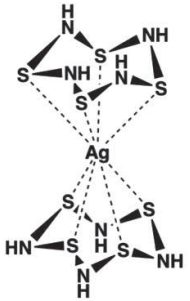

9.20

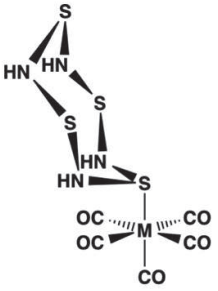

9.21

Chart 9.5. Different coordination modes in metal complexes of $S_4(NH)_4$.

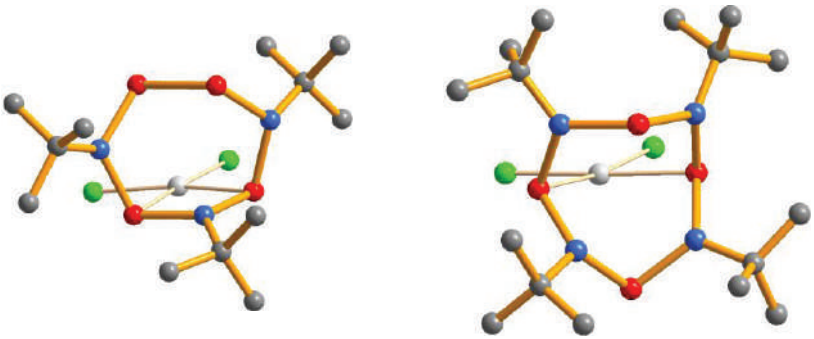

(a) (b)

Figure 9.2. Molecular structures of (a) $[PdCl_2\{Se_4(N^tBu)_3\}]$ and (b) $[PdCl_2\{Se_4(N^tBu)_4\}]$.[34]

The reaction of $^tBuN{=}Se{=}N^tBu$ with $[PdCl_2(NCPh)_2]$ in THF produces the complexes $[PdCl_2\{Se_4(N^tBu)_3\}]$ and $[PdCl_2\{Se_4(N^tBu)_4\}]$.[34] In the former adduct the seven-membered ring $Se_4(N^tBu)_3$ is *Se,Se′*-chelated to palladium *via* the selenium atoms that have two nitrogen neighbours (Fig 9.2a), while the bidentate coordination mode for the eight-membered ring $Se_4(N^tBu)_4$ involves two antipodal selenium atoms (Fig. 9.2b). Ring expansion of the six-membered ring $Se_3(N^tBu)_3$ to give cyclic tetramer $Se_4(N^tBu)_4$ occurs in the presence of $[PdCl_2(NCPh)_2]$, according to ^{77}Se NMR monitoring of this process.[34]

References

1. T. Y. Takeshita and T. H. Dunning, Jr., *J. Phys. Chem. A*, **119**, 1446 (2015).
2. (a) M. Herberhold and W. Bühlmeyer, *Angew. Chem. Int. Ed. Engl.*, **23**, 80 (1984); (b) M. Herberhold, *Comments Inorg. Chem.*, **7**, 53 (1988); (c) M. Herberhold, U. Bertholdt and W. Milius, *Z. Naturforsch.*, **50B**, 1252 (1995); (d) M. Herberhold, U. Bertholdt, W. Milius and B. Wrackmeyer, *Z. Naturforsch.*, **51B**, 1283 (1996).
3. W. J. Middleton, *J. Am. Chem. Soc.*, **88**, 3842 (1966).
4. (a) M. R. Bryce, J. N. Heaton, P. C. Taylor and M. Anderson, *J. Chem. Soc., Perkin Trans.*, **1**, 1935 (1994); (b) M. R. Bryce, J. Becher and B. Fält-Hansen, *Adv. Heterocycl. Chem.,* **1**, 55 (1992).
5. M. R. Bryce and A. Chesney, *J. Chem. Soc., Chem. Commun.*, 195 (1995)
6. H. G. Heal, *The Inorganic Heterocyclic Chemistry of Sulfur, Nitrogen and Phosphorus*, Academic Press (1980).
7. H. G. Heal and J. Kane, *Inorg. Synth.*, **11**, 184 (1968).
8. R. Steudel and F. Rose, *J. Chromatogr.*, **216**, 399 (1981).
9. J. Bojes, T. Chivers and I. Drummond, *Inorg. Synth.*, **18**, 203 (1978).
10. G. Brauer, *Handbook of Preparative Inorganic Chemistry,* 2nd Edition, Academic Press (1963), Vol. 1, p. 411.
11. H-J. Hecht, R. Reinhardt, R. Steudel and H. Bradacek, *Z. Anorg. Allg. Chem.*, **426**, 43 (1976).
12. C.-C. Wang, Y.-Y. Hong, C.-H. Ueng and Y. Wang, *J. Chem. Soc., Dalton Trans.*, 3331 (1992).
13. D. Gregson, G. Klebe and H. Fuess, *J. Am. Chem. Soc.*, **110**, 8488 (1988).
14. T. Chivers, M. Edwards, D. D. McIntyre, K. J. Schmidt and H. J. Vogel, *Mag. Reson. Chem.*, **30**, 177 (1992).
15. T. Chivers and I. Drummond, *Inorg. Chem.*, **13**, 1222 (1974).
16. T. Chivers, F. Edelmann, U. Behrens and R. Drews, *Inorg. Chim. Acta*, **116**, 145, (1986).
17. R. Faggiani, R. J. Gillespie, C. J. L. Lock and J. D. Tyrer, *Inorg. Chem.*, **17**, 2975 (1978).
18. W. I. Gordon and H. G. Heal, *J. Inorg. Nucl. Chem.*, **32**, 1863 (1970).
19. B. B. Stone and M. L. Nielsen, *J. Am. Chem. Soc.*, **81**, 3580 (1959).
20. A. L. MacDonald and J. Trotter, *Can. J. Chem.*, **51**, 2504 (1973)
21. V. A. Ogurtsov and O. A. Rakitin, *Molbank*, **2019**, M1091, (2019).
22. R. Jones, D. J. Williams and J. D. Woollins, *Angew. Chem. Int. Ed. Engl.*, **24**, 760 (1985).

23. K. Bergemann, M. Kustos., P. Krüger and R. Steudel, *Angew. Chem. Int. Ed. Engl.*, **34**, 1330 (1995).
24. R. Steudel, O. Schumann, J. Buschmann and P. Luger, *Angew. Chem. Int. Ed. Engl.*, **37**, 492 (1998).
25. R. Steudel, K. Bergemann, J. Buschmann and P. Luger, *Angew. Chem. Int. Ed. Engl.*, **35**, 2537 (1996).
26. T. Chivers and R. S. Laitinen, *Dalton Trans.*, **46**, 1357 (2017).
27. T. Chivers, R. Oilunkaniemi and R. S. Laitinen, in *Selenium and Tellurium Chemistry*, Eds. J. D. Woollins and R. Laitinen, Springer-Verlag (2011), Ch. 5, pp. 103–122.
28. T. Chivers and R. S. Laitinen, in *Handbook of Chalcogen Chemistry: New Perspectives in Sulfur, Selenium and Tellurium*, Ed. F. Devillanova, Royal Society of Chemistry (2006), Ch. 4, pp. 223–285.
29. T. Maaninen, H. M. Tuononen, G. Schatte, R. Suontamo, J. Valkonen, R. Laitinen and T. Chivers, *Inorg. Chem.,* **43**, 2097 (2004).
30. T. Maaninen, T. Chivers, R. Laitinen, G. Schatte and M. Nissinen, *Inorg. Chem.*, **39**, 5341 (2000).
31. T. Maaninen, T. Chivers, R. Laitinen and E. Wegelius, *Chem. Commun.*, 759 (2000).
32. H. W. Roesky, K.-L. Weber and J. W. Bats, *Chem. Ber.*, **117**, 2686 (1984).
33. A. J. Karhu, O. J. Pakkanen, J. M. Rautiainen, R. Oilunkaniemi, T. Chivers and R. S. Laitinen, *Inorg. Chem.*, **54**, 4990 (2015).
34. M. Risto, A. Eironen, E. Männistö, R. Oilunkaniemi, R. S. Laitinen and T. Chivers, *Dalton Trans.*, 8473 (2009).
35. A. J. Karhu, O. J. Pakkanen, J. M. Rautiainen, R. Oilunkaniemi, T. Chivers and R. S. Laitinen, *Dalton Trans.*, **45**, 6210 (2016).
36. A. Maaninen, J. Konu, R. S. Laitinen, T. Chivers, G. Schatte, J. Pietikäinen and M. Ahlgrén, *Inorg. Chem*., **40**, 3539 (2001).
37. T. Chivers, X. Gao and M. Parvez, *J. Am. Chem. Soc*., **117**, 2359 (1995).
38. R. J. Ramsay, H. G. Heal and H. Garcia-Fernandez, *J. Chem. Soc., Dalton Trans*., 237 (1976).
39. M. B. Hursthouse, K. M. A. Malik and S. N. Nabi, *J. Chem. Soc.*, *Dalton Trans*., 355 (1980).
40. G. Schmid, R. Greese and R. Boese, *Z. Naturforsch*., **37B**, 620 (1982).

Chapter 10

Acyclic Organic Chalcogen-Nitrogen Compounds

10.1 Introduction

In this chapter the chemistry of acyclic organic derivatives containing a chalcogen-nitrogen functional group as the central feature will be discussed. The simplest examples are monomeric thionitroso compounds RNS and their selenium analogues RNSe, which are described in Sec. 9.2 in the context of the corresponding cyclic oligomers $(RNE)_x$ (x = 3, E = Se, Te; x = 4, E = S, Se). Consequently, the first sections of this chapter will discuss organic chalcogenylamines RNEO (E = S, Se, Te) and, subsequently, *N*-thiosulfinylamines RN=S=S. The commercially available *N*-sulfinylamines RNSO (R = trityl) and the related *N*-sulfinyl-*O*-hydroxylamines RONSO (R = ^{t}Bu, 4-PhC_6H_4) are useful reagents for the synthesis of sulfur(VI)-nitrogen compounds with potential applications in the pharmaceutical and agrochemical industries.

Chalcogen(IV) diimides RN=E=NR (E = S, Se, Te) represent a very widely studied class of chalcogen-nitrogen compounds for which detailed structural comparisons for the three chalcogens can be made. These acyclic chalcogen(IV)-nitrogen compounds have an extensive reaction chemistry including the formation of a wide variety of metal complexes.[1,2] In addition, investigations of their reactivity have led to the synthesis of imido analogues of binary sulfur-oxygen species such as SO_3, $[SO_3]^{2-}$ and $[SO_4]^{2-}$, *i.e.*, $S(NR)_3$, $[S(NR)_3]^{2-}$ and $[S(NR)_4]^{2-}$, respectively, which exhibit a rich coordination chemistry.[3]

The foregoing compounds all contain imido groups (NR) attached to a chalcogen(IV) centre. Another important class of acyclic organochalcogen-nitrogen compounds incorporates an amido group (NR_2) linked to a chalcogen(II) centre, *e.g.*, $E(NR_2)_2$ (E = S, Se, Te). These compounds have a well-developed chemistry and there are notable differences between the behaviour of the heavier chalcogen derivatives and that of sulfur analogues, *e.g.*, in the use of tellurium(II) amides in organic synthesis.

The final sections of this chapter will discuss the chemistry of organochalcogen-compounds in which an RE or R_2E group is attached to a nitrogen centre. This category includes (a) organochalcogen azides $R_{4-n}E(N_3)_n$ (n = 1, 2, 3; E = S, Se, Te), (b) trisulfenamides $(RS)_3N$ and the related radicals $[(RS)_2N]^{\bullet}$, (c) chalcogen(IV) monoimides $Ph_2E{=}NH$ (E = S, Se), and (d) the isomers $Ph_2S{=}NX$ (X = Cl, Br) and $Ph_2XS{\equiv}N$ (X = F, OR).

10.2 Organic Chalcogenylamines, RNEO (E = S, Se, Te)

10.2.1 *Synthesis and structures*

Thionyl imide, HNSO, is a thermally unstable gas which polymerises readily. It can be prepared *in situ* in CH_2Cl_2 by protonation of K[NSO] with stearic acid and isolated as an adduct with $B(C_6F_5)_3$ (Sec. 6.4).[4] Organic derivatives RNSO have higher thermal stability, especially when R is an aryl or the bulky alkyl group CPh_3 (Tr). A typical synthesis involves the reaction of a primary amine or, in some cases, a silylated amine with thionyl chloride. For example, *N*-sulfinyltritylamine, TrNSO, can be obtained as a white solid on a 10-gram scale in essentially quantitative yield from the reaction of commercially available tritylamine with thionyl chloride in the presence of triethylamine in diethyl ether at 0°C;[5a] the *tert*-octyl derivative ^{t}OctNSO is prepared in a similar manner in 97% yield (Eq. 10.1).[5b]

$$RNH_2 + SOCl_2 + 2NEt_3 \rightarrow RNSO + 2[Et_3NH]Cl \qquad (10.1)$$
$$(R = Ph_3C, \textit{tert}\text{-octyl})$$

The synthesis of the versatile synthon Me_3SiNSO involves the reaction of thionyl chloride with tris(trimethylsilyl)amine at 70°C in the presence of $AlCl_3$ (Eq. 10.2).[6] Me_3SiNSO is a thermally stable liquid (b.p. 105–107°C), which can be used as an NSO transfer reagent to prepare (a) alkali-metal salts M[NSO] (N = Na, K, Rb, Cs)[7] by reaction with potassium *tert*-butoxide, (b) $[(Me_2N)_3S][NSO]$ upon treatment with $[(Me_2N)_3S][Me_3SiF_2]$[8] or (c) chalcogen(II) derivatives $E(NSO)_2$ *via* reactions with chalcogen halides (SCl_2, E = S;[9a] Se_2Cl_2, E = Se[9b]).

$$(Me_3Si)_3N + SOCl_2 \rightarrow Me_3SiNSO + 2Me_3SiCl \qquad (10.2)$$

N-sulfinyl-*O*-hydroxylamines RONSO represent a related class of synthetically useful sulfinylamines. These reagents can be used as precursors to sulfur(VI)-nitrogen compounds with applications in the pharmaceutical industry and agrochemistry (Sec. 10.2.2).[10a] The biphenyl derivative 4-PhC_6H_4ONSO, is obtained as a white solid in quantitative yield by the reaction of biphenylhydroxylamine with thionyl chloride in the presence of triethylamine in diethyl ether at 0°C (Scheme 10.1a),[10b] while the alkyl derivative ^{t}BuONSO, a colourless liquid, can be isolated in 57% yield from the reaction of commercially available *O*-*tert*-butylhydroxylamine hydrochloride with thionyl chloride under similar conditions (Scheme 10.1b).[10c]

Organic sulfinylamines have planar, *cis* structures in the solid state and in solution, as determined by X-ray crystallography and ^{15}N NMR

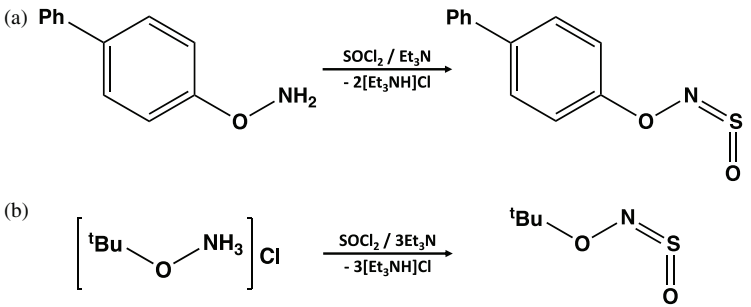

Scheme 10.1. Synthesis of *N*-sulfinyl-*O*-hydroxylamines.

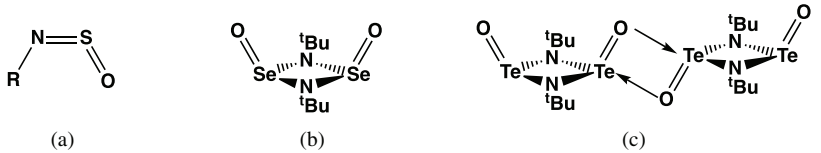

Chart 10.1. (a) Monomeric (b) dimeric and (c) tetrameric chalcogenylamines.

spectroscopy, respectively (Chart 10.1a). The trityl derivative Ph_3CNSO is the only alkyl derivative to have been structurally characterised in the solid state; the S=N and S=O bond lengths are 1.492(1) and 1.450(1) Å, respectively.[11] In contrast to ^{t}BuNSO, the selenium analogue has a dimeric structure $OSe(\mu\text{–}N^tBu)_2SeO$ (Chart 10.1b) in which the two exocyclic oxo substituents are in a *cis* configuration with respect to the Se_2N_2 ring;[12a] the unsymmetrical imido-oxo system *cis*-^{t}BuNSe$(\mu\text{–}N^tBu)_2$SeO has also been structurally characterised.[12b] The Se–N bond lengths in these dimers are in the range 1.86–1.94 Å, slightly longer than the single-bond value of 1.86 Å; the Se=O bond lengths of 1.62–1.63 Å are indicative of double bonds. The tellurium analogue $(^t\text{BuNTeO})_n$ has not been isolated, but the tetrameric unit shown in Chart 10.1c was obtained as a complex in which the strong Lewis acid $B(C_6F_5)_3$ is coordinated to the terminal oxygen atoms.[12c] The increasing reluctance for the heavier chalcogens to form double bonds with NR or O in chalcogenylamines parallels the well-established trend for chalcogen dioxides, *viz.*, SO_2 is a monomeric gas, SeO_2 is a two-dimensional polymer with both single and double SeO bonds, and $(TeO_2)_\infty$ is a three-dimensional polymer with only Te–O single bonds.

10.2.2 *Synthetic applications*

The sulfinylamines TrNSO (Tr = CPh_3) and 4-PhC_6H_4ONSO are both commercially available, attesting to their growing importance for the preparation of sulfur(VI)-nitrogen compounds for applications in medicinal and agrochemistry, *e.g.*, sulfonimidamides, sulfondiimines, sulfoximes, and sulfonamides.[13] Medicinally useful sulfonimidamides have been prepared by the combination of *N*-sulfinyltritylamine (Ph_3CNSO, TrNSO) with a Grignard reagent and chlorination of the resultant anionic

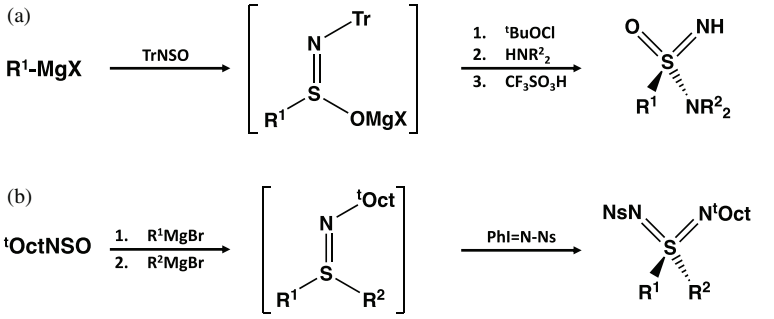

Scheme 10.2. Synthesis of (a) sulfonimidamides and (b) sulfondiimines from *N*-sulfinylamines.

sulfinamide with *tert*-butyl hypochlorite to generate a sulfonimidoyl chloride followed by the addition of a secondary amine and, subsequently, trifluoromethanesulfonic acid (Scheme 10.2a).[5a] The synthesis of sulfondiimines (the diaza analogues of sulfones) requires the use of ^{t}OctNSO rather than TrNSO in a reaction with two Grignard reagents to generate a sulfilimine followed by *S*-imination with the iodinane PhI=N–Ns (Ns = 4-$NO_2C_6H_4SO_2$) in the presence of $[Rh_2(OAc)_4]$ as catalyst (Scheme 10.2b).[5b]

Unlike the preparation of sulfonimidamides from iminosulfur oxydifluorides RN=S(O)F_2 described in Sec 8.3.2, the procedure shown in Scheme 10.2a requires an oxidation step to convert S(IV) to S(VI). However, a more efficient synthesis of sulfonimidamides employs *N*-sulfinyl-*O*-hydroxylamines as an *in situ* source of highly electrophilic sulfinyl nitrenes RS(O)N (Sec 10.10), which react readily with nitrogen or carbon nucleophiles.[10a,b] Thus, reaction of 4-PhC_6H_4ONSO with a Grignard reagent in THF at low temperature followed by addition of a secondary amine results in the rapid formation (<15 min) of sulfonimidamides (Scheme 10.3).[10a,b] Alternatively, the treatment of 4-PhC_6H_4ONSO with a Grignard reagent followed quickly by the addition of another Grignard reagent produces sulfoximes (Scheme 10.3).[10a,b]

Sulfonamides $RS(O)_2NH_2$ are widely used pharmaceuticals, for example in the treatment of epilepsy, high blood pressure, arthritis and glaucoma.[10a,c,13] A new synthesis of these drugs employs the stable

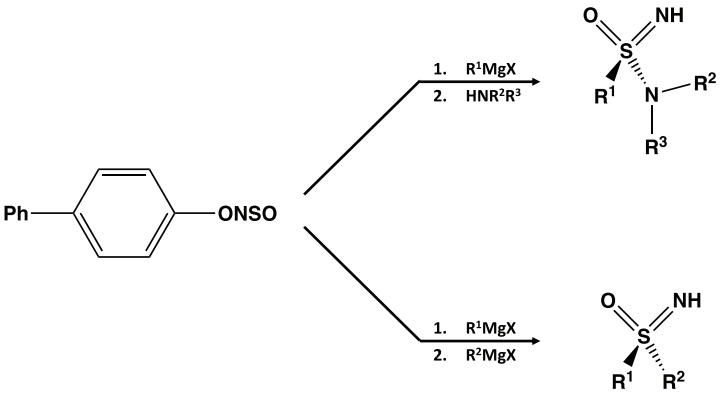

Scheme 10.3. Synthesis of (a) sulfonimidamides and (b) sulfoximes from 4-PhC_6H_4ONSO.

N-sulfinyl-*O*-hydroxylamine ^{t}BuONSO in a one-pot reaction with Grignard or organolithium reagents in THF at −78°C (Eq. 10.3).[10a,c] A wide variety of primary sulfonamides with alkyl or (hetero)aryl substituents can be prepared in 40–85% yields using this procedure.

$$RM + {}^t\text{BuONSO} \rightarrow RS(O)_2NH_2 \quad (M = MgBr, Li) \tag{10.3}$$

An alternative new procedure for the high-yield synthesis of a large variety of sulfonamides of the type $ArS(O)_2NHR'$ (Ar = aryl) is the reaction of the corresponding sulfonyl fluoride with a primary amine in the presence of 1-hydroxybenzotriazole as a catalyst.[14]

N-Sulfinylamines ArNSO were found to be more effective than isocyanates RNCO for oxo-imido exchange reactions with Group 15 or 16 metal oxochlorides when the aryl group is either sterically bulky or strongly electron-withdrawing, *e.g.*, C_6F_5 (Eq. 10.4).[15a] *N*-Sulfinylamines are also effective for the direct imidation of lactones using a titanium imido catalyst.[15b]

$$MO_2Cl_2 + 2C_6F_5NSO \rightarrow M(NC_6F_5)_2Cl_2 + 2SO_2 \quad (M = Cr, Mo, W) \tag{10.4}$$

10.2.3 *Metal complexes*

A number of transition-metal complexes of RNSO ligands have been structurally characterised.[16] Three bonding modes, $\pi(N,S)$, $\sigma(S)$-trigonal and $\sigma(S)$-pyramidal, have been observed (Chart 10.2). Side-on (N,S) coordination is favoured by electron-rich (d^8 or d^{10}) metal centres, while the $\sigma(S)$-trigonal mode is preferred for less electron-rich metal centres (or those with competitive strong π-acid co-ligands). As expected $\pi(N,S)$ coordination results in a significant lengthening of the S–N bond, whereas there are no substantial changes in the structural parameters of the RNSO ligand in the $\sigma(S)$-trigonal bonding mode.[16]

The reactions of *N*-sulfinylamines with Frustrated Lewis Pairs (FLPs) reveal new aspects of the coordination chemistry of the NSO functionality. A zirconium/phosphorus FLP system reacts with PhNSO to give an adduct in which the phosphine Lewis base adds to the N atom while the Lewis acidic Zr^+ centre coordinates to both the S and O atoms (**10.1**) (Scheme 10.4).[17]

In the case of boron/phosphorus FLPs the addition of ArNSO (Ar = *p*-tolyl) can occur in an inter- or intra-molecular fashion.[18] Thus, the

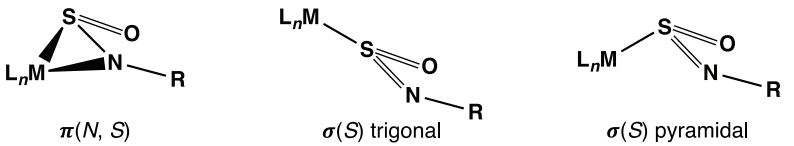

Chart 10.2. Common bonding modes for RNSO ligands.

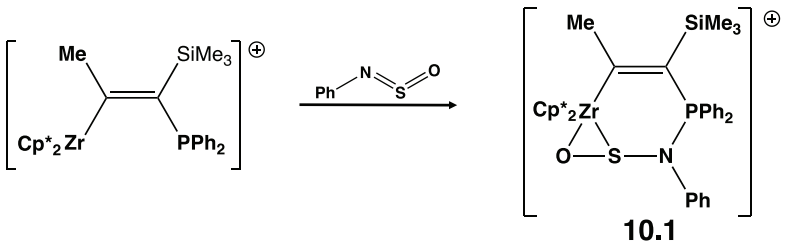

Scheme 10.4. Addition reaction of a Zr/P Frustrated Lewis Pair with PhNSO.

reaction of ArNSO with a mixture of P^tBu_3 and $B(C_6F_5)_3$ produces an adduct in which a bridging NSO group links the P and B centres *via* the N and O atoms, respectively (**10.2**) (Scheme 10.5a). In a similar manner the ethylene-linked P/B species $Mes_2PCH_2CH_2B(C_6F_5)_2$ undergoes addition with ArNSO to give a seven-membered ring with a PNSOB sequence (**10.3**) (Scheme 10.5b). This cyclic adduct is a useful *in situ* source of sulfur monoxide SO, *e.g.*, in reaction with an *N*-heterocyclic carbene to give the corresponding sulfine (>C=S=O).[18]

In another variation of the reactions of *N*-sulfinylamines with FLPs, the treatment of PhNSO with the geminal Sn/P system $(F_5C_2)_3SnCH_2P^tBu_2$ results in cleavage of the S–N bond to give a sulfur monoxide adduct with a cyclic SnCPSO motif (**10.4**) together with a phenylnitrene (PhN) adduct of the FLP (**10.5**) (Scheme 10.6).[19]

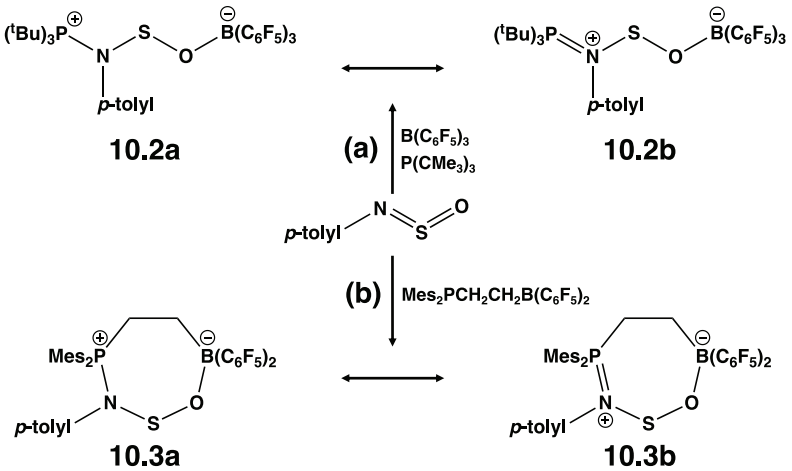

Scheme 10.5. (a) Intermolecular and (b) intramolecular addition of ArNSO to a B/P Frustrated Lewis Pair.

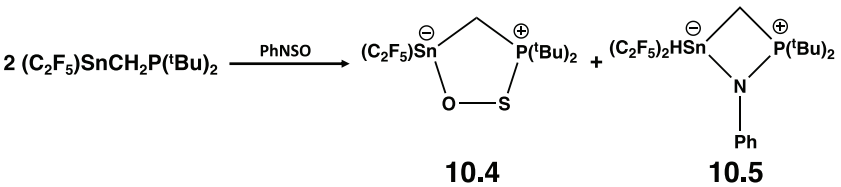

Scheme 10.6. Cleavage reaction of a Sn/P FLP with PhNSO.

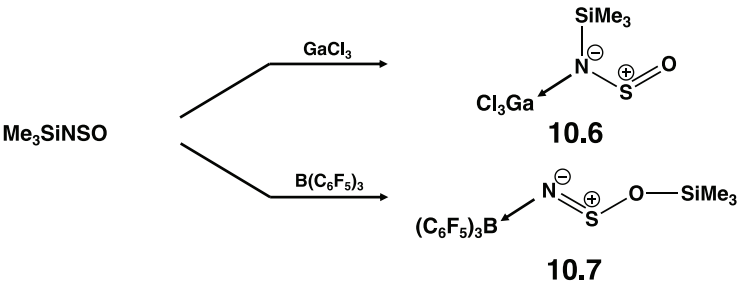

Scheme 10.7. Formation of adducts of Me_3SiNSO with $GaCl_3$ and $B(C_6F_5)_3$.

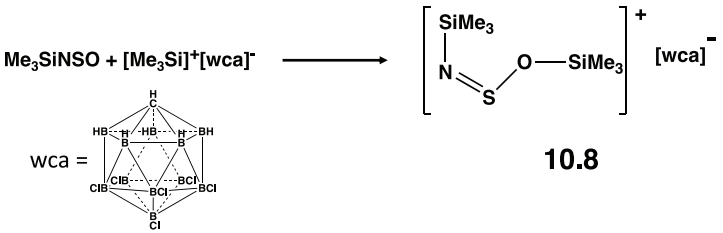

Scheme 10.8. Synthesis of a $[Me_3SiNSOSiMe_3]^+$ salt with a weakly coordinating anion (wca).

The reactions of Me_3SiNSO with several Lewis acids have also been investigated. Both $GaCl_3$ and $B(C_6F_5)_3$ readily form 1:1 adducts at low temperatures in CH_2Cl_2 (Scheme 10.7).[4] The X-ray structures of these adducts revealed different bonding modes for the Lewis acids. Thus, $GaCl_3$ forms an *N*-bonded adduct (**10.6**) whereas the larger $B(C_6F_5)_3$ acceptor engenders a structural rearrangement in which the Me_3Si group undergoes an N→O transfer (**10.7**) (Scheme 10.7).[4]

The reaction of Me_3SiNSO with a trimethylsilylium salt of a weakly coordinating anion $[Me_3Si][CHB_{11}H_5Cl_6]$ in toluene at room temperature generates a salt of the iminosulfonium cation $[Me_3Si–N=S–OSiMe_3]$ $[CHB_{11}H_5Cl_6]$ in modest yield (**10.8**) (Scheme 10.8).[4] In the solid state this cation exhibits *N,O* coordination. However, multinuclear NMR spectra indicate the co-existence of *N,O* and *N,N*-bonded isomers in solution. The cation $[Me_3Si–N=S–OSiMe_3]^+$ is an isoelectronic analogue of the sulfur(IV) diimide $Me_3SiN=S=NSiMe_3$ (Sec. 10.4).

10.3 *N*-Thiosulfinylamines, RNSS

Dithionitro compounds RNS_2 with a branched structure analogous to that of nitro compounds RNO_2 are unknown. However, several *N*-thiosulfinylamines RN=S=S have been isolated and structurally characterised. The first *N*-thiosulfinylamine 4-$Me_2NC_6H_4N$=S=S was obtained as a deep violet solid (λ_{max} 510 nm) in low yield by the reaction of phosphorus pentasulfide with *N*,*N*′-dimethyl-4-nitrosoaniline; it decomposes to the corresponding azobenzene and sulfur on heating to 200°C.[20] Several *N*-thiosulfinyl anilines with bulky *ortho* substituents attached to the nitrogen atom, *e.g.*, 2,4,6-$R_3C_6H_2$ (R = Me, ^{t}Bu, $CH(SiMe_3)_2$) (**10.9**) (Chart 10.3), are isolated in high yields from the reaction of the corresponding aniline with S_2Cl_2 in diethyl ether in the presence of NEt_3.[21–24] However, upon mild thermolysis these derivatives are prone to intramolecular cyclisation involving the *ortho*-alkyl group. Subsequently, bowl-shaped aryl groups with two *m*-terphenyl substituents, Bmt and Bpq (see Fig. 7.5), were found to provide higher thermal stability for the –N=S=S functionality,[21] as described in Sec. 7.7 for *S*-nitrosothiols. For example, BpqNSS did not decompose upon heating at 100°C for seven days.[24]

Sulfur-nitrogen compounds containing the SNSS functionality have also been prepared and structurally characterised. For example, $Ph_3PNSNSS$ (**10.10**)[25] is obtained as deep red crystals by heating the six-membered ring Ph_3P=N–S_3N_3 in boiling acetonitrile. This *N*-bonded derivative of the $[SNSS]^-$ anion (Sec. 5.6.3) adopts a planar *cis,trans* structures with short (*ca.* 1.91 Å) terminal S–S bonds.

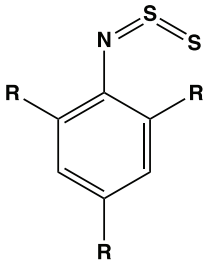

10.9 R = Me, ^{t}Bu, $CH(SiMe_3)_2$

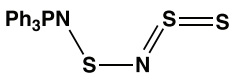

10.10

Chart 10.3. *N*-Thiosulfinylamino derivatives.

10.4 Chalcogen Diimides, RN=E=NR (E = S, Se Te)

10.4.1 *Synthesis*

The reactions of primary amines with sulfur(IV) or selenium(IV) halides provide a facile route to the corresponding chalcogen diimides RN=E=NR (E = S, Se), which are of interest from the structural viewpoint, as reagents in organic synthesis and as ligands for transition metals.[1,2,16] The first sulfur(IV) diimide ^{t}BuN=S=N^{t}Bu was prepared *ca.* 65 years ago by the reaction of *tert*-butylamine with SCl_4 generated *in situ* (Eq. 10.5).[26] Similarly, ^{t}BuN=Se=N^{t}Bu is prepared from the reaction of $SeCl_4$ with *tert*-butylamine.[27] Selenium(IV) diimides are markedly less thermally robust than their sulfur analogues. For example, ^{t}BuN=Se=N^{t}Bu decomposes at room temperature to give a mixture of cyclic selenium imides and ^{t}BuN=N^{t}Bu. (Sec. 9.4).[28]

$$6\,{}^{t}\mathrm{BuNH_2} + \mathrm{ECl_4} \rightarrow {}^{t}\mathrm{BuN{=}E{=}N^{t}Bu} + 4\,{}^{t}\mathrm{BuNH_3Cl} \qquad (10.5)$$
$$(\mathrm{E = S, Se})$$

The corresponding tellurium(IV) diimide ^{t}BuNTe(μ-N^{t}Bu)$_2$TeN^{t}Bu is obtained in good yields from the reaction of lithium *tert*-butylamide with $TeCl_4$ in THF (Eq. 10.6).[29–31] In toluene solution this reaction also produces the cyclic tellurium(II) imide (TeN^{t}Bu)$_3$.[30] The dimer ^{t}BuNTe(μ-N^{t}Bu)$_2$TeN^{t}Bu is obtained as an orange air-sensitive solid, which can be purified by vacuum sublimation at *ca.* 90°C.

$$2\mathrm{TeCl_4} + 8\mathrm{LiNH}{}^{t}\mathrm{Bu} \rightarrow {}^{t}\mathrm{BuNTe}(\mu\text{-}\mathrm{N}{}^{t}\mathrm{Bu})_2\mathrm{TeN}{}^{t}\mathrm{Bu} + 8\mathrm{LiCl} + 4\,{}^{t}\mathrm{BuNH_2} \qquad (10.6)$$

The synthesis of the versatile reagent *N,N′*-bis(trimethylsilyl) sulfur(IV) diimide $Me_3SiN{=}S{=}NSiMe_3$ is described in Sec. 2.3 and Eq. 2.3.[32] The selenium analogue $Me_3SiN{=}Se{=}NSiMe_3$ is obtained in a similar manner by treatment of $SeOCl_2$ with $LiN(SiMe_3)_2$, but it decomposes at ambient temperature.[33] The thermal stability of selenium(IV) diimides is enhanced by the presence of supermesityl groups in Mes*N=Se=NMes*.[34]

10.4.2 *Structures*

Three different conformations are possible for monomeric chalcogen diimides (Chart 10.4). Structural determinations of ^{t}BuN=S=N^{t}Bu (m.p. −28°C) reveal a *cis,trans* conformation in the solid state at low temperature and in the gas phase with mean *d*(S=N) = 1.536 and 1.551 Å, respectively.[35] By contrast, in the gas phase $Me_3SiNSNSiMe_3$ adopts a *cis,cis* arrangement with *d*(S=N) = 1.536 Å.[36] *Ab initio* and DFT molecular orbital computations of the relative energies of the three different conformers for RN=E=NR (E = S, Se; R = H, Me, ^{t}Bu, $SiMe_3$) predict that, with the exception of R = H, the *cis,trans* isomer is the most stable conformation for the majority of chalcogen(IV) diimides.[37] Although this is the most common isomer for sulfur(IV) diimides, the *cis,cis* isomer is observed in solutions of some *N*-aryl derivatives ArN=S=NAr (Ar = 2,4,6-$C_6H_2Br_3$, 2,6-$C_6H_3Me_2$, C_6F_5).[38]

Structural determinations of selenium diimides(IV) in the solid state are limited to two monomeric examples. The bulky alkyl derivative Ad=Se=NAd (Ad = adamantyl)[14] adopts the *cis,trans* conformation consistent with conclusions based on ^{1}H and ^{13}C NMR studies for ^{t}BuN=Se=N^{t}Bu in solution.[39] On the other hand, both DFT calculations and an approximate crystal structure determination for the bulky aryl derivative Mes*N=Se=NMes* indicate a *trans,trans* conformation.[34] Cyclodimerisation of ^{t}BuN=Se=N^{t}Bu occurs in the presence of group 12 dihalides MCl_2 (M = Cd, Hg) to give metal complexes of the *N,N′*-chelated dimer ^{t}BuNSe(μ-N^{t}Bu)$_2$SeN^{t}Bu (Sec. 10.4.4).[40]

In contrast to the monomeric structures of RN=E=NR (E = S, Se), the tellurium analogues adopt dimeric structures. The *tert*-butyl derivative ^{t}BuNTe(μ-N^{t}Bu)$_2$TeN^{t}Bu has a *cis,endo,endo* arrangement of terminal ^{t}Bu

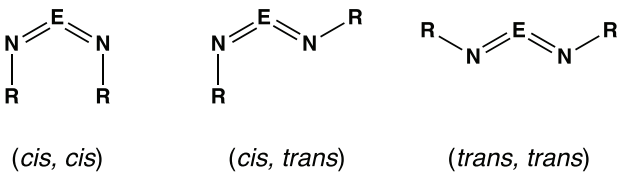

Chart 10.4. Conformational isomers of monomeric chalcogen diimides (E = S, Se); the *syn,anti* or *E,Z* systems of nomenclature may also be used to describe these isomers.

groups with respect to the Te_2N_2 ring,[30] whereas a *trans,exo,exo* arrangement of the exocyclic groups is observed for the unsymmetrical derivatives $RTeN(\mu\text{-}NR')_2TeNR$ ($R = PPh_2NSiMe_3$; $R' = {}^t$Bu, ^{t}Oct) in the solid state (Chart 10.5).[31] The influence of the chalcogen on the energetics of the cyclodimerisation process for chalcogen(IV) diimides is discussed in the next section.

Sulfur(IV) diimides of the type ArE–N=S=N–EAr (E = S, Se) and Me_2P–N=S=N–PMe_2 have been investigated with regard to the influence of interactions between the terminal heteroatom substituents on the configuration of the sulfur(IV) diimide (Chart 10.6).[41,42] The aryl derivatives ArS–N=S=N–SAr (Ar = Ph, 4-ClC_6H_4) adopt a planar *cis,cis* configuration (**10.11**) with an S···S distance that is significantly shorter than the sum of van der Waals radii for two sulfur atoms. Calculations at the DFT/B3LYP level indicate that an intermolecular contact in the solid state, *i.e.*, packing forces, rather than an intramolecular interaction may explain the preference for the *cis,cis* configuration.[41] The calculated packing energies indicate only a small energetic preference (<5 kJ mol^{-1}) for the *cis,cis* over the *cis,trans* configuration (**10.12**).[43] The selenium analogues ArSe–N=S=N–SeAr (Ar = Ph, C_6F_5) also adopt the *cis,cis* configuration in the solid state;[41,43] however, variable-temperature ^{77}Se studies in solution

Chart 10.5. Conformational isomers of tellurium(IV) diimide dimers.

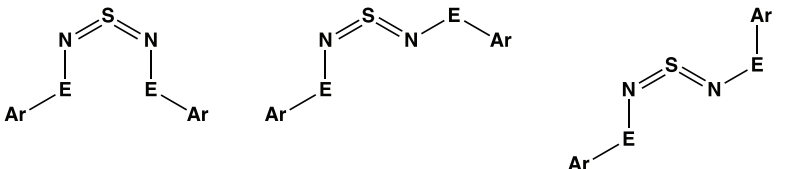

Chart 10.6. The *cis,cis*, *cis,trans-anti,anti*, and *cis,trans-anti,syn* isomers of ArE–N=S=N–EAr (E = S, Se).

revealed the presence of both *cis,cis* and *cis,trans* isomers for the Ar = Ph derivative.[41] A unique example of the *cis,trans* configuration is found in the solid state for the Ar = 4-ClC_6F_4 derivative as a result of Se···Cl interactions.[44] In contrast to the symmetrical heteroatom di-substituted sulfur(IV) diimides, the monosubstituted compounds ArS–N=S=NH (Ar = 4-MeC_6H_4, 2,4,6-$^tBuC_6H_2$) adopt a *cis,trans* configuration in the solid state.[45,46] The phosphorus-substituted sulfur(IV) diimide Me_2P–N=S=N–PMe_2 has not been prepared, but it is predicted by quantum chemical calculations to prefer the *cis,cis* configuration.[42]

10.4.3 *Cyclodimerisation and cycloaddition*

The calculated dimerisation energies for the [2 + 2] cycloaddition of two $E(NR)_2$ (E = S, Se, Te; R = H, Me, ^{t}Bu, $SiMe_3$) molecules (Scheme 10.9) reveal that this process is strongly endergonic for sulfur diimides, approximately energy neutral for selenium diimides and strongly exergonic for tellurium diimides,[47,48] consistent with the experimentally determined crystal structures (Sec. 10.4.2). The results of various calculations for the methyl derivatives $E(NMe)_2$ are depicted in Fig. 10.1. The propensity for the heavier chalcogen imides to undergo cyclodimerisation is also evident in the structures of the hybrid imido-oxo systems of the type RNEO as discussed in Sec. 10.2.1 (Chart 10.1).

The presence of Group 12 metal chlorides MCl_2 (M = Hg, Cd) has a significant effect on the dimerisation energy for selenium diimides. The reaction of ^{t}BuN=Se=N^{t}Bu with $HgCl_2$ or $CdCl_2$ in THF produces high yields of MCl_2 complexes of the dimer ^{t}BuNSe(μ-N^{t}Bu)$_2$SeNtBu (Eq. 10.7).[40] DFT calculations indicate that the activation energy for the [2 + 2] cyclodimerisation process of ^{t}BuN=Se=N^{t}Bu is significantly lowered by

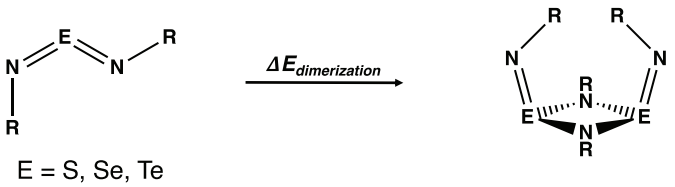

Scheme 10.9. Dimerisation of chalcogen diimides.

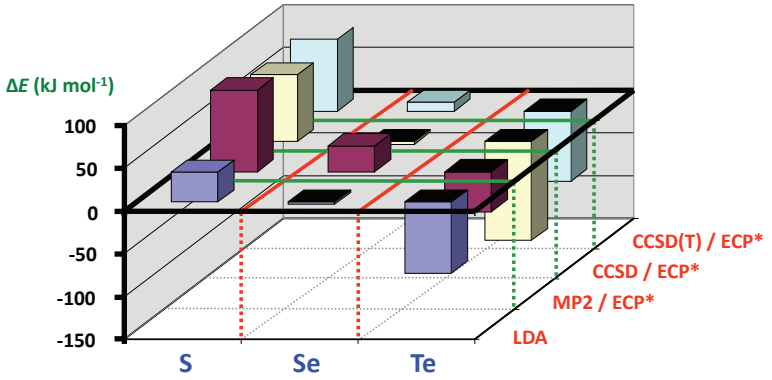

Figure 10.1. Cyclodimerisation energies of $E(NMe)_2$ (E = S, Se, Te).[47,48] [Adapted with permission from R. S. Laitinen, *Phosphorus Sulfur Silicon Relat. Elem.,* **180**, 777 (2005). Copyright 2005 Taylor & Francis].

the presence of Group 12 metal dichlorides, whereas complexation of monomeric ^{t}BuN=Se=N^{t}Bu is preferred for Group 10 metal dihalides MCl_2 (M = Pd, Pt) (Secs. 10.4.2 and 10.4.4).[40]

$$2\,^t\text{BuN=Se=N}^t\text{Bu} + \text{MCl}_2 \rightarrow [\text{MCl}_2\{^t\text{BuNSe}(\mu\text{-N}^t\text{Bu})_2\text{SeN}^t\text{Bu}\}] \quad (10.7)$$
(M = Cd, Hg)

The DFT calculations also show that the activation energy for the dissociation of ^{t}BuNSe(μ-N^{t}Bu)$_2$SeN^{t}Bu into monomers is sufficiently high to explain the observation that the dimer, once formed, is persistent in THF solution.[40]

10.4.4 *Metal complexes*

Monomeric sulfur(IV) diimides have an extensive coordination chemistry as might be anticipated from the availability of three potential donor sites and two π-bonds.[1,16] In addition, they are prone to fragmentation to produce complexes of RNS (thionitroso) ligands. However, under mild conditions sulfur(IV) diimides may form complexes with coordinatively unsaturated metal centres without rupture of the –N=S=N– unit. Four modes of coordination have been identified or invoked as intermediates in fluxional processes (Chart 10.7).

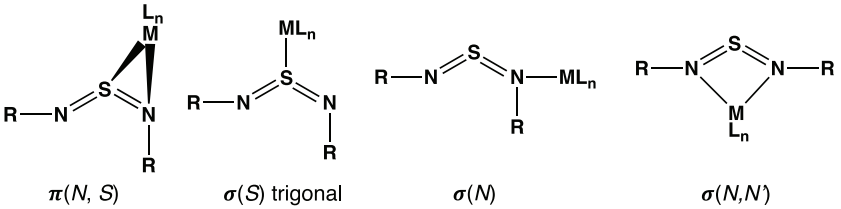

Chart 10.7. Coordination modes for monomeric sulfur(IV) diimides.

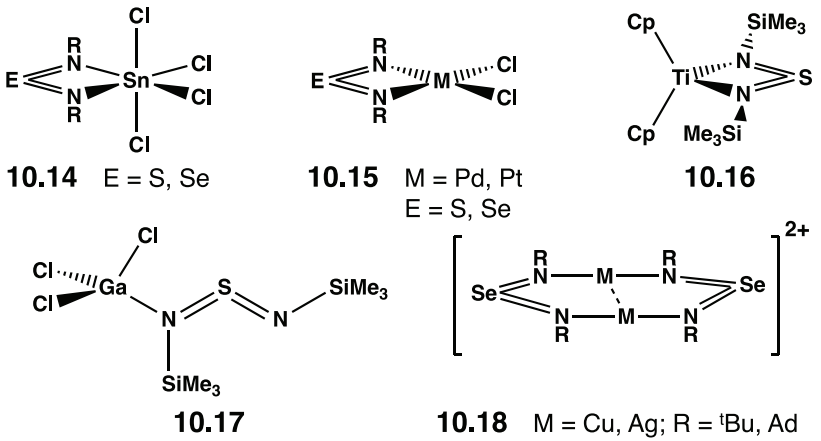

Chart 10.8. Metal complexes of chalcogen(IV) diimide monomers.

N,N′-Chelation is commonly observed for both transition-metal and main-group metal complexes of chalcogen (IV) diimides.[49] Some representative examples are $[SnCl_4\{E(N^tBu)_2\}]$ (**10.14**, E = S, Se),[50,51] $[MCl_2\{E(N^tBu)_2\}]$ (**10.15,** M = Pd, Pt; E = S, Se)[52,53] and $[Cp_2Ti\{S(NSiMe_3)_2\}]$[54] (**10.16**) (Chart 10.8). However, $\sigma(N)$-coordination is observed in the $GaCl_3$ adduct of $Me_3SiN{=}S{=}NSiMe_3$ (**10.17**).[55] Selenium(IV) diimides may also act as bridging ligands in the dinuclear coinage metal complexes $[M_2\{\mu\text{-}N,N'\text{-}Se(NR)_2\}_2]^{2+}$ (**10.18**, M = Cu, Ag; R = ^{t}Bu, Ad), which exhibit close M···M contacts.[56]

The dimeric structure of tellurium(IV) diimides enables these versatile ligands to act in a chelating or bridging bonding mode. For example, *N,N′*-chelated complexes are formed with $HgCl_2$[57] or $CoCl_2$[58] and a structurally analogous $HgCl_2$ complex is observed for dimeric selenium(IV)

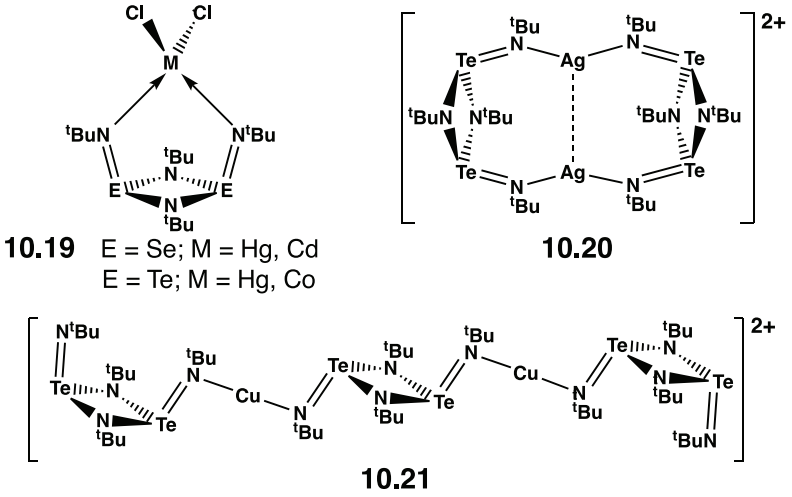

Chart 10.9. Metal complexes of chalcogen(IV) diimide dimers.

diimides (**10.19**, Chart 10.9).[40] With Ag^+, however, two metal ions bridge two tellurium diimide ligands in the *cis,exo,exo* conformation to give a non-linear (*ca.* 163°) N–Ag–N arrangement indicative of a metallophilic attraction (**10.20**). The versatility of tellurium(IV) diimide dimers as ligands is illustrated in the reaction with copper(I) trifluoromethanesulfonate, which brings about a *cis*→*trans* isomerisation of the ligand to give a complex in which two Cu^+ ions form linear bridges between three tellurium diimide ligands and the central ligand is in the *trans* conformation (**10.21**).[59]

10.4.5 *Redox behaviour*

In early work sulfur(IV) diimides were shown to undergo one-electron reduction either chemically by alkali metals[60] or electrochemically[61] to form short-lived radical anions $[S(NR)_2]^{\bullet-}$, which exhibit five-line (1:2:3:2:1) EPR spectra consistent with coupling of the unpaired electron with two equivalent nitrogen centers.[60] A mechanism involving the centrosymmetric association and rearrangement of two sulfur diimide radical anions has been proposed to account for the scrambling process that occurs when a small amount of an alkali metal is added to a mixture of

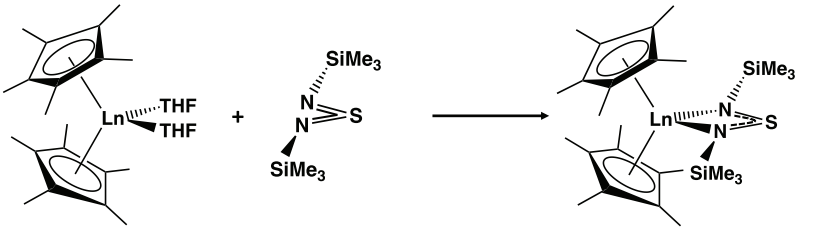

10.22 Ln = Sm, Eu, Yb

Scheme 10.10. Synthesis of lanthanide complexes of a sulfur diimide radical anion.

two symmetrical sulfur diimides.[62] Very recently, the half-life of the radical anion $[Me_3SiN{=}S{=}NSiMe_3]^{\bullet-}$ generated electrolytically in CH_2Cl_2 at 233 K was found to be 9.6 seconds.[63]

The redox reaction of $Me_3SiN{=}S{=}NSiMe_3$ with lanthanide(II) complexes $[LnCp^*_2(THF)_2]$ produced the adducts $[LnCp^*_2(Me_3SiN{=}S{=}NSiMe_3)]$ (**10.22**, Ln = Sm, Eu,Yb) (Scheme 10.10), the first structurally characterised complexes of sulfur(IV) diimide radical anions.[63] The S–N bond lengths in the *N,N′*-chelated complexes **10.22** are elongated by *ca.* 0.10 Å compared with the free ligand, consistent with occupation of the π^* SOMO of the radical anion. In addition, magnetic measurements indicate the presence of Ln^{3+} cations in these complexes, indicating a one-electron redox process.

10.4.6 *Synthetic applications*

Bis(trimethylsilyl)sulfur(IV) diimide $Me_3SiN{=}S{=}NSiMe_3$ is a widely used reagent for the synthesis of both inorganic and organic sulfur-nitrogen compounds containing an –N=S=N– unit. This versatility stems from the facile elimination of Me_3SiX (X = halide) in reactions of this reagent with halogenated substrates or the formation of anions by treatment with bases such as KO^tBu. Some selected examples are shown in Scheme 10.11.

The allylic amination of olefins or 1,3-dienes by the selenium(IV) diimide TsN=Se=NTs (Ts = *p*-toluenesulfonyl), which was prepared from $SeCl_4$ and two equivalents of *p*-toluenesulfonamide in CH_2Cl_2, was reported 45 years ago.[71a,b] A more reactive aminating agent is formed

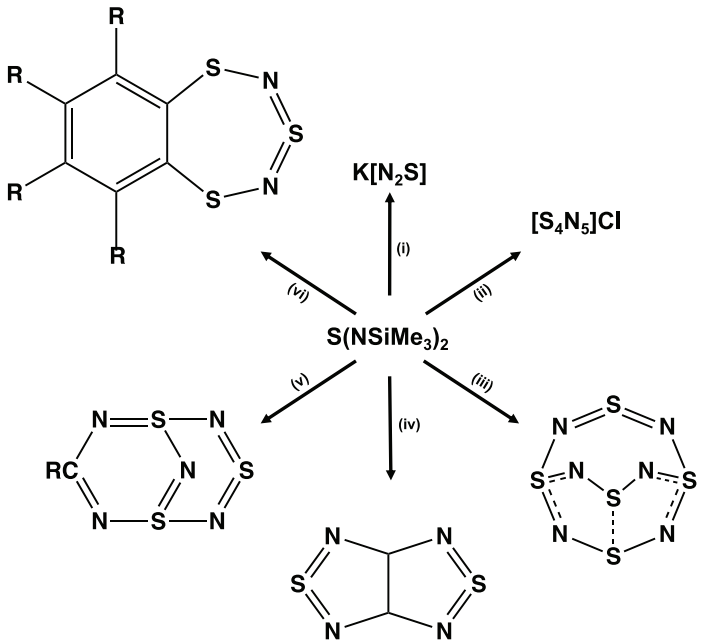

Scheme 10.11. Preparation of sulfur-nitrogen compounds from $Me_3SiNSNSiMe_3$: (i) KO^tBu[64] (ii) $(NSCl)_3$[65] (iii) 1,5-$S_4N_4Cl_2$[66] (iv) 3,4-difluoro-1-thia-2,5-diazole[67] (v) (RCN)$(NSCl)_2$[68,69] and (vi) 1,2-$C_6R_4(SCl)_2$.[70]

when anhydrous chloramine-T (TsNClNa) is stirred with elemental selenium in CH_2Cl_2[71a,b] and, subsequently, the more soluble NsNClNa (Ns = 2-nitrobenzenesulfonyl) was used to prepare NsN=Se=NNs.[71c] Although the identity of this selenium-containing aminating reagent has not been established, it is commonly referred to as TsN=Se=NTs.[72] This reagent has been used to convert triisopropylsilyl enol ethers to α-*N*-tosylamino derivatives[73] and, more recently, in the multi-step synthesis of the natural products daphnezomines A and B.[74]

10.5 Diimidosulfinates, $[RS(NR')_2]^-$

Monoanionic diimidosulfinates $[RS(NR')_2]^-$ are bidentate, heteroallyl ligands (**10.23**) (Chart 10.10), *cf.* amidinates, $RC(NR')_2]^-$, or diiminophosphinates, $[R_2P(NR')_2]^-$. Early work on this class of anionic

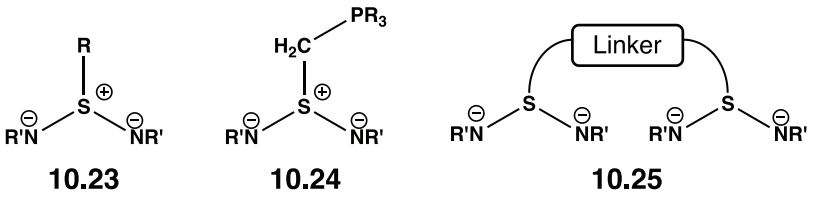

Chart 10.10. Diimidosulfinates (**10.23**), Janus head diimidosulfinates (**10.24**) and linker-bridged bis(diimidosulfinates) (**10.25**).

sulfur-nitrogen compounds has been discussed in reviews.[3,72] Lithium derivatives have been known for more than 50 years;[75a] they are generated by addition of RLi reagents to one of the S=N bonds of a sulfur(IV) diimide (Eq. 10.8) and this reaction has been used to prepare heteroaryl derivatives.[75b,c] The methyl derivative $[CH_3S(N^tBu)_2]^-$ can be deprotonated by MeLi to produce the dianion $[CH_2S(N^tBu)_2]^{2-}$ (methylenediimidosulfite) formally isoelectronic with $[SO_3]^{2-}$ (Eq. 10.9).[76] The bonding in $[CH_2S(N^tBu)_2]^{2-}$ is discussed in Sec. 4.6.

$$RLi + R'N{=}S{=}NR' \rightarrow Li[RS(NR')_2] \qquad (10.8)$$

$$Li[CH_3S(N^tBu)_2] + MeLi \rightarrow Li_2[CH_2S(N^tBu)_2] + CH_4 \qquad (10.9)$$

The approach represented by Eq. 10.8 has also been used to prepare diimidosulfinates with phosphorus- or nitrogen-containing side-arms that expand the coordinative ability of these multidentate ligands.[77,78] Such diimidosulfinates, *e.g.*, $[R_2PCH_2S(NR')_2]^-$ (**10.24**) are described as Janus head ligands since the *P* and *N,N′* coordination sites point in opposite directions.[79] The side-arm in these ligands can be extended by oxidation of the phosphorus(III) centres with oxygen, sulfur or selenium.[79] Dilithium reagents such as $[LiCH_2N(Me)CH_2N(Me)CH_2Li]$,[81] 9,10-dilithioanthracene[82a] or 4,4′-dilthiumbiphenyl[82b] have been used to generate linker-bridged bis(diimidosulfinates) (**10.25**) by reactions with two equivalents of $^tBuN{=}S{=}N^tBu$.

Heavier alkali-metal derivatives are prepared by treatment of sulfinimidamides R′NS(R)N′(H)R with MH (M = Na, K) or the metal (M = Cs, Rb).[83] In a similar approach alkaline earth-metal complexes are obtained

by deprotonation of $PhS(NSiMe_3)N(H)SiMe_3$ with $[M\{N(SiMe_3)_2\}]$ (M = Ca, Sr, Ba).[84] The versatile coordination ability of the diimidosulfinate ligand is illustrated by the variety of structures that have been established for alkali-metal derivatives, which include step-shaped ladders, eight-membered rings and ion-solvated complexes.[72] Structure-determining factors include the size and electronic properties of the R groups as well as the size or solvation of the alkali-metal cation in $M[RS(NR')_2]$. Grignard reagents RMgX[85] and Me_2Zn[86] also undergo addition to the S=N bond of sulfur(IV) diimides. Magnesium derivatives of the type $[Mg(thf)_2X\{(NR')_2SR\}]$ (X = Cl, Br) are either monomeric or dimeric depending on the steric requirements of the R group,[85] while the zinc complex $[MeZn\{(\mu\text{-}NSiMe_3)_2SMe\}]_2$ is a boat-shaped dimer (**10.26**) (Chart 10.11).[86] *N,N'*-chelated complexes of diimidosulfinates, **10.27** and **10.28** (Chart 10.11), are obtained by salt elimination reactions of lithium reagents $Li[RS(NR')_2]$ with the appropriate Group 4 or 14 metal halides.[86,87] The structures of the lithium derivative of a Janus head ligand

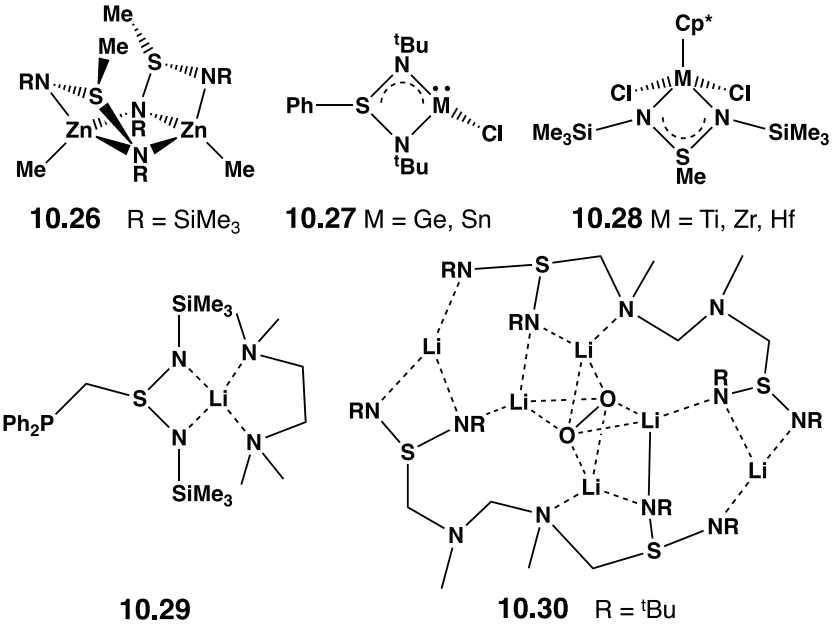

Chart 10.11. Metal complexes of diimidosulfinates.

(**10.29**) and a complex in which Li_2O_2 is entrapped by a linker-bridged bis(diimidosulfinate) (**10.30**) are also shown in Chart 10.11.[88]

10.6 Triimidochalcogenites, $[E(NR)_3]^{2-}$ (E = S, Se, Te)

Dianions of the type $[E(N^tBu)_3]^{2-}$, isoelectronic with chalcogenite ions EO_3^{2-} (E = S,[89] Se,[90] Te[91]), are easily made by the nucleophilic addition of $LiNH^tBu$ to the chalcogen diimide followed by deprotonation with a second equivalent of $LiNH^tBu$ (Eq. 10.10). In these one-pot reactions the lithium reagent behaves both as a nucleophile and as a base.

$$4LiNH^tBu + 2E(N^tBu)_2 \rightarrow [Li_2\{E(N^tBu)_3\}]_2 + 2H_2N^tBu \quad (10.10)$$
(E = S, Se, Te)

The dilithium triimidochalcogenites $[Li_2\{E(N^tBu)_3\}]_2$ (E = S, Se, Te) form dimeric structures in which two pyramidal $[E(N^tBu)_3]^{2-}$ dianions are bridged by four lithium cations to form distorted, hexagonal prisms (**10.31a–c**) (Chart 10.12). Lithium halides disrupt the dimeric structures of the sulfur and selenium derivatives to give distorted cubes in which a molecule of the lithium halide is entrapped by a $Li_2[E(N^tBu)_3]$ monomer (**10.32a**, **b**) (Chart 10.12). A fascinating feature of the dimeric clusters $[Li_2\{E(N^tBu)_3\}]_2$ is the formation of intensely coloured [deep blue (E = S) or green (E = Se)] solutions upon contact with air. The EPR spectra of these solutions are consistent with one-electron oxidation accompanied by removal of one Li^+ ion from the cluster to give neutral radicals in which the dianion $[E(N^tBu)_3]^{2-}$ and the radical monoanion $[E(N^tBu)_3]^{\bullet-}$ are bridged by three Li^+ (**10.33a**, **b**) (Chart 10.12).[92–94]

Although redox processes are sometimes observed in metathetical reactions of the dianions $[E(NtBu)_3]^{2-}$ (E = S, Se) with metal halides,[3,95] the behaviour of the pyramidal triimidotellurite dianion $[Te(NtBu)_3]^{2-}$ in these reactions differs substantially from that of the lighter chalcogens, as illustrated by the examples in Scheme 10.12.[96] For example, metathesis with $PhBCl_2$ gives the monomeric tellurium imide **10.34** stabilised by an *N,N′*-chelated boraamidinato ligand $[PhB(N^tBu)_2]^{2-}$.[91] By contrast, reaction with $InCl_3$ produces the dimeric cluster **10.35**, which incorporates

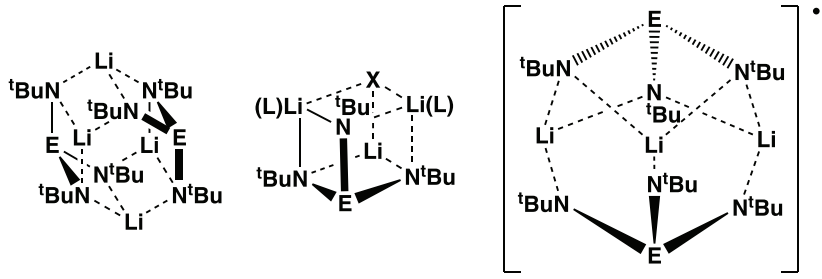

10.31a E = S
10.31b E = Se
10.31c E = Te

10.32a E = S
10.32b E = Se

10.33a E = S
10.33b E = Se

Chart 10.12. Structures of $[Li_2\{E(N^tBu)_3\}]_2$, $[Li_3X\{E(NtBu)_3\}]$ and $[Li_3\{E(NR)_3\}_3]^{\bullet}$.

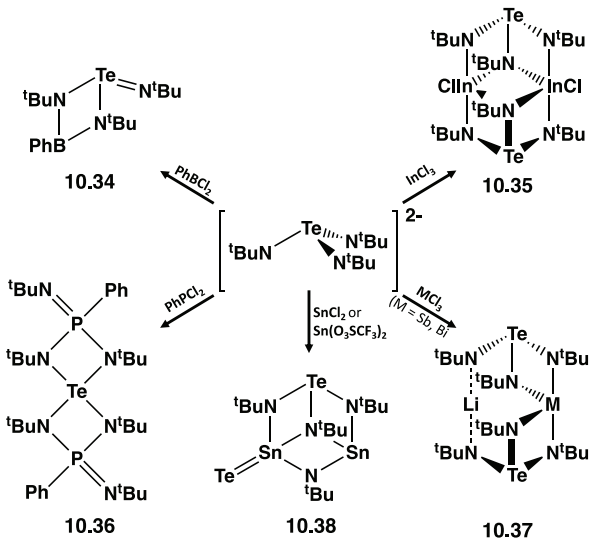

Scheme 10.12. Reactions of the $[Te(N^tBu)_3]^{2-}$ dianion with *p*-block element halides.

two tridentate $[Te(N^tBu)_3]^{2-}$ ligands bridged by two five-coordinate InCl units in an arm-chair structure.[97] Redox behaviour is also observed in the reaction of $[Te(N^tBu)_3]^{2-}$ with $PhPCl_2$ with the formation of elemental tellurium and the neutral spirocyclic complex **10.36** in which the

tellurium(IV) centre is chelated by two $[PhP(N^tBu)_3]^{2-}$ ligands.[91] By contrast, metathesis with heavier group 15 trichlorides produces the spirocyclic monoanions **10.37** in which two $[Te(N^tBu)_3]^{2-}$ dianions are chelated to the Sb or Bi centre, and charge balance is achieved by the presence of a Li^+ counter-ion.[98] An especially intriguing outcome of such redox processes is the formation of the stannatellone **10.38** from reactions with Sn(II) salts.[99]

10.7 Sulfur Triimides, $S(NR)_3$, and Triimidosulfonates, $[RS(NR')_3]^-$

The first sulfur(VI) triimide $S(NSiMe_3)_3$ was prepared by the reaction of NSF_3 with $LiN(SiMe_3)_2$.[101] The oxidation of the trisimidosulfite $[Li_2\{S(N^tBu)_3\}]_2$ with halogens is a convenient route to $S(N^tBu)_3$.[92] The derivatives $S(NR)_3$ (**10.39**, R = $SiMe_3$, ^{t}Bu) (Chart 10.13) have trigonal planar structures, *cf.* SO_3, with short S–N bond lengths in the range 1.50–1.52 Å and an NSN bond angle of 120°.[102,103] The SN vibrations in the Raman spectrum of $S(N^tBu)_3$ occur at much lower wave numbers (640–920 cm^{-1}) than expected for a covalent S=N bond, indicating that the bonding is predominantly electrostatic (S^+–N^-).[103] This conclusion is supported by electron density measurements (Sec. 4.6 and Fig. 4.4).[104]

Although the reactions of RLi reagents (R = ^{n}Bu, ^{t}Bu) with $S(N^tBu)_3$ failed to generate the triimidosulfonates of the type $[RS(NR')_3]^-$ (**10.40**, Chart 10.13),[105] this approach was successful for heteroaryl derivatives (R = EC_4H_3, E = MeN, S, Se).[106] The lithium triimidosulfonate $Li[Ph_2PCH_2S(N^tBu)_3]$ with a pendent PPh_2 group has been prepared from the sulfur(VI) triimide $S(N^tBu)_3$ and $[Li(tmeda)(CH_2PPh_2)]$.[107a] Metathetical reactions of this reagent with both main group and transition-metal dihalides MX_2 produce homoleptic complexes $[M\{Ph_2PCH_2S(N^tBu)_3\}_2]$ (M = Mn, Ni, Zn)[107a] or the monosubstituted derivatives $[MX\{Ph_2PCH_2S(N^tBu)_3\}]$ (M = Ge, X = Cl; M = Sn, X = Br).[107b] In all these complexes the

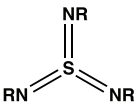

10.39 R = ^{t}Bu, $SiMe_3$

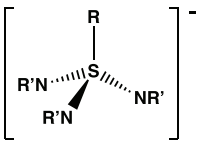

10.40

Chart 10.13. Structures of $S(NR)_3$ and $[RS(NR')_3]^-$.

$[Ph_2PCH_2S(N^tBu)_3]^-$ ligand participates in *N,N′*-chelation with no coordination of the phosphorus side-arm to the metal centre. Paramagnetic, trigonal complexes $[M\{N(SiMe_3)_2\}\{Ph_2PCH_2(N^tBu)_3\}]$ (M = Fe, Co) have also been structurally characterised.[107c]

The methylenetriimidosulfate dianion $[CH_2S(N^tBu)_3]^{2-}$, isoelectronic with $[S(N^tBu)_4]^{2-}$ (Sec. 10.8), is prepared by deprotonation of $[CH_3S(N^tBu)_3]^-$ with methyllithium in the presence of TMEDA (Eq. 10.11).[108]

$$[(thf)_2Li_2\{(N^tBu)_3SMe\}_2] + MeLi \rightarrow [(tmeda)_2Li_2\{H_2CS(N^tBu)_3\}] + CH_4 \quad (10.11)$$

10.8 Tetraimidosulfates, $[S(N^tBu)_4]^{2-}$, and Tetraimidosulfuric Acid, $H_2[S(N^tBu)_4]$

The tetraimidosulfate dianion $[S(NtBu)_4]^{2-}$, isoelectronic with SO_4^{2-}, is prepared by a methodology similar to that employed for the synthesis of triimidosulfites (Eq. 10.8). The reaction of the sulfur triimide $S(N^tBu)_3$ with two equivalents of $LiNH^tBu$ produces the monomeric complex $[Li_2(thf)_4S(N^tBu)_4]$ (**10.41**) (Eq. 10.12) in which solvation of both Li^+ ions by two THF molecules prevents further aggregation (Chart 10.14).[109] The four S–N bond lengths in the $S(N^tBu)_4$ unit are equal at *ca.* 1.60 Å. More recently, lithium complexes of asymmetric hydrogen tetraimidosulfate anions $[(N^tBu)_2(NH^tBu)S(NAr)]^-$ (Ar = 2,6-diisopropylphenyl, 2,5-dimethylphenyl) were prepared by reactions of $S(N^tBu)_3$ with an equimolar mixture of ^nBuLi and $ArNH_2$.[110]

$$S(N^tBu)_3 + 2LiNH^tBu \rightarrow [(thf)_4Li_2\{S(N^tBu)_4\}] + H_2N^tBu \quad (10.12)$$

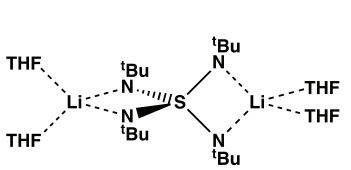

10.41 R = ^{t}Bu, $SiMe_3$

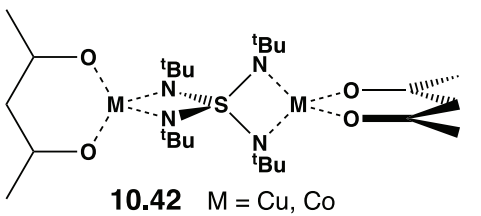

10.42 M = Cu, Co

Chart 10.14. Bimetallic lithium, copper and cobalt complexes of $[S(N^tBu)_4]^{2-}$.

Although a barium(II) complex of $[S(N^tBu)_4]^{2-}$ was prepared and structurally characterised in early work,[103] transition-metal complexes of this dianionic ligand were not reported until 2014 when Cu(I), Cd(I) and Zn(II) derivatives were obtained *via* metathetical reactions of $[(thf)_4Li_2S(N^tBu)_4]$ with metal halides.[111a] The $[S(N^tBu)_4]^{2-}$ dianion behaves as a tetradentate, bridging ligand in all known metal complexes, *e.g.*, $[(acac)M(\mu\text{-}N^tBu)_2S(\mu\text{-}N^tBu)_2M(acac)]$ (M = Cu, Co; **10.42**)[112] (Chart 10.14). The bimetallic cobalt complex exhibits antiferromagnetic coupling between the two Co^{2+} cations.[111b] The bimetallic dysprosium complex $[\{(thf)_2Li(\mu\text{-}N^tBu)_2S(\mu\text{-}N^tBu)_2DyCl_2\}_2{\cdot}ClLi(thf)_2]$ behaves as a single-molecule magnet in the absence of a DC field, while the monometallic lanthanide complexes $[(thf)_2Li(\mu\text{-}N^tBu)_2S(\mu\text{-}N^tBu)_2LnCl_2(thf)_2]$ (Ln = Dy, Tb) show slow magnetic relaxation under applied DC fields.[111c]

The diprotonation of $[S(N^tBu)_4]^{2-}$ with $[^tBuNH_3]Cl$ in THF at room temperature produces the thermally unstable tetraimidosulfuric acid $H_2[S(N^tBu)_4]$ as colourless crystals (Eq. 10.13).[112]

$$[(thf)_4Li_2\{S(NtBu)_4\}] + 2[^tBuNH_3]Cl \rightarrow H_2[S(N^tBu)_4] + 2H_2N^tBu + 2LiCl \qquad (10.13)$$

The X-ray analysis of $H_2[S(N^tBu)_4]$ reveals a distorted tetrahedral structure with S–N (imido) and S–N(H) (amido) bond lengths of 1.527 and 1.648 Å, respectively; the N–S–N and (H)N–S–N(H) bond angles are 127.8° and 100.8° (Fig. 10.2).[112] An electron density determination

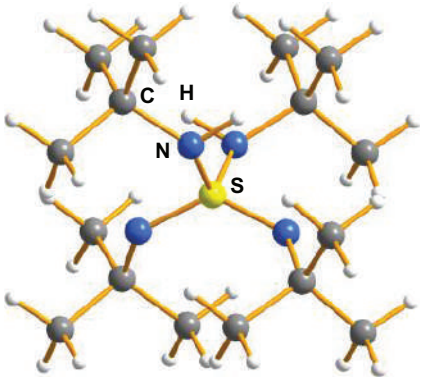

Figure 10.2. Crystal structure of $H_2[S(N^tBu)_4]$.[112]

established that the S–N(imido) and S–N(H)(amido) bonds are all strongly polarised single bonds, *cf.* $S(N^tBu)_3$ (Sec. 4.6);[104] the polarisation is greater for the S–N(imido) bonds.[112]

10.9 Chalcogen Diamides, $E_x(NR_2)_2$ (E = S, Se, Te; x = 1–4)

10.9.1 *Synthesis*

Sulfur diamides (diaminosulfanes), $S_x(NR_2)_2$ (x = 1–4; R = alkyl), are generally obtained by the reaction of sulfur chlorides with an aliphatic secondary amine. Two routes have been used to prepare disulfanes of the type $S_2(NR_2)_2$ or $S_2(HNAr)_2$: (a) treatment of a secondary alkylamine with NaOH in aqueous CH_2Cl_2 followed by addition of S_2Cl_2 (R = Et; NR_2 = morpholinyl, piperidinyl) or (b) reaction of a primary arylamine with S_2Cl_2 in anhydrous diethyl ether in the presence of pyridine.[113] The insecticidal activity of these sulfur-nitrogen compounds has been investigated.[113]

The monoselanes $Se(NR_2)_2$ (R = Me, Et) have also been prepared.[114] Polyselanes $Se_x(NR_2)_2$ (x = 2–4, NR_2 = morpholinyl; x = 4, NR_2 = piperidinyl) are formed in the reaction of elemental selenium with the boiling amine in the presence of Pb_3O_4.[115] The acyclic tellurium(II) diamide $Te(NMe_2)_2$ is obtained by treatment of $TeCl_4$ with $LiNMe_2$.[116a] The homoleptic tellurium(II) triazenide $[\{N(N^{Dipp})_2\}_2Te]$ has been prepared by deprotonation of the triazene with $[Te\{N(SiMe_3)_2\}_2]$ (*vide infra*).[116b]

In early work the reactions of $LiN(SiMe_3)_2$ with SCl_2, Se_2Cl_2 or $TeCl_4$ in hexane or diethyl ether were shown to produce the silylated amino derivatives $E[(N(SiMe_3)_2]_2$ (E = S, Se. Te) (Sec. 2.3, Eqs. 2.3–2.5).[117,118] Subsequently, the corresponding polysulfanes and polyselanes $E_x[N(SiMe_3)_2]_2$ (E = S, Se; x = 2–4) were obtained as inseparable mixtures from reactions of $LiN(SiMe_3)_2$ with SCl_2 and elemental sulfur or Se_2Cl_2 and elemental selenium.[119] More recently, the polysulfanes $S_x[N(SiMe_3)_2]_2$ (x = 3–5) were prepared by the rapid reaction of $NaN(SiMe_3)_2$ with *cyclo*-S_8 in THF at 25°C. The three components were separated by chromatography and identified by high resolution mass spectroscopy (HRMS) (Sec. 3.8.1, Fig. 3.16).[120] The major product is the tetrasulfane $S_4[N(SiMe_3)_2]_2$ (Eq. 10.14). The pure trisulfane $S_3[N(SiMe_3)_2]_2$ is obtained as an orange-yellow oil in low yield from the reaction of $HN(SiMe_3)_2$ with S_2Cl_2 (Eq. 10.15).[119] The reaction of hexamethyldisilazane $HN(SiMe_3)_2$ with

elemental sulfur in toluene at 135°C produces the polymer $[SN(SiMe_3)]_n$, which was identified by HRMS (Sec. 3.8.1).[121]

$$S_8 + NaN(SiMe_3)_2 \rightarrow (Me_3Si)_2N–S–S–S–S–N(SiMe_3)_2 \quad (10.14)$$

$$S_2Cl_2 + HN(SiMe_3)_2 \rightarrow (Me_3Si)_2N–S–S–S–N(SiMe_3)_2 \quad (10.15)$$

Treatment of $LiN(SiMe_3)_2$ with a mixture of SCl_2 and fluorenone in toluene produces the sulfur(II) diimide $C_{12}H_8$=N–S–N=$C_{12}H_8$.[122] The related derivative Ph_2C=N–S–N=C_2Ph was prepared earlier from $LiN=CPh_2$ and S_2Cl_2.[123]

10.9.2 *Structures*

The series $E[N(SiMe_3)_2]_2$ (E = S, Se, Te)[117,118] display E–N bond lengths of 1.72, 1.87 and 2.05 Å, respectively, indicative of chalcogen-nitrogen single bonds. The <NEN bond angles of 109.6°, 108.0° and 105.8°, respectively, reflect the increasing *s* character of the lone pair on the chalcogen. In contrast to the monomeric structure of $Te[N(SiMe_3)_2]_2$, the dimethylamino derivative $[Te(NMe_2)_2]_\infty$ has a polymeric structure with intermolecular Te···N contacts of 2.96 Å that give rise to trapezoidal Te_2N_2 rings.[116a] The bidentate triazenide ligands in $[\{N(N^{Dipp})_2\}_2Te]$ are *N*,*N*′-coordinated asymmetrically to the Te(II) centre with *d*(Te–N) = 2.17, 2.40 Å and 2.16, 2.62 Å.[116b] The X-ray structures of the polyselanes $Se_x(NR_2)_2$ (x = 2–4, NR_2 = morpholino; x = 4, NR_2 = piperidino) exhibit typical single Se–N bond lengths in the range 1.82–1.85 Å.[115]

The mean S–N bond lengths in $C_{12}H_8$=N–S–N=$C_{12}H_8$ and Ph_2C=N–S–N=CPh_2 of 1.656(2) and 1.675(2) Å, respectively,[122,123] are consistent with a sulfur(II) centre in these diimides, *cf.* *d*(SN) = 1.53–1.54 Å in sulfur(IV) diimides RN=S=NR (R= ^{t}Bu, $SiMe_3$) (Sec. 10.4.2).

Although metal complexes of polysulfanes $S_x[N(SiMe_3)_2]$ (x = 3–5) are unknown, the yttrium complex $[Y\{(Me_3SiN)_2(\eta^2\text{-}S_3N(SiMe_3)\}]$ has been isolated in low yield and structurally characterised. This unusual complex features the unique $[(Me_3Si)_2NSSS]^-$ ligand bonded to the metal centre in an η^2-fashion.[124]

10.9.3 *Reactions*

Silylated amino derivatives $E[(N(SiMe_3)_2]_2$ (E = S, Se) are useful reagents for the synthesis of other chalcogen-nitrogen compounds. For example,

reaction of $S[(N(SiMe_3)_2]_2$ with an equimolar mixture of SCl_2 and SO_2Cl_2 is a convenient synthesis of S_4N_4 (Sec. 5.5.1 and Eq. 5.1).[125]

The polysulfanes $S_x[N(SiMe_3)_2]_2$ (x = 3–5) have been used to prepare both inorganic and organic sulfur-nitrogen compounds, *e.g.*, reaction of the trisulfide $S_3[(N(SiMe_3)_2]_2$ with a mixture of S_2Cl_2 and SO_2Cl_2 produces S_4N_2 in 72% yield (Sec. 5.3.3).[119] Polysulfanes have also been employed to introduce bridging polysulfide units in the synthesis of natural products. Thus, a mixture of $S_3[(N(SiMe_3)_2]_2$ and $NaN(SiMe_3)_2$ in THF provides a source of –S–S– or –S–S–S–S– bridges in biologically active diketopiperazines.[120,126] The combination of $KN(SiMe_3)_2$ and elemental sulfur in THF has been used as an *in situ* source of polysulfanes to generate an –S–S–S–S– link between two β-diketimines.[127]

The polar Te–N bond in tellurium(II) amides is readily susceptible to protolysis by weakly acidic reagents. For example, the reaction of $[Te(NMe_2)_2]_\infty$ with two equivalents of Ph_3CSH produces the monomeric tellurium (II) thiolate $Te(SCPh_3)_2$.[116a] Alkynyl tellurides may be prepared by the reaction of terminal acetylenes with arenetellurenamides (Eq. 10.16).[128] Dialkynyl tellurides $(RC{\equiv}C)_2Te$ are obtained in moderate yield by the one-pot reaction of $TeCl_4$ with $LiN(SiMe_3)_2$, followed by the addition of a terminal acetylene.

$$C_6H_5TeN^iPr_2 + RC{\equiv}CH \rightarrow RC{\equiv}CTeC_6H_5 + HN^iPr_2 \qquad (10.16)$$

The unique radical cation $[Te\{N(SiMe_3)_2\}_2]^{\bullet+}$ is formed as the $[AsF_6]^-$ salt by oxidation of $Te[N(SiMe_3)_2]_2$ with AsF_5. This deep blue salt is monomeric in the solid state with d(Te–N) = 1.97 Å, *cf.* 2.10 Å for a Te–N single bond. The broad singlet in the EPR spectrum indicates that the unpaired electron is located primarily on the tellurium atom.[129]

10.10 Organochalcogen Azides and Nitrenes

Organosulfenyl azides RSN_3 cannot be isolated, but they are of interest as precursors to the corresponding sulfenyl nitrenes RSN. For example, the trifluoromethyl derivative CF_3SN_3, prepared from CF_3SCl and trimethylsilyl azide, acts as a source of monomeric CF_3SN which may be trapped by hexachlorocyclopentadiene to give $C_5Cl_6{=}NSCF_3$.[130] The thermal instability of sulfenyl azides has been exploited in the synthesis of

benzo-1,3-dithia-2-azolium chloride from the reaction of 1,2-arenedisulfenyl dichloride with trimethylsilyl azide (Sec. 2.5.2 and Scheme 2.8).

Benzenesulfinyl azide $PhS(O)N_3$ was obtained from the reaction of benzenesulfinyl chloride with sodium azide in acetonitrile below 35°C more than 50 years ago.[131] This thermally unstable orange-brown solid decomposes to produce the six-membered ring $[NS(O)Ph]_3$, *cf.* [NS(O)Cl] (Sec. 8.9) *via* the purported intermediate phenylsulfinyl nitrene PhS(O)N.[131] Very recently, sulfinyl hydroxylamines RONSO have been shown to be excellent sources of sulfinyl nitrenes that can be used for the synthesis of sulfoximes and sulfinimidamides *via* reactions with carbon or nitrogen nucleophiles (Sec. 10.2.2).[10] This reactivity stems from the highly electrophilic character of sulfinyl nitrenes as evident from the zwitterionic resonance form **B** in Scheme 6.2.

Arylsulfonyl azides $ArS(O)_2N_3$ are prepared by reaction of sodium azide with the corresponding sulfonyl chorides or, in some cases, by addition of trimethylsilyl azide to a sulfonyl fluoride.[132a] They are widely used as *in situ* reagents in organic synthesis, *e.g.*, for diazo transfer or azidation reactions.[132b] The preparation and structure of trifluoromethylsulfonyl azide $CF_3SO_2N_3$ are described in Sec. 6.2.1 (Fig. 6.1). This reagent has been employed for the preparation of organic azides from primary amines, but FSO_2N_3 is a safer and more versatile choice for conducting this transformation (Sec. 6.2.2). Flash vacuum pyrolysis of $CF_3SO_2N_3$ is an important source of short-lived S,N,O radicals, which are characterised as matrix-isolated species (Sec. 6.3).

Covalent arylselenium(II) azides $RSeN_3$ are obtained from reactions of the corresponding chlorides ArSeCl with trimethylsilyl azide, but they decompose above 0°C to form diselanes ArSeSeAr. However, the presence of intramolecular coordination, *e.g.*, $2\text{-}Me_2NC_6H_4SeN_3$, or a very bulky aryl substituent stabilises arylselenium(II) and aryltellurium(II) azides so that solid-state structures may be determined, as discussed in Sec. 15.2 (Fig. 15.2).[133,134]

Organoselenium(IV) azides with two or three azido groups attached to tellurium, $R_2Se(N_3)_2$ (R = alkyl, Ph, $2,4,6\text{-}Me_3C_6H_2$) and $RSe(N_3)_3$ [R = alkyl, $2,4,6\text{-}R_3C_6H_2$ (R = Me, ^{t}Bu)], are obtained by reactions of the corresponding organoselenium(IV) fluorides and Me_3SiN_3 in CH_2Cl_2, but these organoselenium(IV) azides can only be handled at low

temperatures.[135] By contrast, the analogous organotellurium(IV) azides, $R_2Te(N_3)_2$ (R = alkyl, Ph, C_6F_5) and $RTe(N_3)_3$ (R = alkyl, 2,4,6-$Me_3C_6H_2$), which are prepared in a similar manner (Eq. 10.17), have sufficient thermal stability to allow structural characterisation in the solid state.[136] Organotellurium(IV) azides form polymeric networks *via* weak Te···N interactions in the range 2.8–3.3 Å resulting in seven- or eight-coordination at the tellurium atom.[136]

$$RTeF_3 + 3Me_3SiN_3 \rightarrow RTe(N_3)_3 + 3Me_3SiF \qquad (10.17)$$

10.11 Trisulfenamides, $(RS)_3N$, and the Radical $[(PhS)_2N]^{\bullet}$

Tribenzenesulfenamide $(PhS)_3N$ is obtained as a pale yellow solid by the treatment of the sodium salt of dibenzenesulfenamide, generated *in situ*, with acetic anhydride.[137] The perfluorinated analogue $(C_6F_5S)_3N$ is prepared by the reaction of $(C_6F_5S)_2NH$ and C_6F_5SCl in diethyl ether.[138]

The solid-state structures of $(PhS)_3N$[139] and $(C_6F_5S)_3N$[138] and the gas-phase structure of $(CF_3S)_3N$[140] all show nearly planar S_3N units, implying the involvement of the nitrogen lone pair in π-bonding. On the other hand, the S–N bond lengths of *ca.* 1.80 Å are longer than typical single-bond values. Tribenzenesulfenamide decomposes at *ca.* 80°C to give PhSSPh and N_2 *via* the intermediate formation of the purple, nitrogen-centred radical $[(PhS)_2N]^{\bullet}$ (**3.13**). This radical is also generated by the oxidation of $(PhS)_2NH$ with lead dioxide.[137] The characteristic three-line (1:2:1) EPR spectra of the *N*-centred radicals $[(RS)_2N]^{\bullet}$ (R = Ph, CF_3) are discussed in Sec. 3.4.1.

10.12 Sulfimide, $Ph_2S{=}NH$, and Monohalogenated Isomers, $Ph_2S{=}NX$ (X = Cl, Br) and $Ph_2FS{\equiv}N$

The prototypical sulfimide $Ph_2S{=}NH$ acts as a versatile ligand in forming complexes with a variety of transition metals. Unusual bonding arrangements or hydrogen bonding to counter-anions may be observed, especially in copper complexes.[141,142] For example, *trans*-$[CuCl_2(Ph_2SNH)_2]$ crystallises in either square-planar or *pseudo*-tetrahedral arrangements,

although neither form shows significant intermolecular interactions.[141] More dramatically, salts with the composition $[Cu(Ph_2S{=}NH)_4][Cu(Ph_2S{=}NH)_5][X]_4$ (X = BF_4, NO_3) are rare examples of a homoleptic complex containing both four- and five-coordinate metal centres in the unit cell.[142]

The monohalogenated derivatives of $Ph_2S{=}NH$ exist as structural isomers reminiscent of the two structural arrangements established for the trihalogenated compounds $F_3S{\equiv}N$ and $F_2S{=}NX$ (X = Cl, F) (Chart 8.3). The monochloro and monobromo derivatives are prepared by reactions of $Ph_2S{=}NH$ with *N*-bromo- or *N*-chloro-succinimide in an inert solvent; they exist as *N*-halosulfimides $Ph_2S{=}NX$ (**10.43**, X = Cl, Br) (Chart 10.15) with a sulfur(IV) centre.[143] The monofluoro derivative is obtained by the treatment of Ph_2SNBr with tetrabutylammonium fluoride.[144] It has been identified as the thiazyne $Ph_2FS{\equiv}N$ (**10.44**, X = F) with a sulfur(VI) centre on the basis of spectroscopic data and reactions with sodium alkoxides to give *S*-alkoxythiazynes $Ph_2(OR)S{\equiv}N$ (**10.44**, X = OR) (Chart 10.15), which have been structurally characterised, *e.g.*, d(S≡N) = 1.441 Å in $Ph_2(OPr)S{\equiv}N$.[145] Similarly, the reaction of $Ph_2FS{\equiv}N$ with PhLi produces $Ph_3S{\equiv}N$ as described in Sec. 8.3.1 (Eq. 8.8).

S,S-Diphenyl *S*-fluorothiazyne serves as a building block for the generation of sulfur(VI)-nitrogen chains. Thus, reaction of two equivalents of $Ph_2FS{\equiv}N$ with $Ph_2S{=}NH$ in the presence of a base produces high yields of $N{\equiv}S(Ph)_2{-}N{=}S(Ph)_2{=}N{-}(Ph)_2S{\equiv}N$ (Eq. 10.18), a unique example of a sulfur-nitrogen chain with two terminal $S^{VI}{\equiv}N$ functionalities, *d*(S≡N) = 1.457(2) Å.[146]

$$Ph_2S{=}NH + 2Ph_2FS{\equiv}N \rightarrow N{\equiv}S(Ph)_2{-}N{=}S(Ph)_2{=}N{-}(Ph)_2S{\equiv}N \quad (10.18)$$

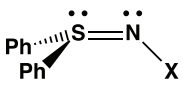

10.43 X = Cl, Br

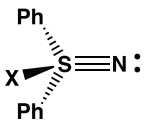

10.44 X = F, OR

Chart 10.15. *N*-halosulfimides (**10.43**) and *S*-fluoro- or *S*-alkoxy-thiazynes (**10.44**).

The reaction of Ph_2SNBr with elemental selenium in dichloromethane on a small scale produces a high yield of pure Se_4N_4 (Sec. 5.5.1).[147] The combination of equimolar amounts of Ph_2SNBr and Ph_2Se gives the mixed chalcogen cation $[Ph_2S{=}N{=}SePh_2]^+$ as a bromide salt.[148] The all-selenium analogue $[Ph_2Se{=}N{=}SePh_2]^+$ has been isolated as a tetraphenylborate salt and structurally characterised, *d*(Se–N) = 1.802(2) and 1.814(2) Å, *cf.* 1.87 Å for a Se–N single bond, and the bond angle <SeNSe is 109.63(8)°.[149]

References

1. R. S. Laitinen and T. Chivers, in *Frontiers of Selenium and Tellurium Chemistry: From Small Molecules to Biomolecules and Materials*, Eds. J. D. Woollins and R. S. Laitinen, Springer (2011), Ch. 8, pp. 179–199.
2. T. Chivers and R. S. Laitinen, in *Selenium and Tellurium Reagents — In Chemistry and Materials Science*, Eds. R. S. Laitinen and R. Oilunkaniemi, de Gruyter (2019), Ch. 4, pp. 123–150; *Phys. Sci. Rev.*, **4**(5), 20170125 (2019).
3. D. Stalke, *Chem. Commun*., **48**, 9559–9573 (2012).
4. R. Labbow, D. Michalik, F. Reiss, A. Schulz and A. Villinger, *Angew. Chem. Int. Ed*., **55**, 7680 (2016).
5. (a) T. Q. Davies, A. Hall and M. C. Willis, *Angew. Chem. Int. Ed*., **56**, 14937 (2017); (b) Z.-X. Zhang, T. Q. Davies and M. C. Willis, *J. Am. Chem. Soc*., **141**, 13022 (2019).
6. E. Parkes and J. D. Woollins, *Inorg. Synth.*, **25**, 48 (1989).
7. S. Mann and M. Jansen, *Z. Anorg. Allg. Chem*., **621**, 153 (1995).
8. W. Heilemann and R. Mews, *Chem. Ber*., **121**, 461 (1988).
9. (a) D. A. Armitage and A. W. Sinden, *Inorg. Chem*., **11**, 1151 (1972); (b) A. Haas, J. Kasprowski, K. Angermund, P. Betz, C. Kruger, Y.-H. Tsay and S. Werner, *Chem. Ber*., **124**, 1895 (1991).
10. (a) T. Q. Davies and M. C. Willis, *Chem. Eur. J*., **27**, 8918 (2021); (b) T. Q. Davies, M. J. Tilby, J. Ren, N. A. Parker, D. Skolc, A. Hall, F. Duarte and M. C. Willis, *J. Am. Chem. Soc*., **142**, 15445 (2020); (c) T. Q. Davies, M. J. Tilby, D. Skolc, A. Hall and M. C. Willis, *Org. Lett.*, **22**, 9495 (2020).
11. K. O. Christe, M. Gerken, R. Haiges, S. Schneider, T. Schroer, F. S. Tham and A. Vij, *Solid State Sci*., **4**, 1529 (2002).

12. (a) T. Maaninen, R. Laitinen and T. Chivers, *Chem. Commun*., 1812 (2002); (b) T. Maaninen, R. Laitinen, T. Chivers, G. Schatte and M. Nissinen, *Inorg. Chem*., **39**, 5341 (2000); (c) T. Chivers, G. Schatte, H. Tuononen, R. Suontamo, R. Laitinen and J. Valkonen, *Inorg. Chem*., **44**, 443 (2005).
13. (a) P. K. Chinthakindi, T. Naicker, N. Thota, T. Govender, H. G. Kruger and P. I. Arvidsson, *Angew. Chem. Int. Ed*., **56**, 4100 (2017); (b) V. Bizet, C. M. M. Hendriks and C. Bolm, *Chem. Soc. Rev*., **44**, 3378 (2015); (c) V. Bizet, R. Kowalczyk and C. Bolm, *Chem. Soc. Rev*., **43**, 2424 (2014).
14. M. Wei, D. Liang, X. Cao, W. Luo, G. Ma, Z. Lui and L. Li, *Angew. Chem. Int. Ed*., **60**, 7397 (2021).
15. (a) K. A. Rufanov, J. Kipke and J. Sundermeyer, *Dalton Trans*., **40**, 1990 (2011); (b) A. V. Rumyantsev, A. V. Pichugov, N. S. Bushkov, D. Yu. Aleshin, T. V. Strelkova, O. L. Lependina, P. A. Zhizhko and D. N. Zarubin, *Chem. Commun*., **57**, 2625 (2021).
16. A. F. Hill, *Adv. Organomet. Chem*., **36**, 159 (1994).
17. X. Xu, G. Kehr, C. G. Daniliuc and G. Erker, *J. Am. Chem. Soc*., **136**, 12431 (2014).
18. L. Longobardi, V. Wolter and D. W. Stephan, *Angew. Chem. Int. Ed*., **54**, 809 (2015).
19. P. Holtkamp, T. Glodde, D. Poier, B. Neumann, H.-G. Stammler and N. W. Mitzel, *Angew. Chem. Int. Ed*., **59**, 17388 (2020).
20. D. H. R. Barton and M. J. Robson, *J. Chem. Soc.*, *Perkin Trans.*, **1**, 1245 (1974).
21. K. Goto and T. Kawashima, *J. Synth. Org. Chem. Japan*, **63**, 1157 (2005).
22. Y. Inagaki, R. Okazaki and N. Inamoto, *Bull. Chem. Soc. Jpn*., **52**, 1998 (1979); (b) Y. Inagaki, R. Okazaki and N. Inamoto, *Bull. Chem. Soc. Jpn*., **52**, 2002 (1979).
23. Y. Inagaki, T. Hosogai, R. Okazaki and N. Inamoto, *Bull. Chem. Soc. Jpn*., **53**, 205 (1980).
24. K. Goto, G. Yamamoto, B. Tan and R. Okazaki, *Tetrahedron Lett*., **42**, 4875 (2011).
25. T. Chivers, A. W. Cordes, R. T. Oakley and P. N. Swepston, *Inorg. Chem*., **20**, 2376 (1981).
26. W. Goehring and G. Weis, *Angew. Chem*., **68**, 687 (1956).
27. K. B. Sharpless, T. Hori, L. K. Truesdale and C. O. Dietrich, *J. Am. Chem. Soc*., **98**, 269 (1976).
28. T. Maaninen, T. Chivers, R. Laitinen, G. Schatte and M. Nissinen, *Inorg. Chem*., **39**, 5341 (2000).

29. T. Chivers, N. Sandblom and G. Schatte, *Inorg. Synth*., **34**, 42 (2004).
30. T. Chivers, X. Gao and M. Parvez, *J. Am. Chem. Soc*., **117**, 2359 (1995).
31. T. Chivers, X. Gao and M. Parvez, *J. Chem. Soc*., *Chem. Commun*., 2149 (1994).
32. C. P. Warrens and J. D. Woollins, *Inorg. Synth*., **25**, 43 (1989).
33. F. Fockenberg and A. Haas, *Z. Naturforsch*., **41B**, 413 (1986).
34. T. Maaninen, H. M. Tuononen, K. Kosunen, R. Oilunkaniemi, J. Hiitola, R. Laitinen and T. Chivers, *Z. Anorg. Allg. Chem*., **630**, 1947 (2004).
35. S. L. Hinchley, P. Trickey, H. E. Robertson, B. A. Smart, D. W. H. Rankin, D. Leusser, B. Walfort, D, Stalke, M. Buhl and S. J. Obrey, *J. Chem. Soc*., *Dalton Trans*., 4607 (2002).
36. D. G. Anderson, H. E. Robertson, D. W. H. Rankin and J. D. Woollins, *J. Chem. Soc*., *Dalton Trans*., 859 (1989).
37. H. M. Tuononen, R. J. Suontamo, J. U. Valkonen, R. S. Laitinen and T. Chivers, *Inorg. Chem*., **42**, 2447 (2003).
38. (a) I. Yu. Bagryanskaya, Y. Gatilov, M. M. Shakirov and A. V. Zibarev, *Mendeleev Commun*., 136 (1994); (b) I. Yu. Bagryanskaya, Y. Gatilov, M. M. Shakirov and A. V. Zibarev, *Mendeleev Commun*., 167 (1994).
39. B. Wrackmeyer, B. Distler, S. Gerstmann and M. Herberhold, *Z. Naturforsch*., **48B**, 1307 (1993).
40. A. J. Karhu, J. M. Rautiainen, R. Oilunkaniemi, T. Chivers and R. S. Laitinen, *Inorg. Chem*., **54**, 9499 (2015).
41. K. Tersago, M. Mandano, C. Van Alsenoy, I. Yu. Bagryanskaya, M. K. Kovalev, A. Yu. Makarov, Y. V. Gatilov, M. M. A. V. Zibarev and F. Blockhuys, *Chem. Eur. J*., **11**, 4544 (2005).
42. K. M. Bal, J. Cautereels and F. Blockhuys, *J. Mol. Struct*., **1132**, 102 (2017).
43. K. Tersago, I. Yu. Bagryanskaya, Y. V. Gatilov, S. A. Gromilov, A. Yu. Makarov, M. Mandano, C. Van Alsenoy, A. V. Zibarev and F. Blockhuys, *Eur. J. Inorg. Chem*., **2007**, 1958 (2007).
44. A. G. Makarov, I. Yu. Bagryanskaya, Y. V. Gatilov, N. V. Kuratieva, A. Yu. Makarov, M. M. Shakirov, A. V. Alexeyev, K. Tersago, C. Van Alsenoy, F. Blockhuys and A. V. Zibarev, *Eur. J. Inorg. Chem*., **2010**, 4801 (2010).
45. R. Jones, *Acta Crystallogr*., **C71**, 456 (2015).
46. I. Yu. Bagryanskaya, Y. V. Gatilov, M. M. Shakirov and A. V. Zibarev, *Mendeleev Commun*., **12**, 167 (2002).
47. N. Sandblom, T. Ziegler and T. Chivers, *Inorg. Chem*., **37**, 354 (1998).
48. T. Maaninen, H. M. Tuononen, G. Schatte, R. Suontamo, J. Valkonen, R. Laitinen and T. Chivers, *Inorg. Chem*., **43**, 2097 (2004).

49. T. Chivers and R. S. Laitinen, in *Handbook of Chalcogen Chemistry: New Perspectives in Sulfur, Selenium and Tellurium*, Ed. F. Devillanova, Royal Society of Chemistry, 2nd Edition (2013), Ch. 4, pp. 191–237.
50. H. W. Roesky, H.-G. Schmidt, M. Noltemeyer and G. M. Sheldrick, *Chem. Ber*., **116**, 1411 (1983).
51. J. Gindl, M. Björgvinsson, H. W. Roesky, C. Freire-Erdbrügger and G. M. Sheldrick, *J. Chem. Soc.*, *Dalton Trans*., 811 (1993).
52. M. Risto, A. Eironen, E. Männistö, R. Oilunkaniemi, R. S. Laitinen and T. Chivers, *Dalton Trans*., 8473 (2009).
53. A. J. Karhu, M. Risto, J. M. Rautiainen, R. Oilunkaniemi, R. S. Laitinen and T. Chivers, *Can. J. Chem*., **94**, 342 (2016).
54. K. Kaleta, M. Ruhmann, O. Theilmann, S. Roy, T. Breweriea, P. Arndt, A. Villinger, E. D. Jemmis, A. Schulz and U. Rosenthal, *Eur. J. Inorg. Chem*., **2012**, 611 (2012).
55. C. Hubrich, A. Schulz and A. Villinger, *Z. Anorg. Allg. Chem*., **633**, 2362 (2007).
56. M. Risto, T. T. Takaluoma, T. Bajorek, R. Oilunkaniemi, R. S. Laitinen and T. Chivers, *Inorg. Chem*., **48**, 6271 (2009).
57. T. Chivers and G. Schatte, *Can. J. Chem*., **81**, 1307 (2003).
58. M. Risto, J. Konu, R. Oilunkaniemi, R. S. Laitinen and T. Chivers, *Polyhedron*, **29**, 871 (2010).
59. T. Chivers, M. Parvez and G. Schatte, *Angew. Chem. Int. Ed. Engl*., **38**, 2217 (1999).
60. J. A. Hunter, B. King, W. E. Lindsell and M. A. Neish, *J. Chem. Soc.*, *Dalton Trans*., 880 (1980).
61. G. Brands and A. Golloch, *Z. Naturforsch*., **37B**, 1137 (1982).
62. K. Bestari, R. T. Oakley and A. W. Cordes, *Can. J. Chem*., **69**, 94 (1991).
63. S. V. Klementyeva, N. P. Gritsan, M. M. Khusniyarov, A. Witt, A. A. Dmitriev, E. A. Suturina, N. D. D. Hill, T. L. Roemmele, M. T. Gamer, R. T. Boeré, P. W. Roesky, A. V. Zibarev and S. N. Konchenko, *Chem. Eur. J*., **23**, 1278 (2017).
64. M. Herberhold and W. Ehrenreich, *Angew. Chem. Int. Ed. Engl*., **21**, 633 (1982).
65. T. Chivers, L. Fieklding, W. G. Laidlaw and M. Trsic, *Inorg. Chem*., **18**, 3379 (1979).
66. W. S. Sheldrick, M. N. S. Rao and H. W. Roesky, *Inorg. Chem*., **19**, 538 (1980).

67. A. Yu. Makarov, I. G. Irtegova, N. V. Vasolieva, I. Yu. Bagryanskaya, T. Borrmann, Yu. V. Gatilov, E. Lork, R. Mews, W.-D. Stohrer and A, V. Zibarev, *Inorg. Chem*., **44**, 7194 (2005).
68. T. Chivers, J. F. Richardson and N. R. M. Smith, *Inorg. Chem*., **25**, 272 (1980).
69. C. Knapp, E. Lork, T. Borrman, W.-D. Stohrer and R. Mews, *Eur. J. Inorg. Chem*., **2003**, 3211 (2003).
70. A. W. Cordes, M. Hojo, H. Koenig, M. C. Noble, R. T. Oakley and W. T. Pennington, *Inorg. Chem*., **25**, 1137 (1986).
71. (a) K. B. Sharpless, T. Hori, L. K. Truesdale and C. O. Dietrich, *J. Am. Chem. Soc*., **98**, 269 (1976); (b) K. B. Sharpless and S. P. Singer, *J. Org. Chem*., **41**, 2504 (1976); (c) M. Bruncko, T. A. V. Khong and K. B. Sharpless, *Angew. Chem. Int. Ed. Engl*., **35**, 454 (1996).
72. R. Fleischer and D. Stalke, *Coord. Chem. Rev*., **176**, 431 (1998).
73. P. Magnus, J. Lacour, I. Coldham, B. Mugrage and W. B. Bauta, *Tetrahedron*, **51**, 11087 (1995).
74. G. Xu, J. Wu, L. Li, Y. Lu and C. Li, *J. Am. Chem. Soc*., **142**, 15240 (2020).
75. (a) O. J. Scherer and R. Schmitt, *J. Organomet. Chem*., **16**, P11 (1969); (b) C. Selinka, S. Deurlein, T. Hauser and D. Stalke, *Inorg. Chim. Acta*, **357**, 1873 (2004): (c) J. T. E. Meyer, T. Schulz, S. K. Pandey and D. Stalke, *Inorg. Chem*., **49**, 2743 (2010).
76. (a) B. Walfort, R. Bertermann and D. Stalke, *Chem. Eur. J*., **7**, 1424 (2001); (b) S. Deurlein, D. Leusswer, U. Fierler, H. Ott and D. Stalke, *Organometallics*, **27**, 2306 (2008).
77. M. M. Meinholz, S. K. Pandey, S. M. Deurlein and D. Stalke, *Dalton Trans*., **40**, 1662 (2011).
78. M. M. Meinholz, M. Klemmer, E. Kriemen and D. Stalke, *Chem. Eur. J*., **17**, 9415 (2011).
79. M. M. Meinholz and D. Stalke, *Eur. J. Inorg. Chem*., **2011**, 4578 (2011).
80. M. M. Meinholz and D. Stalke, *Z. Anorg. Allg. Chem*., **637**, 2233 (2011).
81. M. M. Meinholz, E. Carl, E. Kriemen and D. Stalke, *Chem. Commun*., **47**, 10948 (2011).
82. (a) T. Schulz and D. Stalke, *Z. Naturforsch*., **65B**, 701 (2010); (b) T. Schulz, D.-R. Dauer and D. Stalke, *Z. Naturforsch*., **65B**, 711 (2010).
83. F. Pauer and D. Stalke, *J. Organomet. Chem*., **418**, 127 (1991).
84. R. Fleischer and D. Stalke, *J. Organomet. Chem*., **550**, 173 (1998).
85. T. Schulz, S. Deuerlein and D. Stalke, *Eur. J. Inorg. Chem*., 2178 (2010).

86. M. Bayram, D. Bläser, C. Wölper and S. Schulz, *Organometallics*, **34**, 3421 (2015).
87. N. Nakata, N. Hosoda, S. Takahashi and A. Ishii, *Dalton Trans*., **47**, 481 (2018).
88. M. M. Meinholz, E. Carl, E. Krieman and D. Stalke, *Chem. Commun*., **47**, 10948 (2011).
89. R. Fleischer, S. Freitag, F. Pauer and D. Stalke, *Angew. Chem. Int. Ed. Engl*., **35**, 205 (1996).
90. T. Chivers, M. Parvez and G. Schatte, *Inorg. Chem*., **35**, 4094 (1996).
91. T. Chivers, X. Gao and M. Parvez, *Angew. Chem. Int. Ed. Engl*., **34**, 2549 (1995).
92. R. Fleischer, S. Freitag and D. Stalke, *J. Chem. Soc.*, *Dalton Trans*., 193 (1998).
93. T. Chivers, M. Parvez and G. Schatte, *Inorg. Chem*., **40**, 540 (2001).
94. J. K. Brask, T. Chivers, B. McGarvey, G. Schatte, R. Sung and R. T. Boeré, *Inorg. Chem*., **37**, 4633 (1998).
95. J. K. Brask and T. Chivers, *Angew. Chem. Int. Ed. Engl*., **40**, 3988 (2001).
96. T. Chivers, *Can. J. Chem*., **79**, 1841 (2001).
97. T. Chivers and G. Schatte, *Eur. J. Inorg. Chem*., **2002**, 2266 (2002).
98. T. Chivers, M. Parvez, G. Schatte and G. P. A. Yap, *Inorg. Chem*., **38**, 1380 (1999).
99. T. Chivers and G. Schatte, *Chem. Commun*., 2264 (2001).
100. O. Glemser and J. Wegener, *Angew. Chem. Int. Ed. Engl*., **9**, 309 (1970).
101. O. Glemser, S. Pohl, F.-M. Tesky and R. Mews, *Angew. Chem. Int. Ed. Engl*., **16**, 789 (1977).
102. S. Pohl, B. Krebs, U. Seyer and G. Henkel, *Chem. Ber*., **112**, 1751 (1979).
103. R. Fleischer, B. Walfort, A. Gbureck, P. Scholz, W. Kiefer and D. Stalke, *Chem. Eur. J*., **4**, 2266 (1998).
104. (a) D. Leusser, J. Henn, J. N. Kocher, B. Engels and D. Stalke, *J. Am. Chem. Soc*., **126**, 1781 (2004); (b) D. Stalke, *Chem. Eur. J*., **17**, 9264 (2011).
105. C. Selinka and D. Stalke, *Eur. J. Inorg. Chem*., **2003**, 3376 (2003).
106. B. Walfort, A. P. Leedham, C. A. Russell and D. Stalke, *Inorg. Chem*., **40**, 5668 (2001).
107. (a) E. Carl and D. Stalke, *Chem. Eur. J*., **20**, 15849 (2014); (b) E. Carl and D. Stalke, *Eur. J. Inorg. Chem*., **2015**, 2052 (2015); (c) J. Jung, C. M. Legendre, S. Demeshko, R. Herbst-Irmer and D. Stalke, *Inorg. Chem*., **60**, 9580 (2021).
108. B. Walfort and D. Stalke, *Angew. Chem. Int. Ed. Engl*., **40**, 3846 (2001).
109. R. Fleischer, A. Rothenberger and D. Stalke, *Angew. Chem. Int. Ed. Engl*., **36**, 1105 (1997).

110. J. Matussek, R. Herbst-Irmer and D. Stalke, *Eur. J. Inorg. Chem*., **2015**, 166 (2015).
111. (a) J. Matussek, R. Herbst-Irmer, I. Objartel and D. Stalke, *Dalton Trans*., **43**, 15944 (2014); (b) J. Jung, C. M. Legendre, R. Herbst-Irmer and D. Stalke, *Inorg. Chem*., **60**, 967 (2021); (c) J. Jung, F. Benner, R. Herbst-Irmer, S. Demir and D. Stalke, *Chem. Eur. J.*, **27**, 12310 (2021).
112. J. Jung, A. Münch, R. Herbst-Irmer and D. Stalke, *Angew. Chem. Int Ed*., **60**, 5679 (2021).
113. R. Sun, Y. Zhang, L. Chen, Y. Li, H. Song, R. Huang, F. Bi and Q. Wang, *J. Agric. Food Chem.*, **57**, 3661 (2009).
114. R. Paetzold and E. Rönsch, *Z. Anorg. Allg. Chem*., **338**, 22 (1965).
115. (a) O. Foss and V. Janickis, *J. Chem. Soc*., *Dalton Trans*., 620 (1980); (b) O. Foss and V. Janickis, *J. Chem. Soc*., *Dalton Trans*., 628 (1980)
116. (a) E. Allan, H. Gornitzka, J. Kracher, M. A. Paver, M.-A. Rennie, C. A. Russell, P. R. Raithby, D. Stalke, A. Steiner and D. S. Wright, *J. Chem. Soc.*, *Dalton Trans*., 1727 (1996); (b) K. R. Flanagan, J. D. Parish, M. A. Fox and A. L. Johnson, *Inorg. Chem*., **58**, 16660 (2019).
117. G. Schubert, G. Kiel and G. Gattow, *Z. Anorg. Allg. Chem*., **574**, 129 (1989).
118. M. Björgvinsson, H. W. Roesky, F. Pauer, D. Stalke and G. M. Sheldrick, *Inorg. Chem*., **29**, 5140 (1990).
119. J. Siivari, A. Maaninen, E. Haapiniemi, R. S. Laitinen and T. Chivers, *Z. Naturforsch*., **50B**, 1575 (1995).
120. (a) K. C. Nicoloau, M. Lu, S. Totokotsopoulos, P. Heretsch, D. Giguère, Y.-P. Sun, D. Sarlah, T. H. Nguyen, I. C. Wolf, D. F. Smee, C. W. Day, S. Bopp and E. A. Winzeler, *J. Am. Chem. Soc*., **134**, 17320 (2012); (b) K. C. Nicoloau, S. Totokotsopoulos, D. Giguère and Y.-P. Sun, *Angew. Chem. Int. Ed. Engl*., **51**, 728 (2012).
121. B. G. Kumar and K. Muraludharan, *J. Mater. Chem*., **21**, 11271 (2014).
122. R. L. Melen, D. J. Eisler, R. A. Hewitt and J. M. Rawson, *Dalton Trans*., **42**, 3888 (2013).
123. M.-T. Averbuch-Pouchot, A. Durif, A. J. Banister, J. A. Durrant and J. Halfpenny, *J. Chem. Soc.*, *Dalton Trans*., 221 (1982).
124. J. F. Corbey, M. Fang, J. W. Ziller and W. J. Evans, *Inorg. Chem*., **54**, 801 (2015).
125. A. Maaninen, J. Siivari, R. S. Laitinen and T. Chivers, *Inorg. Synth*., **33**, 196 (2002).
126. K. C. Nicoloau, S. Totokotsopoulos, D. Giguère, Y.-P. Sun and D. Sarlah, *J. Am. Chem. Soc*., **133**, 8150 (2011).

127. M. Desat and R. Kretschmer, *Dalton. Trans*, **48**, 17718 (2019).
128. T. Murai, K. Nonomura, K. Kimura and S. Kato, *Organometallics*, **10**, 1095 (1991).
129. M. Björgvinsson, T. Heinze, H. W. Roesky, F. Pauer, D. Stalke and G. M. Sheldrick, *Angew. Chem. Int. Ed. Engl*., **30**, 1677 (1991).
130. A. Haas and T. Mischo, *Can. J. Chem*., **67**, 1902 (1989).
131. T. J. Maricich, *J. Am. Chem. Soc*., **90**, 7179 (1968).
132. (a) A. S. Barrow and J. E. Moses, *Synlett*, **27**, 1840 (2016); (b) S. Chen, Y. Yao, W. Yang, Q. Lin, L. Wang, H. Li, D. Chen, Y. Tan and D. Yang, *J. Org. Chem*., **84**, 11863 (2019).
133. (a) T. M. Klapötke, B. Krumm and K. Polborn, *J. Am. Chem. Soc*., **126**, 710 (2004); (b) T. M. Klapötke, B. Krumm, H. Nöth, J. C. Gálvez-Ruiz, K. Polborn. I. Schab and M. Suter, *Inorg. Chem*., **44**, 5354 (2005).
134. K. Srivastava, T. Chakraborty, H. B. Singh, U. P. Singh and R. J. Butcher, *Dalton Trans*., **39**, 10137 (2010).
135. T. M. Klapötke, B. Krumm and M. Scherr, *Inorg. Chem*., **47**, 4712 (2008).
136. (a) T. M. Klapötke, B. Krumm, P. Mayer, H. Piotrowski, O. P. Ruscitti and A. Schiller, *Inorg. Chem*., **41**, 1184 (2002); (b) T. M. Klapötke, B. Krumm, P. Mayer, H. Piotrowski, O. P. Ruscitti, *Inorg. Chem*., **39**, 5426 (2000).
137. D. H. R. Barton, I. A. Blair, P. D. Magnus and R. K. Norris, *J. Chem. Soc*., *Perkin Trans. I*, 1032 (1973).
138. A. Biehl, R. Boese, A. Haas, C. Klare and M. Peach, *Z. Anorg. Allg. Chem*., **622**, 1262 (1996).
139. J. R. Carruthers, K. Prout and D. J. Watkin, *Cryst. Struct. Comm*., **10**, 1217 (1981).
140. C. J. Marsden and L. S. Bartell, *J. Chem. Soc*., *Dalton Trans*., 1582 (1977).
141. (a) P. F. Kelly, A. M. Z. Slawin and K. W. Waring, *J. Chem. Soc.*, *Dalton Trans*., 2853 (1997); (b) P. F. Kelly, S.-M. Man, A. M. Z. Slawin and K. W. Waring, *Polyhedron*, **18**, 3173 (1999).
142. K. E. Holmes and P. F. Kelly, S. H. Dale and M. R. J. Elsegood, *CrystEngComm*, **8**, 391 (2006).
143. T. Yoshimura, N. Furukawa, T. Akasaka and S. Oae, *Tetrahedron*, **33**, 1061 (1977).
144. T. Yoshimura, H. Kita, K. Takeuchi, E. Takata, E. Hasegawa, C. Shimasaki and E. Tsukurimichi, *Chem. Lett*., **21**, 1433 (1992).
145. T. Yoshimura, M. Ohkubo, T. Fujii, H. Kita, Y. Wakai, S. Ono, H. Morita, C. Shimasaki and E. Horn, *Bull. Chem. Soc. Jpn*., **71**, 1629 (1998).
146. T. Fujii, M. Kanno, M. Hirata, T. Fujimoro and T. Yoshimura, *Inorg. Chem*., **44**, 8653 (2005).

147. W. Clegg, S. H. Dale, D. Drennan and P. F. Kelly, *Dalton Trans*., 3140 (2005).
148. S. M. Aucott, M. R. Bailey, M. R. J. Elsegood, L. M. Gilby, K. E. Holmes, P. F. Kelly, M. J. Papageorgiou and S. Pedrσn-Haba, *New J. Chem.*, **28**, 959 (2004).
149. M. R. J. Elsegood, P. F. Kelly, G. Reid and P. M. Staniland, *Dalton Trans*., 3798 (2008).

Chapter 11

Diamagnetic Five-membered Carbon-Nitrogen-Chalcogen Rings: From Fundamentals to Functional Devices

11.1 Introduction

An RC unit is isolobal with S^+ as a substituent in a sulfur-nitrogen system. Consequently, it is not surprising that a number of C,N,S ring systems are known that are isoelectronic with the cyclic binary S–N cations discussed in Chapter 5. The replacement of one or more S^+ substituents by RC groups confers greater stability on the ring system and provides a link between these inorganic heterocycles and benzenoid compounds. Activity in this area of chemistry was stimulated in the 1980s by the theoretical prediction that polymers of the type $(RCNSN)_x$ will have conducting properties similar to those of $(SN)_x$ (Sec. 4.7).[1,2] Subsequently, there have been extensive investigations of C,N,S heterocycles as potential precursors for such polymers and recent investigations have also included the heavier chalcogens.

Chapters 11 and 12 deal with diamagnetic C,N,E (E = S, Se, Te) heterocycles, beginning with five-membered rings in this chapter and continuing with six-membered and larger ring systems in the next chapter. The coverage is limited to ring systems in which the number of heteroatoms exceeds the number of carbon atoms. These diamagnetic ring

systems frequently form paramagnetic C,N,E species upon reduction and the chemistry of these and other neutral and anionic radicals is considered in Chapter 13. Metal complexes of paramagnetic C,N,E heterocycles are described in Chapter 14. The emphasis in these four chapters will be on important developments in the last 15 years together with a comparison of the synthesis, structures and properties of selenium and, especially, tellurium derivatives with those of sulfur analogues. Following the precedent established in the discussion of binary chalcogen-nitrogen species in Chapter 5, this chapter will consider neutral, cationic and anionic five-membered C,N,E rings in that order. The isoelectronic relationship between binary chalcogen-nitrogen species and their carbon-poor C,N,E analogues will be noted when warranted.

11.2 1-Chalcogena-2,5-diazoles and Benzo-2-chalcogena-1,3-diazoles

11.2.1 *Synthesis*

Recent reviews provide detailed discussions of the synthesis,[3] donor-acceptor behaviour,[4] formation of radical-anion salts,[5] usage as fluorescent imaging probes,[6] and luminescent properties of metal complexes of 1-chalcogena-2,5-diazoles[7] $(RC)_2N_2E$ (E = S, Se, Te) and their benzo-fused derivatives, *i.e.*, benzo-2-chalcogena-1,3-diazoles. Applications of benzo-2-chalcogena-1,3-diazoles are discussed in Sec. 11.2.5.

Cyclocondensation reactions of sulfur halides with 1,2-diamines represent the traditional route to 1-thia-2,5-diazoles. Recently, the treatment of vicinal dioximes with S_2Cl_2 and pyridine in acetonitrile has been established as a versatile route to these heterocyclic systems.[3,8] As an example of this approach, the synthesis of a fused diazole from 1,2-diamino-1,2-dioxime involves two simultaneous condensation reactions (Scheme 11.1a).[8a] The mixed chalcogen derivative is obtained by cyclocondensation of 3,4-diamino-1-thia-2,5-diazole with $SeCl_4$ in the presence of pyridine (Scheme 11.1b).[8b]

An alternative route to benzo-2-thia-1,3-diazoles, especially for fluorinated derivatives, employs treatment of *N*-aryl-*N*′-trimethylsilyl sulfur diiimides $ArNSNSiMe_3$ with cesium fluoride in acetonitrile

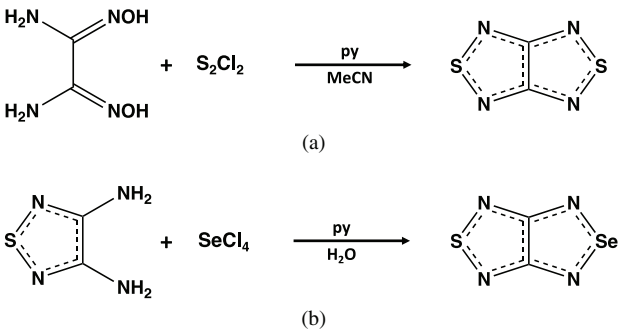

Scheme 11.1. Synthesis of fused chalcogenadiazoles: (a) the S/S system (b) the S/Se system.

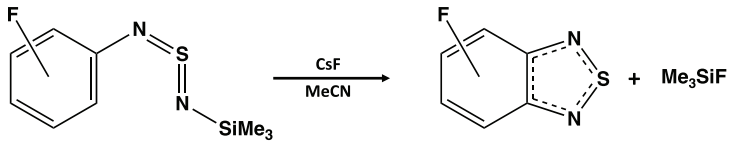

Scheme 11.2. Synthesis of benzo-2-thia-1,3-diazoles *via* nucleophilic ring closure.

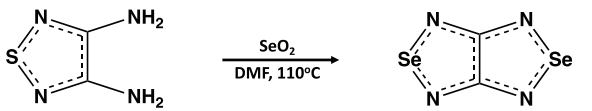

Scheme 11.3. Synthesis of a fused selenadiazole combining cyclocondensation and chalcogen-exchange.

(Scheme 11.2) to generate anions of the type $[ArNSN]^-$ followed by nucleophilic ring closure.[6,9]

1-Selena-2,5-diazoles can normally be obtained *via* cyclocondensation of diamines with $SeCl_4$, $SeOCl_2$ or, preferably, SeO_2.[3] However, the chalcogen-exchange process between a 1-thia-2,5-diazole and SeO_2 in DMF at *ca*. 100°C is an alternative, especially for fused systems. The example shown in Scheme 11.3 combines the cyclocondensation and chalcogen-exchange processes.[10] The cyclocondensation route is also successful for a variety of benzo-2-selena-1,3-diazoles.[3,11]

In early work 1-tellura-2,5-diazole was prepared *via* treatment of the selenium analogue with ethylmagnesium bromide followed by the

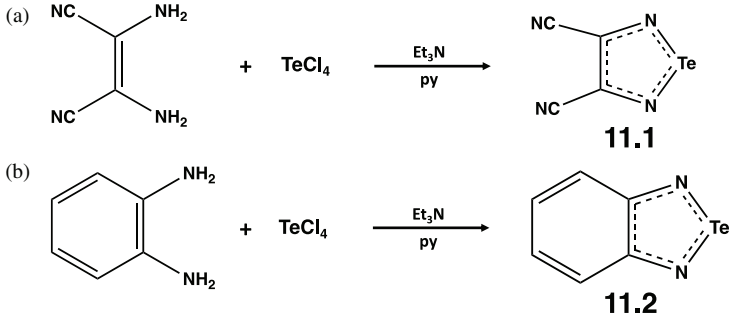

Scheme 11.4. Synthesis of (a) 3,4-dicyano-1-tellura-2,5-diazole and (b) benzo-2-tellura-1,3-diazole *via* cyclocondensation.

addition of tellurium tetrachloride.[12] Cyclocondensation provides a more general route to 1-tellura-2,5-diazoles. For example, reaction of diaminomaleonitile with $TeCl_4$ and an excess of Et_3N in pyridine produces high yields of 3,4-dicyano-1-tellura-3,5-diazole (**11.1** in Scheme 11.4a).[13,14] This telluradiazole has been used as a building block to generate tellurium-containing phthalocyanines (Sec. 11.2.5); a similar strategy was employed previously to prepare phthalocyanines with annulated 1-thia- or 1-selena-2,5-diazole rings.[15] Cyclocondensation of $TeCl_4$ with 1,2-diaminoarenes is also a versatile route to a variety of benzo-2-tellura-1,3-diazoles (**11.2** in Scheme 11.4b).[16,17]

11.2.2 *Structures*

1-Chalcogena-2,5-diazoles and benzo-2-chalcogena-1,3-diazoles can exhibit Lewis acid (acceptor) or Lewis base (donor) behaviour involving either the chalcogen or nitrogen centres, respectively. This ambiphilic character is evident in the structures of the complexes formed between these heterocycles and crown ethers; it may also give rise to secondary bonding (E···N) interactions that result in supramolecular structures as discussed in Secs.15.3.1 and 15.3.2.[18] Computational investigations reveal that this self-association involves a combination of donor-acceptor (covalent) and electrostatic contributions, as well as dispersion forces especially for the sulfur systems.[19] The polarity of the E–N bonds in the heterocycles increases and these bonds become weaker along the series

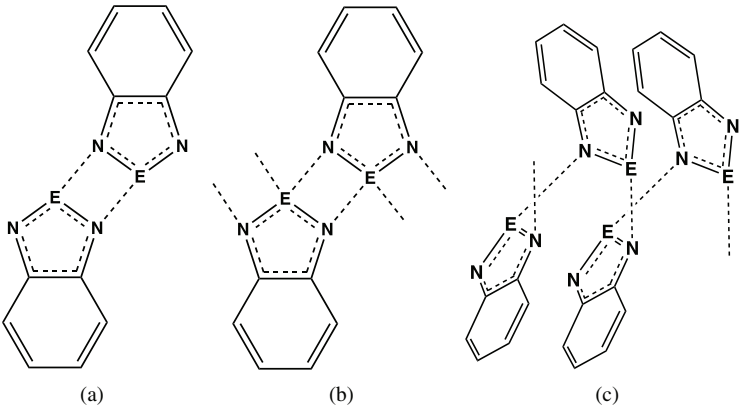

Chart 11.1. Modes of aggregation in benzo-2-chalcogena-1,3-diazoles (E = S, Se, Te): (a) dimer (b) polymer (c) catemer.

S–N, Se–N, Te–N resulting in an enhanced Lewis acidity of the chalcogen centre and, hence, a stronger tendency for self-association for the heavier chalcogens. Consequently, the solid-state structures frequently display intermolecular contacts leading to the formation of dimers or polymers involving a four-membered E_2N_2 unit (E = S, Se, Te), as illustrated for benzo-2-chalcogena-1,3-diazoles in Chart 11.1a and 11.1b, respectively. In some cases, *e.g.*, benzo-2-thia-1,3-diazole and benzo-2-selena-1,3-diazoles, a catemeric structure with single E···N contacts is observed (Chart 11.1c).[20] Enlarging the carbocyclic ring from benzo to phenanthro results in dimeric structures for both the sulfur and selenium systems. However, the S···N distance is only 8% less than the sum of the van der Waals radii for S and N in phenanthro-1-thia-1,5-diazole, whereas d(Se···N) = 2.91 and 2.97 Å for the selenium analogue, *cf.* 3.45 Å for Σr_{vdW}(Se + N).[20] Similarly, the solid-state structures of alkynylated benzo-2-selena-1,3-diazoles show head-to-head dimerisation *via* Se···N interactions in the range 2.87–2.95 Å.[21]

A recent X-ray structural determination of 5,6-dichloro-2,1,3-benzoselenadiazole supported by MP2 calculations revealed a dimeric structure in which the intermolecular selenium-nitrogen contacts [d(Se···N) = 2.829(3) Å] are supplemented by a nitrogen-nitrogen interaction of 2.840 Å, *cf.* 3.32 Å for the sum of van der Waals radii for two N atoms (Fig. 11.1).[22]

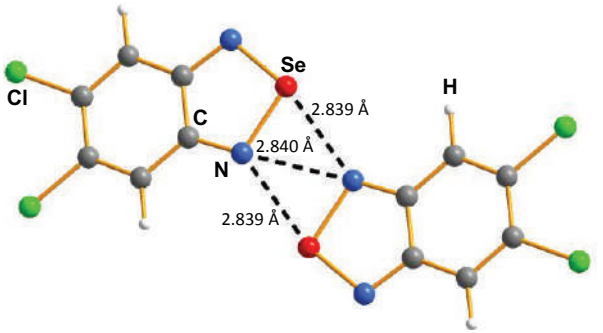

Figure 11.1. Molecular structure of 5,6-dichloro-2,1,3-benzoselenadiazole.[22]

The interaction energies in these associated structures are strongest for tellurium and have been estimated to be as high as 60 kJ mol^{-1} in telluradiazoles.[23] Consequently, the supramolecular structures of telluradiazoles are of especial interest in comparison with those of their sulfur and selenium analogues. The parent benzo-2-tellura-1,3-diazole forms an infinite ribbon structure (Chart 11.1b) with Te···N distances of 2.68–2.72 Å, *cf.* Σr_{vdW}(Te + N) = 3.61 Å.[16a] The stronger interactions in benzo-2-tellura-1,3-diazoles compared to the sulfur or selenium analogues are also evident from their mass spectra. Dimeric species of the type $[M_2H]^+$ were observed in the gas phase for benzo-2-tellura-1,3-diazoles (M), but evidence for associated species was not apparent in the mass spectra of the lighter chalcogen analogues (Sec. 3.8.3).[22] The presence of either bromine or *tert*-butyl substituents on the arene ring, however, restricts the $(Te\cdots N)_2$ association to discrete dimers (Chart 11.1a), as found in the structures of 4,7-dibromobenzo-2-tellura-1,3-diazole (**11.3**)[16a] and 4,6-bis(*tert*-butyl) benzo-2-tellura-1,3-diazole (**11.4**).[24] The Te···N distances in **11.3** and **11.4** are 2.70 and 2.63 Å, respectively.

The perfluorinated derivative 4,5,6,7-tetrafluorobenzo-2-tellura-1,3-diazole is especially intriguing. This tellurium-nitrogen heterocycle exhibits chromotropism in the form of red-orange and yellow crystalline phases, which differ in the nature of the Te···N interactions (Sec. 3.1.1).[25a] The yellow phase is metastable and undergoes an exothermic irreversible transformation to the red polymorph above 100°C. The structures of these two phases are illustrated in Fig. 3.1. The permethylated derivative 4,5,6,7-tetramethylbenzo-2-selena-1,3-diazole has also been obtained in

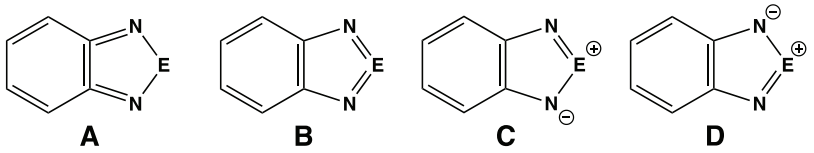

Chart 11.2. Resonance structures for benzo-2-chalcogena-1,3-diazoles (E = S, Se, Te).

two polymorphic forms upon recrystallisation from either ethanol or toluene, respectively.[25b] Further discussion of the supramolecular interactions in benzo-2-chalcogena-1,3-diazoles can be found in Sec. 15.3.2.

The structural parameters in the C_2N_2E ring of benzo-2-chalcogena-1,3-diazoles indicate the importance of the quinoidal resonance form **A** (Chart 11.2). The C=N and C–C distances in benzothiadiazoles are 1.34–1.35 and 1.43–1.44 Å,[26a] *cf.* single-bond values of 1.52 and 1.54 Å, respectively.[26b] Typical S–N, Se–N and Te–N bond lengths fall within the ranges 1.61–1.63, 1.78–1.81 and 2.00–2.05 Å, *cf.* single-bond values of 1.77, 1.91 and 2.10 Å,[26b] consistent with an increase in the contribution from **A** for the heavier chalcogens. Also, the lower electronegativity of Te compared to S and Se (Sec. 1.1) results in larger contributions from the ionic resonance forms **C** and **D** for E = Te.[26c]

11.2.3 *Lewis base (donor) properties*

The ambiphilic character of benzo-2-chalcogena-1,3-diazoles is evident from their behaviour as either Lewis acids (acceptors) or Lewis bases (donors) towards various substrates.[3] This character is dualistic in the sense that σ- and π-molecular orbitals are both involved in the acidic and basic behaviour.[18] A compelling illustration of this characteristic is the formation of 1:1 charge-transfer complexes in which the heterocycle behaves as an electron acceptor and an electron donor, *e.g.*, the red 1:1 complex formed by combination of 4-amino-benzo-2-thia-1,3-diazole and 4-nitro-benzo-2-thia-1,3-diazole, both of which are yellow.[27]

In this section Lewis acid adducts involving the nitrogen centres will be considered first. In early work benzo-2-thia-1,3-diazole (BTD) was shown to form *N*-bonded 1:1 or 1:2 adducts with main group or transition

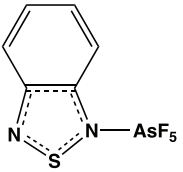

11.5

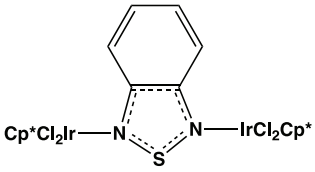

11.6

Chart 11.3. *N*-Bonded complexes of benzo-2-thia-1,3-diazole.

metal acceptors. In the 1:1 adduct with AsF_5, **11.5** (Chart 11.3) coordination of the Lewis acid to one of the nitrogen atoms introduces asymmetry in the heterocyclic ring, *d*(S–N) = 1.63 and 1.58 Å,[28a] *cf.* 1.620 Å in the free ligand.[28b] The quinonoid character of the arene ring of the BTD ligand is still apparent in the adduct. Reactions of BTD or BSD (benzo-2-selena-1,3-diazole) with metal carbonyls produces monodentate *N*-bonded adducts, *e.g.*, $[W(CO)_5(L)]$ (L = BTD or BSD); *N*-coordination is maintained upon one-electron reduction.[29] The reaction of 4-aryl-BTDs with palladium acetate followed by treatment with LiCl and pyridine produced *N*-bonded cyclopalladated products.[30] An example of BTD as a bridging ligand (**11.6** in Chart 11.3) has been isolated from the reaction with $[IrCp^*Cl(\mu\text{-}Cl)]_2$ in a 1:1 molar ratio.[31]

Several studies of transition-metal complexes have revealed the versatility of BSD as a ligand. Reaction of $AgNO_3$ with BSD produced the 1:2 complex $[Ag(BSD)_2(NO_3)]$ containing the supramolecular $[Se\cdots N]_2$ synthon.[32] Subsequently, the addition of $HgCl_2$ to BSD in methanol was shown to generate both 1:1 and 1:2 complexes.[33] The polymeric structure of the latter adduct $[HgCl_2(BSD)_2]_n$ is comprised of a columnar array of $[Hg(\mu\text{-}Cl)_2]_n$ chains flanked by *N*-coordinated BSD ligands that are linked *via* Se···N interactions to a neighbouring chain (Fig. 11.2). The structures of 1:2 complexes of transition-metal dichlorides MCl_2 (M = Mn, Fe, Co, Ni and Cd) with BSD are determined by the size of the metal.[34] The Mn and Cd complexes form infinite chains of metal atoms *N,N′*-bridged by BSD, *cf.* $[HgCl_2(BSD)_2]_n$, whereas the larger ions (Fe, Co, Ni) stabilise infinite chains of metal atoms bridged by chloride ions. The coordination of BSD to the metal in these *N,N′*-bridged complexes has little effect on the geometrical parameters compared to those in the free ligand.[35]

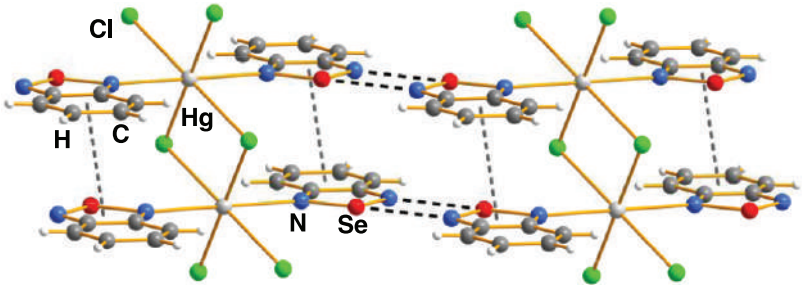

Figure 11.2. Structure of $[HgCl_2(BSD)_2]_n$ showing the intermolecular Se···N interactions.[33]

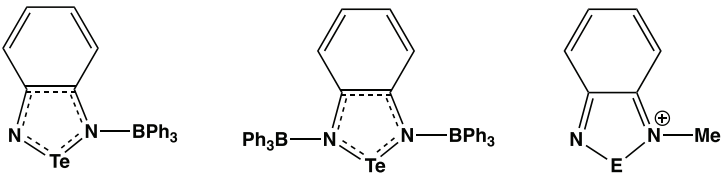

11.7 **11.8** **11.9a** E = S **11.9b** E = Se **11.9c** E = Te

Chart 11.4. Triphenylborane adducts of benzo-2-tellura-1,3-diazole and *N*-methylated benzochalcogenadiazolium cations.

Benzo-2-chalcogena-1,3-diazoles readily undergo adduct formation with Group 13 Lewis acids, *e.g.*, boron trihalides or triphenylborane. Thus, benzo-2-tellura-1,3-diazole forms 1:1 and 1:2 adducts with BPh_3, **11.7** and **11.8**, respectively (Chart 11.4).[36] The *N*-bonded 1:2 adduct **11.8** is a monomer in the solid state with no Te···N SBIs. The Te–N bond lengths in the heterocyclic ring are not significantly different from those in the free ligand. The 1:1 adduct **11.7** has a dimeric structure with Te···N distances of 2.59 and 2.60 Å. By contrast, the formation of a $[Se\cdots N]_2$ unit in 1:1 adducts of benzo-2-selena-1,3-diazole with boron trihalides BX_3 (X = F, Cl, Br) and BPh_3 is precluded by stronger London dispersion forces in the case of BPh_3 and halogen bonding in the BX_3 complexes.[37]

A comparison of the protonation of benzo-2-selena-1,3-diazole and benzo-2-tellura-1,3-diazole in DMSO showed that the pK_a values for the

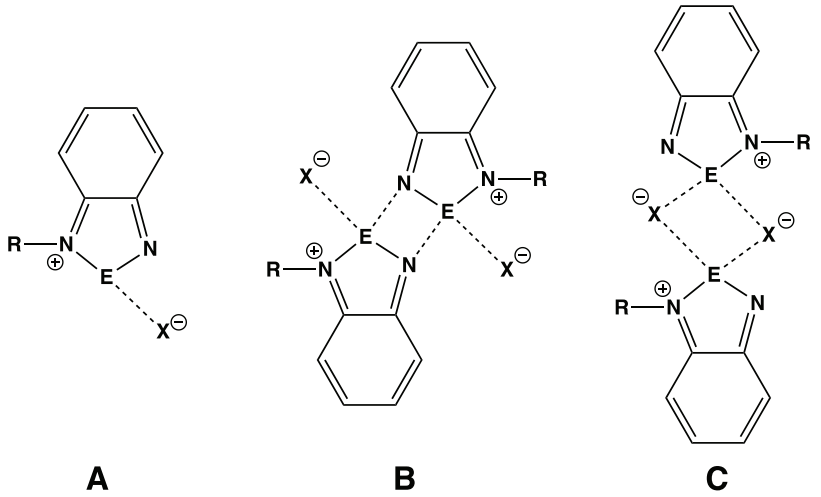

Chart 11.5. Structural arrangements in *N*-alkylated benzochalcogenadiazolium salts.

selenium derivative are well separated while the corresponding values for the tellurium analogue are close together.[38] Consistently, monoprotonated species could not be isolated for benzo-2-tellura-1,3-diazole. However, *N*-methylated benzochalcogenadiazolium cations **11.9a–c** (Chart 11.5) are readily obtained as triflate salts by treatment of the corresponding benzo-2-chalcogena-1,3-diazole with methyl triflate.[39] In the solid state *N*-methylbenzothiadiazolium triflate (**11.9a**) exists as a single ion pair with no cation-cation contacts in the solid state (**A** in Chart 11.5), whereas the Se and Te analogues (**11.9b** and **11.9c**) form centrosymmetric dimers (**B** in Chart 11.5).[38] The Te···N contact of 2.42 Å in **11.9c** is significantly stronger than that in benzo-2-tellura-1,3-diazole (2.70 Å). Replacement of the triflate anion by iodide in these salts has interesting structural consequences.[21] *N*-Methylbenzothiadiazolium iodide exhibits both the dimeric arrangement with an [S···N] synthon (**B** in Chart 11.5) and the ion pair (**A** in Chart 11.5) in its crystal structure, whereas the selenium analogue adopts a dimeric structure with bridging iodide anions (**C** in Chart 11.5).[21,40a] In contrast to the tellurium analogues, *N*-alkyl benzo-2-selena-1,3-diazolium salts are stable in air and in neutral or acidic media.

An alternative, efficient route to *N*-alkyl benzo-2-selena-1,3-diazolium salts involves the cyclocondensation of an alkyl-phenylenediamine

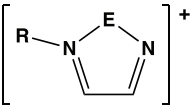

11.10a E = Se
11.10b E = Te

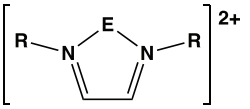

11.11a E = S
11.11b E = Se
11.11c E = Te

Chart 11.6. Alkylated chalcogenadiazolium cations.

with selenous acid, H_2SeO_3, in a mixture of ethanol and trifluoroacetic acid.[40a] This methodology has also been applied to the synthesis of bridged dicationic derivatives of benzo-2-selena-1,3-diazole, *e.g.*, $[H_4C_6NSeN–CH_2–CH_2–NSeNC_6H_4]^{2+}$.[40b]

1-Selena-2,5-diazolium salts **11.10a**[X] (E = Se) are obtained *via* a two-electron redox process between SeX_4 (X = Cl, Br) and *tert*-butylDAB (DAB = 1,4-diaza-1,3-butadiene) (Chart 11.6).[41–43] In the solid state the halide salts are monomeric, but the 1-selena-2,5-diazolium cation dimerises *via* weak Se···N interactions in the $[GaCl_4]^-$ salt. By contrast, the reaction of TeX_4 (X = Cl, Br) with *tert*-butylDAB yields the 1:1 adducts TeX_4·DAB.[42] However, 1-tellura-2,5-diazolium bromide **11.10b**[Br] (E = Te) is isolated as the $[GaBr_4]^-$ salt from the reaction of $TeBr_4$·DAB with Me_3SiOTf followed by anion exchange with KBr and addition of $GaBr_3$.[44] The chalcogen centres in 1-chalcogena-2,5-diazolium cations behave as electron acceptors towards Lewis bases (two-electron donors) such as R_3P, *N*-heterocyclic carbenes or 4-dimethylaminopyridine to give adducts of the type **11.10**·L.[44]

Base-stabilised chalcogen dications of the type **11.11a–c** are formally the result of dialkylation of 1-chalcogena-2,5-diazoles, but these chalcogen analogues of *N*-heterocyclic carbenes are not obtained *via* this route.[45] The highly electrophilic sulfur and selenium dications, **11.11a** and **11.11b**, are prepared by reactions of ECl_2 (E = S, Se) with Me_3SiOTf with $Dipp_2DAB$ (Dipp = 2,6-diisopropylphenyl) and isolated as $[B(C_6F_5)_4]^-$ salts.[46,47] The tellurium analogue **11.11c** is obtained as the triflate salt by ligand exchange between (bipy)$TeCl_2$ and Cy_2DAB followed by treatment with AgOTf.[48] The structural parameters indicate that **11.11a–c** can be considered as ligand (diamine)-stabilised chalcogen dications in which

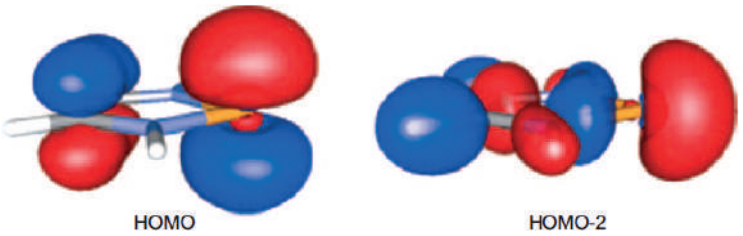

Figure 11.3. The π and σ lone pair orbitals in the model dication $Se[(NH)_2(CH)_2]^{2+}$ **11.11b** (R = H).[45] [Reproduced with permission from T. Chivers and J. Konu, *Angew. Chem. Int. Ed*., **48**, 3025 (2009). Copyright 2009 Wiley-VCH].

the strength of the chalcogen-nitrogen interaction is in the order S–N > Se–N > Te–N.[49] Consistently, theoretical calculations confirm that the chalcogen centres accommodate two lone pairs of electrons with π- and σ-symmetry as expected for an E^{2+} dication (Fig. 11.3).

11.2.4 *Lewis acid (acceptor) properties*

The positive electron affinities of 1-chalcogena-2,5-diazoles and, especially, benzo-2-chalogena-1,3-diazoles determine their strong electron-acceptor behaviour, which is enhanced by the presence of electron-withdrawing substituents, *e.g*., in 3,4-dicyano-1-chalcogena-2,5-diazoles and 4,5,6,7-tetrafluorobenzo-2-tellura-1,3-diazole.[3,4] These heterocycles are readily reduced to radical anions which can be isolated as salts (Sec. 13.8). In this section adduct formation between two-electron donors such as $[PhS]^-$, X^- (X = F, Cl, Br, I), pyridine and *N*-heterocyclic carbenes is discussed. The encapsulation of 1-chalcogena-2,5-diazoles by crown ethers is described in Sec. 15.3.1.

There is a delicate balance between reduction to give radical anions and the formation of an interchalcogen bond in reactions of 1-chalcogena-2,5-diazoles with $[PhE]^-$ (E = S, Se) anions.[8c,50] The first stable complex between a 1-chalcogena-2,5-diazole and an anionic nucleophile was the adduct of 3,4-dicyano-1-selena-2,5-diazole with phenylthiolate $[PhS]^-$ (**11.12** in Chart 11.7), which was isolated as the $[K(18\text{-crown-}6)]^+$ salt.[51] Similar complexes of 3,4-dicyano-1-tellura-2,5-diazole with halide ions X^- (X = F, Cl, Br, I), **11.13**, have also been structurally characterised.[4b,52]

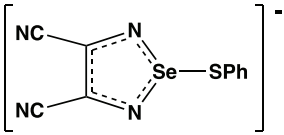

11.12

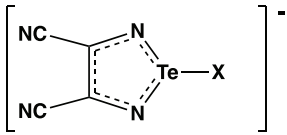

11.13 X = F, Cl. Br, I

Chart 11.7. Chalcogen-bonded adducts of 1-chalcogena-2,5-diazoles with anions.

3,4-Dicyano-1-tellura-2,5-diazole also forms a *bis*-adduct with pyridine.[52]

The Se–S and Te–X distances in the adducts **11.12** and **11.13** are all *ca*. 0.5 Å longer than the sum of the corresponding covalent radii, but *ca*. 1 Å shorter than the sum of the van der Waals radii.[4b,52] Quantum chemical calculations reveal that the coordinate bond in these complexes of 3,4-dicyano-1-chalcogena-2,5-diazoles involves the transfer of electron density from the anion to the heterocycle *via* negative hyperconjugation (*i.e*., from the lone pair molecular orbital on X^- to the σ^* orbital of the E–N bond of the chalcogenadiazole).[4b,54] The energy of the bonding interaction falls within the range 105–360 kJ mol^{-1} and is strongest for the Te-containing heterocycle.[53] The association constants for the interaction of benzo-2-tellura-1,3-diazoles with the Lewis bases X^- (X = Cl, Br, I), NO_3^- and quinuclidine in organic solvents have been determined by using UV-visible and NMR spectroscopy and calculated free energies were found to be as high as 29.2 kJ mol^{-1}. The values were highest for charge-dense Lewis bases (Cl^-) and enhanced by electron-withdrawing substituents on the arene ring of the benzo-2-tellura-1,3-diazole.

Benzo-2-chalcogena-1,3-diazoles readily undergo one-electron reduction with potassium or KC_8 in THF to give the corresponding radical anions, which can be isolated as stable salts with a solvated potassium counter-ion $[K(L)]^+$ (L = THF, 18-crown-6) in the case of the S and Se derivatives (Sec. 13.8). The radical anion of benzo-2-tellura-1,3-diazole (BTD) can be detected by EPR spectroscopy at room temperature, but it decomposes to give the ditellurido $[Te_2]^{2-}$ complex, **11.14**, which undergoes air oxidation to form complex **11.15** in which the tetratellurido $[Te_4]^{2-}$ dianion bridges two telluradiazoles; the dianions **11.14** and **11.15** (Chart 11.8) are isolated as $[K(18\text{-crown-6})]^+$ salts.[54] The isolation and structural characterisation of (a) a trimeric dianionic assembly comprised

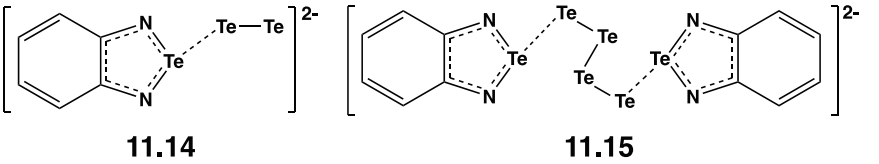

11.14 **11.15**

Chart 11.8. Ditellurido and tetratellurido complexes of benzo-2-tellura-1,3-diazole.

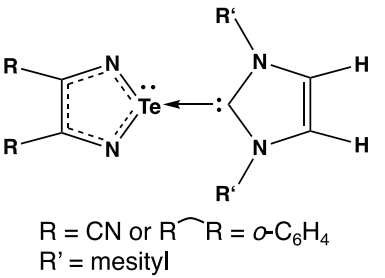

Figure 11.4. Major resonance form of *N*-heterocyclic carbene complexes of **11.1** and **11.2**.

of two BTD radical anions and a neutral BTD molecule and (b) a sterically hindered monomeric BTD radical anion are described in Chapter 13 (see Schemes 13.11 and 13.12, respectively).

Adducts of 3,4-dicyano-1-tellura-2,5-diazole (**11.1** in Scheme 11.4a) and benzo-2-tellura-1,3-diazole (**11.2** in Scheme 11.4b) with neutral two-electron donors, *e.g.*, the *N*-heterocyclic carbene or 1,3-bis(mesityl)imidazole-2-ylidene, have also been isolated and structurally characterised.[55] The mesityl groups in these 1:1 complexes are oriented perpendicularly to the plane of the telluradiazole rings and the C–Te bond lengths are 2.34 and 2.53 Å, respectively, *cf.* sum of covalent radii of Te and C is 2.12 Å. Computational studies of the nature of the C–Te bonding interaction indicate that these complexes can be represented by the resonance form depicted in Fig. 11.4.[55]

11.2.5 *Applications*

The positive electron affinities (acceptor behaviour), optical properties, ambiphilic nature and redox activity of benzo-2-chalcogena-1,3-diazoles

have attracted considerable interest in the incorporation of these chalcogen-nitrogen heterocycles into functional materials.[56] Consequently, the emphasis of recent work has been on derivatives of these heterocycles with potential applications as photovoltaics,[57] organic light-emitting diodes (OLEDs) for flat-panel displays[58a–c] and night-time lighting (candlelight-style OLEDs),[58d,e] field-effect transistors[59] and photoconductors for solar cells.[60] In addition, benzo-2-chalcogena-1,3-diazoles show promise for use as chemical sensors, fluorescent thermometers and probes for locating tumour cells in living systems.[61,62] Several recent articles provide a detailed source of primary publications describing these applications.[3,18,57] More specific reviews on the applications of benzo-2-chalcogena-1,3-diazoles as fluorescence probes or luminescent complexes are also available.[6a,7] In this section some of the molecular assemblies that have been created for specific uses are presented as illustrative examples.

The potential applications of benzo-2-thia-1,3-diazoles in light technology are extensive. Their strong electron-withdrawing properties, together with the ability to introduce a variety of substituents on the carbocyclic ring, are attractive features in the design of materials with a D-A-π-A (D = Donor, A = Acceptor) configuration (**11.16** in Chart 11.9) for use in dye-sensitised solar cells.[63] The acceptor properties can be enhanced by (a) replacement of the benzene ring by pyridine or (b) fluorination of the arene ring. Both these strategies have been investigated for the generation of low band gap polymers.[64] The introduction of pyridine also enables the synthesis of two isomers (**11.17a** and **11.17b**) with different optical and electrochemical properties.[65a]

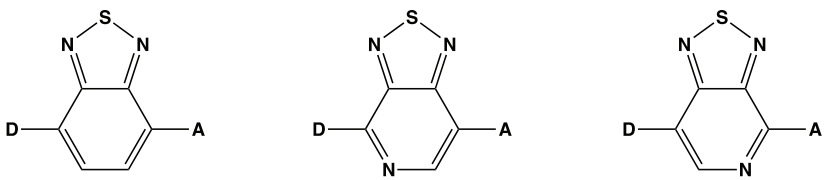

11.16 **11.17a** **11.17b**

Chart 11.9. D-A-π-A configuration in dye-sensitised solar cells and isomers of pyridal-2-thia-1,3-diazole.

More recently, the concept of D-A-π-A organic sensitisers has been extended to benzo-2-selena-1,3-diazoles with triphenylamine or *N*-hexylcarbazole as electronic donors.[65b] The strong electron-withdrawing effect of benzo-2-thia-1,3-diazole also enhances the accepting ability of azaboron dipyrromethene dyes and facilitates electronic communication between the donating and accepting groups in the molecule.[66]

The combination of D and A components in benzo-2-thia-1,3-diazoles is also an efficient way to generate deep red/near infrared (DR/NIR, 650–900 nm) emission in OLEDs because the HOMO-LUMO energy gap can be tuned by appropriate selections of D and A.[67] For example, the electroluminescence of **11.17a** and **11.17b** (D = $(4\text{-}^{t}BuC_6H_4)_2NC_6H_4$ and A = naphthalene), **11.16** (D = $(4\text{-}^{t}BuC_6H_4)_2NC_6H_4$ and A = quinoline) and **11.16** (D = $(4\text{-}^{t}BuC_6H_4)_2$N-2-py and A = naphthalene) have been compared.[67] The emission wavelength of these four isomers was found to vary from yellow to deep red.

A variety of alkynyl-substituted benzo-2-chalcogena-1,3-diazoles have also been investigated in the context of OLEDs.[68] The halogenated phenazino-thiadiazoles (**11.18a**, **b** in Chart 11.10) show efficient electron transport and these materials form polycrystalline thin films upon spin-casting from solution.[68d] In addition to the influence on solid-state structures, the replacement of S by Se in alkynyl-substituted benzo-2-chalcogena-1,3-diazole lowers the HOMO-LUMO energy gap, primarily due to a change in the energy of the HOMO.[68b,c] Arylselenium-functionalised alkynyl benzo-2-thia-1,3-diazoles have also been prepared and their biomolecular interactions were studied.[69]

The emission behaviour of a series of alkynyl-benzothiadiazoles with butterfly (**11.19a**) or linear (**11.19b**) shapes have been compared for both D-A-π-D (R = R′ = MeO, Me_2N, Ph_2N) and D-A-π-A arrangements of the substituents (R = MeO, Me_2N; R′ = CN).[70] The linear compounds emitted brighter light in pristine powders with higher quantum yields, whereas the butterfly-shaped compounds are brighter emitters in crystals and also exhibited mechanochromic character.

Benzo-2-chalcogena-1,3-diazoles are sensitive fluorophores for possible applications as components of fluorescent polymeric thermometers.[71] Benzo-2-selena-1,3-diazoles have also been shown to be fluorescent sensors for anions or cations (Chart 11.11). Thus, the diarylamino derivative

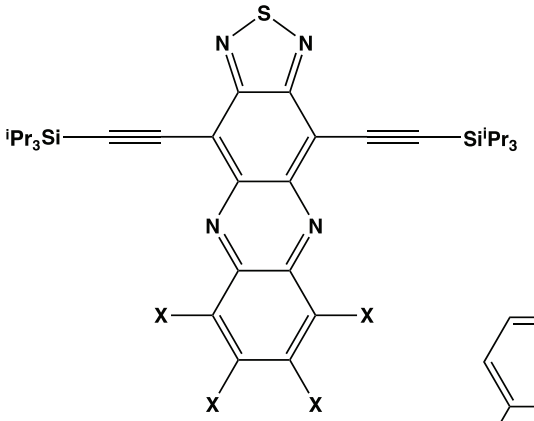

11.18a X = F
11.18b X = Cl

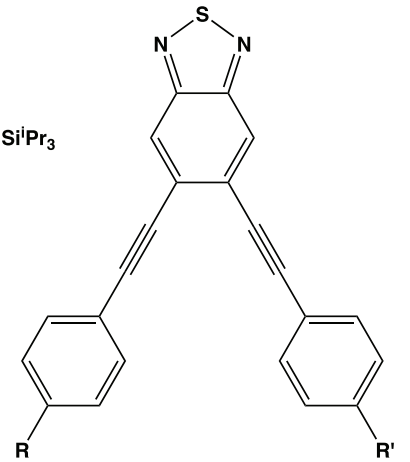

11.19a

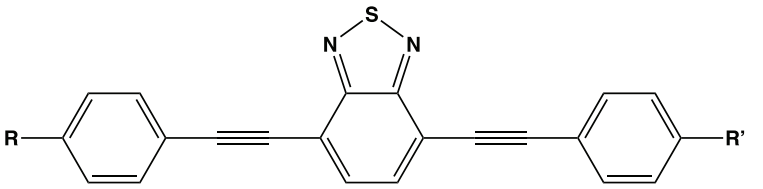

11.19b

Chart 11.10. Alkynyl-substituted benzo-2-thia-1,3-diazoles for OLEDs.

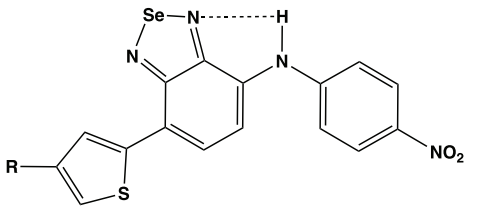

11.20

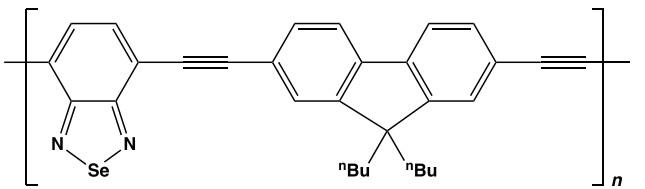

11.21

Chart 11.11. Benzo-2-selena-1,3-diazoles as fluorescent sensors for anions and cations.

11.20[72a] and the conjugated polymer **11.21**[72b] are selective and highly sensitive probes for the detection of fluoride ion and Hg^{2+}, respectively. Fluorescent, water-soluble bis-triazolyl benzochalcogenadiazoles behave as sensors for Cu^{2+}, Ni^{2+} and Ag^{+} with the selenium derivatives exhibiting stronger affinity for these metal ions than their sulfur analogues.[73]

Porphyrazines (phthalocyanine analogues) that incorporate annulated 1-chalcogena-2,5-diazoles have been prepared for all three of the heavier chalcogens, as exemplified by the tellurium derivative **11.22**, which is obtained as a magnesium complex by reaction of 3,4-dicyano-1-tellura-2,5-diazole with magnesium butoxide in *n*-butanol (Scheme 11.5).[15] The tellurium-containing complex **11.22** forms strongly conducting thin films.

The incorporation of moderate steric repulsion within the supramolecular ribbon polymers of 1-tellura-2,5-diazoles engenders a distortion and, hence, removes the inversion centre from the $[Te\cdots N]_2$ ring. This characteristic can be repeated through the lattice creating a non-centrosymmetric crystal with second-order non-linear optical (NLO) properties. 3,4-Dicyano-1-tellura-2,5-diazole (**11.1**) and 5,6-dichlorobenzo-2-tellura-1,3-diazole were investigated as an initial test of this proposition, but their second harmonic generation efficiency is modest.[74] However, it was found that 5-benzoylbenzo-2-tellura-1,3-diazole forms an acentric crystal, suggesting that this approach may lead to more efficient NLO materials.[74]

In the context of biomedical applications, several halogenated (F, Cl) benzo-2-selena-1,3-diazoles exhibit strong apoptotic cytotoxicity and are

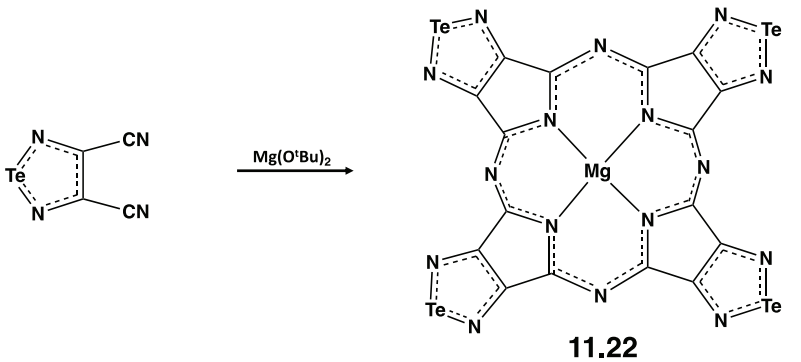

Scheme 11.5. Synthesis of a 1-tellura-2,5-diazole-fused porphyrazine.

considered to be leading candidates for the development of new anticancer drugs.[75]

11.3 1,2-Dithia-3-azolium Salts

The 1,2-dithia-3-azolium cation $[(RC)_2NS_2]^+$ is a 6π-electron heterocycle, isoelectronic with the binary sulfur-nitrogen dication $[S_3N_2]^{2+}$ (Sec. 5.8.4). The dichloro derivative **11.23** (R = Cl) has been prepared with a chloride counter-ion (Appel's salt) by reaction of $ClCH_2CN$ with S_2Cl_2.[76a] Reductive coupling of **11.23** with triphenylantimony produces the fulvalene derivative **11.24** (Scheme 11.6). Electroxidation of **11.24** in the presence of tetrahedral counterions generates a series of 1:1 cation radical salts [**11.24**][X] (X = BF_4^-, ClO_4^-, FSO_3^-), which form ladder-like arrays of cation radicals reminiscent of the *trans*-antarafacial salts of $[S_3N_2]^{\bullet+}$ (Chart 4.5); they behave as Mott insulators.[76b]

In general, however, 1,2-dithia-3-azolium salts are less stable than the benzo-fused derivatives, which are known as Herz salts.[3] These cationic systems are important as precursors to the corresponding radicals *via* one-electron reduction; the fascinating conducting and magnetic properties of these radicals are discussed in Sec. 13.2.[77]

The original preparation of Herz salts from the reaction of aromatic amines with an excess of S_2Cl_2 is the best route to benzo-1,2-dithia-3-azolium salts (Scheme 11.7).[3] When the arylamine incorporates a very bulky *ortho*-R group, however, *N*-sulfinylamines ArNSS may be obtained (Sec. 10.3). An alternative to the Herz reaction involves the condensation reaction between thionyl chloride and an *ortho*-aminothiophenol.[78] This approach has been exploited to generate a benzo-bis(1,2-dithia-3-azolium)

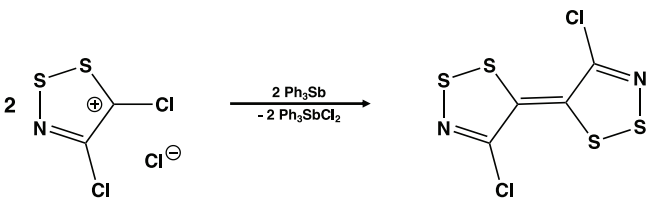

11.23 **11.24**

Scheme 11.6. Synthesis of a fulvalene from 4,5-dichloro-1,2-dithia-3-azolium chloride.

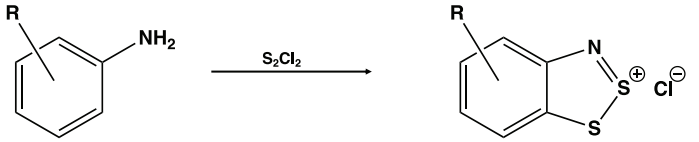

Scheme 11.7. Synthesis of benzo-1,2-dithia-3-azolium chloride.

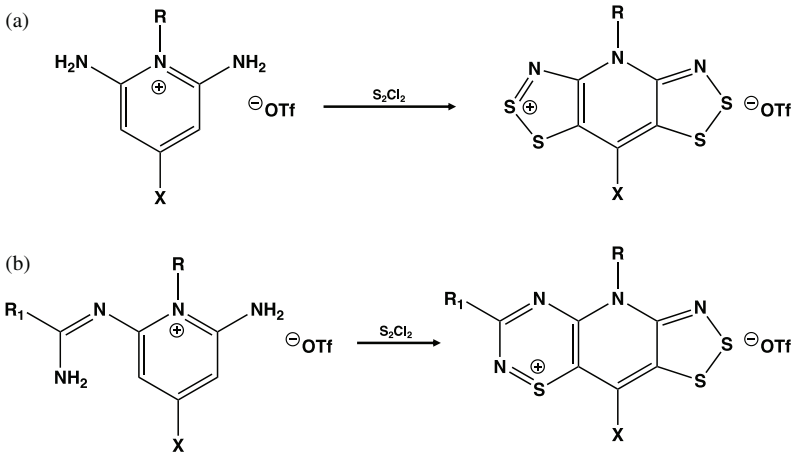

Scheme 11.8. Examples of "double Herz" cyclocondensation reactions.

salt.[79,80] The treatment of benzo-1,3-dithia-2,4-diazines with SCl_2 can be used for the synthesis of Herz salts when the method shown in Scheme 11.7 is not available.[81]

A "double Herz" cyclocondensation reaction of an *N*-alkylated 2,6-diamino-pyridine with S_2Cl_2 produces the antiaromatic (16π-electron) *N*-alkylated *bis*(dithiazolium) salts (Scheme 11.8a), which are essential precursors to the corresponding radicals (Sec. 13.2.1).[82] This methodology has been extended to the synthesis of cations based on *bis*(thiadiazine)[83a,b] and hybrid thiadiazinyl-dithiazole (Scheme 11.8b)[83c] or thiazinyl-dithiazole frameworks.[83d]

Heavy chalcogen analogues of benzo-1,2-dithia-3-azolium salts (**11.25a**, E = Se; **11.25b**, E = Te) have been obtained by the cyclocondensation reactions of *N,N,S*-trisilylated derivative of *ortho*-aminothiophenol with chalcogen tetrahalides (Scheme 11.9).[84] The chloride salts are readily

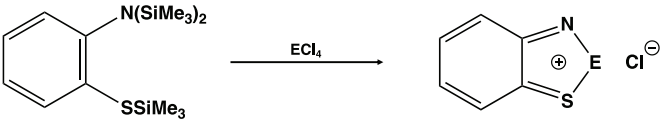

11.25a E = Se
11.25b E = Te

Scheme 11.9. Synthesis of heavy chalcogen analogues of Herz salts.

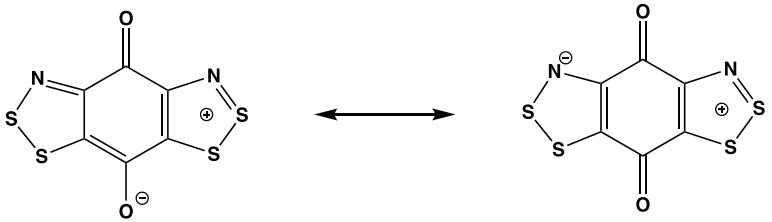

11.26a **11.26b**

Chart 11.12. Resonance forms for benzoquinone-*bis*-1,2-dithia-3-azole.

converted to $[GaCl_4]^-$, $[TeCl_5]^-$ or $[OTf]^-$ complexes. The Se-containing salt [**11.25a**][$GaCl_4$] crystallises as an ion pair, but the Te analogues [**11.25b**][X] (X = [$GaCl_4$], [$TeCl_5$] or [OTf]) exhibit strong anion-cation interactions with Te···N distances of 2.53–2.55 Å. A computational study of benzo-1,2-dichalcogena-3-azolium cations $[C_6H_4NEE']^+$ (E = E′ = S, Se; E = S, E′ = Se) revealed a delocalisation of the positive charge over both the heterocycle and the carbocycle with a bond order in both rings between 1 and 2.[85] NICS values are consistent with the description of these C,N,E heterocycles as 10π-electron systems.[85]

Benzoquinone-bridged bis-1,2-dithia-3-azole and selenium analogues have been investigated as potential molecular semiconductors (Sec. 13.2).[86] The synthesis of benzoquinone-*bis*-1,2-dithia-3-azole involves a double Herz condensation process using 1,4-dihydroxy-2,5-diamonobenzene followed by a deprotonation step to give the zwitterionic product **11.26** (Chart 11.12).[86a] Benzoquinone-*bis*-1,2-dithia-3-azole is a closed shell, antiaromatic 16π-electron system with a small HOMO-LUMO band gap that becomes smaller upon application of pressure (8 GPa) to produce an organic molecular metal with $\sigma_{RT} > 10^1$ S cm^{-1}.[86a] Reaction of **11.26** with SeO_2 results in the replacement of the *N*-bonded

sulfur atom by selenium in each of the dithiazole rings.[86b] Benzoquinone-*bis*-1-thia-2-selena-3-azole is obtained in one nanocrystalline and two crystalline phases. One of the crystalline phases is an organic metal with $\sigma_{RT} \sim 10^2$ S cm^{-1} at 6 GPa.[86b] Benzoquinone-*bis*-1,2-dithia-3-azole **11.26** has been shown to be an excellent anode for organic batteries.[87]

11.4 1,2-Dichalcogena-3,5-diazolium Salts

The first examples of the 1,2-dithia-3,5-diazolium salts were obtained from the treatment of organic nitriles with $(NSCl)_3$.[88] This reaction was subsequently shown to proceed by the intermediate formation of six-membered ring systems of the type $RCN_3S_2Cl_2$ which, upon thermolysis, undergoes ring contraction to yield the five-membered $[RCNSSN]^+$ cation.[89] This methodology has been largely replaced by syntheses based on the cyclocondensation of trisilylated amidines with sulfur dichloride, which can also be employed for 1,2-diselena-3,5-diazolium salts by using $SeCl_2$ generated *in situ* from comproportionation of Se and $SeCl_4$ (Scheme 11.10).[90–92] This route was successful for the preparation of the prototypal systems $[HCNEEN]^+$ (E = S, Se).[93] It is also readily extended to the synthesis of multi-dichalcogenadiazolium cations such as 1,3- or 1,4-$C_6H_4(CNEEN)_2]^{2+}$ (E = S, Se)[90,94] and $[1,3,5\text{-}C_6H_3(CNSSN)_3]^{3+}$.[95] Other spacer groups that have been employed in the construction of these multifunctional cations include 2,5-furan[96] and 2,5-thiophene.[97]

An alternative synthesis of $[RCNSSN]^+$ (R = aryl) salts invokes the use of lithium amidinates $Li[RC(NSiMe_3)_2]$, which can be generated by reactions of (a) nitriles with lithium hexamethyldisilanide or (b) bis(trimethylsilyl)carbodiimide with an organolithium reagent in diethyl ether at room temperature (Scheme 11.11).[98] The latter method is especially useful for the preparation of bulky derivatives (*e.g.*, R = 2,4,6-$(CF_3)_3C_6H_2$) or those with polyaromatic substituents (*e.g.*, R = 1′-pyrenyl).[99,100] However, the LiCl by-product of these reactions can be

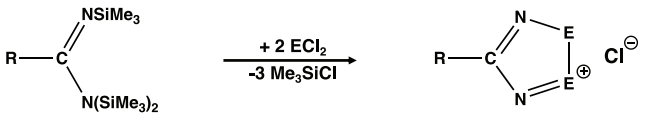

Scheme 11.10. Synthesis of 1,2-dichalcogena-3,5-diazolium salts *via* cyclocondensation.

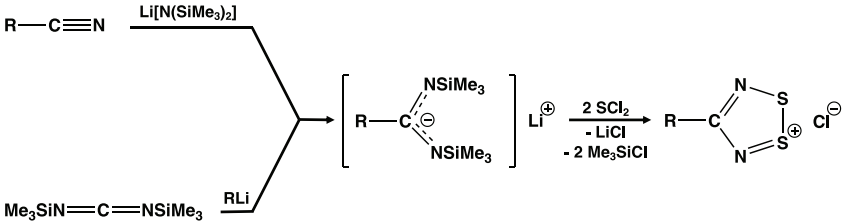

Scheme 11.11. Synthesis of 1,2-dichalcogena-3,5-diazolium salts *via* lithium amidinates.

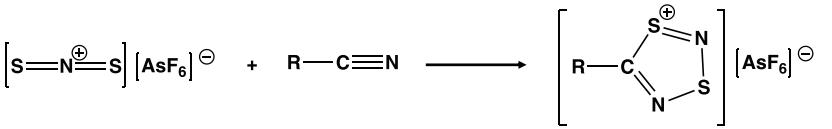

Scheme 11.12. Synthesis of 1,3-dithia-2,4-diazolium salts *via* cycloaddition.

difficult to separate from insoluble 1,2-dithia-3,5-diazolium salts. The chloro derivative [ClCNSSN]Cl is prepared by the direct reaction of $Me_3SiN{=}C{=}NSiMe_3$ with S_2Cl_2.[101]

Recent studies of 1,2-dithia-3,5-diazolium salts have focused on their use as precursors to the corresponding radicals *via* one-electron reduction.[98] The synthesis, molecular and electronic structures, and properties of 1,2-dithia-3,5-diazolyl radicals are discussed in Sec. 13.4.

11.5 1,3-Dithia-2,4-diazolium Salts

The 1,3-dithia-2,4-diazolium cation is prepared by the cycloaddition of the $[SNS]^+$ cation to the C≡N triple bond of organic nitriles (Scheme 11.12).[102] This methodology may also be applied to the synthesis of molecules containing more than one 1,3,2,4-dithiadiazolyl ring, *e.g.*, by the reaction of 1,3-, 1,4-, or 1,5-$C_6H_4(CN)_2$ with two equivalents of $[SNS][AsF_6]$ to give the corresponding dications 1,3-, 1,4-, or 1,5-$[C_6H_4(CNSNS)_2]^{2+}$.[103] The double addition of $[SNS]^+$ to cyanogen produces the dication $[(SNSNC)–(CNSNS)]^{2+}$ [104] and the triple addition of $[SNS]^+$ to the tricyanomethide anion $[C(CN)_3]^-$ proceeds in a stepwise

fashion to give the dication $[C(CNSNS)_3]^{2+}$.[105] The versatility of this approach is further illustrated by the cycloaddition of $[SNS]^+$ to SF_5CN[106] and $Hg(CN)_2$[107] to give the corresponding 1,3-dithia-2,4-diazolium mono- and dications, respectively.

11.6 1-Thia-2,3,4-triazole-5-thiolate Salts

The cyclic forms of 1-thia-2,3,4-triazole $HCSN_3$ (**11.27**) and the nitrogen-rich sulfur nitride SN_4 are isoelectronic, 6π-electron systems. Attempts to prepare SN_4 by reaction of an $[NS]^+$ salt with cesium azide produced the polymer $(SN)_x$ (Sec. 5.7.2). However, the reaction of CS_2 with sodium azide generates the sodium salt of the $[SCSN_3]^-$ anion **11.28**, which was first isolated more than 100 years ago.[108] Treatment of $[Na][SCSN_3]$ with concentrated HCl in water produces the *N*-protonated derivative **11.29** as a temperature-sensitive white solid (Chart 11.13).[109,110]

Deprotonation of **11.29** with alkali-metal or ammonium hydroxides in water provides an improved synthesis of a series of $[M][SCSN_3]$ salts (Eq. 11.1), which are of limited thermal stability.[110] For example, the cesium salt decomposes at room temperature to give cesium thiocyanate according to Eq. 11.2.

$$MOH + HCS_2N_3 \rightarrow M[SCSN_3] + H_2O \qquad (11.1)$$

$$Cs[SCSN_3] \rightarrow Cs[SCN] + N_2 + 1/8S_8 \qquad (11.2)$$

X-ray structures of the ammonium and tetramethylammonium salts reveal that the heterocyclic anion **11.28** is a planar, five-membered ring.[110] In aqueous solution the ^{14}N NMR spectra of salts of **11.28** exhibit three

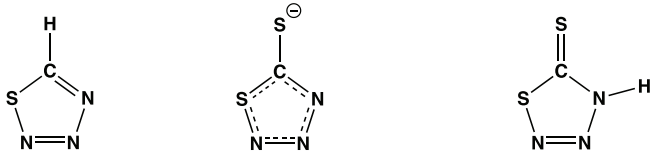

11.27 **11.28** **11.29**

Chart 11.13. 1-Thia-2,3,4-triazole derivatives.

well-separated resonances in the ranges 60–73, 4–6 and –22 to –42 ppm, consistent with the cyclic structure.[109,110] The reaction of the sodium salt of **11.28** with methyl iodide in water produced the covalent methyl derivative $MeSCSN_3$ as a colourless crystalline solid stable in the dark at 0°C for weeks.[110] The Se and Te analogues of **11.28** are unknown, but the cyclic structure is calculated to be of lower energy than the acyclic azido alternative for these heavy chalcogen derivatives by 49.4 and 43.5 kJ mol^{-1}, respectively.[110]

References

1. M.-H. Whangbo, R. Hoffmann and R. B. Woodward, *Proc. Roy. Soc. London, Ser. A*, **366**, 23 (1979).
2. M. P. Cava, M. V. Lakshmikantham, R. Hoffmann and R. M. Williams, *Tetrahedron*, **67**, 6771 (2011).
3. O. A. Rakitin and A. V. Zibarev, *Asian J. Org. Chem*., **7**, 2396 (2018).
4. (a) A. V. Lonchakov, O. A. Rakitin, N. P. Gritsan and A. V. Zibarev, *Molecules*, **18**, 9850, (2013): (b) N. A. Semenov, A. V. Lonchakov, N. P. Gritsan and A. V. Zibarev, *Russ. Chem. Bull*., **64**, 499 (2015).
5. A. V. Zibarev and R. Mews, in *Frontiers of Selenium and Tellurium Chemistry: From Small Molecules to Biomolecules and Materials*, Eds. J. D. Woollins and R. S. Laitinen, Springer (2011), Ch. 6, pp. 123–149.
6. (a) B. A. D. Neto, P. H. P. R. Carvalho and J. R. Correa, *Acc. Chem. Res.*, **48**, 1560 (2015); (b) B. A. D. Neto, A. A. M. Lapis, E. N. da Silva Junior and J. Dupont, *Eur. J. Org. Chem*., **2013**, 228 (2013).
7. T. S. Sukikh, D. S. Ogienko, D. A. Bashirov and S. N. Konchenkoa, *Russ. Chem. Bull*., **68**, 651 (2019).
8. (a) L. S. Konstantinova, E. A. Knyazeva, N. V. Obruchnikova, N. V. Vasileva, I. G. Irtegova, Y. V. Nelyubina, I. Yu. Bagryanskaya, L. A. Shundrin, Z. Yu. Sosnovskaya, A. V. Zibarev and O. A. Rakitin, *Tetrahedron*, **70**, 5558 (2014); (b) I. Yu. Bagryanskaya, N. P. Gritsan, V. N. Ikorskii, I. G. Irtegova, A. V. Lonchakov, E. Lork, R. Mews, V. I. Ovcharenko, N. A. Semenov, N. V. Vasilieva and A. V. Zibarev, *Eur. J. Inorg. Chem*., **2007**, 4751 (2007).
9. A. G. Makarov, N. Yu. Selikhova, A. Yu. Makarov, V. S. Malkov, I. Yu. Bagryanskaya, Y. V. Gatilov, A. S. Knyazev, Y. G. Slizhov and A. V. Zibarev, *J. Fluorine Chem*., **165**, 123 (2014).

10. L. S. Konstantinova, E. A. Knyazeva, A. A. Nefyodov, P. S. Camacho, S. E. M. Ashbrook, J. D. Woollins, A. V. Zibarev and O. A. Rakitin, *Tetrahedron Lett*., **56**, 1107 (2015).
11. (a) T. F. Mikhailovskaya, A. G. Makarov, N. Yu. Selikhova, A. Yu. Makarov, E. A. Pritchina, I. Yu. Bagryanskaya, E. V. Vorontsova, I. D. Ivanov, V. D. Tikhova, N. P. Gritsan, Yu. G. Slizhov and A. V. Zibarev, *J. Fluorine Chem*., **183**, 44 (2016); (b) A. G. Makarov, N. Yu. Selikhova, A. Yu. Makarov, V. S. Malkov, I. Yu. Bagryanskaya, V. Gatilov, A. S. Knyazev, Yu. G. Slizhov and A. V. Zibarev, *J. Fluorine Chem*., **165**, 123 (2014).
12. V. Bertini and F. Lucchesini, *Synthesis*, 681 (1982).
13. A. F. Cozzolino, Q. Yang and I. Vargas-Baca, *Cryst. Growth Des*., **10**, 4959 (2010).
14. N. A. Semenov, N. A. Pushkarevsky, J. Beckmann, P. Finke, E. Lork, R. Mews, I. Yu. Bagryanskaya, Y. V. Gatilov, S. N. Konchenko, V. G. Vasiliev and A. V. Zibarev, *Eur. J. Inorg. Chem*., **2012**, 3693 (2012).
15. (a) P. A. Stuzhin, M. S. Mikailov, E. S. Yurina, M. I. Bazanov, O. I. Koifman, G. L. Pakhomov, V. V. Travkin and A. A. Sinelshchikova, *Chem. Commun*., **48**, 10135 (2012); (b) M. P. Donzello, C. Ercolani and P. A. Stuzhin, *Coord. Chem. Rev*., **250**, 1530 (2006).
16. (a) A. F. Cozzolino, J. F. Britten and I. Vargas-Baca, *Cryst. Growth Des*., **6**, 181 (2006); (b) A. F. Cozzolino and I. Vargas-Baca, *J. Am. Chem. Soc*., **40**, 4966 (2005); (c) A. F. Cozzolino, I. Vargas-Baca, S. Mansour and A. H. Mahmoudkhani, *J. Organomet. Chem*., **692**, 2654 (2007).
17. N. A. Pushkarevsky, E. A. Chulanova, L. A. Shundrin, A. I. Smolentsev, G. E. Salnikov, E. A. Pritchina, A. M. Genaev, I. G. Irtegova, I. Yu. Bagryanskaya, S. N. Konchenko, N. P. Gritsan, J. Beckmann and A. V. Zibarev, *Chem. Eur. J.*, **25**, 806 (2019).
18. E. A. Chulanova, E. A. Radiush, I. K. Shundrina, I. Yu. Bagryanskaya, N. A. Semenov, J. Beckmann, N. P. Gritsan and A. V. Zibarev, Cryst. *Growth Des.*, **20**, 5868 (2020).
19. A. F. Cozzolino, P. J. W. Elder, L. M. Lee and I. Vargas-Baca, *Can. J. Chem*., **91**, 338 (2013).
20. J. Alfuth, B. Zadykowicz, A. Sikorski, T. Poloński, K. Eichstaedt and T. Olszewska, *Materials*, **13**, 4908 (2020).
21. B. D. Lindner, B. A. Coombs, M. Schaffroth, J. U. Engelhart, O. Tverskoy, F. Rominger, M. Hamburger and U. H. F. Bunz, *Org. Lett*., **15**, 666 (2013).
22. M. Michalczyk, M. Malik, W. Zierkiewicz and S. Scheiner, *J. Phys. Chem. A*, **125**, 657 (2021).

23. A. F. Cozzolino, G. Dimopoulos-Italiano, L. M. Lee and I. Vargas-Baca, *Eur. J. Inorg. Chem*., **2013**, 2751 (2013).
24. T. Chivers, X. Gao and M. Parvez, *Inorg. Chem*., **35**, 9 (1996).
25. (a) A. F. Cozzolino, P. S. Whitefield and I. Vargas-Baca, *J. Am. Chem. Soc*., **132**, 17265 (2010); (b) K. Eichstaedt, A. Wasileska, B. Wicher, M. Gdaniec and T. Polonski, *Cryst. Growth Des*., **16**, 1282 (2016).
26. (a) S. Langis-Barsetti, T. Maris and J. D. Wuest, *J. Org. Chem*., **82**, 5034 (2017); (b) P. C. Ho, J. Z. Wang, F. Meloni and I. Vargas-Baca, *Coord. Chem. Rev.*, **422**, 21364 (2020); (c) E. A. Pritchina, N. P. Gritsan, O. A. Rakitin and A. V. Zibarev, *Targets Heterocycl. Syst*., **23**, 143 (2019).
27. (a) D. A. Bashirov, T. S. Sukikh, N. V. Kuratieva, E. A. Chulanova, I. V. Yushina, N. P. Gritsan, S. N. Konchenko and A. V. Zibarev, *RSC Adv*., **4**, 28309 (2014); (b) E. A. Chulanova, E. A. Pritchina, L. A. Malaspina, S. Grabowsky, F. Mostaghimi, J. Beckmann, I. Yu. Bagryanskaya, M. V. Shakova, L. S. Konstantinova, O. A. Rakitin, N. P. Gritsan and A. V. Zibarev, *Chem. Eur. J.*, **23**, 852 (2017).
28. (a) A. Apblett, T. Chivers and J. F. Richardson, *Can. J. Chem*., **64**, 849 (1986); (b) T. Suzuki, T. Tsuji, T. Okubo, A. Okada, Y. Obana, T. Fukushima, T. Miyashi and Y. Yamashita, *J. Org. Chem.,* **66**, 8954 (2001).
29. (a) W. Kaim and S. Kohlman, *Inorg. Chim. Acta*, **101**, L21 (1985); (b) S. Plebst, M. Bubrin, D. Schweinfurth, S. Zalis and W. Kaim, *Z. Naturforsch*., **72B**, 839 (2017).
30. F. S. Mancilha, L. Barloy, F. S. Rodembusch, J. Dupont and M. Pfeffer, *Dalton Trans*., **40**, 10535 (2011).
31. D. A. Bashirov, T. S. Sukhikh, N. V. Kuratieva, D. Yu. Naumov, S. N. Konchenko, N. A. Semenov and A. V. Zibarev, *Polyhedron*, **42**, 168 (2012).
32. A.-J. Zhou, S.-L. Zheng, Y. Fang and M.-L. Tong, *Inorg. Chem*., **44**, 4457 (2005).
33. C. J. Milios, P. V. Ioannou, C. P. Raptopoulou and G. S. Papaestathiou, *Polyhedron*, **28**, 3199 (2009).
34. L. M. Lee, P. J. W. Elder, P. A. Dube, J. E. Greedan, H. A. Jenkins, J. F. Britten and I. Vargas-Baca, *CrystEngComm*, **15**, 7434 (2013).
35. A. C. Gomes, G. Biswas, A. Banerjee and W. L. Duax, *Acta Crystallogr*., **C45**, 73 (1989).
36. A. F. Cozzolino, A. D. Bain, S. Hanhan and I. Vargas-Baca, *Chem. Commun*., 4043 (2009).
37. J. Lee, L. M. Lee, Z. Arnott, H. Jenkins, J. F. Britten and I. Vargas-Baca, *New J. Chem*., **42**, 10555 (2018).

38. L. M. Lee, P. J. W. Elder, A. F. Cozzolino, Q. Yang and I. Vargas-Baca, *Main Group Chem*., **9**, 117 (2010).
39. M. Risto, R. W. Reed, C. M. Robertson, R. Oilunkaniemi, R. S. Laitinen and R. T. Oakley, *Chem. Commu*n., 3278 (2008).
40. (a) L. M. Lee, V. B. Corless, M. Tran, H. Jenkins, J. F. Britten and I. Vargas-Baca, *Dalton Trans*., **45**, 3285 (2016); (b) L. M. Lee, V. B. Corless, H. Luu, A. He, H. Jenkins, J. F. Britten, F. A. Pani and I. Vargas-Baca, *Dalton Trans*., **48**, 12541 (2019).
41. J. L. Dutton, J. J. Tindale, M. C. Jennings and P. J. Ragogna, *Chem. Commun*., 2474 (2006).
42. J. L. Dutton, A. Sutrisno, R. W. Schurko and P. J. Ragogna, *Dalton Trans*., 3470 (2008).
43. (a) J. L. Dutton and P. J. Ragogna, *Coord. Chem. Rev*., **255**, 1414 (2011); (b) J. L. Dutton and P. J. Ragogna, in *Selenium and Tellurium Chemistry: From Small Molecules to Biomolecules and Materials*, Eds. J. D. Woollins and R. S. Laitinen, Springer (2011), Ch. 8, pp. 179–199.
44. J. L. Dutton and P. J. Ragogna, *Inorg. Chem.*, **48**, 1722 (2009).
45. T. Chivers and J. Konu, *Angew. Chem. Int. Ed*., **48**, 3025 (2009).
46. (a) C. D. Martin, M. C. Jennings, M. J. Ferguson and P. J. Ragogna, *Angew. Chem. Int. Ed*., **48**, 2210 (2009); (b) C. D. Martin and P. J. Ragogna, *Inorg. Chem*., **49**, 4324 (2010).
47. J. L. Dutton, H. M. Tuononen, M. C. Jennings and P. J. Ragogna, *J. Am. Chem. Soc.*, **128**, 12624 (2006).
48. J. L. Dutton and P. J. Ragogna, *Chem. Eur. J*., **16**, 12454 (2010).
49. H. M. Tuononen, R. Roesler, J. L. Dutton and P. J. Ragogna, *Inorg. Chem*., **46**, 12374 (2007).
50. (a) V. N. Ikorskii, I. G. Irtegova, E. Lork, A. Yu. Makarov, R. Mews, V. I. Ovcharenko and A. V. Zibarev, *Eur. J. Inorg. Chem*., **2006**, 3061 (2006); (b) A. Yu. Makarov, I. G. Irtegova, N. V. Vasilieva, I. Yu. Bagryanskaya, T. Borrmann, Yu. V. Gatilov, E. Lork, R. Mews, W.-D. Stohrer and A. V. Zibarev, *Inorg. Chem*., **44**, 7194 (2005).
51. E. A. Suturina, N. A. Semenov, A. V. Lonchakov, I. Yu. Bagryanskaya, Y. V. Gatilov, I. G. Irtegova, N. V. Vasilieva, E. Lork, R. Mews, N. P. Gritsan and A. V. Zibarev, *J. Phys. Chem. A*, **115**, 4851 (2011).
52. N. A. Semenov, A. V. Lonchakov, N. A. Pushkarevsky, E. A. Suturina, V. V. Korolev, E. Lork, V. G. Vasiliev, S. N. Konchenko, J. Beckmann, N. P. Gritsan and A. V. Zibarev, *Organometallics*, **33**, 4302 (2014).

53. G. E. Garrett, G. L. Gibson, R. N. Straus, D. S. Seferos and M. S. Taylor, *J. Am. Chem. Soc*., **137**, 4126 (2015).
54. N. A. Pushkarevsky, E. A. Chulanova, L. A. Shundrin, A. I. Smolentsev, G. E. Salnikov, E. A. Pritchina, A. M. Genaev, I. G. Irtegiva, I. Yu. Bagryanskaya, S. N. Konchenko, N. P. Gritsan, J. Beckmann and A. V. Zibarev, *Chem. Eur. J.*, **25**, 806 (2019).
55. N. A. Pushkarevsky, P. A. Petrov, D. S. Grigoriev, A. I. Smolentsev, L. M. Lee, F. Kleemiss, G. E. Salnikov, S. N. Konchenko, I. Vargas-Baca, S. Grabowsky, J. Beckmann and A. V. Zibarev, *Chem. Eur. J*., **23**, 10987 (2017).
56. (a) D. Xia, X. Guo, L. Chen, M. Baumgarten, A. Keerthin and K. Müllen, *Angew. Chem. Int. Ed*., **55**, 941 (2016); (b) D. Xia, X-Y. Wang, X. Guo, M. Baumgarten, M. Li and K. Müllen, *Cryst. Growth Des*., **16**, 7124 (2016).
57. J. Du, M. C. Biewer and M. C. Stefan, *J. Mater. Chem*., **4**, 15771 (2016).
58. (a) F. Ni. Z. Wu, Z. Zhu, T. Chen, K. Wu, C. Zhong, K. An, D. Wei, D. Ma and C. Yang, *J. Mater. Chem. C*, **5**, 1363 (2017); (b) Y. Zhang, Z. Chen, X. Wang, J. He, J. Wu, H. Liu, J. Song, J. Qu, W. T-K. Chan and W-Y. Wong, *Inorg. Chem*., **57**, 14208 (2018); (c) Y. Zhang, Z. Chen, J. Song, J. He, X. Wang, J. Wu, S. Chen, J. Qu and W-Y. Wong, *J. Mater. Chem. C*, **7**, 1880 (2019); (d) V. M. Korshunov, T. N. Chmovzh, E. A. Knyazeva, I. V. Tyadakov, L. V. Mikhalchenko, E. A. Varaksina, R. S. Saifutyarov, I. C. Avetissov and O. A. Rakitin, *Chem. Commun*., **55**, 13354 (2019); (e) V. M. Korshunov, T. N. Chmovzh, I. S. Golovanov, E. A. Knyazeva, L. V. Mikhalchenko, R. S. Saifutyarov, I. C. Avetissov, J. D. Woollins, I. V. Tyadakov, and O. A. Rakitin, *Dyes Pigm*., **185**, 108917 (2020).
59 X. Zhang, H. Bronstein, A. J. Kronemeijer, J. Smith, Y. Kim, R. J. Kline, L. J. Richter, T. D. Anthopoulos, H. Sirringhaus, K. Song, M. Heeney, W. Zhang, I. McCulloch and D. M. DeLongchamp, *Nat. Commun*., **4**, 2238 (2013).
60. J. Chen, C-L. Dong, D. Zhao, Y-C. Huang, X. Wang, L. Samad, L. Dang, M. Shearer, S. Shen and L. Guo, *Adv. Mater*., **29**, 1606198 (2017).
61. (a) T. O. Carvalho, P. H. P. R. Carvalho, J. R. Correa, B. C. Guido, G. A. Medeiros, M. N. Eberlin, S. E. Coelho, J. B. Domingos and B. A. D. Neto, *J. Org. Chem*., **84**, 5118 (2019); (b) P. H. P. R. Carvalho, J. R. Correa, K. L. R. Paiva, M. Baril, D. F. S. Machado, J. D. Scholten, P. E. N. de Souza, F. H. Veiga-Souza, J. Spencer and B. A. D. Neto, *Org. Chem. Front*., **6**, 2371 (2019).

62. C. H. Silveira, M. G. Fronza, R. A. Balaguez, A. M. E. Larroza, L. Savegnago, D. F. Back, B. A. Iglesias and D. Alves, *Dyes Pigm*., **185**, 108910 (2021).
63. Y. Wu and X. Zhu, *Chem. Soc. Rev*., **42**, 2039 (2013).
64. (a) H. Zhou, L. Yang, S. C. Price, K. J. Knight and W. You, *Angew*. *Chem. Int. Ed.*, **49**, 7992 (2010); (b) H. Zhou, L. Yang, A. C. Stuart, S. C. Price, S. Liu and W. You, *Angew*. *Chem. Int. Ed*., **50**, 2995 (2011); (c) M. Wang, X. Hu, P. Liu, W. Li, X. Gong, F. Huang and Y. Cao, *J. Am. Chem. Soc*., **133**, 9638 (2011).
65. (a) S. Chaurasia, C-Y. Hsu, H.-H. Chou and J. T. Lin, *Org. Electron*., **15**, 378 (2014); (b) E. A. Knyazeva, W. Wu, T. N. Chmovzh, N. Robertson, J. D. Woollins and O. A. Rakitin, *Sol. Energy*, **144**, 134 (2017).
66. S. David, H-J. Chang, C. Lopes, C. Brännlund, B. Le Guennic, G. Berginc, E. Van Stryland, M. V. Bondar, D. Hagan, D. Jacquemin, C. Andraud and O. Maury, *Chem. Eur. J.*, **27**, 3517 (2021).
67. Y. Zhang, Z. Chen, J. Sing, J. He, X. Wang, J. Wu, S. Chen, J. Qu and W.-Y. Wong, *J. Mater*. *Chem. C*, **7**, 1880 (2019).
68. (a) A. L. Appleton, S. Miao, S. M. Brombosz, N. J. Berger, S. Barlow, S. R. Marder, B. M. Lawrence, K. I. Hardcastle and U. H. F. Bunz, *Org. Lett*., **11**, 5222 (2009); (b) B. A. Coombs, B. D. Lindner, R. M. Edkins, F. Rominger, A. Beeby and U. H. F. Bunz, *New. J. Chem.*, **36**, 550 (2012); (c) B. D. Lindner, B. A. Coombs, M. Schaffroth, J. U. Engelhart, O. Tverskoy, F. Rominger, M. Hamburger and U. H. F. Bunz. *Org. Lett.*, **15**, 666 (2013); (d) B. D. Lindner, F. Paulus, A. L. Appleton, M. Schaffroth, J. U. Engelhart, K. M. Schelkle, O. Tverskoy, F. Rominger, M. Hamburger and U. H. F. Bunz, *J. Mater. Chem. C*, **2**, 9609 (2014).
69. C. H. Silveira, M. G. Fronza, R. A. Balaguez, A. M. E. Larroza, L. Savegnago, D. F. Back, B. A. Iglesias and D. Alves, *Dyes Pigm*., **185**, 108910 (2021).
70. Z. Wang, Z. Peng, K. Huang, P. Lu and Y. Wang, *J. Mater*. *Chem. C*, **7**, 6706 (2019).
71. S. Uchiyama, K. Kimura, C. Gota, K. Okabe, K. Kawamoto, N. Inada, T. Yoshihara and S. Tobita, *Chem. Eur. J*., **18**, 9552 (2012).
72. (a) C. Saravanan, S. Easwaramoorthi, C-Y. Hsiow, K. Wang, M. Hayashi and l. Wang, *Org. Lett.*, **16**, 354 (2014); (b) D. Li, M. Liu, J. Chen, J. Ding, X. Huang and H. Wu, *Macromol. Chem. Phys*., **215**, 82 (2014).
73. J. J. Bryant, B. D. Lindner and U. H. F. Bunz, *J. Org. Chem*., **78**, 1038 (2013).

74. A. F. Cozzolino, Q. Yang and I. Vargas-Baca, *Cryst. Growth Des*., **10**, 4959 (2010).
75. (a) D. O. Prima, E. V. Vorontsova, A. G. Makarov, A. Yu. Makarov, I. Yu. Bagryanskaya, T. F. Mikhailovskaya, Y. G. Slizhov and A. V. Zibarev, *Mendeleev Commun*., **27**, 439 (2017); (b) D. O. Prima, A. G. Makarov, I. Yu. Bagryanskaya, A. E. Kolesnokov, L. V. Zargarova, D. S. Baev, T. F. Eliseeva, L. V. Politanskaya, A. Yu. Makarov, Yu. G. Slizhov and A. V. Zibarev, *ChemistrySelect*, **4**, 2383 (2019).
76. (a) R. Appel, H. Janssen, M. Siray and F. Knoch, Chem. Ber., **118**, 1632 (1985); (b) T. M. Barclay, L. Beer, A. W. Cordes, R. C. Haddon, M. I. Itkis, R. T. Oakley, K. E. Preuss and R. W. Reed, *J. Am. Chem. Soc*., **121**, 6657 (1999).
77. Yu. M. Volkova, A. Yu. Makarov, E. A. Pritchina, N. P. Gritsan and A. V. Zibarev, *Mendeleev Commun*., **30**, 385 (2020).
78. L. D. Huestis, M. L. Walsh and N. Hahn, *J. Org. Chem*., **30**, 2763 (1965).
79. T. M. Barclay, A. W. Cordes, J. D. Goddard, R. C. Mawhinney, R. T. Oakley, K. E. Preuss and R. W. Reed, *J. Am. Chem. Soc*., **119**, 12136 (1997).
80. L. Beer, J. L. Brusso, A. W. Cordes, R. C. Haddon, M. E. Itkis, K. Kirschbaum, D. S. MacGregor, R. T. Oakley, A. A. Pinkerton and R. W. Reed, *J. Am. Chem. Soc*., **124**, 9498 (2002).
81. F. Blockhuys, N. P. Gritsan, A. Yu. Makarov, K. Tersago and A. V. Zibarev, *Eur. J. Inorg. Chem*., **2008**, 655 (2008).
82. (a) L. Beer, R. T. Oakley, J. R. Mingie, K. E. Preuss and N. J. Taylor, *J. Am. Chem. Soc*., **122**, 7602 (2000); (b) L. Beer, J. L. Brusso, A. W. Cordes, R. C. Haddon, M. E. Itkis, K. Kirschbaum, D. S. MacGregor, R. T. Oakley, A. A. Pinkerton and R. W. Reed, *J. Am. Chem. Soc*., **124**, 9498 (2002).
83. (a) L. Beer, R. C. Haddon, M. E. Itkis, A. A. Leitch, R. T. Oakley, R. W. Reed, J. F. Richardson and D. G. Vander Veer, *Chem. Commun*., 1218 (2005); (b) A. A. Leitch, R. T. Oakley, R. W. Reed and L. K. Thompson, *Inorg. Chem*., **46**, 6261 (2007); (c) S. M. Winter, A. R. Balo, R. J. Roberts, K. Lekin, A. Assoud, P. A. Dube and R. T. Oakley, *Chem. Commun*., **49**, 1603 (2013); (d) P. Vasko, J. Hurmalainen, A. Mansikkamäki, A. Peuronen, A. Mailman and H. M. Tuononen, *Dalton Trans*., **46**, 16004 (2017).
84. M. Risto, A. Assoud, S. M. Winter, R. Oilunkaniemi, R. S. Laitinen and R. T. Oakley, *Inorg. Chem*., **47**, 10100 (2008).
85. A. Yu. Makarov, F. Blockhuys, I. Yu. Bagryanska, Y. V. Gatilov, M. M. Shakirov and A. V. Zibarev, *Inorg. Chem*., **52**, 3699 (2013).

86. (a) A. Mailman, A. A. Leitch, W. Yong, E. Steven, S. M. Winter, R. C. M. Claridge, A. Assoud, J. S. Tse, S. Desgreniers, R. A. Secco and R. T. Oakley, *J. Am. Chem. Soc*., **139**, 2180 (2017); (b) K. Lekin, A. A. Leitch, A. Assoud, W. Yong, J. Desmarais, J. S. Tse, S. Desgreniers, R. A. Secco and R. T. Oakley, *Inorg. Chem*., **57**, 4757 (2018).
87. M. R. Tuttle and S. Zhang, *Chem. Mater*., **32**, 255 (2020).
88. (a) G. G. Alange, A. J. Banister, B. Bell and P. W. Millen, *J. Chem. Soc., Perkin Trans*. 1, 1192 (1979); (b) A. J. Banister, N. R. M. Smith and R. G. Hey, *J. Chem. Soc., Perkin Trans*. 1, 1181 (1983).
89. A. Apblett and T. Chivers, *Inorg. Chem*., **28**, 4544 (1989).
90. P. Del Bel Belluz, A. W. Cordes, E. M. Kristof, P. V. Kristof, S. W. Liblong and R. T. Oakley, *J. Am. Chem. Soc*., **111**, 9276 (1989).
91. A. W. Cordes, R. C. Haddon, R. T. Oakley, L. F. Schneemeyer, J. V. Waszczak, K. M. Young and N. M. Zimmerman, *J. Am. Chem. Soc*., **113**, 582 (1991).
92. A. I. Taponen, J. W. L. Wong, K. Lekin, A. Assoud, C. M. Robertson, M. Lahtinen, R. Clérac, H. M. Tuononen, A. Mailman and R. T. Oakley, *Inorg. Chem*., **57**, 13901 (2018).
93. A. W. Cordes, C. D. Bryan, W. M. Davis, R. H. de Laat, S. H. Glarum. J. D. Goddard. R. C. Haddon, R. G. Hicks, D. K. Kennepohl, R. T. Oakley, S. R. Scott and N. P. C. Westwood, *J. Am. Chem. Soc*., **115**, 7232 (1993).
94. M. P. Andrews, A. W. Cordes, D. C. Douglass, R. M. Fleming, S. H. Glarum, R. C. Haddon, P. Marsh, R. T. Oakley, T. T. M. Palstra, L. F. Schneemeyer, G. W. Trucks, R. R. Tycko, J. V. Waszczak, W. W. Warren, K. M. Young and N. M. Zimmerman, *J. Am. Chem. Soc*., **113**, 3559 (1991).
95. A. W. Cordes, R. C. Haddon, R. G. Hicks, R. T. Oakley, T. T. M. Palstra, L. F. Schneemeyer and J. F. Waszczak, *J. Am. Chem. Soc*., **114**, 5000 (1992).
96. A. W. Cordes, C. M. Chamchoumis, R. G. Hicks, R. T. Oakley, K. M. Young and R. C. Haddon, *Can. J. Chem*., **70**, 919 (1992).
97. A. W. Cordes, R. C. Haddon, C. D. MacKinnon, R. T. Oakley, G. W. Patenaude, R. W. Reed, T. Rietveld and K. E. Vajda, *Inorg. Chem*., **35**, 7626 (1996).
98. M. A. Nascimento and J. R. Rawson, in *Encyclopedia of Inorganic and Bioinorganic Chemistry*, John Wiley & Sons (2019), doi:10.1002/9781119951438.eibc2640.
99. A. Alberola, C. S. Clarke, D. A. Haynes, S. I. Pascu and J. M. Rawson, *Chem. Commun*., 4726 (2005).

100. Y. Beldjoudi, M. A. Nascimento, Y. J. Cho, H. Yu, H. Aziz, D. Tonouchi, K. Eguchi, M. M. Matsushita, K. Awaga, I. Osorio-Roman, C. P. Constantinides and J. M. Rawson, *J. Am. Chem. Soc*., **140**, 6260 (2018).
101. H.-U. Höfs, J. W. Bats, R. Gleiter, G. Hartmann, R. Mews, M. Eckert-Maksić, H. Oberhammer and G. M. Sheldrick, *Chem. Ber*., **118**, 3781 (1985).
102. (a) G. K. MacLean, J. Passmore, M. N. S. Rao, M. J. Schriver, P. S. White, D. Bethell, R. S. Pilkington and L. H. Sutcliffe, *J. Chem. Soc., Dalton Trans*., 1405 (1985); (b) S. Parsons and J. Passmore, *Acc. Chem. Res*., **27**, 101 (1994).
103. A. J. Banister, J. M. Rawson, W. Clegg and S. L. Birkby, *J. Chem. Soc., Dalton Trans*., 1099 (1991).
104. S. Parsons, J. Passmore, M. J. Schriver and P. S. White, *J. Chem. Soc., Chem. Commun*., 369 (1991).
105. A. J. Banister, I. Lavender, J. M. Rawson and W. Clegg, *J. Chem. Soc., Dalton Trans*., 859 (1992).
106. J. Jacobs, S. E. Ulic, H. Willner, G. Schatte, J. Passmore, S. V. Sereda and T. S. Cameron, *J. Chem. Soc., Dalton Trans*., 383 (1996).
107. A. J. Banister, I. Lavender, S. E. Lawrence, J. M. Rawson and W. Clegg, *J. Chem. Soc., Chem. Commun*., 29 (1994).
108. F. Sommer, *Ber. Dtsch. Chem. Ges*., **48**, 1833 (1915).
109. M.-J. Crawford, T. M. Klapötke, P. Klüfers, P. Mayer and P. S. White, *J. Am. Chem. Soc*., **122**, 9052 (2000).
110. M.-J. Crawford, T. M. Klapötke, P. Mayer and M. Vogt, *Inorg. Chem*., **43**, 1370 (2004).

Chapter 12

Diamagnetic Six-, Seven- and Eight-membered Carbon-Nitrogen-Chalcogen Rings

12.1 Introduction

This chapter is a continuation of the preceding discussion of diamagnetic five-membered carbon-nitrogen-chalcogen ring systems, which is now extended to include heterocycles with six or more atoms in the ring, as well as bicyclic systems. The isolobal relationship between an RC unit and S^+ as a substituent in a sulfur-nitrogen ring is still apposite (Sec. 4.8.1). Thus, a number of these larger neutral heterocycles have isoelectronic analogues among the cyclic binary S–N cations described in Chapter 5 and the concept of aromaticity is invoked in discussions of their electronic structures. Early work in this area was inspired by the intriguing notion that macrocycles or polymers incorporating –(R)CNSN– repeating units would have unusual conducting properties.[1a] Such polymers incorporating three-coordinate carbon have not been achieved, but S–N chains with aryl or heteroaryl linkages are insulators.[1b] From an experimental viewpoint the synthesis, structures and reactions of the antiaromatic 12π-electron benzo-1,3-dichalogena-2,4-diazines has been the most active area of recent investigations (Sec. 12.2.1).[2] Theoretical work has focused on the concept of "pancake bonding" in the dimerisation of 8π-electron 1,3-dithia-2,4,6-triazines (Secs. 4.10 and 12.2.2),[3] as well as the nature of weak intramolecular chalcogen-chalcogen interactions in bicyclic

molecules such as 1,5-dithia-2,4,6,8-tetrazocines (Secs. 4.9 and 12.4.1).[4] Six-, seven- and eight-membered rings will be discussed in that order. Ring systems that incorporate two-coordinate sulfur or selenium will be considered first followed by those that contain three- or four-coordinate chalcogen atoms.

12.2 Benzo-1,3-dichalcogena-2,4-diazines

12.2.1 *Synthesis*

In keeping with the discussion of benzo-2-chalcogena-1,3-diazoles and benzo-1-chalcogena-2,5-diazoles in the previous chapter (Sec. 11.2), benzo-1,3-dichalcogena-2,4-diazines are considered here to be six-membered rings because they are benzo-fused derivatives of the unknown dithiatriazine 1,3,2,4-$(HC)_2S_2N_2$,[2] which would be an 8π-electron system isoelectronic with $[S_3N_3]^+$ (Sec. 5.8.5). The parent benzodithiadiazine **12.1** (R = H), an inorganic naphthalene analogue, is obtained as a volatile deep-blue solid by the reaction of $C_6H_5NSNSiMe_3$ with SCl_2, followed by an intramolecular ring closure of the intermediate $C_6H_5NSNSCl$ with elimination of HCl (Schemes 2.3 and 12.1).[5] This procedure is successful for a wide variety of benzo-1,3-dithia-2,4-diazines, but the yields vary from very low for **12.1** (R = 7-I) to moderate for **12.1** (R = 6-F).[2,6,7] Low yields are the result of further reaction with SCl_2 to form benzo-1-dithia-2,3-azolium chlorides and this reaction can be used as an alternative to the traditional synthesis of Herz salts (Sec. 11.3).[2,8]

An alternative route to benzo-1,3-dithia-2,4-diazines for polyfluorinated derivatives involves nucleophilic ring closure. For example, the

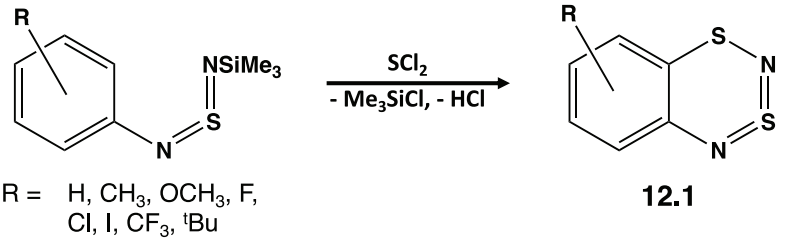

Scheme 12.1. Synthesis of benzo-1,3-dichalcogena-2,4-diazines by electrophilic ring closure.

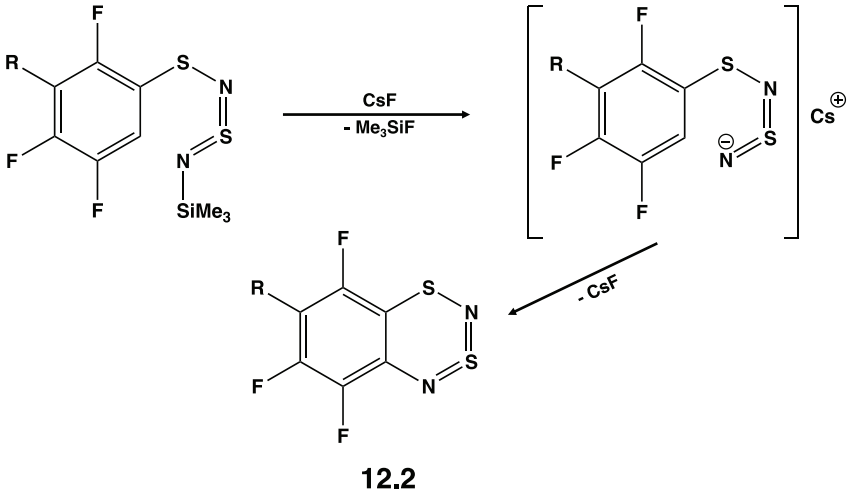

12.2

Scheme 12.2. Synthesis of tetrafluorobenzo-1,3-dithia-2,4-diazine by nucleophilic ring closure.

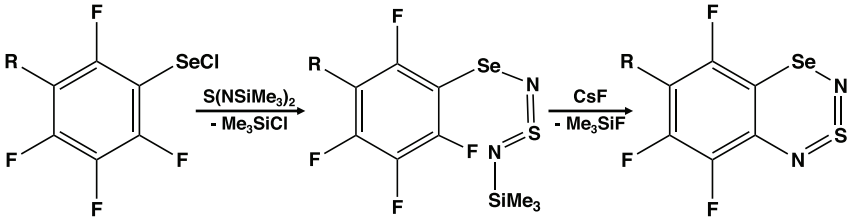

12.3 R = F, H

Scheme 12.3. Synthesis of polyfluorinated benzo-3-thia-1-selena-2,4-diazines by nucleophilic ring closure.

tetrafluoro derivative **12.2** (R = F) is prepared by treatment of $C_6F_5SNSNSiMe_3$ with CsF in acetonitrile (Scheme 12.2).[7,9] Difluoro- and trifluoro-benzodithiadiazines of **12.1** have been obtained by both methods depicted in Schemes 12.1 and 12.2.[2,7]

Mixed chalcogen systems, *e.g.*, polyfluorinated benzo-3-thia-1-selena-2,4-diazines can also be prepared by nucleophilic cyclisation. Thus, treatment of RC_6F_4SeCl with $Me_3SiN{=}S{=}NSiMe_3$ produces $RC_6F_4SeNSNSiMe_3$ (R = F, H), which reacts with cesium fluoride in acetonitrile to give benzo-3-thia-1-selena-2,4-diazines in low (**12.3**, R = F) or moderate (**12.3**, R = H) yields (Scheme 12.3).[10]

12.2.2 *Molecular and electronic structures*

X-ray structural investigations of the heterocycles **12.1** (R = H) and **12.2**, as well as a large number of mono-, di- and tri-substituted benzodithiadiazines, reveal a structural dichotomy indicative of the influence of packing effects. The prototypical **12.1** (R = H) and its 5-CF_3, 6-F, 7-Br, 7-OCH_3, 5,6,7-F_3 and 5,6,8-F_3 derivatives all have essentially planar structures in the solid state.[2,5–9,11] By contrast, the dithiadiazine ring in the tetrafluoro analogue **12.2** (R = F) and 5-Br, 5-OCH_3, 6-CH_3, 8-Br, 5,7-^{t}Bu$_2$ and 6,8-F_2 derivatives of **12.1** is bent about the S···N axis by varying amounts (in the range 4°–26°). The mixed chalcogen derivative benzo-3-thia-1-selena-2,4-dithiadiazine **12.3** (R = F) is also slightly folded about the Se···N axis, but the crystal packing differs significantly from that in **12.2** (R = F).[10] The increased number of intermolecular short contacts in **12.3** (R = F) result in channel-like cavities that encapsulate molecular N_2.

The influence of packing effects is removed by carrying out gas-phase structural determinations by electron diffraction (Sec. 3.1.2). Interestingly, the structure of **12.1** (R = H) is non-planar and the 5,6,7-F_3 derivative deviates only slightly from planarity in the gas phase, whereas the structures of **12.2** (R = F) and the 6,8-F_2 derivative of **12.1** are planar.[12,13] Theoretical studies indicate that the variation of the heterocyclic ring conformation in different phases can be attributed to packing effects; strong intermolecular interactions lead to a planar conformation in the solid state, whereas weak interactions do not perturb folded conformations.[14]

The low first ionisation energies and enhanced magnetic shielding of the ^{1}H NMR resonances of benzo-1,3-dichalcogena-2,4-diazines are consistent with antiaromaticity. In that context the electronic structures of these carbon-chalcogen-nitrogen heterocycles have been investigated by a wide variety of quantum chemical calculations.[7,12,13,15,16] The following findings are pertinent: (a) in a planar conformation the carbocycle and the ESN_2 (E = S, Se) unit form a 12π-electron system, (b) calculated NICS(0) values (Sec. 4.3) are negative for the carbocylic ring, but positive for the heterocyclic ring consistent with aromaticity and antiaromaticity, respectively, and (c) fluorination of the carbocyclic ring increases the NICS(0) values for that ring from –6.7 to –11.8 ppm and for the heterocyclic ring from 10.7 to 14.9 ppm (a –C=C– unit is common to both rings). These

findings lead to the general conclusion that benzo-1,3-dichalcogena-2,4-diazines can be classified as conjugated nonaromatic molecules.[2]

12.2.3 *Reactions*

Thermolysis of benzo-1,3-dichalcogena-2,4-diazines in *dilute* hydrocarbon solutions at 150°C produces persistent Herz radicals (Sec. 13.2) in nearly quantitative yields (Scheme 12.4).[17–19] This methodology provides an alternative to the reduction of 1,2,3-benzodiazolium salts for the preparation of Herz radicals. By contrast, the thermolysis of **12.1** (R = H) or **12.2** (R = F) in *concentrated* (0.5 M) hydrocarbon solvents at 150–170°C generates a mixture of carbon-sulfur-nitrogen heterocycles, including some fused polycyclic systems that were isolated in very low yields by column chromatography and structurally characterised.[20]

Similar to the behaviour of **12.1** (R = H) upon thermolysis in dilute solutions (Scheme 12.4), photolysis with UV irradiation at 313 or 365 nm results in ring contraction to form the corresponding Herz radical and dinitrogen.[21] The intermediates formed in this photochemical process were characterised in a matrix isolation study in argon at 12 K by using IR and UV-visible spectroscopy supported by quantum chemical calculations.[22] The intermediate **12.4** can be represented by singlet nitrene RS–N and thiazyl RS≡N resonance structures (Scheme 12.5), *cf.* photolysis of S_4N_4 (Sec. 6.9).

The reactions of **12.1** (R = H) or **12.2** (R = F) with triphenylphosphine PPh_3 result in ring contraction to produce an iminophosphorane **12.5** featuring a chiral S(IV) centre (Scheme 12.6) which, in the case of **12.1**

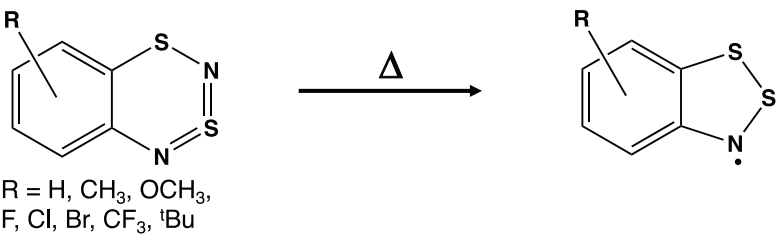

Scheme 12.4. Thermolysis of benzo-1,3-dichalcogena-2,4-diazines in hydrocarbon solvents.

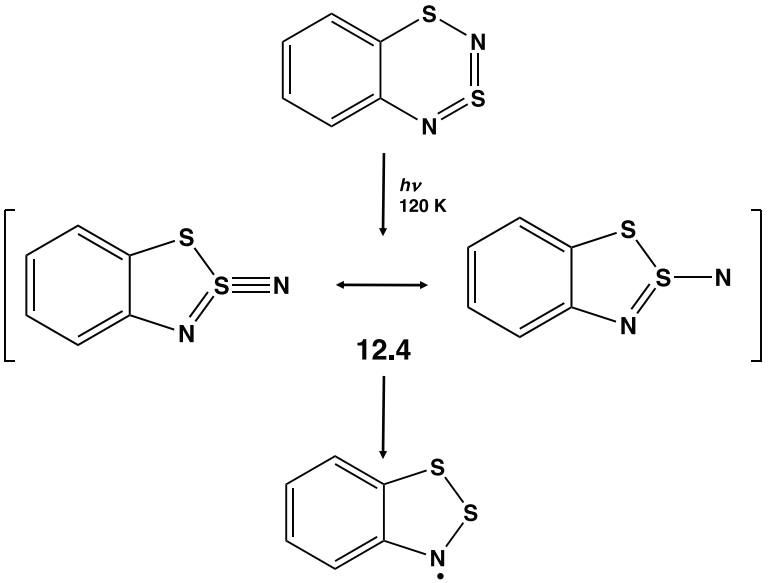

Scheme 12.5. A nitrene intermediate formed in the photolysis of **12.1** (R = H).

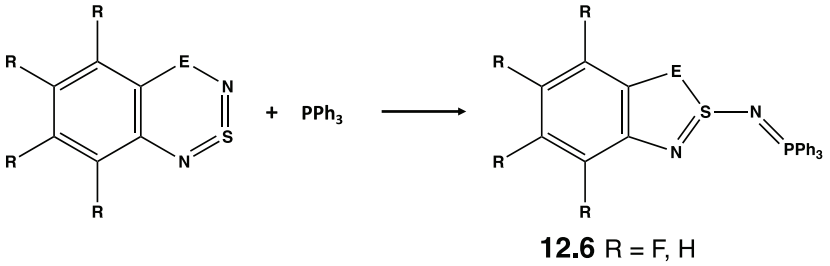

Scheme 12.6. Ring contraction upon reaction of benzo-1,3-dichalcogena-2,4-diazines with PPh_3.

(R = H), can be considered as the PPh_3 adduct of the nitrene intermediate **12.4** formed upon photolysis (Scheme 12.5).[23–25] This ring contraction also occurs rapidly at low temperatures for the 6,7-F_2 and 6,8-F_2 derivatives of **12.1**, as well as the 5,6,8-F_3 derivative of **12.1** and the mixed chalcogen system **12.3** (X = H).[24,25]

The redox behaviour of **12.1** (R = H), **12.2** (R = F) and various alkylated and fluorinated derivatives of **12.1** has been studied by cyclic

voltammetry. The radical anions are highly unstable, whereas the radical cations in the hydrocarbon series are relatively long-lived and could be characterised by EPR spectroscopy.[26]

12.3 1-Chalcogena-2,4,6-triazinyl derivatives

E-Monohalogenated 1-chalcogena-2,4,6-triazinyl derivatives (**12.7**, E = S, Se) are important precursors for the corresponding 7π-electron radicals, $[(RC)_2N_3E]^{\bullet}$ (**12.8**, E = S, Se) (Chart 12.1), which are discussed in Sec. 13.2. Reduction of **12.8** (E = S, R = Ph) by sodium in liquid ammonia produces the anion, which has been isolated as the protonated derivative **12.9** (E = S, R = Ph).[27]

The *E*-monohalogenated derivatives **12.7** (E = S, Se; R = Ph), are best prepared by the condensation of imidoyl amidines with SCl_2 or $SeCl_4$, respectively (Scheme 12.7).[28] In the case of the selenium derivative, the

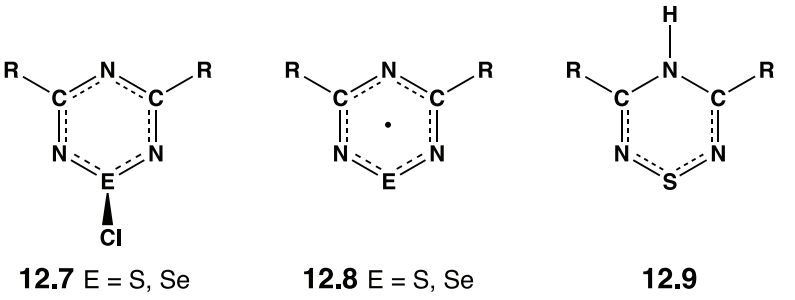

Chart 12.1. 1-Chalcogena-2,4,6-triazinyl derivatives.

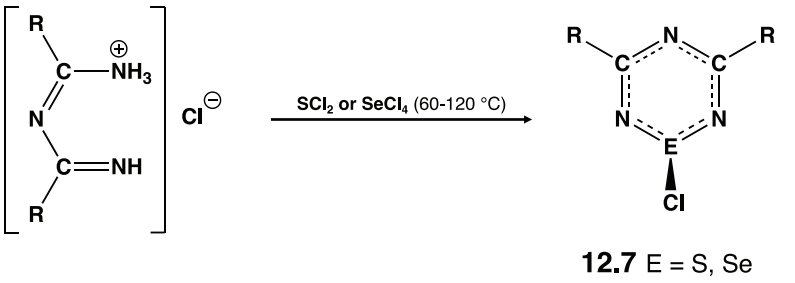

Scheme 12.7. Synthesis of *E*-monochloro-1-chalcogena-2,4,6-triazines.

initial product is heated at 60°C and then at 120°C in order to generate **12.7** (E = Se, R = Ph).[29] Similar methodology has been used to prepare the bis(thienyl) derivative **12.7** (E = S, R = C_4H_3S),[30] as well as unsymmetrical derivatives of the type (ArC)(CF_3C)N_3SCl (Ar = 4-XC_6H_4, X = H, Me, OMe, Cl, CF_3) in high yields.[31]

The related cyanuric-thiazyl system $(ClC)_2N_3SCl$ (**12.10**, X = Cl) (Chart 12.2) is obtained in good yield by the reaction of sodium dicyanamide with thionyl chloride in DMF.[32] This trihalogenated heterocycle reacts with sodium alkoxides or aryloxides with preferential substitution at sulfur.[32b] Trisubstitution can be achieved without ring degradation to give $[(RO)C]_2N_3S(OR)$ (R = Me, Et, CH_2CF_3, Ph). The reaction of **12.10** (X = Cl) with trialkylamines results in cleavage of a C–N bond of the tertiary amine and regiospecific substitution of the dialkylamino group on the carbon atoms of the heterocycle.[33] For example, treatment of **12.10** (X = Cl) with tetramethylmethylenediamine produces $[(Me_2N)C]_2N_3SCl$. The oxidation of **12.10** (X = Cl) with a mixture of $KMnO_4$ and $CuSO_4$. xH_2O (x = 4–6) produces the hybrid cyanuric-sulfanuric ring **12.11** as a low-melting solid.[32b] The S–Cl bond length and mean S–N bond distances of 1.99 and 1.58 Å, respectively, for this four-coordinate sulfur(VI) system[32c] are both significantly shorter than the values of 2.13 and 1.62 Å found for the analogous sulfur (IV) heterocycle **12.10** (X = Cl).[34] The gas-phase structure of the corresponding trifluoro derivative **12.10** (X = F) has been determined by electron diffraction [d(S–N) = 1.59 Å].[35]

S-Alkyl functionalisation of the 1-thia-2,4,6-triazine ring has been achieved by using the protonated bis(2-pyridyl) derivative **12.12** as a precursor to either an anionic or a cationic intermediate, **12.13** and **12.14**, respectively (Scheme 12.8).[36] Hydrolysis of **12.13** in dichloromethane or treatment of **12.14** with sodium hydride in THF produces the

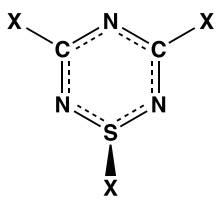

12.10 X = Cl, F

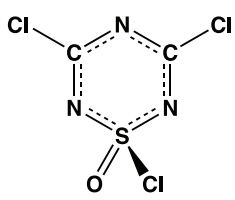

12.11

Chart 12.2. Six-membered cyanuric-thiazyl and -sulfanuric rings.

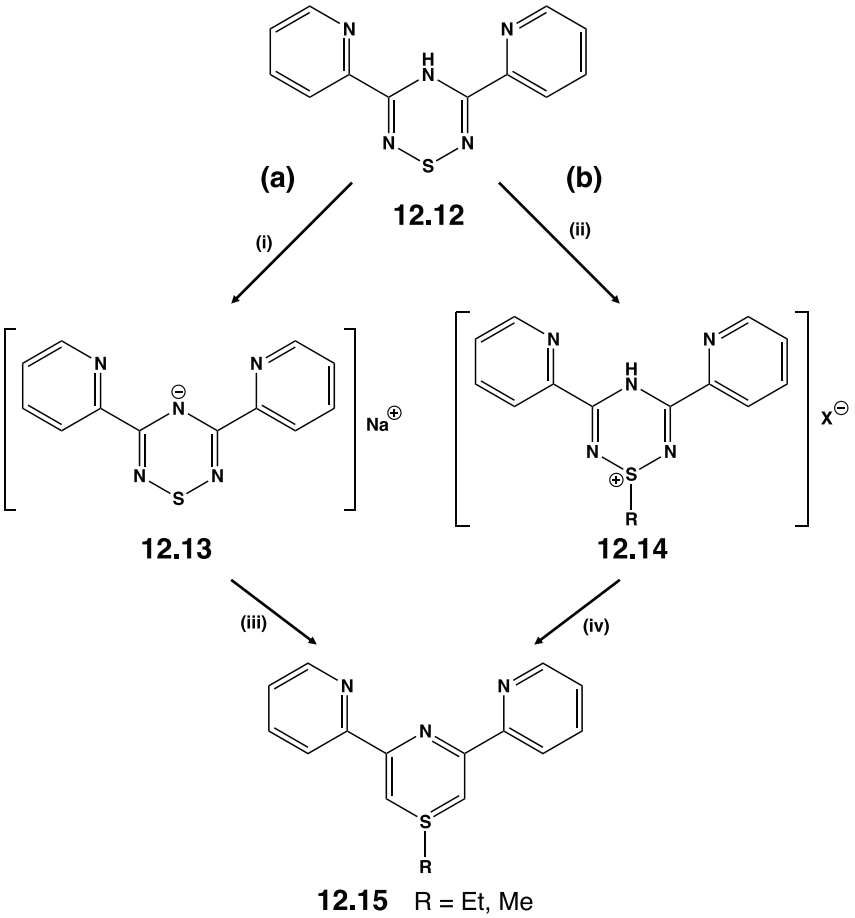

Scheme 12.8. Synthesis of *S*-alkyl-bis(2-pyridyl)thiatriazines *via* (a) anionic or (b) cationic intermediates: (i) NaH (ii) $[Et_3O][BF_4]$ or MeOTf (iii) H_2O.

S-alkyl derivatives **12.15** in high yields.[37] These protocols have been extended to generate derivatives in which two 1-thia-2,4,6-triazinyl ring are joined by a $-(CH_2)_n-$ linkage (n = 4, 5, 6, 8, 10).[38]

12.4 1,5-Dithia-2,4,6-triazines

The six-membered 1,5-dithia-2,4,6-triazine ring **12.16** is an 8π-electron system isoelectronic with $[S_3N_3]^+$ (Sec. 5.8.5) (Chart 12.3). This

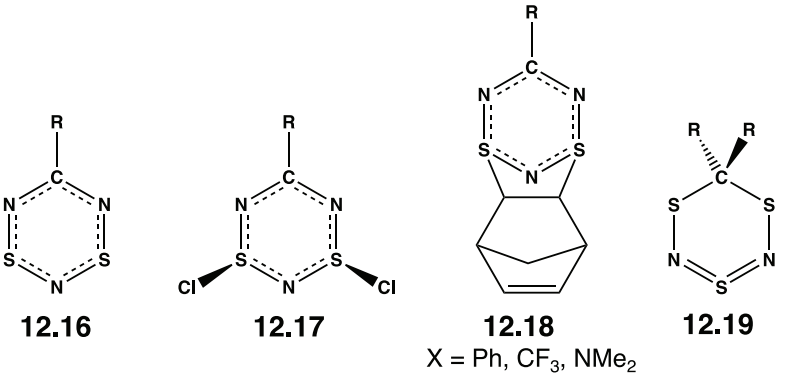

Chart 12.3. Six-membered RCN_3S_2 and RCN_3S_3 ring systems.

heterocycle is prepared by reduction of the corresponding *S,S'*-dichloro derivatives **12.17**, which can be generated in two ways: (a) chlorination of the bicyclic systems RCN_5S_3 (Sec. 12.10) with gaseous chlorine[39–41] or (b) the treatment of organic nitriles RCN with $(NSCl)_3$ (Scheme 2.5). The latter reactions are slow at room temperature for R = ^{t}Bu, CCl_3, CF_3, Ph, but proceed efficiently on mild heating in CCl_4 for dialkylcyanamides to produce **12.17** (R = NMe_2, NEt_2, N^iPr_2).[42] The X-ray structures of **12.17** (R = CF_3,[43] Ph,[44] NMe_2,[45] NEt_2[46]) reveal a *cis* arrangement of the two chlorine substituents in axial positions with S–Cl bond lengths ranging from *ca.* 2.10 Å (R = CF_3) to *ca.* 2.21 Å (R = NMe_2, NEt_2). As in the case of the cyclotrithiatriazine $(NSCl)_3$ (Sec. 8.7), this arrangement is stabilised by negative hyperconjugation (nitrogen lone pair → S–Cl σ^* bond).[48]

The reduction of yellow *S,S'*-dichloro derivatives **12.17** to the corresponding dark red, 1,5-dithia-2,4,6-triazines **12.16** can be achieved conveniently with $SbPh_3$ (R = aryl, CF_3) [3,39–41] or $Hg(SiMe_3)_2$ (R = NMe_2).[43–48] In the solid state the 8π-electron heterocycles **12.16** exist as cofacial dimers with S···S separations in the range of 2.5–2.6 Å.[3,14] ^{1}H NMR studies indicate that the dimeric structure is maintained in solution.[3] The dimerisation process is discussed in the context of "pancake bonding" in Sec. 4.10 (Fig. 4.17).[3,49,50] Although examples of monomeric **12.16** have not been isolated, the norbornadiene adducts **12.18** (R = Ph, CF_3, NMe_2) are readily formed, *cf.* $[S_3N_3]^+$ (Sec. 4.8). Selenium analogues of **12.16** are unknown.

12.5 1,3,5-Trithia-2,4-diazines

1,3,5-Trithia-2,4-diazines (**12.19**) (Chart 12.3) were first obtained from the reaction of S_4N_4 with diazoalkanes.[51] For example, the parent system **12.19** (R = H) was isolated as a red solid in 40% yield after passing diazomethane into a hot dichloromethane solution of S_4N_4. 1,3,5-Trithia-2,4-diazines are more conveniently synthesised from 1,1-bis(sulfenyl chlorides) $ClS–C(R)_2–SCl$ and $Me_3SiNSNSiMe_3$.[52] The six-membered ring in **12.19** adopts a half-chair conformation with long S–N bonds (1.67 Å) connecting the $–SCH_2S–$ and –N=S=N–units, in which the sulfur-nitrogen distances are *ca.* 1.55 Å.[51] These structural parameters are similar to those of the binary sulfur nitride S_4N_2 (Sec. 5.6.3), with which **12.19** (R = H) is isoelectronic.

12.6 1,3,5-Trithia-2,4-diazepines and Benzotrithiadiazepine Isomers

1,3,5-Trithia-2,4-diazepines are seven-membered, 10π-electron systems isoelectronic with $[S_4N_3]^+$ (Sec. 5.8.6). Benzo-1,3,5-trithia-2,4-diazepine **12.20** (R = H) is obtained as bright-yellow crystals by the reaction of benzo-1,2-bis(sulfenyl chloride) with $Me_3SiNSNSiMe_3$ (Scheme 12.9a).[5]

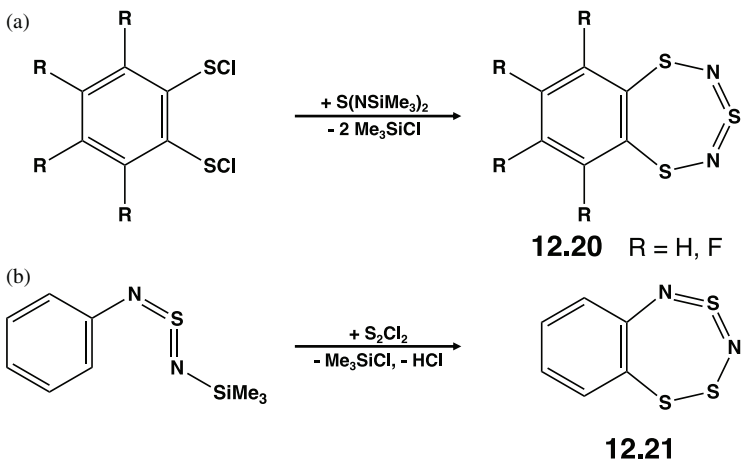

Scheme 12.9. Synthesis of benzotrithiadiazepine isomers.

The tetrafluoro derivative **12.20** (R = F) has been prepared by a similar procedure.[53] The isomeric benzo-1,2,4-trithia-3,5-diazepine (**12.21**) is obtained from the reaction of $PhNSNSiMe_3$ and S_2Cl_2, followed by intramolecular cyclisation (Scheme 12.9b).[54] The isomer **12.21** has also been identified as one of the products of the thermolysis of **12.1** (R = H).[20]

The parent 1,3,5-trithia-2,4-diazepine $(HC)_2N_2S_3$ (**12.22**) (Chart 12.4) is synthesised by cyclocondensation of $ClSCH(Cl)CH_2SCl$ with $Me_3SiNSNSiMe_3$.[55a] The seven-membered ring in **12.22** is planar and the bond lengths indicate complete delocalisation.[55b] The ^1H NMR spectrum of **12.22** in $CDCl_3$ shows a singlet in the aromatic region at δ 7.76.[55b] Cyclic voltammetry shows that **12.22** is more difficult to reduce and slightly easier to oxidise than the eight-membered ring **12.25** (R = H) (Chart 12.5).[56] The heterocycle **12.22** is inert to protic and Lewis acids and, as befits an aromatic system, it does not partake in cycloaddition reactions.[3] However, the benzo derivative **12.20** (R = H) undergoes reversible *S,S'*-cycloaddition with norbornadiene.[5] The parent heterocycle **12.22** undergoes standard electrophilic aromatic substitution reactions at carbon.

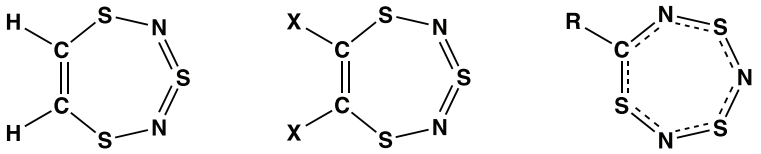

Chart 12.4. Seven-membered carbon-nitrogen-sulfur rings.

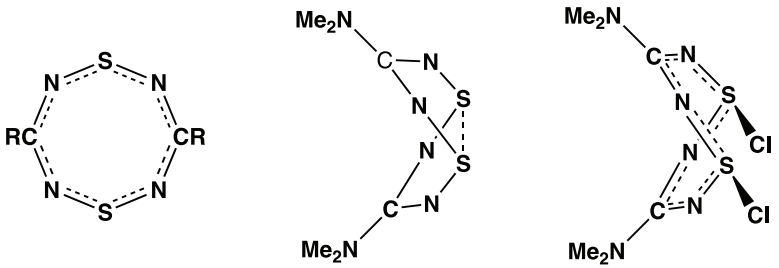

Chart 12.5. 1,5-Dithia-2,4,6,8-tetrazocines and an *S,S'*-dichloro derivative.

Thus, the disubstituted derivatives **12.23** (X = Br, NO_2, HgOAc) may be prepared by reactions of **12.22** with *N*-bromosuccinimide, $[NO_2][BF_4]$ or mercury(II) acetate, respectively. Precise X-ray structures of **12.23** (X = NO_2, CN) have been determined recently.[57]

12.7 1,3,5-Trithia-2,4,6-triazepines

The seven-membered 1,3,5,2,4,6-CN_3S_3 ring **12.24** (Chart 12.4) is also a 10π-electron system. It was first obtained as the ester **12.24** (R = CO_2Me), which is a minor product of the reaction of S_4N_4 with dimethylacetylene dicarboxylate.[58a] A precise X-ray structural determination of **12.24** (R = CO_2Me) has confirmed the planar structure with S–N bond lengths in the range 1.548(4)–1.607(4) Å.[57] A deformation density analysis of **12.24** (X = NO_2) reveals the partial ionic nature of the sulfur-nitrogen bonds in this heterocycle (Sec. 4.6).[57] The parent 1,3,5-trithia-2,4,6-triazepine **12.24** (R = H) is obtained as a colourless solid by carefully heating the ester with aqueous HCl followed by decarboxylation.[58b] The ^{1}H NMR resonance of **12.24** (R = H) occurs at δ 9.03 in $CDCl_3$ [*cf.* δ 9.70 for **12.25** (R = H)], indicating a diamagnetic ring current and aromatic character.[58b]

12.8 1,5-Dithia-2,4,6,8-tetrazocines

1,5-Dithia-2,4,6,8-tetrazocines, **12.25** (R = Ph) and **12.26** (Chart 12.5), were first prepared by the cyclocondensation of benzamidine or dimethylguanidine, respectively, with SCl_2 in the presence of a base.[59] The yields are low, however, and air oxidation of the corresponding dithiadiazolium salts $[ArCN_2S_2]X$ in the presence of $SbPh_3$ is a better alternative for the synthesis of aryl derivatives of **12.25**.[60] By the use of two different dithiadiazolium salts, this method can be adapted to generate unsymmetrically substituted dithiatetrazocines.[61] The reduction protocol has also been used to prepare 1,5-dithienyl derivatives of **12.25**, which are of interest for their optoelectronic properties.[62,63] 30 years after the seminal discovery of **12.25** (R = Ph), the parent 1,5-dithia-2,4,6,8-tetrazocine **12.25** (R = H) was obtained by the reaction of $[HCN_2S_2]Cl$ with *N,N,N′*-tris(trimethylsilyl) formamidine in acetonitrile at reflux, but the yields are low.[56]

The structures of 1,5-dithia-2,4,6,8-tetrazocines are notably dependent upon the nature of the group attached to carbon. The parent molecule **12.25** (R = H) and the diphenyl derivative in **12.25** (R = Ph) both exhibit planar heterocyclic rings with bond lengths that are consistent with a fully delocalised 10π-electron aromatic system (*cf.* $[S_4N_4]^{2+}$, Sec. 5.8.6).[56] Additional evidence of delocalisation comes from the EPR spectrum of the electrochemically generated anion radical of **12.25** (R = Ph), which reveals equal hyperfine coupling to all four nitrogen nuclei (Sec. 3.4.2, Fig. 3.11).[64] By contrast, the bis(dimethylamino) derivative **12.26** adopts a folded structure with d(S···S) = 2.43 Å.[59] Alternative explanations for this ring folding are discussed in Sec. 4.9.3.[65,66] Dithiatetrazocines with exocyclic N(Me)Bu groups exhibit both *cis/trans* and ring inversion isomerism on the NMR time scale.[67]

The aromaticity of **12.25** (R = H) is indicated by a ^{1}H NMR chemical shift of 9.70 ppm and an intense optical absorption band at λ_{max} 349 nm (in MeOH).[56] Consistent with its aromatic character, the planar ring **12.25** (R = Ph) has high thermal stability and is chemically unreactive. For example, it does not react with *n*-butyllithium, *m*-chloroperbenzoic acid or N_2O_4.[59,68] Furthermore, it exhibits no basic properties towards $HClO_4$.[40] By contrast, the folded ring **12.26** is readily oxidised and serves as an informative model for understanding the processes involved in the oxidation of sulfur-nitrogen heterocycles containing transannular S···S bonds. Two types of stereochemistries are involved in these oxidation processes. Reaction with Cl_2 or Br_2 produces an *exo,endo* geometry, as in the dichlorinated derivative **12.27**, whereas fluorination or reaction with the radical $[(CF_3)_2NO]^{\bullet}$ results in an *exo,exo* substitution pattern.[69] These different outcomes are the result of polar and radical oxidation mechanisms, respectively. The folded ring system **12.26** acts as an *S,S'*-bidentate ligand towards platinum upon reaction with $Pt(PPh_3)_4$.[70] It also behaves as a weak Lewis base *N*-donor towards Pt(II).[71]

12.9 The 1,3,5-trithia-2,4,6,8-tetrazocine cation

This eight-membered 1,3,5-trithia-2,4,6,8-tetrazocine monocation **12.28** (Chart 12.6) is a hybrid of the dication $[S_4N_4]^{2+}$ (Sec. 5.8.6) and

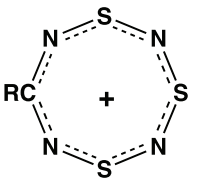

12.28

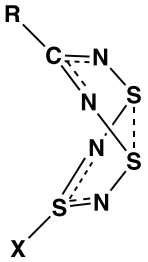

12.29

Chart 12.6. The 1,3,5-trithia-2,4,6,8-tetrazocine monocation and *S*-substituted derivatives.

1,5-dithia-2,4,6,8-tetrazocines **12.25**. In early work the $[CF_3CN_4S_3]^+$ cation (**12.28**, R = CF_3) was isolated in very low yields with either $[S_3N_3O_4]^-$ or $[AsF_6]^-$ counter-ions.[72,73] A more general route involves the reaction of the bicyclic systems RCN_5S_3 with the mercury(II) salt $[Hg(SO_2)_2][AsF_6]_2$ in liquid SO_2, which yields **12.28** (R = CF_3, Ph, 2-FC_6H_4, 2,6-$F_2C_6H_3$, NMe_2) as yellow or orange solids.[74]

The heterocyclic ring in the four derivatives **12.28** (R = CF_3, Ph, 2-FC_6H_4, 2,6-$F_2C_6H_3$) has an almost planar structure with S–N bond distances in the range 1.53–1.57 Å, consistent with a delocalised 10π-electron system.[73,75] The NICS(0) value of –17.2 for **12.28** (R = CF_3) indicates aromatic character; this value is reduced to –10.4 by the electron-donating dimethylamino group in **12.28** (R = NMe_2).[75] The eight-membered CN_4S_3 ring in **12.28** (R = NMe_2) is bent but, unlike the related dithiatetrazocine **12.26**, it does not exhibit a transannular S···S interaction. By contrast, the *S*-chloro derivative $Me_2NCN_4S_3Cl$ (**12.29**, R = NMe_2, X = Cl) has a folded structure with *d*(S···S) = 2.43 Å (Chart 12.6), identical to the value found for **12.26**. Folded structures with transannular S···S interactions in the range 2.41–2.46 Å are also observed for many other neutral 1,3,5-trithia-2,4,6,8-tetrazocines, *e.g.*, **12.28**, R = CF_3, X = $NEPh_3$, E = P, As; R = NMe_2, X = $NPPh_3$; R = 4-R′C_6H_4 (R′ = H, Cl, Me, OMe, CF_3), X = $NPPh_3$ or $NP(C_6H_4OMe\text{-}4)_3$.[73,76,77] Radical anions of the type $[RCN_4S_3]^{\bullet-}$ were detected at –50°C in CH_2Cl_2 by using the SEEPR technique (Sec. 3.4.2). These short-lived species decompose rapidly to the corresponding five-membered neutral radicals, *e.g.*, $[4\text{-}CF_3C_6H_4CN_2S_2]^{\bullet}$.[77]

12.10 Bicyclic Carbon-Nitrogen-Sulfur Ring Systems

A wide range of derivatives of the bicyclic ring systems RCN_5S_3 (**12.30**, R = alkyl, aryl, CF_3, NR'_2, Cl) have been prepared and structurally characterised.[73–78] The preferred synthesis for derivatives with R = Cl, CX_3 (X = F, Cl) or R'_2N (R′ = alkyl) involves the reaction of *S,S*′-dichlorodithiatriazines (**12.17**) with $Me_3SiNSNSiMe_3$ (Scheme 12.10a).[75,78] Aryl derivatives, on the other hand, are obtained by the reactions of trisilylated benzamidines with $(NSCl)_3$ (Scheme 12.10b).[79,80] A modification of the second route that employs lithium *N,N*'-bis(trimethylsilyl)amidines is necessary to prepare derivatives with electron-withdrawing aryl substituents such as C_6F_5 or 4-NCC_6H_4.[78]

The molecular structure of the bicyclic framework in **12.30** is best described as a dithiatriazine bridged by an –N=S=N– group. The bond lengths in the latter unit are 1.54–1.55 Å, indicative of double bonds, while the "connecting" S–N bonds (1.72–1.75 Å) reflect single-bond character and the S–N bonds in the remaining S_3N_3 unit fall within the intermediate range of 1.58–1.64 Å.[78,81] The exocyclic substituent R has only a minor effect on the structural parameters within the CN_5S_3 framework. Two fundamentally different packing arrangements are observed in the solid state: (a) stacking of RCN_5S_3 molecules and (b) face-to-face dimerisation of S_3N_3 subunits. Although these interactions are undoubtedly electrostatic in origin, there is no obvious correlation with the nature

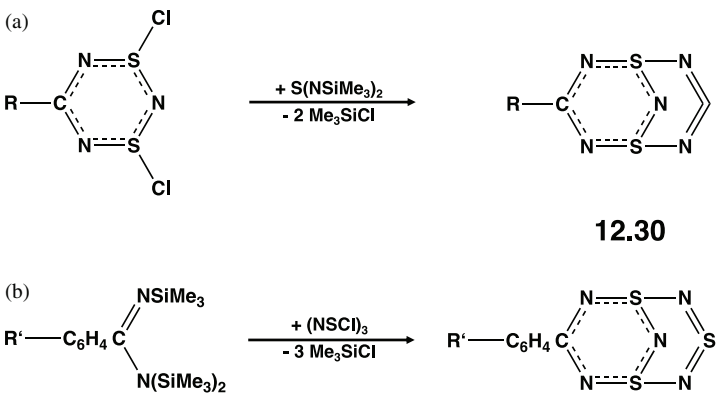

Scheme 12.10. Two routes for the synthesis of bicyclic ring systems RCN_5S_3.

of the R substituent attached to carbon. The aryl-substituted derivatives **12.30** (R = aryl) form 2:1 inclusion complexes with aromatic fluorocarbons or hydrocarbons.[82] The parallel-displaced arrangement of the aromatic rings of the host and guest in these complexes is typical of the non-covalent π-stacking interactions of the arene-polyfluoroarene type.

The bicyclic compounds **12.30** are susceptible to either nucleophilic or electrophilic attack. For example, reactions with the nucleophiles EPh_3 (E = P, As) transform **12.30** (R = Ph) into the monocyclic eight-membered ring **12.29** (R = Ph, X = $NEPh_3$).[77,83] The five nitrogen donor sites in RCN_5S_3 offer a rich coordination chemistry for this multifunctional ligand, as demonstrated by studies of the interaction of the trifluoromethyl derivative **12.30** (R = CF_3) with transition-metal ions. In contrast to protonation, which occurs at a nitrogen atom linked to the carbon centre,[84] the trifluoromethyl derivative **12.30** (R = CF_3) behaves as an *N*-monodentate ligand through the bridgehead nitrogen atom towards hard transition-metal cations (*e.g.*, Co^{2+}, Ni^{2+}, Cu^{2+}, Zn^{2+}, Cd^{2+} and Ag^{+}) as well as AsF_5. Consistently, calculations confirm that the largest negative charge resides on the bridgehead nitrogen atom. An *N,N'*-bridging mode involving the bridging nitrogen atom and a nitrogen atom next to the ring carbon atom has also been observed for Ag^{+} and Cd^{2+} complexes.[85] By contrast, the Hg^{2+} cation converts **12.30** (R = CF_3, NMe_2, Ph) to the corresponding cationic eight-membered rings **12.28** (R = CF_3) (Sec. 12.9).[74]

References

1. (a) M. P. Cava, M. V. Lakshmikantham, R. Hoffmann and R. M. Williams, *Tetrahedron*, **67**, 6771 (2011); (b) G. Wolmershäuser, J. Fuhrmann, R. Jotter, T. Wilhelm and O. J. Scherer, *Mol. Cryst. Liq. Cryst*., **118**, 435 (1985).
2. (a) F. Blockhuys, N. P. Gritsan, A. Yu. Makarov, K. Tersago and A. V. Zibarev, *Eur. J. Inorg. Chem*., **2008**, 655 (2008); (b) Yu. M. Volkova, A. Yu. Makarov, S. B. Zikirin, A. M. Genaev, I. Yu. Bagryanskaya and A. V. Zibarev, *Mendeleev Commun*., **27**, 19 (2017).
3. R. T. Boeré, *ACS Omega*, **3**, 18170 (2018).
4. R. Gleiter, G. Haberhauer and S. Woitschetzki, *Chem. Eur. J*., **20**, 13801 (2014).
5. A. W. Cordes, M. Hojo, H. Koenig, M. C. Noble, R. T. Oakley and W. T. Pennington, *Inorg. Chem*., **25**, 1137 (1986).

6. A. Yu. Makarov, S. N. Kim, N. P. Gritsan, I. Yu. Bagryanskaya, Yu. V. Gatilov and A. V. Zibarev, *Mendeleev Commun*., **15**, 14 (2005).
7. A. Yu. Makarov, I. Yu. Bagryanskaya, F. Blockhuys, C. Van Alsenoy, Yu. V. Gatilov, V. V. Knyazev, A. M. Maksimov, T. V. Mikhalina, V. E. Platonov, M. M. Shakirov and A. V. Zibarev, *Eur. J. Inorg. Chem*., **2003**, 77 (2003).
8. A. Yu. Makarov, I. Yu. Bagryanskaya, Yu. V. Gatilov, T. V. Mikhalina, M. M. Shakirov, L. N. Shchegoleva and A. V. Zibarev, *Heteroatom Chem*., **12**, 563 (2001).
9. A. V. Zibarev, Yu. V. Gatilov and A. O. Miller, *Polyhedron*, **11**, 1137 (1992).
10. A. Yu. Makarov, K. Tersago, K. Nivesanond, F. Blockhuys, C. Van Alsenoy, M. K. Kovalev, I. Yu. Bagryanskaya, Yu. V. Gatilov, M. M. Shakirov and A. V. Zibarev, *Inorg. Chem*., **45**, 2221 (2006).
11. I. Yu. Bagryanskaya, Yu. V. Gatilov, A. Yu. Makarov, A. M. Maksimov, A. O. Miller, M. M. Shakirov and A. V. Zibarev, *Heteroatom Chem*., **10**, 113 (1999).
12. A. R. Turner, F. Blockhuys, C. Van Alsenoy, H. E. Robertson, S. L. Hinchley, A. V. Zibarev, A. Yu. Makarov and D. W. H. Rankin, *Eur. J. Inorg. Chem*., **2005**, 572 (2005).
13. F. Blockhuys, S. L. Hinchley, A. Yu. Makarov, Yu. V. Gatilov, A. V. Zibarev, J. D. Woollins and D. W. H. Rankin, *Chem. Eur. J*., **7**, 3592 (2001).
14. I. Yu. Bagryanskaya, E. V. Bartaschevich, D. K. Nikulov, Yu. V. Gatilov and A. V. Zibarev, *J. Struct. Chem*., **50**, 127 (2009).
15. J. Oláh, F. Blockhuys, T. Veszprémi and C. Van Alsenoy, *Eur. J. Inorg. Chem*., **2006**, 69 (2006).
16. K. Tersago, C. De Dobbelaere, C. Van Alsenoy and F. Blockhuys, *Chem. Phys. Lett.,* **434**, 200 (2007).
17. A. Yu. Makarov, S. N. Kim, N. P. Gritsan, I. Yu. Bagryanskaya, Yu. V. Gatilov and A. V. Zibarev, *Mendeleev Commun*., **15**, 14 (2005).
18. I. V. Vlasyuk, V. A. Bagryansky, N. P. Gritsan, Yu. N. Molin, A. Yu. Makarov, Yu. V. Gatilov, V. V. Shcherbukhin, and A. V. Zibarev, *Phys. Chem. Chem. Phys*., **3**, 409 (2001).
19. V. A. Bagryansky, I. V. Vlasyuk, Yu. V. Gatilov, A. Yu. Makarov, Yu. N. Molin, V. V. Shcherbukhin and A. V. Zibarev, *Mendeleev Commun.*, **10**, 5 (2000).
20. V. V. Zhivonitko, A. Yu. Makarov, I. Yu. Bagryanskaya, Yu. V. Gatilov, M. M. Shakirov and A. V. Zibarev, *Eur. J. Inorg. Chem*., **2005**, 4099 (2005).
21. N. P. Gritsan, S. N. Kim, A. Yu. Makarov, E. N. Chesnokov and A. V. Zibarev, *Photochem. Photobiol. Sci*., **5**, 95 (2006).

22. N. P. Gritsan, E. A. Pritchina, T. Bally, A. Yu. Makarov and A. V. Zibarev, *J. Phys. Chem. A*, **111**, 817 (2007).
23. A. V. Zibarev, Y. V. Gatilov, I. Yu. Bagryanskaya, A. M. Maksimov and A. O. Miller, *J. Chem. Soc., Chem. Commun*., 299 (1993).
24. A. Yu. Makarov, V. V. Zhivonitko, A. G. Makarov, S. B. Zikirin, I. Yu. Bagryanskaya, V. A. Bagryansky, Y. V. Gatilov, I. G. Irtegova, M. M. Shakirov and A. V. Zibarev, *Inorg. Chem*., **50**, 3017 (2011).
25. T. D. Grayfer, A. Yu. Makarov, I. Yu. Bagryanskaya, I. G. Irtegova, Yu. V. Gatilov and A. V. Zibarev, *Heteroatom Chem*., **26**, 42 (2015).
26. N. V. Vasilieva, I. G. Irtegova, N. P. Gritsan, L. A. Shundrin, A. V. Lonchakov, A. Yu. Makarov and A. V. Zibarev, *Mendeleev Commun*., **17**, 161 (2007).
27. R. T. Boeré, A W. Cordes, P. J. Hayes, R. T. Oakley, R. W. Reed and W. T. Pennington, *Inorg. Chem*., **25**, 2445 (1986).
28. P. J. Hayes, R. T. Oakley, A. W. Cordes and W. T. Pennington, *J. Am. Chem. Soc*., **107**, 1346 (1985).
29. R. T. Oakley, R. W. Reed, A. W. Cordes, S. L. Craig and J. B. Graham, *J. Am. Chem. Soc*., **109**, 7745 (1987).
30. N. J. Yutronkie, A. A. Leitch, I. Korobkov and J. L. Brusso, *Cryst. Growth Des.*, **15**, 2524 (2015).
31. R. T. Boeré, T. L. Roemmele and X. Yu, *Inorg. Chem*., **50**, 5123 (2011).
32. (a) J. Geevers, J. T. Hackman and W. P. Trompen, *J. Chem. Soc. C*, 875 (1970); (b) T. Chivers, D. Gates, X. Li, I. Manners and M. Parvez, *Inorg. Chem*., **38**, 70 (1999); (c) T. J. Clark, T. Chivers, A. J. Lough and I. Manners, *Acta Crystallogr*., **E60**, O2402 (2004).
33. T. V. V. Ramakrishna, A. J. Elias and A. Vij, *Inorg. Chem*., **38**, 3022 (1999).
34. S-J. Chen, U. Behrens, E. Fischer, R. Mews, F. Pauer, G. M. Sheldrick, D. Stalke and W-D. Stohrer, *Chem. Ber.*, **126**, 2601 (1993).
35. E. Fischer, E. Jaudas-Prezel, R. Maggiulli, R. Mews, H. Oberhammer, R. Paape and W-D. Stohrer, *Chem. Ber*., **124**, 1347 (1991).
36. A. A. Leitch, I. Korobkov, A. Assoud and J. L. Brusso, *Chem. Commun*., **50**, 4934 (2014).
37. E. Kleisath, N. J. Yutronkie, I. Korobkov, B. M. Gabidullin and J. L. Brusso, *New J. Chem*., **40**, 4472 (2016).
38. N. J. Yutronkie, P. Tami, S. Singh, E. Kleisath, B. M. Gabidullin, R. Davis and J. L. Brusso, *New J. Chem*., **41**, 2268 (2017).
39. R. T. Boeré, C. L. French, R. T. Oakley, A. W. Cordes, J. A. J. Privett, S. L. Craig and J. B. Graham, *J. Am. Chem. Soc*., **107**, 7710 (1985).
40. A. W. Cordes, S. L. Craig, J. A. J. Privett, R. T. Oakley and R. T. Boeré, *Acta Crystallogr*., **42C**, 508 (1986).

41. R. T. Boeré, J. Fait, K. Larsen and J. Yip, *Inorg. Chem*., **31**, 1417 (1992).
42. A. Apblett and T. Chivers, *Inorg. Chem*., **28**, 4544 (1989).
43. H-U. Höfs, G. Hartmann, R. Mews and G. M. Sheldrick, *Z. Naturforsch*., **39B**, 1389 (1984).
44. J. B. Graham, A. W. Cordes, R. T. Oakley and R. T. Boeré, *Acta Crystallogr*., **42C**, 992 (1986).
45. H. W. Roesky, P. Schäfer, M. Noltemeyer and G. M. Sheldrick, *Z. Naturforsch*., **38B**, 347 (1983).
46. T. Chivers, J. F. Richardson and N. R. M. Smith, *Inorg. Chem*., **25**, 47 (1986).
47. E. Jaudas-Prezel, R. Maggiulli, R. Mews, H. Oberhammer, T. Paust and W.-D. Stohrer, *Chem. Ber*., **123**, 2123 (1990).
48. T. Chivers, F. Edelmann, J. F. Richardson, N. R. M. Smith, O. True, Jr., and M. Trsic, *Inorg. Chem*., **25**, 2119 (1986).
49. G. Haberhauer and R. Gleiter, *Chem. Eur. J*., **22**, 8646 (2016).
50. Z. Cui, H. Lischka, H. Z. Benebru and M. Kertesz, *J. Am. Chem. Soc*., **136**, 12958 (2014).
51. R. M. Bannister, R. Jones, C. W. Rees and J. D. Williams, *J. Chem. Soc., Chem. Commun*., 1546 (1987).
52. R. M. Bannister and C. W. Rees, *J. Chem. Soc., Perkin Trans.1*, 509 (1990).
53. I. Yu. Bagryanskaya, H. Bock, Yu. V. Gatilov, A. Haas, M. M. Shakirov, B. Salouki and A. V. Zibarev, *Chem. Ber*., **130**, 247 (1997).
54. A. Yu. Makarov, M. M. Shakirov, K. V. Shuvaev, I. Yu. Bagryanskaya, Y. V. Gatilov and A. V. Zibarev, *Chem. Commun*., 1774 (2001).
55. (a) J. L. Morris and C. W. Rees, *J. Chem. Soc., Perkin Trans. 1*, 211 (1987); (b) J. L. Morris and C. W. Rees, *J. Chem. Soc., Perkin Trans. 1*, 217 (1987).
56. K. H. Moock, K. M. Wong and R. T. Boeré, *Dalton Trans*., **40**, 11599 (2011).
57. R. Jones, *Acta Crystallogr*., **C70**, 60 (2014).
58. (a) S. T. A. K. Daley and C. W. Rees, *J. Chem. Soc., Perkin Trans. 1*, 203 (1987); (b) P. J. Dunn, J. L. Morris and C. W. Rees, *J. Chem. Soc., Perkin Trans. 1*, 1745 (1988).
59. I. Ernest, W. Holick, G. Rihs, D. Schomburg, G. Shoham, D. Wenkert and R. B. Woodward, *J. Am. Chem. Soc*., **103**, 1540 (1981).
60. R. T. Boeré, K. H. Moock, S. Derrick, W. Hoogerdijk, K. Preuss, J. Yip and M. Parvez, *Can. J. Chem*., **71**, 473 (1993).
61. A. D. Bond, D. A. Haynes and J. M. Rawson, *Can. J. Chem*., **80**, 1507 (2002).

62. S. S. Afjeh, A. A. Leith, I. Korobkov and J. L. Brusso, *RSC Adv.*, **3**, 23438 (2013).
63. F. Magnan, I. Korobkov and J. Brusso, *New. J. Chem.*, **39**, 7272 (2015).
64. R. T. Boeré, A. M. Bond, T. Chivers, S. W. Feldberg and T. L. Roemmele, *Inorg. Chem.*, **46**, 5596 (2007).
65. R. T. Oakley, *Prog. Inorg. Chem.*, **36**, 1 (1988).
66. R. Gleiter, G. Haberhauer and S. Witschetzki, *Chem. Eur. J.*, **20**, 13801 (2014).
67. R. A. Pascal, Jr. and R. P. L'Esperance, *J. Am. Chem. Soc.*, **116**, 5167 (1994).
68. M. Amin and C. W. Rees, *J. Chem. Soc. Perkin Trans. 1*, 2495 (1989).
69. R. T. Boeré, A. W. Cordes, S. L. Craig, R. T. Oakley and R. W. Reed, *J. Am Chem. Soc.*, **109**, 868 (1987).
70. T. Chivers, K. S. Dhathathreyan and T. Ziegler, *J. Chem. Soc., Chem. Commun.*, 86 (1989).
71. T. Chivers and R. W. Hilts, *Inorg. Chem.*, **31**, 5272 (1992).
72. H-U. Höfs, G. Hartmann, R. Mews and G. M. Sheldrick, *Angew. Chem. Int. Ed.*, **23**, 988 (1984).
73. C. Knapp, E. Lork, R. Maggiulli, P. G. Watson, R. Mews, T. Borrmann, W. D. Stohrer and U. Behrens, *Z. Anorg. Allg. Chem.*, **630**, 1235 (2004)
74. C. Knapp, P. G. Watson, E. Lork, D. H. Friese, R. Mews and A. Decken, *Inorg. Chem.*, **47**, 10618 (2008).
75. T. Chivers, J. F. Richardson and N. R. M. Smith, *Inorg. Chem.*, **25**, 272 (1986).
76. R. T. Boeré, A. W. Cordes and R. T. Oakley, *J. Am. Chem. Soc.*, **109**, 7781 (1987).
77. X. Yu, T. L. Roemmele and R. T. Boeré, *ChemElectroChem*, **5**, 968 (2018).
78. C. Knapp, E. Lork, T. Borrman, W-D. Stohrer, and R. Mews, *Eur. J. Inorg. Chem.*, **2003**, 3211 (2003).
79. (a) R. T. Boeré, C. L. French, R. T. Oakley, A. W. Cordes, J. A. J. Privett, S. L. Craig and J. B. Graham, *J. Am. Chem. Soc.*, **107**, 7710 (1985); (b) A. W. Cordes, S. L. Craig, J. A. J. Privett, R. T. Oakley and R. T. Boeré, *Acta Crystallogr.*, **42C**, 508 (1986).
80. R. T. Boeré, J. Fait, K. Larsen and J. Yip, *Inorg. Chem.*, **31**, 1417 (1992).
81. R. Maggiulli, R. Mews, W-D. Stohrer, M. Noltemeyer and G. M. Sheldrick, *Chem. Ber.*, **121**, 1881 (1988).
82. C. Knapp, E. Lork, R. Mews and A. V. Zibarev, *Eur. J. Inorg. Chem.*, **2004**, 2446 (2004).

83. R. T. Boeré, A. W. Cordes and R. T. Oakley, *J. Am. Chem. Soc*., **109**, 7781 (1987).
84. C. Knapp, E. Lork, R. Maggiulli, P. G. Watson, R. Mews. T. Borrmann, W.-D. Stohrer and U. Behrens, *Z. Anorg. Allg. Chem*., **630**, 1235 (2004).
85. C. Knapp and R. Mews, *Eur. J. Inorg. Chem.*, **2004**, 3536 (2004).

Chapter 13

Paramagnetic Carbon-Nitrogen-Chalcogen Rings: Magnetic Materials

13.1 Introduction

Paramagnetic systems have been a major focus of investigations of carbon-nitrogen-chalcogen (C,N,E where E = S, Se, Te) heterocycles over the past 15 years in view of their unusual magnetic and conducting properties that give rise to potential applications as functional materials, *e.g.*, as molecular switches. As a reflection of the intense interest in these novel materials, this area of chalcogen-nitrogen chemistry has been well-served by a number of general reviews.[1–6] In particular, a book chapter provides a comprehensive description of the early work on neutral, cyclic C,N,E radicals through to the end of 2008[7a] and that coverage has been extended to 2012.[7b] In addition, a wide range of articles have addressed the structures and properties of specific classes of paramagnetic C,N,E heterocycles, *viz.*, benzo-1,2-dichalcogena-3-azolyl radicals, 1,2-dithia-3,5-diazolyl radicals,[9,10] 1-chalcogena-2,5-diazolidyl radical anions,[11,12] and 1-thia-2,3,4-triazolyl radical cations.[13] Several recent book chapters and reviews also provide detailed discussions of the unique magnetic and electrical properties of cyclic chalcogenazyl radicals.[14–18]

In this chapter the most important aspects of the synthesis, molecular and electronic structures, properties and potential applications of neutral, cationic and anionic five- and six-membered paramagnetic C,N,E rings are discussed. Where appropriate, an emphasis will be placed on significant differences in structures and properties of selenium- and

tellurium-containing systems compared with those of their sulfur analogues. In most cases, these radicals are produced by one-electron reduction of diamagnetic heterocycles described in Chapters 11 and 12. Metal complexes of neutral paramagnetic C,N,E heterocycles are covered in the subsequent Chapter 14.

13.2 Monocyclic and Resonance-Stabilised 1,2-Dichalcogena-3-azolyl Radicals

1,2-Dithia-3-azolyl radicals were first identified in solution by EPR spectroscopy in the early 1980s. Since the late 1990s, developments in synthetic methods for benzo-fused derivatives, sometimes named Herz radicals, as well as bridged bis(1,2-dithia-3-azolyls) and their selenium analogues, have fuelled an explosive growth in this area of heterocyclic carbon-nitrogen-chalcogen chemistry. The intriguing conducting and magnetic properties of these paramagnetic materials are discussed in very recent reviews.[8,18]

13.2.1 *Synthesis*

1,2-Dithia-3-azolyl radicals (DTAs) can be monocyclic or fused to another ring. Monocyclic systems undergo carbon-centred reactivity, but they can be stabilised by steric protection or the attachment of an electron-withdrawing substituent in the 5-position, *e.g.*, **13.1**[19] and **13.2**[20] (Chart 13.1). Fusion with aromatic carbocycles gives rise to more stable derivatives, *e.g.*, benzo-fused 1,2-dithia-3-azolyls (BDTAs), also known as Herz radicals), *e.g.*, the prototypical derivative **13.3** and the naphthalene analogue **13.4**.[21] In addition, resonance effects may enhance stability through delocalisation of spin density. This feature gives rise to conducting materials with unique magnetic properties, as evidenced by extensive investigations of bis(1,2-dithia-3-azolyls) bridged by an *N*-containing heterocycle, **13.5**,[22–30] or an oxobenzene linkage, **13.6**.[31–41]

1,2,3-DTAs are prepared by either (a) one-electron reduction of the corresponding dithiazolium salts (Sec. 11.3), *e.g.*, with Zn, Sn, Mg, Cu, $SbPh_3$ or (b) thermolysis or photolysis of benzo-1,3-dithia-2,4-diazines

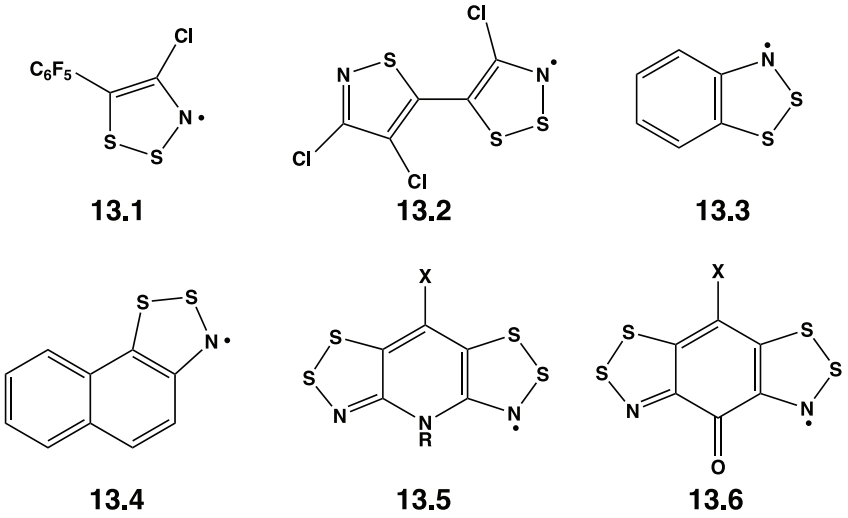

Chart 13.1. Stable monocyclic, fused and bridged 1,2-dithia-3-azolyl radicals.

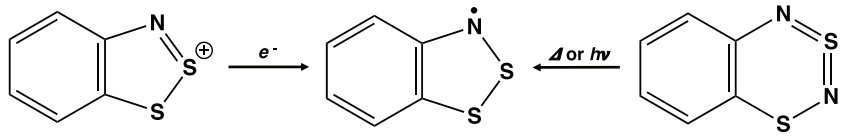

Scheme 13.1. Synthetic approaches to benzo-1,2-dithia-3-azolyl radicals.

(Sec. 12.2), as depicted in Scheme 13.1.[7] Many derivatives of the fused systems (**13.3** and **13.4**) and the bridged systems (**13.5** and **13.6**) in which one or both of the sulfur atoms are replaced by selenium have been synthesised by these methods in order to investigate the influence of the presence of the heavier chalcogen on their structures and magnetic or conducting properties.[8,17,18,42] To date, no tellurium analogues of 1,2,3-DTAs have been isolated.

13.2.2 *Molecular structures and properties*

Monocyclic 1,2,3-DTAs are 7π-electron systems isoelectronic with the binary radical cation $[S_3N_2]^{\bullet+}$ (Sec. 5.8.4). The singly occupied π-SOMO in these radicals is antibonding with respect to the CSSN fragment of the

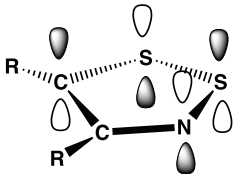

Figure 13.1. The π-SOMO of 1,2-dithia-3-azolyl radicals.

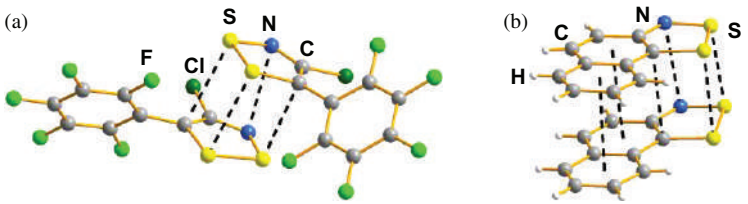

Figure 13.2. π^*–π^* Dimerisation in (a) monocyclic and (b) fused 1,2-dithia-3-azolyl radicals.

ring with no contribution from the carbon atom adjacent to nitrogen (Fig. 13.1).[2]

Non-fused 1,2,3-DTAs exhibit a propensity for σ-dimerisation. However, steric protection or extended π-conjugation inhibits σ-bond association in favour of a π^*–π^* interaction as illustrated in Fig. 13.2 for the monocyclic and fused radicals, **13.1** and **13.4**, respectively.[19,42,43] The inter-ring S···S distances of 3.2–3.3 Å in these dimers are generally longer than the corresponding interaction in dimers of the other paramagnetic C,N,S heterocycles discussed in this chapter. By contrast, the thiazole-substituted 1,2,3-DTA **13.2** exists in the solid state as a radical.[20] Experimental (EPR spectra) and computational studies (DFT calculations) show that the replacement of S by Se in **13.3** causes only minor perturbations in the electronic structures of these 1,2,3-BDTA radicals.[44] In the solid state, however, this exchange results in a strengthening of secondary bonding interactions leading to increased electrical conductivity and magnetic exchange interactions.[8] In addition, stronger spin-orbit coupling for the selenium atom results in significant magnetic anisotropy.

Detailed investigations of the influence of crystal structures on the magnetic and conducting properties of pyridine-bridged

bis(1,2-dithia-3-azolyls) of the type **13.5** have been carried out in attempts to identify a monocyclic C,N,E (E = S, Se) radical that exhibits metallic behaviour. Such a material should have a low value of the Coulomb barrier U, where U = Ionisation Potential – Electron Affinity, and an easily accessible LUMO. The substituent at N in the resonance-stabilised radicals **13.5** inhibits π^*–π^* dimerisation and all derivatives of pyridine-bridged bis(1,2-dithia-3-azolyls) adopt slipped π-stacked structures and retain their paramagnetism in the solid state. The slippage leads to the evolution of poorly developed band structures (σ_{RT} 10^{-5}–10^{-6} S cm^{-1}) and more localised electronic structures. Their magnetic behaviour is controlled by the magnitude and sign of the weak intermolecular exchange interactions within and between the herringbone-packed slipped π-stacks. Depending on the choice of R and X groups, and hence the nature of this slippage, weak antiferromagnetic or ferromagnetic responses are observed, but no indication of magnetic ordering has been found.[22–25] However, metamagnetism has been reported for **13.5** (R = Me, X = H).[45]

A series of *C*-fluorinated pyridine-bridged bis(1,2-dithia-3-azolyls) **13.5** (X = F) with *N*-alkyl substituents of increasing length have been synthesised and structurally characterised. For the longer alkyl chains (R = Bu, Pn, Hx) the adjacent columns of π-stacked radicals are bridged by short intermolecular F···S contacts that create spin-ladder arrays and antiferromagnetic behaviour.[28] Pyridine-bridged bis(1,2-dithia-3-azolyls) can be polymorphic as exemplified by the *N*-methyl-4-phenyl derivative **13.5** (R = Me, X = Ph).[30] In this case, the α- and β-phases both show slipped π-stacks of undimerised radicals and the crystal packing arrangements result in a predominantly antiferromagnetic response. In the high symmetry (trigonal) α-phase there is no clear indication of antiferromagnetic ordering above 2 K.

The introduction of an additional heteroatom in heterocyclic-bridged bis(1,2-dithia-3-azolyls) results in subtle structural variations involving a delicate balance between stable π-stacked radicals and various σ-bonded structures. For example, the pyrazine-bridged derivative **13.7** is polymorphic and exhibits a tendency to dimerise in the solid state *via* either C–C σ-bond formation in α-**13.7** (Fig. 13.3a) or a 4-centre-6-electron S---S–S---S arrangement in β-**13.7** (Fig. 13.3b).[26] The *N*-methyl analogue of **13.7** does not dimerise at room temperature; its structure is comprised of

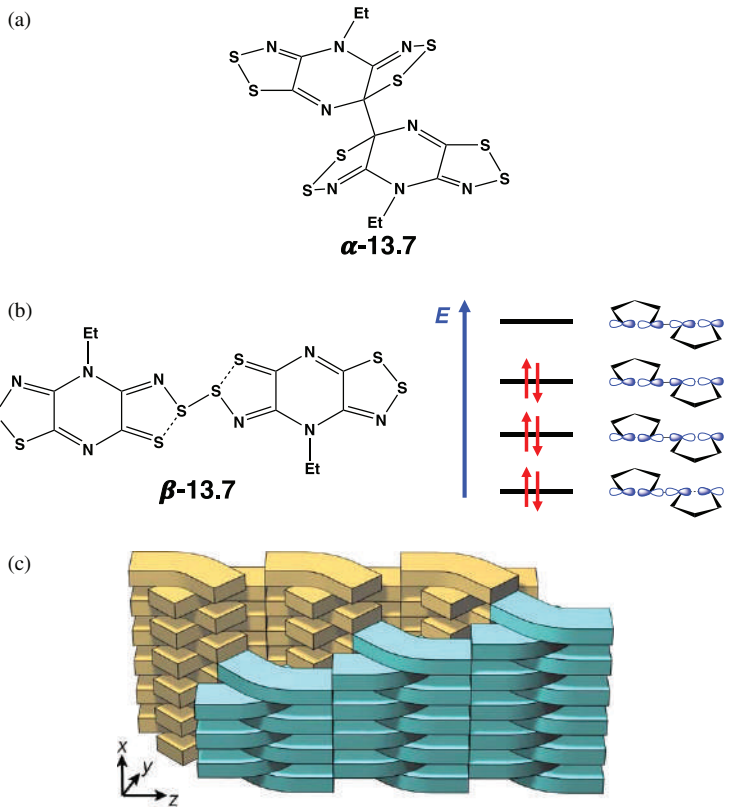

Figure 13.3. (a) Dimerisation modes of pyrazine-bridged bis(1,2-dithia-3-azolyl) **13.7** (a) C–C or (b) 4-centre-6-electron S---S–S---S σ-bonding in β-**13.7**,[26] (c) π-stack arrays in *N*-methyl analogue of **13.7**.[27] [Reproduced with permission from A. A. Leitch, C. E. McKenzie, R. W. Reed, C. M. Robertson, J. F. Britten, X. Yu, R. A. Secco and R. T. Oakley, *J. Am. Chem. Soc.*, **129**, 7903 (2007). Copyright 2007 American Chemical Society].

evenly-spaced, superimposed alternating ABABAB π-stack arrays (Fig. 13.3c). Accordingly, this material shows high temperature conductivity ($\sigma = 10^{-3}$ S cm^{-1}).[27]

Some pyridine-bridged bis(1,2-dithia-3-azolyls) **13.5** also afford dimers in which the radicals are linked by hypervalent S---S–S---S σ-bonds in the solid state, as found for **13.7**. These systems are of interest for their potential applications in switching devices. For example, in the case of **13.5** (R = Et, Me; X = F), reversible spin-crossover between

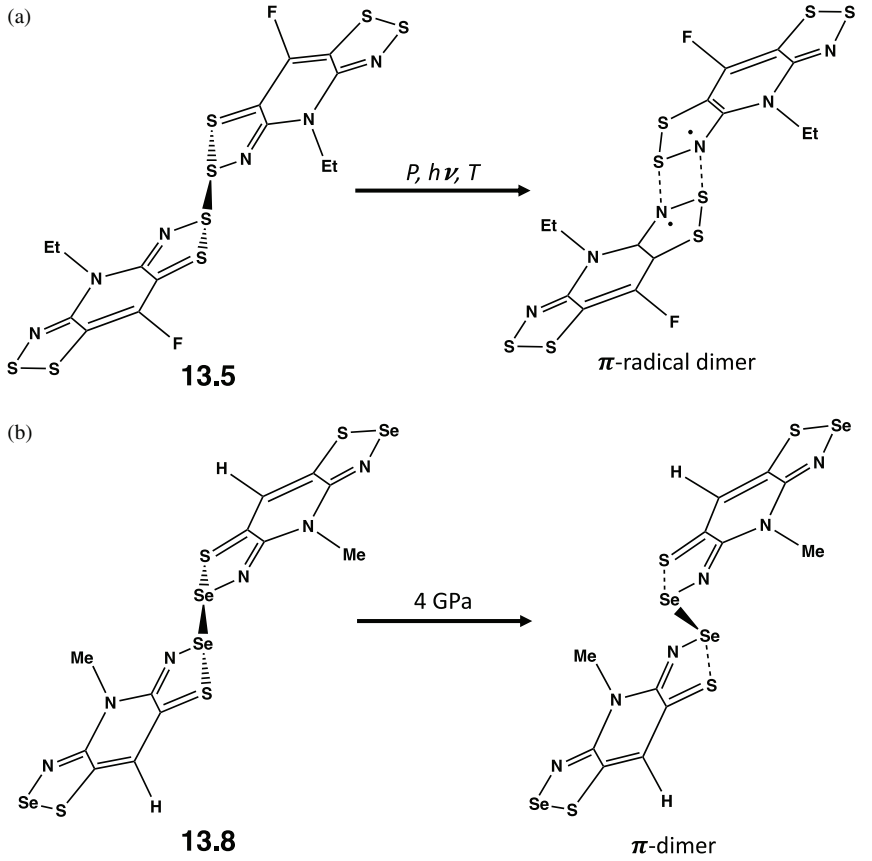

Scheme 13.2. (a) Reversible heat-, light- or pressure-induced opening of the σ-dimer phase of **13.5** (R = Et, X = F) to a π-radical dimer, (b) pressure-induced buckling of the selenium-based (SSeN) analogue of **13.8** (R = Me, X = H).

diamagnetic dimer and paramagnetic radical forms can be induced by heat, light or pressure (Scheme 13.2a).[46]

In the σ-dimer of the selenium-based (SSeN) analogue **13.8** (R = Me, X = H) the hypervalent S---Se–Se---S linkage is stronger,[47] and cannot be ruptured by heat or light (Scheme 13.2b). However, the σ-dimer becomes a distorted π-dimer upon application of pressure (~5 GPa).[48] This structural transformation results in a narrowing of the electronic band gap leading to a dramatic (10^6-fold) increase in electrical conductivity and formation of a metallic state.

Apart from the examples noted above, the incorporation of selenium into the 1- and 2- positions of bis(1,2-dithia-3-azolyls) does not lead to dimerisation in the solid state. In some cases, for a given choice of R and X substituents, isostructural families of four radicals (SSN, SSeN, SeSN, SeSeN) are produced, which all behave as Mott insulators. While the conductivity of the purely sulfur-based derivatives is limited, it increases significantly with incorporation of selenium, and highly correlated metal states can be generated with the application of pressure.[49–52] At ambient pressure many of the selenium-containing variants exhibit magnetically ordered phases, ordering either as spin-canted antiferromagnets (SC-AFM) or bulk ferromagnets (FM).[53–58] A summary of ordering temperatures (Curie Temperature, T_C, for FMs, Neel Temperature, T_N, for SC-AFMs), and coercive fields H_c for derivatives of **13.9** is provided in Table 13.1. In general, ordering temperatures increase with selenium content. The T_C values found for **13.9g** (17 K) and **13.9h** (17.5 K) are the highest observed

Table 13.1. Ordering temperatures (T_N or T_C) and coercive field H_c at 2 K for derivatives of pyridine-bridged bis(1,2-dichalcogena-3-azolyls) **13.9.**

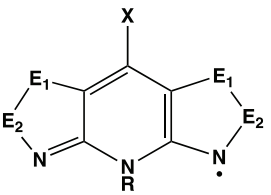

13.9

Radical	E_1	E_2	R	X	Magnetic Order	H_c (Oe) at 2 K
13.9a	Se	S	Et	H	SC-AFM, T_N = 13.0 K	130
13.9b	Se	Se	Et	H	SC-AFM, T_N = 27 K	390
13.9c	S	Se	Et	Cl	FM, T_C = 12.8 K	250
13.9d	S	Se	Et	Br	FM, T_C = 14.1 K	230
13.9e	S	Se	Et	Me	FM, T_C = 13.6 K	320
13.9f	Se	S	Et	Cl	SC-AFM, T_N = 14 K	66
13.9g	Se	Se	Et	Cl	FM, T_C = 17 K	1370
13.9h	Se	Se	Et	Br	FM, T_C = 17.5 K	1600
13.9i	Se	Se	Et	I	FM, T_C = 10.5 K	387

for any organic (*p*-block) radical ferromagnet. Significantly, their large coercive fields H_c, which are characteristic of hard magnets, *i.e.*, magnets that retain magnetisation in the absence of an applied field, reflect greater anisotropic exchange interactions due to spin-orbit coupling arising from spin density on the heavy selenium atom.[17] The T_C values of the halo-substituted bis(1,2-diselena-3-azolyl) radicals **13.9g–i** are all increased by the application of pressure, reaching 21 K at 1 GPa for **13.9g**,[59] 24 K at 2 GPa for **13.9h**,[60] and 27.5 K at 2 GPa for **13.9i**.[29] At greater pressures and with the expected increase in intermolecular hopping, magnetic ordering is lost and highly correlated bad metal states are produced.

The oxo-bridged radicals **13.6** differ from the *N*-alkylpyridine bridged materials **13.9** in two ways. The first is the so-called multi-orbital effect, *i.e.*, the presence of a low-lying π-LUMO that reduces the effective onsite Coulomb potential and enhances intersite ferromagnetic exchange interactions.[17] As a result, a remarkable number of magnetically ordered phases, typically spin-canted antiferromagnets, have been found for radicals of this type. The other important feature of these radicals involves the structure-building influence of multi-centre supramolecular synthons, which leads to packing patterns based on a chain-like arrays of radicals instead of the herringbone motifs commonly found for **13.9**.

The effect of the substituent X on the magnetic properties and conducting behaviour of the oxobenzene-bridged bis(1,2-dithia-3-azolyls) has been studied in detail for the derivatives **13.6a** (X = H),[34,35] **13.6b** (X = F),[33] **13.6c** (X = Cl),[32] **13.6d** (X = I),[36] **13.6e** (X = Me)[30,31] and **13.6f** (X = Ph) (Chart 13.2).[30,31] The influence of crystal structures and, in particular, the role of weak secondary bonding interactions (S···O and S···N) on the

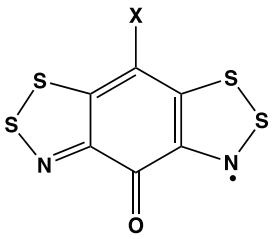

13.6

13.6a	X = H	**13.6f**	X = Ph
13.6b	X = F	**13.6g**	X = NO_2
13.6c	X = Cl	**13.6h**	X = O^-
13.6d	X = I	**13.6i**	X = OMe
13.6e	X = Me	**13.6j**	X = OEt

Chart 13.2. Oxobenzene-bridged bis(1,2-dithia-3-azolyls).

observed magnetic behaviour has been discussed in detail in a recent review on thiazyl magnets.[18] The prototypical derivative **13.6a** is a Mott insulator and exhibits a conductivity σ_{RT} of 6×10^{-3} S cm^{-1} (RT = 300 K).[35] Mott insulators should conduct electricity according to band theory, but in practice they are insulators. The application of pressure induces changes in the crystal structure and transport properties of **13.6a** and three phases have been identified.[35] With compression greater than 4 GPa the conductivity increases threefold, and the thermal activation energy is reduced to zero, heralding the formation of a metallic state. The halogeno-substituted derivatives, **13.6b** and **13.6c**, are both spin-canted antiferromagnets.[32,33] The fluoro-substituted radical **13.6b** exhibits a high conductivity $\sigma_{RT} = 6 \times 10^{-2}$ S cm^{-1} and undergoes a Mott insulator-to-metal transition under a pressure of 3 GPa,[33] and at 6 GPa a Fermi liquid state is produced.[35] The EtCN solvate of the iodo-substituted derivative **13.6d** displays strong ferromagnetic interactions between 100 K and 300 K and orders as a spin-canted antiferromagnet below 35 K.[36]

The introduction of a nitro group stabilises the LUMO in **13.6g** (X = NO_2) and hence lowers the effective Coulombic barrier to charge transfer.[38] The MeCN solvate of **13.6g** forms superimposed π-stacked arrays and exhibits Pauli-like magnetic properties, but the conductivity σ_{RT} = 0.04 S cm^{-1} indicates a Mott insulating ground state. Under pressure the charge gap between the Mott insulator and metallic states can be closed at 6 GPa.[38] The properties of the benzoquino-bridged material **13.6h** (X = O) are particularly interesting. This derivative, which is isoelectronic with **13.6b** (X = F), is a closed shell antiaromatic 16π-electron zwitterion with a small HOMO-LUMO gap. It behaves as a semiconductor with $\sigma_{RT} = 1 \times 10^{-3}$ S cm^{-1}. Application of pressure up to 8 GPa closes the band gap to form a molecular metal with $\sigma_{RT} > 10$ S cm^{-1}.[39] The alkoxy derivatives **13.6i** (X = OMe) and **13.6j** (X = OEt) exhibit strong antiferromagnetic interactions and Mott insulating behaviour with lower room-temperature conductivities, σ_{RT} ~1×10^{-4} and ~1×10^{-3} S cm^{-1}, respectively, than the fluoro analogue **13.6b** (*vide infra*).[40]

13.2.3 *Reactions*

Benzo-1,2-dichalcogena-3-azolyl radicals, *e.g.*, **13.3**, are stable in the solid state and persistent in solution at room temperature, although the

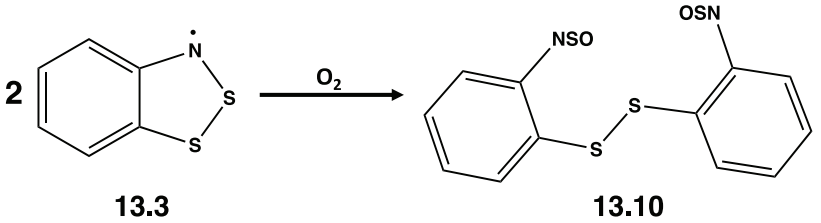

Scheme 13.3. Reaction of benzo-1,2-dithia-3-azolyl radical with O_2.

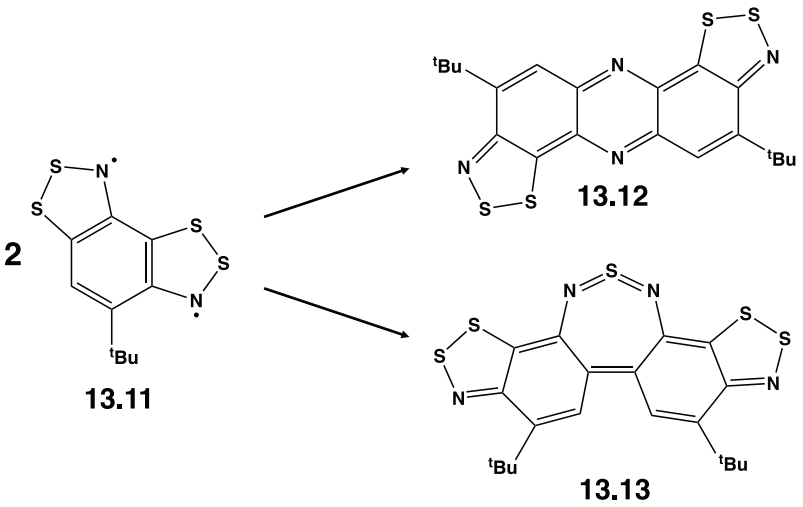

Scheme 13.4. Formation of pentacyclic bis(1,2-dithia-3-azoles) by self-condensation of the diradical **13.11**.

stability of selenium derivatives is lower than that of sulfur analogues.[7,42] However, the reaction of **13.3** with O_2 in hydrocarbon solvents occurs *via* a radical process to give a disulfide with *ortho*-NSO substituents (**13.10**, Scheme 13.3).[63,64]

The diradical **13.11**, generated *in situ*, undergoes self-condensation to give the phenazine-bridged bis(1,2-dithia-3-azole) **13.12** as the major product and small amounts of another pentacyclic bis(1,2-dithia-3-azole) **13.13** (Scheme 13.4).[65] Both **13.12** and **13.13** are near-IR dyes with visible absorption bands at λ_{max} = 689 and 796 nm, respectively. Cyclic voltammetry combined with UV-visible spectroscopy reveals five different oxidation states for **13.12** ranging from dication to dianion, each with a

different colour. Chemical oxidation of **13.12** with 4-$CH_3C_6H_4ICl_2$ generates the dicationic salt [**13.12**][$Cl]_2$, which is converted to [**13.12**][$GaCl_4]_2$ by treatment with $GaCl_3$.[65] Comproportionation of **13.11** with [**13.12**][$GaCl_4]_2$ produces the corresponding salt of the radical monocation [**13.12**][$GaCl_4$].

13.2.4 *Charge-transfer complexes*

The X-ray structural parameters of 3,4-dichlorobenzo-bis(1,2-chalcogena-3-azoles) (**13.14a** and **13.14b**) are consistent with a quinoidal structure rather than the alternative diradical formulation (Chart 13.3).[66] A variety of charge-transfer complexes of **13.14a**, **b** and the naphtho-bis(1,2-dithia-3-azole) **13.15** of varying stoichiometries have been generated by electrooxidation. In early work the radical cations [**13.14a**]$^{\bullet+}$ and [**13.14b**]$^{\bullet+}$ were shown by EPR spectroscopy to be stable towards disproportionation in solution. Further oxidation of these radical cations with $PhICl_2$ in liquid SO_2 produced the dications, which were isolated and structurally characterised as $[AlCl_4]^-$ salts.[66] Recently, the 1:1 radical cation salt [**13.14a**][$GaBr_4$] was generated by the one-electron electrooxidation of **13.14a** in dichloroethane in the presence of [Bu_4N][$GaBr_4$].[67] The X-ray structure of [**13.14a**][$GaBr_4$] showed the radical cations to be located at the triangular corners of a trigonal lattice, a rare example of a kagome basket structure (Fig. 13.4). The low-temperature magnetic properties of this material are consistent with a spin-frustrated system.

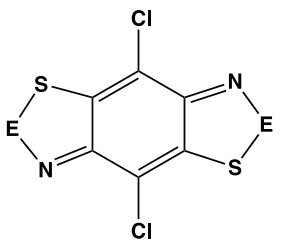

13.14a E = S
13.14b E = Se

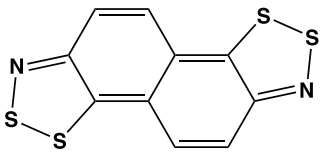

13.15

Chart 13.3. Quinoidal bis(1,2-dithia-3-azoles).

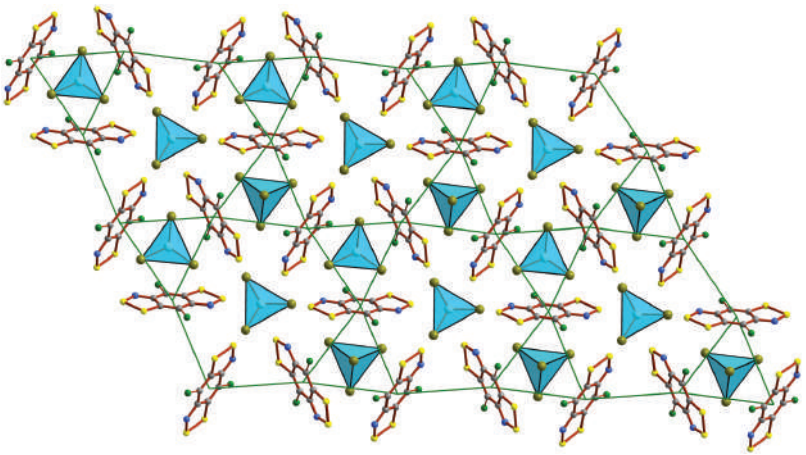

Figure 13.4. Structure of [**13.14a**][$GaBr_4$] in the *ab* plane showing the kagome basket arrangement of radical cations at corner-sharing triangles.[67]

In contrast to the behaviour of **13.14a**, the electrochemical oxidation of **13.15** in a 1:1 mixture of 1,2-dichloroethane and CS_2 in the presence of an electrolyte, [Bu_4N][BF_4] or [Bu_4N][MCl_4], produces either the 3:2 or 3:1 radical anion salts, [**13.15**]$_3$[BF_4]$_2$[68] or [**13.15**]$_3$[MCl_4] [M = Ga, Fe],[69] respectively. The mixed valence salt [**13.15**]$_3$[BF_4]$_2$ is comprised of π^*–π^* dimers [**13.15**]$_2^{2+}$ and neutral **13.15** molecules; it has a conductivity value of $\sigma \sim 10^{-2}$ S cm^{-1}.[68] The 3:1 salts [**13.15**]$_3$[MCl_4] are semiconductors with $\sigma_{RT} \sim 0.5$ S cm^{-1}.[69b]

13.3 Monocyclic and Resonance-Stabilised 1,3-Dithia-2-azolyl Radicals

Monocyclic 1,3-dithia-2-azolyl (DTA) radicals **13.16** were identified as a product of reactions of alkynes with S_4N_4 or S_4N_2 by EPR spectroscopy more than 40 years ago and early investigations of the chemistry of benzo-fused derivatives **13.17** (Chart 13.4) have been discussed in a review article.[70] Recent work on these radical systems has been focused on the synthesis, redox behaviour and the conducting and magnetic properties of a wide variety of resonance-stabilised derivatives, which are described in several more recent reviews.[15,16,18]

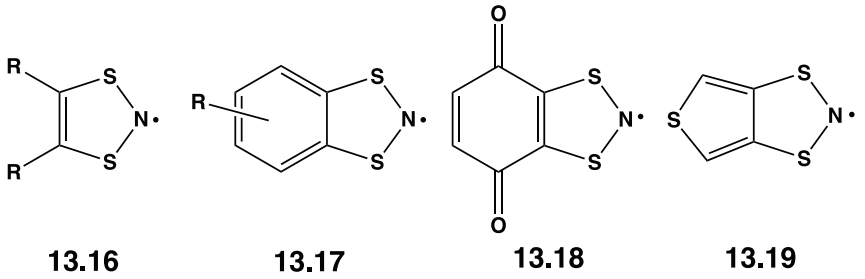

Chart 13.4. Examples of monocyclic and fused 1,3-dithia-3-azolyls.

13.3.1 *Synthesis*

Both monocyclic and benzo-fused 1,3-dithia-2-azolyl radicals (1,3,2-BDTAs) are normally prepared by one-electron reduction of the corresponding cations, *e.g.*, **13.16** (R = CF_3)[71] and **13.17** (R = H, Me),[72] respectively. For monocyclic derivatives the cationic precursors are generated by cycloaddition of $[SNS]^+$ and alkynes (Sec. 5.8.2, Scheme 5.6) and this method has been adapted for the preparation of quinone-fused dithiazolyls, *e.g.*, **13.18**.[73] The synthesis of the cationic precursors of benzo-fused derivatives involves the preparation of 1,2-bis(sulfenyl chlorides) from the corresponding 1,2-dithiols followed by cyclocondensation with Me_3SiN_3 (Sec. 2.5.2, Scheme 2.6); the cations are then reduced with metals such as silver powder. This approach has also been used for the preparation of the thiopheno-1,3-dithia-2-azolyl radical **13.19**.[74] Since 1,2-dithiols have limited commercial availability, alternative methods for the synthesis of 1,2-bis(sulfenyl chlorides) have been developed, *viz.*, (a) reaction of 1,2-dihaloarenes with ^{t}BuSNa followed by deprotection of sulfur with Cl_2[75] or (b) preparation of tetrathiocins from 1,2-dialkoxyarenes and S_2Cl_2 and subsequent oxidation with SO_2Cl_2.[76] These methods provide access to 1,3,2-BTDAs (**13.17**) with either electron-withdrawing (R = CN, CF_3)[75] or electron-donating (R = OR′; R′ = alkyl) groups.[76]

13.3.2 *Molecular structures and properties: Bistability*

The SOMO of the 1,3,2-DTAs **13.16** and **13.17** is heavily concentrated on the SNS portion of the ring.[2] In **13.19** *ca.* 10% of the spin density is

delocalised onto the thiophene ring according to EPR data and DFT calculations.[71] The gas-phase structure of monomeric **13.16** (R = CF_3), a green paramagnetic liquid, has been determined by electron diffraction (Sec. 3.1.2). In the solid state monocyclic 1,3,2-DTAs crystallise as cofacial, diamagnetic dimers; however, **13.16** (R = CF_3) adopts a tilted structure with weak N···N and S···S contacts of 2.86 and 3.17 Å, respectively.[77] The substituent on the arene ring has a marked influence on the structures of 1,3,2-BDTAs. The prototypical derivative **13.17** (R = H) forms a centrosymmetric (*trans*-antarafacial) dimer with average *d*(S···S) = 3.17 Å,[78] whereas the corresponding S···S contacts in the 4-methyl derivative **13.17** (R = Me) are longer than the sum of the van der Waals radii for sulfur (3.6 Å) and dimerisation is not observed.[79] The cyano derivative **13.17** (R = 4-CN) is polymorphic.[75d,80] The low-temperature phase is a diamagnetic dimer and adopts a *cis*-cofacial dimer with intra-dimer distances *d*(S···S) = 3.26–3.35 Å, but undergoes a phase transition upon warming above 250 K to form a paramagnetic phase which adopts a regular π-stack with *d*(S···S) = 3.66 Å, reflecting the close thermodynamic balance between monomeric and dimeric phases. The dimeric phase is enthalpically more stable and the transition to the paramagnetic phase appears to be driven by entropy.

This ability of π-stacked DTA radicals to undergo reversible phase transition between diamagnetic and paramagnetic phases has been a major driving force for recent studies of 1,3,2-DTA radicals. These bistable molecules have potential uses in electronic devices such as switching units and thermal sensors or for information storage; the 1,3,2-DTAs are particularly prone to such thermally driven radical interconversions. In **13.17** (R = 4-CN) the structural and magnetic responses to dimer opening and radical closing occur at the same temperature. In many cases, however, the temperature for these interconversions is different yielding a region of magnetic bistability wherein the thermodynamically stable and metastable forms can co-exist. The paramagnetic heterocycles **13.20**, **13.21** and **13.22** (Chart 13.5) are typical examples of 1,3,2-DTA radicals that exhibit this magnetic hysteresis.[81–85] These three radicals exhibit high-temperature crystal structures based on regular π-stacked arrays of radicals; on cooling they form distorted π-stacks of cofacial or pancake dimers (Sec. 4.10).

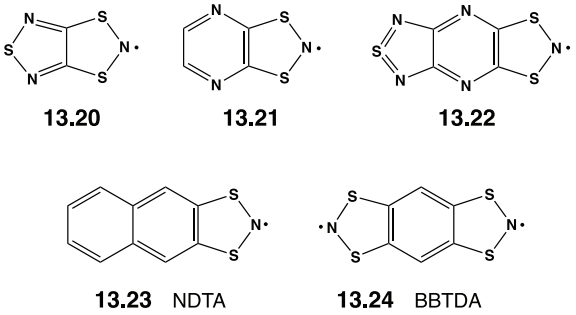

Chart 13.5. Magnetically bistable 1,3-dithia-2-azolyl radicals.

Magnetic bistability in the bicyclic radical **13.20** was first recognised in 1999.[82] A wide thermal hysteresis loop (230–305 K) involving the high-temperature 1D stacks of radicals (the paramagnetic phase) and the low-temperature dimer (the diamagnetic phase) was observed. The transition from the low-temperature phase to the high-temperature phase is not only driven thermally, but can also be driven by light irradiation[86] or upon the application of pressure.[87] Recent *ab initio* molecular dynamics simulations and X-ray diffuse scattering data indicate that the high-temperature polymorph is the result of a fast intra-stack pair-exchange dynamics in which these radicals continually exchange with the adjacent radical involved in the formation of an eclipsed dimer.[88,89] This concept has been developed further through a consideration of the different magnetic behaviour of 4-cyano-BTDA **13.17** (R = CN) and the bicyclic radical **13.20**, which are examples of non-bistable and bistable materials, respectively.[90] Both derivatives exhibit low-temperature diamagnetic and high-temperature paramagnetic structures. The computational results show that the regular π-stacks (Fig. 13.5a) are not potential energy minima, but average structures arising from a dynamic interconversion between two degenerate dimeric structures (Fig. 13.5b). However, bistability is not generated by this intra-stack exchange process alone. While a change in space group is not a necessary requirement for a first order phase transition, when there is a space group change the transition must be first order. In the case of **13.20** and **13.21** the transition is manifested by the breaking and reforming of intermolecular contacts. This leads to an activation

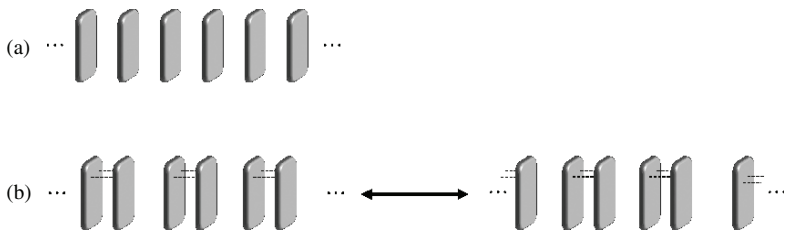

Figure 13.5. Arrangement of (a) regular and (b) dimerised π-stacks of 1,3-dithia-2-azolyl radicals.

energy for the phase transition which is typically manifested in bistability in the spin-switching behaviour. Several mechanisms for these abrupt phase transitions have been proposed comprising plate slippage and domino cascade,[85] exemplified by **13.20**. Conversely, the second-order nature of the phase transition in **13.17** (R = CN), for which both phases adopt the $P2_1/c$ space group, has no substantial change in inter-stack close contacts and is more gradual.[90]

The naphtho-fused derivative NDTA **13.23** (Chart 13.5) also exhibits bistability over a range of 60 K as a result of a radical-dimer interconversion, but the paramagnetism is incompletely quenched.[91a] In 2018 low-temperature crystallographic data for **13.23** were obtained by using synchrotron radiation and revealed that half the NDTA radicals dimerise in the solid state *via* a rare example of an N–N bonded σ-dimer.[91b]

The reversible interconversion between diamagnetic and paramagnetic phases associated with these bistable materials requires only small molecular displacements within the crystal lattice. When the structures of monomeric and dimeric phases are substantially different reversible solid-state transformations appear suppressed. In 1990 it was shown that the prototypical, dimeric 1,3,2-BDTA melts at ~90°C and from the melt a second monomeric phase **13.3** is produced.[78] Subsequent magnetic measurements revealed the metastable radical phase exhibited antiferromagnetic ordering at 11 K.[92]

The incorporation of 1,3,2-BDTA and the 5-methyl derivative (MBDTA) into a porous host has been achieved *via* gas-phase diffusion.[93] The dimeric structure is retained for BDTA, whereas MBDTA is

monomeric on the basis of EPR spectra and powder X-ray diffraction. The guests can be removed by solvent extraction with CH_2Cl_2.

13.3.3 *Charge-transfer complexes*

Charge-transfer complexes of 1,3,2-BDTA (**13.17**) exhibit a variety of magnetic and electrical properties.[15] The adduct BDTA·TCNQ (TCNQ = tetracyanoquinone) was first prepared in 1984 by either (a) direct reaction of the radical **13.17** with TCNQ in acetonitrile or (b) salt metathesis between [BDTA]Cl and LiTCNQ in water; a conductivity of $\sigma_{RT} \sim 0.5$ S cm^{-1} was reported for a powdered sample.[72a] Black, needle-like crystals of BDTA·TCNQ form a segregated stacking structure with a short contact between the donor and acceptor columns; this complex exhibits semiconductor behaviour.[15] A series of charge-transfer complexes of $[BDTA]_n[M(mnt)_2]$ ($n = 1$, M = Ni; $n = 2$, M = Cu, Co; mnt = maleonitriledithiolate) were also obtained *via* salt metathesis.[15] In the Ni and Cu complexes the cation and anion are not bonded to one another, whereas in the cobalt complex $[BDTA]_2[M(mnt)_2]$ the two BDTA ligands are *S*-coordinated to the metal centre as illustrated in Fig. 14.8 (Sec. 14.4). The 1:1 nickel complex shows ferromagnetic coupling between the alternating stacks of $[BDTA]^+$ cations and $[Ni(mnt)_2]^-$ monoanions.[94] The 2:1 copper complex consists of an alternating stack of head-to-head $[BDTA]^+$ dimers and a planar $[Cu(mnt)_2]^{2-}$ dianion; short S···S contacts between the stacks give rise to an ideal one-dimensional magnetic material.[95] The structure of the 2:1 cobalt complex is similar to that of the copper complex at 253 K, but this salt undergoes a phase transition at 190 K that leads to competing behaviour of BDTA as a cation and a ligand.[96]

Polymorphs of a particular salt are often observed. For example, there are two diamagnetic and one paramagnetic phase of $[BBDTA][GaCl_4]$ (BBDTA = benzo-bis(dithiazolyl) diradical, **13.24** in Chart 13.5).[101] All of these charge-transfer complexes exhibit long-range magnetic order and their diverse magnetic behaviour is attributed to the different alignments of the $[BBDTA]^{\bullet+}$ radical cations.[104] A detailed discussion of their structures and magnetic properties can be found in a recent review.[18]

The chloride salt of the $[BBDTA]^{\bullet+}$ radical cation, [BBDTA]Cl, exhibits paramagnetic behaviour with strong antiferromagnetic interactions at room temperature and a paramagnetic-to-diamagnetic phase transition with no thermal hysteresis at *ca.* 150 K.[104] The magnetic interactions between the neighbouring $[BBDTA]^{\bullet+}$ radical cations in the π-stacking columns are much stronger than the magnetic interactions between the columns in this salt.[104] A gold complex of $[BBTDA]^{\bullet+}$ radical cations with linear $[Au(CN)_2]^-$ anions is comprised of π-stacked columns with short intercolumnar contacts. This complex exhibits ferromagnetic ordering at 8.2 K.[105] The radical cation salt [BBDTA][$FeCl_4$] exists as an acetonitrile solvate which exhibits antiferromagnetic order at 6.3 K, but desolvates to form a new phase which shows enhanced magnetisation at 44 K suggestive of ferrimagnetic ordering.[102]

13.4 1,2-Dichalcogena-3,5-diazolyl Radicals

The first 1,2-dichalcogenyl-3,5-diazoyl radicals were prepared and structurally characterised more than 40 years ago and early work was comprehensively reviewed in 1995.[106] The chemistry of sulfur systems (DTDAs) and their selenium analogues (DSDAs) up to 2004 was discussed in the first edition of this book and as part of more general review articles and book chapters published during 2007–2013.[2,7a,b] An authoritative account of the synthesis, electronic and crystal structures, properties and reactions of 1,2,3,5-DTDAs appeared in 2019.[10] More specialised reviews have focused on pancake bonding (Sec. 4.10),[107] crystal engineering concepts,[9] and the physical properties of these carbon-nitrogen-chalcogen radicals.[14,18] The rich coordination chemistry of these paramagnetic heterocyclic ligands is discussed in Chapter 14.

13.4.1 *Synthesis*

The necessary precursors to 7π-electron 1,2,3,5-DTDA or DSDA radicals are the corresponding 6π-electron 1,2,3,5-DTDA cations. Synthetic approaches to these cations are discussed in Sec. 11.4 (Scheme 11.11).

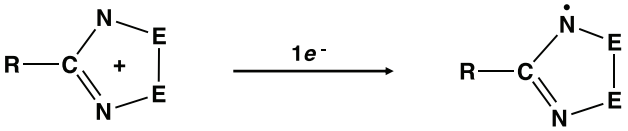

Scheme 13.5. Synthesis of 1,2,3,5-dichalcogenadiazolyl radicals.

For soluble radicals, one-electron reduction of the corresponding cations (Scheme 13.5) can be achieved by using metals such as Ag powder or a Zn/Cu couple. The use of 0.5 equivalents of Ph_3Sb in CH_2Cl_2 is effective for the production and separation of poorly soluble radicals, since both Ph_3Sb and Ph_3SbCl_2 are soluble in that solvent.[108] For radicals that are sufficiently volatile to be separated from Ph_3SbCl_2 by sublimation, a mechanochemical technique can be used for this reduction.[109]

13.4.2 *EPR spectra and electronic structures*

Although some 1,2,3,5-DTDAs and 1,2,3,5-DSDAs have been characterised as monomers in the solid state, *e.g.*, the sterically hindered derivatives $[2,4,6\text{-}(F_3C)_3C_6H_2CNSSN]^{\bullet}$[110] and $[3\text{-}NC\text{-}5\text{-}^{t}BuC_6H_3CNSeSeN]^{\bullet}$,[111] as well as some polyfluorinated aryl derivatives such as $[p\text{-}NCC_6F_4C_6F_4CNSSN]^{\bullet}$ and $[p\text{-}O_2NC_6F_4CNSSN]^{\bullet}$,[112] the vast majority of these radicals are dimers in crystalline form (Sec. 13.4.3). Computational studies on these dimers have proved challenging as the ground state electronic configuration is a diradicaloid singlet. Benchmark studies using the CCSD(T)/6-311g++(d,p) level of theory have computed dissociation energies of 12 and 15 kJ mol^{-1} for the prototypical dimers $[HCNSSN]_2$ and $[HCNSeSeN]_2$, respectively.[113] Experimental EPR and UV-visible studies on DTDA radicals in solution reveal more substantial dimerisation energies of *ca.* 35 kJ mol^{-1} and these dimeric 1,2,3,5-DTDAs readily dissociate to give monomers in dilute solutions.[114] Information about the spin density distribution in the heterocyclic ring can be gleaned from EPR spectroscopy. The EPR spectra of 1,2,3,5-DTDAs display 1:2:3:2:1 quintets arising from hyperfine coupling to two equivalent nitrogen centres (^{14}N, $I = 1$, $a_N \sim 5.0$ G). The singly occupied molecular orbital (SOMO) of DTDA radicals is a π^* orbital with a node at carbon. Consequently, the R substituent is expected to have little

influence on the EPR parameters of these paramagnetic species. Consistently, the second derivative EPR spectrum of the prototypical DTDA $[HCNSSN]^{\bullet}$ in toluene at 169 K reveals only a weak hyperfine coupling to the exocyclic hydrogen atom ($a_H = 0.55$ G).[112] Computational studies indicate that the prototypical DTDA, $(HCNSSN)_2$, has promising potential as an external field-driven optical switch.[115]

Computational and EPR studies on the monomer $[p\text{-}O_2NC_6F_4C\text{-}NSSN]^{\bullet}$, supported by single-crystal neutron diffraction data, indicate that the spin density is almost entirely located in sulfur and nitrogen p_z orbitals perpendicular to the ring with only a small negative spin density on the carbon atom.[111]

13.4.3 *Crystal structures*

A large number of dimeric 1,2,3,5-DTDAs (>85) and 1,2,3,5-DSDAs (>25) have been structurally characterised by X-ray crystallography.[10,111,116] The formation of dimers results from π^*–π^* interactions that are strongly directional; the MO depictions of these interactions are depicted in Fig. 4.11. Five dimerisation motifs with different orientations of the two monomers have been structurally established in the solid state (Chart 13.6).[116a] The most common mode of dimerisation is *cis*-cofacial,

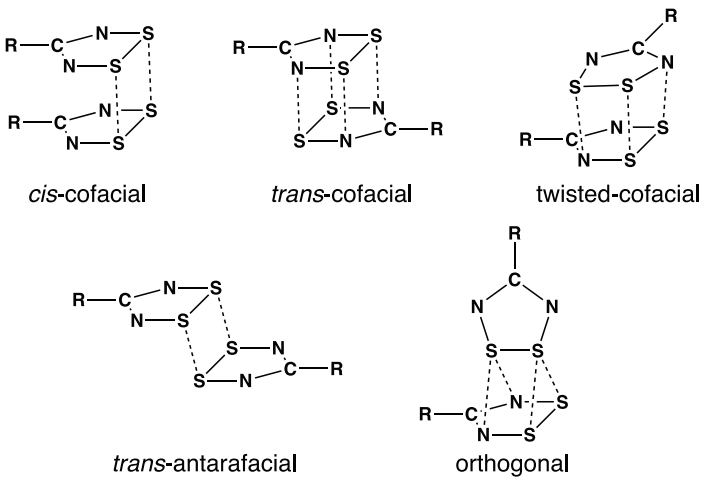

Chart 13.6. Dimeric arrangements of 1,2,3,5-DTDAs.

while the orthogonal arrangement is rare. Three of these motifs, *cis*-cofacial, orthogonal and *trans*-antarafacial are also observed for polyfluoroaryl 1,2,3,5-DSDAs, $(p\text{-}XC_6F_4CNSeSeN)_2$ (X = F, Cl, Br, CF_3, NO_2, CN) dimers.[116b] The dimerisation energies for 1,2,3,5-DSDAs are larger than those of their sulfur analogues. Since the chalcogen-nitrogen bonds are strongly polar ($^{\delta+}E\text{–}N^{\delta-}$) (E = S, Se) electrostatics also play an important role in the self-assembly of these structures.[116c] Single crystals of the β phase of the paramagnetic $[4\text{-}NCC_6F_4CNSSN]^{\bullet}$ radical are bendable owing to strong CN· · ·S interactions forming supramolecular chains of radicals but weak inter-chain interactions between radicals.[116d]

The presence of structure-directing groups in derivatives of the type $p\text{-}XC_6R_4DTDA$ (X = CN, NO_2, R = H, F) can lead to supramolecular chains *via* $CN^{\delta-}\cdots S^{\delta+}$ or $NO_2^{\delta-}\cdots S^{\delta+}$ interactions.[9] Hydrogen bonding may also play a role in the formation of 3D networks as is evident in the structure of 4-(2′-benzimidazolyl)DTDA (**13.25**, Chart 13.7).[117] A 1:1 co-crystal of a DTDA dimer with triphenylstibine, $[(4\text{-}CF_3C_6H_4)CNSSN]_2{\cdot}SbPh_3$, has also been structurally characterised.[118] In this adduct the DTDA adopts a *cis*-cofacial arrangement and there are short contacts between the S–S units and the carbon atoms of one of the aryl groups of the stibine.

While the observed geometries of DTDA dimers can be understood in terms of maximising the SOMO-SOMO interactions between two monomers (pancake bonding, Sec. 4.10), there is a fine balance between the bonding interaction arising from orbital overlap and the repulsive electrostatic and dispersion terms which arise at distances less than the sum of the van der Waals radii.[118] The build-up of electron density between the two radicals has been confirmed through the determination of high values of the electron density at the bond critical points in the dimers $(Ar_FCNSSN)_2$ ($Ar_F = C_6F_5$, NC_5F_4).[119]

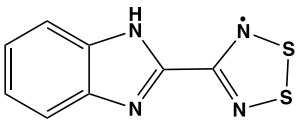

13.25

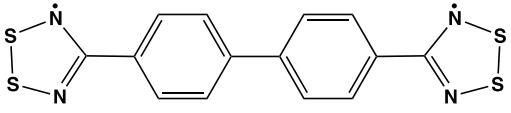

13.26

Chart 13.7. DTDA derivatives that undergo phase transitions.

Polymorphs are often observed for DTDAs and DSDAs. For example, five polymorphs of the chlorinated derivative $(ClCNSSN)_2$[120,121] and four polymorphs of 9′-anthracenyl-DTDA[122] have been structurally characterised. This phenomenon is illustrated for the α- and β-phases of the dimer $\{[3,5\text{-}F(CF_3)C_6H_3]CNSSN\}_2$ in Fig. 3.2. Several DTDA derivatives undergo phase transitions between different polymorphs in the solid state. For example, the benzimidazole derivative **13.25** exhibits a first-order transition at *ca.* 270 K with a narrow window of thermal hysteresis between diamagnetic dimeric and paramagnetic monomeric states.[115] The 4,4′-biphenyl diradical **13.26** undergoes two first-order transitions at 306 and 359 K involving subtle changes in intermolecular interactions (Chart 13.7).[123]

13.4.4 *Properties and reactions*

The physical properties of DTDAs, *e.g.*, photoconductivity, non-linear optical switching, magnetic and fluorescence behaviour have been investigated in view of their potential applications. The biradical **13.27** and 1′-pyrenyl-DTDA **13.28** (Chart 13.8) both exhibit a photoconducting response.[124,125] The conductivity of these paramagnetic materials increases approximately twofold upon irradiation at 532 nm and 455 nm, respectively.[124,125] The possible influence of substrates on the physical properties of DTDAs is implied by the significant change in packing that occurs when **13.27** is coated on a Cu(111) surface.[126]

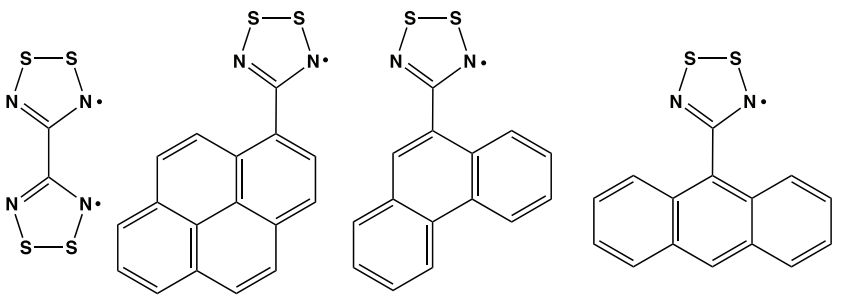

Chart 13.8. Photo-conducting and fluorescent DTDAs.

The influence of packing on the physical properties of DTDA radicals is illustrated by the two polymorphs of *p*-NCC_6F_4CNSSN, both of which have chain structures linked by $CN^{\delta-}\cdots S^{\delta+}$ interactions. Pure samples of the α- and β-phases of this DTDA are obtained by carefully controlled sublimation.[127] The α-phase shows minor field-dependent behaviour of the magnetic susceptibility at low temperature, but no clear evidence for long-range order,[127] whereas the β-phase undergoes long-range magnetic order as a canted antiferromagnet below 36 K.[128a,b] An increase in pressure to 1600 kPa leads to shorter intermolecular contacts in the β-phase and strengthening of the magnetic communication leading to ordering at 70 K.[128c] The radical *p*-$NO_2C_6F_4CNSSN$ has been found to order as an organic ferromagnet at 1.3 K.[128d]

The isostructural dimers $(NEENC_6H_4NEEN)_2$ (E = S, Se) are small band gap semiconductors as a result of a small HOMO-LUMO band gap. The application of pressure (~10 GPa) on these pancake π-dimers widens this gap to an extent that offsets the effect of band broadening.[129] This behaviour differs from that observed for some hypervalent σ-dimers of bis-selenathiazolyls, which undergo metallisation near 5 GPa as a result of pressure-induced closure of the HOMO-LUMO gap (Sec. 13.2.2).[49]

The luminescent and fluorescent properties of DTDA derivatives that incorporate polyaromatic substituents, *e.g.*, pyrene (**13.28**), phenanthrene (**13.29**) and anthracene (**13.30**) (Chart 13.8), have attracted recent attention. Both **13.28** and **13.29** are blue-light emitters in solution and in polymer matrices with quantum efficiencies of 50% and 11%, respectively, with the more emissive radical **13.28** being successfully incorporated into a prototype OLED device.[124,130] In contrast to the pancake dimers formed by **13.28** and **13.29**, the nearly orthogonal arrangement of the 9-anthracenyl and DTDA rings in **13.30** pre-empts dimerisation.[122] Consequently, this derivative is a unique example of the combination of the paramagnetic properties of the radical with the emissive behaviour of a polyaromatic hydrocarbon.

In the context of designing radical-radical co-crystals that behave as ferrimagnetic materials, the structure-directing interactions of the E–E bond (E = S, Se) in 1,2,3,5-DTDAs and DSDAs with electronegative groups have been invoked. In that context 2:1 co-crystals of $[C_6F_5CNEEN][TEMPO]$ (E = S, Se) and the 2:2 co-crystal $[PhCNSSN]_2[MBDTA]_2$

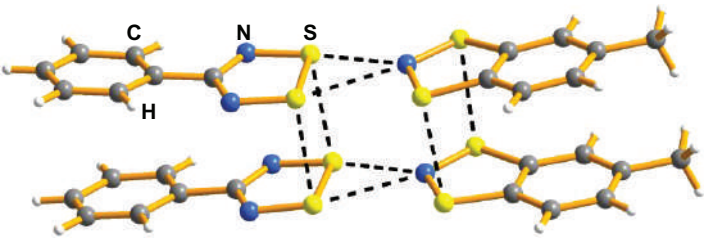

Figure 13.6. Crystal structure of $[PhCNSSN]_2[MBDTA]_2$.[131]

(MBDTA = methyl benzodithiadiazolyl) have been prepared and structurally characterised.[131] The favourable $^{\delta+}S\cdots N^{\delta-}$ interaction and the dimeric structure of $[PhCNSSN]_2[MBDTA]_2$ are illustrated in Fig. 13.6. Although MBDTA itself does not form a π^*–π^* dimer, this benzo-1,3-dithia-2-azolyl is dimerised in the 2:2 co-crystal owing to a combination of these electrostatic interactions and the propensity of DTDA radicals to dimerise.[131] This tendency prevents the formation of ferrimagnetic materials.

Two aspects of the host-guest chemistry of 1,2,3,5-DTDAs have been established. Firstly, DTDAs can be incorporated as guests into either porous[132,133] or non-porous hosts.[134] These inclusion complexes are prepared by a gas-phase diffusion process in which the vapour of the radical produced by vacuum sublimation is passed through a sample of the host material. EPR spectra and magnetic measurements indicate that the radicals exist predominantly as dimers in these inclusion complexes.[132] The reactivity of these radical guests appears to be somewhat diminished, as evidenced by incomplete oxidation upon treatment with I_2 at 40°C.[133] The DTDAs can be recovered from the frameworks by solvent extraction.[132,133] Conversely, 1,2,3,5-DTDAs, *e.g.*, $[CF_3(F)C_6H_3CNSSN]_2$, may also serve as hosts for small molecules such as N_2, CO_2, Ar and SO_2, when sublimed under a partial atmosphere of one of these gases.[135]

13.5 1,3-Dithia-2,4-diazolyl Radicals

1,3-Dithia-2,4-diazolyl radicals (1,3,2,4-DTDAs), $[RCNSNS]^{\bullet}$ (**13.31**) (Chart 13.9) are prepared by one-electron reduction of the corresponding cations, which are obtained *via* cycloaddition between the $[SNS]^+$ cation and organic nitriles as described in Sec. 11.5.[2] Similar reduction

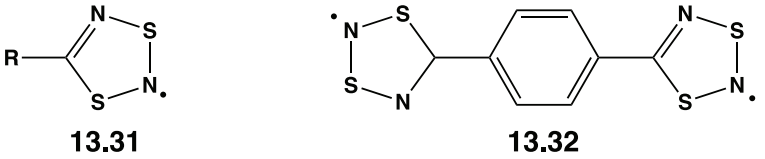

Chart 13.9. 1,3-Dithia-2,4-diazolyl radicals and diradicals.

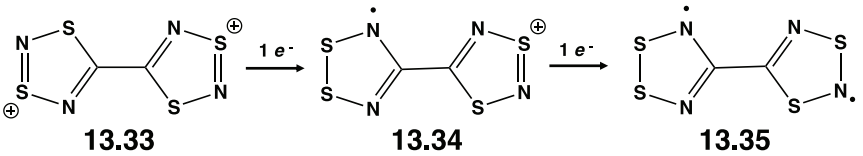

Scheme 13.6. Isomerisation of a 1,3,2,4-DTDA radical into the 1,2,3,5-isomer.

methodology is used for the synthesis of diradicals with a phenylene spacer, *e.g.*, 1,4-$[C_6H_4(CNSNS)_2]^{\bullet\bullet}$ (**13.32**), which has a polymeric structure involving π^*–π^* interactions between the heterocyclic rings.[136]

1,3,2,4-DTDA radicals are unstable with respect to isomerisation to the 1,2,3,5-isomers both in solution[137a] and in the solid state.[137b] The isomerisation is a photochemically symmetry-allowed process, which is thermally symmetry forbidden. The rearrangement is conveniently monitored by EPR spectroscopy since 1,3,2,4-DTDAs exhibit a 1:1:1 triplet, whereas the 1,2,3,5-isomers give rise to a 1:2:3:2:1 quintet.[137] The proposed mode of association required for rearrangement is observed in the solid-state structure of diradical **13.32** which undergoes thermal isomerisation at 145°C. The one-electron reduction of the dication $[SNSNC–CNSNS]^{2+}$ (**13.33**) to give the radical cation $[NSSNC–CNSNS]^{\bullet+}$ (**13.34**) in which the radical ring has rearranged to the 1,2,3,5-isomer is an example of this characteristic behaviour (Scheme 13.6). Further reduction of **13.34** with ferrocene produces the mixed diradical $[NSSNC–CNSNS]^{\bullet\bullet}$ (**13.35**), which forms a cofacial, centrosymmetric dimer in the solid state.[138]

13.6 1-Chalcogena-2,4,6-triazinyl Radicals

The first detailed studies of 7π-electron 1-chalcogena-2,4,6-triazinyl radicals TTAs (T = thia) and STAs (S = selena) involving the symmetrical

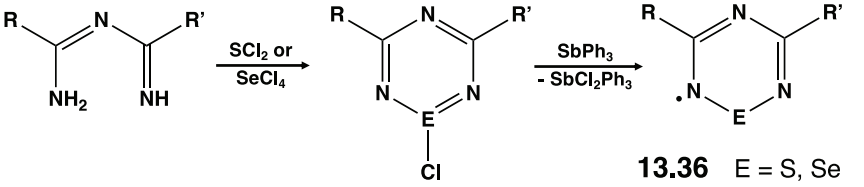

Scheme 13.7. Synthesis of 1-chalcogena-2,4,6-triazinyl radicals from imidoylamidines.

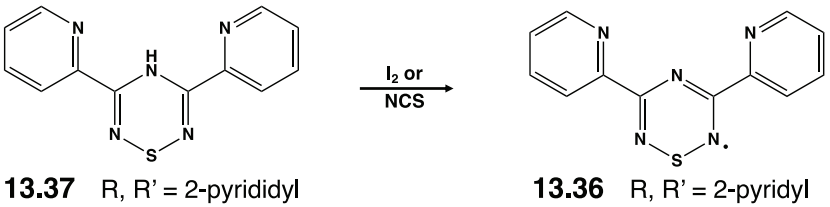

Scheme 13.8. Synthesis of 3,5-bis(2-pyridyl)-TTA.

derivatives **13.36** (E = S, Se; R = R′ = Ph) were reported in the mid-1980s.[139] The synthesis of the radicals **13.36** requires the initial preparation of *S*-chloro- or *Se*-chloro-chalcogenatriazines by cycloocondensation of imidoylamines with SCl_2 or $SeCl_4$ followed by reduction with triphenylantimony (Scheme 13.7). This methodology has been adapted for the preparation of unsymmetrical derivatives **13.36** [E = S, R = CF_3, R′ = *p*-XC_6H_4 (X = H, Cl, CH_3, CF_3, OCH_3)].[140]

Although the route shown in Scheme 13.7 is effective for the synthesis of the thienyl-substituted TTA derivative **13.36** (E = S, R = R′ = 2-thienyl),[141] a different approach is necessary for the preparation of the bis(2-pyridyl)-substituted TTA radical **13.36** (E = S, R = R′ = 2-pyr), which is of interest as a tridentate ligand for transition-metal complexes (Sec. 14.2.1). This derivative may be obtained by oxidation of 1-thia-2,4,6-triazine (TTAH, **13.37**) with either iodine[142] or *N*-chlorosuccinimide (NCS) (Scheme 13.8).[143] The synthesis of *S*-alkylated derivatives of 3,5-bis(2-pyridyl)-1-thia-2,4,6-triazines can be achieved *via* deprotonation of **13.37** with sodium hydride to give the corresponding anion followed by treatment with an alkyl iodide as described in Sec. 12.3 (Scheme 12.8).[144]

The electron density of the SOMO of TTA and STA radicals is primarily located on the unique nitrogen atom and the NEN unit (Fig. 13.7a).

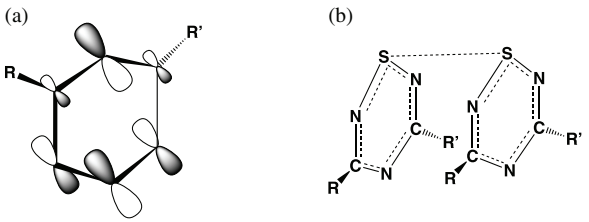

Figure 13.7. (a) SOMO and (b) dimeric structure of 1-thia-2,4,6-triazinyl radical (**13.36**, E = S).

In the solid state these radicals form diamagnetic cofacial dimers with S···S distances in TTAs of 2.59–2.67 Å, which are significantly shorter than the π^*–π^* interactions in other dimeric thiazyl radicals (Fig. 13.7b).[139a,140,141] The Se···Se distance in the dimer of the STA **13.36** (E = Se, R = R′ = Ph) is 2.79 Å.[139b]

The TTA dimers dissociate readily in solution and EPR spectroscopy is a valuable technique for the identification of the monomeric radicals (Sec. 3.4.1).[140,145,146] For symmetrically substituted derivatives **13.36** (R = R′) the EPR spectra exhibit slightly larger hyperfine couplings (a_N) to the unique nitrogen atoms compared to those of the symmetrically equivalent pair of nitrogen atoms (0.41–0.49 mT *vs*. 0.33–0.39 mT), except for R = R′ = 4-$MeOC_6H_4$ for which accidental equivalence of all three nitrogen centres is observed.[145,146] In the case of unsymmetrical TTA radicals (**13.36**, R ≠ R′) three distinct a_N values are generally observed.[140] EPR spectroscopy was used to detect the formation of **13.36** (R = R′ = Ar) as an initial product of the photolysis of the eight-membered rings 1,5-$ArC(NSN)_2CAr$ (Ar = Ph, 4-MeC_6H_4) by loss of an NS fragment.[147]

13.7 1,2,3-Trithia-4-azolium Radical Cations

The first salt of a 1,2,3-trithia-4-azolium radical cation $[F_3CCNSSS]$ $[AsF_6]$ (**13.38**, R = CF_3) was reported in 1992[148] and the chemistry of this class of paramagnetic C,N,S heterocycle was reviewed in 2013.[13] The original synthesis involved the cycloaddition of CF_3CN to the *in situ* reagent $[S_3]^{\bullet+}$, which is generated from an equimolar mixture of $[S_4][AsF_6]_2$ and $[S_8][AsF_6]_2$ in liquid SO_2 (Scheme 13.9a). This methodology has

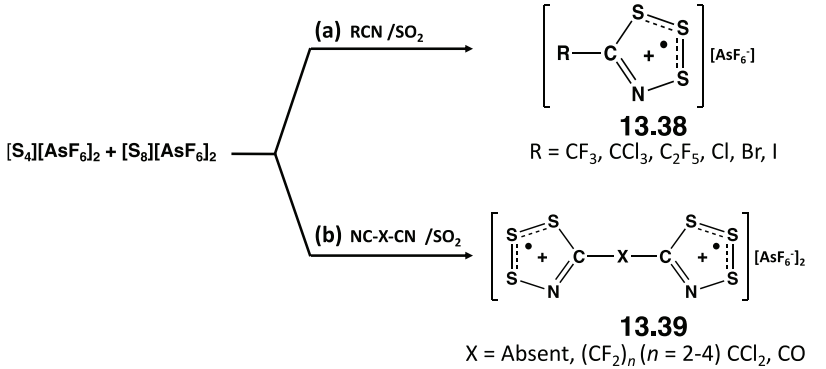

Scheme 13.9. Synthesis of (a) 1,2,3-trithia-4-azolium cation radicals and (b) diradical cations.

subsequently been used for the preparation of other halogenated derivatives **13.38** (R = CCl_3, C_2F_5, Cl, Br, I),[149,150] but it is ineffective for the synthesis of derivatives with protonic substituents on carbon. A family of diradical cations **13.39** have been obtained in a similar manner from cyanogen NC–CN and a variety of other bridged dinitriles NC–X–CN as shown in Scheme 13.9b.[13,151,152]

The $[RCNSSS]^{\bullet+}$ radical cations are 7π-electron species isoelectronic with neutral 1,3-dithia-2,5-diazolyl radicals $[RCNSNS]^{\bullet}$ (Sec. 13.5) by replacement of an N atom with S^+. The electron density in the SOMO of $[RCNSSS]^{\bullet+}$ is primarily located on the three sulfur atoms with only low spin density on the nitrogen atom (Fig. 13.8a). Consequently, the solution EPR spectra are usually comprised of a single line with no hyperfine splitting to nitrogen at room temperature.[13,148–152] In the solid state the structures of $[RCNSSS]^{\bullet+}$ salts are notably dependent on the substituent on carbon.[13] For example, the trichloromethyl derivative **13.38** (R = CCl_3) forms a one-dimensional chain with very weak S···S contacts (3.853 Å) between the chains.[149] By contrast, the halo-derivatives **13.38** (R = Cl, Br, I) all form π^*–π^* dimers with a *trans*-antarafacial arrangement and d(S···S) = 3.150–3.167 Å (Fig. 13.8b). These radicals have singlet ground states, but EPR spectroscopy has identified low-lying triplet states.[150]

The most remarkable derivative of the 1,2,3-trithia-4-azolyl ring system is the diradical dication $[SSSNC–CNSSS]^{2\bullet 2+}$, **13.39** (X = absent), in

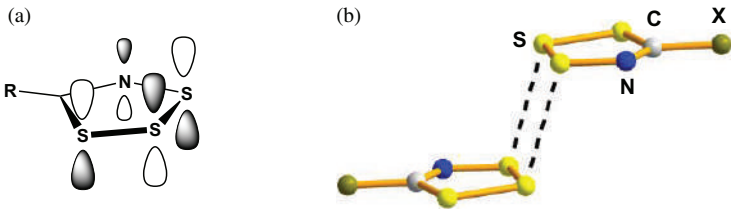

Figure 13.8. (a) SOMO and (b) dimeric structure of $[RCNSSS]^{\bullet+}$ radical cations (**13.38**, R = Cl, Br, I).[150]

which two radical cations are joined by a C–C single bond. This material is paramagnetic in all states.[13,151] The radical centres are disjoint with essentially degenerate open-shell singlet and triplet states. In the solid state the weak π^*–π^* contacts, d(S···S) = 3.31–3.46 Å, propagate very strong antiferromagnetic radical-radical interactions.[151] EPR spectra have confirmed the presence of a thermally accessible triplet state.

13.8 2-Chalcogena-1,3-diazolyl Radical Anions

Investigations of the synthesis and structures of radical anions of benzo-2-chalcogena-1,3-diazoles have provided poignant examples of the influence of the heavier chalcogens, especially tellurium, on the properties of carbon-containing chalcogen-nitrogen heterocycles. A combination of cyclic voltammetry and DFT calculations revealed that, in contrast to the trend towards lower electronegativities for the heavier chalcogens (Sec. 1.1), the electron acceptor ability of benzo-2-chalcogena-1,3-diazoles increases along the series S < Se < Te.[153] Although the radical anions of benzo-2-thia-1,3-diazoles **13.40a** and benzo-2-selena-1,3-diazoles **13.40b** were identified under CV conditions in solution by their EPR spectra in the 1960s,[154] they were not isolated as thermally stable salts until more than 40 years later. They were obtained by chemical reduction of the neutral precursor with potassium metal or KC_8 in THF or THF/18-crown-6 and isolated with $[K(THF)]^+$ or $[K(18\text{-crown-6})]^+$ counter-ions (Scheme 13.10).[153,155] The solid-state structure of the selenium-containing system [K(THF)][**13.40b**] consists of polymeric chains in which quasi-octahedral K^+ ions are coordinated to four N atoms of the radical anions

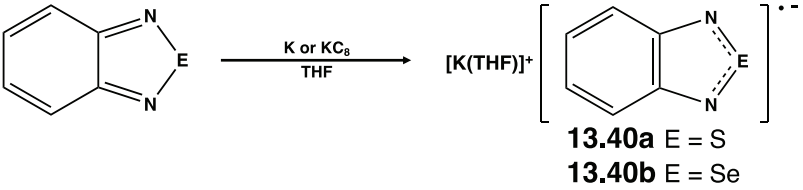

Scheme 13.10. Synthesis of salts of benzo-2-chalcogena-1,3-diazolyl radical anions.

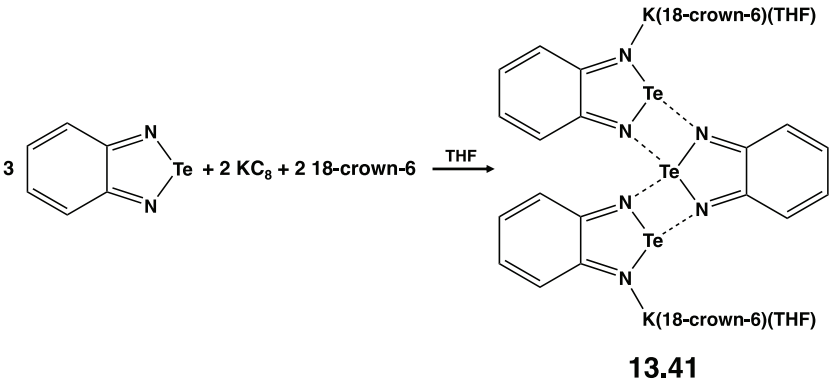

Scheme 13.11. Synthesis of $[K(18\text{-crown-6})(THF)]_2[C_6H_4NTeN]_3$.

and two O atoms of THF molecules.[153] By contrast, the K^+ ions in [K(18-crown-6)][**13.40b**] are sequestered by the 18-crown-6 ligand, which inhibits the formation of a coordination network.[153] Upon contact with air, the salts of **13.40a** and **13.40b** decompose quickly in solution to produce the chalcogenacyanate ions $[ECN]^-$ (E = S, Se). Fluorinated derivatives of the radical anions **13.40a** and **13.40b** have been produced by electrochemical reduction and characterised by EPR spectroscopy.[156]

The EPR spectrum of the radical anion of benzo-2-tellura-1,3-diazole (**13.40c**, E = Te) was not reported until 2019; it could only be obtained after chemical reduction of the neutral precursor with KC_8 in THF in the presence of 18-crown-6.[153] Initial attempts to isolate salts of **13.40c** (E = Te) resulted in decomposition to give a ditellurido complex of benzo-2-tellura-1,3-diazole, as described in Sec. 11.2.4 (Chart 11.6).[153] Subsequently, this reduction protocol was shown to produce a trimeric dianion **13.41** comprised of two radical anions **13.40c** (E = Te) and one

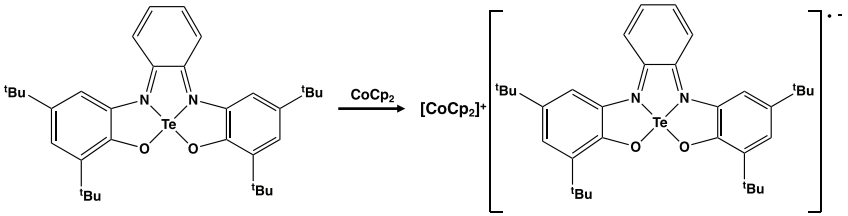

13.42 **13.43**

Scheme 13.12. Synthesis of a radical anion of a sterically hindered benzo-2-tellura-1,3-diazole.

neutral benzo-2-tellura-1,3-diazole molecule (Scheme 13.11).[157] The Te–N bond lengths in the three C_2N_2Te rings of **13.41** are in the range 2.019–2.096 Å, slightly longer than the values of 1.987–2.014 Å in benzo-2-tellura-1,3-diazole.[158] The different outcome of the reduction of benzo-2-tellura-1,3-diazole compared to that of the sulfur and selenium analogues is attributed to the strong secondary bonding interactions in **13.41**; three of the Te···N contacts are remarkably short (2.25–2.38 Å), while the fourth is unusually long (2.90 Å).[157] In the solid state **13.41** is diamagnetic due to strong antiferromagnetic coupling.

The one-electron reduction of the sterically hindered benzo-2-tellura-1,3-diazole **13.42** with cobaltocene produces the cobaltocinium salt of the corresponding radical anion **13.43** (Scheme 13.12), which was characterised by single-crystal X-ray diffraction.[159] The EPR spectrum of **13.43** in THF solution at room temperature exhibits a 1:2:3:2:1 quintet arising from hyperfine splitting with two equivalent ^{14}N nuclei.[159]

13.9 Radical Anions of Bicyclic 1-Chalcogena-2, 5-diazoles

Bicyclic radical anions in which a C–C bond is bridged by two NEN units (**13.44a**, E = S; **13.44b**, E = Se) (Chart 13.10) are readily obtained upon electrochemical or chemical reduction of the neutral precursor. Thermally stable salts of **13.44a** have been generated by using the following reducing agents: KO^{t}Bu,[160] [M(18-crown-6)][SPh] (M = Li, Na, K),[161] $CoCp_2$,[162] $CrCp^*_2$,[163] $Cr(\eta^6\text{-}C_7H_8)_2$,[164] and $MoMes_2$.[165] One-electron reduction with

13.44a E = S
13.44b E = Se

13.45

Chart 13.10. Monomeric radical anions and a dimeric dianion of a bicyclic 1-chalcogena-2,5-diazole.

the thiolate [K(18-crown-6)][SPh] has also been employed to produce the selenium analogue **13.44b**.[166] The salts of these radical anions with crown ether-encapsulated alkali-metal cations or $[S(NMe_2)_3]^+$, $[CoCp_2]^+$, $[CrCp_2*]^+$, $[Cr(\eta^6\text{-}C_7H_8)_2]^+$, and $[MoMes_2]^+$ cations are monomeric in the solid state. These salts are homospin where only the anions are paramagnetic and heterospin where both ions are paramagnetic. Both homospin and heterospin salts exhibit antiferromagnetic interactions in their spin systems.[160–166] However, when 1,1,2,2-tetrakis(dimethylamino)ethene is used as the reducing agent a black diamagnetic π-dimer comprised of the dianion **13.45** and $[(Me_2N)_2C\text{–}C(NMe_2)_2]^{2+}$ dications is isolated.[167] The interplanar separation in this dimer is 3.25 Å.

References

1. K. Awaga, T. Tanaka, T. Shirai, M. Fujimori, Y. Suzuki, H. Yoshikawa and W. Fujita, *Bull. Chem. Soc. Jpn.*, **79**, 25 (2006).
2. J. M. Rawson, A. Alberola and A. Whalley, *J. Mater. Chem.*, **16**, 2560–2575 (2006).
3. R. G. Hicks, in *Stable Radicals: Fundamental and Applied Aspects of Odd-Electron Compounds*, Ed. R. B. Hicks, John Wiley & Sons (2010), Ch. 9, pp. 317–380.
4. N. P. Gritsan, A. Yu. Makarov and A. V. Zibarev, *Appl. Magn. Reson.*, **41**, 449–466 (2011).
5. O. A. Rakitin, *Russ. Chem. Rev.*, **80**, 647–659 (2011).
6. R. T. Boeré and T. L. Roemmele, in *Comprehensive Inorganic Chemistry II,* Ed. T. Chivers, Elsevier (2013), Vol. 1, Ch. 1.14, pp. 375–411.
7. (a) J. M. Rawson and A. Alberola, in *Handbook of Chalcogen Chemistry: New Perspectives in Sulfur, Selenium and Tellurium*, Ed. F. A. Devillanova,

Royal Society of Chemistry (2007), Ch. 12.1, pp. 733–762; (b) J. M. Rawson and J. J. Hayward, in *Handbook of Chalcogen Chemistry: New Perspectives in Sulfur, Selenium and Tellurium*, Ed. F. A. Devillanova, Royal Society of Chemistry (2013), 2nd Edition, Ch. 11.1, pp. 69-98.

8. Y. M. Volkova, A. Yu. Makarov, E. A. Pritchina, N. P. Gritsan and A. V. Zibarev, *Mendeleev Commun*., **30**, 385–394 (2020).
9. D. A. Haynes, *CrystEngComm*, **13**, 4793–4805 (2011).
10. M. A. Nascimento and J. M. Rawson, in *Encyclopedia of Inorganic and Bioinorganic Chemistry*, John Wiley & Sons (2019), doi:10.1002/9781119951438.eibc2640.
11. (a) N. P. Gritsan and A. V. Zibarev, *Russ. Chem. Bull*., **60**, 2131 (2011); (b) E. A. Chulanova, N. A. Semenov, N. A. Pushkarevsky, N. P. Gritsan and A. V. Zibarev, *Mendeleev Commun*., **28**, 453 (2018); (c) E. A. Pritchina, N. P. Gritsan, O. A. Rakitin and A. V. Zibarev, *Targets Heterocycl. Syst.*, **23**, 143 (2019).
12. A. V. Zibarev and R. Mews, in *Frontiers of Selenium and Tellurium Chemistry: From Small Molecules to Biomolecules and Materials*, Eds. J. D. Woollins and R. S. Laitinen, Springer (2011), Ch. 6, pp. 123–149.
13. K. V. Shuvaev and J. Passmore, *Coord. Chem. Rev*., **257**, 1067–1091 (2013).
14. J. M. Rawson, J. Luzon and F. Palacio, *Coord. Chem. Rev*., **249**, 2631–2641 (2005).
15. (a) K. Awaga, Y. Umezono, W. Fujita, H. Yoshikawa, H. Cui, H. Kobayashi, S. Staniland and N. Robertson, *Inorg. Chim. Acta*, **361**, 3761 (2008); (b) K. Awaga, K. Nomura, H. Kishida, W. Fujita, H. Yoshikawa, M. M. Matsushita, L. Hu, Y. Shuku and R. Suiza, *Bull. Chem. Soc. Jpn*., **87**, 234 (2014).
16. S. M. Winter, S. Hill and R. T. Oakley, *J. Am. Chem. Soc*., **137**, 3720 (2015).
17. J. M. Rawson and C. P. Constantinides, in *World Scientific Reference on Spin in Organics*, Ed., J. S. Miller, World Scientific (2018), Vol. 4, pp. 95–124.
18. D. Yuan, W. Liu and X. Zhu, *Chem*., **7**, 1 (2021).
19. T. M. Barclay, L. Beer, A. W. Cordes, R. T. Oakley, K. E. Preuss, N. J. Taylor and R. W. Reed, *Chem. Commun*., 531 (1999).
20. L. Beer, A. W. Cordes, R. C. Haddon, M. E. Itkis, R. T. Oakley, R. W. Reed and C. M. Robertson, *Chem. Commun*., 1872 (2002).
21. T. M. Barclay, A. W. Cordes, R. C. Haddon, M. E. Itkis, R. T. Oakley, R. W. Reed and J. F. Richardson, *J. Am. Chem. Soc*., **121**, 969 (1999).
22. L. Beer, J. L. Brusso, A. W. Cordes, R. C. Haddon, M. E. Itkis, K. Kirschbaum, D. S. MacGregor, R. T. Oakley, A. A. Pinkerton and R. W. Reed, *J. Am. Chem. Soc*., **124**, 9498 (2002).

23. L. Beer, J. L. Brusso, A. W. Cordes, E. Godde, R. C. Haddon, M. E. Itkis, R. T. Oakley and R. W. Reed, *Chem. Commun*., 2563 (2002).
24. L. Beer, J. F. Britten, J. L. Brusso, A. W. Cordes, R. C. Haddon, M. E. Itkis, D. S. MacGregor, R. T. Oakley, R. W. Reed and C. M. Robertson, *J. Am. Chem. Soc*., **125**, 14394 (2003).
25. L. Beer, J. F. Britten, O. P. Clements, R. C. Haddon, M. E. Itkis, K. M. Matkovich, R. T. Oakley and R. W. Reed, *Chem. Mater*., **16**, 1564 (2004).
26. A. A. Leitch, C. E. McKenzie, R. T. Oakley, R. W. Reed, J. F. Richardson and L. D. Sawyer, *Chem. Commun.*, 1088 (2006).
27. A. A. Leitch, C. E. McKenzie, R. W. Reed, C. M. Robertson, J. F. Britten, X. Yu, R. A. Secco and R. T. Oakley, *J. Am. Chem. Soc*., **129**, 7903 (2007).
28. K. Lekin, J. W. L. Wong, S. M. Winter, A. Mailman P. A. Dube and R. T. Oakley, *Inorg. Chem*., **52**, 2188 (2013).
29. K. Lekin, K. Ogata, A. Maclean, A. Mailman, S. M. Winter, A. Assoud, M. Mito, J. S. Tse, S. Desgreniers, N. Hirao, P. A. Dube and R. T. Oakley, *Chem. Commun*., **52**, 13877 (2016).
30. N. J. Yutronkie, D. Bates, P. A. Dube, S. M. Winter, C. M. Robertson, J. L. Brusso and R. T. Oakley, *Inorg*. *Chem*., **58**, 419 (2019).
31. (a) X. Yu, A. Mailman, P. A. Dube, A. Assoud and R. T. Oakley, *Chem. Commun*., 47, 4655 (2011); (b) X. Yu, A. Mailman, K. Lekin, A. Assoud, P. A. Dube and R. T. Oakley, *Cryst. Growth Des*., **12**, 4655 (2011).
32. (a) X. Yu, A. Mailman, K. Lekin, A. Assoud, C. M. Robertson, B. C. Noll, C. F. Campana, J. A. K. Howard, P. A. Dube and R. T. Oakley, *J. Am. Chem. Soc*., **134**, 2264 (2012); (b) X. Yu, A. Mailman, K. Lekin, A. Assoud, P. A. Dube and R. T. Oakley, *Cryst. Growth Des.*, **12**, 2485 (2012).
33. (a) A. Mailman, S. M. Winter, X. Yu, C. M. Robertson, W. Yong, J. S. Tse, R. A. Secco, Z. Liu, P. A. Dube, J. A. K. Howard and R. T. Oakley, *J. Am. Chem. Soc*., **134**, 9886 (2012); (b) S. M. Winter, A. Mailman, R. T. Oakley, K. Thirunavukkuarasu, S. Hill, D. E. Graf, S. W. Tozer, J. S. Tse, M. Mito and H. Yamaguchi, *Phys. Rev*. *B*, **89**, 214403 (2014).
34. (a) J. W. L. Wong, A. Mailman, S. M. Winter, C. M. Robertson, R. J. Holmberg, M. Murugesu, P. A. Dube and R. T. Oakley, *Chem. Commun*., **50**, 785 (2014); (b) J. W. L. Wong, A. Mailman, K. Lekin, S. M. Winter, W. Yong, J. Zhao, S. V. Garimella, J. Tse, R. A. Secco, S. Desgreniers, Y. Ohishi, F. Borondics and R. T. Oakley, *J. Am. Chem. Soc*., **136**, 1070 (2014).
35. D. Tian, S. M. Winter, A. Mailman, J. W. L. Wong, W. Yong, H. Yamaguchi, Y. Jia, J. S. Tse, S. Desgreniers, R. A. Secco, S. R. Julian, C. Jin, M. Mito, Y. Ohishi and R. T. Oakley, *J. Am. Chem. Soc*., **137**, 14136 (2015).

36. A. Mailman, S. M. Winter, J. W. L. Wong, C. M. Robertson, A. Assoud, P. A. Dube and R. T. Oakley, *J. Am. Chem. Soc*., **137**, 1044 (2015).
37. L. Postulka, S. M. Winter, A. G. Mihailov, A. Mailman, A. Assoud, C. M. Robertson, B. Wolf, M. Lang and R. T. Oakley, *J. Am. Chem. Soc*., **138**, 10738 (2016).
38. A. Mailman, J. W. L. Wong, S. M. Winter, R. C. M. Claridge, C. M. Robertson, A. Assoud, W. Yong, E. Steven, P. A. Dube, J. S. Tse, S. Desgreniers, R. A. Secco and R. T. Oakley, *J. Am. Chem. Soc*., **139**, 1625 (2017).
39. A. Mailman, A. A. Leitch, W. Yong, E. Steven, S. M. Winter, R. C. M. Claridge, A. Assoud, J. S. Tse, S. Desgreniers, R. A. Secco and R. T. Oakley. *J. Am. Chem. Soc*., **139**, 2180 (2017).
40. A. Mailman, C. M. Robertson, S. M. Winter, P. A. Dube and R. T. Oakley, *Inorg. Chem*., **58**, 6495 (2019).
41. Y. M. Volkova, A. Yu. Makarov, S. B. Zikirin, A. M. Genaev, I. Yu. Bagryanskaya and A. V. Zibarev, *Mendeleev Commun*., **27**, 19 (2017).
42. A. W. Cordes, J. R. Mingie, R. T. Oakley, R. W. Reed and H. Zhang, *Can. J. Chem*., **79**, 1352 (2001).
43. R. T. Oakley, R. W. Reed, C. M. Robertson and J. F. Richardson, *Inorg. Chem*. **44**, 1837 (2005).
44. (a) A. V. Pivtsov, L. V. Kulik, A. Yu. Makarov and F. Blockhuys, *Phys. Chem. Chem. Phys*., **13**, 3873 (2011); (b) A. Yu. Makarov, F. Blockhuys, I. Yu. Bagryanskaya, Y. V. Gatilov, M. M. Shakirov and A. V. Zibarev, *Inorg. Chem*., **52**, 3699 (2013).
45. S. M. Winter, K. Cvrkalj, P. A. Dube, C. M. Robertson, M. R. Probert, J. A. K. Howard and R. T. Oakley, *Chem. Commun*., 7306 (2009).
46. (a) H. Phan, K. Lekin, S. M. Winter, R. T. Oakley and M. Shatruk, *J. Am. Chem. Soc*., **135**, 15674 (2013); (b) K. Lekin, H. Phan, S. M. Winter, J. W. L. Wong, A. A. Leitch, D. Laniel, W. Yong, R. A. Secco, J. S. Tse, S. Desgreniers, P. A. Dube, M. Shatruk and R. T. Oakley, *J. Am. Chem. Soc*., **136**, 8050 (2014).
47. L. Beer, J. L. Brusso, R. C. Haddon, M. E. Itkis, A. A. Leitch, R. T. Oakley, R. W. Reed and J. F. Richardson, *Chem. Commun*., 1543 (2005).
48. A. A. Leitch, X. Yu, C. M. Robertson, R. A. Secco, J. S. Tse and R. T. Oakley, *Inorg. Chem*., **48**, 9874 (2007).
49. J. S. Tse, A. A. Leitch, X. Yu, X. Bao, S. Zhang, Q. Liu, C. Jin, R. A. Secco, S. Desgreniers, Y. Ohishi and R. T. Oakley, *J. Am. Chem. Soc*., **132**, 4876 (2010).

50. K. Lekin, S. M. Winter, L. E. Downie, X. Bao, J. S. Tse, S. Desgreniers, R. A. Secco, P. A. Dube and R. T. Oakley, *J. Am. Chem. Soc*., **132**, 16212 (2010).
51. (a) J. L. Beer, J. L. Brusso, R. C. Haddon, M. E. Itkis, R. T. Oakley, R. W. Reed, J. F. Richardson, R. A. Secco and X. Yu, *Chem. Commun*., 5745 (2005): (b) L. Beer, J. L. Brusso, R. C. Haddon, M. E. Itkis, H. Kleinke, A. A. Leitch, R. T. Oakley, R. W. Reed, J. F. Richardson, R. A. Secco and X. Yu, *J. Am. Chem. Soc*., **127**, 18159 (2005).
52. J. L. Brusso, S. Derakhsan, M. E. Itkis, H. Kleinke, R. C. Haddon, R. T. Oakley, R. W. Reed and J. F. Richardson, C. M. Robertson and L. K. Thompson, *Inorg. Chem*., **45**, 10958 (2006).
53. A. A. Leitch, X. Yu, S. M. Winter, R. A. Secco, P. A. Dube and R. T. Oakley, *J. Am. Chem. Soc*., **131**, 7112 (2009).
54. J. L. Brusso, K. Cvrkalj, A. A. Leitch, R. T. Oakley, R. W. Reed and C. M. Robertson, *J. Am. Chem. Soc*., **128**, 15080 (2006).
55. A. A. Leitch, J. L. Brusso, K. Cvrkalj, R. W. Reed, C. M. Robertson, P. A. Dube and R. T. Oakley, *Chem. Commun*., 3368 (2007).
56. C. M. Robertson, D. J. T. Myles, A. A. Leitch, R. W. Reed, B. M. Dooley, N. L. Frank, P. A. Dube, L. K. Thompson and R. T. Oakley, *J. Am. Chem. Soc*., **129**, 12688 (2007).
57. C. M. Robertson, A. A. Leitch, K. Cvrkalj, R. W. Reed, D. J. T. Myles, P. A. Dube, and R. T. Oakley, *J. Am. Chem. Soc*., **130**, 8414 (2008).
58. C. M. Robertson, A. A. Leitch, K. Cvrkalj, D. J. T. Myles, R. W. Reed, P. A. Dube and R. T. Oakley, *J. Am. Chem. Soc*., **130**, 14791 (2008).
59. X. Yu, A. Mailman, P. A. Dube, A. Assoud and R. T. Oakley, *Chem. Commun*., **47**, 4655 (2011).
60. M. Mito, Y. Komorida, H. Tsuruda, J. S. Tse, S. Desgreniers, Y. Ohishi, A. A. Leitch, K. Cvrkalj, C. M. Robertson and R. T. Oakley, *J. Am. Chem. Soc*., **131**, 16012 (2009).
61. H. Tsuruda, M. Mito, H. Deguchi, S. Takagi, A. A. Leitch, K. Lekin, S. M. Winter and R. T. Oakley, *Polyhedron*, **30**, 2997 (2011).
62. A. A. Leitch, K. Lekin, S. M. Winter, L. E. Downie, H. Tsuruda, J. S. Tse, M. Mito, S. Desgreniers, P. A. Dube, S. Zhang, Q. Liu, C. Jin, Y. Ohishi and R. T. Oakley, *J. Am. Chem. Soc*., **133**, 6051 (2011).
63. A. Yu. Makarov, S. N. Kim, N. P. Gritsan, I. Yu. Bagryanskaya, Yu. V. Gatilov and A. V. Zibarev, *Mendeleev Commun*., **15**, 14 (2005).
64. N. P. Gritsan, S. N. Kim, A. Yu. Makarov, E. N. Chesnokov and A. V. Zibarev, *Photochem. Photobiol. Sci*., **5**, 95 (2006).

65. A. Yu. Makarov, Y. M. Volkova, L. A. Shundrin, A. A. Dmitriev, I. G. Irtegova, I. Yu. Bagryanskaya, I. K. Shundrina, N. P. Gritsan, J. Beckmann and A. V. Zibarev, *Chem. Commun*., **56**, 727 (2020).
66. T. M. Barclay, A. W. Cordes, J. D. Goddard, R. C. Mawhinney, R. T. Oakley, K. E. Preusss and R. W. Reed, *J. Am. Chem. Soc*., **119**, 12136 (1997).
67. L. Postulka, S. M. Winter, A. G. Mihailov, A. Mailman, A. Assoud, C. M. Robertson, B. Wolf, M. Lang and R. T. Oakley, *J. Am. Chem. Soc*., **138**, 10738 (2016).
68. T. M. Barclay, I. J. Burgess, A. W. Cordes, R. T. Oakley and R. W. Reed, *Chem. Commun*., 1939 (1998).
69. (a) K. Okamoto, T. Tanaka, W. Fujita, K. Awaga and T. Inabe, *Angew. Chem. Int. Ed*., **45**, 4516 (2006); (b) K. Okamoto, T. Tnaka, W. Gujita and K. Awaga, *Phys. Rev. B*, **76**, 075328 (2007).
70. J. M. Rawson and G. D. McManus, *Coord. Chem. Rev*., **189**, 135 (1999).
71. H. Du, R. C. Haddon, I. Krossing, J. Passmore, J. M. Rawson and M. J. Schriver, *Chem. Commun*., 1836 (2002).
72. (a) G. Wolmershäuser, M. Schnauber and T. Wilhelm, *J. Chem. Soc*., *Chem. Commun*., 573 (1984); (b) G. Heckmann, R. Johann, G. Kraft and G. Wolmershäuser, *Synth. Met*., **41–43**, 3287 (1991).
73. (a) A. Decken, A. Mailman, J. Passmore, J. M. Raitiainen, W. Scherer and E. W. Scheidt, *Dalton Trans*., 868 (2011); (b) A. Decken, A. Mailman and J. Passmore, *Chem. Commun*., 6077 (2009); (c) A. Decken, A. Mailman, S. M. Mattar and J. Passmore, *Chem. Commun*., 2366 (2005).
74. A. Alberola, R. D. Farley, S. M. Humphrey, G. D. McManus, D. M. Murphy and J. M. Rawson, *Dalton Trans*., 3838 (2005).
75. (a) A. Alberola, D. J. Eisler, L. Harvey and J. M. Rawson, *CrystEngComm*, **13**, 1794 (2011); (b) A. Alberola, O. P. Clements, R. J. Collis, L. Cubbitt, C. M. Grant, R. J. Less, R. T. Oakley, J. M. Rawson, R. W. Reed and C. M. Robertson, *Cryst. Growth Des*., **8**, 155 (2008); (c) A. Alberola, R. J. Collis, R. J. Less and J. M. Rawson, *J. Organomet. Chem*., **692**, 2743 (2007); (d) A. Alberola, J. Burley, R. J. Collis, R. J. Less and J. M. Rawson, *J. Organomet. Chem*., **692**, 2750 (2007).
76. A. Alberola, D. J. Eisler, R. J. Less, E. Navarro-Moratalla and J. M. Rawson, *Chem. Commun*., **46**, 6114 (2010).
77. S. Brownridge, H. B. Du, S. A. Fairhurst, R. C. Haddon, H. Oberhammer, S. Parsons, J. Passmore, M. J. Schriver, L. H. Sutcliffe and N. P. C. Westwood, *J. Chem. Soc*., *Dalton Trans*., 3365 (2000).

78. E. G. Awere, N. Burford, R. C. Haddon, S. Parsons, J. Passmore, J. V.Waszczak and P. S. White, *Inorg. Chem*., **29**, 4821 (1990).
79. G. D. McManus, J. M. Rawson, N. Feeder, F. Palacio and P. Oliete, *J. Mater. Chem*., **10**, 2001 (2000).
80. A. Alberola, R. J. Collis, S. M. Humphrey, R. J. Lees and J. M. Rawson, *Inorg. Chem*., **45**, 1903 (2006).
81. T. M. Barclay, A. W. Cordes, N. A. George, R. C. Haddon, M. E. Itkis, M. Mashuta, R. T. Oakley, G. W. Patenaude, R. W. Reed, J. F. Richardson and H. Zhang, *J. Am. Chem. Soc*., **120**, 352 (1998).
82. W. Fujita and K. Awaga, *Science*, **286**, 261 (1999).
83. G. D. McManus, J. M. Rawson, N. Feeder, J. van Duijn, E. J. L. McInnes, J. J. Novoa, R. Burriel, F. Placio and P. Oliete, *J. Mater. Chem*., **11**, 1992 (2001).
84. J. L. Brusso, O. P. Clements, R. C. Haddon, M. E. Itkis, A. A. Leitch, R. T. Oakley, R. W. Reed and J. F. Richardson, *J. Am. Chem. Soc*., **126**, 8256 (2004).
85. J. L. Brusso, O. P. Clements, R. C. Haddon, M. E. Itkis, A. A. Leitch, R. T. Oakley, R. W. Reed and J. F. Richardson, *J. Am. Chem. Soc*., **126**, 14692 (2004).
86. P. Naumov, J. P. Hill, K. Sakurai, M. Tanaka and K. Ariga, *J. Phys. Chem. A*, **111**, 6449 (2007).
87. T. Tanaka, W. Fujita and K. Awaga, *Chem. Phys. Lett*., **393**, 150 (2004).
88. S. Vela, F. Mota, M. Deumal, R. Suizu, Y. Shuku, A. Mizuno, K. Awaga, M. Shiga, J. J. Novoa and J. Ribas-Arino, *Nature Commun*., **5**, 4411 (2014).
89. S. Vela, M. Deumal, M. Shiga, J. J. Novoa and J. Ribas-Arino, *Chem. Sci*., **6**, 2731 (2015).
90. S. Vela, M. B. Reardon, C. E. Jakobsche, M. M. Turnbull, J. Ribas-Arino and J. J. Novia, *Chem. Eur. J*., **23**, 3479 (2017).
91. (a) T. M. Barclay, A. W. Cordes, N. A. George, R. C. Haddon, R. T. Oakley, T. T. M. Palstra, G. W. Patenaude, R. W. Reed, J. F. Richardson and H. Zhang, *Chem. Commun*., 873 (1997); (b) D. Bates, C. M. Robertson, A. A. Leitch, P. A. Dube and R. T. Oakley, *J. Am. Chem. Soc*., **140**, 3846 (2018).
92. W. Fujita, K. Awaga, Y. Nakazawa, K. Saito and M. Sorai, *Chem. Phys. Lett*., **352**, 348 (2002).
93. S. V. Potts, L. J. Barbour, D. A. Haynes, J. M. Rawson and G. O. Lloyd, *J. Am. Chem. Soc*., **133**, 12948 (2011).
94. Y. Umezono, W. Fujita and K. Awaga, *Chem. Phys. Lett*., **409**, 139 (2005).

95. S. Staniland, W. Fujita, Y. Umezono, K. Awaga, P. J. Camp, S. J. Clark and N. Robertson, *Inorg. Chem*., **44**, 546 (2005).
96. Y. Umezono, W. Fujita and K. Awaga, *J. Am. Chem. Soc*., **128**, 1084 (2006).
97. T. M. Barclay, A. W. Cordes, R. H. de Laat, J. D. Goddard, R. C. Haddon, D. Y. Jeter, R. C. Mawhinney, R. T. Oakley, T. T. M. Palstra, G. W. Patenaude, R. W. Reed and N. P. C. Westwood, *J. Am. Chem. Soc*., **119**, 2633 (1997).
98. W. Fujita, K. Takahashi and H. Kobayashi, *Cryst. Growth Des*., **11**, 575 (2011).
99. W. Fujita, R. Kondo, S. Kagoshima and K. Awaga, *J. Am. Chem. Soc*., **128**, 6016 (2006).
100. W. Fujita, K. Kikuchi and K. Awaga, *Angew. Chem. Int. Ed*., **47**, 9480 (2008)
101. (a) W. Fujita and K. Awaga, *Chem. Phys. Lett*., **357**, 385 (2002); (b) W. Fujita and K. Awaga, *Chem. Phys. Lett*., **388**, 186 (2004); (c) M. Mito, M. Fujino, H. Deguchi, S. Takagi, W. Fujita and K. Awaga, *Polyhedron*, **24**, 2501 (2005); (d) W. Fujita and K. Kikuchi, *Asian J. Chem*., **4**, 400 (2009).
102. W. Fujita, K. Awaga, M. Takahashi, M. Takeda and T. Yamazaki, *Chem. Phys. Lett*., **362**, 97 (2002).
103. K. Suzuki, T. Kodama, K. Kikuchi and W. Fujita, *Chem. Lett*., **39**, 1096 (2010).
104. W. Fujita and K. Kikuchi, *Eur. J. Inorg. Chem*., **2014**, 93 (2014).
105. W. Fujita, *Dalton Trans*., **44**, 903 (2015).
106. J. M. Rawson, A. J. Banister and I. Lavender, *Adv. Het. Chem*., **62**, 137 (1995).
107. K. E. Preuss, *Polyhedron*, **79**, 1 (2014).
108. C. D. Bryan, A. W. Cordes, J. D. Goddard, R. C. Haddon, C. D. MacKinnon, R. C. Mawhinney, R. T. Oakley, T. T. M. Palstra and A. S. Perel, *J. Am. Chem. Soc*., **118**, 330 (1996).
109. S. W. Robinson, D. Haynes and J. M. Rawson, *CrystEngComm*, **15**, 10205 (2013).
110. A. Alberola, C.S. Clarke, D. A. Haynes, S. I. Pascu and J. M. Rawson, *Chem. Commun*., 4726 (2005).
111. R. T. Boeré and N. D. D. Hill, *CrystEngComm*, **19**, 3698 (2017).
112. (a) A. Alberola, R. J. Less, F. Placio, C. M. Pask and J. M. Rawson, *Molecules*, **9**, 771 (2004); (b) J. Luzon, J. Campo, F. Placio, G. J. McIntyre, J. M. Rawson, R. J. Less, C. M. Pask, A. Alberola, R. D. Farley, D. M. Murphy and A. E. Goeta, *Phys. Rev. B*, **81**, 144429 (2010).

113. (a) M. Kertesz, *Chem. Eur. J*., **25**, 400 (2019); (b) H. Z. Beneberu, Y.-H. Tian and M. Kertesz, *Phys. Chem. Chem. Phys*., **14**, 10713 (2012).
114. (a) W. V. F. Brooks, N. Burford, J. Passmore, M. J. Schriver and L. H. Sutcliffe, *J. Chem. Soc.*, *Chem. Commun.,* 69 (1987); (b) S. A. Fairhurst, K. M. Johnson, L. H. Sutcliffe, K. F. Preston, A. J. Banister, Z. V. Hauptman and J. Passmore *J. Chem. Soc.*, *Dalton Trans*., 1465 (1986).
115. H. Matsui, M. Yamane, T. Tonami, T. Nagami, K. Watanabe, R. Kishi, Y. Kitagawa and M. Nakano, *Mater. Chem. Front*., **2**, 785 (2018).
116. (a) Y. Beldjoudi, R. Sun, A. Arauzo, J. Campo. R. J. Less and J. M. Rawson, *Cryst. Growth Des*., **18**, 179 (2018); (b) R. L. Melen, R. J. Less, C. M. Pask and J. M. Rawson, *Inorg. Chem*., **55**, 11747 (2016); (c) D. A. Haynes and J. M. Rawson, *Eur. J. Inorg. Chem*., 3554 (2018); (d) P. Commins, A. B. Dippenaar, L. Li, H. Hara, D. A. Haynes and P. Naumov, *Chem. Sci*., **12**, 6188 (2021).
117. M. B. Mills, T. Wohlhauser, B. Stein, W. R. Verduyn, E. Song, P. Dechambenoit, M. Rouzières, R. Clérac and K. E. Preuss, *J. Am. Chem. Soc*., **140**, 16904 (2018).
118. R. T. Boeré, *CrystEngComm*, **18**, 2748 (2016).
119. (a) S. Domagala, K. Kose, S. W. Robinson, D. A. Haynes and K. Woźniak, *Cryst. Growth Des*., **14**, 4834 (2014); (b) S. Domagala and D. A. Haynes, *Cryst. Growth Des*., **16**, 7116 (2014).
120. (a) A. D. Bond, D. A. Haynes, C. M. Pask and J. M. Rawson, *J. Chem. Soc., Dalton Trans*., 2522 (2002): (b) C. S. Clarke, S. I. Pascu and J. M. Rawson, *CrystEngChem*, **6**, 79 (2004).
121. C. Knapp, E. Lork, K. Gupta and R. Mews, *Z. Anorg. Allg. Chem*., **631**, 1640 (2005).
122. Y. Beldjoudi, A. Arauzo, J. Campo, E. L. Gavey, M. Pilkington, M. A. Nascimento and J. M. Rawson, *J. Am. Chem. Soc*., **141**, 6875 (2019).
123. R. Suizu, A. Iwasaki, Y. Shuku and K. Awaga, *J. Mater. Chem. C*, **3**, 7938 (2015).
124. Y. Beldjoudi, M. A. Nascimento, Y. J. Cho, H. Yu, H. Aziz, D. Tonouchi, K. Eguchi, M. M. Matsushita, K. Awaga, I. Osorio-Roman, C. P. Constantinides and J. M. Rawson, *J. Am Chem. Soc*., **140**, 6260 (2018).
125. A. Iwasaki, L. Hu, R. Suizu, K. Nomura, H. Yoshikawa, K. Aaga, Y. Noda, K. Kanai, Y. Ouchi, K. Seki and H. Ito, *Angew. Chem. Int. Ed*., **48**, 4022 (2009).
126. M. Yamamoto, R. Suizu, S. Dutta, P. Mishra, T. Nakayama, K. Sakamoto, K. Wakabayashi, T. Uchihashi and K. Awaga, *Sci. Rep*., **5**, 18359 (2015).

127. Y. Beldjoudi, A. Arauzo, F. Palacio, M. Pilkington and J. M. Rawson, *J. Am. Chem. Soc*., **138**, 16779 (2019).
128. (a) F. Palacio, G. Antorrena, M. Castro, R. Burriel, J. M. Rawson, J. N. B. Smith, N. Bricklebank, J. Novoa and C. Ritter, *Phys. Rev. Lett*., **79**, 2338 (1997); (b) M. Deumal, J. M. Rawson, A. E. Goeta, J. A. K. Howard, R. C. B. Copley, M. A. Robb and J. J. Novoa, *Chem. Eur. J*., **16**, 2741 (2010); (c) R. I. Thomson, C. M. Pask, G. O. Lloyd, M. Mito and J. M. Rawson, *Chem. Eur. J*., **18**, 8629 (2012); (d) A. Alberola, R. J. Lees, C. M. Pask, J. M. Rawson, F. Palacio, P. Oliete, C. Paulsen. A. Yamaguchi, R. D. Farley and D. M. Murphy, *Angew. Chem. Int. Ed*., **42**, 4782 (2003).
129. W. Yong, K. Lekin, R. P. C. Bauer, J. S. Tse, S. Desgreniers, R. A. Secco, N. Hirao and R. T. Oakley, *Inorg. Chem*., **58**, 3550 (2019)
130. Y. Beldjoudi, I. Osorio-Roman, M. A. Nascimento and J. M. Rawson, *J. Mater. Chem. C*, **5**, 2794 (2017).
131. M. A. Nascimento, E. Heyer, J. J. Clarke, H. J. Cowley, A. Alberola, N. Stephaniuk and J. M. Rawson, *Angew. Chem. Int. Ed*., **58**, 1371 (2019).
132. H. J. Cowley, J. J. Hayward, D. R. Pratt and J. M. Rawson, *Dalton Trans*., **43**, 1332 (2014).
133. N. T. Stephaniuk, E. M. Haskings, A. Arauzo, J. Campo and J. M. Rawson, *Dalton Trans*., **48**, 16312 (2019).
134. V. I. Nikolayenko, L. J. Barbour, A. Arauzo, J. Campo, J. M. Rawson and D. A. Haynes, *Chem. Commun*., **53**, 11310 (2017).
135. C. S. Clarke, D. A. Haynes, J. M. Rawson and A. D. Bond, *Chem. Commun*., 2774 (2003).
136. A. J. Banister, J. M. Rawson, W. Clegg and S. L. Birkby, *J. Chem. Soc*., *Dalton Trans*., 1099 (1991).
137. (a) J. Passmore and X. Sun, *Inorg. Chem*., **35**, 1313 (1996): (b) C. Aherne, A. J. Banister, A. W. Luke, J. M. Rawson and R. J. Whitehead, *J. Chem. Soc*., *Dalton Trans*., 1277 (1992).
138. T. S. Cameron, M. T. Lemaire, J. Passmore, J. M. Rawson, K. V. Shuvaev and L. K. Thompson, *Inorg. Chem*., **44**, 2576 (2005).
139. (a) P. J. Hayes, R. T. Oakley, A. W. Cordes and W. T. Pennington, *J. Am. Chem. Soc*., **107**, 1346 (1985); (b) R. T. Oakley, R. W. Reed, A. W. Cordes, S. L. Craig and J. B. Graham, *J. Am. Chem. Soc*., **109**, 7745 (1987).
140. R. T. Boeré, T. L. Roemmele and X. Yu, *Inorg. Chem*., **50**, 5123 (2011).
141. N. J. Yutronkie, A. A. Leitch, I. Korobkov and J. L. Brusso, *Cryst. Growth Des*., **15**, 2524 (2015).
142. A. A. Leitch, I. Korobkov, A. Assoud and J. L. Brusso, *Chem. Commun*., **50**, 1934 (2014).

143. K. L. M. Harriman, I. Kühne, A. A. Leitch, I. Korobkov, R. Clérac, M. Murugesu and J. L. Brusso, *Inorg. Chem*., **55**, 2268 (2016).
144. E. Kleisath, N. J. Yutronkie, I. Korobkov, B. M. Gabidullin and J. L. Brusso, *New J. Chem*., **40**, 4472 (2016).
145. R. T. Boeré and T. Roemmele, *Phosphorus*, *Sulfur and Silicon*, **107**, 1346 (2004).
146. R. T. Boeré, R. T. Oakley, R. W. Reed and N. P. C. Westwood, *J. Am. Chem. Soc*., **111**, 1180 (1989).
147. N. P. Gritsan, K. V. Shuvaev, S. N. Kim, C. Knapp, R. Mews, V. A. Bagryanskya and A. V. Zibarev, *Mendeleev Commun*., **17**, 204 (2007).
148. T. S. Cameron, R. C. Haddon, S. M. Mattar, S. Parsons, J. Passmore and A. P. Ramirez, *Inorg. Chem*., **31**, 2274 (1992).
149. A. Decken, S. M. Mattar, J. Passmore, K. V. Shuvaev and L. K. Thompson, *Inorg. Chem*., **45**, 3878 (2006).
150. T. S. Cameron, A. Decken, R. M. Kowalczyk, E. J. L. McInnes, J. Passmore, J. M. Rawson, K. V. Shuvaev and L. K. Thompson, *J. Chem. Soc.*, *Chem. Commun*., 2277 (2006).
151. T. S. Cameron, A. Decken, F. Grein, C. Knapp, J. Passmore, J. M. Rautiainen, K. V. Shuvaev, R. C. Thompson and D. J. Wood, *Inorg. Chem*., **49**, 3861 (2010).
152. A. Decken, M. Ebdah, R. M. Kowalczyk, C. P. Landee, E. J. I. McInnes, J. Passmore, K. V. Shuvaev and L. K. Thompson, *Inorg. Chem*., **46**, 7756 (2007).
153. N. A. Pushkarevsky, E. A. Chulanova, L. A. Shundrin, A. I. Smolentsev, G. E. Salnikov, E. A. Pritchina, A. M. Genaev, I. G. Irtegoa, I. Yu. Bagryanskaya, S. N. Konchenko, N. P. Gritsan, J. Beckmann and A. V. Zibarev, *Chem. Eur. J*., **25**, 806 (2019).
154. E. T. Strom and G. A. Russell, *J. Am. Chem. Soc*., **87**, 3326 (1965).
155. S. N. Konchenko, N. P. Gritsan, A. V. Lonchakov, U. Radius and A. V. Zibarev, *Mendeleev Commun*., **19**, 7 (2009).
156. N. V. Vasylieva, I. G. Irtegova, N. P. Gritsan, A. V. Lonchakov, A. Yu. Makarov, L. A. Shundrin and A. V. Zibarev, *J. Phys. Org. Chem*., **23**, 536 (2010).
157. N. A. Pushkarevsky, A. I. Smolentsev, A. A. Dimitriev, I. Vargas-Baca, N. P. Gritsan, J. Beckmann and A. V. Zibarev, *Chem. Commun.,* **56**, 1113 (2020).
158. P. A. Petrov, E. M. Kadilenko, T. S. Sukhikh, I. V. Eltsov, A. L. Gushchin, V. A. Nadolinny, M. N. Sokolov and N. P. Gritsan, *Chem. Eur. J*., **26**, 14688 (2020).

159. A. F. Cozzolino, J. F. Britten and I. Vargas-Baca, *Cryst. Growth Des*., **6**, 181 (2006).
160. A. Yu. Makarov, I. G. Irtegova, N. V. Vasilieva, I. Yu. Bagryanskaya, T. Borrmann, Y. V. Gatilov, E. Lork, R. Mews, W.-D. Stohrer and A. V. Zibarev, *Inorg. Chem*., **44**, 7195 (2005).
161. V. N. Ikorskii, I. G. Irtegova, E. Lork, A. Yu. Makarov, R. Mews, V. I. Ovcharenko and A. V. Zibarev, *Eur. J. Inorg. Chem*., **2006**, 3061 (2006).
162. S. N. Konchenko, N. P. Gritsan, A. V. Lonchakov, I. G. Irtegova, R. Mews, V. I. Ovcharenko, U. Radius and A. V. Zibarev, *Eur. J. Inorg. Chem*., **2008**, 3833 (2008).
163. N. A. Semenov, N. A. Pushkarevsky, A. V. Lonchakov, A. S. Bogomyakov, E. A. Pritchina, E. A. Suturina, N. P. Gritsan, S. N. Konchenko, R. Mews, V. I. Ovcharenko and A. V. Zibarev, *Inorg. Chem*., **49**, 7558 (2010).
164. N. A. Semenov, N. A. Pushkarevsky, E. A. Suturina, E. A. Chulanova, N. V. Kuratieva, A. S. Bogomyakov, I. G. Irtegova, N. V. Vasilieva, L. S. Konstantinova, N. P. Gritsan O. A. Rakitin, V. I. Ovcharenko, S. N. Konchenko and A. V. Zibarev, *Inorg. Chem*., **52**, 6654 (2013).
165. N. A. Pushkarevsky, N. A. Semenov, A. A. Dmitriev, N. V. Kuratieva, A. S. Bogomyakov, I. G. Irtegova, N. V. Vasilieva, B. E. Bode, N. P. Gritsan, L. S. Konstantinova, J. D. Woollins, O. A. Rakitin, S. N. Konchenko, V. I. Ovcharenko and A. V. Zibarev, *Inorg. Chem*., **54**, 7007 (2005).
166. I. Yu. Bagryanskaya, Y. V. Gatilov, N. P. Gritsan, V. N. Ikorskii, I. G. Irtegova, A. V. Lonchakov, E. Lork, R. Mews, V. I. Ovcharenko, N. A. Semenov, N. A. Vasilieva and A. V. Zibarev, *Eur. J. Inorg. Chem*., **2007**, 4751 (2007).
167. N. P. Gritsan, A. V. Lonchakov, E. Lork, R. Mews, E. A. Pritchina and A. V. Zibarev, *Eur. J. Inorg. Chem*., **2008**, 1994 (2008).

Chapter 14

Metal Complexes of Carbon-Nitrogen-Chalcogen Radicals: Coordination Modes

14.1 Introduction

The simplest chalcogenazyl radicals $[EN]^{\bullet}$ (E = S, Se) can be stabilised in a wide variety of transition-metal complexes as discussed in Sec. 5.3.2.[1] Metal complexes of paramagnetic carbon-nitrogen-chalcogen heterocycles have attracted attention recently in view of their unusual properties. This chapter chronicles the synthesis, coordination behaviour and properties of metal complexes of the radicals discussed in Chapter 13 and related multidentate ligands. It begins with an account of the metal complexes of 1,2-dichalcogena-3,5-diazolyl radicals, which are the most widely studied C,N,E paramagnetic ligands. This is followed by a description of the preparation and properties of metal complexes of 1,3-dichalcogen-2-azolyl, 1-chalcogena-2,4,6-triazinyl and 1,3-dithia-2-azolyl radicals.

General reviews of this interesting topic were published in 2007[2a] and 2015,[2b] and several other accounts and book chapters include a discussion of specific aspects, notably magnetic properties.[3,4] Charge-transfer complexes that incorporate carbon-nitrogen-chalcogen radical cations and metal-containing counter-anions are discussed in Secs. 13.2.4 and 13.3.3, unless they involve *N*- and/or *S*-coordination linkages between the heterocycle and the metal centre (Sec. 14.4). Similarly, derivatives of bicyclic 1,2-dichalcogen-5-azolyl radical anions with organometallic cations are

described in Sec. 13.9, since they exist as ion-separated salts rather than coordination complexes.

14.2 Transition-Metal Complexes of 1,2-Dichalcogena-3,5-diazolyl Ligands

Early work on metal complexes of 1,2-dichalcogena-3,5-diazolyl radicals explored the use of PhDTDA (Chart 14.1) as a ligand. More recently, the emphasis in investigations of the coordination chemistry of DTDAs has

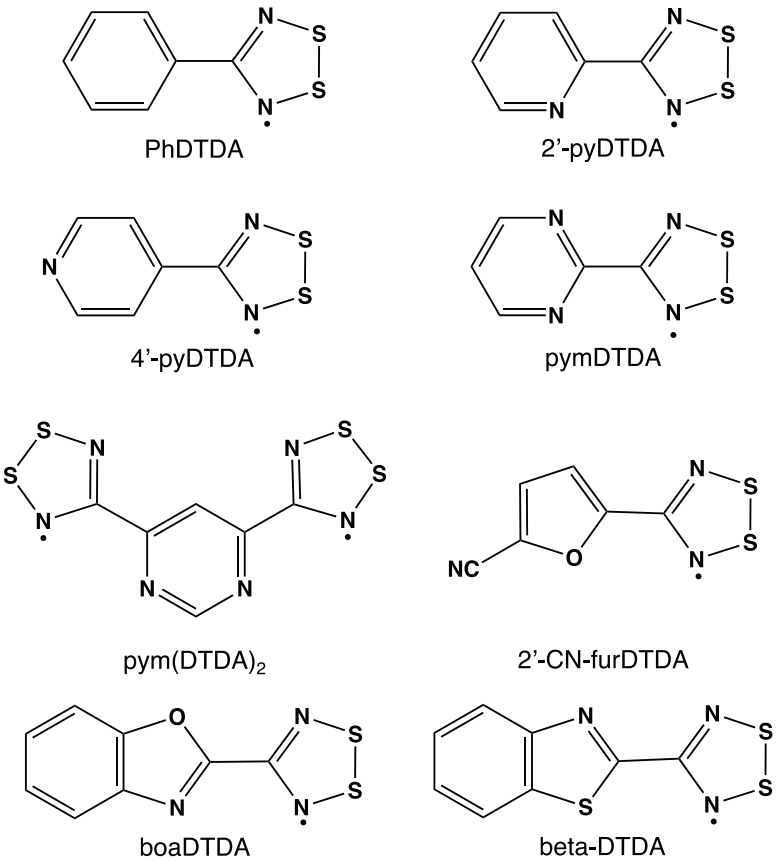

Chart 14.1. DTDA ligands with phenyl and heterocyclic substituents; py = pyridine, pym = pyrimidine, fur = furanyl, boa = benzooxazol-2′-yl, beta = benzothiazole.

been on ligands with heterocyclic substituents attached to the carbon atom of DTDA (Chart 14.1).[2b,3]

These multidentate ligands can coordinate in either a monodentate or chelating mode to first-row transition metals, especially Lewis-acidic $M(hfac)_2$ (hfac = hexafluoroacetonato) complexes. In addition, supramolecular interactions between the metal-DTDA complexes may influence their magnetic properties. These interactions can include pancake bonding (Sec. 4.10). They may also entail electrostatic contacts involving the $S^{\delta+}$ atoms of the DTDA ligand or π-stacking arrangements between the thiazyl ring and the *C*-heterocyclic substituent of a neighbouring complex. This structural variety and the magnetic properties of the metal complexes are illustrated in the subsequent discussion of selected examples, which follows the chronological development of the design of the ligands shown in Chart 14.1.[2b]

14.2.1 *Complexes of phenyl-1,2-dichalcogena-3,5-diazolyl radicals*

The first investigations of coordination complexes of 1,2-dithia-3,5-diazolyl radicals (DTDAs) established that these ligands readily undergo redox reactions with low-valent metal centres.[4] For example, oxidative-addition with $[Pt(PPh_3)_3]$ or $[Ni(Cp)(CO)_2]$ yields the *S,S′*-chelated metal complexes $[Pt(PPh_3)_2(PhDTDA)]$ (**14.1**)[5] and $[Ni_2Cp_2(PhDTDA)]$[6] (**14.2**), respectively (Chart 14.2). The Pt(II) complex of the $[PhDTDA]^{2-}$ ligand **14.1** disproportionates to give the trinuclear complex $[Pt_3(PhDTDA)_3(PPh_3)_4]$ containing two trianionic ligands $[PhDTDA]^{3-}$ and a neutral $[PhDTDA]^{\bullet}$ radical.[5] Alternatively, DTDA radicals can form η^2 π-complexes in which the S–S bond remains intact with values of *d*(S–S) in the range 2.11–2.15 Å. For example, a variety of diamagnetic chromium complexes $[CrCp(CO)_2(4\text{-}XC_6H_4DTDA)]$ (**14.3**, X = Me, Cl, OMe, CF_3) are produced by the reaction of $(4\text{-}XC_6H_4DTDA)_2$ with the 17-electron radical $[CrCp(CO)_3]^{\bullet}$ or by salt metathesis of $[4\text{-}XC_6H_4DTDA]$Cl with $Na[Cr(Cp)(CO)_3]$ (**14.3**, X = OMe, CF_3).[7] In these complexes the DTDA ligand replaces a CO at the metal centre and acts as a three-electron π-donor; both *endo* and *exo* isomers have been structurally characterised for **14.3** (X = Me) (Chart 14.2).

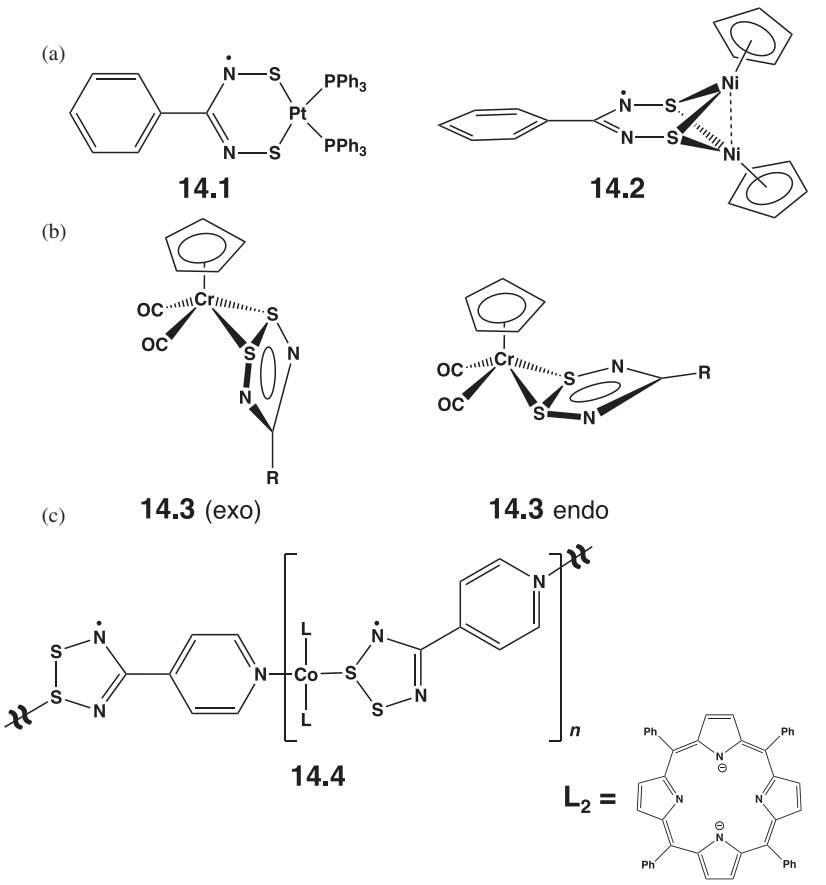

Chart 14.2. Coordination modes of DTDAs: (a) *S,S′*-chelation (b) η^2 π-*S,S′* and (c) monodentate *S*-coordination (L_2 = 5,10,15,20-tetraphenylporphyrinato-ligand).

14.2.2 *Complexes of pyridyl-1,2-dichalcogena-3,5-diazolyl radicals*

The first example of a paramagnetic metal-DTDA complex was the cobalt(II) complex [Co(hfac)$_2$(2′-pyDTDA)] (**14.5**) in which the ligand assumes bidentate coordination (Chart 14.3).[8] This Co(II) complex and the M(II) (M = Fe, Ni) analogues are monomeric in the solid state.[8,9] By contrast, the complexes [M(hfac)$_2$(2′-pyDTDA)] (M = Mn, Cu) both form

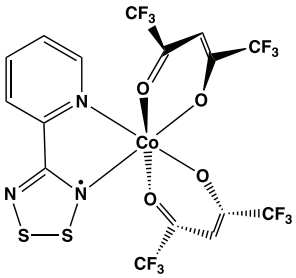

14.5

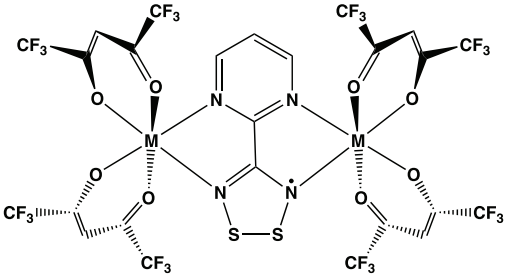

14.6

Chart 14.3. Structures of [Co(hfac)$_2$(2′-pyDTDA)] and [{M(hfac)$_2$}$_2$(pymDTDA)].

pancake bonds in the solid state with either a *cis*-cofacial or twisted-cofacial arrangement of the DTDA ligands for the Mn(II) and Cu(II) complexes, respectively.[10a,b] The magnetic properties of the series [M(hfac)$_2$(2′-pyDTDA)] have been investigated. The Mn(II) and Fe(II) complexes exhibit antiferromagnetic coupling between the magnetic moments of the metal and ligand, whereas the Co(II), Ni(II) and Cu(II) complexes demonstrate ferromagnetic exchange coupling. Curiously, the Mn(hfac)$_2$ complex of the 4′-CN-pyDTDA ligand does not engage in pancake bonding, but the nickel(II) complex of the same ligand forms dimers in the solid state.[10]

A unique example of monodentate *S*-coordination by a DTDA ligand is illustrated in the complex of 4′-pyDTDA with Co(TPP) (TPP = 5,10,15,20-tetraphenylporphyrinato ligand) (**14.4**, Chart 14.2).[11] In this polymeric complex 4′-pyDTDA acts as a bridging ligand with monodentate *S*-coordination to one cobalt centre and *N*-coordination to adjacent cobalt ions *via* the pyridyl nitrogen atom. The S–S distance of 2.12 Å in **14.4** has been used to estimate a charge transfer of *ca.* 0.5 e$^-$ from the cobalt(II) centre to the 4′-pyDTDA ligand.[11]

14.2.3 *Complexes of pyrimidyl-1,2-dichalcogena-3, 5-diazolyl radicals*

The additional N atom in the pyrimidine ring confers a bridging capability on the pymDTDA ligand (Chart 14.1), as illustrated by the structures of

the bimetallic complexes [{M(hfac)$_2$}$_2$(pymDTDA)] (**14.6**, M = Mn, Co, Ni, Zn) (Chart 14.3).[12,13] None of these complexes form pancake bonds in the solid state. The antiferromagnetic coupling in the Mn(II) complex results in an $S = 9/2$ spin ground state, whereas ferromagnetic coupling in the Co(II) and Ni(II) complexes gives rise to $S = 7/2$ and $S = 5/2$ spin ground states, respectively. The Mn(II) and Ni(II) complexes have also been characterised for the selenium-containing pymDSDA ligand.[13] Curiously, the manganese(II) complex [{Mn(hfac)$_2$}$_2$(pymDSDA)] is isomorphous with the sulfur analogue, but the Ni(II) complex of pymDSDA forms dimers in a *trans*-antarafacial conformation.

14.2.4 *Complexes of furanyl-1,2-dichalcogena-3,5-diazolyl radicals*

The 2′-cyano-furanylDTDA radical (Chart 14.1) introduces another aspect of the coordination chemistry of these paramagnetic ligands, namely monodentate *N*-coordination as illustrated by the isostructural series [M(hfac)$_2$(2′-NC-furDTDA)] (**14.7**, M = Mn, Co, Ni).[11] In these complexes the *N*-monodentate ligands are located in axial positions around the pseudo-octahedral metal centre and the two hfac ligands occupy equatorial sites. The cyano substituents coordinate to a second metal centre giving rise to the polymeric arrangement depicted in Chart 14.4.

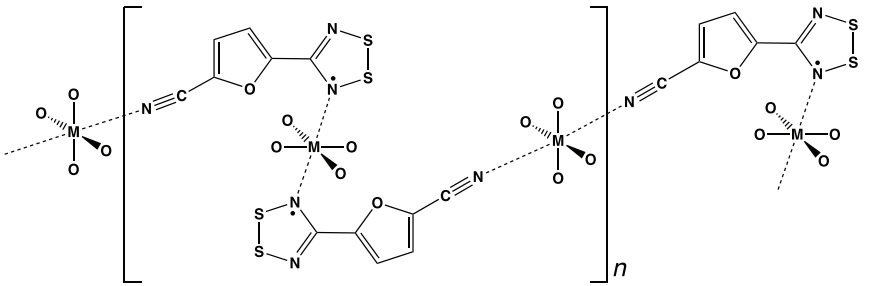

14.7

Chart 14.4. Monodentate *N*-coordination in the polymers [M(hfac)$_2$(2′-NC-furDTDA)] (M = Mn, Co, Ni).

14.2.5 *Complexes of benzoxalo-2-yl-1,2-dichalcogena-3,5-diazolyl radicals*

The different size and shape of the benzoxalo-2-yl substituent in the boaDTDA ligand (Chart 14.1) inhibits the formation of disordered crystal structures, which are often found for other DTDA ligands. Instead of pancake bonding (formation of π-dimers) in the solid state, the $Mn(hfac)_2$ complex of boaDTDA participates in pairwise electrostatic ($S^{\delta+}\cdots O^{\delta-}$) contacts between a DTDA sulfur atom and an hfac oxygen atom of a neighbouring molecule.[14] Antiferromagnetic coupling between the metal and ligand moments in $[Mn(hfac)_2(boaDTDA)]$ is observed ($S = 2$ per molecule). In addition, the $S^{\delta+}\cdots O^{\delta-}$ contacts provide a pathway for magnetic coupling between the pairs of molecules resulting in a high spin ground state ($S_T = 4$ per pair of molecules). By contrast, the nickel(II) complex $[Ni(hfac)_2(boaDTDA)]$ forms a one-dimensional π-stacked staircase arrangement in which the DTDA ring of one molecule interacts with the benzoxalo-2-yl ring of another molecule.[15]

14.2.6 *Complexes of pyrimidyl-bis(1,2-dichalcogena-3,5-diazolyl) radicals*

The influence of electrostatic $S^{\delta+}\cdots O^{\delta-}$ contacts is especially evident in the $Mn(hfac)_2$ complex of the biradical $pym(DTDA)_2$ (Chart 14.1). As indicated in Chart 14.5, the bimetallic complex $[Mn(hfac)_2(pymDTDA)_2]$ (**14.8**) forms 2-dimensional ribbon-like arrays in the solid state as a result of these interactions.[16] Complex **14.8** exhibits a ferromagnetic arrangement of the magnetic moments of neighbouring complexes within a ribbon. In addition, weak antiferromagnetic coupling between the ribbons stabilises an antiferromagnetic ground state.

14.2.7 *Complexes of benzo-1-thia-3-azolyl-1,2-dichalcogena-3,5-diazolyl radical*

The benzothiazole substituent in betaDTDA ligand (Chart 14.1) incorporates an electropositive sulfur centre outside the DTDA ring that can

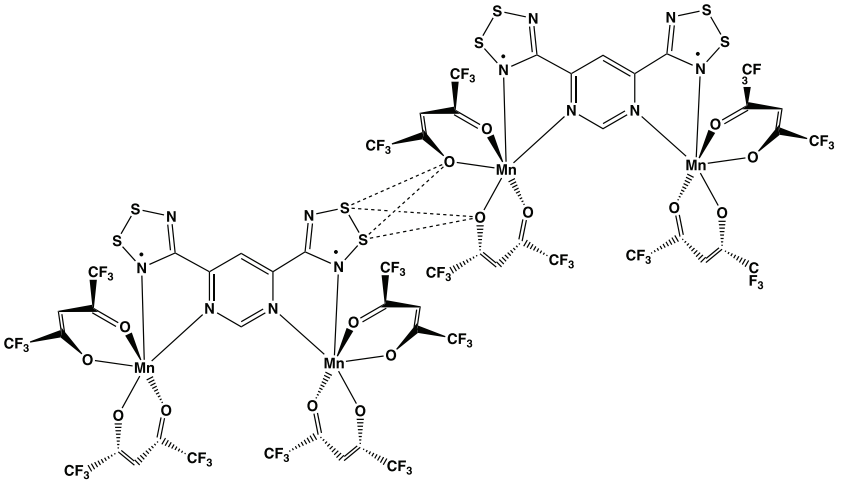

14.8

Chart 14.5. Electrostatic $S^{\delta+}\cdots O^{\delta-}$ contacts in the structure of $[Mn(hfac)_2(pymDTDA)_2]$.

engage in electrostatic intermolecular contacts. The X-ray structure of $[Fe(hfac)_2(betaDTDA)]$ (**14.9**) reveals pancake-bonded dimers with a *cis*-cofacial arrangements of thiazyl rings [d(S···S) ~ 3.5 Å] supplemented by $S^{\delta+}\cdots O^{\delta-}$ contacts between benzothiazole sulfur atoms and neighbouring hfac oxygen atoms (Fig. 14.1).[17] Complex **14.9** shows strong antiferromagnetic coupling between the metal and ligand moments resulting in an $S = 3/2$ ground state that is the only thermally populated ground state below 40 K. Below 4 K, this complex exhibits single-molecule magnet behaviour.

14.3 Lanthanide Metal Complexes of 1,2-Dichalcogena-3,5-diazolyl Ligands

DTDA ligands also coordinate to lanthanide ions as exemplified by the series of complexes $[Ln(hfac)_3(boaDTDA)]$ (**14.10**, Ln = La, Sm, Dy, Gd, Y).[18–20] In these complexes the flexible coordination spheres of Ln^{3+} ions facilitate the bridging capability of DTDA ligands and, hence, the

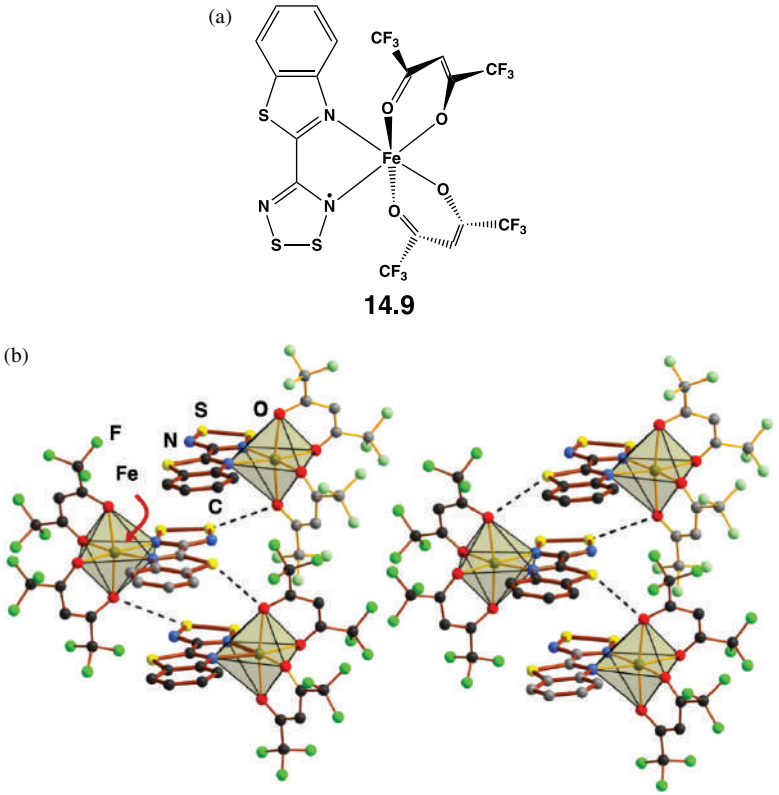

Figure 14.1. (a) Line drawing and (b) π-stacking and $S^{\delta+}\cdots O^{\delta-}$ contacts in the crystal structure of $[Fe(hfac)_2(betaDTDA)]$.[17]

formation of coordination polymers, *e.g.*, $[Ln(hfac)_3(boaDTDA)]_n$ (Ln = La, Sm). For example, the lanthanum complex (Ln = La) forms a one-dimensional polymer with alternating $La(hfac)_3$ and boaDTDA units that exhibits ferromagnetic coupling between the radicals *via* the diamagnetic La(III) ion (Chart 14.6a).[18] The corresponding dysprosium(III) complex forms twisted cofacial dimers with [d(S···S) = 2.90 Å], which has single-molecule magnet properties (Chart 14.6b).[19] The samarium complex has a polymeric structure isomorphous with that of the lanthanum analogue (Chart 14.6a).[20] Interestingly, this soluble, readily sublimable polymer exhibits ferromagnetic ordering with T_C = 3 K.

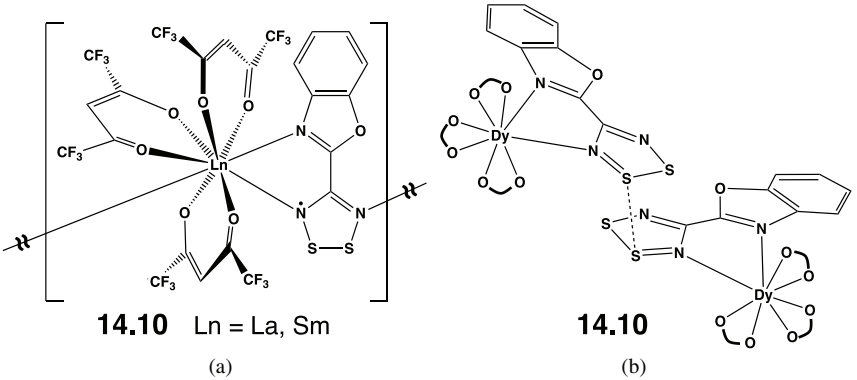

Chart 14.6. (a) Polymeric and (b) dimeric structures of $[Ln(hfac)_3(boaDTDA)]$ complexes.

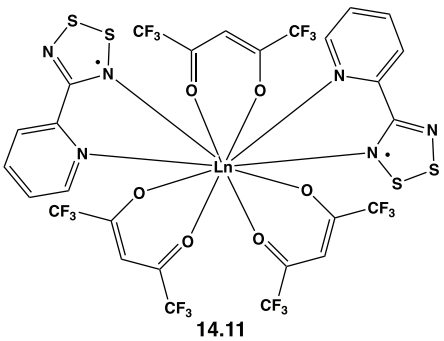

Chart 14.7. Ten-coordination in $[La(hfac)_3(2'\text{-pyDTDA})_2]$.

The ample coordinating ability of a lanthanide metal centre is illustrated well by the ten-coordinate complex $[La(hfac)_3(2'\text{-pyDTDA})_2]$ (**14.11**) incorporating two bidentate 2′-pyDTDA ligands (Chart 14.7).[21] This complex exhibits temperature-dependent structural and magnetic properties. Below 100 K it is diamagnetic, consistent with an f^0 lanthanum(III) ion and pancake bonding of the radical ligands. Upon heating, the 1D polymeric structure undergoes two phase transitions at 160 and 310 K involving cleavage of half and then all of the pancake bonds. These structural changes generate stepwise increases in the paramagnetic susceptibility.[21]

14.4 Transition-Metal Complexes of 1-Thia-2,4,6-triazinyl Radicals

The reactions of $[Cr(Cp)(CO)_2]^{\bullet}$, generated *in situ* from the dimer, with 1-thia-2,4,6-triazinyl (TTA) radicals (Sec. 13.6) yield two 1:1 coordination complexes in which the heterocyclic ring binds to the metal either in an η^1-*S* (**14.12**) or an η^2-*S,N* fashion (**14.13**) (Fig. 14.2).[22] Both **14.12** and **14.13** are obtained for the symmetrical TTA ligand 3,5-$Ph_2C_2N_3S$, whereas only **14.13** is isolated for the unsymmetrically substituted TTA ring 3-Ph-5-CF_3-C_2N_3S.[23] In the *S*-monodentate complex **14.12** the thiazyl ring acts as a one-electron donor. Although it is bonded to the metal *via* the perpendicular *p*-orbital of the sulfur atom, the Cr–S interaction is considered to be a σ-bond on the basis of the bond length and a frontier molecular orbital analysis.[23] In the formation of the bidentate-*S,N* complex **14.13** the TTA ligand displaces CO from the metal centre and behaves as a three-electron π-ligand.[23]

The synthesis of the py_2TTA ligand (**13.36**) is depicted in Scheme 13.10.[24–26] This terpyridine-like ligand introduces a different aspect of the coordination behaviour for this class of TTA ligand. For example, direct reaction of a solution of $FeCl_2$ in MeCN with a $CHCl_3$ solution of the neutral py_2TTA radical produces the 1:1 adduct **14.14** (Scheme 14.1).[24] The iron complex **14.14** may be also prepared by the

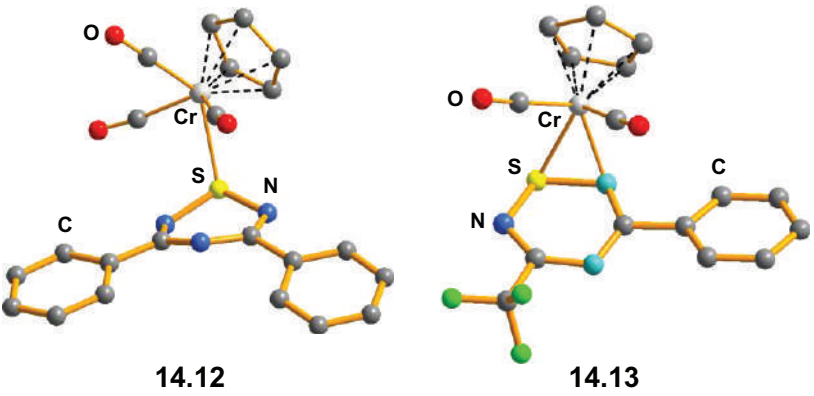

14.12 **14.13**

Figure 14.2. η^1-*S* and η^2-*S,N* chromium complexes of a 1-thia-2,4,6-triazinyl ring.[22]

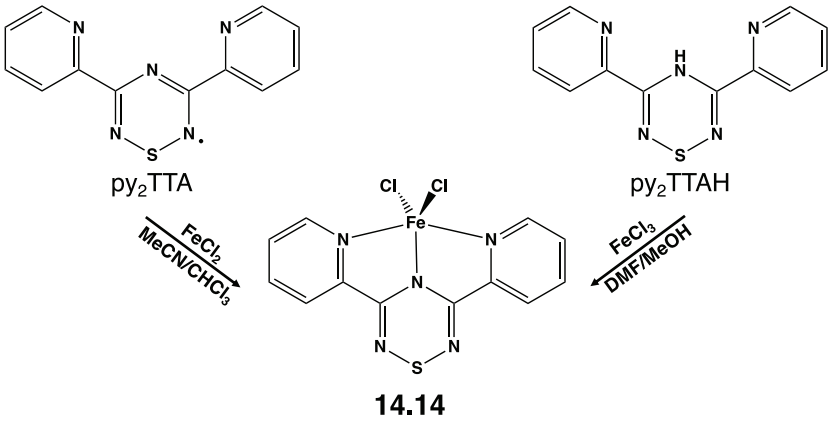

Scheme 14.1. Synthesis of the complex $[Fe(py_2TTA)Cl_2]$.

redox reaction between py_2TTAH and $FeCl_3$ in DMF/methanol on exposure to air for three days (Scheme 14.1).[27] An X-ray structure of **14.14** reveals that the metal centre lies within the plane of the tridentate py_2TTA ligand. The structural, spectroscopic and magnetic measurements, in conjunction with computational analysis, indicate strong electronic interaction between the ligand and the metal leading to an $S = 5/2$ complex.[27]

14.5 Lanthanide Metal Complexes of 1-Thia-2,4,6-triazinyl Radicals

In contrast to the reaction of py_2TTAH with $FeCl_3$ (*vide supra*), the analogous reaction with $Ln(NO_3)_3{\cdot}6H_2O$ (Ln = Dy, Y) results in an *in situ* oxidation of the sulfur centre in the ligand to give the nine-coordinate lanthanide complexes **14.15**.[28] The sulfoxide linkages in **14.15** give rise to the dimeric structure depicted in Chart 14.8. The presence of the S=O group may be attributed to the intermediate formation of the py_2TTA radical in the reaction of py_2TTAH with Ln^{3+} salts, since the radical is readily oxidised in air,[25] whereas py_2TTAH resists oxidation in the absence of a metal.[28] Despite the dimeric structure, the dysprosium complex **14.15** (Ln = Dy) behaves as a mononuclear single-molecule magnet.[28]

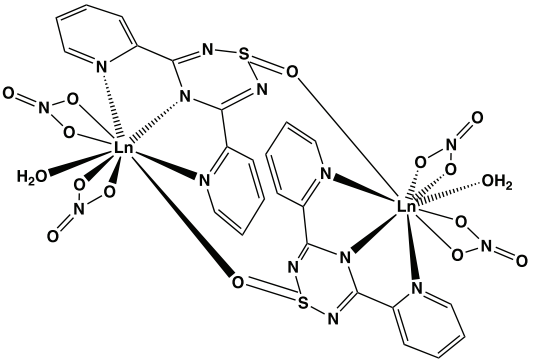

14.15

Chart 14.8. Dimeric structure of $[Ln_2(1\text{-oxo-py}_2TTA)_2(NO_3)_4]$ (Ln = Dy, Y).

14.6 Transition-Metal and Main Group Element Complexes of 1,3-Dithia-2-azolyl Radicals

Both *N*- and *S*-coordination modes have been found in metal complexes of 1,3-dithia-2-azolyl radicals (1,3,2-DTAs). In early work the 1:1 adduct $[Cu(hfac)_2TTTA]_n$ (TTTA = 1,3,5-trithia-2,4,6-triazapentalenyl) (**14.16**) was obtained from the reaction of $[Cu(hfac)_2]$ with TTTA in heptane.[29] The TTTA ligand in this coordination polymer bridges two copper sites *via N*-coordination of the 1,3,2-DTA nitrogen atom and one of the nitrogen atoms of the thiadiazole ring (Fig. 14.3a). This material exhibits ferromagnetic behaviour.[29] In contrast to the ion-separated charge-transfer complexes [BBDTA][GaX_4] (X = Cl, Br; BBDTA = benzo-bis-1,3-dithia-2-azolium) (Sec. 13.3.3), the related complexes with a diamagnetic group 13-centred anion [BBDTA][InX_4] (**14.17**, X = Cl, Br) form one-dimensional coordination polymers.[30, 31] In these complexes the pseudo-octahedral $[InX_4]^-$ anions are bridged *via* the two nitrogen atoms of a $[BBDTA]^{\bullet+}$ radical cation in equatorial positions, as illustrated in Fig. 14.3b. The complexes [BBDTA][InX_4] (X = Cl, Br) exhibit a spin-Peierls transition at 108 K (X = Cl) and 250 K (X = Br).[30,31]

S-coordination is observed in the 2:1 complex formed between benzo-1,3-dithia-2-azolyl radical (BDTA) and $[Co(mnt)_2]$ (mnt^{2-} = maleonitriledithiolate) (**14.18**) (Fig. 14.4).[32–34] The complex **14.18** exhibits a structural

(a)

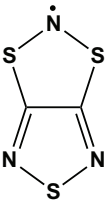

TTTA

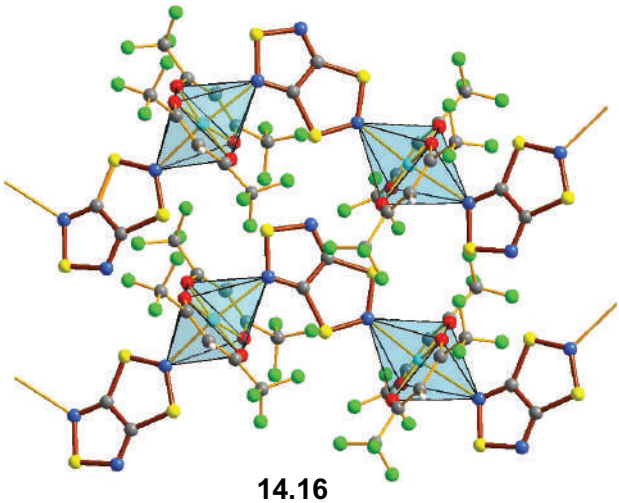

14.16

(b)

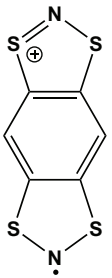

$BBDTA^+$

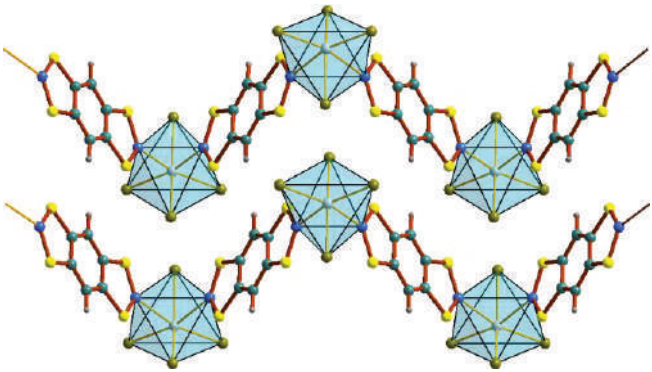

14.17

Figure 14.3. Structures of coordination polymers (a) $[Cu(hfac)_2TTTA]_n$[29] and (b) $[BBDTA][InCl_4]$.[31]

and magnetic phase transition involving the formation and rupture of an *S*-coordination linkage between one of the BDTA molecules and the cobalt ion.[32–34]

Reaction of the methylbenzo-1,3-dithia-2-azolyl (MeBDTA) radical with $M(hfac)_2$ in a 2:1 molar ratio yields the complexes $[M(hfac)_2(MeBDTA)_2]$ (**14.19**, M = Mn, Co, Zn).[35] The *N*-donor monodentate MeBDTA ligands

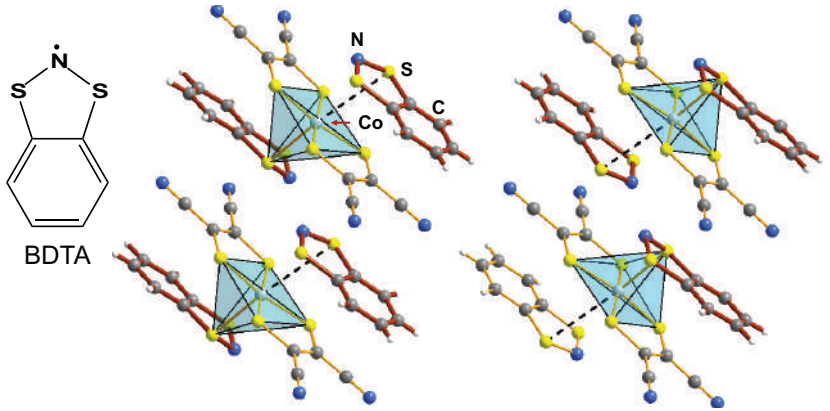

14.18

Figure 14.4. Crystal structure of $[Co(BDTA)_2(mnt)_2]$.[32]

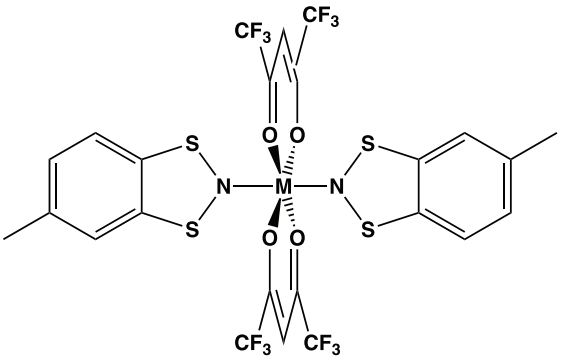

14.18

Chart 14.9. Structure of $[M(hfac)_2(MeBDTA)_2]$ (M = Co, Zn).

assume a *trans* arrangement in these octahedral complexes (Chart 14.9). Strong antiferromagnetic exchange interactions are observed between M(II) ions and the two $S = ½$ radicals for M = Mn, Co, whereas weak

antiferromagnetic interactions between radicals are found for the diamagnetic Zn(II) ion.[35]

References

1. R. T. Boeré and T. L. Roemmele, in *Comprehensive Inorganic Chemistry II,* Ed. T. Chivers, Elsevier (2013), Vol. 1, Ch. 1.14, pp. 375–411.
2. (a) K. E. Preuss, *Dalton Trans*., 2357 (2007); (b) K. E. Preuss, *Coord. Chem. Rev*., **289**, 49 (2015).
3. M. A. Nascimento and J. R. M. Rawson, in *Encyclopedia of Inorganic and Bioinorganic Chemistry*, John Wiley & Sons (2019), doi:10.1002/97811 19952438.eibc2640.
4. A. Døssing, *Coord. Chem. Rev*., **306**, 544 (2015).
5. (a) A. J. Banister, I. B. Gorrell, S. E. Lawrence, C. W. Lehman, I. May, G. Tate, A. J. Blake and J. M. Rawson, *Chem. Commun*., 1779 (1994); (b) A. J. Banister, I. B. Gorrell, J. A. K. Howard, S. E. Lawrence, C. W. Lehman, I. May, J. M. Rawson, B. K. Tanner, C. I. Gregory, A. J. Blake and S. P. Fricker, *J. Chem. Soc., Dalton Trans*., 377 (1997).
6. A. J. Banister, I. B. Gorrell, W. Clegg and K. A. Jorgensen, *J. Chem. Soc. Dalton, Trans*., 1105 (1991).
7. (a) H. F. Lau, V. W. I. Ng, L. L. Koh, G. K. Tan, L. Y. Goh, T. L. Roemmele, S. D. Seagrave and R. T. Boeré, *Angew. Chem. Int. Ed.*, **45**, 4498 (2006); (b) H. F. Lau, P. C. Y. Ang, V. W. I. Ng, S. L. Kuan, L. Y. Goh, A. S. Borisov, P. Hazendonk, T. L. Roemmele, R. T. Boeré and R. D. Webster, *Inorg. Chem*., **47**, 632 (2008).
8. N. G. R. Hearns, K. E. Preuss, J. F. Richardson and S. Bin-Salamon, *J. Am. Chem. Soc*., **126**, 9942 (2004).
9. N. G. R. Hearns, E. M. Fatila, R. Clérac, M. Jennings and K. E. Preuss, *Inorg. Chem*., **47**, 10330 (2008).
10. (a) N. G. R. Hearns, K. D. Hesp, M. Jennings, J. L. Korcok, K. E. Preuss and C. S. Smithson, *Polyhedron*, **26**, 2047 (2007); (b) N. G. R. Hearns, R. Clérac, M. Jennings and K. E. Preuss, *Dalton Trans*., 3193 (2009).
11. D. A. Haynes, L. J. van Laeren and O. Q. Munro, *J. Am. Chem. Soc*., **19**, 14620 (2017).
12. M. Jennings, K. E. Preuss and J. Wu, *Chem. Commun*., 341 (2006).

13. J. Wu, D. J. MacDonald, R. Clérac, I.-R. Jeon, M. Jennings, A. J. Lough, J. Britten, C. Robertson, P. A. Dube and K. E. Preuss, *Inorg. Chem*., **51**, 3827 (2012).
14. E. M. Fatila, J. Goodreid, R. Clérac, M. Jennings, J. Assoud and K. E. Preuss, *Chem. Commun*., **46**, 6569 (2010).
15. E. M. Fatila, R. Clérac, M. Jennings and K. E. Preuss, *Chem. Commun*., **49**, 9431 (2013).
16. E. M. Fatila, R. Clérac, M. Rouzières, D. V. Soldatov, M. Jennings and K. E. Preuss, *J. Am. Chem. Soc*., **135**, 13298 (2013).
17. C. A. Michalowicz, M. B. Mills, E. Song, D. V. Soldatov, P. D. Boyle, M. Rouzières, R. Clérac and K. E. Preuss, *Dalton Trans*., **48**, 4514 (2019).
18. E. M. Fatila, R. Clérac, M. Rouzières, D. V. Soldatov, M. Jennings and K. E. Preuss, *Chem. Commun*., **49**, 6271 (2013).
19. E. M. Fatila, M. Rouzières, M. C. Jennings, A. J. Lough, R. Clérac and K. E. Preuss, *J. Am. Chem. Soc*., **135**, 9596 (2013).
20. E. M. Fatila, A. C. Maahs, M. B. Mills, M. Rouzières, D. V. Soldatov, R. Clérac and K. E. Preuss, *Chem. Commun*., **52**, 5414 (2016).
21. E. M. Fatila, R. A. Mayo, M. Rouzières, M. C. Jennings, P. Dechambenoit, D. V. Soldatov, C. Mathonière, R. Clérac, C. Coulon and K. E. Preuss, *Chem. Mater*., **27**, 4023 (2015).
22. C. Y. Ang, R. T. Boeré, L. Y. Goh, L. L. Koh, S. L. Kuan, G. K. Tan and X. Yu, *Chem. Commun*., 4735 (2006).
23. C. Y. Ang, S. L. Kuan, G. K. Tan, L. Y. Goh, T. L. Roemmele, X. Yu and R. T. Boeré, *Can. J. Chem*., **93**, 181 (2015).
24. A. A. Leitch, I. Korobkov, A. Assoud and J. L. Brusso, *Chem. Commun*., **50**, 1934 (2014).
25. N. J. Yutronkie, A. A. Leitch, I. Korobkov and J. L. Brusso, *Cryst. Growth Des*., **15**, 2524 (2015).
26. K. L. M. Harriman, I. Kühne, A. A. Leitch, I. Korobkov, R. Clérac, M. Murugesu and J. L. Brusso, *Inorg. Chem*., **55**, 2268 (2016).
27. K. L. M. Harriman, A. A. Leitch, S. A. Stoian, F. Habib, J. L. Kneebone, S. I. Gorelsky, I. Korobkov, S. Desgreniers, M. L. Neidig, S. Hill, M. Murugesu and J. L. Brusso, *Dalton Trans*., **44**, 10516 (2015).
28. N. J. Yutronkie, I. A. Kuhne, I. Korobkov, J. L. Brusso and M. Murugesu, *Chem. Commun*., **52**, 677 (2016).
29. W. Fujita and K. Awaga, *J. Am. Chem. Soc*., **123**, 3601 (2001).

30. W. Fujita, K. Awaga, R. Kondo and S. Kagoshima, *J. Am. Chem. Soc*., **128**, 6016 (2006).
31. W. Fujita, K. Kikuchi and K. Awaga, *Angew. Chem. Int. Ed.*, **47**, 9480 (2008).
32. Y. Umezono, W. Fujita and K. Awaga, *J. Am. Chem. Soc*., **128**, 1084 (2006).
33. M. Kepenekian, B. Le. Guennic, K. Awaga and V. Robert, *Phys. Chem. Chem. Phys*., **11**, 6066 (2009).
34. K. Awaga, K. Nomura, H. Kishida, W. Fujita, H. Yoshikawa, M. M. Matsushita, L. Hu, Y. Shuku and R. Suizu, *Bull. Chem. Soc. Jpn*., **87**, 234 (2014).
35. D. Leckie, N. T. Stephaniuk, A. Arauzo, J. Campo and J. M. Rawson, *Chem. Commun*., **55**, 9849 (2019).

Chapter 15

Secondary Bonding Interactions in Chalcogen-Nitrogen Compounds: Supramolecular Assemblies

15.1 Introduction

The concept of a secondary bonding interaction (SBI) refers to weak interatomic contacts.[1] They are also called σ-hole, non-covalent, semi-bonding, nonbonding, weakly bonding, closed-shell, or soft-soft interactions. The SBIs involving chalcogen atoms are now called chalcogen bonding (ChB), which is defined by IUPAC as a supramolecular interaction between an electrophilic region on a Group 16 atom and electron-rich centres with interatomic distances between those of typical single bonds and the sum of van der Waals radii.[2] In the case of chalcogen-nitrogen compounds, SBIs may refer to either *intramolecular* or *intermolecular* interactions.

Weak intramolecular E···E contacts that involve two chalcogen atoms (E = S, Se) of a chalcogen-nitrogen ring system are discussed in Sec. 4.9. They involve a cross-ring π^*-π^* interaction of two NSN units on opposite sides of the ring. Such bicyclic systems typically display S···S distances in the range of 2.4–2.6 Å, *cf.* 2.06 Å for an S–S single bond. In the first part of this chapter *intramolecular* SBIs incorporating a close contact between a donor atom (*i.e.*, nitrogen) and the acceptor chalcogen center (E = S, Se or Te) will be considered. This type of SBI

may involve donation of the lone pair on N to the σ^*(E–X) orbital for organochalcogen(II) derivatives REX (Sec. 15.2.7), a vacant tellurium *p* orbital for organochalcogen(II) cations $[RE]^+$ (Sec.15.2.4) or a σ hole on the chalcogen for organochalogen(IV) cations $[REX_2]^+$ (Sec. 15.2.5). The resulting chalcogen-nitrogen bonds are of variable strength and the E···N distances can range from close to a single-bond value to intermediate between the sum of covalent and van der Waals radii for E and N (see Table 15.1 for benchmark data). Importantly, as discussed in Sec. 15.2, *intramolecular* SBIs can lead to the stabilisation of reactive functional groups, especially for the heavier chalcogens, as has been described in recent reviews of the chemistry of telluroxanes and related organotellurium compounds with a Te=O functionality.[3,4] *Intramolecular* SBIs also facilitate the isolation and structural characterisation of organochalcogen (II and IV) cations.

Intermolecular SBIs in chalcogen-nitrogen compounds may involve either chalcogen-chalcogen or chalcogen-nitrogen contacts. Weak intermolecular chalcogen-chalcogen contacts are most prevalent for cyclic chalcogen-nitrogen radicals, and they are discussed under the rubric of pancake bonding in Sec. 4.10. *Intermolecular* SBIs that entail chalcogen-nitrogen interactions are the focus of Sec. 15.3. Several recent reviews discuss the concept of ChB in the context of chalcogen-nitrogen chemistry[2,5-8] and several more general articles on ChB include sections on selected chalcogen-compounds.[9] The chalcogen atom can potentially provide two depleted electron density regions (σ-holes) typically along the extension of the covalent bond axis and, hence, serves as an electron acceptor rather than a donor. In addition to the fundamental interest in understanding the nature of ChB in chalcogen-nitrogen systems, *intermolecular* SBIs can lead to materials with supramolecular structures that exhibit unique properties as well as novel host-guest chemistry.

Table 15.1. Sums of covalent radii (Σr_{cov}) and van der Waals (Σr_{vdW}) radii (Å).

	Σr_{cov}	Σr_{cvdW}		Σr_{cov}	Σr_{cvdW}
S–N	1.77	3.35	S–S	2.06	3.60
Se–N	1.91	3.45	Se–Se	2.34	3.80
Te–N	2.10	3.61	Te–Te	2.70	4.10

15.2 Intramolecular SBIs: Stabilisation of Reactive Functional Groups

In addition to the installation of sterically bulky groups on the chalcogen atom, the stabilisation of reactive functional groups in organochalcogen(II and IV) compounds has often been achieved by invoking intramolecular heteroatom coordination (N or O) of a side-arm attached to an aromatic scaffold. The most frequently used frameworks are the 2-dimethylaminomethylphenyl (**15.1**), 8-dimethylaminonaphthyl (**15.2**), 2-butyliminomethylphenyl (**15.3**), 2-(2′-pyridyl)phenyl (**15.4**), 2-oxalinylphenyl (**15.5**) and 2-(phenylazo)phenyl (**15.6**) groups (Chart 15.1); the NCN pincer ligand 2,6-bis(dimethylaminomethyl)phenyl (**15.7**) has been employed widely for the stabilisation of cationic selenium and tellurium centres. The significance of intramolecular SBIs increases for the heavier chalcogens. Consequently, this section will focus

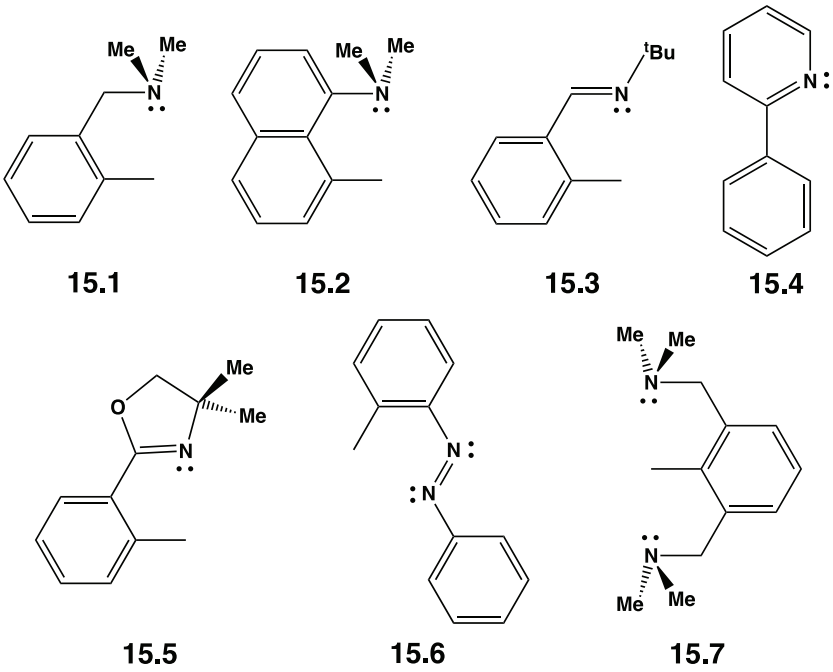

Chart 15.1. *N*-coordinating scaffolds for stabilisation of reactive organochalcogen compounds.

on the stabilisation of reactive functional groups in organoselenium and organotellurium compounds, *i.e.*, halides and azides, derivatives incorporating Te=O functionalities, and cationic species, with an emphasis on solid-state structures. Subsequent sections will consider their electronic structures and solution behaviour.

15.2.1 *Organo-selenium(II) and -tellurium(II) halides and azides*

Although phenylselenium(II) halides PhSeX (X = Cl, Br) are stable commercial products, selenenyl iodides can only be stabilised by sterically protecting substituents or intramolecular heteroatom coordination, *e.g.*, **15.5**SeI.[10a] The Se···N distances in organoselenium(II) halides of the type **15.5**SeX (X = Cl, Br, I),[10a] **15.1**SeX (X = Cl, I)[10b] and **15.1**SeX (X = Cl, I)[10c] are in the range 2.05–2.24 Å, *cf.* 1.91 Å for a Se–N single bond (Table 15.1). These distances are not changed significantly when the pendant Me_2N side-arm in **15.1** is replaced by Et_2N or $E(CH_2CH_2)N$ (E = O, NMe).[10d,e] In addition, the nature of the halide substituent has only a minor influence on the Se···N interaction with the iodides being slightly longer (< 0.1 Å) than the chlorides.[10a,b] However, the replacement of halide by a less electronegative sulfur- or selenium-centred ligand in **15.1**SeX results in a substantial elongation to 2.44–2.47 Å.[10b] The arylselenenyl fluoride **15.1**SeF[11] and the tellurium(II) congener **15.1**TeF[12] could only be characterised in solution by ^{19}F and ^{77}Se or ^{125}Te NMR spectroscopy.

In contrast to their selenium analogues, phenyltellurenyl halides PhTeX (X = Cl, Br), as well as PhTeI, are unstable with respect to disproportionation. However, early work established that aryltellurenyl halides can be stabilised by intramolecular coordination, *i.e.*, an $n^2(N) \rightarrow \sigma^*(Te–X)$ interaction. There is now a substantial body of solid-state structural data available to indicate that the *p*-character of the donor nitrogen ligand has a stronger influence on the strength of this interaction than the electronegativity of the halogen X. Thus, the Te···N distances of 2.355(3) and 2.360(3) Å in the aryltellurenyl chlorides **15.1**TeCl[13] and **15.2**TeCl[14] with sp^3-hybridised nitrogen atoms are significantly longer than the values of 2.203(2) and 2.218(19) Å found for **15.3**TeCl[15] and **15.6**TeCl,[16] which

have sp^2-hybridised donor centres. The effect of the electronegativity of the halide substituent on the intramolecular Te···N contact in aryltellurenyl halides is insignificant, *e.g.*, *d*(Te···N) = 2.210(14) Å in **15.6**TeI.[16] However, the Te···N distance of 2.808(2) Å in the phenyl derivative **15.1**TeC_6H_5[17] is *ca.* 19% longer than that in **15.1**TeCl.[13]

The pentafluorophenyl derivative 2-$Me_2N(CH_2)_3TeC_6F_5$ (**15.8**) provides a unique opportunity to compare the strength of intramolecular Te···N interaction in the solid-state and gas phases.[18] The organotellurium(II) compound **15.8** is prepared by the reaction C_6F_5TeLi and $Me_2N(CH_2)_3Cl$ in THF at −78°C.[18] In the solid state the Te···N distance involving the long dimethylaminopropyl side-arm is 2.639(1) Å. A very weak interaction of Te with the centroid of the C_6F_5 ring produces a dimeric structure (Fig. 15.1a).[18] By comparison, the electron diffraction structure of **15.8** reveals a weaker Te···N interaction of 2.92(3) Å in the gas phase, but only one conformer is present indicating the significance of the intramolecular interaction (Fig. 15.1b).[18]

The presence of intramolecular coordination also stabilises labile arylselenium(II) and aryltellurium(II) azides, *e.g.*, 2-$Me_2NC_6H_4SeN_3$ (**15.1**SeN_3) (Sec. 10.10).[19,20] The incorporation of this feature and a bulky aryl group produces an organoselenium azide (**15.9**) that is thermally stable at room temperature (Fig. 15.2).[21] The mean intramolecular Se···N distance in **15.9** is only marginally shorter (< 0.1 Å) than the mean selenium-azide (Se–N_3) bond length in the slightly unsymmetrical 3c-4e bond system (Sec. 15.2.7).

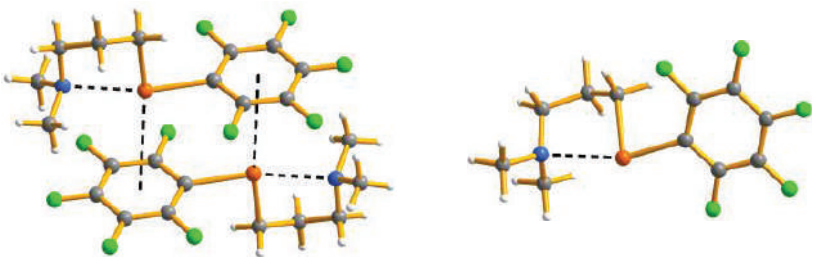

(a) (b)

Figure 15.1. Molecular structures of 2-$Me_2N(CH_2)_3TeC_6F_5$ in (a) solid state (b) gas phase.[18]

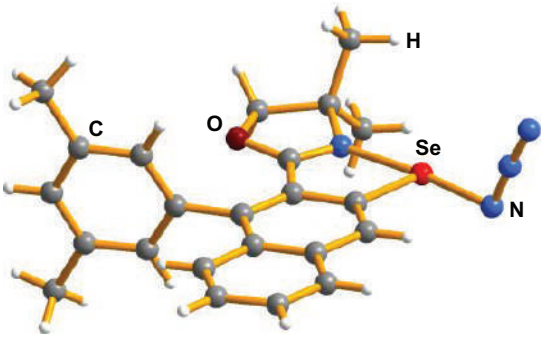

Figure 15.2. Intramolecular N···Se coordination in the organoselenium(II) azide **15.9**.[21]

15.2.2 *Organo-selenium(IV) and -tellurium(IV) trihalides*

The organoselenium(IV) trichloride **15.1**$SeCl_3$ is prepared by chlorination of the diselenide (**15.1**Se–)$_2$ with an excess of SO_2Cl_2.[10b] The intramolecular N···Se distance in the trichloride is *ca.* 0.14 Å longer than that in the monochloride. The trichloride **15.1**$SeCl_3$ decomposes slowly in solution to give the **15.1**SeCl and Cl_2.[10b]

Organotellurium(II) halides are readily oxidised to organotellurium(IV) trihalides by halogens. As in the case of organotellurium(II) halides, a stronger Te···N interaction is observed for N(sp^2) donor atoms in the organotellurium(IV) trihalides, but only modest changes in the intramolecular Te···N distance occur despite the increase in oxidation state. For example, the Te···N distances of 2.360(3) and 2.203(2) Å for **15.2**TeCl[14] and **15.3**TeCl[15] are increased slightly to 2.420(3) and 2.286(1) Å in **15.2**$TeCl_3$ and **15.3**$TeCl_3$,[14,15] respectively. The limited influence of the halide substituent on this interaction in organotellurium(IV) trihalides is evident from the data for the series **15.1**TeX_3 (X = F, Cl, Br, I), which are prepared by the reactions of **15.1**HgCl with $TeCl_4$ (X = Cl) or $TeCl_4$/HBr (X = Br) (Scheme 15.1a)[22] or the treatment of the ditelluride (**15.1**Te–)$_2$ with an excess of XeF_2 (X = F)[12] or iodine (X = I)[22] (Scheme 15.1b). The Te···N distances increase slightly along this series of trihalides: 2.405(4) (X = F),[12] 2.406(3) (X = Cl), 2.434(3) (X = Br) and 2.458(4) Å.[22]

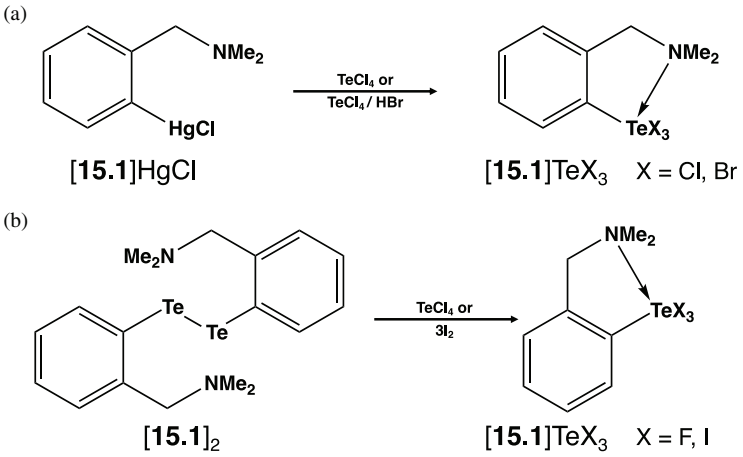

Scheme 15.1. Syntheses of organotellurium(IV) trihalides with intramolecular N···Te coordination.

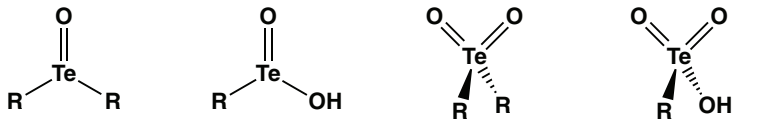

Chart 15.2. Common organotellurium(IV) and organotellurium(VI) compounds with a Te=O group.

15.2.3 *Organotellurium compounds with a Te=O functionality*

Tellurium(IV) compounds containing a Te=O functionality exhibit a strong tendency to oligomerise, *e.g.*, diphenyltellurium oxide exists as a dimer with a four-membered Te_2O_2 ring in the solid state.[3,4] The introduction of intramolecular N···Te coordination has played a key role in the stabilisation of monomeric forms of common organotellurium(IV) and organotellurium(VI) compounds with a Te=O moiety, *e.g.*, telluroxides, tellurinic acids, tellurones and telluronic acids (Chart 15.2),[3,4] as illustrated by the following examples.

The first monomeric diaryltellurium oxide $(2\text{-}Me_2NCH_2C_6H_4)_2TeO$, $(\mathbf{15.1})_2Te{=}O$, was obtained serendipitously by slow hydrolysis of the corresponding diaryltellurium diazide.[23] Oxidation of the telluride $(8\text{-}Me_2NC_{10}H_6)_2Te$, $(\mathbf{15.2})_2Te$, with aqueous hydrogen peroxide produces the corresponding tellurone $(8\text{-}Me_2NC_{10}H_6)_2TeO_2$, $(\mathbf{15.2})_2Te(=O)_2$, rather than the telluroxide $(8\text{-}Me_2NC_{10}H_6)_2Te{=}O$, $(\mathbf{15.2})_2Te{=}O$.[24a] However, comproportionation of the telluride and tellurone generates the monoxide in good yield.[24a] The reaction of $(\mathbf{15.2})_2Te{=}O$ with acetonitrile occurs with oxygen transfer to produce the zwitterionic diaryltelluronium(IV) acetimidate $(\mathbf{15.2})_2Te{=}NC(O)CH_3$ (Eq.15.1), formally comprised of the diaryltellurium dication $[(\mathbf{15.2})_2Te]^{2+}$ and the rare acetimidate dianion.[24b]

$$R_2Te{=}O + CH_3CN \rightarrow R_2Te{=}N{-}C(O){-}CH_3 \qquad (15.1)$$
(R = **15.2**)

The X-ray structures of the telluroxide $(\mathbf{15.1})_2Te{=}O$ and the tellurone $(\mathbf{15.2})Te(=O)_2$ are depicted in Fig. 15.3.[23,24a] The tellurium-oxygen bond length of 1.829(1) Å for the telluroxane and the mean value of 1.822(6) Å for the tellurone represent formal Te=O double bonds. The lack of Te···O SBIs in $(\mathbf{15.1})_2Te{=}O$ is attributed to the double intramolecular *N*-coordination with Te···N distances of 2.755(6) and 2.566(5) Å,[23] *cf.* single-bond value 2.10 Å (Table 15.1). For comparison, the Te···N bond lengths in the acetimidate $(\mathbf{15.2})_2Te{=}NC(O)CH_3$ are 2.704(1) and

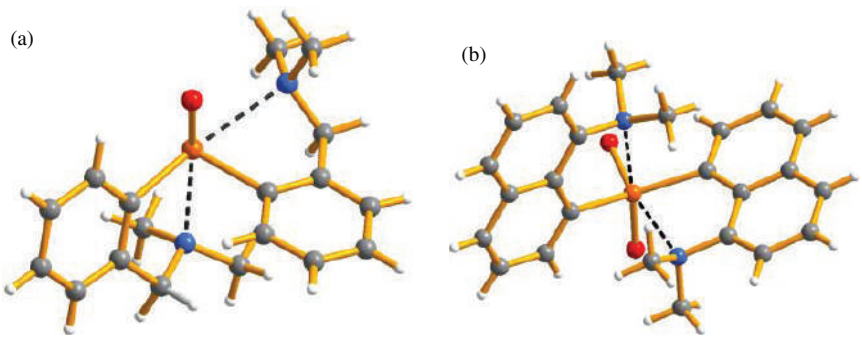

Figure 15.3. Molecular structures of (a) $(2\text{-}Me_2NCH_2C_6H_4)_2TeO$[23] and (b) $(8\text{-}Me_2NC_{10}H_6)_2TeO_2$. Co-crystallised H_2O and H_2O_2 are not shown.[24a]

2.768(1) Å and the polar covalent tellurium-nitrogen bond distance is 2.006(1) Å, significantly smaller than the single-bond value (Table 15.1).[24b] The two Te···N contacts in (**15.2**)$_2$Te(=O)$_2$ are 2.709(7) and 2.762(7) Å.[24a]

The aqueous alkaline hydrolysis of the aryltellurium(IV) trichloride **15.6**$TeCl_3$ at reflux produced the corresponding tellurinic acid **15.1**Te(=O)OH and its sodium salt **15.6**Te(=O)ONa, which were isolated in a 1:3 ratio as a co-crystal.[16] The hydrolysis of **15.2**$TeCl_3$ with three equivalents of NaOH generated the tellurinic anhydride [**15.2**Te(=O)]$_2$(μ-O) (**15.10**), which has a polymeric structure with an N···Te distance of 2.718(6) Å (Chart 15.3).[14] The polymeric structure in **15.10** is cleaved upon treatment with strong aqueous NaOH to give the aryltellurinate [**15.2**TeO_2]$^-$ (**15.11**) as a hydrated sodium salt.[25] The use of the rigid, planar 2-(2′-pyridyl) phenyl (ppy) substituent enabled the isolation and structural characterisation of a monomeric tellurinic acid stabilised by intramolecular N···Te coordination. Thus, treatment of ppy$TeCl_3$ with three equivalents of NaOH produced a high yield of ppyTe(=O)OH (**15.12**) (Chart 15.3).[26] The N···Te distance in **15.12** is 2.411(2) Å indicating a strong intramolecular

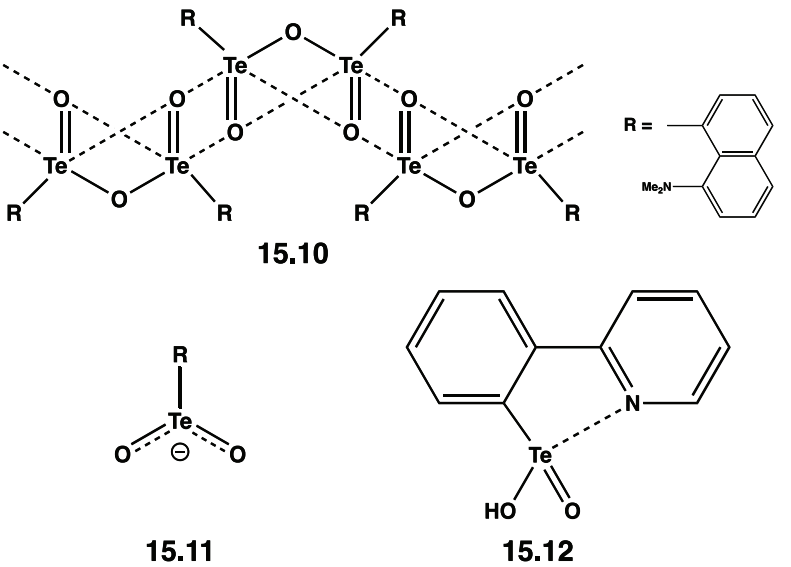

Chart 15.3. The polymeric tellurinic anhydride **15.10**, the tellurinate **15.11** and monomeric tellurinic acid **15.12**.

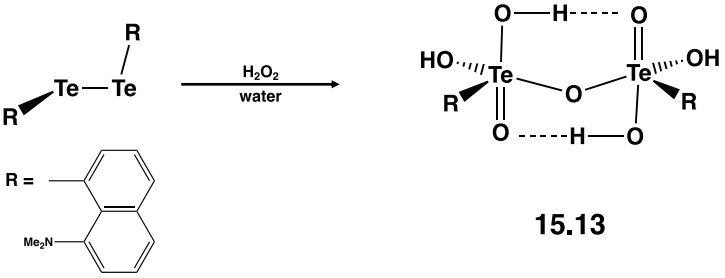

15.13

Scheme 15.2. Synthesis of the dinuclear telluronic acid **15.13**.

interaction with an estimated stabilisation energy of *ca.* 157 kJ mol^{-1} according to DFT calculations.[26]

The treatment of the ditelluride (**15.2**Te–)$_2$ with H_2O_2 in aqueous solution produced the dinuclear telluronic acid [**15.2**Te(=O)$(OH)_2]_2(\mu$-O) (**15.13**) as a tetrahydrate in 34% yield (Scheme 15.2).[27] Intramolecular *N*-coordination in **15.13** (d(N···Te) = 2.376(4) Å) limits this telluronic acid to a single Te–O–Te bridge; the mean Te=O bond length is 1.835(3) Å.[27]

15.2.4 *Organo-selenium(II) and -tellurium(II) cations*

Intramolecular *N*-coordination involving the N,C,N pincer ligand **15.7** has played a key role in the stabilisation of organochalcogen(II) cations RE^+ (E = Se, Te). In early seminal work the hexafluorophosphate salts [**15.7**E] PF_6 (E = Se, Te) were prepared by reactions of (a) **15.7**SeMe with ^{t}BuOCl in anhydrous methanol or (b) **15.7**Te^{n}Bu with bromine (Scheme 15.3a).[28] Subsequently, the selenenium salt [**15.7**Se]PF_6 was obtained in high yield by treatment of the diselenide (**15.7**Se–)$_2$ with two equivalents of XeF_2 in methanol.[11] The hexafluorophosphate salts [**15.7**E]PF_6 (E = Se, Te) were formed upon addition of K[PF_6] to the initial product (Scheme 15.3a).[11,28] More recently, the series of halide salts [**15.7**Se]X (X = Cl, Br, I) were obtained by oxidation of the diselenide (**15.7**Se–)$_2$ with SO_2Cl_2 followed by halide exchange with an excess of potassium bromide or iodide in acetone (Scheme 15.3b).[29,30] Similar methodology has been used to prepare the related organoselenenium chloride salts [2,6-{E(CH_2CH_2) $NCH_2\}_2C_6H_3$Se]$^+Cl^-$ (E = O, NMe);[31] oxidation of the diselenide

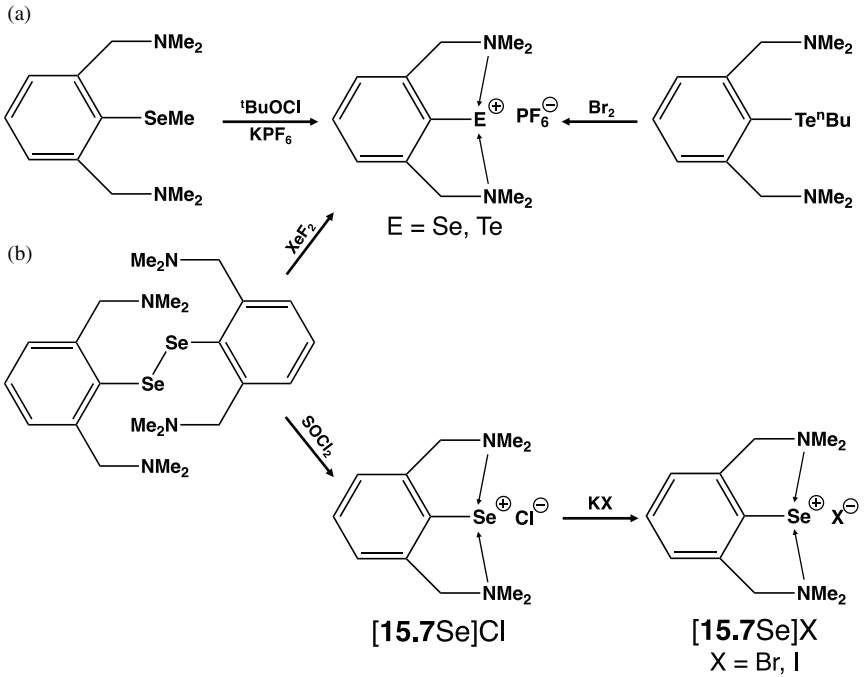

Scheme 15.3. Synthesis of the salts [**15.7**E]X. (a) (E = Se, Te); X = $[PF_6]^-$ (b) E = Se; X = Cl^-, Br^-, I^-.

(**15.7**Se–)$_2$ with $Au(C_6F_5)$(tht) (tht = tetrahydrothiophene) produces the gold complex [**15.7**Se][$Au(C_6F_5)_2$].[31]

The values of the two intramolecular Se···N interactions in the selenenium salts [**15.7**Se]X fall within the narrow range 2.16–2.18 Å indicating a strong interaction, *cf.* 1.91 Å for an Se–N single bond (Table 15.1).[28–31] The geometry at selenium is distorted T-shaped with a bond angle <NSeN of 161–162°.

The tellurenium cation $[2,6\text{-}\{O(CH_2CH_2)NCH_2\}_2C_6H_3Te]^+$ (**15.14**Te^+) was isolated as the $[Hg_2Cl_6]^{2-}$ salt in low yield from the reaction of $[2,6\text{-}\{O(CH_2CH_2)NCH_2\}_2C_6H_3]HgCl$ and tellurium tetrachloride (Chart 15.4).[32] This transmetallation methodology was also employed for the preparation of $[HgX_4]^{2-}$ salts of the tellurenium and selenenium cations **15.15**E^+ (E = Se, Te); ion-separated halide salts [**15.15**Te]X (X = Cl,

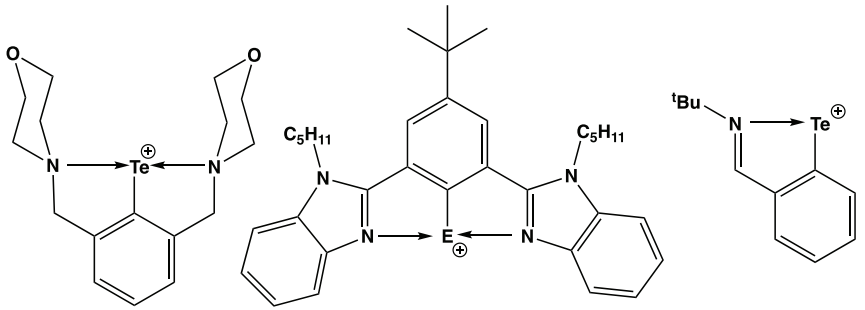

[**15.14**]Te$^+$ [**15.15**]Te$^+$ E = Se, Te [**15.3**]Te$^+$

Chart 15.4. Monoorganotellurenium cations RTe$^+$.

Br) were also isolated in small yields from those reactions.[33] The sp^2-hybridised nitrogen atoms in the N,C,N pincer ligand in **15.15** generate stronger intramolecular E···N interactions (E = Se, Te) than those found for the sp^3-hybridised nitrogen atoms in **15.14**. Thus, the Te···N bond lengths in salts of **15.15**E$^+$ (E = Te) are in the range 2.210(7) –2.287(2) Å,[33] *cf.* 2.354(7) and 2.392(7) for **15.14**Te$^+$.[32] These SBIs are attributed to donation of the lone pair on the N atom to a vacant chalcogen *p* orbital involving an electrostatic contribution that is significantly higher for Te owing to the lower electronegativity of Te compared to that of Se.[33] The sp^2-hybridised donor nitrogen centre in the chelating C,N ligand of salts of [**15.3**Te]X (X = $[O_3SCF_3]^-$, $[SbF_6]^-$, $[Al\{OC(CF_3)_3\}]_4^-$) produces Te···N bond lengths 2.051(4)–2.113(1) Å, *cf.* single-bond value of 2.10 Å.[34]

A palladium complex of an organotellurenium cation $[PdCl_3(TeL)]$ (L= **15.7**) was obtained by reaction of the telluride [(**15.7**)$_2$Te] with sulfuryl chloride followed by K_2PdCl_4 in THF (Eq. 15.2).[35] In this complex the ambiphilic tellurium(II) centre acts as a donor towards the $[PdCl_3]^-$ unit and accepts electrons from the two donor arms of the pincer ligand **15.7** (*d*(Te···N) = 2.337(2) and 2.355(2) Å). By contrast, the reaction of [(**15.7**)$_2$Te] with $HgCl_2$ produces the known organotellurenium cation [**15.7**Te]$^+$ as the $[HgCl_4]^{2-}$ salt.[35]

$$L_2Te + SO_2Cl_2 + K_2PdCl_4 \rightarrow [PdCl_3(TeL)] \quad (15.2)$$
(L = **15.7**)

15.2.5 *Organotellurium(IV) cations*

Organotellurium(IV) cations of the type $[RR'TeX]^+$ (X = Cl, Br, I, OH) in which the highly electrophilic nature of the tellurium centre is attenuated by intramolecular Te···N bonding have been known since the 1990s, *e.g.*, [**15.1**Te(Ph)Br]$^+$.[36] This class of halotelluronium cations are typically prepared by the oxidative addition of halogens to the corresponding ditelluride RR′Te in a 1:1 molar ratio. More recent examples that have been obtained using this methodology include $[(\mathbf{15.6})_2TeI]^+$,[16] $[(\mathbf{15.2})_2TeX]^+$ (X = Cl, Br, I) (Scheme 15.4),[37a] and $[(\mathbf{15.4})_2TeI]^+$.[38] The hexahalotellurate salts $[(\mathbf{15.2})_2TeX]_2[TeX_6]$ were prepared by reaction of two equivalents of $[(\mathbf{15.2})_2TeX]^+X^-$ with TeX_4 in THF.[37b] The aqueous hydrolysis of halotelluronium salts $[(\mathbf{15.2})_2TeX]^+X^-$ produced the corresponding hydroxytelluronium salts $[(\mathbf{15.2})_2TeOH]^+ X^-$ (X = Cl, Br, I).[37] The triflate salt (X = O_3CF_3) was obtained by treatment of the telluroxide$[(\mathbf{15.2})_2Te{=}O]$ with triflic acid.[24] The structure of $[(\mathbf{15.1})_2TeOH]_2 [SiF_6]$ has also been reported.[39]

The geometry around tellurium in diaryl halotelluronium cations is distorted trigonal pyramidal with one donor N atom in an axial position and the other in an equatorial position, as exemplified by the structure of $[(\mathbf{15.2})_2TeBr]^+Br^-$ in Fig. 15.4a.[37a] Consequently, the intramolecular Te···N bond distances are unequal. Typical values are in the ranges 2.43–2.53 Å

Scheme 15.4. General synthesis of diarylhalotelluronium salts.

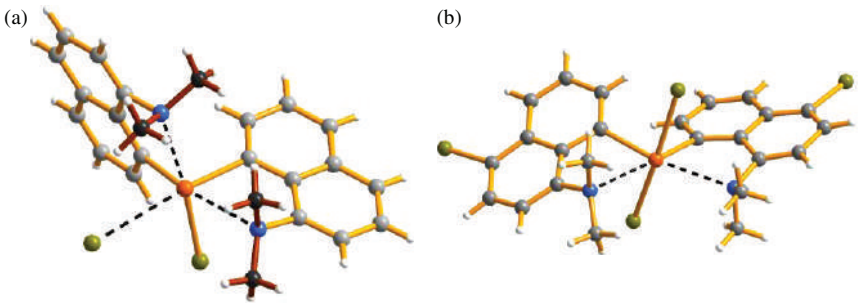

Figure 15.4. Molecular structures of (a) $[(\mathbf{15.2})_2TeBr]^+Br^-$ and (b) [(5-Br-8-$Me_2NC_{10}H_5)_2TeBr_2$]. [37a]

and 2.70–2.80 Å for the axial and equatorial Te···N bonds, respectively. The bromination of the diaryltelluride [(**15.2**)$_2$Te] with three equivalents of Br_2 results in a single electrophilic substitution and formation of [(5-Br-8-$Me_2NC_{10}H_5$)$_2$$TeBr_2$]. The geometry about tellurium in this covalent diaryl dibromide is distorted octahedral with approximately equal Te···N distances in the range 2.73–2.75 Å (Fig.15.4b), and the Te–Br distances are almost equal (2.66 and 2.71 Å), *cf.* 2.59 and 3.41 Å in the ionic compound [(**15.2**)$_2$TeBr]$^+$Br$^-$.[37a]

The structure of [**15.7**$TeBr_2$]$^+$, an example of an aryldihalotellurium(IV) cation, exhibits *d*(Te···N) = 2.372(2) and 2.435(2) Å (Fig. 15.5a).[40] The stabilisation of a diaryltellurium dication by intramolecular Te···N coordination has been achieved by using the 2-(2′-pyridyl)phenyl ligand (ppy) (**15.4** in Chart 15.1). Thus, reaction of [(**15.4**)$_2$TeI][I_3] with an excess of silver perchlorate or silver triflate in acetonitrile produces [(**15.4**)$_2$Te]$^{2+}$[X^-]$_2$ (X = ClO_4, O_3SCF_3] as white crystalline solids in 90% yields (Scheme 15.5).[38] The distorted arrangement of ligands around tellurium in the dication [(**15.4**)$_2$Te]$^{2+}$ includes two strong Te···N interactions of 2.224(2) and 2.229(2) Å (Fig. 15.5b). The stabilisation of these organotellurium(IV) cations is attributed to strong electrostatic interaction of the N lone pair of the ligand with the σ hole of the tellurium centre resulting in short Te···N contacts.[38,40]

15.2.6 *Solution behaviour*

^{77}Se and ^{125}Te NMR chemical shifts can be used to determine the strength of intramolecular E···N bonds in organochalcogen(II) derivatives in

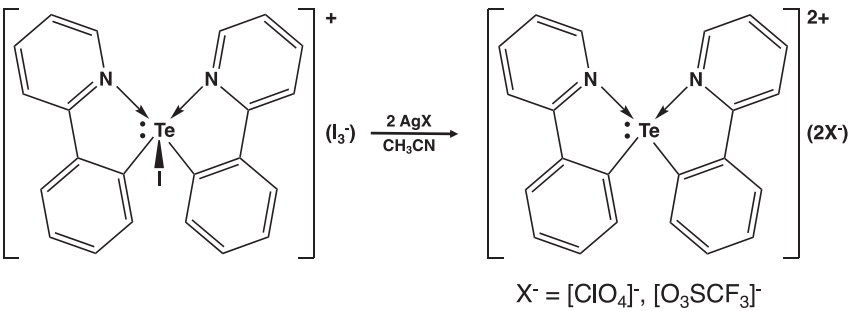

Scheme 15.5. Synthesis of salts of the diaryltellurium dication [(**15.4**)$_2$Te]$^{2+}$.

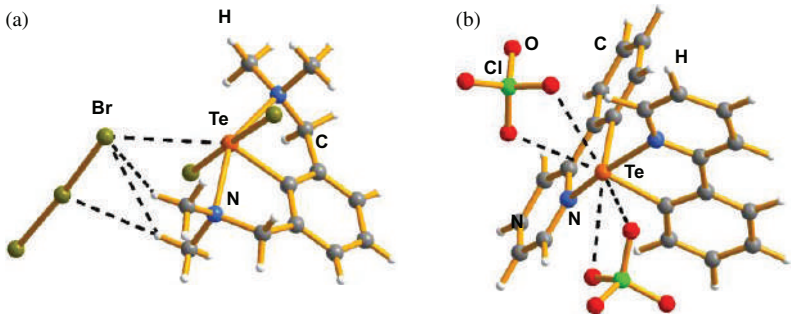

Figure 15.5. Molecular structures of (a) [**15.7**$TeBr_2$]$^+$[Br_3]$^-$ [40] and (b) [(**15.4**)$_2$Te]$^{2+}$[ClO_4]$^-_2$.[38]

solution, since the transfer of electron density from nitrogen to the chalcogen atom results in a substantial downfield chemical shift. For example, the selenenyl monohalides **15.5**SeX (X = Cl, Br, I) with a strong Se···N interaction (d(Se···N) = 2.05–2.13 Å, Sec. 15.2.1) exhibit a downfield shift in the ^{77}Se NMR resonance of 300–400 ppm, compared to the values for the diselenide (**15.5**Se–)$_2$ or **15.5**$SeCH_2Ph$, which have a much weaker Se···N contact (d(Se···N) = 2.75–2.80 Å.[10a] The ^{77}Se chemical shifts for a given series of organoselenium(II) halides RSeX move significantly downfield with the decreasing electronegativity of X, *i.e.*, chloride > bromide > iodide.[10a,c,d,e]

^{77}Se NMR chemical shifts can also give an indication of the ionisation of RSeCl derivatives in solution, which is manifested by a low-field shift on formation of RSe^+. Thus, the δ(^{77}Se) values for covalent derivatives fall within the range 856–1030 ppm,[10c] whereas [2,6-{$O(CH_2CH_2)NCH_2$}$_2$$C_6H_3$Se]$^+$Cl, which is ionic in the solid state, and [**15.7**Se]$^+$[$Au(C_6F_5)_2$]$^-$ (Sec. 15.2.3) exhibit resonances at *ca.* 1200 ppm.[31]

Similar to the trends for RSeCl derivatives, the ^{125}Te NMR resonance for the aryltellurenyl halide **15.3**TeCl (d(Te···N) = 2.203 Å) is observed at 1259 ppm, *ca.* 680 ppm downfield from that of the ditelluride (**15.3**Te–)$_2$ (d(Te···N) = 2.688 Å).[34] The chemical shifts of the related aryltellurenyl cation in salts [**15.3**Te]$^+$X$^-$ (d(Te···N) = 2.066–2.073 Å) are further deshielded to an extent that depends on the strength of the cation-anion interaction in solution [δ(^{125}Te) = 1735–1945 ppm], as discussed in Sec. 3.3 (Table 3.2).[34]

^{125}Te NMR spectroscopy also provides insights into the behaviour of the rare tritelluride **15.2**TeTeTe**15.2** (d(Te···N) = 2.67 Å) in solution.[41] The ^{125}Te NMR spectrum of the pure tritelluride in CD_2Cl_2 at −90°C exhibits resonances at 703 and −295 ppm with the expected relative intensities of 2:1 together with a minor resonance at 433 ppm assigned to the known ditelluride (d(Te···N) = 2.72 Å) and two signals of similar intensity at 764 and 8 ppm attributed to the unknown tetratelluride.[41]

^{125}Te NMR data combined with conductivity studies have elucidated the behaviour of diorganotellurium(IV) dihalides in solution. For example, the covalent dihalides, *e.g.*, $[(5,7\text{-}Cl_2\text{-}8\text{-}Me_2NC_{10}H_4)_2TeCl_2]$ and $[(5\text{-}Br\text{-}8\text{-}Me_2NC_{10}H_5)_2TeBr_2]$, and ionic compounds $[(\mathbf{15.2})_2TeX]^+X^-$ (X = Cl, Br) have been structurally characterised in the solid state (Fig. 15.4).[37a] The ^{125}Te NMR resonance for the dichloride $[(5,7\text{-}Cl_2\text{-}8\text{-}Me_2NC_{10}H_4)_2TeCl_2]$ is shifted more than 150 ppm to high field compared to that of the ionic isomer $[(\mathbf{15.2})_2TeCl]^+Cl^-$, and conductivity studies show that the covalent form does not ionise in solution. By contrast, electrolytic dissociation does occur for the dibromide $[(5\text{-}Br\text{-}8\text{-}Me_2NC_{10}H_5)_2TeBr_2]$ in acetonitrile, as evidenced by the molar conductivity and the observation that $[(5\text{-}Br\text{-}8\text{-}Me_2NC_{10}H_5)_2TeBr_2]$ and $[(\mathbf{15.2})_2TeBr]^+Br^-$ exhibit identical ^{125}Te chemical shifts in CD_3CN.[37a] The ^{125}Te NMR chemical shifts for the series of ionic salts $[(\mathbf{15.2})_2TeX]^+X^-$ (X = Cl, Br, I) are essentially identical (1198, 1197 and 1184 ppm, respectively) and unchanged by replacement of halide counter-ion by $[PF_6]^-$.[37a] The ^{125}Te NMR chemical shift of 1706 ppm for the monoorganodihalotelluronium cation in $[\mathbf{15.7}TeBr_2]^+[Br_3]^-$ is shifted considerably downfield relative to the values for comparable diorganohalotelluronium cations.[40]

15.2.7 *Electronic structures and bonding*

The intramolecular E···N (E = Se, Te) SBI in organochalcogen(II) halides and related derivatives is a consequence of an n^2(N) → σ^*(E–X) interaction in which the lone pair on the nitrogen atom donates electron density into the unoccupied antibonding σ^* orbital of the heavy chalcogen and the substituent X (Fig. 15.6).[1] More electronegative substituents X = Cl, Br, I lower the energy of the σ^*(E–X) orbitals and lead to a stronger n^2(N) → σ^*(E–X) interaction. Although the nature of the halide substituent in REX

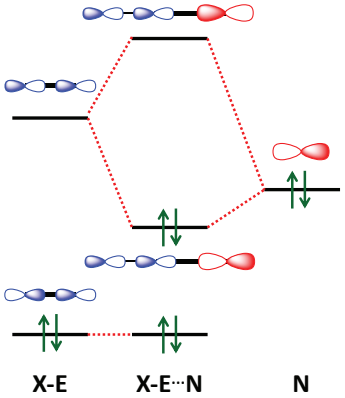

Figure 15.6. Orbital interactions for intramolecular E···N SBIs in REX (E = Se, Te).

derivatives has only a modest influence on the strength of the intramolecular Se···N contact (Sec 15.2.1), the partial occupation of the σ^*(E–X) orbital results in an elongation of the E–X bond.[10] Since the polarisability of atoms increases down the periodic table, the energy difference between σ(E–X) and σ^*(E–X) orbitals decreases. At the same time, the region of positive electrostatic potential on the opposite side of one of the covalent E–X bonds (σ hole), which interacts with the donor atom lone pair, becomes more pronounced when going down the periodic table. Dispersion effects are also more significant in tellurium compounds than in the lighter congeners.[6] This results in stronger SBIs in tellurium compounds compared to those of selenium and sulfur.

The bonding in the cation [**15.7**Se]$^+$ with two pendant *N*-donor arms (Scheme 15.3) involves a 3-centre-4-electron system with two short Se···N distances (Sec. 15.2.3).[29] In the free cation the N···Se···N arrangement is symmetrical and the stabilisation energy resulting from the n^2(N) $\rightarrow$ σ^*(Se–N) interaction is estimated to be 249 kJ mol^{-1}. In the halide salts [**15.7**Se]X this value is reduced to *ca.* 197 (X = I), 177 (X = Br) and 165 (X = Cl) kJ mol^{-1} and the N···Se···N unit becomes progressively asymmetrical.[29] The two principal resonance structures for the free cation [**15.7**Se]$^+$ are depicted in Fig. 15.7.

In organotellurium(II) cations RTe$^+$ that have no substituent X attached to Te, the intramolecular Te···N SBI can be sufficiently strong to

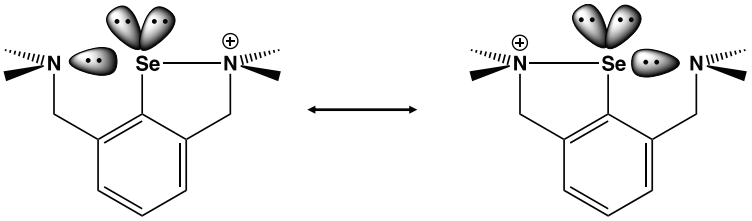

Figure 15.7. Principal resonance structures for the free cation [**15.7**Se]$^{+}$.[28]

generate a tellurium-nitrogen single bond, as exemplified by Te–N distances of 2.05–2.11 Å in salts of **15.3**Te^{+} (Sec. 15.2.4) (Chart 15.4). The five-membered C_3NTe ring in this cation is a Hückel 6π-electron system with aromatic character as judged by calculated NICS values for the parent cation $[HC)_3(HN)Te]^{+}$, which are similar to those of 1-tellura-2,5-diazole.[34]

The intramolecular Te···N SBIs in organotellurium(IV) cations are also very strong. In the aryldibromotellurium monocation [(**15.7**)$TeBr_2$]$^{+}$ (Fig. 15.5a) the donation of the lone pair of electrons on each N atom to the vacant *p* orbital on tellurium results in stabilisation energies of *ca.* 385 and 339 kJ mol^{-1} on the basis of natural bond orbital (NBO) analysis.[40] The two SBIs in the dication [(**15.4**)$_2$Te]$^{2+}$ (Fig. 15.5b) are even stronger with an estimated stabilisation energy of *ca.* 506 kJ mol^{-1} each on the basis of NBO analysis, consistent with Te···N bond lengths that are only *ca.* 0.13 Å longer than the single-bond value (Sec. 15.2.4).[38]

15.3 Intermolecular SBIs: Supramolecular Chemistry

Intermolecular SBIs in chalcogen-nitrogen compounds provide a cogent illustration of the concept of ChB, as discussed in Sec. 15.1. For example, in carbon-poor chalcogen-nitrogen heterocycles ChB can generate supramolecular structures that exhibit unique properties or novel host-guest chemistry. In this section the structures and properties of materials that incorporate diamagnetic C,N,E building blocks, *viz.*, 1-chalcogena-2,5-diazoles, benzo-2-chalcogena-1,3-diazoles, *iso*-tellurazole *N*-oxides, and

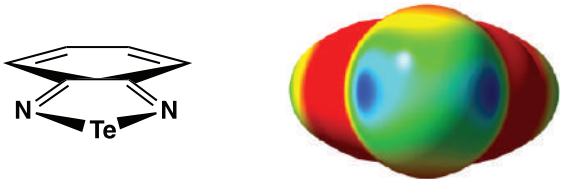

Figure 15.8. Electrostatic potentials on the molecular surface of benzo-2-tellura-1,3-diazole. Red colour indicates negative regions and blue indicates positive regions.[42] [Reproduced with permission from G. E. Garrett, G. L. Gibson, R. N. Straus, D. S. Seferos and M. S. Taylor, *J. Am. Chem. Soc.*, **137**, 4126 (2015). Copyright 2015 American Chemical Society].

benzo-1-chalcogena-3-azoles, are described as examples of this propensity.

The ChB concept in which the chalcogen can provide two regions of depleted electron density (σ-holes) along the extension of the covalent bond axis is illustrated for benzo-2-tellura-1,3-diazole in Fig. 15.8.[42]

15.3.1 *1-Chalcogena-2,5-diazoles*

The X-ray crystal structures of salts of the 1:1 adduct of 3,4-dicyano-1-selena-2,5-diazole (**15.16a**) with the anion $[PhS]^-$,[43] 1:1 complexes of 3,4-dicyano-1-tellura-2,5-diazole (**15.16b**) (Chart 15.5) with halide anions,[44] and a 1:2 complex with pyridine have been determined (Sec. 11.2.4, Chart 11.7).[44] The nature of ChB in this class of compounds has been investigated by a systematic X-ray diffraction and solid-state NMR (^{77}Se and ^{125}Te) investigation of cocrystals of **15.16a** and **15.16b** with tetrabutylammonium halides $[Bu_4N]X$ (X = Cl, Br, I), pyridine *N*-oxide and various pyridine derivatives.[45a] These studies demonstrated the ability of **15.16a** and **15.16b** to form strongly directional, double ChB indicating their promise to serve as supramolecular synthons. For halide ions two classes of adducts were characterised; (a) 1:1 complexes $[(\mathbf{15.16a}X)_2]^{2-}$ (X = Cl, Br) and $[(\mathbf{15.16b}I)_2]^{2-}$ in which the anion acts as a bidentate ChB acceptor (Chart 15.5a) and (b) 1:2 complexes $[\mathbf{15.16b}X_2]^{2-}$ (X = Cl, Br) in which the halide anions are monodentate (Chart 15.5b).[45a]

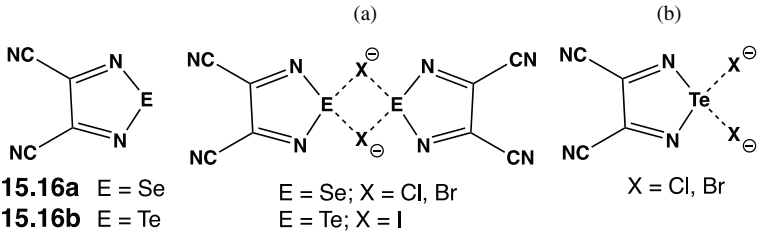

Chart 15.5. (a) 1:1 and (b) 1:2 adducts of 3,4-cyano-1-chalcogena-2,5-diazoles, **15.6a**, **b**, with halide ions.

Pyridine-*N*-oxide forms a 1:1 adduct with **15.16a** and a 1:2 adduct with **15.16b** with structural arrangements analogous to the corresponding halide complexes.[45a] The influence of substituents in pyridine *N*-oxides on the nature of ChB in adducts with **15.16a** and **15.16b** was also investigated.[45b] Without steric hindrance, cocrystals formed between **15.16a** and pyridine *N*-oxides formed a supramolecular tetrameric ChB synthon (Fig. 15.9a), while the corresponding cocrystals of **15.16b** and pyridine *N*-oxides exhibit an open spiral configuration (Fig. 15.9b).[45b]

The macrocycles **15.17a** (E = Se) and **15.17b** (E = Te) incorporating four 1-chalcogena-2,5-diazoles connected by two 1,3-phenylene and two $–CH_2–$ linkers have been synthesised and characterised by solution NMR spectra and ESI mass spectra, but no X-ray structural data were reported (Chart 15.6).[46a] The ChB interactions of **15.17a**, **b** with the anionic surfactant 4-dodecyl-pyridine *N*-oxide were found to be reversible upon the addition of halide ion.[46a] This work has been extended to supramolecular polymers comprised of ChB donors constructed from two tetrameric units of **15.17a** or **15.17b** with a $(–OCH_2–CH_2–)_5$ linker and a bispyridine *N*-oxide bridged by a $–CH_2O(CH_2)_{10}OCH_2–$ group.[46b]

The Lewis ambiphilicity of 1-chalcogena-2,5-diazoles (Sec. 11.2.3) is illustrated by their molecular complexes with crown ethers. The 1:1 complexes of 18-crown-6 with **15.6a**, **15.6b** or benzo-2-selena-1,3-diazole (BSD) have been isolated from THF solutions as pale yellow crystals and structurally characterised by X-ray crystallography.[47] The SBIs in these complexes include charge transfer from O atoms of the crown ether onto

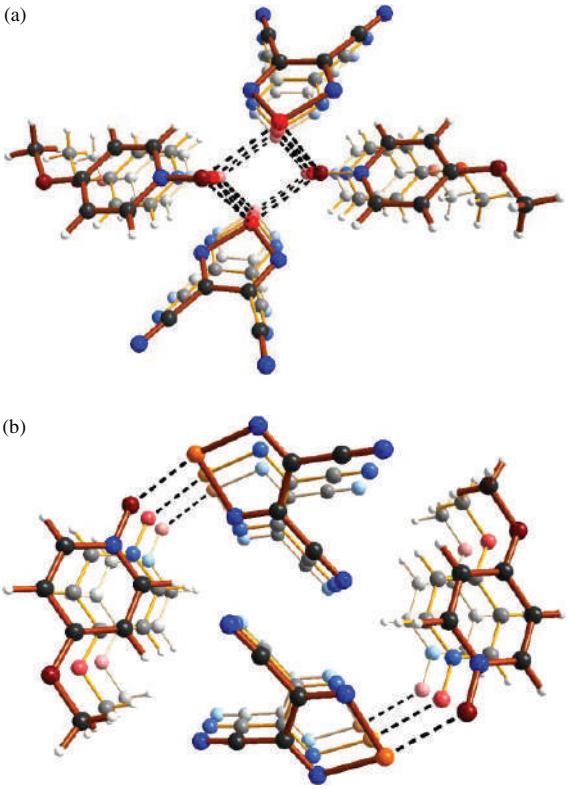

Figure 15.9. Chalcogen bond geometry in cocrystals of 4-methoxypyridine *N*-oxide with (a) **15.16a** and (b) **15.16b**.[45b]

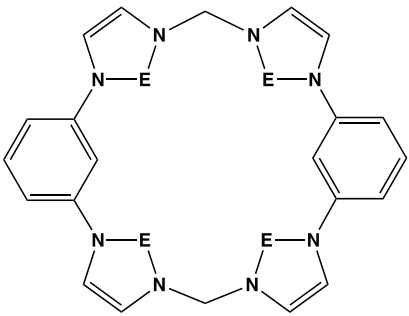

15.17a E = Se
15.17b E = Te

Chart 15.6. Tetrameric 1-chalcogena-2,5-diazoles with $–C_6H_4–$ and $–CH_2–$ linkers.

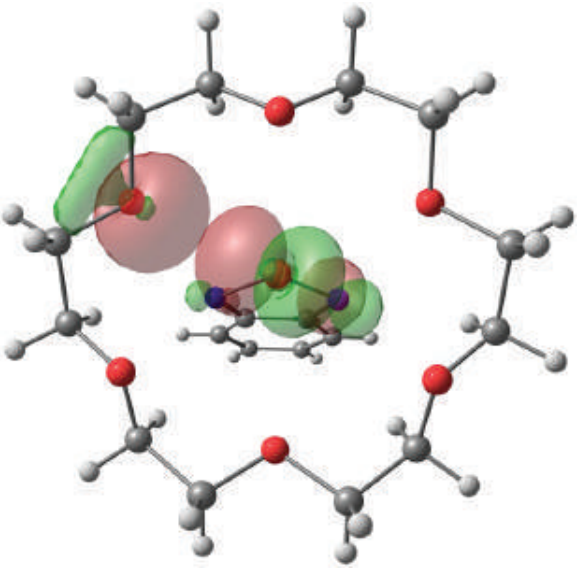

Figure 15.10. One of the two symmetry-related strongly interacting orbitals in [18-c-6][BSD] showing the lone pair of the O atom and Se–N σ^* orbital.[47] [Reproduced with permission from E. A. Chulanova, E. A. Radiush, I. K. Shundrina, I. Yu. Bagryanskaya, N. A. Semenov, J. Beckmann, N. P. Gritsan and A. V. Zibarev, *Cryst. Growth Des*., **20**, 5868 (2020). Copyright 2020 American Chemical Society].

the E atom of the chalcogenadiazole and back donation from E to O, as depicted for [18-c-6][BSD] in Fig. 15.10.[47] The energies of the bonding interactions in these complexes are significantly lower than those of the anionic complexes of **15.16a** and **15.16b** (Chart 15.5).

15.3.2 *Benzo-2-chalcogena-1,3-diazoles*

The fundamental chemistry of benzo-2-thia-1,3-diazoles has received renewed attention recently owing to the potential applications of these chalcogen-nitrogen heterocycles as luminescent materials and as components of thin-film optoelectronic devices such as LEDs, solar cells, field-effect transistors, and biosensors, as discussed in Sec. 11.2.5. For these applications suitable structural arrangements are necessary in order to generate efficient thin films. With this in mind a recent investigation has

focused on developing an understanding of the molecular organisation of compounds with multiple benzothiadiazole units attached to planar and non-planar molecular cores (**15.18**–**15.22**, Chart 15.7).[48] For compounds **15.18**–**15.21** complex structures that are controlled by significant S···N interactions supplemented by C–H···N and/or C–H···O contacts were observed. Polymorphs or solvates were not isolated for these derivatives even when crystallisation was carried out under a variety of conditions. The bis(thiadiazole) **15.18** and the tris(thiadiazole) **15.20** are more easily reduced than the parent benzo-2-thia-1,3-diazole, reflecting the electron-withdrawing influence of the additional thiadiazole ring(s). The main UV

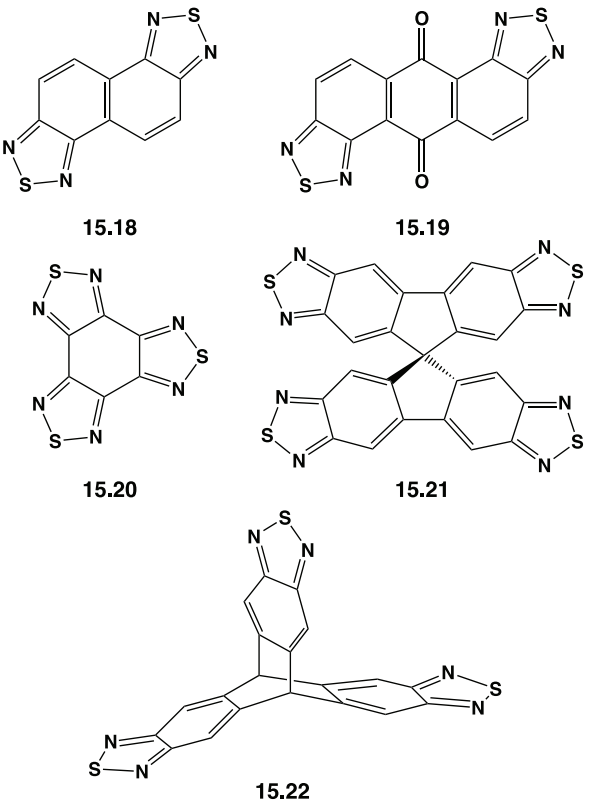

Chart 15.7. Compounds with multiple benzo-2-thia-1,3-diazole units.

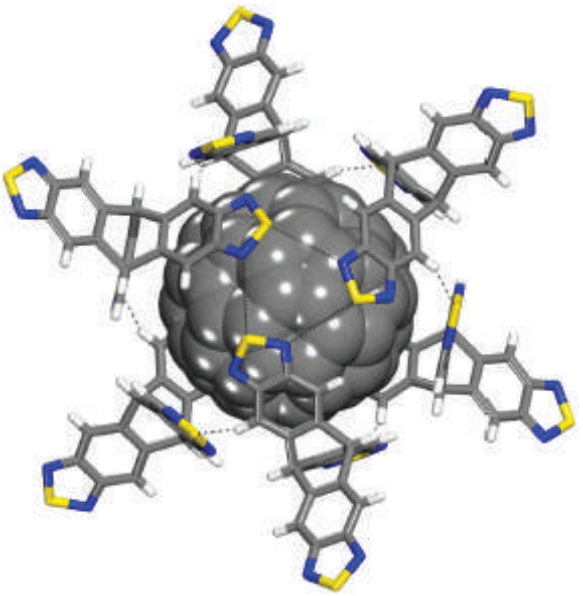

Figure 15.11. Molecular structure of co-crystals of triptycenetris(thiadiazole) (**15.21**) and C_{60}.[48a] [Reproduced with permission from S. Langis-Barsetti, T. Maris and J. D. Wuest, *J. Org. Chem.*, **82**, 5034 (2017). Copyright 2017 American Chemical Society].

absorption band of benzo-2-thia-1,3-diazole is shifted from 310 nm to *ca.* 256 nm (in THF solution) for **15.18** and **15.20**.

In contrast to the structures of **15.18**–**15.21**, the S···N interactions in triptycenetris(thiadiazole) **15.22** are either weak or absent leading to an open structure that is able to act as a host for the fullerenes C_{60} and C_{70} (Fig. 15.11).[48a,b] Interestingly, the bromination of **15.21** occurs selectively to give dibromo, tetrabromo and hexabromo derivatives each with two bromines attached to the same phenyl ring.[48b]

The different strengths of E···N interactions in benzo-2-chalcogena-1,3-diazoles are demonstrated impressively in a comparison of the structures of the supramolecular capsules formed when a benzo-2-thia-1,3-diazole or benzo-2-tellura-1,3-diazole motif is introduced into a resorcin[4]arene cavitand (Chart 15.8).[49] The stronger 2Te–2N square interactions in **15.23a** result in a dimeric capsule in all solvents with 16 short Te···N

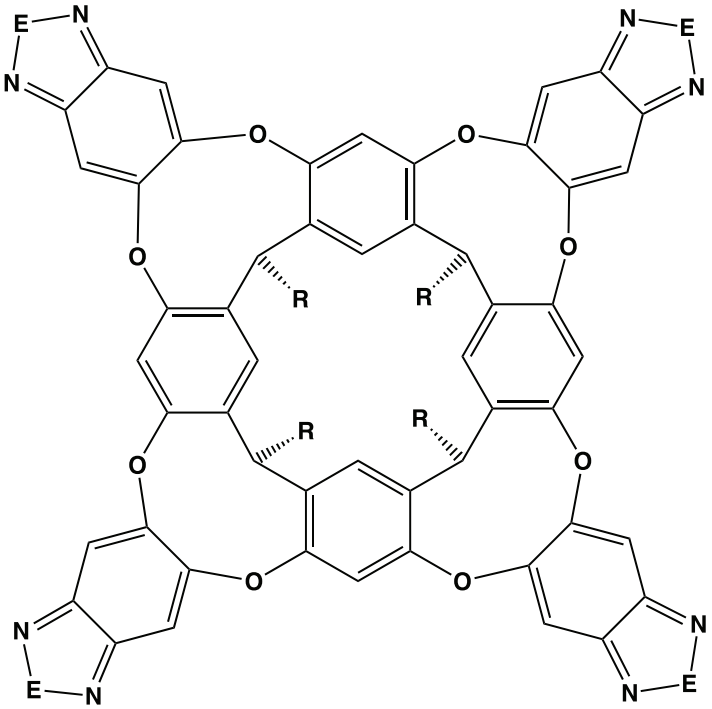

15.23a E = Te
15.23b E = S

Chart 15.8. Benzo-2-chalcogena-1,3-diazole-functionalised resorcin[4]arenes.

distances as revealed by the X-ray crystal structure (d(Te···N) <2.9 Å), and confirmed by ESI-MS (Sec. 3.8.2). By contrast, the sulfur analogue **15.23b** crystallises in solvent-dependent arrangements involving either a shifted 2S–2N square-bonded capsule or an interlocked 1D polymer with an infinite π-π stacking array.[49]

The supramolecular association of benzo-2-thia-1,3-diazoles most commonly results in a square motif (Chart 15.9a), although other weak interactions such as S···S, halogen bonding or hydrogen bonding may compete with the 2S–2N interaction.[50,51] Alternatively, a hexagonal arrangement may be observed, notably when a heteroatom is introduced into the carbocyclic ring, *e.g.*, pyridyl-benzo-2-thia-1,3-diazole (Chart 15.9b). The attachment of substituents such as NO_2 or CN in the 4- or

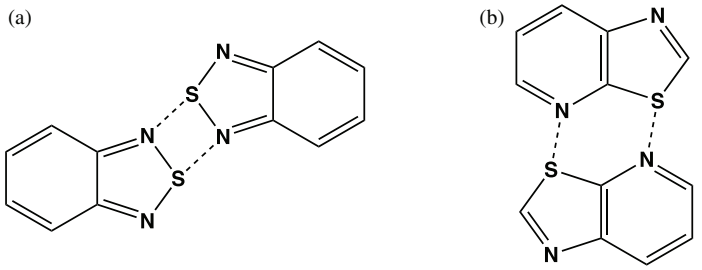

Chart 15.9. (a) Square and (b) hexagonal bonding motifs in benzo-2-thia-1,3-diazoles.

4,7- positions of the carbocyclic ring of benzo-2-thia-1,3-diazole favours the square motif, whereas the C_6F_5 group strengthens the hexagonal interaction.[51] The inclusion of additional N atoms in the carbocylic ring also enhances the hexagonal arrangement.

The proclivity of benzo-2-chalcogena-1,3-diazoles to engage in additional SBIs is illustrated by the formation of co-crystals of benzo-2-selena-1,3-diazole (BSD) with monofunctional hydrogen or halogen bond doors such as pentafluorophenol, pentafluorobenzoic acid or pentafluoroiodobenzene or bifunctional donors, *e.g.*, resorcinol, tetrafluororesorcinol, tetrafluorohydroquinone or 1,4-diiodotetrafluorobenzene.[52] In these co-crystals the nitrogen atoms not involved in the formation of the 2Se–2N interaction act as acceptors of hydrogen or halogen bonds. As representative examples, the tetrameric assembly in the co-crystals of 1:1 complex of BSD with pentafluoroiodobenzene and the supramolecular polymer formed by the 2:1 complex of BSD with 1,4-diiodotetrafluorobenzene are shown in Figs. 15.12a and 15.12b, respectively. Both of these structures involve N···I interactions in the range 2.97–3.10 Å (*cf.* sum of van der Waals radii for N and I = 3.53 Å). The parent benzo-2-selena-1,3-diazole also forms a 1:1 complex with molecular I_2 involving a strong I–I···N interaction [d(N···I) = 2.64 Å] and a very weak I–I···Se contact.[52]

15.3.3 *Iso-tellurazole N-oxides*

Iso-tellurazole *N*-oxides are five-membered tellurium-nitrogen heterocycles, *e.g.*, **15.24**, that form cyclic oligomers *via* supramolecular Te···O

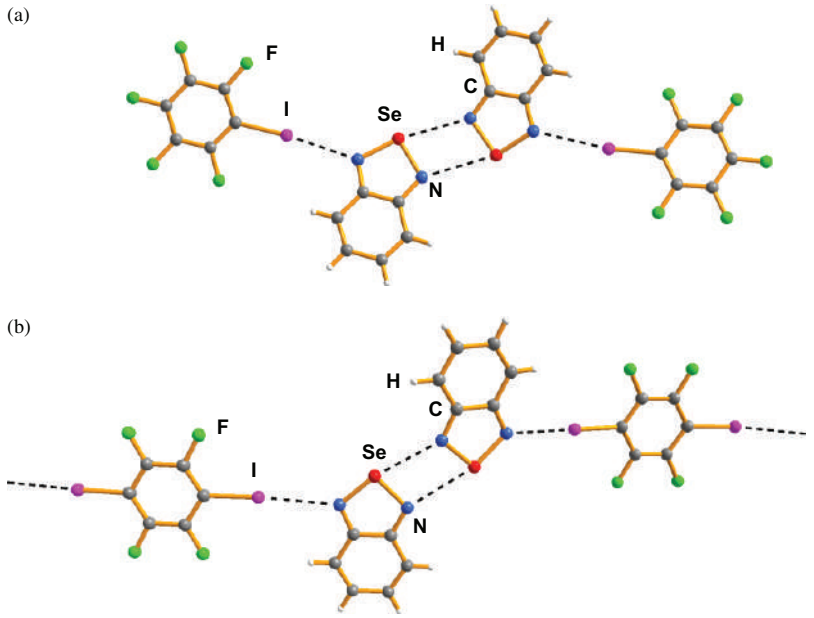

Figure 15.12. Crystal structures of (a) BSD·C_6F_5I and (b) $(BSD)_2$·1,4-$I_2C_6F_4$.[52]

SBIs, *e.g.*, the tetramers **15.25** and hexamers **15.26** (Chart 15.10).[53–55] Ring systems up to the heptamer have been identified in solution on the basis of ESI-MS (Sec. 3.8.2). Two different infinite polymers **15.27** have also been structurally characterised.[54,56]

Chlorination of the tetramer **15.25a** (R = Ph) with SO_2Cl_2 occurs with retention of the auto-associated structure to give the dichloro derivative $(\mathbf{15.24a}Cl_2)_4$ (Fig. 15.13a).[57] The mean Te···O bond length of *ca.* 2.06 Å in this tellurium(IV) derivative is significantly shorter than that in any other tetrameric or hexameric derivatives involving tellurium(II) (Chart 15.10) and close to the sum of covalent radii for Te and O (2.03 Å). DFT-D3 calculations indicate that the stronger ChB donor interactions in the chlorinated derivative are offset by weaker acceptor interactions.[57] The partially chlorinated derivative $(\mathbf{15.24a})_2(\mathbf{15.24a}Cl_2)_2$ (Fig. 15.13b) with alternating tellurium(II) and tellurium(IV) centres was obtained by reaction of **15.25a** (R = Ph) with a stoichiometric amount of SO_2Cl_2 or by mixing $(\mathbf{15.24a})_4$ and $(\mathbf{15.24a}Cl_2)_4$ in a 1:1 ratio; this mixed-valent

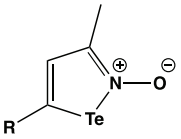

15.24a R = Ph
15.24b R = 3,5-$^{t}Bu_2C_6H_3$

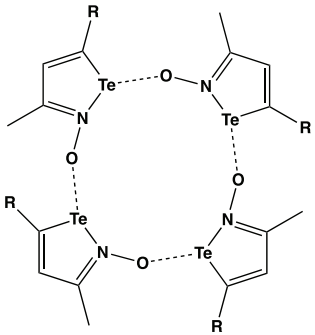

15.25a R = Ph
15.25b R = 3,5-$^{t}Bu_2C_6H_3$

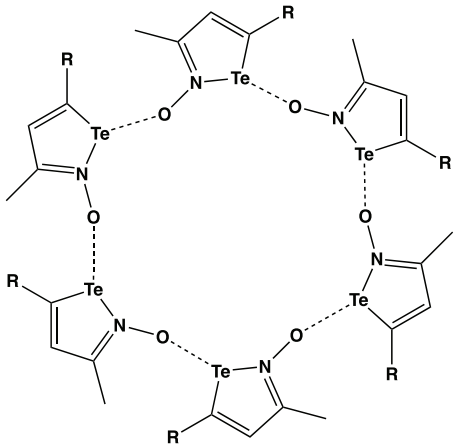

15.26a R = Ph
15.26b R = 3,5-$^{t}Bu_2C_6H_3$

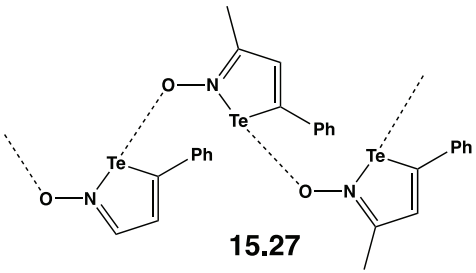

15.27

Chart 15.10. Tetrameric, hexameric and polymeric forms of *iso*-tellurazole *N*-oxides.

tetramer is the thermodynamically favoured arrangement according to DFT calculations.

Although the synthesis of **15.24a** and its cyclic oligomers requires multiple steps,[53] the preparation of the benzo-annulated derivative **15.28a**

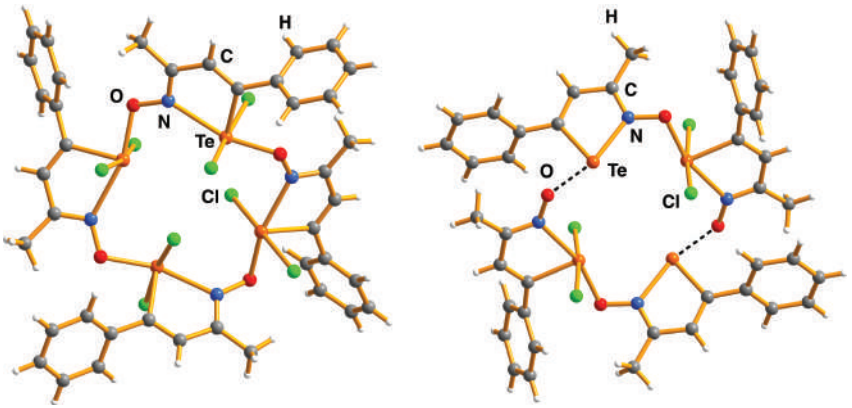

Figure 15.13. Molecular structure of (a) (**15.24a**Cl_2)$_4$ and (b) (**15.24a**)$_2$(**15.24a**Cl_2)$_2$ (the disordered molecule in the asymmetric unit has not been shown for clarity).[57]

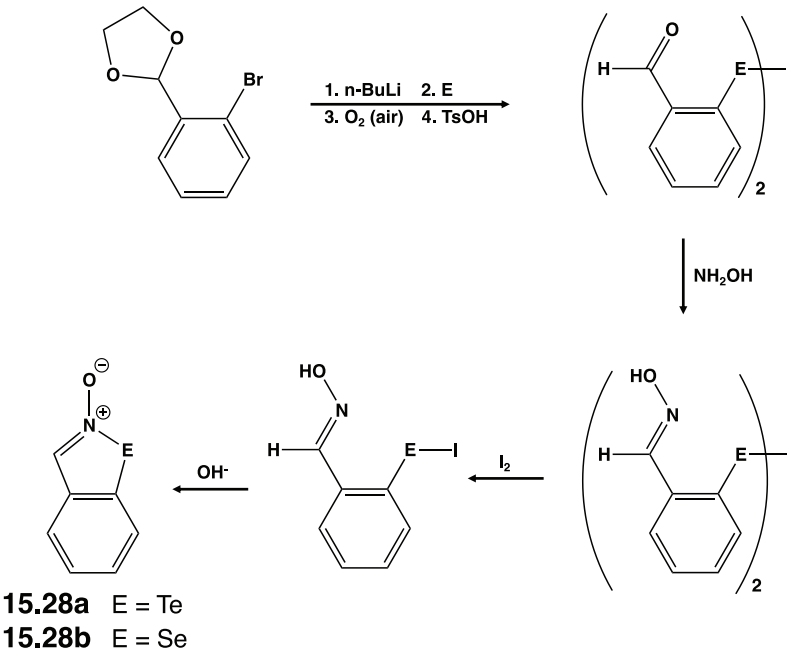

Scheme 15.6. Synthesis of benzo-1,2-chalcogenazole 2-oxides.

is more straightforward and can also be applied to the selenium analogue **15.28b**, as shown in Scheme 15.6.[54] In the solid state **15.28a** forms cyclic tetrameric and hexameric aggregates analogous to **15.25** and **15.26**. By contrast, the selenium congener **15.28b** has a supramolecular polymeric structure analogous to **15.27**.[54] Changing the phenyl group in **15.24a** to 3,5-di-*tert*-butylphenyl (**15.24b**) enhances the solubility of the *iso*-tellurazole *N*-oxide.[58]

Iso-tellurazole *N*-oxides are air-stable and unaffected by water. However, the supramolecular structure is broken up in acidic media to give the adducts **15.24a**·HX (X = Cl, Br).[56] Protonation occurs at the O atom with the formation of Te–X bonds. The Te–N bond lengths in these adducts are in the range 2.17–2.18 Å,[56] *cf.* 2.15 Å in the tetramer **15.25a**.[53] The protonation process is reversible.

The auto-association of *iso*-tellurazole *N*-oxides is a Lewis acid-Lewis base interaction. In that context, the reactions of Lewis acids and Lewis bases with **15.24a** and **15.28a** are of interest. ^{1}H NMR spectra indicate that these *iso*-tellurazole *N*-oxides are remarkably inert towards Lewis bases such as acetonitrile, 4-dimethylamino-pyridine (DMAP), triphenylphosphine and *N*-heterocyclic carbenes.[59] On the other hand, **15.24a** readily forms 1:1 *O*-bonded adducts with Lewis acids BR_3 (**15.29**, R = F, Ph) (Chart 15.11), *cf.* protonation of **15.24a**. These adducts react readily with Lewis bases to give complexes in which the *iso*-tellurazole

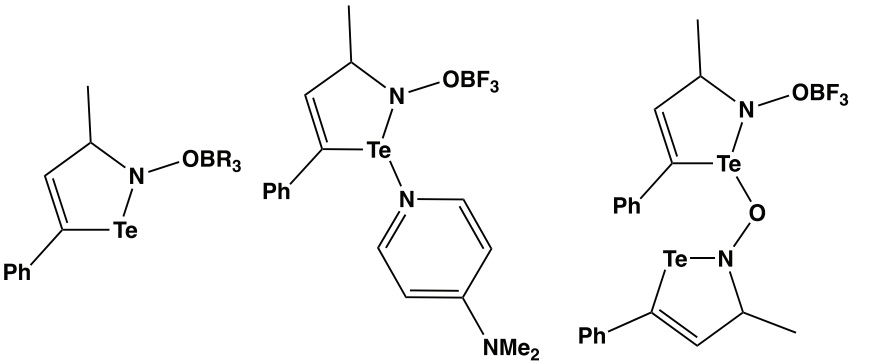

15.29a R = F
15.29b R = Ph

15.30

15.31

Chart 15.11. Lewis acid and Lewis base adducts of iso-tellurazole *N*-oxide **15.24a**.

N-oxide exhibits ambiphilic properties, *e.g.*, **15.30** (Chart 15.11). Of particular interest is the reaction of **15.29a** with **15.24a** to give the complex **15.31** in which the *iso*-tellurazole *N*-oxide acts as both a chalcogen-bond acceptor (Lewis acid) and donor (Lewis base).[59]

The cyclic tetramer **15.25a** forms coordination complexes with transition-metal ions. For example, the complex [Pd(**15.25a**)](BF_4) is readily obtained in quantitative yield by addition of a CH_2Cl_2 solution of **15.24a** to an acetonitrile solution of [Pd($NCCH_3$)$_4$](BF_4).[54] The tetrameric ligand in [Pd(**15.25a**)](BF_4) is in a boat conformation and the metal centre is coordinated to the four tellurium atoms in a slightly distorted square-planar arrangement (Fig. 15.14a). An analogous square-planar platinum(II) complex has been obtained by using the more soluble **15.24b**.[57] The octahedral rhodium(III) complex [$RhCl_2$(**15.25a**)](BF_4) in which the four Te atoms of the tetramer are coordinated in a square arrangement to the metal has also been structurally characterised.[57]

Reactions of *iso*-tellurazole *N*-oxides with monocations of the coinage metals introduce new aspects of their coordination chemistry.[60] For example, treatment of **15.24a** with [Au(Cl)(C_4H_3S)] in CH_2Cl_2 produces the binuclear gold(I) complex [Au_2Cl_2(**15.25a**)], which incorporates two linear Te–Au–Cl units and two very weak Te···Au contacts (Fig. 15.14b).

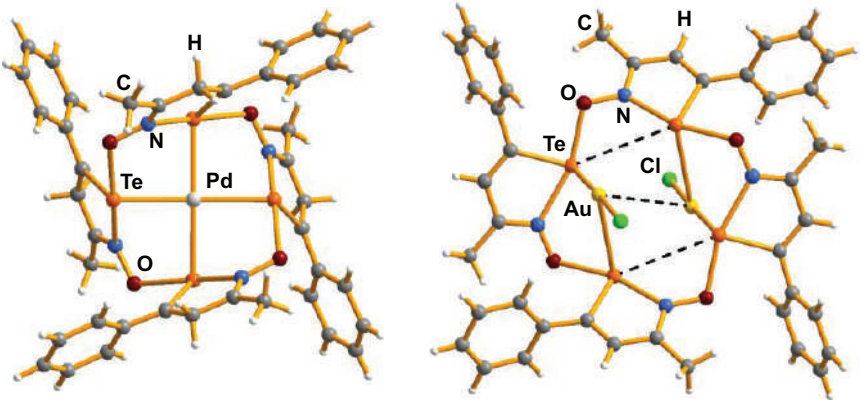

(a) (b)

Figure 15.14. Crystal structures of (a) [Pd(**15.25a**)]$^{2+}$ and (b) [Au_2Cl_2(**15.25a**)].[60]

Silver(I) exhibits a unique preference for coordination to the hexameric ligand in the complex [{$Ag_2(\mu\text{-}CF_3SO_3)_2$(**15.26b**)}$Ag_2(CF_3SO_3)_2$].

Slow diffusion of a $CHCl_3$ solution of **15.24a** into a concentrated solution of C_{60} in CCl_4 produces crystals of the host-guest complex **15.25a**·C_{60}.[54] In contrast to the boat conformation of **15.25a** in the Pd complex, the *iso*-tellurazole rings in this adduct are tilted towards the meridional plane of the macrocycle and there are two very weak Te···C contacts with the fullerene (Fig. 15.15).

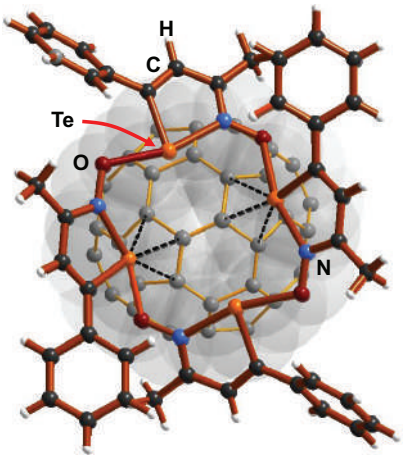

Figure 15.15. Crystal structure of **15.25a**·C_{60}.[54]

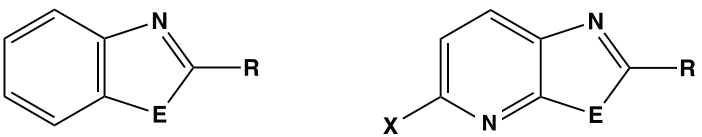

15.32a E = Te
15.32b E = Se

15.33a E = Te
15.33b E = Se

Chart 15.12. 2-Substituted benzo-1,3-chalcogenazoles and chalcogenazolopyridines.

15.3.4 *Benzo-1,3-chalcogenazoles*

Although a direct chalcogen-nitrogen bond is not incorporated within the heterocyclic ring, benzo-1,3-chalcogenazoles (**15.32**, E = Se, Te) (Chart 15.12) provide compelling examples of the influence of strong

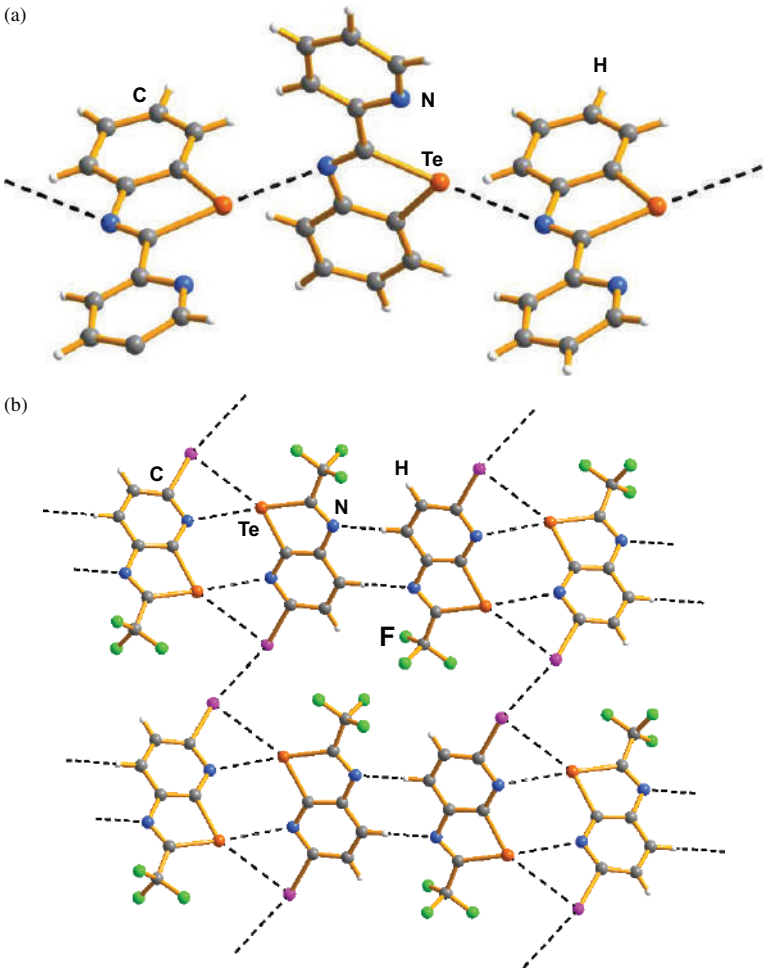

Figure 15.16. X-ray structures of (a) **15.32a** (R = 2-pyridyl) and (b) **15.33a** (R = CF_3, X = I).[63,64]

E···N SBIs on molecular structures and properties.[5] New synthetic routes have been developed for a wide range of these chalcogen-nitrogen heterocycles, including those with heteroatom substituents in the 2-position that can act as chalcogen-bond acceptors through one of the σ holes of the chalcogen, *e.g.*, R = 2-, 3- or 4-pyridyl.[60,61] For example, **15.32a** (R = 2-pyridyl) forms a wire-like structure *via* moderately strong *intramolecular* Te···N contacts (*ca.* 3.23 Å) (Fig. 15.16a).[62] Concomitantly, a stronger *intermolecular* Te···N interaction (*ca.* 3.09 Å) blocks the second σ hole of the chalcogen atom.

Extension of these ideas to the chalcogenazolopyridines **15.33** (Chart 15.12) with R = 2-pyridyl or an electron-withdrawing group produces six-membered rings with two E···N SBIs.[63] In the selenium congeners the weaker Se···N contacts may compete with hydrogen bonding interactions unless R is a strong electron-withdrawing group, *e.g.*, CF_3, C_6F_5. The judicious choice of substituents in the 2- and 5-positions of **15.33** can control the tailoring of supramolecular structures to give either ribbon or wire-like arrangements.[64] For example, the tellurium derivative **15.33a** (R = CF_3, R = I) forms a kinked ribbon involving two weak Te···N SBIs in dimeric units supplemented by two C–H···N hydrogen bonding interactions (Fig. 15.16b).[64] By contrast, the ribbon-like arrangement is held together through only hydrogen bonding in the selenium congener **15.33b** (R = CF_3, R = I) and no Se···N contacts are observed.

References

1. T. Chivers and R. S. Laitinen, *Chem. Soc. Rev*., **44**, 1725 (2015).
2. (a) C. B. Aakeroy, D. L. Bryce, G. R. Desiraju, A. Frontera, A. C. Legon, F. Nicotra, K. Rissanen, S. Scheiner, G. Terraneo, P. Metrangolo and G. Resnati, *Pure Appl. Chem.*, **91**, 1889 (2019); (b) P. C. Ho. J. Z. Wang, F. Meloni and I. Vargas-Baca, *Coord. Chem. Rev*., **422,** 21364 (2020).
3. J. Beckmann and P. Finke, in *Selenium and Tellurium Chemistry: From Small Molecules to Biomolecules and Materials*, Eds. J. D. Woollins and R. S. Laitinen, Springer (2011), Ch. 7, pp. 179–200.
4. K. Srivatava, A. Panda, S. Sharma and H. B. Singh, *J. Organomet. Chem*., **861**, 174 (2018)

5. N. Biot and D. Bonifazi, *Coord. Chem. Rev*., **413**, 213243 (2020).
6. G. Haberhauer and R. Gleiter, *Angew. Chem. Int. Ed*., **59**, 21236 (2020).
7. S. Kolb, G. A. Oliver and D. B. Werz, *Angew. Chem. Int. Ed*., **59**, 22306 (2020).
8. A. F. Cozzolino, P. J. W. Elder, *Coord. Chem. Rev*., **255**, 1426 (2011).
9. (a) M. Fourmigué and A. Dhaka, *Coord. Chem. Rev*., **403**, 213084 (2020); (b) P. Scilabra, G. Terraneo and G. Resnati, *Acc. Chem. Res*., **52**, 1313 (2019); (c) L. Vogel, P. Wonner and S. M. Huber, *Angew. Chem. Int. Ed*., **58**, 1880 (2019); (d) K. T. Mahmudov, M. N. Kopylovich, M. F. C. Guedes da Silva and A. J. L. Pombeiro, *Dalton Trans*., **46**, 10121 (2017).
10. (a) G. Mugesh, A. Panda, H. B. Singh and R. J. Butcher, *Chem. Eur. J*., **5**, 1411 (1999); (b) M. Kulcsar, A. Silvestru, C. Silvestru, J. E. Drake, C. L. B. MacDonald, M. E. Hursthouse and M. E. Light, *J. Organomet. Chem*., **690**, 3217 (2005); (c) A. Panda, G. Mugesh, H. B. Singh and R. J. Butcher, *Organometallics*, **18**, 1986 (1999); (d) A. Pöllnitz, V. Lippolis, M. Arca and A. Silvestru, *J. Organomet. Chem*., **696**, 2837 (2011); (e) M. Kulcsar, A. Beleaga, C. Silvestru, A. Nicolescu, C. Deleanu, C. Todasca and A. Silvestru, *Dalton Trans*., 2187 (2007).
11. H. Polschner and K. Seppelt, *Chem. Eur. J*., **10**, 6565 (2004).
12. A. Hammerl, T. M. Klapötke, B. Krumm and M. Scherr, *Z. Anorg. Allg. Chem*., **633**, 1618 (2007).
13. P. Rakesh, H. B. Singh and R. J. Butcher, *Acta Crystallogr. E*, **E68**, o214 (2012).
14. J. Beckmann, J. Bolsinger and A. Duthie, *Chem. Eur. J*., **17**, 930 (2011).
15. M. Hejda, E. Lork, S. Mebs, L. Dostál and J. Beckmann, *Eur. J. Inorg. Chem*., **2017**, 3435 (2017).
16. K. Srivastava, P. Shah, H. B. Singh and R. J. Butcher, *Organometallics*, **30**, 534 (2011).
17. T. Chakraborty, H. B. Singh and R. J. Butcher, *Acta Crystallogr. E*, **E65**, o2562 (2009).
18. (a) T. Glodde, Y. V. Vishnevsky, L. Zimmermann, H-G. Stammler, B. Neumann and N. W. Mitzel, *Angew. Chem. Int. Ed*., **60**, 1519 (2021); (b) J.-M. Mewes, A. Hansen and S. Grimme, *Angew. Chem. Int. Ed.*, **60**, 13144 (2021); (c) Y. V. Vishnevsky and N. W. Mitzel, *Angew. Chem. Int. Ed*., **60**, 13150 (2021).
19. T. M. Klapötke, B. Krumm and K. Polborn, *J. Am. Chem. Soc*., **126**, 710 (2004).
20. T. M. Klapötke, B. Krumm, H. Nöth, J. C. Gálvez-Ruiz, K. Polborn. I. Schab and M. Suter, *Inorg. Chem*., **44**, 5354 (2005).

21. K. Srivastava, T. Chakraborty, H. B. Singh, U. P. Singh and R. J. Butcher, *Dalton Trans*., **39**, 10137 (2010).
22. F. D. da Silva, C. A. D. P. Simões, S. S. dos Santos and E. S. Lang, *J. Organomet. Chem*., **832**, 66 (2017).
23. T. M. Klapötke, B. Krumm and M. Scherr, *Phosphorus Sulfur Silicon Relat. Elem.*, **184**, 1347 (2009).
24. (a) J. Beckmann, J. Bolsinger, J. Duthie and P. Finke, *Organometallics*, **31**, 238 (2012); (b) O. Mallow, J. Bolsinger, P. Finke, M. Hesse, Y-S. Chen, A. Duthie, S. Grabowsky, P. Luger, S. Mebs and J. Beckmann, *J. Am. Chem. Soc*., **136**, 10870 (2014).
25. J. Beckmann, A. Duthie, T. M. Gesing, T. Koehne and E. Lork, *Organometallics*, **31**, 3451 (2012).
26. R. Deka, A. Sarkar, R. J. Butcher, P. C. Junk, D. R. Turner, G. B. Deacon and H. B. Singh, *Dalton Trans*., **49**, 1173 (2020).
27. J. Beckmann, J. Bolsinger, J. Duthie and P. Finke, *Organometallics*, **31**, 289 (2012).
28. H. Fujihara, H. Mima and N. Furukawa, *J. Am. Chem. Soc*., **117**, 10153 (1995).
29. A. Pop, A. Silvestru, E. J. Juárez-Pérez, M. Arca, V. Lippolis and C. Silvestru, *Dalton Trans*., **43**, 2221 (2014).
30. R. A. Varga, M. Kulcar and A. Silvestru, *Acta Crystallogr. E*, **E66**, o771 (2010).
31. A. Pop and A. Silvestru, *Polyhedron*, **160**, 279 (2019).
32. A. Beleaga, V. R. Bojan, A. Pöllnitz, C. I. Raț and C. Silvestru, *Dalton Trans*., **40**, 8830 (2011).
33. V. Rani, M. Boda, S. Raju, G. N. Patwari, H. B. Singh and R. J. Butcher, *Dalton Trans*., **47**, 9114 (2018).
34. M. Hejda, D. Duvinage, E. Lork, R. Jirásko, A. Lyčka, S. Mebs, L. Dostál and J. Beckmann, *Organometallics*, **39**, 1202 (2020).
35. A. K. Gupta, R. Deka, H. B. Singh and R. J. Butcher, *New J. Chem*., **43**, 13225 (2019).
36. (a) M. R. Detty, A. E. Friedman and M. McMillan, *Organometallics*, **13**, 3338 (1994); (b) M. R. Detty, A. J. Williams, J. M. Hewitt and M. McMillan, *Organometallics*, **14**, 5258 (1995).
37. (a) J. Beckmann, J. Bolsinger, A. Duthie and P. Finke, *Dalton Trans*., **42**, 12193 (2013); (b) J. Bolsinger and J. Beckmann, *Main Group Met. Chem*., **37**, 159 (2014).
38. R. Deka, A. Sarkar, R. J. Butcher, P. C. Junk, D. R. Turner, G. B. Deacon and H. B. Singh, *Organometallics*, **39**, 334 (2020).

39. T. M. Klapötke, B. Krumm and M. Scherr, *Acta Crystallogr. E*, **E63**, o4189 (2007).
40. R. Deka, A. Gupta, A. Sarkar, R. J. Butcher and H. B. Singh, *Eur. J. Inorg. Chem*., **2020**, 4170 (2020).
41. J. Beckmann, J. Bolsinger and A. Duthie, *Organometallics*, **28**, 4610 (2009).
42. G. E. Garrett, G. L. Gibson, R. N. Straus, D. S. Seferos and M. S. Taylor, *J. Am. Chem. Soc*., **137**, 4126 (2015).
43. E. A. Suturina, N. A. Semenov, A. V. Lonchakov, I. Yu. Bagryanskaya, Y. V. Gatilov, I. G. Irtegova, N. V. Vasilieva, E. Lork, R. Mews, N. P. Gritsan and A. V. Zibarev, *J. Phys. Chem. A*, **115**, 4851 (2011).
44. (a) N. A. Semenov, A. V. Lonchakov, N. A. Pushkarevsky, E. A. Suturina, V. V. Korolev, E. Lork, V. G. Vasiliev, S. N. Konchenko, J. Beckmann, N. P. Gritsan and A. V. Zibarev, *Organometallics*, **33**, 4302 (2014); (b) N. A. Semenov, N. A. Pushkarevsky, J. Beckmann, P. Finke, E. Lork, R. Mews, I. Yu. Bagryanskaya, Y. V. Gatilov, S. N. Konchenko, V. G. Vasiliev and A. V. Zibarev, *Eur. J. Inorg. Chem*., **2012**, 3693 (2012).
45. (a) V. Kumar, Y. Xu and D. L. Bryce, *Chem. Eur. J*., **26**, 3275 (2020); (b) Y. Xu, V. Kumar, M. J. Z. Bradshaw and D. L. Bryce, *Cryst. Growth Des*., **20**, 7910 (2020).
46. (a) L. Chen, J. Xiang, Y. Zhao and Q. Yan, *J. Am. Chem. Soc*., **140**, 7079 (2018); (b) R. Zeng, Z. Gong and Q. Yan, *J. Org. Chem*., **85**, 8397 (2020).
47. E. A. Chulanova, E. A. Radiush, I. K. Shundrina, I. Yu. Bagryanskaya, N. A. Semenov, J. Beckmann, N. P. Gritsan and A. V. Zibarev, *Cryst. Growth Des*., **20**, 5868 (2020).
48. (a) S. Langis-Barsetti, T. Maris and J. D. Wuest, *J. Org. Chem*., **82**, 5034 (2017); (b) B. Kohl, C. Over, T. Lohr, M. Vasylyeva, F. Rominger and M. Masterlerz, *Org. Lett*., **16**, 5596 (2014).
49. L.-J. Riwar, N. Trapp, K. Root, R. Zenobi and F. Diederich, *Angew. Chem. Int. Ed*., **57**, 17259 (2018).
50. M. R. Ams, N. Trapp, A. Schwab, J. V. Milić and F. Diederich, *Chem. Eur. J*., **25**, 323 (2019).
51. Y. Lu, W. Li, W. Yang, Z. Zhu, Z. Xu and H. Liu, *Phys. Chem. Chem. Phys*., **21**, 21568 (2019).
52. K. Eichstaedt, A. Wasilewska, B. Wicher, M. Gdaniec and T. Poloński, *Cryst. Growth Des*., **16**, 1282 (2016).
53. J. Kübel, P. J. W. Elder, H. A. Jenkins and I. Vargas-Baca, *Dalton Trans*., **39**, 11126 (2010).

54. P. C. Ho, P. Szydloski, J. Sinclair, P. J. W. Elder, J. Kübel, C. Gendy, L. M. Lee, H. Jenkins, J. F. Britten, D. R. Morim and I. Vargas-Baca, *Nat. Commun*., **7**, 11299 (2016).
55. P. C. Ho, J. Rafique, J. Lee, L. M. Lee, H. A. Jenkins, J. F. Britten, A. L. Braga and I. Vargas-Baca, *Dalton Trans*., **46**, 6570 (2017).
56. P. C. Ho, L. M. Lee, H. Jenkins, J. F. Britten and I. Vargas-Baca, *Can. J. Chem*., **94**, 453 (2016).
57. P. C. Ho, J. Lomax, V. Tomassetti, J. F. Britten and I. Vargas-Baca, *Chem. Eur. J.*, **27**, 10849 (2021).
58. P. C. Ho, R. Bui, A. Cevallos, S. Sequeira, J. F. Britten and I. Vargas-Baca, *Dalton Trans*., **48**, 4879 (2019).
59. P. C. Ho, H. A. Jenkins, J. F. Britten and I. Vargas-Baca, *Faraday Discuss*., **203**, 187 (2017).
60. J. Wang, P. C. Ho, J. F. Britten, V. Tomasetti and I. Vargas-Baca, *New. J. Chem*., **43**, 12601 (2019).
61. A. Kremer, C. Aurisicchio, F. De Leo, B. Ventura, J. Wouters, N. Armaroli, A. Barbieri and D. Bonifazi, *Chem. Eur. J*., **21**, 15377 (2015).
62. A. Kremer, A. Fermi, N. Biot, J. Wouters and D. Bonifazi, *Chem Eur. J*., **22**, 5665 (2016).
63. N. Biot and D. Bonifazi, *Chem. Eur. J*., **24**, 5439 (2018).
64. N. Biot, D. Romito and D. Bonifazi, *Cryst. Growth Des*., **21**, 536 (2021).

Subject Index